

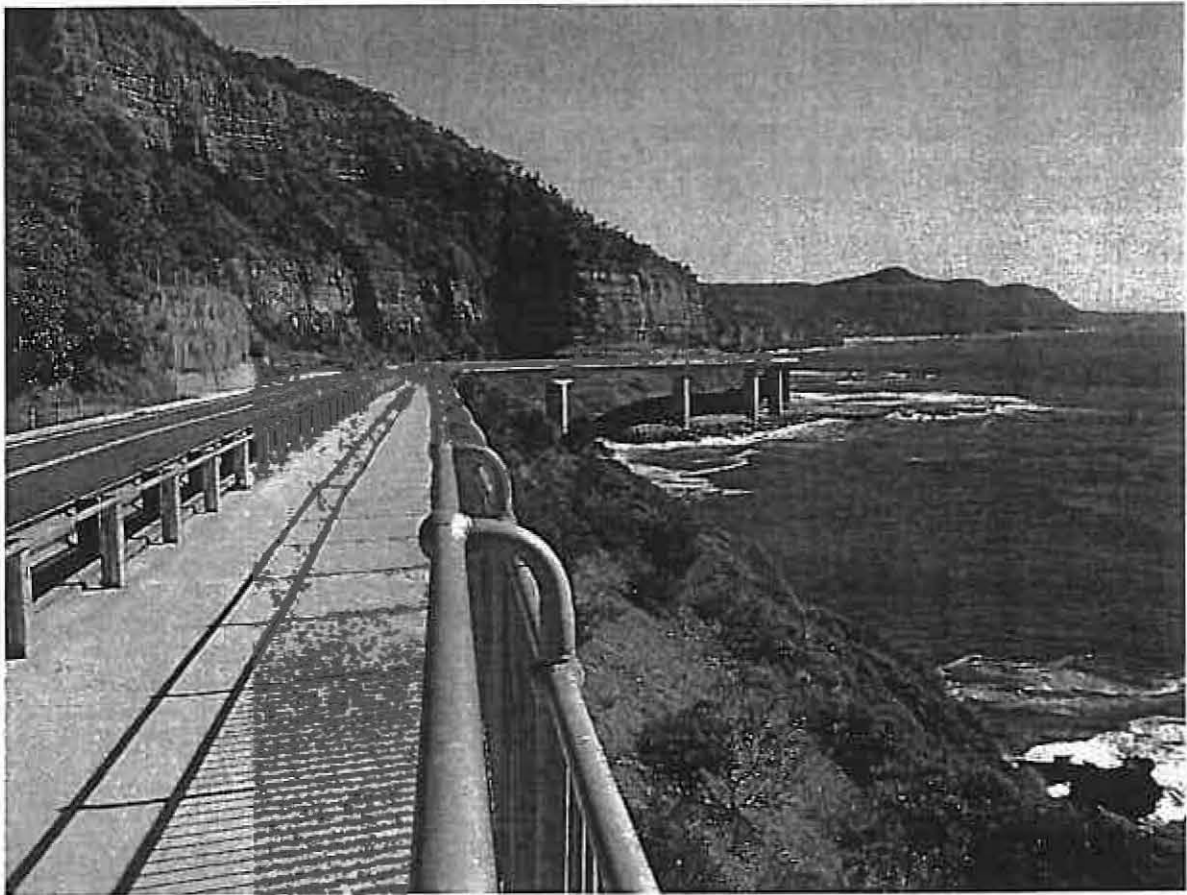
*MALCOLM BOCKING*

**PROCEEDINGS OF THE THIRTY SIXTH  
SYDNEY BASIN SYMPOSIUM**

**on**

**“ADVANCES IN THE STUDY OF THE  
SYDNEY BASIN”**

**27-29 November, 2006**



**University of Wollongong  
NSW 2522 AUSTRALIA**

**Cover Photograph**

SeaCliff Bridge on Lawrence Hargrave Drive, Coalcliff, with the Narrabeen Group cropping behind the bridge, with the Illawarra Coal Measures below it and the Hawkesbury Sandstone in the distance. Looking North.

---

University of Wollongong

---



**SCHOOL  
OF  
EARTH AND ENVIRONMENTAL SCIENCES**

**PROCEEDINGS OF THE THIRTY SIXTH SYDNEY  
BASIN SYMPOSIUM**

**on**

**ADVANCES IN THE STUDY OF THE  
SYDNEY BASIN**

**27-29 November, 2006**

**University of Wollongong  
2522 AUSTRALIA**

Editors: Adrian Hutton and Jonathan Griffin

Authors could elect to have their papers refereed. Part A of this volume contains papers that were refereed by at least two persons. The referees' comments were taken into account when editing the papers. Part B of this volume contains papers that were not refereed.

The organisers would like to thank the following persons for their contribution in reviewing papers included in this volume

**Reviewers**

Paul Carr  
Bryan Chenhall  
Rod Doyle  
Chris Fergusson  
Jonathan Griffin  
Adrian Hutton  
Ray Nolan

ISBN-13: 978-1-74128-123-1

ISBN-10: 1-74128-123-7

The editors, the School of Earth and Environmental Sciences and the referees are not responsible, nor necessarily accept, the facts and opinions given in the papers.

Copyright of the papers in this volume is retained by the authors

**Published by the School of Earth and Environmental Sciences  
University of Wollongong NSW 2522 Australia**

## FOREWORD

Welcome to the 36th Sydney Basin Symposium on *Advances in the Study of the Sydney Basin*. These symposia have a long and distinguished tradition, having been initiated by Professor Claus Diessel and colleagues in the former Department of Geology at the University of Newcastle. This year marks the second time that the Sydney Basin Symposium will be held at the University of Wollongong. It is with great pleasure that the School of Earth & Environmental Sciences is able to host this important event.

In what continues to be a financially challenging time for the university sector, the School of Earth & Environmental Sciences remains very well resourced and especially in terms of research infrastructure. This is largely due to the assiduous efforts of many academics within the School and their successes in obtaining nationally competitive research funds. Since the last Symposium the School has received funds for a state-of-the-art compound-specific radiocarbon dating facility, as well as new equipment for optically stimulated luminescence and amino acid racemisation dating, a new X-ray fluorescence spectrometer, an additional bus for assisting in our field-based teaching activities and a new bank of computers for our spatial analysis laboratories. It is also pleasing to see that the University of Wollongong has recently won the Times Higher Education Supplement inaugural award as "Commonwealth University of the Year". The University of Wollongong was the only short-listed Australian university for this award.

Even a cursory glance at the program for this symposium reveals the exciting diversity of research topics currently being examined within the Sydney Basin province. It is also gratifying to see so many people presenting talks at this meeting.

In many respects, the Sydney Basin, although representing the local field area for many investigators, is increasingly becoming an international stage for research in view of the widespread concerns about anthropogenic influences on recent climate changes. Whilst some people may wish to debate the nuances of causal relationships in understanding the physical basis of recent climatic and environmental changes, what is beyond debate are the very exciting research opportunities that are emerging relating to resource utilization and the development of clean technologies in the use of long-established energy resources. It is hoped that this symposium will also provide an appropriate forum to discuss these important issues.

Many of you will have attended previous Sydney Basin symposia, and hence at this meeting, will have the opportunity to renew old acquaintanceships. For others, it will be an opportunity to possibly establish new research partnerships. Either way, I hope that you gain a lot by attending this symposium

I would particularly like to record the enormous effort that Adrian Hutton has made in organizing this meeting. On behalf of the School of Earth & Environmental Sciences, I would like to welcome you to the University of Wollongong and wish you a very successful and memorable meeting.

Colin V. Murray-Wallace  
Head, School of Earth & Environmental Sciences

## PREFACE

The 36th Sydney Basin Symposium on "Advances in the Study of the Sydney Basin" is back after an absence of three years again, hosted by the University of Wollongong but in a new venue, the Function Centre. Whilst attendance and the number of papers to be presented are down compared to the last Symposium in 2003, the diversity and quality of the papers has not changed. Two days of technical papers have been programmed but without the need to run alternate sessions. It is heartening to see approximately half of the papers will be presented by persons who have not attended a previous Sydney Basin Symposium. We again have the all important Dinner on Tuesday evening and an optional visit to the Science Centre.

The 33rd Symposium heralded the inaugural Kenneth George Mosher Memorial Lecture and we again host it this year. The lecture is in honour of the life and achievements of Ken Mosher a former Chief Geologist with the Joint Coal Board and stalwart of the New South Wales Coal Geology Council and its predecessors. We are privileged to have Emeritus Professor Jim Galbraith as speaker. Jim has had a long association with the mining industry and his thoughts and views are indeed timely.

The field trip will provide an overview of the coastal exposures from Wollongong to Coalcliff providing we access the last two stops weather permitting. At Wollongong Harbour the upper part of the marine Shoalhaven Group crops out. We then progress upwards through the Illawarra Measures with the main coal seams the focus.

As a final note, I gratefully acknowledge the support of Peter Vrahas, Function Coordinator at UNICENTRE. Peter had done all the organising - from the venue, to the lunches and morning tea and the dinner. As with the 35<sup>th</sup> Sydney Basin Symposium, the support of the Coalfields Geology Council of New South Wales is welcomed as the support of the coal industry is needed if the Sydney Basin Symposium is to continue with its normal vigour.

To those attending, please enjoy your symposium and please prepare for the next.

Adrian Hutton,  
Convener

**Major Sponsor**



***Integrated Seismic  
Technologies***

# Table of Contents

## Technical Program

Author	Title	Page
<b>Part A – Refereed Papers</b>		
Beamish, B. and Clarkson, F.	Self-Heating Rates of Sydney Basin Coals - The Emerging Picture	1
Carr, P., Jones, B. and Selleck, B.	The Sydney Basin and Frozen Prawns - The Cool Mineral Connection	9
David, K.	Overview of the Hydrogeology of the Western Coalfield – Ulan Coal Mine Case Study	15
Davis, B., Esterle, J. and Keilar, D.	Determining the Geological Controls on the Spatial Distribution of Phosphorus within Coal Seams Mined at South Walker Creek Mine, Bowen Basin, Central Queensland, Australia	27
Dawson, M., Coxhead, C. and McMinn, A.	Greta Coal Measures in the Werris Creek Area, New South Wales	37
Fergusson, C.	Review of Structure and Basement Control of the Lapstone Structural Complex, Sydney Basin, Eastern New South Wales	45
Griffin, J. and Hutton, A.	Wingecarribee Peat Swamp, Southern Highlands, New South Wales – And Its Water	51
Hatherly, P., Thomson, S and Armstrong, M.	Geophysical Log Analysis for the Southern Sydney Basin	59
Hopley, C. and Jones, B.	Morphological and Stratigraphic Evolution of Wandandian Creek Delta, St Georges Basin, New South Wales	71
Hopley, C. Jones, B. and Puotinen, M.	Morphological Changes, Assessed within a GIS Framework, in the Prograding Macquarie Rivulet Delta, New South Wales	79
Hutton, A.	OH&S Legislation in the Coal Industry – What Prompts Change?	87

- Hutton, A., Johnson, M. and Gentz, M. Petrography of Hawkesbury Sandstone and Water Movement
- Pinetown, K., Saghafi, A. and Grobler, P. Effects of Igneous Intrusions on Coal Measures of the South African Karoo Basin and associated Coal Seam Gas
- Prendergast E., Healy, B., Kyan, D., Demidjuk, Z., McCaughan, G., Woodfull, C. and Munroe, S. Multiple Data Sets Used to Evaluate Geology and Structure: Bowen and Surat Basins Queensland
- Saghafi, A., Faiz, M. and Roberts, D. Gas Reservoir Properties of Sydney Basin Coals and their Impacts on CO<sub>2</sub> Sequestration
- Ward, C., French, D., Heidrich, C. and Bowman, H. Fly Ash – Waste Or Resource?
- Ward, C., Li, Z. and Gurba, L. Rank and Maceral Chemistry of the Greta Coal Measures in the Sydney and Cranky Corner Basins
- Williams, M., Carr, P. and Jones, B. Identification of the Permian-Triassic Boundary in the Southern Sydney Basin
- Part B – Unrefereed Papers**
- Ahmed, M., Volk, H., George, S. and Faiz, M. Organic Geochemical Characteristics of Late Permian Coals From The Southern Sydney Basin, Australia
- Bartlett, K. and Edwards, J. The Use of Acoustic Scanner Results for Mine Design
- Creech, M. RIP: The Wollombi Coal Measures
- Daigle, L. Primary Fabric and Fracture Distribution within the Cordeaux Crininite Intrusive
- Dawson, M. Geology of The Willow Tree-Ardglen Area, New South Wales: A Reappraisal
- Edwards, J., Bartlett, K. Hatherly, P. And Lea, J. Exploration of Coal Deposits
- Esterle, J., Williams, R., Sliwa, R. and Malone, M. Variability in Coal Seam Gas Contents that Impacts on Fugitive Gas Emissions Estimations for Australian Black Coals

McLean, W. and Averkiou, A.	The Port Botany Hawkesbury Sandstone LPG Cavern: An Overview of Cavern Design, Operation and Monitoring	223
McMahon, C.	Exploratory Blend Optimisation Modelling	231
Och, D.	Greater Sydney Region Audit and Gaps Analysis	243
O'Donnell, M. and O'Brien, G. Huttton, A.	Factors Affecting Water-Quality in the Wingecarribee Shire Council Local Government Area	253
Peters, T. and Hendrick, N.	Applications of Seismic Reflection In The Coal Environment	267
Pickel, W.	Organic Petrology – State of the Art (An Overview)	277
Thomson, S., Adam, S. and Hatherly, P.	Enhanced Geological Modelling through Advances in Logging and Interpretation of Inseam Boreholes	279
<b>List of Authors</b>		<b>293</b>

**36<sup>th</sup> SYDNEY BASIN SYMPOSIUM  
2006**

**ADVANCES IN THE STUDY ON THE SYDNEY BASIN**

**Technical Program**

**Monday, 27 November 2006**

<b>08.00 –09.00</b>	<b>REGISTRATION</b>	<b>Function Centre (Building 11)</b>
<b>Symposium Opening</b>		<b>Function Centre (Building 11)</b>
<b>09.00- 09.05</b>	<b>Welcome</b>	<b>Associate Professor Paul Carr</b>
<b>09.05-09.15</b>	<b>Official Opening</b>	<b>Prof Lee Astheimer</b> Pro Vice-Chancellor Research, University of Wollongong
<b>Technical Session 1</b>		<b>Function Centre (Building 11)</b>
<b>Chair – Paul Carr</b>		
<b>09.15-09.40</b>	<b>C McMahon</b>	<b>Exploratory Blend Optimisation Modelling</b>
<b>09.40-10.05</b>	<b>S Thomson, S Adam, P Hatherly</b>	<b>Enhanced Geological Modelling through Advances in Logging and Interpretation of Inseam Boreholes</b>
<b>10.05-10.40</b>	<b>Kenneth George Mosher Memorial Lecture</b> <b>Emeritus Prof. Jim Galvin</b>	<b>The Elevated Role of Geology in Today's World</b>
<b>10.40-11.00</b>	<b>Morning Tea - Function Centre (Building 11)</b>	
<b>11.00-11.25</b>	<b>T Peters, N Hendrick</b>	<b>Applications Of Seismic Reflection In The Coal Environment</b>
<b>11.25-11.50</b>	<b>K Bartlett, J Edwards</b>	<b>The Use of Acoustic Scanner Results for Mine Design</b>
<b>11.50-12.15</b>	<b>P Hatherly, S Thomson, M Armstrong</b>	<b>Geophysical Log Analysis for the Southern Sydney Basin</b>
<b>12.15-12.40</b>	<b>J Edwards, K Bartlett, P Hatherly, J. Lea</b>	<b>Exploration of Coal Deposits</b>
<b>12.40-13.30</b>	<b>Lunch – Function Centre (Building 11)</b>	

## Technical Session 2

### Chair – Chris Fergusson

13.30-13.55 C. Hopley, B Jones

13.55-14.20 W McLean, A Averkiou

14.20-14.45 M O'Donnell, G O'Brien,  
A.Hutton

14.45-15.10 C Hopley, B Jones  
Puotinen, M.

15.10-15.40 **Afternoon Tea - Function Centre (Building 11)**

15.40-16.05 C Ward, D French,  
C Heinrich, H Bowman

16.05-16.30 W Pickel

16.30-16.55 C Ward, Z Li, L Gurba

16.55-17.20 A Hutton, M Johnson,  
M Gentz

## Function Centre (Building 11)

Morphological and Stratigraphic Evolution  
Of The Wandandian Creek Delta,  
St Georges Basin, New South Wales  
The Port Botany Hawkesbury Sandstone  
LPG Cavern: An Overview of Cavern  
Operation And Monitoring.

Factors Affecting Water Quality in the  
Wingecarribee Shire Council Local  
Government Area

Morphological Changes, Assessed with  
a GIS Framework, in the Prograding  
Macquarie Rivulet Delta, New South Wales

Fly Ash – Waste Or Resource?

Organic Petrology – State of the Art  
(An Overview)

Rank and Maceral Chemistry of the Great  
Coal Measures in the Sydney and  
Cranky Corner Basins

Petrography of Hawkesbury Sandstone  
Water Movement

# SELF-HEATING RATES OF SYDNEY BASIN COALS - THE EMERGING PICTURE

Basil Beamish<sup>1</sup> and Fiona Clarkson<sup>2</sup>

<sup>1</sup>Director, Spontaneous Combustion Testing Laboratory  
The University of Queensland, St Lucia Qld 4072

<sup>2</sup>Research Scientist  
Simtars, PO Box 467, Goodna Qld 4300

## ABSTRACT

Adiabatic oven tests provide a simple and accurate measure of the intrinsic spontaneous combustion propensity of coal. Coal rank and mineral matter have significant effects on self-heating rate. Modifying effects such as coal start temperature also need to be considered when making an overall risk assessment of the potential of a hot spot forming. Lower in-mine temperatures of the Sydney Basin mean that coals with a medium to high intrinsic spontaneous combustion propensity, as determined by adiabatic testing, will have an overall lower risk rating than the same coal being mined in the Bowen Basin. Coking coals also display a substantially lower self-heating rate than steaming coals of the same rank.

## INTRODUCTION

The self-heating of coal is due to a number of complex exothermic reactions that occur once the coal is exposed to air. This self-heating process will continue provided that there is a sufficient air supply and the heat produced is not dissipated. The parameters that control a coal's propensity for self-heating have been the subject of many investigations. Relationships between coal properties (rank, mineral matter content, maceral composition, and moisture content) and self-heating indices have been published in a number of studies (Humphreys *et al.* 1981; Moxon & Richardson 1985; Singh & Demirbilek 1987; Barve & Mahadevan 1994; Beamish *et al.* 2001; Beamish 2005; Beamish & Blazak 2005; Beamish & Hamilton 2005).

Humphreys *et al.* (1981) found a simple relationship between the coal self-heating index parameter,  $R_{70}$  and coal rank for Queensland coals. However, work by Beamish *et al.* (2001) and Beamish (2005) on New Zealand and Australian coals covering a wider range of coal rank showed that the rank relationship with  $R_{70}$  coal self-heating rate is non-linear. Beamish & Blazak (2005) also showed that  $R_{70}$  values decrease significantly with increasing mineral matter content, as defined by the ash content of the coal.

To date there is little published data on the self-heating properties of Sydney Basin coals. Singh *et al.* (2003) and Moreby (1997 & 2005) have presented case history studies on a longwall operation in the Hunter Valley, describing the approaches to spontaneous combustion management planning. The self-heating parameters proposed by Singh *et al.* (2003) for risk assessment were a combination of intrinsic and extrinsic factors fed into an expert systems approach. The starting intrinsic parameters were the initial rate of heating (IRH) and total temperature rise (TTR). Values for these parameters were obtained from a set of statistical equations developed by Singh & Demirbilek (1987).

The purpose of this paper is to present results on a selection of Sydney Basin coals taken from the large  $R_{70}$  database that has been developed at The University of Queensland and for coals from both Australia and overseas. Significant differences are identified between coking coal and steaming coals of the same rank. A discussion is presented on the interpretation of the  $R_{70}$  parameter to evaluate the spontaneous combustion propensity of coal and its ability to develop a hot spot taking into account effects of extrinsic parameters. In particular, the impact of coal start temperature is illustrated that highlights the significant difference this extrinsic factor has on coals being mined in the Sydney Basin compared to coals being mined in the Bowen Basin.

## COAL SAMPLES AND $R_{70}$ TESTING PROCEDURE

### Sample characteristics

The coal samples tested in this study have been supplied either as fresh core samples from exploration and mining areas or as fresh lumps from developing mine faces. They cover a rank range from high volatile C bituminous to high volatile A bituminous (Table 1). The majority of samples are from the Wittingham Coal Measures of the Hunter Valley (C, B, C, D, E, H and I), but two sets of samples are from the Newcastle Coal Measures (G and G). When viewed on a Suggate rank plot (Suggate, 1998 & 2000) the samples plot between 11.7 to 13.7 (Figure 1). Coal E is substantially different in coal type to the rest of the samples. This coal is mined as a coking coal product and as such has a significant vitrinite content (>70%). The other samples plot at the lower end or just below the Zealand coal band, which is consistent with a lower vitrinite content (Suggate, 1998).

### $R_{70}$ test procedure

The  $R_{70}$  testing procedure essentially involves drying a 150g sample of <212 $\mu$ m crush at 110°C under nitrogen for approximately 16 hours. Whilst still under nitrogen, the sample is cooled to 40°C before being transferred to an adiabatic oven. Once the coal temperature is equilibrated at 40°C under a nitrogen flow in the adiabatic oven, oxygen is passed through the sample at 50mL/min. A data logger records the temperature rise due to the self-heating of the coal. The time taken for the coal temperature to reach 70°C is calculated as the self-heating rate index ( $R_{70}$ ), which is in units of °C/h and is a good indicator of the intrinsic reactivity towards oxygen.

### RELATIONSHIP BETWEEN COAL RANK, ASH CONTENT AND $R_{70}$ VALUE

As the  $R_{70}$  value is obtained on a dry basis, the best way to graphically represent the data is to plot it against the ash content (on a dry basis, Figure 2). The ash content is closely related to the mineral matter in the coal, which is the inorganic constituents of the coal that modify coal behaviour in many combustion processes. In the case of the coal self-heating, mineral matter acts as a diluent, effectively creating a heat sink due to its heat capacity (Barnes *et al.* 1988). Mineral matter may also create blockage of access to oxidation sites, leading to a lower self-heating rate of the coal even further (Beamish & Arisoy in prep). A general trend of decreasing  $R_{70}$  value with increasing ash content can be seen in Figure 2 for all of the samples tested.

In terms of rank, the high volatile A bituminous coals have  $R_{70}$  values less than 4°C/h whereas nearly all of the high volatile C/B bituminous coals have  $R_{70}$  values greater than 4°C/h (Figure 2). Coal E has an extremely low  $R_{70}$  value for the rank of coal. This is a soft coking coal from the Wittingham Coal Measures and has  $R_{70}$  values that are even lower than the high volatile A bituminous coals.

## SELF-HEATING RATES

than coal H, which has a much higher Suggate rank. (12.0 cf 13.0, respectively). A similar trend of extremely low  $R_{70}$  values has been noted for other coking coals of equivalent rank, in particular premium coking coals from the South Island of New Zealand. These New Zealand coals have extremely high crucible swelling numbers ( $>9$ ) and their  $R_{70}$  values are less than  $0.5^{\circ}\text{C/h}$ .

A possible explanation for this low self-heating rate is that coking coals contain a predominance of vitrinite. It is well documented that vitrinite is highly microporous (Unsworth *et al.* 1989; Gamson *et al.* 1993; Beamish & Crosdale 1998). As a result, it is more difficult for air to gain access to these pores to enable surface interactions to take place.

### INTERPRETING $R_{70}$ VALUES IN TERMS OF PROPENSITY FOR SPONTANEOUS COMBUSTION

#### **Intrinsic spontaneous combustion propensity classification**

Interpreting the significance of the  $R_{70}$  value for determining spontaneous combustion propensity has often been problematical for mining operations in the Sydney Basin, particularly as there is a wider range of coals being mined than when the test was first developed for Queensland coals in the late 70's (Humphreys 1979). Moreby (1997) reports that a coal with an  $R_{70}$  value below  $0.5^{\circ}\text{C/h}$  is considered to be low propensity,  $0.5$ - $0.8^{\circ}\text{C/h}$  medium propensity, while coals with an  $R_{70}$  value higher than  $0.8^{\circ}\text{C/h}$  are considered to be highly prone to spontaneous combustion. Using this classification would indicate that all the Sydney Basin samples in this study except Coal I have a high propensity for spontaneous combustion.  $R_{70}$  values in the UQ database have been measured as high as  $35^{\circ}\text{C/h}$  for an Indonesian sub-bituminous C coal. Therefore, a more refined classification scheme is needed to cover this range. A simple scheme is shown in Table 2, which uses a self-heating rate doubling to distinguish between classes. This doubling effect of self-heating rate is somewhat analogous to the Arrhenius kinetics often applied to coal oxidation modelling. Boundaries for each of these classes have been superimposed on Figure 2 to show which class each of the coals falls into. Coals A, B and C have a very high intrinsic spontaneous combustion propensity. Coals D, F and G have a high intrinsic spontaneous combustion propensity. Coals E and H have a medium intrinsic spontaneous combustion propensity and Coal I has a low-medium spontaneous combustion propensity.

#### **Mining analogues**

Knowing the intrinsic reactivity of a coal with respect to other known coals is a good starting point to assess the risk of spontaneous combustion. Consequently, Figure 2 also provides the opportunity to identify mining analogues that can be used to assist with future spontaneous combustion management planning. For example, coals C and D come from a longwall mining operation in the Hunter Valley that has a history of self-heating events. Coal A is from a seam that overlies coal C. Hence, it can be seen from the substantial increase in self-heating rate of Coal A, that it would pose a significant risk in terms of spontaneous combustion, particularly if this coal is building into a pile in the goaf behind the longwall.

Coal B (Figure 2) is from a Greenfield site in the Hunter Valley and consequently, spontaneous combustion management plans are already being developed from the test data obtained to date based on the mining analogy with coals C and D.

### Modifying effect of coal start temperature on self-heating rate

The  $R_{70}$  value is based on a 40°C coal start temperature. In-mine temperatures of Basin coals are not likely to be this high. Therefore to assess the effect of start temp on coal self-heating rate, one of the Newcastle coals was tested at the normal  $R_{70}$  temperature and a duplicate sample was tested at a lower start temperature. The curves for each of these tests are shown in Figure 3. The average self-heating rate at 70°C changes from 3.97°C/h at 40°C to 2.73°C/h at 33°C. This is equivalent to approximate doubling of the self-heating rate for every 10°C rise in temperature consistent with the Arrhenius kinetics of coal oxidation. If this factor is applied to the Basin results, each of the coals would reduce by at least one or two intrinsic spontaneous combustion propensity classes depending on the in-mine temperature. Consequently the same coal being mined in the Bowen Basin would be a greater spontaneous combustion risk due to the higher in-mine temperatures experienced there.

### Other modifying influences on spontaneous combustion risk

The modifying influences of other factors also need to be considered when assessing the meaning of an  $R_{70}$  value in terms of hot spot development. For example, Coal G in the new longwall mining operation in the Newcastle District. To date there has been no history of self-heating incidents, consistent with previous experience of mining this coal. Bulk tests of this coal also indicated a low propensity to develop a hot spot. Given the  $R_{70}$  rating of this coal (Class IV – high propensity) this appears to be anomalous. However, given that laboratory test is a measure of the coals reactivity to oxygen at fine particle size, it is remembered that in bulk coal, hot spot development is dependent on particle size. Coal G has a very low Hardgrove Grindability Index (HGI). Consequently, production of a large amount of coal fines is reduced. Hence, hot spot development is inhibited as a result of this additional factor.

Beamish & Hamilton (2005) have shown that the accelerated effect of coal reactivity does not take place until the moisture content of the coal drops to approximately 50% of the maximum holding capacity. This is due to the competing influences of heat loss through evaporation and blocking of access to oxidation sites by the moisture. Hence, Coal A, which has a high moisture content, will require a considerable time to develop a hot spot due to this. However, the high self-heating rate of the coal still dominates the spontaneous combustion risk assessment. These competing influences are best examined using numerical modelling. Preliminary work has begun using data from the  $R_{70}$  self-heating curves to extract kinetic parameters as input to a moist coal model (Arisoy *et al.* 2006). Further refinement of this work is in progress using data from coals in the UQ  $R_{70}$  database.

### CONCLUSIONS

Coal self-heating is a complex process. To determine the risk of spontaneous combustion requires a good appreciation of the influence of various factors, both intrinsic and extrinsic. One way to assess spontaneous combustion propensity is to conduct laboratory tests on samples from the seam of interest to obtain self-heating rate parameters. One parameter frequently used in the Australian coal industry is the  $R_{70}$  self-heating rate value of the coal. A comprehensive classification scheme has been developed using this parameter and other parameters and analogues are readily identified for Greenfield sites.

$R_{70}$  values are strongly affected by rank and mineral matter. In addition, the ambient temperature of the coal needs to be taken into consideration when interpreting this parameter.

particularly when making comparisons between coals mined in the Sydney Basin and Bowen Basin. There are also differences between coking and steaming coals, which have not been given as much consideration as they should. Other modifying parameters such as moisture content and production of fines need to be considered when assessing the risk of a hot spot developing. Numerical modelling can be used to achieve this, but the modelling must incorporate data specific to the coal being mined. Consequently, in any final mine assessment there is no substitute for hard data from laboratory testing.

#### ACKNOWLEDGEMENTS

Permission to publish these results has been granted by UniQuest Pty Limited and Simtars. Funding for this work has also been provided by ACARP project C12018. The authors would like to thank the coal companies who supported this project and provided fresh samples for testing.

#### REFERENCES

- ARISOY A., BEAMISH B. B. & ÇETEGEN E. 2006. Modelling spontaneous combustion of coal. *Turkish Journal of Engineering & Environmental Sciences* 30, 193-201.
- BARVE S. D. & MAHADEVAN V. 1994. Prediction of spontaneous heating liability of Indian coals based on proximate constituents. *Proceedings 12<sup>th</sup> International Coal Preparation Congress*, pp557-562, Cracow, Poland.
- BEAMISH B. B. 2005. Comparison of the R<sub>70</sub> self-heating rate of New Zealand and Australian coals to Suggate rank parameter. *International Journal of Coal Geology* 64, 139-144.
- BEAMISH B. B. & ARISOY A. (in prep). Effect of mineral matter on coal self-heating rate.
- BEAMISH B. B. & BLAZAK D. G. 2005. Relationship between ash content and R<sub>70</sub> self-heating rate of Callide Coal. *International Journal of Coal Geology* 64, 126-132.
- BEAMISH B. B. & HAMILTON G. R. 2005. Effect of moisture content on the R<sub>70</sub> self-heating rate of Callide Coal. *International Journal of Coal Geology* 64, 133-138.
- BEAMISH B. B. & CROSDALE P. J. 1998. Instantaneous outbursts in underground coal mines: an overview and association with coal type. in *Coalbed Methane: From Coal-Mine Outbursts to a Gas Resource*, R.M. Flores (ed), Special Issue, *International Journal of Coal Geology* 35, 27-55.
- BEAMISH B. B., BARAKAT M. A. & ST GEORGE J. D. 2001. Spontaneous-combustion propensity of New Zealand coals under adiabatic conditions. *International Journal of Coal Geology* 45, 217-224.
- GAMSON P. D., BEAMISH B. B. & JOHNSON D. P. 1993. Coal microstructure and micropermeability and their effects on natural gas recovery. *Fuel* 72, 87-99.
- HUMPHREYS D. 1979. A study of the propensity of Queensland coals to spontaneous combustion, ME Thesis, Department of Mining and Metallurgical Engineering, The University of Queensland, Australia.
- HUMPHREYS D., ROWLANDS D. & CUDMORE J. F. 1981. Spontaneous combustion of some Queensland coals. *Proceedings Ignitions, Explosions and Fires in Coal Mines Symposium*, pp5-1 – 5-19, The AusIMM Illawarra Branch, Melbourne, Australia.
- MOREBY R. 2005. Management of seam gas emission and spontaneous combustion in a highly gassy, thick and multi seam coal mine – A learning experience. *Proceedings 8th International Mine Ventilation Congress*, pp. 39-45, The AusIMM, Melbourne, Australia.
- MOREBY R. 1997. Dartbrook coal - Case study. *Proceedings 6th International Mine Ventilation Congress*, pp. 39-45, The Society of Mining, Metallurgy and Exploration Inc., Littleton, USA.

- MOXON N. T. & RICHARDSON S. B. 1985. Development of a self-heating index for coal. *Coal Preparation* 2, 91-105.
- SINGH R. N. & DEMIRBILEK S. 1987. Statistical appraisal of intrinsic factors affecting spontaneous combustion of coal. *Mining Science and Technology* 4, 155-165.
- SINGH R. N., SHONHARDT J.A. & PORTER I. 2003. Spontaneous combustion risk management in longwall mining in New South Wales. Proceedings of Mining Risk Management Conference, The AusIMM, Melbourne, Australia, 165-174.
- SMITH A. C., MIRON Y. & LAZZARA P. 1988. *Inhibition of Spontaneous Combustion of Coal*. US Bureau of Mines Report of Investigation, RI 9196.
- SUGGATE R. P. 2000. The Rank ( $S_r$ ) scale: its basis and its application as a maturity index for all coals. *New Zealand Journal of Geology and Geophysics* 43, 521-553.
- SUGGATE R. P. 1998. Analytical variation in Australian coals related to coal type and rank. *International Journal of Coal Geology* 37, 179-206.
- UNSWORTH J. F., FOWLER C. S. & JONES L. F. 1989. Moisture in coal – 2. Maceral effects on pore structure. *Fuel* 68, 18-26.

Table 1. Analytical and rank data for coal samples

	IM (%, adb)	Ash (%, db)	VM (%, dmmf)	CV (Btu/lb, mmmf)	ASTM Rank	Suggate Rank
Coal A	9.0	11.8	35.0	12858	hvCb	11.7
Coal B	4.5	15.0	40.6	13942	hvBb	11.7
Coal C	5.5	13.8	38.8	13577	hvBb	11.8
Coal D	5.0	12.9	35.0	13660	hvBb	11.9
Coal E	2.1	6.8	42.8	14853	hvAb	12.0
Coal F	2.8	27.0	36.3	14080	hvAb	12.5
Coal G	1.6	15.8	31.7	14452	hvAb	12.6
Coal H	2.1	14.6	36.5	14675	hvAb	13.0
Coal I	1.9	15.6	31.4	14827	hvAb	13.7

## SELF-HEATING RATES

**Table 2.** Intrinsic spontaneous combustion propensity (ISCP) classification based on  $R_{70}$  self-heating rate values

ISCP Class	$R_{70}$ values	Propensity rating
Class I	$R_{70} < 0.5$	Low
Class II	$0.5 \leq R_{70} < 1$	Low – medium
Class III	$1 \leq R_{70} < 2$	Medium
Class IV	$2 \leq R_{70} < 4$	High
Class V	$4 \leq R_{70} < 8$	Very high
Class VI	$8 \leq R_{70} < 16$	Extremely high
Class VII	$R_{70} \geq 16$	Exceptionally high

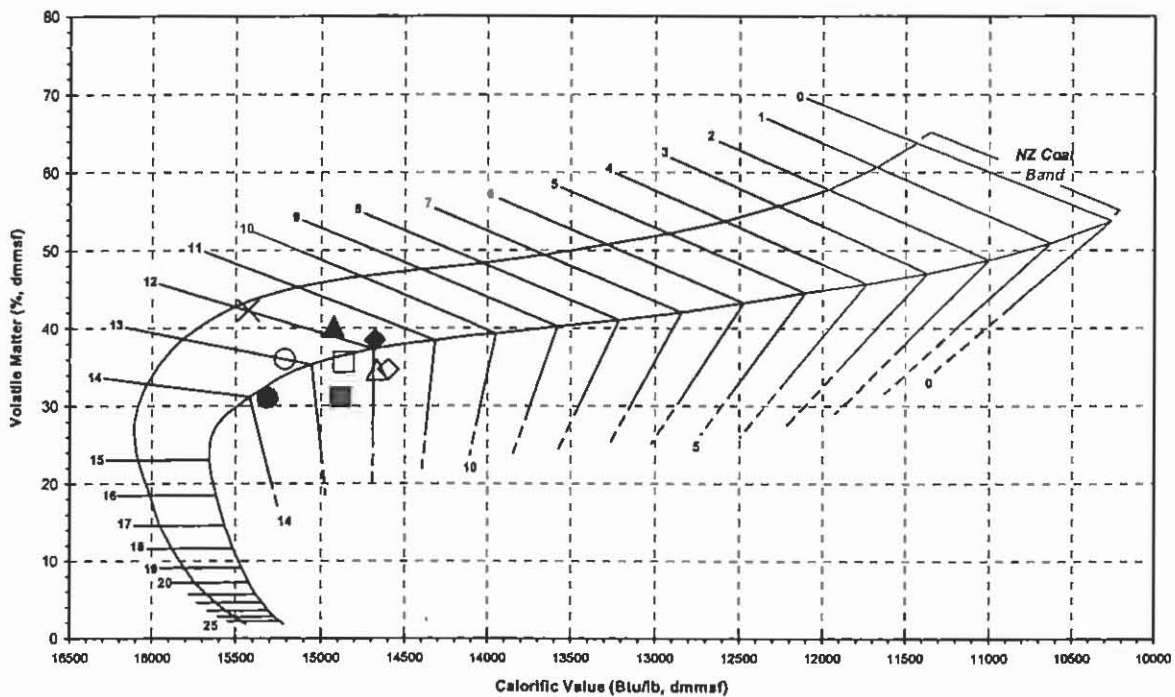


Figure 1. Suggate rank plot of Sydney Basin coal samples (see Figure 2 for legend)

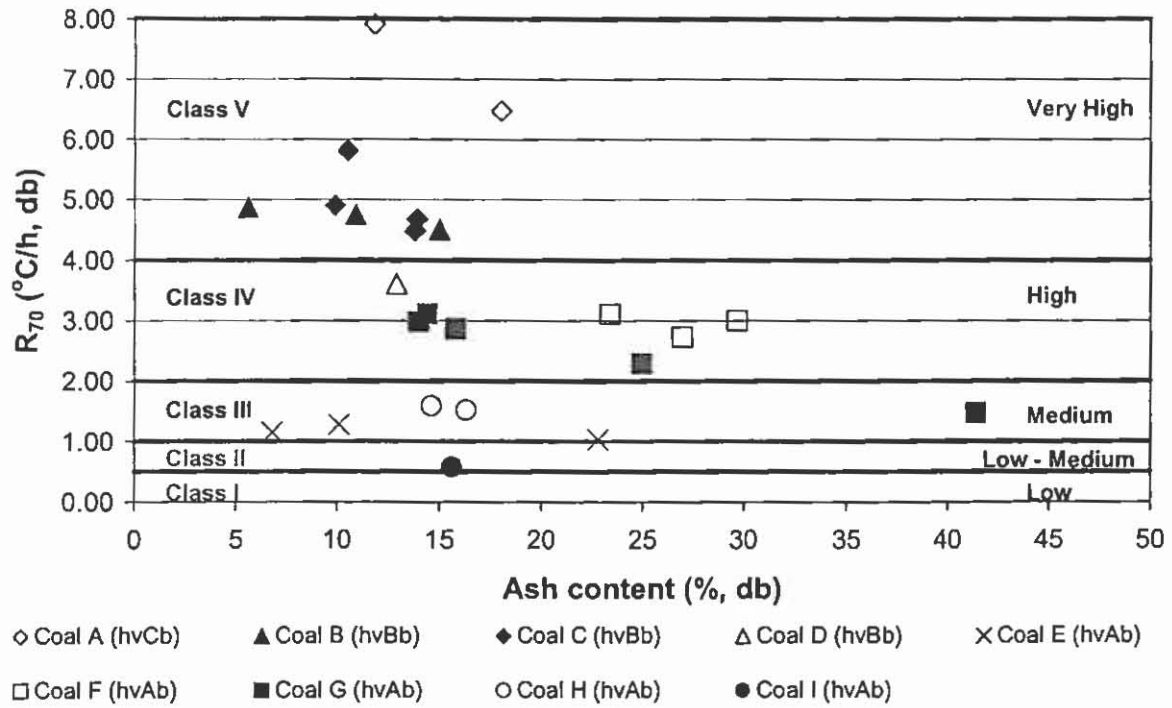


Figure 2. Relationship between ash content, coal rank and  $R_{70}$  self-heating rate for Sydney Basin coals

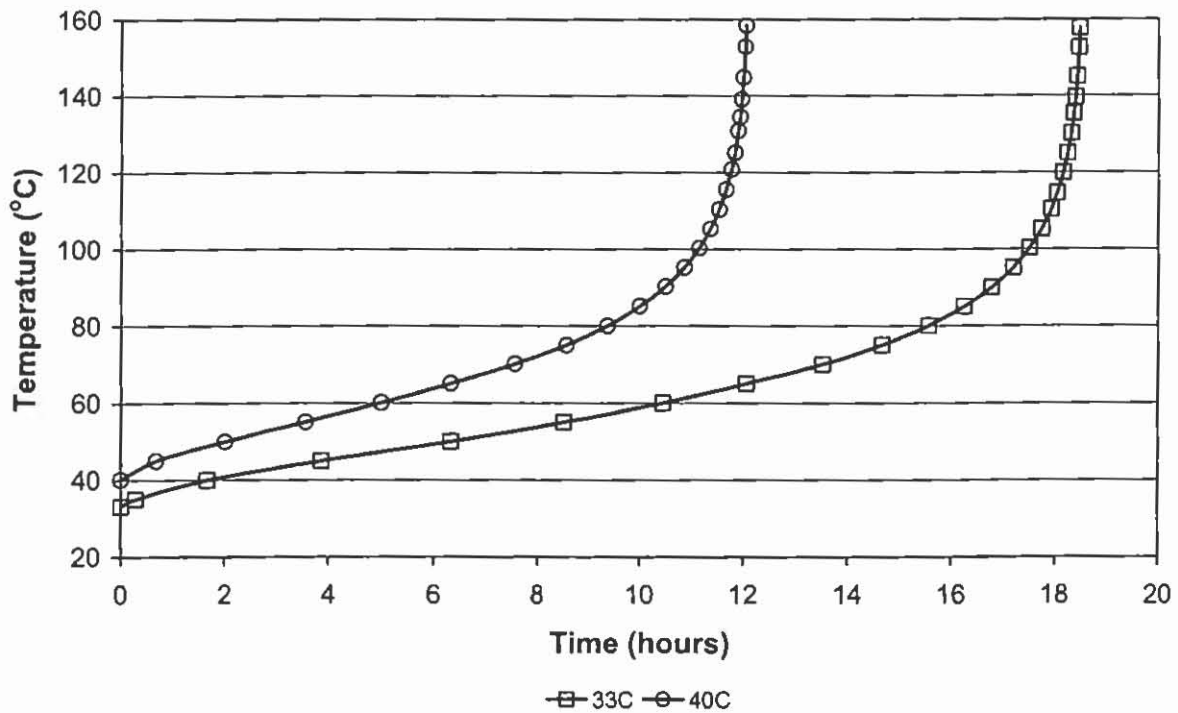


Figure 3. Adiabatic self-heating curves of Newcastle coal from start temperatures of 33°C and 40°C.

# THE SYDNEY BASIN AND FROZEN PRAWNS - THE COOL MINERAL CONNECTION

Paul Carr<sup>1</sup>, Brian Jones<sup>1</sup> and Bruce Selleck<sup>2</sup>

<sup>1</sup>School of Earth and Environmental Sciences

<sup>2</sup>Department of Geology  
Colgate University, Hamilton, NY, 13346-1398, USA

## ABSTRACT

Calcite pseudomorphs after ikaite (glendonite) are common in the Permian marine sequences of the Sydney Basin and have been recorded from more than 30 localities representing six major glendonite-forming intervals. Recognition of glendonites in Sydney Basin strata provides unequivocal evidence for coldwater deposition. Stable isotope signatures of modern ikaite suggest carbonate precipitation in equilibrium with ambient seawater and are consistent with derivation of carbonate from methane oxidation. Review of published data suggests that while Holocene glendonite may provide reliable isotopic records of the conditions of ikaite crystallisation, precipitation of later calcite cement within the glendonite structure reduces the significance of the isotopic signature as an indicator of primary depositional conditions. Stable isotope data from Sydney Basin glendonites indicate that diagenetic processes have obscured whatever primary carbonate isotope signal might have been preserved.

## INTRODUCTION

Glendonite is but one of several names used for a group of pseudomorphs that have been recorded from a wide range of geographic locations and in strata ranging from Precambrian to Recent in age. Samples from the original locality at Glendon in the northern Sydney Basin were presented to James Dwight Dana, the eminent American mineralogist, during his visit to Australia in 1839-40 and were later described and figured in his report on the geology of New South Wales (Dana 1849). The name "glendonite", however, was not proposed until more than fifty years later when David *et al.* (1905) published a detailed description of the occurrence, morphology and significance of glendonites from Glendon and three other localities in the Sydney Basin. The aim of the current paper is to describe the occurrence and distribution of glendonites in the Sydney Basin, and to assess their significance for paleoclimatic reconstructions and as a proxy for Permian seawater isotopic compositions.

## PRECURSOR MINERAL

The identity of the precursor mineral to glendonites has been the subject of considerable debate throughout the last century with the majority of studies relying on crystallographic data for mineral identification. Several minerals including anhydrite (CaSO<sub>4</sub>), aragonite (CaCO<sub>3</sub>), celestite (SrSO<sub>4</sub>), gaylussite (CaCO<sub>3</sub>•Na<sub>2</sub>CO<sub>3</sub>•5H<sub>2</sub>O), glauberite (Na<sub>2</sub>SO<sub>4</sub>•CaSO<sub>4</sub>), gypsum (CaSO<sub>4</sub>•2H<sub>2</sub>O), sulphur (S) and thenardite (Na<sub>2</sub>SO<sub>4</sub>) have been suggested as possible precursors, with glauberite and thenardite probably being the most favoured choices. The lack of agreement between the early investigators about the identify of the precursor mineral for glendonites and other similar pseudomorphs is not surprising due to the ambiguity of the crystallographic data and because the most likely forerunner was not discovered in nature

until relatively recently.

Synthetically produced calcium carbonate hexahydrate ( $\text{CaCO}_3 \cdot 6\text{H}_2\text{O}$ ) had been known to chemists before James Dana visited the Hunter Valley and described the original glendonites, but it was not found in nature until the mineral ikaite was discovered in the very cold waters of Ikka Fjord, southern Greenland (Pauly 1963). This discovery provided the first indication of the identity of the elusive precursor mineral and also vindicated the suspicions held by at least some mineralogists more than a century ago. According to Edward Dana (1884), who investigated the thinolites (*i.e.* glendonites) from Lake Lahontan, Nevada, "the original mineral was one which does not appear thus far to have been observed in its natural condition, although, as will be shown later, it probably has occurred abundantly at numerous other localities." Following the discovery of ikaite it took nearly another two decades before Kaplan (1979) recognized that the composition, morphology and distribution of this new mineral matched those required for the precursor for glendonites. Ikaite has now received widespread acceptance as the precursor mineral for glendonites and related pseudomorphs (*e.g.* Suess *et al.* 1982; Carr *et al.* 1989; Swainson & Hammond 2001).

### IKAITE OCCURRENCES

In the last two decades ikaite has been recognized in a wide range of facies ranging from lakes to estuaries, shallow-marine shelves and deep oceanic basins. All occurrences, however, are characterized by cold, alkaline conditions and, for at least some occurrences, elevated phosphate concentrations in precipitating waters. These elevated phosphate levels apparently suppress precipitation of other calcium carbonate polymorphs (Buchardt *et al.* 2001). Ikaite crystals rapidly degrade to calcite plus water when warmed above 4°C (Bischoff *et al.* 1993) and may result in the generation of calcite aggregates whose external form pseudomorphs the ikaite crystal morphology. The limited stability of ikaite makes it a robust indicator of coldwater conditions and thus the recognition of its pseudomorphs in the geological record is of great paleoclimatic significance.

The restricted temperature stability and rapid conversion of ikaite to pseudomorphic calcite aggregates (*i.e.* glendonites) provides the potential for using the stable isotopic characteristics of glendonite calcite as a proxy for water isotope chemistry in the depositional or early burial setting. The current model for the stable isotopic evolution of Phanerozoic seawater is based on biogenic carbonate records and the availability of another proxy for seawater chemistry would be of considerable value in validating the long-term trends (Veizer *et al.* 1999). Conversion of ikaite to calcite, however, involves a significant volume decrease resulting in development of high porosity and the potential for later precipitation of void-filling calcite under physical and chemical conditions that may be very different from the original depositional setting. This limits the reliability of stable isotopic results unless the primary calcite phase that was formed from ikaite conversion can be recognized and analyzed.

### FROZEN PRAWN CONNECTION

Ikaite appears to be a rare mineral but its occurrence is probably much more common than generally realized. A common, albeit anthropogenic, example is the white spots that develop in the shell of frozen prawns during storage. X-ray diffraction analysis indicates that the mineral component of these white spots is ikaite (Mikkelsen *et al.* 1999).

**SYDNEY BASIN GLENDONITES**

Glendonites are common in the Sydney Basin and have been recorded from more than 30 separate geographic localities (Carr *et al.* 1989) representing six major glendonite-forming intervals – the Allandale Formation, upper Pebbley Beach Formation, Wandrawandian Siltstone-Branxton Formation, Berry-Mulbring Siltstones, Broughton Formation, and Kulnura Marine Tongue in the lower Illawarra Coal Measures. All glendonite occurrences in the Sydney Basin have several features in common. In particular, all occur in dark grey, carbonaceous, Permian marine strata. The glendonites are restricted to particular stratigraphic intervals within each formation and tend to occur in several glendonite-bearing horizons within a stratigraphic interval several 10s of metres thick. These horizons are composed of mudstone, siltstone, or rarely, very fine-grained sandstone that is commonly bioturbated. The glendonites are prismatic or stellate with randomly-oriented long axes, and may partially or completely enclose fossils or pebbles. Glendonite-bearing beds are commonly overlain by sandy and/or fossiliferous beds that contain abundant rounded and less common subangular dropstones.

Glendonites in the Sydney Basin consist of brown to amber, blocky calcite crystals, 2-50 microns across, that form diffuse agglomerations and more regular dendritic arrays. This amber to brown calcite is interpreted as the calcite that formed during the early conversion of ikaite to calcite (*cf.* Greinert & Derkachev 2004). Pore space within the brown to amber calcite network is filled with clear, millimeter- to micron-scale, secondary calcite. Brachiopods associated with glendonites in the Sydney Basin are well-preserved, with apparently minimal recrystallization and loss of primary microfabric. Joints within the glendonite-bearing units are mineralized with calcite and rare quartz that are probably related to later tectonic or burial phenomena, but some may be related to hydrothermal fluid systems developed near basalt flows coeval with sediment deposition.

**STABLE ISOTOPIC DATA**

Stable isotope analyses were carried out on hand-picked separates and bulk glendonite samples, together with samples of biogenic calcite (brachiopods), calcite spar from mineralized joints, and samples of coalified wood from the Sydney Basin. Samples of glendonites and associated biogenic carbonate from elsewhere were also analysed and the new data were integrated with published data to assess the reliability of glendonites as climate proxies and as records of stable isotopic chemistry of waters in the depositional setting.

The stable isotope signatures of modern (transformed) ikaite define distinctive trends. Most ikaite samples have a narrow range of  $\delta^{18}\text{O}_{\text{PDB}}$  (+1 to +4.5‰) consistent with precipitation from normal marine waters at temperatures within the mineral's stability field. The broader range of  $\delta^{13}\text{C}_{\text{PDB}}$  (-19 to -32‰) reflects mixing of relatively depleted carbonate from methane oxidation with relatively enriched seawater carbonate. Data for samples from the type locality in Ikka Fjord define a different array resulting in precipitation from waters formed by mixing of meteoric, submarine spring water with seawater (Buchardt *et al.* 2001).

Stable isotope data for Sydney Basin brachiopods have a restricted range well within the range of Permian biogenic low-magnesium calcite reported in numerous studies as summarized by Veizer *et al.* (1999). The modest spread of the Sydney Basin data may suggest some recrystallization or filling of brachiopod shell punctae by later diagenetic cement.

Sydney Basin glendonite bulk samples and hand-picked separates form a broad array, particularly in terms of  $\delta^{18}\text{O}_{\text{PDB}}$  (-5.2 to -21.4‰). The lack of any glendonite  $\delta^{18}\text{O}_{\text{PDB}}$  values more enriched than -5‰ may indicate initial precipitation from relatively depleted waters from mixed meteoric-seawater sources. Alternatively, the relative depletion in  $\delta^{18}\text{O}_{\text{PDB}}$  of glendonites compared to the brachiopod samples, may reflect physical mixing of a more depleted phase analogous to the late spar cement in mineralized joints. The separated amber calcite, which is presumed to represent the primary calcite from the transformation of ikaite during early burial, shows no significant difference from the bulk glendonite samples or the white/clear spar. This suggests that the scale of intergrowth of primary calcite and later spar is much finer than the mm-scale fragments that were separated by hand-picking.

### IMPLICATIONS OF GLENDONITE OCCURRENCES

Glendonites are robust indicators of cold conditions but not reliable indicators of palaeolatitude. The glendonite-bearing formations in the Sydney Basin are predominantly very fine-grained and represent periods of slow deposition where water depths were below storm wave base on an open continental shelf (lower three intervals) or in a protected seaway (upper three intervals). Between the glendonite-bearing formations coarser sand-dominated successions represent shallower water offshore and shoreface facies (e.g. Le Roux & Jones 1994; Herbert 1995; Tye *et al.* 1996). The presence of glendonites in the Pebbley Beach Formation (and possibly the Allandale Formation) may represent deposition under icehouse conditions during the last major phase of Gondwanan glaciation (Fielding *et al.* 2006). The relatively common occurrence of glendonites through the upper part of the Sydney Basin marine succession, however, indicates that cold conditions (<4°C) must have persisted at least periodically through most of the mid to Late Permian to allow the growth of ikaite crystals. Cold conditions with seasonal ice are also indicated throughout this succession by the presence of rounded erratic dropstones. Most of the formations (including the icehouse Pebbley Beach Formation) also contain wood fragments that have been washed into, and preserved in, the cold marine waters, thus indicating that the adjacent landmass supported a woody flora and the climate must have been only seasonally cold. The occurrence of glendonites in the deeper water phases of Sydney Basin deposition is probably the result of tectonic downwarping of the basin rather than glacio-eustatic sea level changes that would suggest they formed during interglacial periods.

### REFERENCES

- BISCHOFF, J. L., FITZPATRICK, J. A. & ROSENBAUER, R. J. 1993. The solubility and stabilisation of Ikaite ( $\text{CaCO}_3 \cdot 6\text{H}_2\text{O}$ ) from 0° to 25°: Environmental and palaeoclimatic implications for thinolite tufa. *Journal of Geology* 101, 21-33.
- BUCHARDT, B., ISRAELSON, C., SEAMAN, P. & STOCKMANN, G. 2001. Ikaite tufa towers in Ikka Fjord, southwest Greenland: their formation by mixing of seawater and alkaline springwater. *Journal of Sedimentary Research* 71, 176-189.
- CARR, P. F., JONES, B. G. & MIDDLETON, R. G., 1989. Precursor and formation of glendonites in the Sydney Basin. *Australian Mineralogist* 4, 3-12.
- DANA, E. S. 1884. A crystallographic study of the thinolite of Lake Lahontan. *United States Geological Survey Bulletin* 12, 429-450.
- DANA, J. D. 1849. *United States Exploring Expedition. During the years 1838, 1839, 1840, 1841, 1842. Under the command of Charles Wilkes, U.S.N. Vol. X. Geology*, C. Sherman, Philadelphia.

## COOL MINERAL CONNECTION

- DAVID, T. W. E., TAYLOR, T. G., WOOLNOUGH, W. G. & FOXALL, H. G. 1905. Occurrence of the pseudomorph glendonites in New South Wales. *Records of the Geological Survey of New South Wales* 8, 162-179.
- FIELDING, C. R., BANN, K. L., MACEACHERN, J. A., TYE, S. C. & JONES, B. G. 2006. Cyclicity in the nearshore marine to coastal, Lower Permian Pebbley Beach Formation, southern Sydney Basin, Australia: a record of relative sea-level fluctuations at the close of the Late Palaeozoic Gondwanan ice age. *Sedimentology* 53, 435-463.
- GREINERT, J. & DERKACHEV, A. 2004. Glendonites and methane-derived Mg-calcites in the Sea of Okhotsk, eastern Siberia: Implications of a venting-related ikaite/glendonite formation. *Marine Geology* 204, 129-144.
- HERBERT, C. 1995. Sequence stratigraphy of the Late Permian coal measures in the Sydney Basin. *Australian Journal of Earth Sciences* 42, 391-405.
- KAPLAN, M. E. 1979. Calcite pseudomorphs (pseudogaylussite, jarrowite, thinolite, glendonite, gennoishi, White Sea hornlets) in sedimentary rocks. Plenum Publishing Corporation 1980. Translated from *Lithologiya I Poleznye* 5, 125-141.
- LE ROUX, J. P. & JONES, B. G. 1994. Lithostratigraphy and depositional environment of the Nowra Sandstone in the southwestern Sydney Basin, Australia. *Australian Journal of Earth Sciences* 41, 191-203.
- MIKKELSEN, A., ANDERSON, A. B., ENGELSEN, S. B., HANSEN, H. C., LARSEN, O. & SKIBSTED L. H. 1999. Presence and dehydration of ikaite, calcium carbonate hexahydrate, in frozen shrimp shell. *Journal of Agriculture and Food Chemistry* 47, 911-917.
- PAULY, H. 1963. Ikaite, a new mineral from Greenland. *Arctic* 16, 263-264.
- SUESS, E., BALZER, W., HESSE, K-F., MULLER, P. J., UNGERER, C. A., & WEFER, G. 1982. Calcium carbonate hexahydrate from organic-rich sediments of the Arctic Shelf: Precursors of glendonites. *Science* 216, 1128-1130.
- SWAINSON, I. P. & HAMMOND, R. P. 2001. Ikaite,  $\text{CaCO}_3 \cdot 6\text{H}_2\text{O}$ : Cold comfort for glendonites as palaeothermometers. *American Mineralogist* 86, 1530-1533.
- TYE, S. C., FIELDING, C. R. & JONES, B. G. 1996. Stratigraphy and sedimentology of the Permian Talaterang and Shoalhaven Groups in the southernmost Sydney Basin, New South Wales. *Australian Journal of Earth Sciences* 43, 57-69.
- VEIZER, J., ALA, D., KAREM, A., BRUCKSCHEN, P., BUHL, D., BRUHN, F., CARDEN, G., DIENER, A., EBNETH, S., GODDERIS, Y., JASPER, T., KORTE, C., PAWELLEK, F., PODLAHA, O. & STRAUSS, H. 1999.  $^{87}\text{Sr}/^{86}\text{Sr}$ ,  $\delta^{13}\text{C}$  and  $\delta^{18}\text{O}$  evolution of Phanerozoic seawater. *Chemical Geology* 161, 59-88.



# OVERVIEW OF THE HYDROGEOLOGY OF THE WESTERN COALFIELD – ULAN COAL MINE CASE STUDY

**Katarina David**

Senior Hydrogeologist, Parsons Brinckerhoff,  
GPO Box 5394, Sydney, NSW 2000

## **ABSTRACT**

Stratigraphy of the north-western coalfields consists of six aquifers; the shallow Quaternary alluvium associated with the rivers, Tertiary basalt, Cretaceous-Jurassic sandstone in the north, Triassic sandstone, Permian sediments of which Ulan coal seam aquifer is of most interest and the deepest aquifer, the Marrangaroo conglomerate. Each of the aquifers has own geochemical signature. Ulan Coal Mine is located on the northwestern margin of the Sydney Basin and extracts coal from Ulan seam in both open cut and underground operations. The majority of groundwater information is provided by the Ulan Mine where the monitoring exists for all five aquifers. There is limited information available on the aquifers regionally. This is mainly due to the mine being isolated in this region but also because there are no major rivers and no significant water demands that would initiate any further groundwater developments and investigations. The majority of drillholes within that region were drilled as part of the coal exploration program and did not particularly target aquifers. Regionally existing groundwater information is available for the shallow alluvium associated with Goulburn and Talbragar River on the southern and northern side of the mine lease, respectively. The alluvial groundwater flow is generally towards and along the river, as the Goulburn River flows to the east and the Talbragar River flows to the west. The groundwater flow of the other aquifers is influenced by the location of regional recharge areas, geology and the dip of the stratigraphic units. The groundwater chemistry reflects the characteristics of each of the formations. A recent mine drilling program provides new information which allows more detailed interpretation and reveals the characteristics of the Cretaceous- Jurassic aquifer. Regionally, the importance of this aquifer lies in water supply capacity for the towns to the north of Ulan Mine.

## **INTRODUCTION**

The Western Coalfields lie on the western margin of the Sydney basin. Regional hydrogeological characterization is scarce. Groundwater is increasingly becoming an important management issue for users in this area. The general objective of this project is to gain better knowledge and understanding of the groundwater resources (both quality and quantity) of the area by using the data available from Ulan Coal Mine in this assessment.

Hydrogeological and hydrogeochemical characterization provided in this project aims at assessing the groundwater origin, identifying the processes controlling groundwater flow and chemistry in space and time. This report focuses on the geological and hydrogeological conditions, the relationship between the groundwater types and description of the results of the hydrogeological and geochemical program.

The hydrogeological and geochemical characterization program involved: (1) analysis of groundwater gauging of the piezometers on and off the mine site, (2) analysis of geochemical data collected from over 15 piezometers over a period of over 15 years, (3) geochemical characterization of all hydrogeochemical units. The data used in this process included the following sources: DNR database and current and historic data available from Ulan Coal Mine. The approach used to study the multiple aquifer system in the western coalfields was to determine the hydrogeology starting from water levels and flow directions, and to determine the hydrogeochemistry of groundwater for all hydrogeologic units looking at their origin and following the flow path.

**STUDY AREA**

The area includes the western edge of the Western Coalfields, in particular the area covered by Ulan mine and exploration lease extending to the north to the Talbragar River, to the west to Gulgong, to the south bounded by granite outcrop and to the east adjoining the Hunter Valley (Figure 1). This paper uses the hydrogeological data available from Ulan mine and any available data from neighboring areas.

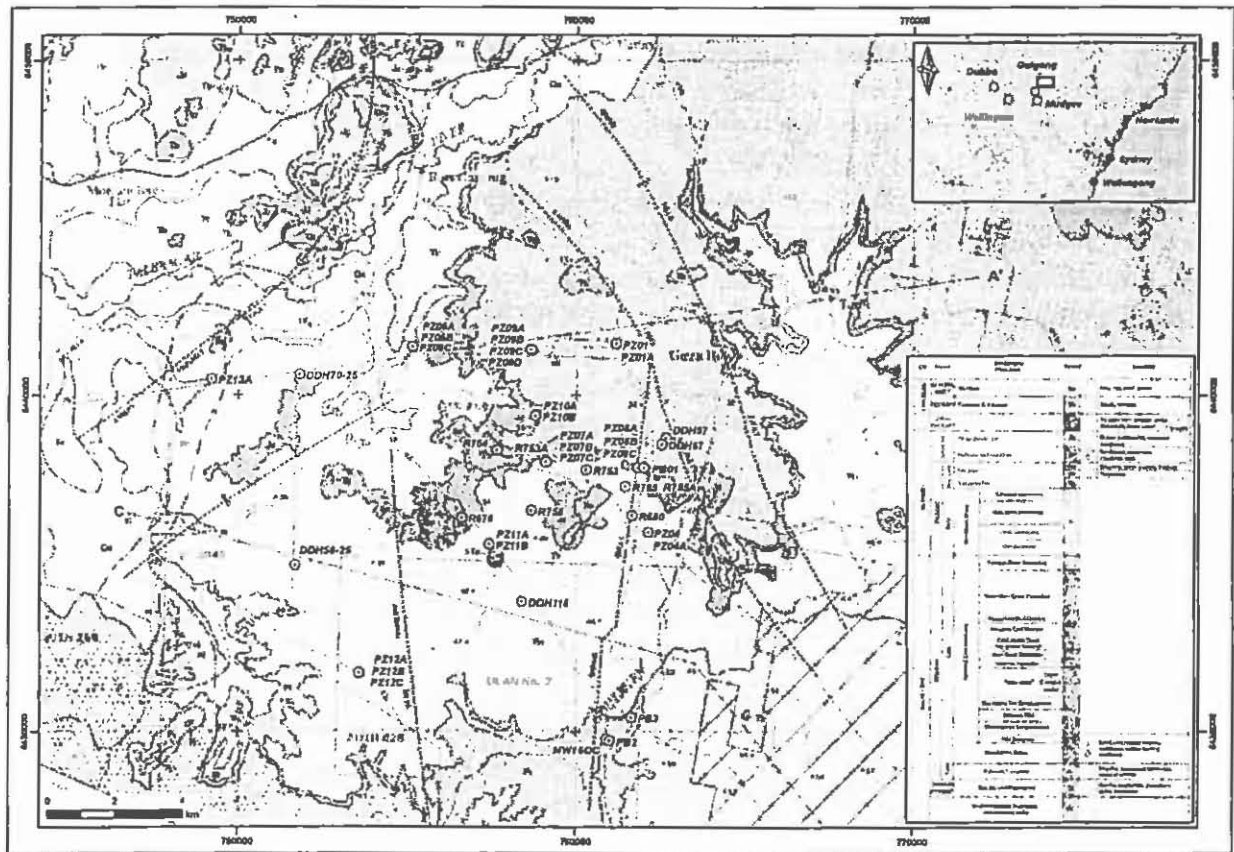


Figure 1. Location map with piezometer location

**GEOLOGICAL SETTING**

The basement of the sedimentary sequence is represented by the Gulgong Granite which crops out to the southwest of the area. It is characterized by a deeply weathered profile. The granite occurs in phases represented mostly as dykes and veins. Thin Quaternary alluvium, comprising clay, silt, sand and gravel is deposited adjacent to the Goulburn and Talbragar Rivers.

## WESTERN COALFIELDS HYDROGEOLOGY

The late Permian Illawarra Coal Measures overlie granite basement. The Illawarra coal measures form the western boundary of the Western Coalfields and crop out to the south of the project area. The thickness of this unit increases eastwards from the western margin of the Basin. The depositional environment includes swamps, deltas, lagoons, and fluvial and alluvial fan deposits. Yoo(1993) recorded an average dip of 1 degree to the east-northeast. The Illawarra Coal Measures are divided into four groups, and of interest to this study is the lower Cullen Bullen Formation as it hosts the mining interval of the Ulan Seam (Geological Survey, 1999). The basal unit of this subgroup is the Marrangaroo Conglomerate, an approximately 10m thick unit which thins to the east (Lohe *et al*, 1992). The Illawarra coal measures form gentle landforms which are covered by highly weathered sandy clay soils. The lithology includes mudstone, laminated siltstone, medium grained quartz sandstone, conglomerate, coal, carbonaceous mudstone and rhyolitic tuff.

Overlying the Permian sediments are fluvial sediments of the Triassic Narrabeen Formation. This group forms an extensive plateau bounded by cliff forming escarpments in the area from Wollar to Rylstone. It is characterized by the lower lithic and upper quartzose facies comprising conglomerate and sandstone units. The depositional environment is typical of alluvial fans (Cameron *et al*, 1993). At the project site the Triassic Sandstone crops out over the central and northern area and forms the elevated range.

Cropping out in the north and overlying the Triassic group sandstones are Jurassic Purlawaugh Formation sandstones. The Jurassic sediment sequence crops out to the north of the project area and is probably part of the Surat Basin (part of the Great Artesian Basin). The Purlawaugh Formation is conformably overlain by the coarse grained fluvial sandstone mapped as Pilliga Formation (Geological Survey of NSW, 1999) but is probably Cretaceous in age (Martin, H, 1981). This formation is intruded by the Tertiary basalt. The thickness of the unit varies from 30m to 50m and is well exposed beside the Talbragar River. The formation comprises massive medium to very coarse grained to conglomeratic quartzose sandstone.

Tertiary basalt unconformably overlies the Pilliga Sandstone in the northern area and comprises large unconnected areas of basalt flow that cap the central area of the site.

### HYDROGEOLOGICAL CHARACTERISTICS

Over the western coalfields the groundwater occurs in: (1) Unconsolidated *sediments*: non-cemented sands and gravels commonly found in alluvial valleys and sand dune systems, (2) *Sedimentary rock*: consolidated formations such as sandstones, siltstone and shales, both within pore space in the rock matrix, and within fractures and joints. (3) *Fractured rock*: igneous rocks and fractured sedimentary rocks

Locally, there are six main aquifer systems in the area at Ulan, as follows:

- Quaternary alluvial aquifers along drainage lines
- Tertiary basalt
- Jurassic-Cretaceous sandstone – Pilliga Sandstone and Purlawaugh Sandstone
- Triassic sandstone – Narrabeen Group
- Coal seams within the Permian Illawarra Coal Measures – Ulan Coal Measures
- Marrangaroo Conglomerate – within the Permian Sedimentary sequence.

The schematic conceptual hydrogeology model is shown on Figure 2.

## Alluvium

Properties of alluvial aquifers vary regionally and locally depending on the extent and thickness of the alluvial deposits and the nature of the sediments. These aquifers generally occur along the floors of valleys and are derived from streams draining the ranges in the north of the Ulan Mine and across the divide in the north catchment. Fairly extensive areas of unconsolidated sands and gravels occur along the Goulburn River, Ulan Creek and the Talbragar River and most of the larger creeks. In places these are up to 20 metres thick.

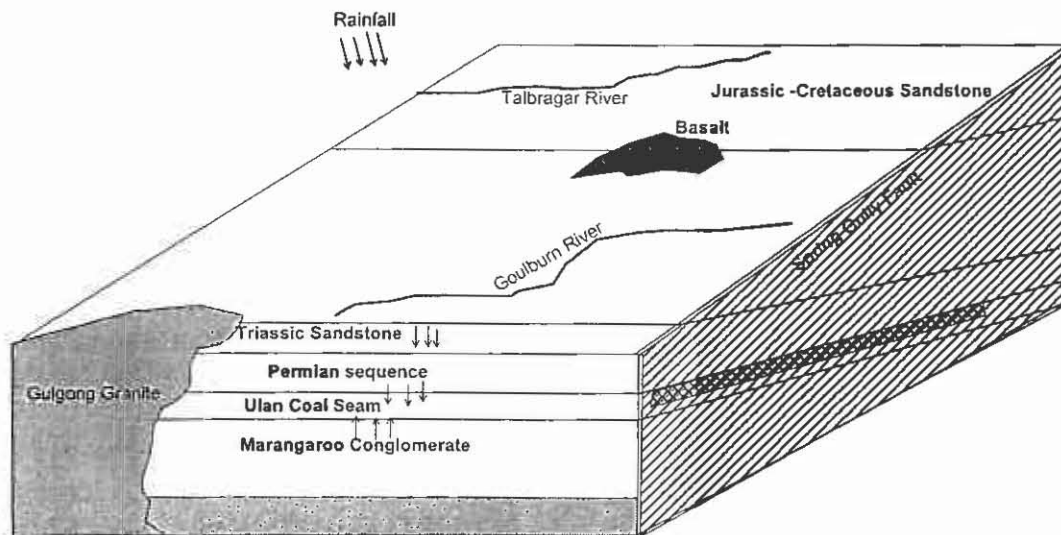


**Figure 2. Conceptual groundwater models of the western coalfields (Ulan area)**

Groundwater flow is through primary intergranular flow. Sand and gravel deposits are more permeable than clay-rich deposits and can produce high yielding bores and wells. Typically, these aquifers are bounded at depth by low permeability strata (rock) that restricts or prevents the downward movement of rainfall recharge. Salinity is generally low in the alluvial formations. Measured water levels in the piezometers installed in Goulburn River alluvium in 2004 and 2005 indicate there is hydraulic connection with surface water.

## Basalt

The Tertiary basalt forms a cap on top of Triassic sandstone in the central area. Groundwater occurs at discrete horizons within the sequence where the more permeable or fractured layers occur. The basalt attains up to approximately 100 metres in thickness. Basalts are typically reactive rocks and hence can produce groundwater containing high levels of total dissolved solids. Water levels range from 7 to 30 metres below ground surface and yields range from 0.09 to 1 L/s (PB, 2005). At Ulan this is a minor aquifer which may provide recharge to the underlying sandstone. Anecdotal evidence indicates that the water storages on the local properties are generally built in basalt.

## Jurassic-Cretaceous

The Cretaceous Sandstone, crops out to the north of the study area and forms a multilayered aquifer system. Groundwater occurs at discrete horizons within the sequence where the more permeable or fractured layers occur. Very little is known about the aquifer in this area however it is a high yielding formation to the north and northeast where both irrigators and town water supply are sourced from this unit. The sandstone is underlain by the Purlawaugh Formation consisting of lithic labile sandstone interbedded with siltstone and mudstone. These sandstones have low porosity and permeability (Hawke and Bourke, 1984) and the

## WESTERN COALFIELDS HYDROGEOLOGY

Purlawaugh Formation was regionally classified by Habermehl (1980) as a confining unit. The older Jurassic sandstone is expected to be semi-confined where it outcrops to the north of the study area because of the layered nature of the strata and the presence of siltstone and shale horizons. Groundwater quality is typically fresh and water is suitable for domestic use, irrigation and stock watering.

Two piezometers recently installed into this unit indicate that the Cretaceous-Jurassic aquifer may be unconfined and recharged directly by rainfall. The depth to water level varies from 37m to 62 m influenced mostly by topography. The rise in the water levels following the rainfall period (12/05 to 3/06) is noticed in PZ10B, the southern of the two piezometers. The change in water level may be also due to the increased vertical seepage through the overlying basalt. The groundwater flow direction is difficult to establish, however based on the dip of the strata and the measured water levels it is expected to be in a northerly direction. No information exists on the permeability of this aquifer.

### **Triassic**

Triassic sandstone aquifers of the Narrabeen Group underlie the Jurassic sandstone aquifers in the region. The Narrabeen Group forms a complex, layered aquifer system, to the north of Ulan area with groundwater occurring in vertically discrete horizons, with limited downward movement between these (Wolley, 1980). Groundwater movement is poorly understood but is expected to be quite variable, occurring as both primary intergranular flow and secondary fracture flow. Aquifers are likely to be confined. Yields are typically low and water quality fresh to brackish (Woolley, 1980). The Narrabeen Group crops out over most of the study area, the central area forms a recharge zone for this aquifer system which elsewhere in the north underlies the Jurassic-Cretaceous sandstone. The Narrabeen Group comprises interbedded sandstone and shale aquifer units.

Permeability of this aquifer has been tested over the years by undertaking packer tests, pump tests and slug tests. The results shown in Figure 3 indicate that permeability ranges from 0.05 m/d to 6m/d with decreases correlating with increasing depth of testing.

The interpretation of the flow direction and gradient was provided based on the information from 12 piezometers including both historical and recent data. The groundwater flows in an easterly direction with gradient of 0.005 being uniform throughout the study area. This is not in agreement with the dip of this layer to the northeast. The time series data for the period from 2001 onwards indicates only minor change over time with variation generally within one meter. The depth to water is guided by the topography, being within 20m in the topographically lower areas and up to 120m in topographically higher areas. Variation in the depth to groundwater may also indicate the change from unconfined conditions at the outcrop areas to the confined conditions downdip in the northeast direction.

### **Illawarra Coal Measures**

Illawarra Coal Measures form a sequence of interbedded sandstone, siltstone, claystone, coal and conglomerate. Due to the expected higher salinity of this formation and the depth to access the coal measures, no bores have been drilled to exploit this formation's water. The groundwater reservoir properties of the Coal Measures are thus known from coal exploration holes and piezometers installed at the Ulan mine site. The Ulan seam is mined at Ulan therefore a great deal of information is available for this unit. Groundwater occurs in vertically discrete horizons, with little vertical movement between layers in undisturbed environments. The hydraulic properties of the coal seam depend on the degree of cleat

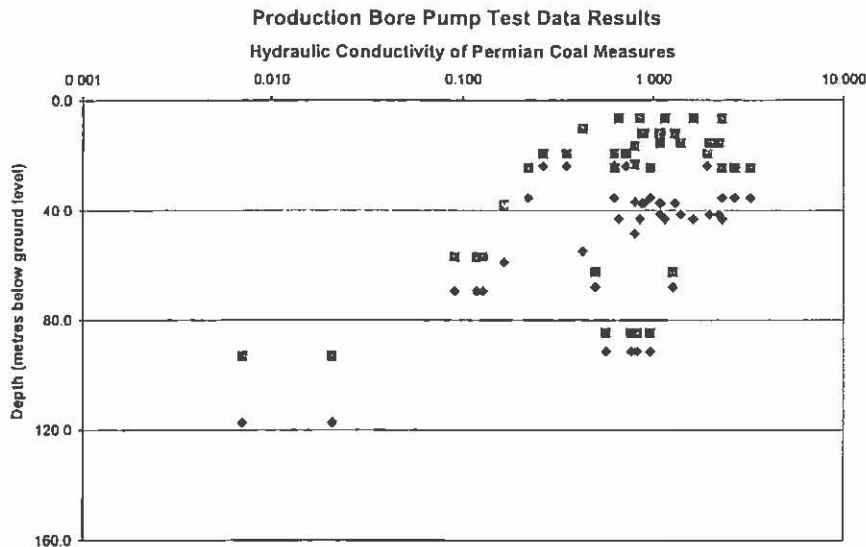


Figure 3 Permeability Range of Permian aquifer

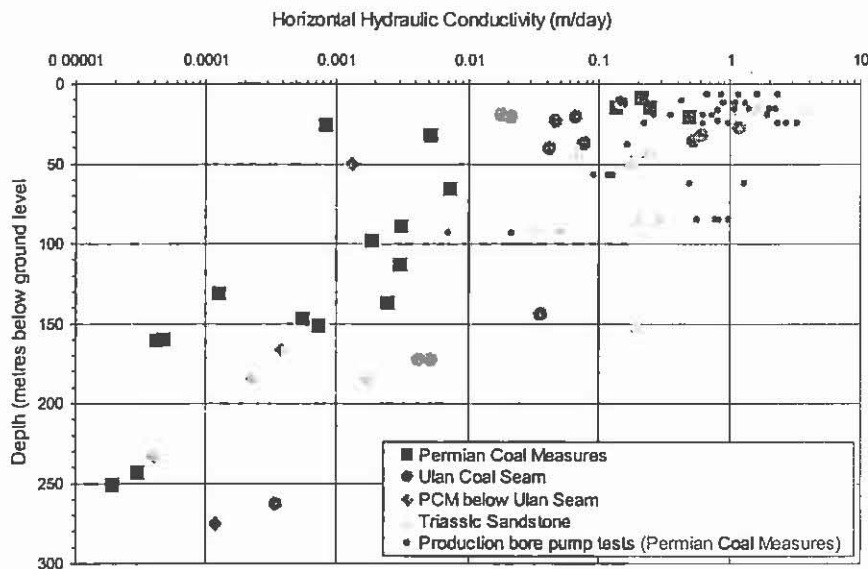


Figure 4. Permeability of aquifers versus depth

**Relationship between the aquifers**

The establishment of the relationship between the series of aquifers present in the western coalfields has been made possible through the recently completed hydrogeology program by Ulan Mine. The program involved installation of a series of piezometer nests where each of the piezometers is installed in a separate hole and screened in a different aquifer. The contour maps created for the aquifers indicate that the water pressure is generally downwards except for the Marrangaroo conglomerate where in the hydraulic gradient is upwards in some areas.

The general groundwater flow direction is interpreted to be mostly in a northeasterly direction. This direction of flow is consistent with the dip of the layers which is at around 2 to 3 degrees to the north-north-east. Each of the six aquifers is unique and is not in hydraulic connection with others. The presence of pressure gradient difference of over 50 m between different aquifers confirms this statement.

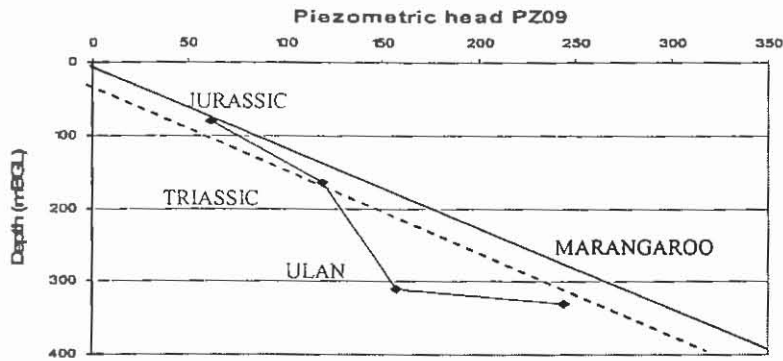


Figure 5. Piezometric head versus depth of aquifer

Piezometer PZ09 (Figure 5) shows the plot of groundwater head elevation water versus depth of aquifers. The departure off the straight line indicates the presence of aquitards within the Permian measures above the Ulan Seam. This is consistent with the geological log data showing the presence of siltstone, shale and other less permeable strata within the Illawarra Coal Measures. Alternatively this could be explained as mine dewatering effect causing a decrease in groundwater levels; however the distance to active mining area is significant.

## GEOCHEMISTRY

A series of historical mine water quality data were combined with the data from the recently undertaken Ulan mine hydrogeological program. The water chemistry results were evaluated to compare multiple aquifer systems and to assess geological and hydrogeological influences on water quality.

### Groundwater Quality

The data for alluvium, Triassic, Ulan Seam and Marrangaroo aquifers and rainfall was plotted on a Piper trilinear plot and also presented on a spatial basis for each of the aquifers depending upon the salinity. The data are presented in Figure 6.

#### Alluvium

The water samples in alluvium refer to historical data from late 1990s. The waters are sourced from the river and creek alluvium and the water type is typically Na-Cl-Ca-Mg-SO<sub>4</sub> dominated. The EC of water (being a good proxy for salinity) ranges from 180 uS/cm to 7737 uS/cm for 25 samples. The mean value is 2395 uS/cm. There is great variability in the proportion of each of the major ions depending mostly on the location where the sample was taken. The presence of SO<sub>4</sub> as a less dominant ion is significant as sulphate does not appear in any of samples taken from other aquifers. This may be due to mixing with local runoff from old mined areas where pyrite is exposed to air. This water plots close to rainfall data on a Piper plot, indicating aquifer is recharged by direct rainfall.

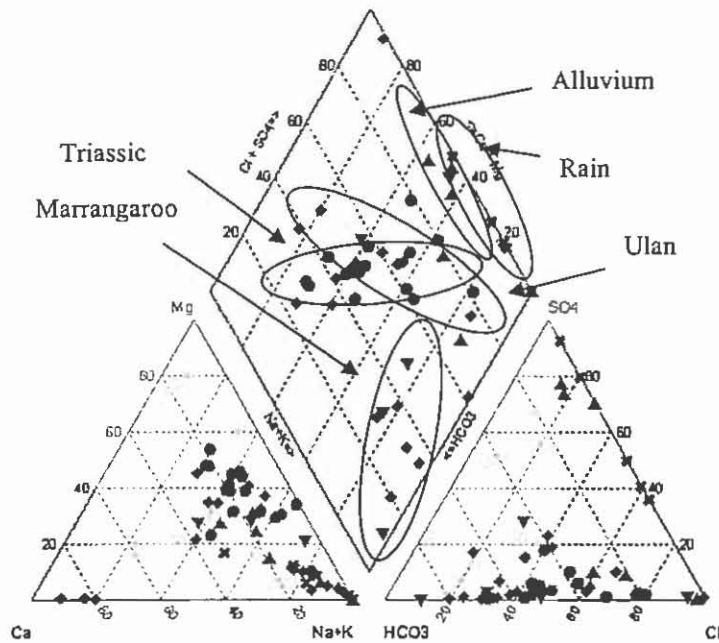


Figure 6. Piper plot showing different water types

### Triassic

The water in Triassic has the following characteristics:

- The water is generally soft with the exception of the R676
- The Piper plot classifies the water as Mg-Na-  $\text{HCO}_3$ -Cl and Na-Mg-Cl-  $\text{HCO}_3$  (R753, PZ04A and PZ07C) with the exception of PZ06C which is Na-K-Cl-  $\text{CO}_3$  (Figure 6)
- The proportionally high bicarbonate is characteristic of freshly recharged waters
- EC ranges from 170 uS/cm to 1600 uS/cm with the values above 500 uS/cm in the central area and below 500 uS/cm in the piezometers to the south and north. The historic mean of the 36 samples taken since 1980s is 384 uS/cm
- pH ranges from 5.4 to 9.8 but is generally around neutral 6.8 to 7.3.

There is noted change in water quality with time (2001 to 2005), with shift from Na-Mg-Ca- $\text{HCO}_3$ -Cl water to Na-Mg-  $\text{HCO}_3$ -Cl in R753A and R676 due to calcite precipitation. The water quality in R755 has not changed during this time period.

The water from this aquifer has elevated iron compared to the other aquifers at the same location. This is typical of the Triassic sandstone units elsewhere in the Sydney Basin.

### Ulan Seam

The water from Ulan Seam has the following characteristics:

- The hardness ranges from 40 mg/L to 1580 mg/L with the mean value around 280 mg/L
- The EC ranges from 64 uS/cm to 8120 uS/cm with the mean of 835 uS/cm and only two values below 500mg/L to the east and west of the mine lease. Analysis of the historical data including 11 samples yields a mean of 547 uS/cm.
- The Piper plot classifies the water as Na-Mg-Ca-  $\text{HCO}_3$  and Na-  $\text{HCO}_3$  type, with the exception of DDH58-50 being Na-K-Cl-  $\text{HCO}_3$
- The change is noticed over time with a shift from Na-  $\text{HCO}_3$ -Cl water to Na-Mg-Cl- $\text{HCO}_3$  in R755

- pH ranges from 6.4 to 12.5
- high potassium concentration compared to Triassic sandstone is noticeable in all nested piezometer locations
- low iron concentration in all samples and higher nitrogen values than Triassic sandstone.

A shift in water quality over time in some piezometers in the centre of the study area from Na-HCO<sub>3</sub>-Cl to Na-Mg-Ca-HCO<sub>3</sub>-Cl is noticed. Where the Ulan seam is close to surface such as in MW160C the shift is Na-Cl-HCO<sub>3</sub> to Na-HCO<sub>3</sub>-Cl where the aquifer is recharged directly by rainfall.

The occurrence of Na and HCO<sub>3</sub> as dominant ions can be explained by the effects of ion exchange and calcite dissolution. For this type of water to occur at such depth the CO<sub>2</sub> must have been generated within the groundwater flow system at depths well below the water table (Freeze and Cherry, 1979). This process requires the presence of anaerobic bacteria and is identified by the smell of the H<sub>2</sub>S gas. This explanation is supported by the typically low SO<sub>4</sub> concentrations found in the samples but also the presence of the “rotten egg” smell during recent drilling.

#### **Marrangaroo Conglomerate**

The water from Marrangaroo Conglomerate is characterized by the following:

- Historical data for 14 samples taken from this unit indicates EC ranges from 280 uS/cm to 625 uS/cm with a mean of 741 uS/cm
- The limited water samples have classified this water as Na-Mg-Cl and Na-Mg-K-HCO<sub>3</sub>-Cl
- pH taken on 18 samples varies from 5.2 to 9.

The available analysis exist for two events in the 1990s and 2005, however the water composition does not seem to have changed significantly over the period.

#### **DISCUSSION AND CONCLUSIONS**

The detailed hydrogeological investigations undertaken recently by the Ulan Mine together with the historical and limited recent geochemistry data has provided the insight into the behaviour and connection of the aquifers in the region.

The system of multiple aquifers in the 400m thick sequence indicates that each of the aquifers is a separate unit and only minor leakage and connection exists under natural conditions ie they are essentially disconnected. This is further confirmed by recent installation (Ulan coal mine) of the multilevel piezometers, where each of the aquifers measures a different head. The hydraulic gradient in all aquifers is downward, with the exception of the Marrangaroo Conglomerate. The alluvial aquifer is unconfined throughout the project area while the Permian aquifer and Ulan Seam are only unconfined in the south of the study area where they outcrop. With the dip of the layers of 2-3 degrees to the northeast they become confined with increasing thickness of the overlying sediments. The aquifer in the Marrangaroo conglomerate appears to have upward hydraulic gradient in the areas away from the current mining influence. The Jurassic and Triassic sediments are unconfined where they crop out in the center of the study area, but become confined along dip in the northerly direction.

Apart from the differences in the hydraulic properties, the differences in the water chemistry indicate that aquifers are generally not hydraulically interconnected; however some mixing

## WESTERN COALFIELDS HYDROGEOLOGY

may be occurring between Triassic and Permian waters. The alluvium has a higher proportion of bicarbonates typical for the fresh recharged waters. The EC can be high and sulphates are present in the water. This may be due to sampling locations being close to open cut mines and being affected by the oxidation of the pyrite. No data exist at present for the quality of the Jurassic-Cretaceous aquifer, but further to the north the water from this aquifer is used for town water supply. The water from the Triassic aquifer has the best water quality overall with low salinity and only minor iron concentration. This is typical of the sandstones in the Sydney basin. The Permian and Ulan Seam water is of medium salinity and generally Na-Mg-Ca-HCO<sub>3</sub> dominated. The presence of HCO<sub>3</sub> in the aquifer at that depth is unusual. The source of this cation is probably due to an exchange process and the Ca abundance is due to calcite dissolution. Another possible explanation is the mixing of water from different aquifers which probably occurs from the downward leakage (which can be recognised in the Piper Plot) from the Triassic aquifer. The groundwater quality of the Marrangaroo conglomerate is poorer than the Ulan Seam, the salinity is generally higher and the composition is different with Na-Mg-Cl. This is more typical of the groundwater moving very slowly with minimal recharge.

Ongoing water level and water quality monitoring will help provide further understanding into these aquifer systems.

### ACKNOWLEDGEMENTS

The author would like to thank Ulan Mine for allowing the use and publication of the groundwater data. Acknowledgment goes to Mr. John Ross for the review of this paper.

### REFERENCES

- BECKET, J., 1988. The Hunter Coalfield – Notes to Accompany the 1:100,000 Hunter Coal field Geological Map, Geological Survey Report No. GS 1988/051. Department of Minerals and Energy.
- MCKIBBIN D AND SMITH P.C. 2000. Sandstone Hydrogeology of the Sydney Region. A paper given at the 15<sup>th</sup> Australian Geological Convention. Sandstone City – Sydney's Dimension Stone and other Sandstone Geomaterials. EEHSG Geological Society of Australia. Monograph No. 5. Ed. By G.H. McNally & B.J. Franklin.
- GEOLOGICAL SURVEY OF NSW, 1999. Dubbo 1:250,000 Geological Series Sheet, SI 55-4. and Explanatory Notes, Mineral Resources NSW.
- HABERMEHL, M. A. 1980. The Great Artesian Basin, Australia. *BMR Journal of Australian Geology and Geophysics* 5, 9-38.
- FREEZE R.A. AND CHERRY, J.A 1979 Groundwater, Prentice Hall, Inc., Upper Saddle River, NJ 07458, USA.
- LOHE, E.M., MCLENNAN, T.P.T., SULLIVAN, T.D., SOOLE, K.P., MALLET, C.W., 1992 Sydney Basin –Geological Structure and Mining Conditions, Assessment for Mine Planning, External Report No. 20, NERDDEC Project, CSIRO.
- MARTIN, H.A, 1981 An Early Cretaceous Age for Subsurface Pilliga Sandstone in the Spring Ridge District, Mooki Valley, *Journal and Proceedings, Royal Society of New South Wales*, 114, pp. 29-31.
- MCKIBBIN, D., SMITH, P.C. 2000 Sandstone City , Sydney's Dimension Stone and Other Sandstone Materials , Symposium Proceedings, UTS , Sydney, July 2000
- PARSONS BRICKERHOFF, 2005. Hydrogeological Assessment – Merriwa Coal Seam Gas Project, Sydney Gas.
- WOOLLEY, D.R. 1980. Groundwater. In: Geology of the Sydney 1:100,000 Sheet 9130 Ed. By C. Herbert.

---

DAVID

# DETERMINING THE GEOLOGICAL CONTROLS ON THE SPATIAL DISTRIBUTION OF PHOSPHORUS WITHIN COAL SEAMS MINED AT SOUTH WALKER CREEK MINE, BOWEN BASIN, CENTRAL QUEENSLAND, AUSTRALIA

Brooke Davis<sup>1</sup>, Joan Esterle<sup>2</sup>, Dave Keilar<sup>3</sup>

<sup>1</sup>BMA Coal, Brisbane, Qld

<sup>2</sup>University of Queensland Earth Sciences  
St. Lucia Campus, Qld 4072

<sup>3</sup> BMA Coal, South Walker Creek Mine, Nebo, Qld

## ABSTRACT

Phosphorus content greater than 0.07% within metallurgical coals is a problem as it makes steel brittle. The occurrence and maceral affinity of phosphorus within coal seams has been previously investigated, but the geological factors controlling its spatial distribution are still poorly understood. This study focused on the Main seam at South Walker Creek Mine, where phosphorus contents range from 0.007% to 0.261% across the entire mine.

Tightly sampled company data illustrates that phosphorus contents for total seam composites increase within faulted anticlinal areas. Splitting in the seam roof and floor are coincident with folding and the seam is also intruded on a flank of the anticline. Isopleth maps of composite seam phosphorus content show the highest values haloing the faults, but not the intrusions. Extensive low phosphorus domains are associated with synclinal areas relatively free of faulting. Within the seam, high phosphorus increments are common at the roof and floor contacts in the low domain. High phosphorus increments become increasingly frequent and thicker up dip towards the crest of the anticline and transgress lithotype boundaries. In this high to ultrahigh domain, the high phosphorus increments occur adjacent to and commonly above stone partings that themselves are low in phosphorus content.

Detailed ash mineralogy and petrographic analysis of two borecores located within the ultrahigh phosphorus zone displayed no relationship between phosphorus content, lithotype or maceral composition. This corroborates the trends observed above. However, SEM-EDS analysis of high phosphorus samples suggests that the main phosphorus-bearing mineral phase is authigenic apatite that commonly resides in the cell-lumens of semifusinite macerals in association with kaolinite. Less commonly, apatite was observed cross cutting kaolinite and calcite-filled cleats suggesting that it is a younger mineral phase. The distribution of phosphorus and the paragenesis of apatite suggest epigenetic mineralisation due to fluid migration along permeable pathways provided by the faults and coal/rock interfaces.

Although the source of phosphorus could be remobilisation from within the coal itself, the underlying volcanogenic sandstones of the Fort Cooper Coal Measures potentially supplied the phosphorus required to precipitate apatite; whereas the dykes and sills were likely sources of the calcium which also precipitated as calcite, ankerite and gypsum proximal to the intrusives. It is possible that mildly acidic, low-temperature, hydrothermal fluids transported the phosphorus up faults and traversed stone-coal contacts and into the Main seam.

**INTRODUCTION**

South Walker Creek Mine produces multiple products for pulverised coal injection, coke and thermal coal. It is located 35km west of the town of Nebo on the north-eastern flank of the Bowen Basin (Figure 1.). The Permian Age Elphinstone Coal Measures that are stratigraphically equivalent to the Rangal Coal Measures are the target interval.

The Main seam (MA) is the most economic seam at South Walker Creek Mine. Its thickness ranges from 10.5 to 14m and consists of dull to dull-banded coal with minor mudstone bands. This seam splits to the north and south of the central portion of Walker pit into the Mains Tops (MT, MT1 & MT2) and Mains Bottoms (MB) and the combined unit of MB2 (MB +MT2). The MA Seam is the lateral equivalent of the Leichhardt Seam, with the MB2 daughter split commonly known as the Elphinstone Seam. Ranging from 15-60m below the MA seam is the uneconomic Hynds Seam (Figure 2.), whose lateral equivalent is the Vermont Seam.

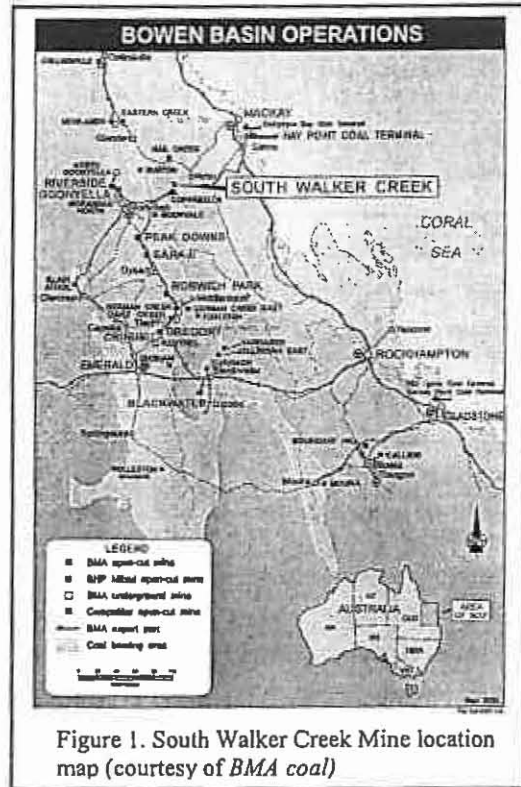


Figure 1. South Walker Creek Mine location map (courtesy of BMA coal)

To the north coal plies near the roof and floor of the MB2 seam split away into the Mains Floor Rider (MF) and the Mains Roof Ryder (MR) seams, leaving the MB2 as the main mineable seam. Within the MB2 seam, low-, high- and ultrahigh-phosphorus domains have been defined for both raw and washed product coal (Figure 3.). The objective of this study was to determine the geological controls on phosphorus distribution in the MB2 seam within Mulgrave Pit.

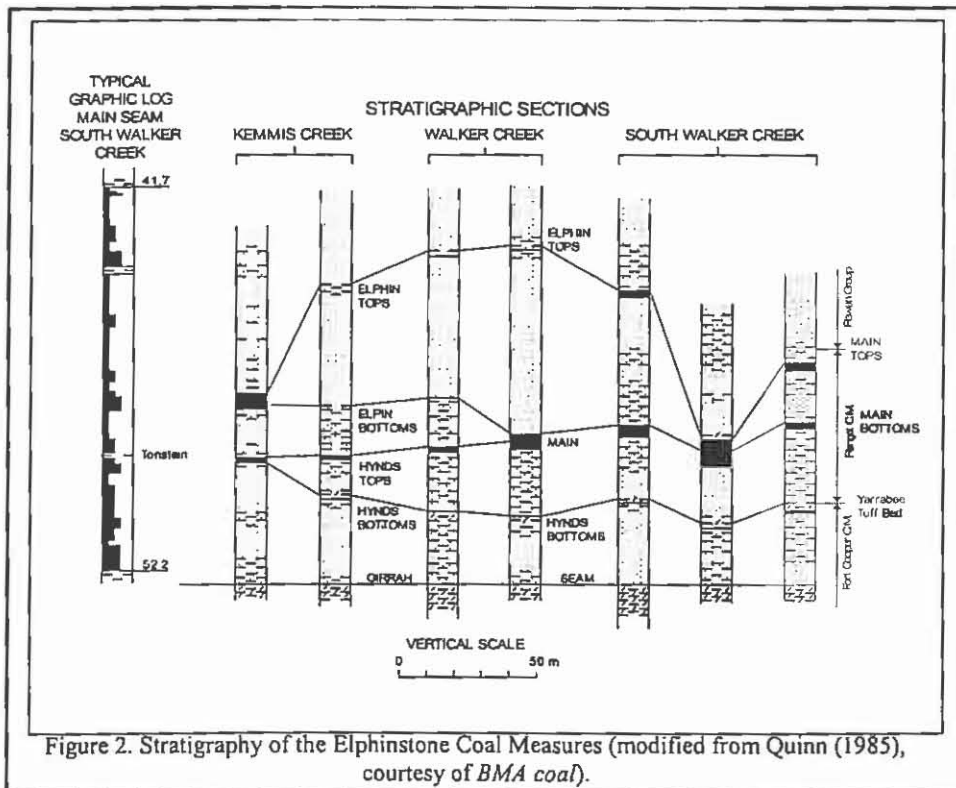


Figure 2. Stratigraphy of the Elphinstone Coal Measures (modified from Quinn (1985), courtesy of BMA coal).

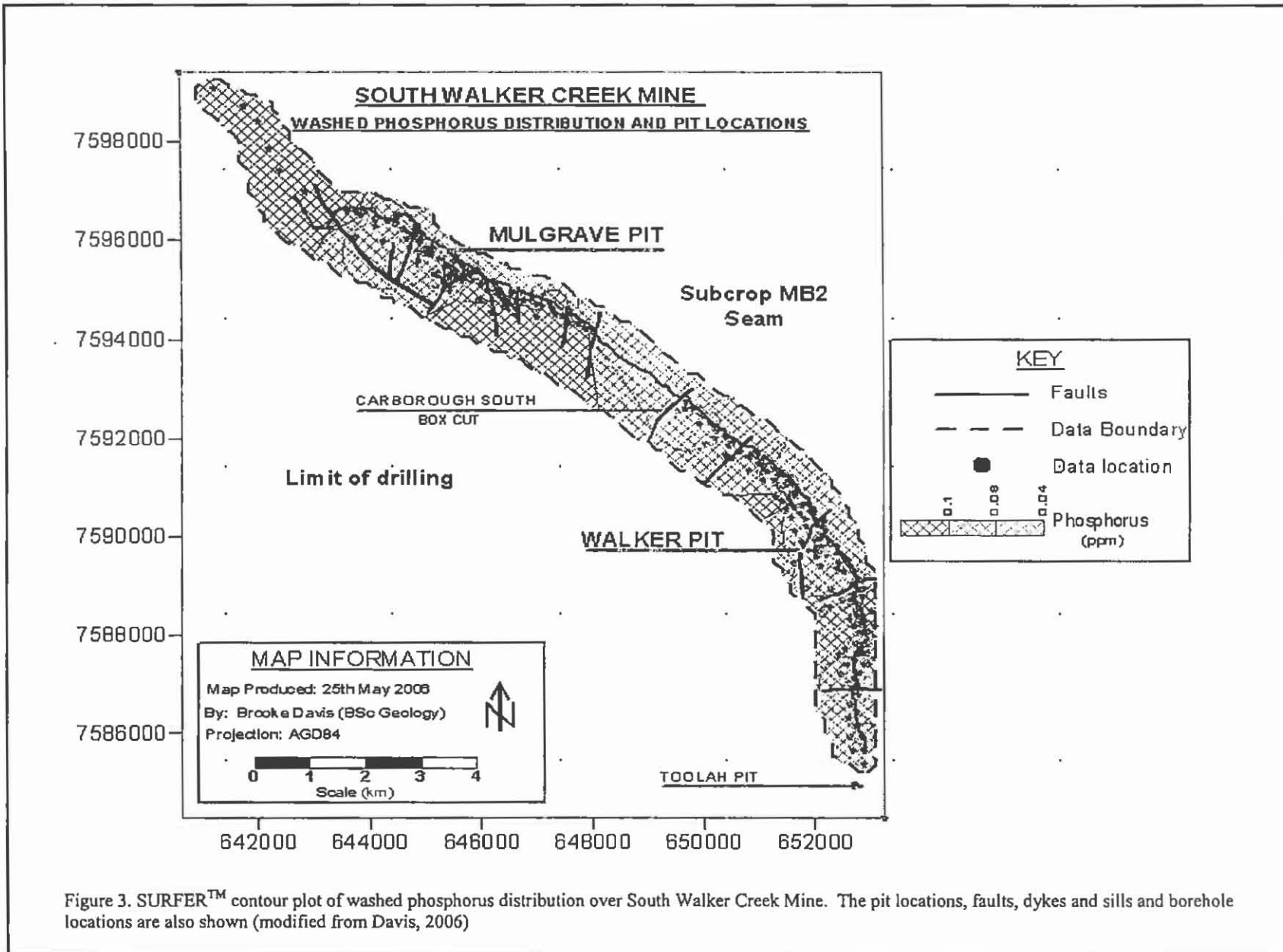


Figure 3. SURFER™ contour plot of washed phosphorus distribution over South Walker Creek Mine. The pit locations, faults, dykes and sills and borehole locations are also shown (modified from Davis, 2006)

## DATA CAPTURE AND ANALYSES

### Company drilling data

Existing company data were utilized to determine the vertical and lateral phosphorus distributions relative to other elements and geological features, such as:

1. MB2 seam thickness;
2. MF and MR splitting patterns;
3. Structure (faults and folds);
4. Intrusions (dykes and sills);
5. Depth of weathering; and
6. Base of Tertiary.

Company data, including phosphorus and ash mineralogy of contiguous 50cm samples from ~100 boreholes, were available to the study. Ash mineralogy was interpreted from element oxide data derived from x-ray fluorescence, while the phosphorus contents were determined by ash digestion. Isopleth maps of these data were analysed in conjunction with isopach maps of coal and interburden thicknesses as well as the position and severity of dykes and faults. This method was used to determine the depositional/post-depositional controls on the spatial distribution of high-phosphorus contents within the MB2 seam. Negligent differences between phosphorus contents for both raw coal and washed product at floats 1.6g/cc demonstrated that the phosphorus is more likely associated with the coal rather than the rock. Therefore, using results from the washed coal only did not bias distributions.

### Detailed core analyses

Two sets of twin cored holes (100mm diameter) (company core: 11851 and 11834, UQ core: 11852 and 11835) were obtained for the MB2 seam at two locations within the ultra high phosphorus zone, down dip of the Mulgrave Pit.

All four cores were brightness logged, though their sampling regimes varied. The company cores were sampled on contiguous 50cm increments to contribute to the current database. These samples were analysed by proximate and ultimate analysis as well as for total sulphur and phosphorus contents. The phosphorus results from the company cores were used to guide sampling of the twin UQ cores. This was achieved by correlating the high phosphorus zones across to the UQ cores by utilising the brightness logs. The lithotypes within these correlative zones were then contiguously sub-sampled to investigate the occurrence of phosphorus mineralisation relative to coal composition.

The lithotype sub-samples from UQ core 11835 (total 45 samples) were crushed to <1mm and split into representative samples for petrography, proximate analysis and x-ray fluorescence. UQ core 11852 was held in reserve, later the highest phosphorus zones correlative to company core 11851 were block sampled to examine maceral, phyteral and cleat associations. The grain and block samples were mounted in epoxy resin, set ground and polished for petrographic analysis.

Petrographic analysis of grain mounts validated the megascopic designation of coal lithotypes by their maceral composition. Analysis was conducted under white light using oil immersion lenses of 100x and 500x magnifications. Two-hundred and fifty

## GEOLOGICAL CONTROLS ON PHOSPHORUS

grains were counted per grain mount, with every fifth block counted twice to check for repeatability.

Three sub-samples with the highest  $P_2O_5\%$  contents (2228, 2237 and 2242) as well as a sub-sample proximal to the roof of the MB2 seam (2209) were chosen to be analysed by scanning electron microprobe (SEM) analysis. This was to determine the main-phosphorus bearing mineral/s, their associations with maceral assemblage, other minerals and features such as cleats.

### RESULTS AND DISCUSSION

Cross-correlations of phosphorus and ash mineralogy data did not yield strong relationships between elements or discriminate any phosphorus-bearing minerals. Reasonable relationships between Mn and Fe, Ca and Mg, S and Ca and Mg, and Na and Ba were observed. These poor correlations are most likely due to multiple sources of elements such as calcium. Mineral associations for these elements include calcite, ankerite and gypsum, their contents increase proximal to the intrusions.

Phosphorus contents for the total seam increased adjacent to the faults but not the intrusions, seam splitting zones or proximal to the base of Tertiary and base of weathering (Figures 4. and 5.). A southeast trending cross section of the MB2 seam illustrates the vertical and lateral variability of phosphorus contents within seam (Figure 6.).

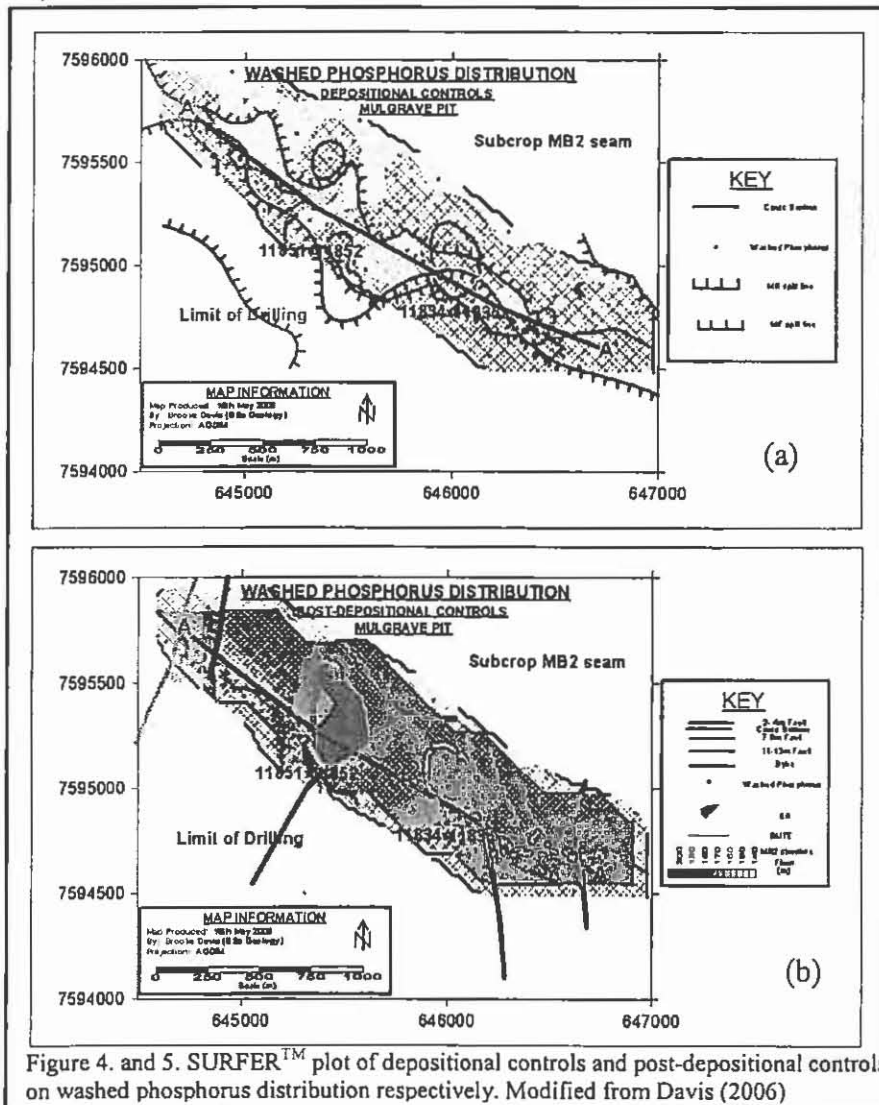
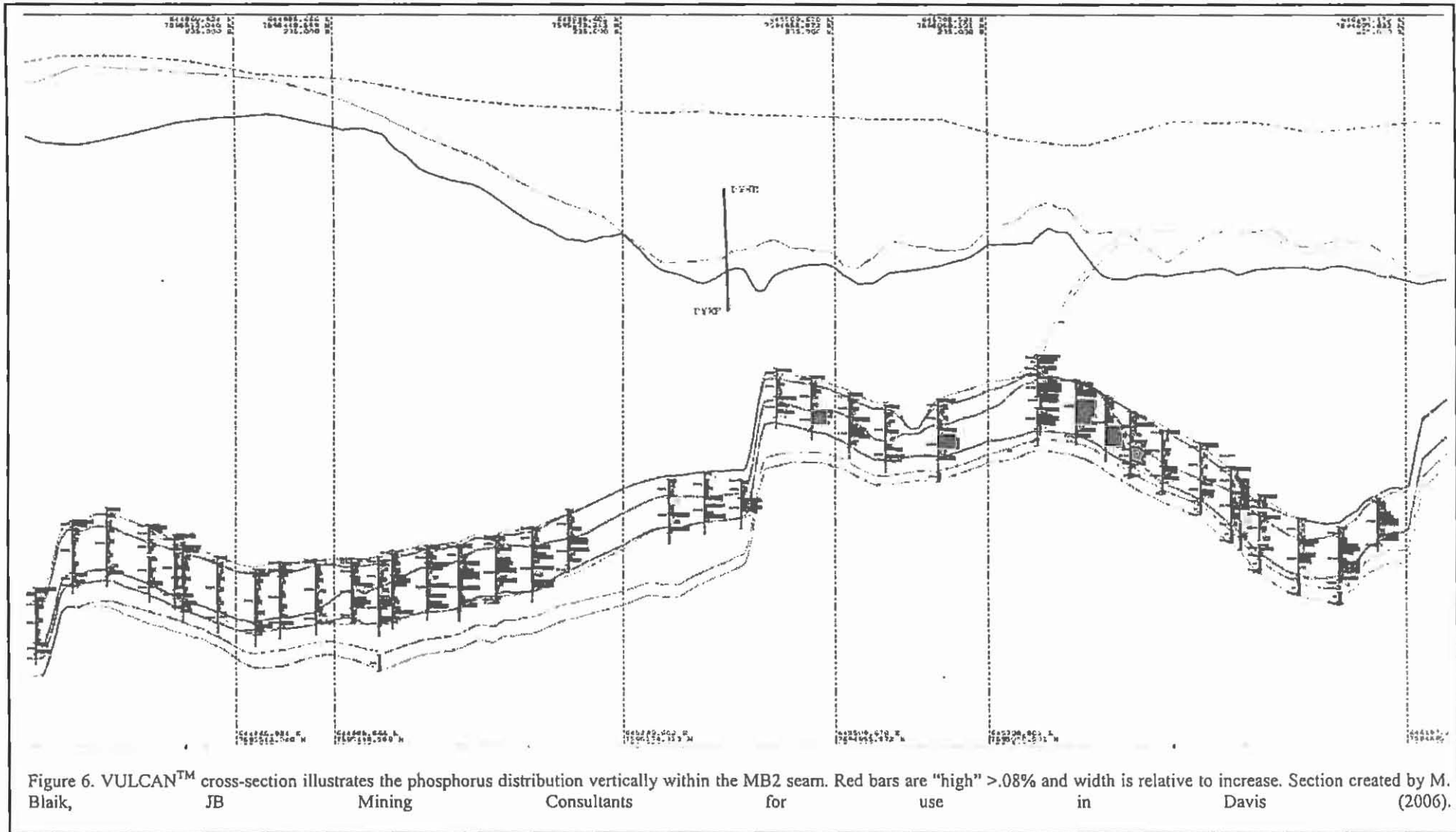


Figure 4. and 5. SURFER™ plot of depositional controls and post-depositional controls on washed phosphorus distribution respectively. Modified from Davis (2006)



The MB2 seam dips to the southwest. Along strike it gently folds into a syncline in the northwest and an anticline in the southeast. In the syncline, total seam phosphorus contents are generally low except at the roof and floor of the seam. As the anticline is approached toward the southeast, increments of high phosphorus contents gradually increase in frequency and thickness in the mid sections of the coal seam, transgressing lithotype boundaries until the anticline is saturated with phosphorus. These high phosphorus increments are associated with coal surrounding and generally above stone partings. The partings themselves are low in phosphorus content and dominantly consist of Si, Al and Ca. The poor correlation between maceral composition and phosphorus contents (Figure 7.) corroborates the observation that phosphorus mineralisation transgresses lithotype boundaries and does not have an affinity for a particular maceral group and/or sub-group.

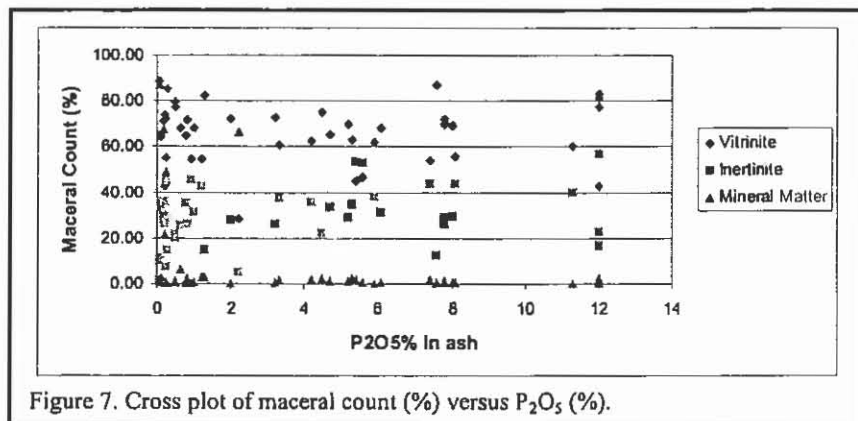


Figure 7. Cross plot of maceral count (%) versus P<sub>2</sub>O<sub>5</sub> (%).

Optically, the main mineral groups observed were carbonates and clays. SEM techniques successfully identified kaolinite, calcite and apatite as the dominant mineral assemblage; where apatite constituted 40% of mineral matter analysed. The apatite and kaolinite were frequently observed residing in the cell lumens of semifusinite macerals. This relationship has been observed by others (e.g. Rao 1997). Less commonly apatite was observed in open spaces within telovitrinite and calcite-dominated veins; and cross-cutting a cleat infilled with kaolinite (Figures 8.a, b, and c). The cross-cutting relationships of apatite to kaolinite and calcite suggest apatite is the youngest mineral phase.

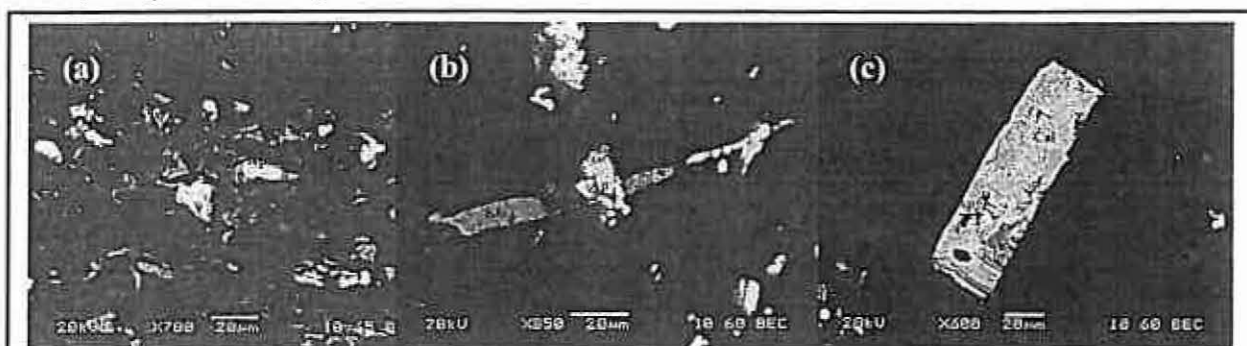


Figure 8. SEM images (a) apatite and kaolinite infill in the cell lumen of semifusinite maceral, (b) apatite cross-cutting kaolinite infilled cleat and (c) Calcite-dominated fracture with apatite in a hole within the calcite.

The paragenesis of apatite and the association of high phosphorus contents with faults and coal-rock roof, floor and parting contacts have led to the interpretation that high phosphorus zones are the result of phosphorus-rich, acidic fluids migrating along permeable pathways in the coal. Conversely, the occurrence of apatite within the cell lumens of the semifusinite macerals more than the cleats is perplexing, as this relationship would suggest early authigenesis (Ward 1994; Ryan 1995; Ward 2002). It is believed that upon the death of a plant, phosphorus is released as soluble PO<sub>4</sub><sup>-</sup> and complexes with calcium ions available in the interstitial waters. Authigenic

apatite is thought to precipitate within the cell lumens of inertinite macerals due to their increased pore size (Ward 1996; Esterle 1999). Additional interaction with Al, Sr and Ba, which are believed to be associated with igneous bodies or tuffaceous partings, may result in the precipitation of the goyazite-crandallite group, but these minerals were not observed.

In an alternative model, the phosphorus could have been liberated due to the dissolution of phosphorus-rich feldspars, preferentially albite, from the underlying volcanogenic sandstones of the tuffaceous Fort Cooper Coal Measures (Huang 1999; Michaelsen et al. 2000). These phosphorus-rich fluids could have migrated up the faults, along the roof, floor and coal-parting contacts and eventually precipitated within the coal itself. It is likely that the apatite formed as a result of phosphorus-bearing solutions reacting with calcium-bearing rocks. The gypsum, ankerite and calcite that halo the dykes and sills were likely sources for the calcium ions required to precipitate apatite out of solution (Golab 2004; Querol 1997; Bjorlykke 1993). It has been concluded that K-, Mg- and Fe- depleted, mildly acidic and relatively low-temperature fluids liberated phosphorus and calcium ions from the surrounding lithology, with faults and fractures acting as possible conduits to fluid flow.

#### ACKNOWLEDGEMENTS

The authors would like to thank BHP Billiton Mitsubishi Alliance for their financial assistance and BHP Billiton Mitsui Coal for enabling the authors to access company data and the mine site.

#### REFERENCES

1. BJORLYKKE, K. (1993). "Fluid flow in sedimentary basins." *Sedimentary Geology* 86(1-2): 137 - 158.
2. DAVIS, B.A. (2006). "Determining the geological controls on the spatial distribution of phosphorus within coal seams mined at South Walker Creek Mine, Bowen Basin, Central Queensland, Australia." University of Queensland Honours Thesis, Brisbane, Australia.
3. ESTERLE, J.S. (1999). Controls on phosphorus variability at the minescale. Proceedings of the Thirty third Newcastle Symposium on Advances in the study of the Sydney Basin, Newcastle.
4. GOLAB, A.N, CARR, P.F. (2004). "Changes in geochemistry and mineralogy of thermally altered coal, Upper Hunter Valley, Australia." *International Journal of Coal Geology* 57: 197 - 210.
5. HUANG, X, WANG, X., LIU, C. AND CHEN, Y. (1999). "The P<sub>2</sub>O<sub>5</sub> content of feldspars from the Yashan granites, Jiangzi Province, South China." *Chinese Science Bulletin* 44(13): 1245 - 1248.
6. HULEATT, M.B. (1991). Handbook of Australian black coals: geology, resources, seam properties, and product specifications. *Bureau of Mineral Resources, Australia, Resource Report 7*. A. G. L. Paine. Canberra, Bureau of Mineral Resources, Geology and Geophysics.
7. MICHAELSEN, P, HENDERSON, R.A. (2000). "Sandstone petrofacies expressions of multiphase basinal tectonics and arc magmatism: Permian - Triassic north Bowen Basin, Australia." *Sedimentary Geology* 136: 113 - 136.
8. QUEROL, X, ALASTUEY, A., LOPEZ-SOLER, A., PLANA, F., FERNANDEZ-TURIEL, J.J., ZENG, R., XU, W., ZHUANG, X. AND SPIRO, B. (1997). "Geological Controls on the Mineral Matter and Trace Elements of Coals from the Fuxin Basin,

## GEOLOGICAL CONTROLS ON PHOSPHORUS

- Liaoning Province, Northeast China." *International Journal of Coal Geology* 34: 89 - 109.
9. RAO, P.D, WALSH, D.E. (1997). "Nature and distribution of phosphorus minerals in Cook Inlet coals, Alaska." *International Journal of Coal Geology* 33: 19 - 42.
  10. RYAN, B.D, GRIEVE, D.A. (1995). "Source and distribution of phosphorus in British Columbia coal seams." Geological fieldwork 1996: Ministry of Energy, Mines and Petroleum Resources Paper: 277 - 294.
  11. WARD, C.R (2002). "Analysis and significance of mineral matter in coal seams." *International Journal of Coal Geology* 50: 135-168.
  12. WARD, C.R, CHRISTIE, P. J. (1994). "Clays and Other Minerals in Coal Seams of the Moura Baralaba Area, Bowen Basin, Australia." *International Journal of Coal Geology* 25: 287 - 309.
  13. WARD, C.R., CORCORAN, J.F., SAXBY, J.D. AND READ, H.W. (1996). "Occurrence of phosphorus minerals in Australian coal seams." *International Journal of Coal Geology* 30: 185 - 210.



# GRETA COAL MEASURES IN THE WERRIS CREEK AREA, NEW SOUTH WALES

M.W. Dawson<sup>1,2</sup>, C. Coxhead<sup>3</sup> and A. McMinn<sup>4</sup>

<sup>1</sup> Department of Earth Sciences  
University of New England, NSW 2351.

<sup>2</sup> Whitehaven Coal Mining  
Boggabri Road, Gunnedah, NSW 2380.

<sup>3</sup> Glennies Creek Colliery  
Middle Fallbrook Road, Singleton, NSW 2330.

<sup>4</sup> Institute of Antarctic and Southern Ocean Studies  
University of Tasmania, TAS 7005.

## ABSTRACT

An outlier of the Greta Coal Measures and Maitland Group, crops out approximately three kilometres south of Werris Creek in the Werrie Basin, New South Wales. In this area the Greta Coal Measures constitute two lithological formations (Skeletar Formation and Rowan Formation) that host eight coal members (From base: Glenara Coal Member, Faithful Coal Member, Friendly Coal Member, Eurunderee Coal Member, Doyles Hill Coal Member, Cintra Coal Member, Britton Coal Member, Aberglen Coal Member). The Maitland Group constitutes one formation (Railway View Conglomerate) and hosts the Narrawolga Coal Member). A framework of 5 cored and 29 open boreholes, all with geophysical logs, has been used to assemble a sequence stratigraphic interpretation.

Over 750 000 tonnes of coal was mined from the old Werris Creek Colliery between 1925 and 1963 by board and pillar methods. Mining recommenced in May 2005 by open cut methods at a rate of 1.5 million tonnes per annum with pre-mining reserves totalling 9.8 million tonnes.

Palynology from nine samples throughout the Greta Coal Measures indicates an age range from Early Permian Stage 3b? to Upper Stage 4a showing time equivalence to the Greta Coal Measures in the Musswellbrook anticline area to the south.

A second-order sequence boundary represented by a disconformity with the underlying Werrie Basalt marks the lower of two sequence boundaries within the Greta Coal Measures. The colluvial to fluvial to estuarine Skeletar Formation occupies the initial lowstand and transgressive system tract with a maximum flooding surface occurring just above the Skeletar-Rowan Formation boundary. The deltaic Rowan Formation occupies three cycles of highstand then transgressive systems indicated by repetitions of increasing and decreasing marine influence. Another second-order sequence boundary marked by an erosional base on the alluvial Railway View Conglomerate occurs, with the lowstand, transgressive and highstand systems tracts almost indistinguishable within this unit. The top of the Railway View Conglomerate is not observed. A sequential thinning and disappearance of lower coal seams towards the northeast of the basin indicates a palaeotopographic high.

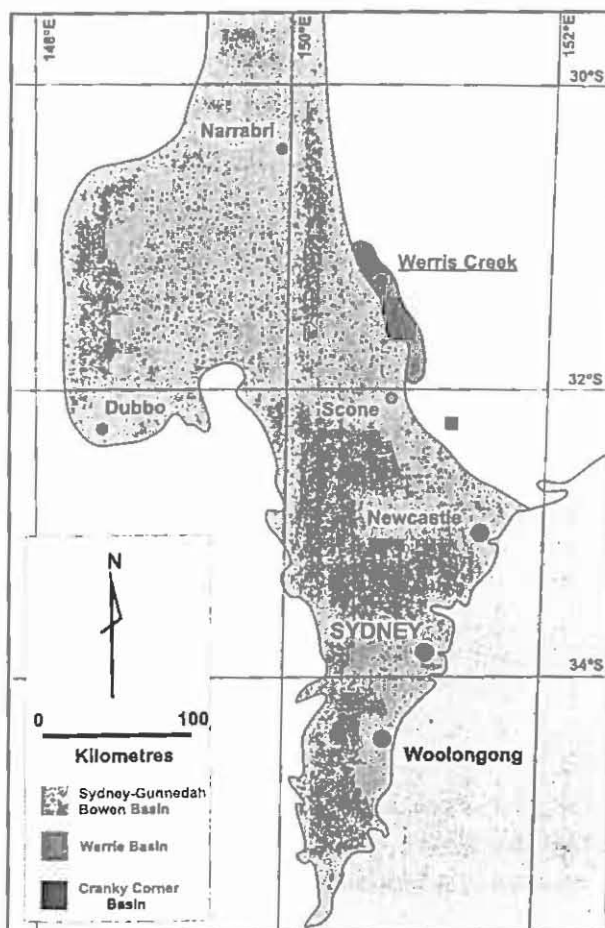
## INTRODUCTION

An outlier of Early Permian Greta Coal Measures occurs approximately three kilometres south of Werris Creek (Figure 1). Outcrop of the Greta Coal measures occurs at the intersection of two oblique (north-south and east-west trending) upright synclines (Carey

1934) to form an elliptical 'basin' shape with dimensions three kilometres north-south by two kilometres east-west. Recent exploration in this area has defined significant open-cut reserves of low-sulphur and low-ash export thermal coal product, and provided new geological data to undertake a detailed sedimentological investigation. The sedimentology is investigated as part of a project to form a regional sequence stratigraphic interpretation of the Greta Coal Measures in the Werrie Basin.

### REGIONAL SETTING, PREVIOUS WORK AND MINING HISTORY

The Werrie Basin is a structural basin containing Permian sedimentary and volcanic rocks that unconformably overlies Middle Cambrian (Cawood 1980) to earliest Permian (Roberts et al 2006) basement of the Tamworth Belt, Southern New England Orogen (Gilligan and Brownlow 1988). Briefly, the Werrie Basin consists of the basal terrestrial Temi Formation that comprises up to 220 metres of mudstones, sandstones, pebble conglomerates and minor felsic to intermediate volcanics and coal (Roberts et al 2005, Hanlon 1948). Overlying the Temi Formation are a series mafic to intermediate volcanics and associated intrusives (Werrie Basalt and Warrigundi Igneous Complex) up to two kilometres thick that were deposited in both marine and terrestrial regimes (Carey 1935; Hanlon 1947). The Werrie Basalt is unconformably overlain by late Early Permian coal-bearing sequence of the Willow Tree Formation (Oversby 1971; Pratt 1996) (herin renamed the Greta Coal Measures - Werris Creek outlier). Conformably overlying the Willow Tree Formation is the early Late Permian marine conglomerates and sandstones of the Borambil Creek Formation. This unit consists of basal, poorly-sorted conglomerates and diamictites with sandy and fossiliferous horizons (Hanlon 1948). The youngest unit in the Werrie Basin is the Late Permian Toll Bar Formation. This unit is both terrestrial and marine containing sandstone, siltstone, mudstone and coal with localised pods of limestone (Hanlon 1948).



Raggat (1933) was the first to note coal from a water bore (cable bore) at the Werris Creek outlier (formerly 'Colliery Basin'; Carey 1935). From 1925 to 1963 the Greta Coal Measures were worked in the northeastern part of the outlier for approximately 750 000 tonnes of coal by board and pillar methods. Mining operations ceased due to the cancelling of contracts for the supply of steaming coal for locomotives. Pratt (1996) identified a remnant resource of 1.4 Million tonnes, which remained in the pillars of the old workings. Renewed exploration at the Werris Creek outlier recommenced in 2000 with the granting of EL5993. Subsequently, thick coal sequences were discovered in the southern part of the Werris Creek outlier with a pre-mining reserve of 9.8 Million tonnes delineated (Department of Primary Industries 2005). Open-cut mining commenced in May 2005 at a nominal capacity of 1.5 Million tonnes per annum.

Figure 1 The location of Werris Creek. Werrie Basin, New South Wales.

## GRETA COAL MEASURES, WERRIS CREEK.

### METHODS

Fieldwork entailed inspection of exploration percussion and cored drilling with geophysical logs as well as exposures in the walls of the opencut at Werris Creek Colliery. The core and associated geophysical logs were subject to a standard sedimentary lithofacies analysis and will be discussed further in Dawson (in prep). All coordinates discussed in this paper are in Australian Geodetic Datum 1966.

### LITHOLOGY

Two lithostratigraphic units within the Greta Coal Measures (Skeletal Formation and Rowan Formation) and one lithostratigraphic unit from the Maitland Group (Railway View Conglomerate) are recognised at Werris Creek. Table 1 shows the stratigraphic relationships at the Werris Creek outlier. The Skeletal Formation consists of colluvial/alluvial dark-grey, kaolinitic, well-rounded, orthomictic, granule to pebble conglomerate (pelletoidal clayrock) intercalated with intraformational sandstone, coal and minor claystone and siltstone towards the top of the unit. It occurs above the Werrie Basalt and below the Rowan Formation with a maximum thickness of 24 metres. The Glenara Coal Member (4-8 m) occurs toward the top of the unit. Typically, the Skeletal Formation contains numerous upward fining cycles comprising poorly-sorted granule conglomerate with an erosional base, up to one metre thick in the lower cycles. These are overlain by up to 70 centimetres of trough cross-bedded sandstone that fines upward into siltstone and generally thin coal. A progressive thinning of the Skeletal Formation can be observed a maximum of 24 metres in rotary hole WC19 (AMG56 275613mE 6523251mN; south) to 0 metres in the cable bore (Raggatt 1933; northwest). Syneresis cracks and minor bioturbation is recorded in the interval above the Glenara Coal Member and below the Rowan Formation.

**Table 1. Revised stratigraphic nomenclature of the Werrie Basin at Werris Creek.**

<b>MAITLAND GROUP</b>	<b>Railway View Conglomerate</b>	Narrawolga Coal Member
<b>GRETA COAL MEASURES</b>	<b>Rowan Formation</b>	Aberglen Coal Member
		Britton Coal Member
		Cintra Coal Member
		Doyles Hill Coal Member
		Eurunderee Coal Member
		Friendly Coal Member
		Faithful Coal Member
	<b>Skeletal Formation</b>	Glenara Coal Member
<b>WERRIE BASALT</b>		
<b>TEMI FORMATION</b>		

Overlying the Skeletal Formation are lithic sandstones, siltstone and conglomerate with seven correlatable coal seams which constitutes the Rowan Formation. Clasts of jasper, green chert and felsic volcanics are common in the conglomeratic phases of the Rowan Formation. Commonly, the upper contact of the Rowan Formation is not observed, however the one fully cored section of the Rowan Formation exists in cored hole WC39C (AMG56 275297mE 65240679mN). The thickness of the Rowan Formation in WC39C is 86 metres. Coal seams within the Rowan Formation include:- Faithful Coal Member (3-5 m), Friendly Coal Member (0.4-0.7 m), Eurunderee Coal Member (4-6 m), Doyles Hill Coal Member (1-2 m), Cintra Coal Member (3-5 m), Britton Coal Member (1-2 m) and Aberglen Coal Member (1-3 m). Bioturbation is present in the Rowan Formation in a number of intervals throughout the section. The lowermost of is the interval directly overlying the Skeletal Formation, and may

be equivalent to the brackish estuarine Ayrdale Sandstone Member of Boyd and Leckie (2000), indicating a marine transgression. In cored hole WC31C (AMG56 275337mE 6523760mN) a marine interval of 95 centimetres thick containing drop pebbles and a high sulphur content is observed directly beneath the Cintra Coal Member. Two correlatable siderite horizons (Palaeosols) exist in the Rowan Formation. The lower of these occurs between the Friendly Coal Member and Eurunderee Coal Member, whereas the upper siderite horizon occurs between the Doyles Hill Coal Member and Cintra Coal Member. At the 'cable bore' of Raggatt (1933) the Eurunderee Coal Member occurs approximately two metres above the Werrie Basalt. This type of relationship implies that more than 40 metres of palaeorelief occurs at the Werris Creek outlier, as the Skeletar Formation and lower part of the Rowan Formation are absent.

The Railway View Conglomerate comprises massive orthomictic pebble to cobble conglomerate with rare siltstone and coal. Clasts are predominantly well-rounded felsic volcanics that are comparable to felsic ignimbrites from the Currabubula Formation, Tamworth Belt (Roberts et al 2005). Coal within the Railway View Conglomerate is manifest as the Narrawolga Coal Member (2-4 m). The top of the Railway View Conglomerate is not observed, however the unit is in excess of 100 metres thick.

#### AGE OF THE GRETA COAL MEASURES AT WERRIS CREEK

At the Werris Creek outlier the Greta Coal Measures contain both *Glossopteris* and *Gangamopteris*, indicating an Early Permian age. Palynology has been undertaken to further constrain the age, with slide mounts of nine samples from cored hole WC30C (AMG56 275592mE 6523615mN) prepared at the University of Queensland. Overall the pollen yields were low, but were quite diverse in assemblage. A spore/polen distribution chart of the examined slides can be observed in Table 2. Palynostratigraphic nomenclature discussed herein are that of Price (1983).

The presence of *Verrucosiporites pseudoreticulatus* and an absence of *Thymospora cicatricosa* in the samples within the Skeletar Formation (100.0 m and 104.3 m) indicate that the samples belong to palynological zone Stage 3b. This age may be similar to that of the Skeletar Formation in the Musswellbrook anticline, as no definitive palynology for this unit has been undertaken in the Musswellbrook anticline area (McMinn 1980a,b). Otherwise, it is quite possible that the lower two samples are actually lower Stage 4 as the key taxa *Phaselisporites cicatricosus* is rare. The appearance of *Thymospora cicatricosa* at 86.8 metres in the Rowan Formation indicates the start of lower Stage 4 zone, and the presence of *Praecolpatites sinuosus* at 55.1 metres indicates the start of upper Stage 4a zone. This age range for the Rowan Formation is similar to that observed in the Musswellbrook Anticline area (McMinn 1980a). The Railway View Conglomerate has not been sampled for palynological assessment. Overall, the Greta Coal Measures range in age from Permian palynological zones Stage 3b? to upper Stage 4a.

#### SEQUENCE STRATIGRAPHY

Sequence stratigraphy has already been investigated for the Greta Coal Measures in the Musswellbrook anticline, Lochinvar anticline and Cranky Corner Basin by a number of authors (Boyd and Leackie 2000, Van Heeswijck 2001). A summary of the lithologies, geophysics, depositional environment, palynology and sequence stratigraphy of the referenced cored hole WC30C can be observed in Figure 2. A second-order sequence boundary marking the start of the Greta Coal Measures is represented by a disconformity at

GRETA COAL MEASURES, WERRIS CREEK.

the boundary between the Skeletal Formation and the underlying Werrie Basalt. However, some portion of the palaeorelief may be attributable to an inherent uneven surface of the underlying Werrie Basalt. Where thickest, the immature peletiodal claystone is typical of an incised valley fill poor-sorting. The colluvial to fluvial to estuarine Skeletal Formation occupies the initial lowstand and transgressive system tracts.

**Table 2.** Spore/pollen distribution chart of samples from WC30C (AMG56 275592mE 6523615mN).

	Depth (m)								
	Rowan Fmn							Skeletal Fmn	
	23.2	36.8	53.7	55.1	64.3	78.9	86.8	100.0	104.3
<i>Acanthotriletes teretangulatus</i>	X	X	X	X				X	
<i>Allsporites australis</i>									
<i>Apicuatissporites cornutus</i>		X					X	X	X
<i>Bascanisporites undosus</i>				X					
<i>Barakarites rotatus</i>									
<i>Cannanoropollis diffusus</i>	X		X	X		X	X	X	X
<i>Calamnospora</i> spp.									
<i>Circulisporea parvus</i>									
<i>Cycadophites follicularis</i>	X		X			X	X		X
<i>Dulhuntylspora dulhuntyi</i>									
<i>Dulhuntylspora parvithola</i>									
<i>Gondisporites</i>									
<i>Granulatisporites frustulentus</i>									
<i>Granulatisporites micronodosus</i>			X	X		X	X	X	X
<i>Granulatisporites trisinus</i>		X	X	X		X		X	
<i>Indotradites splendens</i>		X	X	X		X		X	
<i>Lelotriletes directus</i>	X	X	X	X	X	X	X	X	X
<i>Limlitsporites moerensis</i>		X	X	X			X		
<i>Lundbladisporea lphilegna</i>									
<i>Marsupipollenites triradiatus</i>	X	X	X	X	X	X	X	X	X
<i>Microbaculispora tentula</i>	X	X	X	X	X	X	X	X	
<i>Osmundacladites</i> spp.									
<i>Plattysaccus leschikii</i>									
<i>Plicatipollenites malabarensis</i>	X	X	X	X			X		X
<i>Praecolpites sinuosus</i>				X					
<i>Protohaploxylinus</i> spp.	X	X	X	X	X	X			
<i>Pteruchipollenites gracilis</i>				X	X			X	
<i>Punctatisporites gretensis</i>	X	X	X	X		X	X	X	
<i>Retusotriletes nigrifolius</i>		X	X	X			X		
<i>Scheuringipollenites maximus</i>	X	X	X	X	X	X	X		X
<i>Scheuringipollenites ovatus</i>	X	X	X	X	X	X	X		X
<i>Secaripollenites bullatus</i>									
<i>Striatopodocarpites cancellatus</i>	X	X		X	X	X	X		X
<i>Striatoabietites multistriatus</i>		X	X	X	X		X		X
<i>Thymospora cicatricosa</i>	X	X	X			X	X		
<i>Verrucosisporites pseudoreticulatus</i>		X	X			X	X	X	X
<i>Vitreisporites signatus</i>					X		X		X

The river-dominated deltaic Rowan Formation comprises three cycles of increasing then decreasing marine influence, determined by variations in the occurrence of sedimentological features such as bioturbation, syneresis cracks, sulphur content. This is common for the Rowan Formation in the Musswellbrook anticline area and indicates sediment supply was approximately equal to basin subsidence (Boyd and Leakie 2000). Furthermore, no erosional surfaces with significant (>10 m) relief have been identified in the Rowan Formation. A sequence stratigraphic interpretation of this is a series of alternating highstand and transgressive systems with no lowstand. This occurs when a prograding delta is offset by an

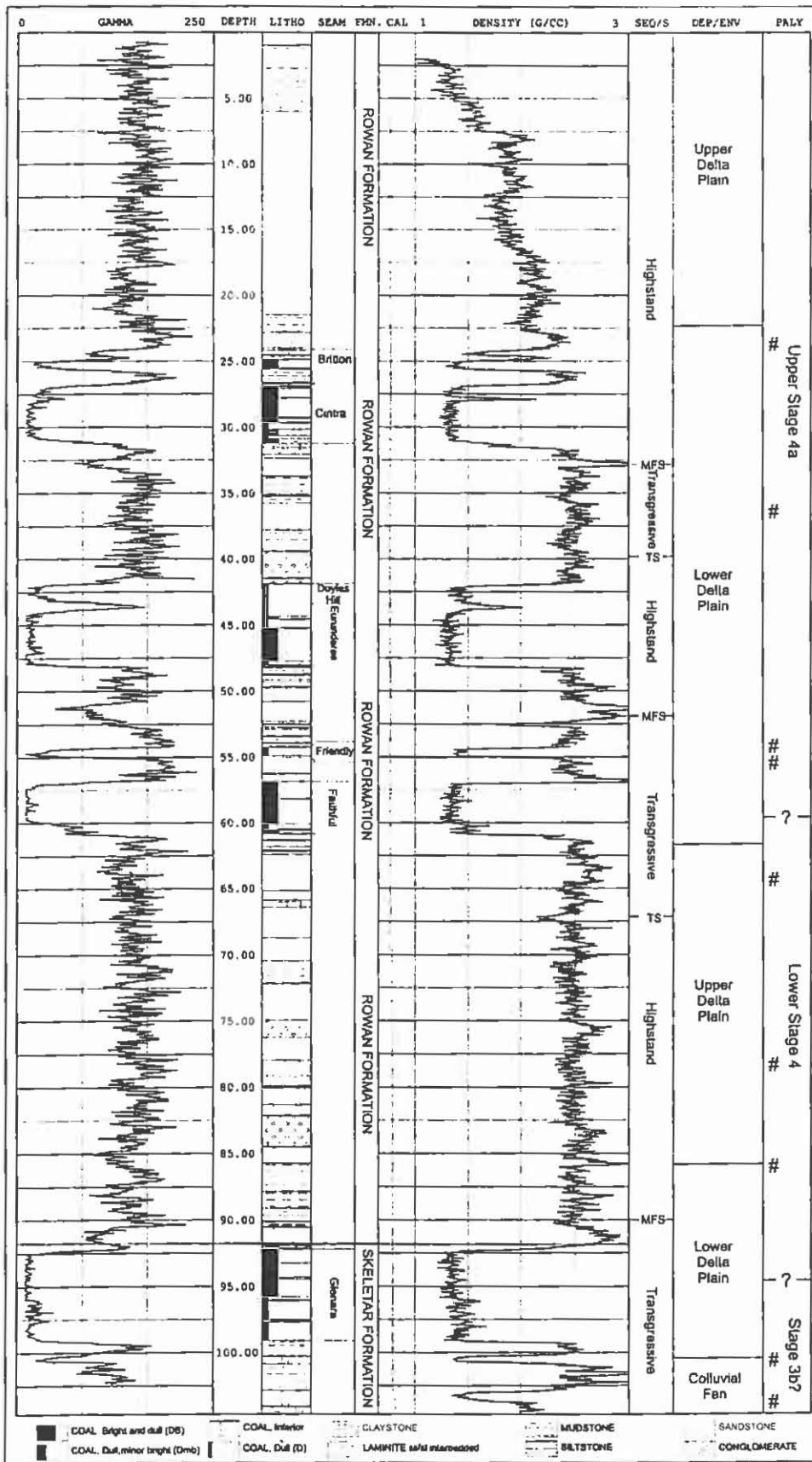


Figure 2. Graphic log of WC30C (AMG56 275592mE 6523615mN).

## GRETA COAL MEASURES, WERRIS CREEK.

equal amount of marine transgression. A similar sedimentological situation has been proposed for the Rowan Formation in the Muswellbrook anticline area (Boyd and Leake 2000).

A second-order sequence boundary marked by an erosional base on the alluvial Railway View Conglomerate occurs. This boundary shows an easily identifiable increase in clast size and change in clast composition. The amount of erosion at the base of the Railway View Conglomerate cannot be ascertained easily as no coal seams or marker horizons within the Rowan Formation are eroded. From limited drill core data, the lowstand, transgressive and highstand systems tracts are almost indistinguishable within this unit, as the unit is comprised, almost wholly, of massive pebble to cobble conglomerate.

### CORRELATION

Due to the remarkable similarities in lithology, depositional environment and age, the Skeletar and Rowan Formations within the Greta Coal Measures at Werris Creek can be correlated directly with those in the Muswellbrook anticline area. This implies that the isolated Greta Coal Measures outlier at Werris Creek identified in this study was once part of a series of continuous, west-flowing, high-energy delta plains. The delta plains may have stretched from north of Werris Creek to south of Muswellbrook. The Railway View Conglomerate may be equivalent to the 'terrestrial' Branxton Formation (Beckett 1988) or Jasdec Park Sandstone Member (Boyd and Leake 2000), which formed during a brief marine regression then transgression.

### CONCLUSIONS

The outlier of Greta Coal Measures at Werris Creek contains two formations (Skeletar Formation and Rowan Formation) and eight correlatable coal members. An Early Permian age determined from palynology of the Greta Coal Measures extends from Stage 3b? (Skeletar Formation) to Upper Stage 4a (upper Rowan Formation). Deposition environments range from early colluvium to a river-dominated delta plain. Direct correlations have been identified between the Greta Coal Measures at the Werris Creek outlier and the Greta Coal Measures at the Muswellbrook anticline.

### ACKNOWLEDGEMENTS

Thanks to Daniel Mantle and Peter Colls (University of Queensland) for preparing slides for palynology. Jeff Brownlow (New South Wales Department of Primary Industries) is thanked for his insights into the geology of Werrie Basin. Creek Resources is thanked for allowing access to drilling information and site visits.

### REFERENCES

- BECKETT J. 1988. The Hunter Coalfield. Notes to accompany the 1:100 000 Geological Map, *Geological Survey of New South Wales, Report GS1988/51*.
- BOYD R. & LECKIE D. 2000. The Greta Coal Measures in the Muswellbrook Anticline area, New South Wales. *Australian Journal of Earth Sciences* 47, 259-279.
- CAREY S.W. 1934. The Geological Structure of the Werrie Basin. *Journal and proceedings of the Linnean Society of New South Wales* 59. 351-374.
- CAREY S.W. 1935. Note on the Permian Sequence in the Werrie Basin. *Journal and proceedings of the Linnean Society of New South Wales* 60. 447-456.
- CAWOOD P.A. 1980. Geological development of the New England Fold Belt in the Woolomin-Nemingha and Wisemans Arm regions. The evolution of a Palaeozoic fore-arc terrain, PhD thesis, University of Sydney.

- DEPARTMENT OF PRIMARY INDUSTRIES. 2005. New South Wales Coal Industry Profile. New South Wales Department of Primary Industries, Maitland.
- GILLIGAN L.B. & BROWNLOW J.W. (Eds) 1987. *Tamworth-Hastings 1:250 000 metallogenic map. Sheets SH 56-13, SH 56-14 (plus parts of SI 56-1 and SI 56-2). Mineral deposit data sheets and metallogenic study.* Geological Survey of New South Wales, 438 pp.
- HANLON F.N. 1947. Geology of the north-western coalfield. *Department of Mines New South Wales, Annual report.* 107-108.
- HANLON F.N. 1948. Geology of the north-western coalfield. Part II. Geology of the Willow Tree—Temi district. *Royal Society of New South Wales, Journal and Proceedings* **81**, 291-297.
- LOUGHNAN, F.C. 1973. Kaolinite clayrocks of the Koogah Formation New South Wales. *Geological Society of Australia, Journal* **20(3)**. 329-341.
- McMINN A. 1980. Palynology of DM Balmoral DDH1, Greta Coal Measures, East Musswellbrook Drilling Program. (Unpubl.) *Geological Survey of New South Wales, Report GS1980/196*, 4pp.
- McMINN A. 1980. Palynology of DM Brougham DDH1 and DM Brougham DDH 5, East Musswellbrook Drilling Program. (Unpubl.) *Geological Survey of New South Wales, Report GS1980/272*, 4pp.
- OFFENBERG A.C. 1971. *Tamworth 1:250,000 Geological Sheet SH 56-13*, Geological Survey of New South Wales, Sydney.
- PRATT W. 1996. Coal resources of the Werrie Basin NSW. Department of Mineral Resources, *GS1996/528*, pp19.
- PRICE P. 1983. A Permian palynostratigraphy for Queensland. In Permian geology of Queensland. Geological Society of Australia, Queensland Division, 155-213.
- RAGGATT H.G. 1933. Notes on the geology of the Quirindi-Werris Creek district. *Department of Mines New South Wales, Annual report.* 107-108.
- ROBERTS J., OFFLER R. & FANNING M. 2006. Carboniferous to Lower Permian stratigraphy of the southern Tamworth Belt, southern New England Orogen, Australia: boundary sequences of the Werrie and Rouchel blocks. *Australian Journal of Earth Sciences* **53(2)**. 249-284.
- VAN HEESWIJCK A. 2001. Sequence stratigraphy of coal-bearing high energy clastic units: the Maitland – Cessnock – Greta Coalfield and Cranky Corner Basin. *Australian Journal of Earth Sciences* **48(3)**. 417-426.

# REVIEW OF STRUCTURE AND BASEMENT CONTROL OF THE LAPSTONE STRUCTURAL COMPLEX, SYDNEY BASIN, EASTERN NEW SOUTH WALES

Christopher L. Fergusson

School of Earth and Environmental Sciences  
University of Wollongong, NSW 2522, Australia

## ABSTRACT

In the western Sydney Basin, the Lapstone Structural Complex is a major north-trending association of monoclines and faults that forms the frontal ridge of the Blue Mountains Plateau. At Kurrajong Heights, the Lapstone Structural Complex is dominated by an east-facing monocline with a gently dipping central limb containing several different homoclinal segments. At the Hawkesbury Lookout section, strata are steeply dipping to near vertical along the main east-facing monocline. The Lapstone Structural Complex has been related to either steep east-dipping extensional faulting or to moderate to steep west-dipping contraction faults. Strike-slip displacement may also have played a role in its development. The Hawkesbury Lookout section is interpreted in the subsurface as a moderately west-dipping thrust fault. The historical development of the Lapstone Structural Complex has been difficult to resolve although palaeomagnetic data from the southern part are indicative of Late Cretaceous to Cenozoic deformation. Neotectonic activity may also have occurred along the structure. Basement to the Sydney Basin is the eastern Lachlan Fold Belt, which includes moderately west-dipping faults that may have been reactivated as thrust faults in the present-day stress regime. These structures provide a potential analogue for a basement-controlled fault that has generated the Lapstone Structural Complex.

## INTRODUCTION

This account presents a brief review of the Lapstone Structural Complex in the western Sydney Basin (Figure 1). Two cross sections are shown for Kurrajong Heights and Hawkesbury Lookout and these complement the structural outline of the Lapstone Structural Complex given by Branagan and Pedram (1990, 1997). The Lapstone Structural Complex is a significant feature but its understanding has been limited by various contradictory data on its historical development and also by its overall classification as one of contractional, extensional and/or strike-slip association. Additionally, it has been considered controlled by an underlying basement structure and this is considered herein with reference to potentially active faults in the Lachlan Fold Belt to the west and southwest of the Sydney Basin.

## BACKGROUND

The Lapstone Structural Complex is an association of east-facing monoclines, high-angle faults, and fracture zones to the west of Sydney (Branagan & Pedram 1990, 1997). Its development was considered syndepositional during the Permian and Triassic periods by Pickett and Bishop (1992) as units thicken immediately to the east of the complex (see also seismic interpretation in Australian Oil & Gas Corporation Ltd 1966). An upper limit to tilting associated with monocline development was based on the cross-cutting Jurassic Nortons Basin diatreme near Wallacia which is apparently undeformed (Pickett & Bishop

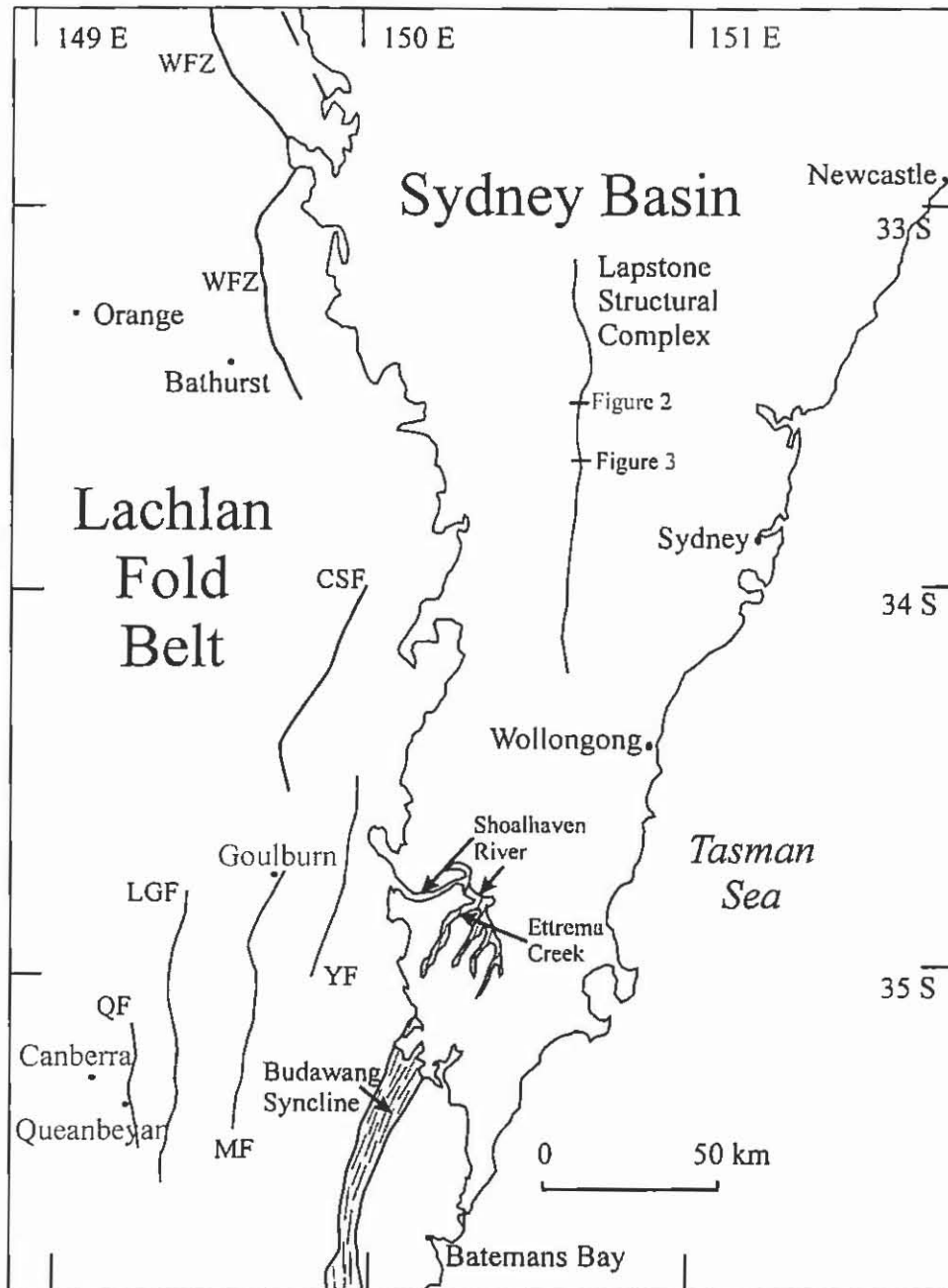


**Figure 1** Sydney Basin and major structures in the adjoining Lachlan Fold Belt (after Scheibner 1997). Lapstone Structural Complex is marked along with locations of Figures 2 and 3. Faults in Lachlan Fold Belt: CSF = fault on western margin of Cockbundoon Syncline, LGF = Lake George Fault, QF = Queanbeyan Fault, MF = Mulwaree Fault, YF = Yarralaw Fault, WFZ = Wiagdon Fault Zone.

1992). Palaeomagnetic data indicate that tilting associated with the Lapstone Structural Complex affected the mid-Cretaceous overprint magnetisation at Tahmoor and that therefore much of the deformation post-dated the mid Cretaceous (Schmidt *et al.* 1995). A lack of tilting of Miocene magnetisation was determined for the monocline at Lapstone (Bishop *et al.* 1979). These constraints are consistent with an Early Tertiary age for the Lapstone Structural Complex suggested by Branagan and Pedram (1990) and supported by studies of the sub-

## LAPSTONE STRUCTURAL COMPLEX

basalt topography and modelling in the Blue Mountains (van der Beek *et al.* 2001). Numerous earthquakes have occurred and indicate that the Lapstone Structural Complex may still be active (Brown & Gibson 2004). Neotectonic deformation in southeastern Australia is now recognised as being more prominent than previously considered (Sandiford 2003).

### STRUCTURE OF THE LAPSTONE MONOCLINE

The Lapstone Structural Complex varies along its length with monocline(s), high-angle faults and minor structures such as thrusts, minor folds, tectonic breccias and joints (Branagan & Pedram 1990, 1997). An east-facing monocline is well developed along much of the complex as at Kurrajong Heights where the central, gentle limb of the monocline consists of several segments with different dips to the east (Figure 2). Much steeper dips on the monocline occur below the Hawkesbury Lookout. Here, strata west of the monocline are flat and gradually increase in dip up to *ca* 15° to the east before crossing a fault onto the steeply dipping near vertical central limb (Figure 3, Branagan & Pedram 1990, figure 7).

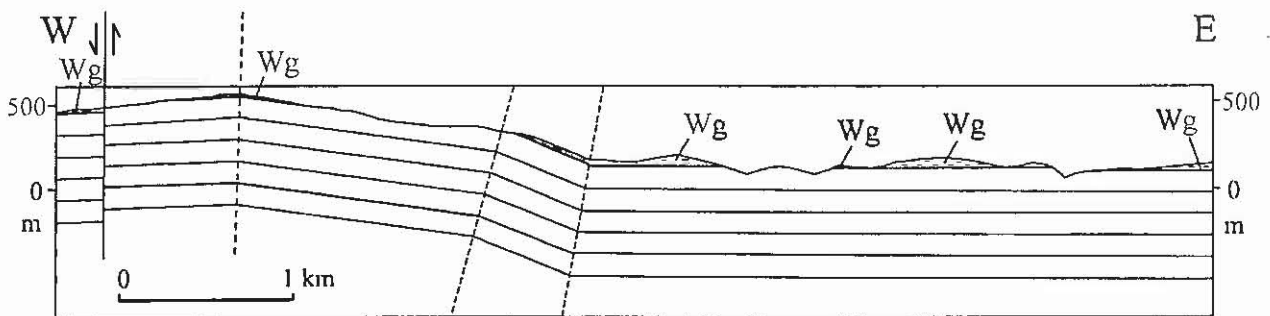


**Figure 2** West to east cross section through the Lapstone Structural Complex at Kurrajong Heights. Wg = Wianamatta Group (underlying units not labelled). Vertical scale = horizontal scale. Cross section is constrained by the contact between the Wianamatta Group and the underlying Hawkesbury Sandstone as shown on the Penrith 1:100 000 Geological Sheet (Clarke & Jones 1991).

### Interpretation

Monoclines, such as those of the Colorado Plateau, have been attributed to contractional deformation along thrust faults at depth (Bump & Davis 2003). But they are also related to deformation in rock strata overlying steeply dipping extensional faults in underlying basement (Withjack & Callaway 2000). Herbert (1989) noted from seismic data that high-angle reverse faults were associated with the Lapstone Structural Complex but that the en echelon geometry of these faults implies a strike-slip component. The cross sections shown above have been constructed from surface dip and stratigraphic data following Suppe's (1985) kink-band method. Available seismic data have not been used in their construction. The gentle nature of the monocline at Kurrajong Heights is difficult to interpret and could be related to either a contractional or extensional regime. For the Hawkesbury Lookout section, the zone of ductile deformation in the central limb of the monocline implies that a moderately west-dipping thrust fault occurs at depth with approximately 500 m of net slip. This thrust fault dips 50° to the west, some 20° less steep than the main high-angle reverse fault recognised by Herbert (1989) from seismic data to the south of Yellow Rock Lookout (~3 km south of Hawkesbury Lookout). Dips of reverse faults in other sections shown in Herbert (1989) are of the order of 55–65° mainly to the west. From this we may infer that contractional faulting was responsible for the Lapstone Structural Complex but the excessive dips in contrast to most thrust faults in

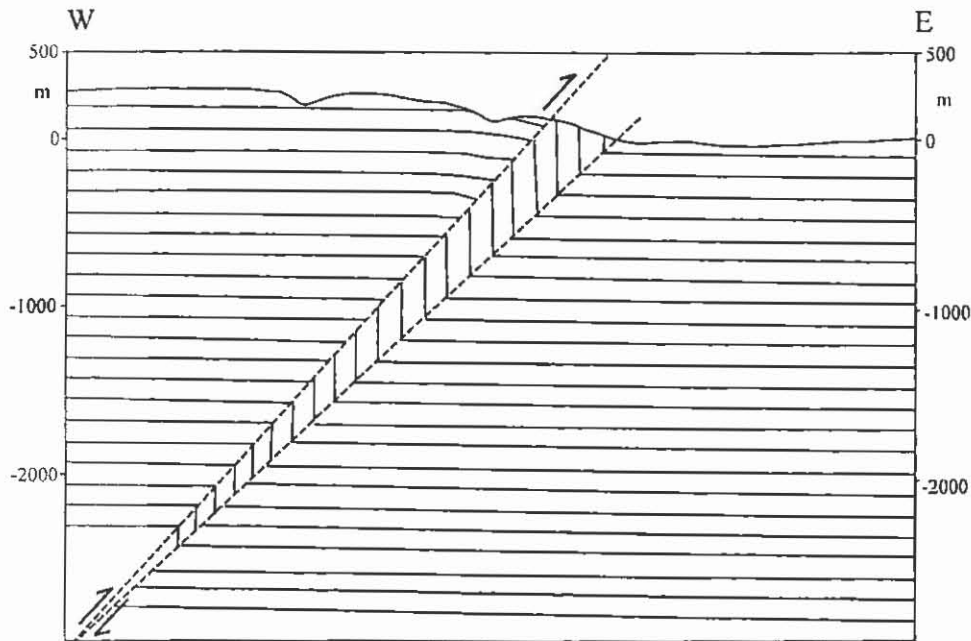


**Figure 3** West to east cross section through the Lapstone Structural Complex at the Hawkesbury Lookout (note that stratigraphy is omitted but the surface exposure is in the Hawkesbury Sandstone). Vertical scale = horizontal scale.

undeformed strata (i.e.  $<35^\circ$ , following Anderson's classification of faults) are anomalous unless these structures have a listric geometry. The dips of reverse faults portrayed by Herbert (1989) could be accounted for by reactivation of west-dipping normal faults but this is clearly inconsistent with any inferred normal faults associated with deposition and/or Mesozoic rifting as these would be east-dipping. It is considered that strike-slip movement could have played only a local role in structural development of the Lapstone Structural Complex.

### **BASEMENT CONTROL**

It has been suggested that the Lapstone Structural Complex was controlled by reactivation of the western margin of the Budawang Syncline (the Eden-Comerong-Yalwal Rift) in the underlying Lachlan Fold Belt especially where this was intersected by elements of the east-trending Lachlan Lineament (Branagan & Pedram 1990). The structure of the Budawang Syncline exposed at the Shoalhaven River and Ettrema Creek has been described by Cooper (1992). The western margin of the Budawang Syncline is locally faulted and other faults occur within it although no evidence has been found indicating reactivation of these faults in the present-day stress field. West of the Sydney Basin, faults are west dipping and include structures such as the Wiagdon Fault Zone, Mulwaree Fault, and Yarralaw Fault (Fergusson & Vandenberg 1990). The Lake George Fault, northeast of Canberra, has spectacular topographic expression and has been related to Tertiary normal faulting (Abell 1991). It is associated with a thin (up to 165 m) late Tertiary succession in Lake George that indicates development of the depression east of the fault in the last  $\sim 10$  Ma (Abell 1989). Most other faults in the region show little sign of Tertiary reactivation although some have limited topographic expression with subdued fault scarps consistent with some local neotectonic activity. A pre-existing west-dipping thrust in the basement under the western Sydney Basin, perhaps analogous to the Lake George Fault further west, may have controlled development of the Lapstone Structural Complex. This structure would have been reactivated in the Late

## LAPSTONE STRUCTURAL COMPLEX

Neogene east-west contractional regime that has affected southeastern Australia (Sandiford 2003; Brown & Gibson 2004).

### DISCUSSION AND FUTURE DIRECTIONS

Earthquake activity in southeastern Australia is concentrated in a broad zone between Sydney and Melbourne in the southeastern highlands as well as in other regions such as the Mt Lofty and Flinders Ranges (Brown & Gibson 2004). Seismicity has been related to a contractional regime reflecting east-west convergence across the Australian-Pacific plate boundary in the South Island of New Zealand that has developed in the Late Neogene (Sandiford 2003). Slip rates along faults in southeast Australia are low (metres per million years, Brown & Gibson 2004) and it is therefore not surprising that neotectonic faulting remains difficult to establish. Many earthquakes cannot be tied to source faults. Given the clear topographic expression of the Lapstone Structural Complex, and faults such as the Lake George Fault, these structures may be at least partly related to the Late Neogene contractional tectonic setting. Suggestions of an extensional origin for both these structures need to be critically re-evaluated. A Late Neogene age for the Lapstone Structural Complex is apparently contradicted by untilted Miocene magnetisation at Lapstone (Bishop *et al.* 1979) but it does provide a plausible explanation for the problematic Rickabys Creek Gravel at Glenbrook and elsewhere (cf. Pickett & Bishop 1992).

Given the great antiquity of much of the landscape in eastern Australia, the lack of evidence for notable tectonic events in the latest Cretaceous to latest Palaeogene and recent evidence of Late Neogene deformation and uplift in southeastern Australia (Sandiford 2003), it is important to re-evaluate the role of reactivation and neotectonic activity on structures such as the Lake George Fault, Mulwaree Fault and Lapstone Structural Complex. The present-day seismicity of southeastern Australia indicates that thrust faulting is active and therefore west-dipping structures with potential evidence for neotectonic activity should be carefully examined. More cross sections drawn to depth incorporating seismic and borehole data are needed to determine if these structural geometries are viable.

### ACKNOWLEDGEMENTS

An earlier draft of this contribution has also been submitted to the proceedings of a workshop held on the Lapstone Structural Complex in Sydney in 2005. Dr Dan Clarke is thanked for organising the workshop on the Lapstone Structural Complex. Dr David Branagan kindly commented on a draft of this manuscript. Dr Hossein Memarian is thanked for many discussions on Sydney Basin structure. I am most grateful to the late Professor Peter Coney for showing me the Colorado Plateau and its monoclines in 1993.

### REFERENCES

- ABELL R. S. 1991. *Geology of the Canberra 1:100 000 Sheet area, New South Wales and Australian Capital Territory*. Bureau of Mineral Resources, Geology and Geophysics, Bulletin 233.
- AUSTRALIAN OIL & GAS CORPORATION LTD 1966. Putty-Oakdale seismic survey, PEL 102 and PEL 103, Sydney Basin. Geological Survey of New South Wales, Report SS048 (unpub.).
- BISHOP P., HUNT P. & SCHMIDT P. W. 1982. Limits to the age of the Lapstone Monocline, N.S.W.— a palaeomagnetic study. *Journal of the Geological Society of Australia* 29, 319–326.

- BRANAGAN D. F. & PEDRAM H. 1990. The Lapstone Structural Complex, New South Wales. *Australian Journal of Earth Sciences* **37**, 23–36.
- BRANAGAN D. F. & PEDRAM H. 1997. Engineering geology of a sandstone escarpment: the Blue Mountains, Sydney Basin NSW. In: McNally G. ed. *Collected Case Studies in Engineering Geology, Hydrogeology and Environmental Geology. Third Series*, pp. 38–52. Environmental, Engineering and Hydrogeology Specialist Group, Geological Society of Australia and Conference Publications.
- BROWN A. & GIBSON G. 2004. A multi-tiered earthquake hazard model for Australia. *Tectonophysics* **390**, 25–43.
- BUMP A. P. & DAVIS G. H. 2003. Late Cretaceous–early Tertiary Laramide deformation of the northern Colorado Plateau, Utah and Colorado. *Journal of Structural Geology* **25**, 421–440.
- CLARKE N. R. & JONES D. C. eds. 1991. *Penrith 1:100 000 Geological Sheet 9030*. New South Wales Geological Survey, Sydney.
- COOPER G. T. 1992. Early Carboniferous back-arc deformation in the Lachlan Fold Belt, Shoalhaven River–Ettrema Creek area, NSW. *Australian Journal of Earth Sciences* **39**, 529–537.
- FERGUSSON C. L. & VANDENBERG A. H. M. 1990. Middle Palaeozoic thrusting in the eastern Lachlan Fold Belt, southeastern Australia. *Journal of Structural Geology*, **12**, 577–589.
- HERBERT C. 1989. The Lapstone Monocline-Nepean Fault – a high angle reverse fault system. Advances in the study of the Sydney Basin. Proceedings of the 23<sup>rd</sup> Symposium, University of Newcastle, Department of Geology, 179–186.
- PICKETT J. W. & BISHOP P. 1992. Aspects of landscape evolution in the Lapstone Monocline area, New South Wales. *Australian Journal of Earth Science*, **39**, 21–28.
- SANDIFORD M. 2003. Neotectonics of southeastern Australia: linking the Quaternary faulting record with seismicity and *in situ* stress. In: Hillis R. R. & Müller R. D. eds. *Evolution and Dynamics of the Australian Plate*, pp. 107–119. Geological Society of Australia Special Publication **22**, and Geological Society of America Special Paper **372**.
- SCHEIBNER E. 1997. *Stratotectonic map of New South Wales, scale 1:1 000 000*. Geological Survey of New South Wales, Sydney.
- SCHMIDT P. W., LACKIE M. A. & ANDERSON J. C. 1995. Palaeomagnetic evidence for the age of the Lapstone Monocline, NSW. *Australian Coal Geology* **10**, 13–22.
- SUPPE J. 1985. *Principles of Structural Geology*. Prentice-Hall, New Jersey.
- VAN DER BEEK P., PULFORD A. & BRAUN J. 2001. Cenozoic landscape development in the Blue Mountains (SE Australia): lithological and tectonic controls on rifted margin morphology. *Journal of Geology* **109**, 35–56.
- WITHJACK M. A. & CALLAWAY S. 2000. Active normal faulting beneath a salt layer: an experimental study of deformation pattern in the cover sequence. *American Association of Petroleum Geologists Bulletin* **84**, 627–651.

# WINGECARRIBEE PEAT SWAMP, SOUTHERN HIGHLANDS, NEW SOUTH WALES – AND ITS WATER

Jonathan Griffin and Adrian Hutton

School of Earth and Environmental Sciences  
University of Wollongong  
Wollongong NSW 2522

## ABSTRACT

The Wingecarribee peat deposit was Australia's largest intact mainland peat deposit until a combination of factors in 1998 resulted in the collapse and erosion of the peat. Starting in 2001, the water table in the swamp has been monitored in four transects of pipes, with three transects of pipes in the dissected peat and one shorter transect of pipes in one of the two relatively stable arms.

In this paper we present data from monitoring of the water levels in two of the transects, one located in an unaltered arm and the second located in part of the severely altered section of the swamp. Our data show that the water table is closely related to the rainfall with the table rising significantly after heavy rain. The channel which was eroded through the peat during the collapse is being revegetated with herbaceous plants and this has caused the water table in this part of the swamp to rise and for the higher water levels to spread laterally into areas previously without a water table above the clay substrate. Unless a catastrophic event removes the vegetation, this build of initially living but later decaying plant matter will continue, with a positive prognosis for the viability of the peat.

Preliminary analysis of rainfall and evaporation data show that in the evolution and the revival of the peat the net evaporation to rainfall budget is important.

## INTRODUCTION

Wingecarribee Swamp is approximately 5 km long (east to west) and 750 m wide and is elevated 670 m above sea level. The swamp lies 3 km west of Robertson (Figure 1) and approximately 20 km west of the Illawarra Escarpment, New South Wales, and is part of the Warragamba Hydrological Catchment that supplies the bulk of Sydney's water supply. The catchment covers an area of 40 km<sup>2</sup> with the main feeder creek, Caalang Creek, bringing the bulk of surface runoff to the swamp. It was also believed that the peat received significant quantities of water through seepage from the adjacent grazing and agricultural land.

The swamp hosted the largest pristine montane peat deposit on mainland Australia until August 1998, when erosion and mass slumping after a major rainfall event (Figure 2) resulted in structural failure and loss of a considerable part of the peat.

Wingecarribee Swamp lies in the gently sloping upper catchment valley of the Wingecarribee River. Prior to the collapse of the swamp in 1998, the swamp acted as a natural filter that trapped sediments, nutrients and heavy metals, especially from nearby agricultural land. The

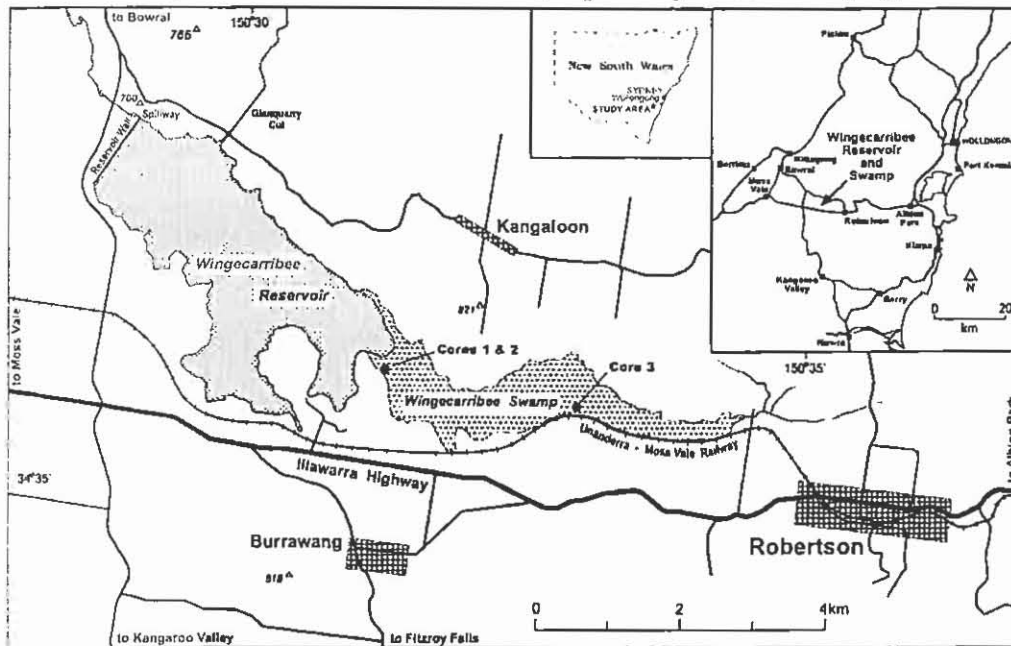


Figure 1. Location of Wingecarribee Swamp.

swamp also acted as a screen to reduce water velocity of the flow into the reservoir. Until the collapse water input was thought to have been maintained primarily by groundwater springs at the junction of the Hawkesbury Sandstone and the overlying basalt (Hope & Southern 1984; Fiander 1993).

The peat collapse of August 1998 resulted in the hydrology of the swamp being dramatically altered. Large fractures and gaps appeared between sizeable blocks of peat, exposing the previously hidden stratigraphy in slump scars. The surface peat at the eastern area of the swamp was highly desiccated and has minimal moisture content.

An Australian Water Technologies review (AWT 1998) of the swamp collapse suggested that the effect of the altered hydrological regime on Wingecarribee Swamp is likely to be catastrophic. For example, the swamp was thought to no longer be able to reduce peak flows into the Wingecarribee Reservoir, the large amount of drying peat had considerably increased the risk of fire and the altered hydrology was thought to probably have a negative impact on species reliant on specific water levels (Kodala 1998).

Honours theses by Smith (2000) and Hales (2001) provided some baseline data on the physical nature of the peat, the remaining thickness of peat, depth to the watertable and age of the peat. The substrate below the peat is commonly a white clay to grey carbonaceous clay that has developed through weathering of the Hawkesbury Sandstone. An interesting feature is that in many cores taken by Smith (2000) there appears to have been little accumulation of organic matter in the clay and the boundary between the overlying peat and clay is very sharp.

## WINGECARRIBEE PEAT

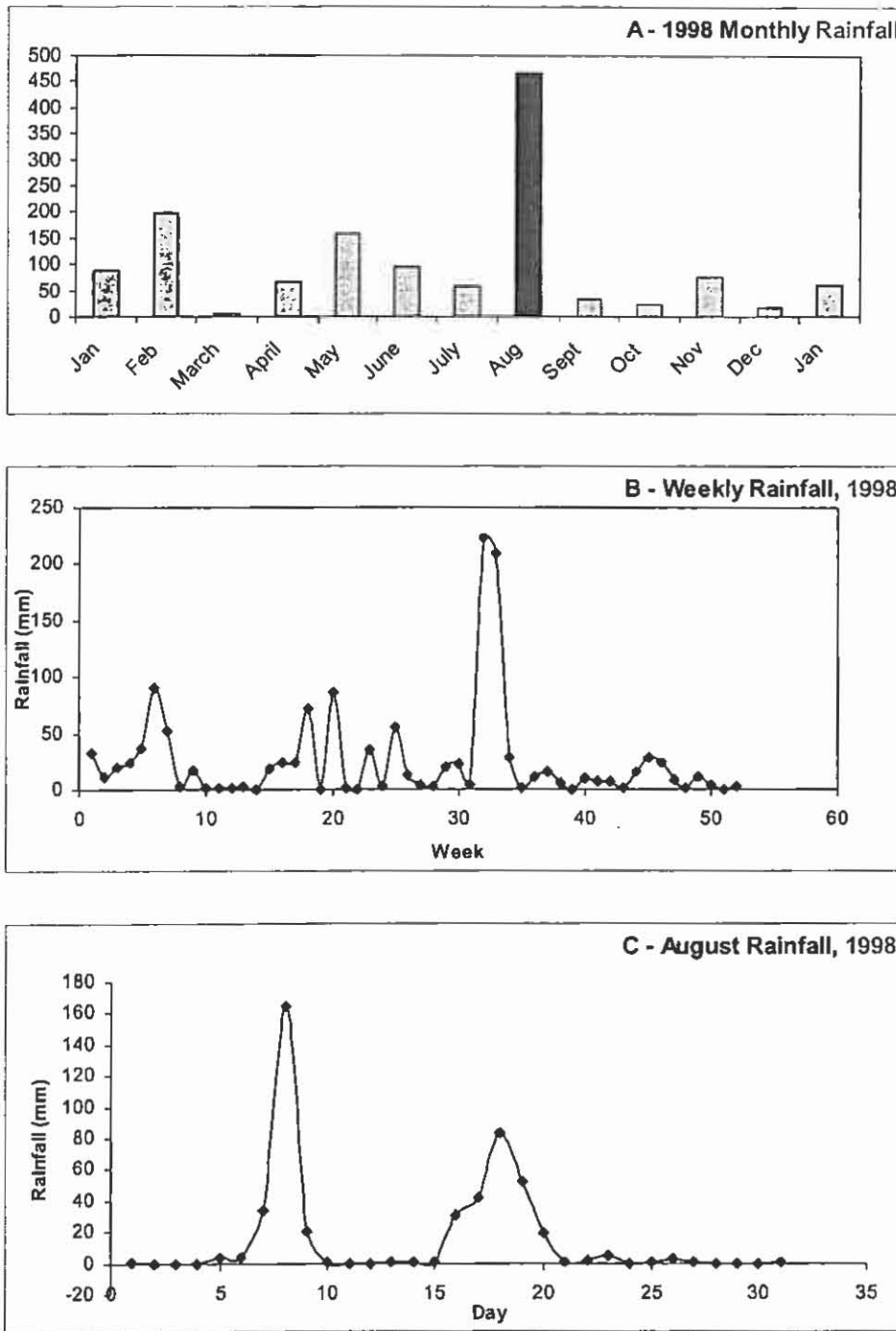


Figure 2. Rainfall data for Wingecarribee Reservoir wall showing the large rainfall event, 8 August 1998 preceding the collapse of the swamp (compiled from data in Smith 2000).

Since 2001, the level of water in four transects of open-ended 5 cm diameter pipes has been monitored to assess the influence of rainfall on water levels. It is aimed to use these results to determine the prospect for peat survival and to relate to coal formation.

### CAN THE PEAT SURVIVE?

The accumulation of organic matter only takes place when the rate of production exceeds the rate of loss due to decay and removal (Hope & Southern 1984). The ratio of production to loss

is slightly positive in most peat deposits, giving accumulation rates of between 0.1 and 1 mm per year (Hope & Southern 1984). Physico-chemical changes in the peat such as decay, decomposition or humification are usually rapid following deposition but slow down later (Clymo 1983). Humification, perhaps the most important process in an aggrading peat mire, is the loss of organic matter, physical structure and change in the chemical nature of peat (Clymo 1983), and is in effect a measure of the extent to which plant structure is visible.

Smith (2000) reported that peat formation is promoted by various external factors including:

- low temperatures
- acidic conditions
- available water
- light
- limited nutrients
- absence of removal mechanisms (erosion, fire or grazing).

Lowe and Walker (1997) provided an account of peat accumulation in which there is a chronological sequence starting with the sequential build-up from an open water environment to a swamp environment, termed 'hydroseral succession'. The accumulation of plant material in lakes eventually fills them and allows fen plants and then bog plants to invade. Sediments gradually change in character from mud to peat (Lowe & Walker 1997). According to Lowe and Walker (1997), the rate of hydroseral succession depends on:

- the size of the lake,
- the size of the catchment,
- the rate of sediment supply, and
- the level of productivity within the lake.

Australian peat develops in areas with low topography and moderate to high rainfall with little seasonal variation (DMR 1995). In New South Wales, these conditions are confined to the coastal strip and the highlands of the Great Dividing Range. Because Australia is a temperate to sub-tropical area with unreliable rainfall and relatively subdued relief (Hope & Southern 1984), the country is deprived of peatlands relative to other countries. Peatlands that exist in Australia do so in the coldest and wettest areas with abundant rainfall (Hope & Southern 1984) such as Tasmania and the Southern Highlands of New South Wales.

Once peat has accumulated, loss takes place primarily by decay and this occurs when the peat is exposed and dries out. The four transects of pipes were put in the monitor the water to determine if over the short term (two to five years) the water table dropped.

Figures 3 and 4 show the water levels in pipes from an arm of the swamp where the effects of collapse were negligible and in the eastern half of the swamp where the effects of collapse were severe respectively, over a period of 23 months. At Pipe 1 and Pipe 3 the water level

## WINGECARRIBEE PEAT

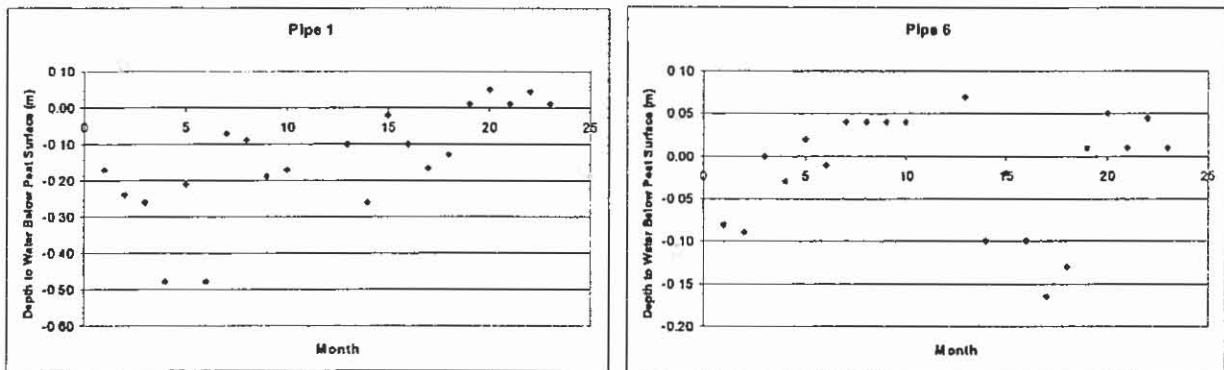


Figure 3. Depth of water table below the peat surface for two pipes in Transect 1, located in an arm where there no effects of the collapse. (Pipe 1 is located on the edge of the peat and is emplaced in the soil substrate; Pipe 6 is located in the centre of the arm where the peat is approximately 5 m thick. Month 1 is January 2005)

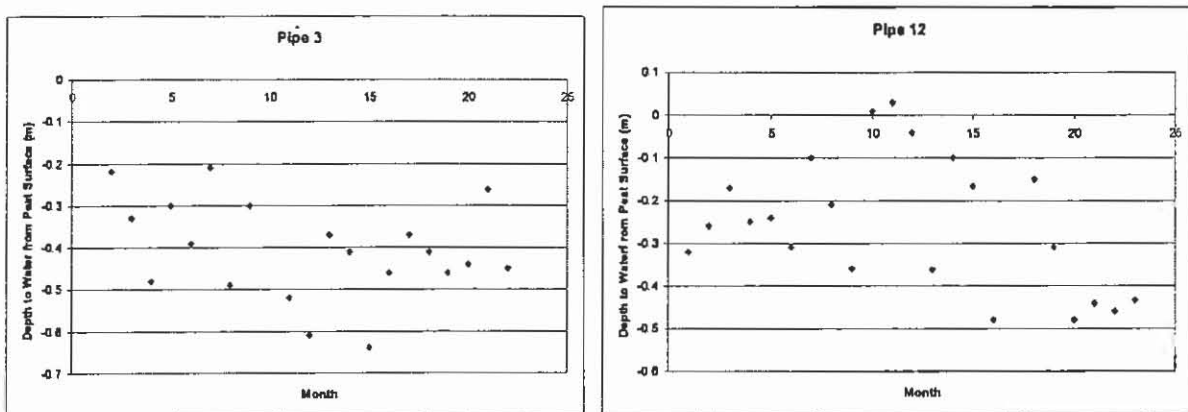


Figure 4. Depth of water table below the peat surface for two pipes in Transect 3 which is located in the eastern part of the swamp where effects of the collapse were severe. (Pipe 3 is located on the southern side of the swamp and Pipe 12 is located on the northern side of the swamp. Month 1 is January 2005))

fluctuates more than in the other two pipes. More importantly, Pipes 6 and 12 show the water table above the surface after periods of heavy rain. These data are typical for the unaltered arm and the northern side of the swamp (similar data was obtained for the other two transects)

The data suggest that on the northern side of the swamp and in the two unaltered arms, the water table recovers, especially after heavy rainfall. Thus although there is likely to be annual lowering of the water table in these sections of the swamp, the water budget is sufficient to maintain high water tables for the longer term. It is suspected that surface inflow of water from the northern side of the swamp is greater than the surface inflow on the southern side. The prognosis for the peat in these areas is good. This is in spite of the Southern Highlands, as with most parts of New South Wales, having the 'worst drought in history'.

On the other hand, on the southern side of the swamp the water table is probably well below the average levels prior to the collapse. In addition, it is likely that although the water levels do rise significantly after heavy rainfall, the higher water table is only temporary and soon drops. The prognosis for the peat on the southern side, and in some parts of the northern side

where the effects of mining caused as much disruption to the peat as on the southern side, is poor and there may be, in the long term, substantial loss of peat as it dries out and decays.

One additional point that is encouraging for the viability of the swamp is the change in the nature of the creek that was eroded through the swamp during the collapse. The areas of the swamp that were covered by the mine pond prior to the collapse and central axial part of the swamp adjacent to the erosional channel have been exposed to the clay basement. When data were first collected, in 2000, the erosional channel was a typical 'creek' with a significant flow of water over a sandy to clayey bed and with relatively well defined banks on either side of the channel. Most of the water flow was concentrated through the exposed channel.

However, over the past two to three years, herbaceous vegetation has started to grow in the 'creek' channel and more recently has encroached across the channel. As a consequence, no longer is there a well defined stream channel and the water level in the former channel has risen to well above the heights when there was a well defined channel. Now the water flows through the vegetation which has hindered the flow, causing the rise in the water levels, and also causing the water to flow across/through areas adjacent to the former channel. The effect has been to cause a rise in the water table in the former channel area.

Based on these recent observations, the prognosis for the swamp is also positive. It is postulated that unless there is a major catastrophic event to remove the vegetation in the former erosional channel, vegetation will continue to grow and build up resulting in further rises in the water table in this part of the swamp.

### **INFLUENCE OF RAINFALL**

Wingecarribee Swamp is at 670 m above sea level and is at the headwaters of the Wingecarribee River system, which covers an area of 40 km<sup>2</sup> and is part of the Warragamba Catchment, the main water supply for Sydney. Prior to this study it was hypothesised that the swamp water budget was from surface water from rainfall that fell on the swamp and water entering mostly through the main feeder creek Caalang Creek, the surrounding hills, and groundwater primarily from springs at the junction of the Hawkesbury Sandstone and the Robertson Basalt (Hope and Southern 1984; Fiander 1993). Caalang Creek, adds approximately 5.3 mega-litres per day of water from the upper catchment to the swamp.

The dramatic rise in the water levels after heavy rain and the relatively sudden drop shortly after the rain ceases, suggests that little water enters the swamp from either deep springs below the swamp. Rainfall appears to be the main water supplier.

An examination of the rainfall and evaporation data for Wingecarribee Reservoir wall are pertinent (Figure 5). The data show that during the winter months of the year, the rainfall is in excess of the evaporation but during the hotter summer months, evaporation is higher than rainfall. For the period shown in the graphs, evaporation was approximately 1950 mm and the rainfall 1400 mm resulting in excess evaporation. This should suggest that the swamp should have a negative water budget and a declining water table. However, we suspect that the living and dead herbaceous cover across the swamp restricts evaporation with evaporation probably being less over the swamp than is instrumentally recorded at the reservoir wall. Another important factor is the winter excess rainfall is probably more than sufficient to allow a high water table, necessary for peat viability, to be re-established each year.

## WINGECARRIBEE PEAT

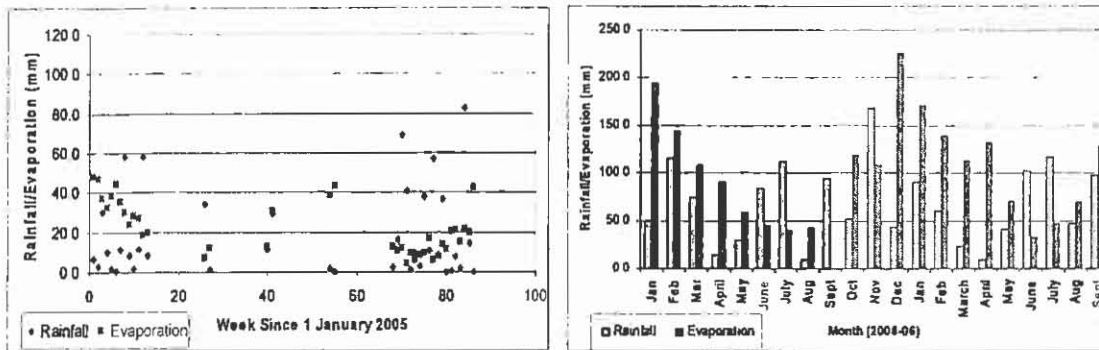


Figure 5. Weekly and monthly rainfall and evaporation at the Wingecarribee Reservoir wall.

### CONCLUSIONS

The Wingecarribee peat deposit has been derived mostly from herbaceous plants with no evidence of a forest stage and subsequent incorporation of large amounts of woody material into the peat. Monitoring of the water levels in four transects across the swamp, located in both unaltered and severely altered parts of the swamp, post the 1998 collapse, show that the water table is closely related to the rainfall with the table rising significantly after heavy rain. The erosional channel is being revegetated with herbaceous plants and this has caused the water table in this part of the swamp to rise and for the higher water levels to spread laterally into areas previously without a water table above the clay substrate. Unless a catastrophic event removes the vegetation, this build of initially living but later decaying plant matter will continue, with a positive prognosis for the viability of the peat.

One important factor in the evolution and the revival of the peat is the evaporation to rainfall budget.

### ACKNOWLEDGEMENTS

We greatly acknowledge the cooperation of personal at Sydney Water Catchment offices in allowing this study to be undertaken and especially the Burrawang office for supplying rainfall and evaporation data. Travel for this project was partly funded by the GeoQuest research group, University of Wollongong.

### REFERENCES

- AUSTRALIAN WATER TECHNOLOGIES. 1998. *Draft Literature Review for the Wingecarribee Swamp, with particular reference to the recent peat swamp collapse*. Sydney Water Corporation. AWT, Sydney.
- CLYMO G. C. 1983. Peat. In: *Ecosystems of the World 4A: Mires: Swamp, Bog, Fen and Moor – General Studies*. (Gore, A.J.P. ed. Elsevier Scientific Publishing Company, Amsterdam.
- DEPARTMENT OF MINERAL RESOURCES. 1995. *Peat*. Minfact Information Sheet 215, June 1995.
- FIANDER H. J. 1993. *Brief Study of the Drainage Behaviour of Wingecarribee Swamp*. Toby Fiander and Associates, Castle Hill.
- HALES, B. 2001. *Physical and Geochemical Environments of the Wingecarribee Swamp, NSW*. Unpublished Honours thesis, University of Wollongong.
- HOPE, G. AND SOUTHERN, W. 1984. *Organic Deposits of the Southern Tablelands Region, New South Wales*. Unpublished report of the National Parks and Wildlife Service, NSW.

- KODELA P.G. 1998. *Wingecarribee Swamp and Reservoir wetland complex: preliminary re-assessment of its heritage values and the Ramsar criteria after the August 1998 environmental damage, including concepts for rehabilitation and management*. Royal Botanic Gardens, Sydney.
- LOWE J.J & WALKER, M. J. C. 1997. *Reconstructing Quaternary Environments*. Addison Wesley Longman, Essex.
- SMITH, E.A., 2000. *An Evolutionary History of Wingecarribee Swamp, NSW, and Ensuing Management Implications*. Unpublished Honours thesis, University of Wollongong.

# GEOPHYSICAL LOG ANALYSIS FOR THE SOUTHERN SYDNEY BASIN

Peter Hatherly<sup>1</sup>, Scott Thomson<sup>2</sup> and Michael Armstrong<sup>3</sup>

<sup>1</sup>School of Geosciences  
University of Sydney

<sup>2</sup>CoalBed Concepts  
205 Dobell Dr, Wangi Wangi

<sup>3</sup>BHP Billiton Illawarra Coal  
PO Box 514 Unanderra, NSW 2526

## ABSTRACT

This paper describes a method for quantitatively interpreting geophysical logs, a feature of which is the ability to cross-check on the validity of the derived values of porosity and shaliness. The method has been used to interpret geophysical logs from exploration boreholes drilled in the Appin area by BHP Billiton Illawarra Coal. Results from three of these holes are discussed to demonstrate the method and the geological interpretations that can be made. The Hawkesbury Sandstone is revealed as a quartz rich sandstone while the constituents of the clastic rocks of the Narrabeen Group and the Illawarra Coal Measures contain greater proportions of lithic and volcanic fragments. Discrimination between the Narrabeen Group and Illawarra Coal Measures is also possible. Individual units can be investigated by studying composition and lateral variability. The existence of a strong horizontal stress field in the Narrabeen Group and Illawarra Coal Measures is also evident.

## INTRODUCTION

For many years, BHP Billiton Illawarra Coal have acquired geophysical logs from exploration boreholes drilled to support their mining operations in the Southern Coalfield. Holes are typically drilled to the Tongarra Coal, approximately 100 m below the Bulli seam which is mined in the Appin, West Cliff and Douglas Collieries. The logs typically acquired are natural gamma, density, caliper, sonic, neutron, resistivity and verticality. More recently, acoustic scanner and full waveform sonic logs in the form of a single channel cement bond log have also been obtained. These logs have been acquired by just the one logging contractor, Precision Energy Services (formerly Reeves Wireline).

As with most geophysical logging, exploration staff use the logs to validate formation and unit depths, thickness, internal fabric and intersections with major units. Some of the logs, principally the acoustic logs – sonic, full waveform sonic and acoustic scanner are also used for geotechnical evaluations (MacGregor, 2004). UCS is estimated from the sonic logs and acoustic scanner logs are used to map stress related breakout and to map fractures.

Direct comparison of UCS values determined from laboratory tests with estimates from sonic logs indicated a variation of  $\pm 20\%$  in strength.

In two recent ACARP funded projects, Hatherly et al (2001, 2004) investigated more quantitative means of making geotechnical assessments using interpretation methods developed by the petroleum industry. In Hatherly et al (2001), the approach was to quantify

the composition of clastic rocks in terms of quartz, clay and porosity and to then estimate UCS. This provided only a marginal improvement in UCS estimation. In Hatherly et al (2004), an alternative approach was adopted. Rather than attempting to directly estimate rock strength, the approach was to derive a geophysical rock mass rating scheme. While this work is the subject of on-going research, the overall interpretation scheme can already be used for geological interpretations. This application is demonstrated in this paper.

### AN APPROACH TO QUANTITATIVE GEOPHYSICAL LOG INTERPRETATION

The approach to geophysical log interpretation described by Hatherly et al (2004) involves:

1. A check on the quality of the logs to ensure that the raw log values are reasonable and that there are no depth errors. Sections within the hole where there is significant caving need to be identified, as do sections where casing is still present.
2. Calculation of the porosity from the density log by equation 1. If the porosities are unreasonable (i.e. less than zero or unrealistically high), the calculation should be repeated with a different value for the matrix density.
3. Determination from the natural gamma log of typical values (end points) for a clean sandstone and a shale followed by calculation of shaliness using equation 2.
4. Calculation of velocity using equation 3 and an assumed gradient for the effective pressure. The calculated velocity should then be compared with the observed velocity. If the match between the measured and observed velocities is unacceptable, the process needs to be repeated with different values of porosity, shaliness and pressure (steps 2 to 4).
5. Independent checking of the shaliness using the neutron log (equation 4) and calculation of velocity (equation 3).

$$\phi_D = \frac{\rho_{ma} - \rho}{\rho_{ma} - \rho_f} \quad \text{equation 1}$$

$$V_{shale} = \frac{\gamma - \gamma_{sandstone}}{\gamma_{shale} - \gamma_{sandstone}} \quad \text{equation 2}$$

$$v = 5.77 - 6.94\phi - 1.73\sqrt{V_{shale}} + 0.446(\sigma - e^{-16.7\sigma}) \quad \text{equation 3}$$

$$V_{shale} = \frac{\phi_N - \phi_D}{\phi_{NSh} - \phi_{DSH}} \quad \text{equation 4}$$

In these equations:

$\rho$  = measured density (t/m<sup>3</sup>)

$\rho_{ma}$  = density of the rock fraction (matrix density).

$\rho_f$  = density of the pore fluid (1 in the case of pure water).

$\phi$  = porosity

$\phi_D$  = porosity derived from density log

$V_{shale}$  = volume of 'shale' = clay and other fine grained components, not the grains.

$\gamma$  = gamma log response (measured in API)

$\sigma$  = effective pressure (measured in kilobars) = confining pressure minus pore pressure.

$v$  = P-wave velocity (measured in km/s)

$\phi_N$  = porosity from a calibrated neutron log

$\phi_{DSH}$  = porosity of pure shale determined from the density log

## GEOPHYSICAL LOG ANALYSIS

$\phi_{Nsh}$  = 'porosity' of pure shale determined from the neutron log.

The basis of equations 1, 2 and 4 is described in standard logging texts (for example Hearst et al, 2000; Rider, 2000; and Asquith and Krygowski, 2004). Equation 3 is from Eberhart-Phillips et al (1989) and was empirically derived through laboratory testing.

Successful geophysical log interpretation using this approach requires the selection of appropriate values for the constants in equations 1, 2 and 4. The matrix density in equation 1 requires careful consideration and need not be 2.65 as would be the case for a pure quartz sand. The natural gamma and neutron porosity values needed for clean sands and pure shales are referred to as "end points". The choice of these may vary according to the types of sands and clays present. Once the log interpretation yields shale determinations that are consistent and there is agreement between the calculated and observed velocities, the interpretation can be considered to be robust. Constructing cross-plots between the different logs to derive these parameters can assist with the determination of end points.

Non-clastic lithologies can also be identified. Coals are evident on the basis of their low densities, carbonates will have high densities and tuffs may have unusually high natural gamma readings. The presence of non-potassic clay minerals such as kaolinite which have low gamma counts can also be indicated by comparison of the gamma based and neutron based shale values. Another relevant aspect of the log interpretation concerns the provision of a qualitative indication of the presence of gas bearing sandstones. Such sandstones are typified by porosity determinations from the density log (equation 1) that are significantly higher than those for the neutron log. In such circumstances, a porosity cross-over is said to have occurred. In Armstrong et al (2006) there is a discussion of this aspect of geophysical log interpretation in the Southern Coalfield.

### GEOLOGY OF THE APPIN AREA

The general geology of the Southern Coalfield is described by Armstrong et al (1995) and Moffitt (2000). Table 1 details the relevant portion of the geological section as described by Moffitt (2000), together with typical unit thicknesses from Myer (2006). Fielding et al (2001) describe a unified depositional history for the entire Bowen-Gunnedah-Sydney Basins. Deposition for the section from the Tongarra Coal through to the Wianamatta Group and their equivalents, occurred from about 260 to 230 million years ago when the basins were undergoing foreland loading associated with thrusting from New England Fold Belt (Fielding et al, 2001). Following Fielding et al (2001), the relevant aspects of the depositional history through this section of the Southern Sydney Basin are as follows:

1. The Late Permian Tongarra Coal is from a late phase of a depositional cycle that began with a flooding event represented by the deposition of the Erins Vale Formation.
2. This was followed by another flooding cycle that commenced with the Bargo Claystone. General basin-wide NS alluvial drainage was established and lithic sediments derived from the rising New England Fold Belt formed the dominant sediment source. During this cycle, the overlying coal seams formed. Basin wide tuffs were also deposited.
3. For the Triassic Narrabeen Group, the New England Fold Belt remained the primary sediment source, but the absence of coal and increase in colouration is attributed to the end of Permian extinction event that occurred sometime after the formation of the

Bulli Coal. Herbert (1997) suggests that there was a south easterly marine connection for the Southern Sydney Basin and that the westward lensing out of the various claystone units can be interpreted in terms of a general 2<sup>nd</sup> order rise in sea level that continued over a 6 million year period through to the deposition of the Hawkesbury Sandstone. Superimposed on this are four minor 3<sup>rd</sup> order fluctuations in sea level, each of approximately 1.5 million year duration.

4. For the overlying Hawkesbury Sandstone, the source of sediments was quartzitic material from the Lachlan Fold Belt to the west.
5. The uppermost part of the geological section is the Wianamatta Group and for this, the sediment source returned to the New England Fold Belt with an associated accumulation of lithic and volcanic material.

Group	Formation	Thickness
Wianamatta Group	Ashfield Shale	
	Hawkesbury Sandstone	184 m
Narrabeen Group	Newport Formation	13 m
	Garie Member	3 m
	Bald Hill Claystone	28 m
	Bulgo Sandstone	141 m
	Stanwell Park Claystone	7 m
	Scarborough Sandstone	58 m
	Wombarra Claystone	49 m
	Coal Cliff Sandstone	22 m
	Illawarra Coal Measures	Bulli Coal
Loddon Sandstone		7 m
Balgownie Coal		1 m
Lawrence Sandstone		8 m
Eckersley Formation		20 m
Wongawilli Coal		10 m
Kembla Sandstone		8 m
Allans Creek Formation		20 m
Darke Forest Sandstone		9 m
Bargo Claystone		14 m
Tongarra Coal		2 m

Table 1. Typical section and thicknesses for the Appin area (adapted from Moffitt, 2000; and Myer, 2006).

From the point of view of the geophysical logs, the matrix densities and the shale and sand end-points for the various geological units can be expected to vary according to the depositional environment and the source of the sediments.

### GEOPHYSICAL LOG INTERPRETATION FOR THE APPIN AREA

Geophysical logs from 70 boreholes have been studied with most efforts concentrated on the lower parts of the Narrabeen Group overlying the Bulli Coal. However, the full sections of some boreholes have also been investigated. Results from three of these holes - S1488, S1733 and S1768 are discussed in this paper. These holes are at the locations shown in Figure 1. The geophysical logging occurred in July 2003, August 2005 and February 2006 respectively.

## GEOPHYSICAL LOG ANALYSIS

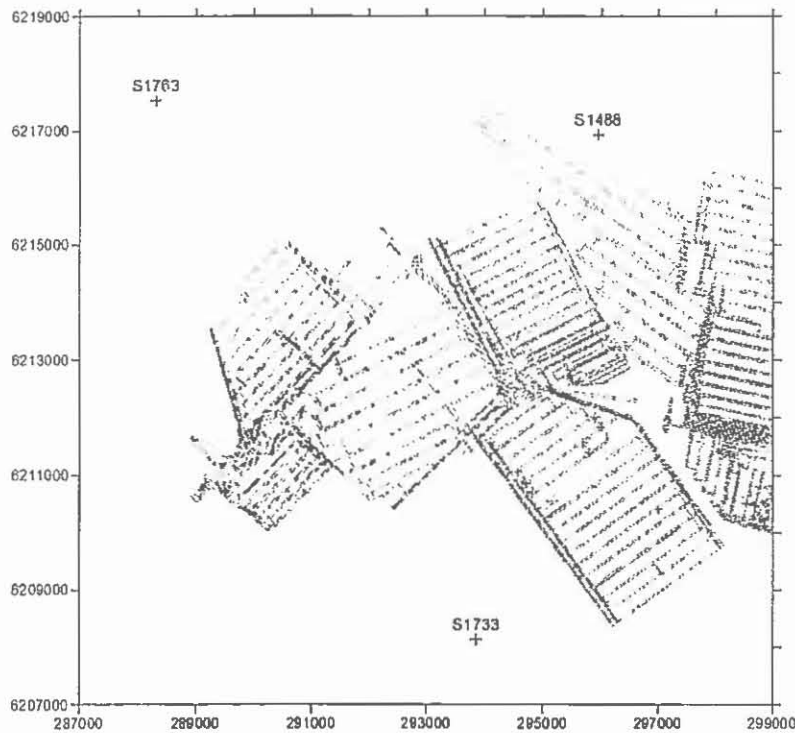


Figure 1. Mine workings in the Appin area and the locations of boreholes S1733, S1748 and S1763.

To illustrate the interpretation procedure, results from borehole S1488 are shown in Figure 2 and 3. Table 2 lists the end-points and other parameters required in these calculations and for Figure 2, the values used were those listed for the Narrabeen Group in this hole. In Figure 2a, calculated shale values based on equations 2 and 4 are compared. In the Illawarra Coal Measures, there is an obvious discrepancy between the two sets of values. Comparison of the observed and calculated velocities based on the two different sets of shale values in Figures 2b and 2c also shows a discrepancy and suggests that the correct shale values are those calculated from the neutron and density porosity logs (equation 4). Results for the Hawkesbury Sandstone are not shown but these similarly exhibit discrepancies between the calculated shale values and also between the calculated and observed velocities.

	Hawkesbury Sandstone			Narrabeen Group			Illawarra Coal Measures		
	S1488	S1763	S1733	S1488	S1763	S1733	S1488	S1763	S1733
matrix density (t/m <sup>3</sup> )	2.65	2.65	2.65	2.72	2.70	2.72	2.70	2.70	2.75
gamma sand (API)	10	10	10	35	35	35	35	35	35
gamma shale (API)	200	200	200	180	180	180	280	250	250
shale neutron porosity (fraction)	0.2	0.11	0.12	0.28	0.22	0.2	0.28	0.22	0.2
effective pressure (MPa/km)	15	15	15	25	25	25	25	25	25

Table 2. End-points and other parameters used for the geophysical log interpretation.

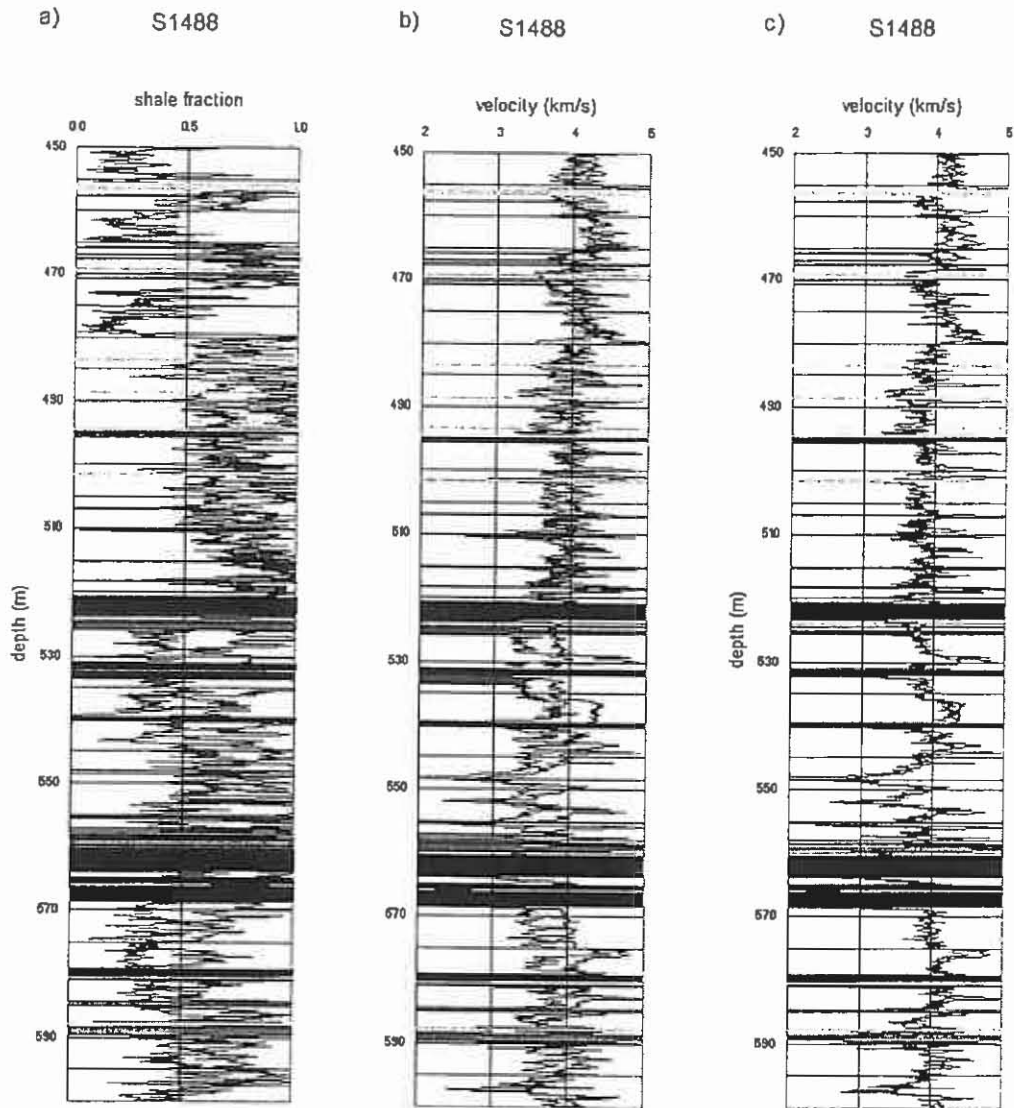


Figure 2. Initial geophysical log analysis for a part of borehole S1488. The end-points and other parameters used for the calculations are those given for the Narrabeen Group in Table 1. The Illawarra Coal Measures start at 522 m. Representation of coloured bars: black = coal, dark blue = dense zones with density greater than chosen matrix density, green = zones with gamma values greater than 1.25 gamma shale (= tuff?), sky blue = zones where holes have caved, red = zones where free gas is inferred to be present.

- a) In blue are the shale values calculated from the natural gamma log. In mauve are the shale values calculated from the neutron porosity and density porosity logs.
- b) In blue is the observed sonic log. In mauve is the sonic log calculated from the density porosity and shale from the natural gamma.
- c) In blue is the observed sonic log. In mauve is the sonic log calculated from the density porosity and the shale calculated from the neutron/density porosity logs.

# GEOPHYSICAL LOG ANALYSIS

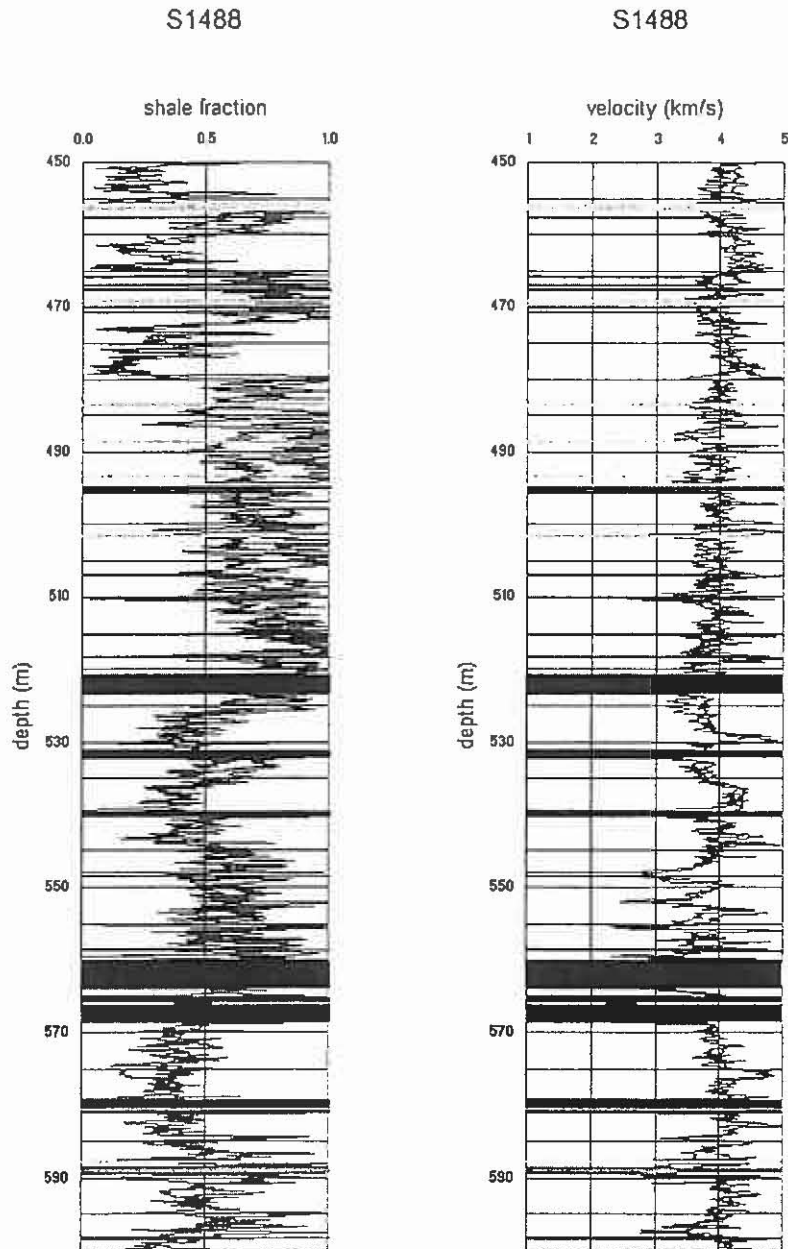


Figure 3. *Left.* Shale contents from the natural gamma log (blue) and the neutron/density porosity combinations (mauve). Below the Bulli Coal, the end-points and other parameters used for the geophysical log interpretation were revised to those values listed for the Illawarra Coal Measures in Table 2. The calculated shale values below the Bulli Coal are now in agreement. *Right.* Observed velocities, in blue and in mauve, those calculated using the revised gamma shale and density porosity values. The calculated and observed velocities are now in close agreement over this section of the hole. This part of the log interpretation can therefore be judged to be robust.

The end points and other parameters were therefore adjusted in the manner described above until agreement was reached between the shale values and between the observed and calculated velocities. Figure 3 shows the final results for the section of hole shown in Figure 2. The end-points and other parameters are listed in Table 2. Because there is general agreement for the shale and velocity criteria, the log interpretation is judged to be robust.

Figures 4 and 5 show final results for basal 200 m sections of the three holes using the parameters listed in Table 2. The shale comparisons are not shown. However, the fact that there is agreement between the observed and calculated velocities which are shown in Figure 4 and are based on the gamma shale determinations (equation 2) indicates that the values of the shaliness that were used are appropriate.

In Figure 5, the calculated values for density porosity and shaliness (gamma shale) are shown in fractional form. In this format, correlation between the various formations can be considered. Note the consistency in the character of the various units below the Bulli Coal. On the other hand, there is much more variability above the Bulli Coal. The Coal Cliff Sandstone is not present as an identifiable unit and there is considerable variability in the Wombarra Claystone and, to a lesser extent, within the Scarborough Sandstone. Note also the suggestions of strata gas that are shown by the red bars in parts of the Scarborough Sandstone, but not elsewhere.

The influence of the effective pressure is not illustrated by these figures. Its impact is to introduce base-line shifts to the overall calculated velocity. If the effective pressure was only due to lithostatic loading, it would have a value of approximately 15 MPa per km depth of burial. The values used here are higher than this except in the Hawkesbury Sandstone. These values are necessary to achieve the general agreement between the calculated and observed velocities.

## DISCUSSION

Given that the log interpretation process has provided values of porosity and shaliness that are consistent with the geophysical logs, there are numerous observations that can be made concerning the results shown in Figure 5 and the values of the end-points required to achieve consistent interpretations.

### *Illawarra Coal Measures*

The named formation members are readily identified on the basis of changes in the shaliness. Some, e.g. the Bargo Claystone and the Allans Creek Formation are also associated with lower sonic velocities. Porosities throughout this part of the Illawarra Coal Measures remain reasonably constant (about 10%). The consistency in the overall character of the log interpretations suggests that over the area covered by these holes, the depositional conditions have remained laterally constant. The high values required for the gamma shale end points suggest that the rock grains are more lithic/volcanic, and possibly tuffaceous. This suggestion is also supported by the fact that slightly higher matrix densities are required compared to the Narrabeen Group.

While effective pressure is used in equation 3 rather than true deviatoric stress, it is evidently adequate for current purposes. The requirement for a higher value in the Illawarra Coal Measures (and Narrabeen Group) is likely to be due to the high horizontal stresses present in

## GEOPHYSICAL LOG ANALYSIS

this area which have been recorded to be in excess of three times the vertical at coal seam depths (Hebblewhite et al, 2000).

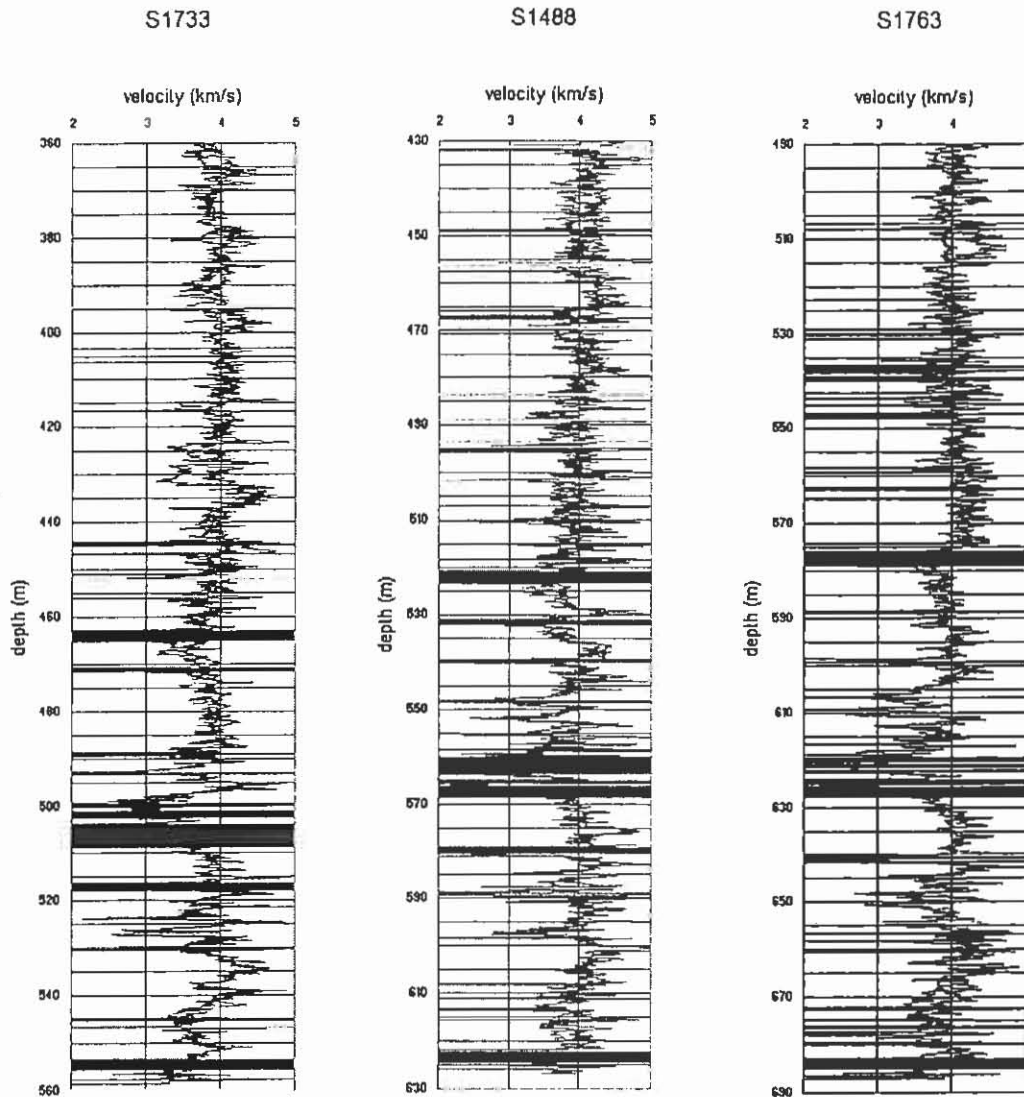


Figure 4. Observed (blue) and calculated velocities (mauve) using the gamma shale determinations for the three boreholes. A 200 m section from the Scarborough Sandstone (Narrabeen Group) through to the Illawarra Coal Measures as far as the base of the holes below the Tongarra Coal are shown. The end-points and other parameters used for the geophysical log interpretation are those listed in Table 2. There is generally good agreement between the observed and calculated velocities. The log interpretations for these three holes can therefore be judged to be robust.

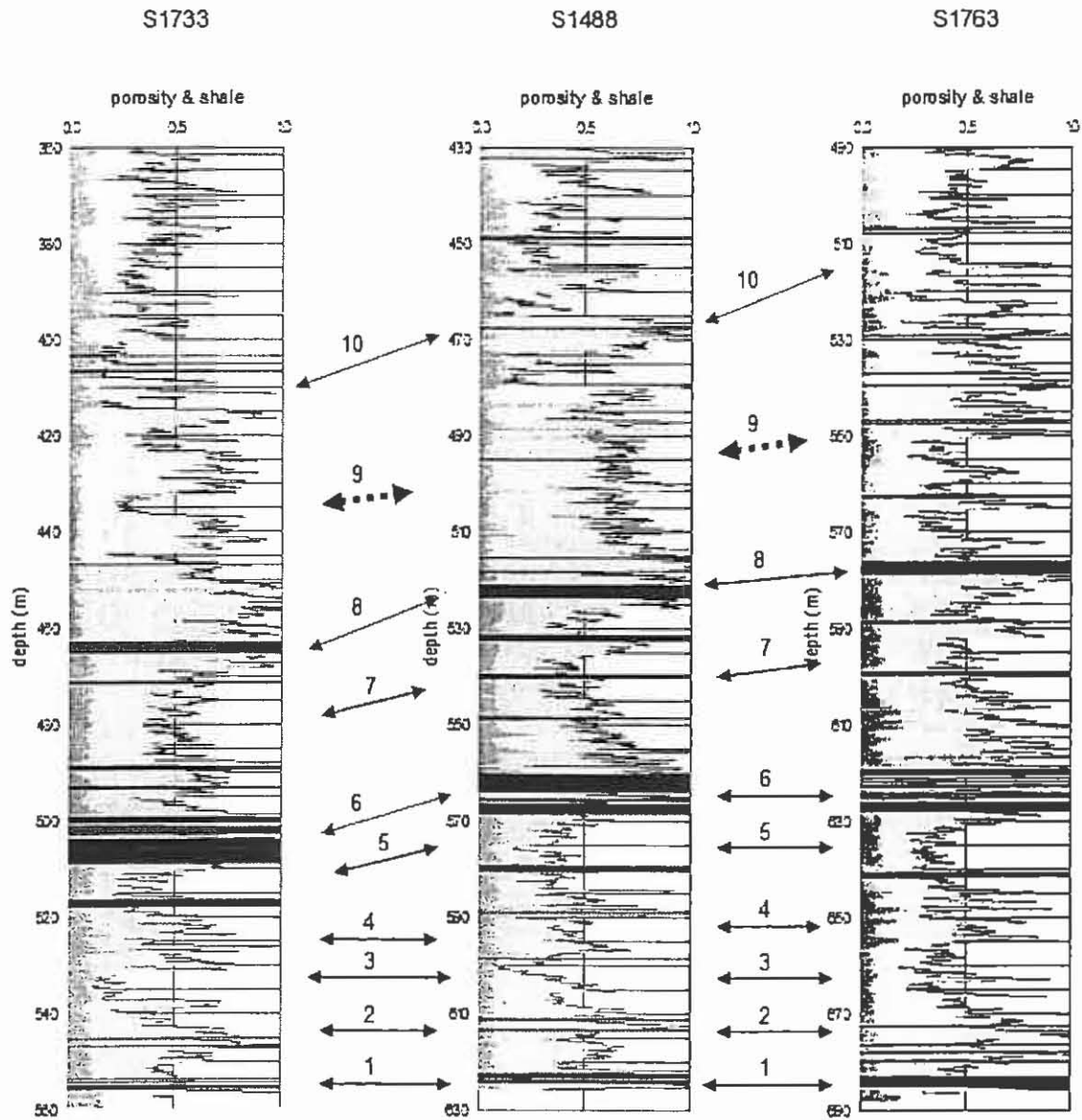


Figure 5. Fractional density derived porosity (blue) and gamma derived shale values (tan) for the three holes. 1 = Tongarra Coal; 2 = Bargo Claystone; 3 = Darkes Forest Sandstone; 4 = Allans Creek Formation; 5 = Kembla Sandstone; 6 = Wongawilli Coal; 7 = Lawrence Sandstone; 8 = Bulli Coal; 9 = Wombarra Claystone; 10 = Scarborough Sandstone.

*Narrabeen Group*

The values shown for the Narrabeen Group in Table 2 are valid through to the Bulgo Sandstone. Within the Wombarra Claystone and Scarborough Sandstone section shown in Figure 5, porosities are lower than in the Illawarra Coal Measures. There is also considerable variability in the shaliness of the Wombarra Claystone, both laterally and vertically. The patterns are supportive of Herbert's (1997) suggestion of a marine connection and the use of the principles of sequence stratigraphy to interpret the depositional environment. Subtle changes in the source of the sediments and/or the impact of the end of Permian extinction event may also be indicated by the need for a reduced matrix density and gamma shale value and the more variable porosity.

## GEOPHYSICAL LOG ANALYSIS

Results for the overlying Bald Hill Claystone are not shown. However this unit which is rich in kaolinite and haematite (Loughnan, 1970) is easily identified as a region where the log analysis procedure fails. Gamma signatures are very low and densities are high.

### *Hawkesbury Sandstone*

While results for this unit have not been given, it is typified by sandstones with high porosities and low shale values with only the occasional shale bands. The low matrix density ( $2.65 \text{ t/m}^3$ ) and low gamma sand values (10 API) are consistent with this sandstone being quartz rich with grains derived from the Lachlan Fold Belt. Of the units assessed by the procedure described in this paper, the Hawkesbury Sandstone is the least confidently characterised. The neutron porosity logs in particular, do not show the same behaviour as the deeper formations. Another observation is that the value for the effective pressure required to bring the calculated and observed velocities into general agreement is the value for lithostatic loading only. This suggests that in the Hawkesbury Sandstone, the horizontal stresses are not as great as in the underlying strata.

### *Calibration issues*

As noted above, while these three holes were logged by the same contractor, the logging occurred at different times. Questions therefore arise as to whether the geophysical tools were performing to the same specifications on each occasion. While the log interpretation procedure described in this paper allows for variations in tool performance by virtue of the need to determine end points and other variables, it would be preferable if the performance of the tools could be assured through a combination of calibration tests against known standards and the logging of 'check' holes designed to allow repeat logging over time.

Another operational issue concerns the choice of logging intervals. All of the logs analysed in this paper were acquired at centimeter (cm) intervals but for the interpretations, the logs were resampled to 10 cm intervals. While there may be an argument for obtaining closely sampled logs for coal seam analysis and for geotechnical purposes, geological assessments of the type undertaken here do not require such detailed logging.

## CONCLUSIONS

The method for geophysical log interpretation of clastic rocks described in this paper is based on cross-checking shale determinations and implied velocities using the derived values of porosity, shaliness and an assumed effective pressure. Through such checking, greater confidence can be placed on the values of porosity and shaliness. Further geological information can also be obtained from the end-points and constants derived for the calculations.

In the Appin area in the Southern Sydney Basin, the major units of the Illawarra Coal Measures can be easily identified on the interpreted geophysical logs. Similar depositional conditions appear to have existed across this area at any one time. In the Narrabeen Group, regional correlation of individual units within the Wombarra Claystone is not possible. Depositional conditions were therefore varied laterally. Different end-points and constants are also required for the Illawarra Coal Measures, the Narrabeen Group and the Hawkesbury Sandstone. The highest matrix densities and gamma shale values are required for the Illawarra Coal Measures. This implies a different provenance for these strata to that for the Hawkesbury Sandstone. Below the Hawkesbury Sandstone, the effective stress is also higher than that due to lithostatic loading alone. This is presumed to be due to high horizontal stresses.

**ACKNOWLEDGEMENTS**

Financial support from the Australian Coal Association Research Program has allowed development of the geophysical log interpretation techniques. Greg Poole of BHP Billiton Illawarra Coal was instrumental in setting up this study and providing the high quality geophysical logs that have been used. The paper is published with the permission of BHP Billiton Illawarra Coal.

**REFERENCES**

- ARMSTRONG, M., BAMBERRY, W.J., HUTTON, A.C. AND JONES, B.G., 1995. Sydney Basin - Southern Coalfield. In Ward, C.R., Harrington, H.J., Mallett, C.W., and Beeston, J.W. (Editors): Geology of Australian coal basins. *Geological Society of Australia Coal Geology Group Special Publication*, 1, 213-230.
- ARMSTRONG, M., HATHERLY, P. AND THOMSON, S., 2006. Determining the controls for strata gas and oil distribution within sandstone reservoirs overlying the Bulli seam. *Proceedings Coal2006*, Wollongong, NSW.
- ASQUITH, G. AND KRYGOWSKI, D., 2004. Basic well log analysis (2<sup>nd</sup> edition), AAPG Methods in Exploration Series 16, AAPG, Tulsa.
- EBERHART-PHILLIPS, E., HAN, D.H. AND ZOBACK, M.D., 1989. empirical relationships among seismic velocity, effective pressure, porosity & clay content in sandstone. *Geophysics*, 54, 82-89.
- FIELDING, C.R., SLIWA, R., HOLCOMBE, R.J. AND JONES, A., 2001. A new palaeogeographic synthesis for the Bowen, Gunnedah and Sydney Basins of eastern Australia. *PESA Eastern Australian Basins Symposium*, 269-278.
- HATHERLY, P., MEDHURST, T., ZHOU, B. AND HUA, G., 2001. Geotechnical evaluation for mining – assessing rock mass conditions using geophysical logging. Final report – ACARP Project C8022b.
- HATHERLY, P., SLIWA, R., TURNER, R. AND MEDHURST, T., 2004. Quantitative geophysical log interpretation for rock mass characterisation. Final report – ACARP Project C11037.
- HEARST, J.R., NELSON, P.H. AND PAILLETT, F.L., 2000. Well logging for physical properties. John Wiley and Sons, 2<sup>nd</sup> edition.
- HEBBLEWHITE, B., WADDINGTON, A. AND WOOD, J., 2000. Regional horizontal surface displacements due to mining beneath severe surface topography. 19<sup>th</sup> International Ground Control in Mining Conference, Morgantown, USA. August, 2000.
- HERBERT, C., 1997. Sequence stratigraphic analysis of Early and Middle Triassic alluvial and estuarine facies in the Sydney Basin, Australia. *Australian Journal of Earth Sciences*, 44, 125-143.
- LOUGHNAN, F.C., 1970. Flint clay in the coal-barren Triassic of the Sydney Basin, Australia. *Journal of Sedimentary Petrology*, 40, 822-828.
- MACGREGOR, S., 2004. Maximising in-situ stress measurement data from borehole breakout using acoustic scanner and wireline tools. Final report – ACARP Project C1009.
- MOFFITT, R.S., 2000. A compilation of the geology of the Southern Coalfield: notes to accompany the 1:100 000 Southern Coalfield geological map. Geological Survey of NSW, Report No. GS1998/277.
- MYER, T., 2006. Surface goaf hole drainage trials at Illawarra Coal. *Proceedings Coal2006*, Wollongong, NSW.
- RIDER, M., 2000. The geological interpretation of well logs, Whittles Publishing, 200 p.

# MORPHOLOGICAL AND STRATIGRAPHIC EVOLUTION OF WANDANDIAN CREEK DELTA, ST GEORGES BASIN, NEW SOUTH WALES

Carl A Hopley and Brian G Jones

School of Earth and Environmental Sciences  
University of Wollongong  
Wollongong NSW 2522

## ABSTRACT

Wandandian Creek delta in southern New South Wales shows a history from subaerial exposure during the last glacial maximum to an array of prograding Holocene deltaic facies. Subaerial exposure during the last glacial maximum promoted development of leached and mottled Pleistocene strata and palaeosols. The incised palaeo-creek was partially filled with poorly sorted fluvial sand. The post-glacial marine transgression impounded the western portion of St Georges Basin flooding the palaeo-valley and prodelta lagoonal mud was deposited from approximately 7 ka. Progradation of the delta into the study area commenced approximately 3.5 ka to 4 ka ago and is marked by an upward-coarsening prograded deposit of sandy silt and sand. Continued sedimentation, in conjunction with channel avulsion and meandering, formed vertically accreted mouth bars, levees and floodplains adjacent to the distributary channels.

## INTRODUCTION

This paper presents the findings of a comprehensive stratigraphic and morphological study of Wandandian Creek delta's evolution throughout the Holocene. The delta evolution was reconstructed based on interpretation of spatially selected sub-surface vibracores and drill holes, that resulted in the identification of several facies ranging from Pleistocene channel-fill fluvial sand to modern subaerially exposed levee deposits. Amino acid racemisation (AAR), lead 210 ( $^{210}\text{Pb}$ ), accelerated mass spectrometry (AMS) and conventional radiocarbon ( $^{14}\text{C}$ ) dating techniques were used to establish the geochronology of the delta.

## REGIONAL SETTING

The Wandandian Creek delta is located approximately 200 km south of Sydney and is actively prograding into western St Georges Basin (Fig 1). Outcrops of the Snapper Point Formation and the Wandrawandian Siltstone occur on the southwestern and northwestern shores of the delta respectively. Due to the long sinuous entrance channel, tidal variation within St Georges Basin is restricted to 0.04 m in the central basin (Webb *et al.* 1996). Picnic Point, the easternmost boundary of the delta shelters it from wind-wave reworking for much of the year. The headwaters of Wandandian Creek on the Tianjara Range are located approximately 25 km west of St Georges Basin (Windley 1986). Climate is generally warm with maximum rainfall occurring from late summer through to autumn (Bradshaw 1987). The average rainfall for the area is 1300 mm/year with an annual runoff estimated at 400 mm (Webb *et al.* 1993). Since 1952 a total of four major flood events and nine minor flood events occurred within the St Georges Basin catchment area (Webb *et al.* 2001). The majority of the soils within the catchment area are readily eroded (Webb *et al.* 1993).

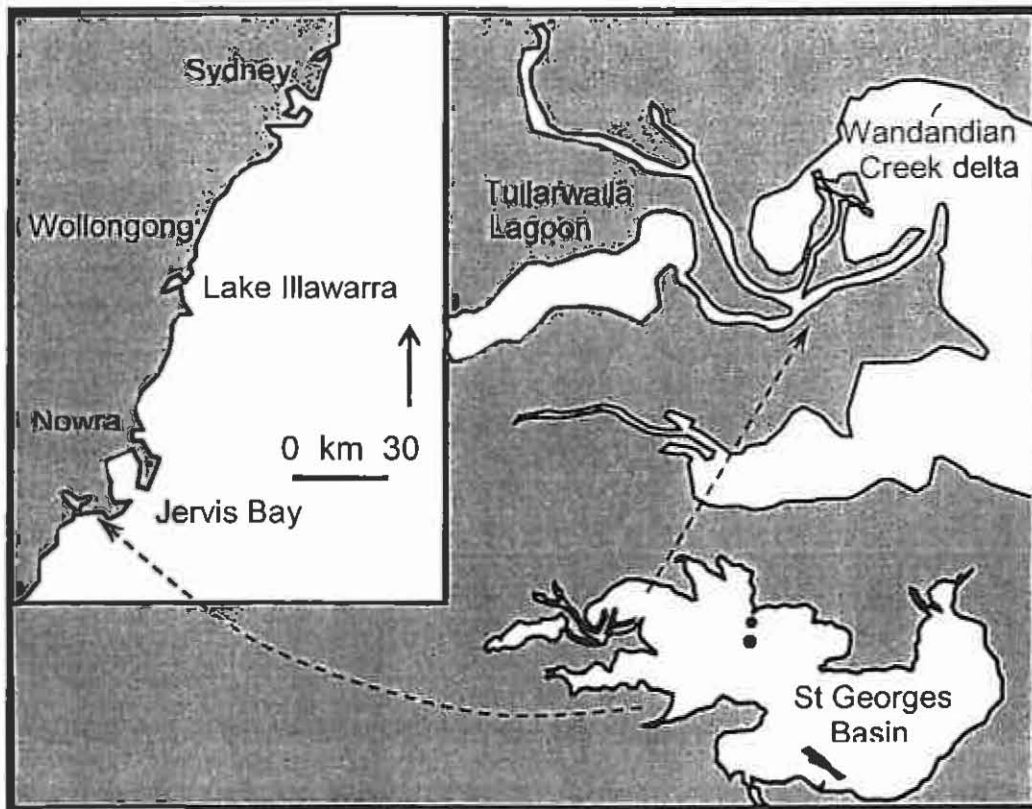


**Figure 1:** Location of Wandandian Creek delta

Europeans first settled the area in the 1830s, clearing the land for agricultural purposes. However much of the catchment area was not impacted due to the steep terrain. The most significant anthropogenic modification was the dredging of the lower creek in the late 1960s to 1970s although the exact time-frame, location or the amount of sediment removed are unknown.

## **METHODS**

Subsurface sedimentological and facies data were acquired using a combination of vibracorer (16 cores; Fig 2), a truck mounted drill rig fitted with solid augers (two holes), push coring (two cores), the digging of pits (5 pits) and an interpreted seismic trace. The sampling sites were spatially selected using field reconnaissance, topographic maps and both historic and recent orthorectified aerial photographs to provide the basis for constructing an accurate stratigraphic evolutionary model. The seismic trace was collected using a  $\frac{1}{4}$  second 200 joule, Geo-acoustics boomer with a Benthos 20 element streamer.

The cores collected were logged, sub-sampled and the macro-fossil components removed for geochronological assessment. Samples were assessed for colour using a Munsell soil colour chart within 24 hours of sampling on a cleaned face to minimise the impacts of oxidisation. Sedimentological analysis was completed using a Malvern Mastersizer 2600 laser particle size analyser and X-ray diffraction (XRD) analysis. The combination of sedimentological data and the visual logs resulted in the identification of several distinct facies within the Wandandian Creek delta area.

Ten *Anadara trapezia* and *Notospisula trigonella* macrofossils sampled at depths greater than 50 cm were analysed, in the University of Wollongong's amino acid racemisation (AAR) laboratory, following Murray-Wallace (1993) and Sloss *et al.* (2004a, b).  $^{210}\text{Pb}$  dating of core WCPb1 (Fig. 2) was conducted at ANSTO to establish the recent prodelta sedimentation rates. AMS and  $^{14}\text{C}$  dating was completed by the University of Waikato radiocarbon dating laboratory with the reported ages corrected for the marine reservoir effect and converted to sidereal years.

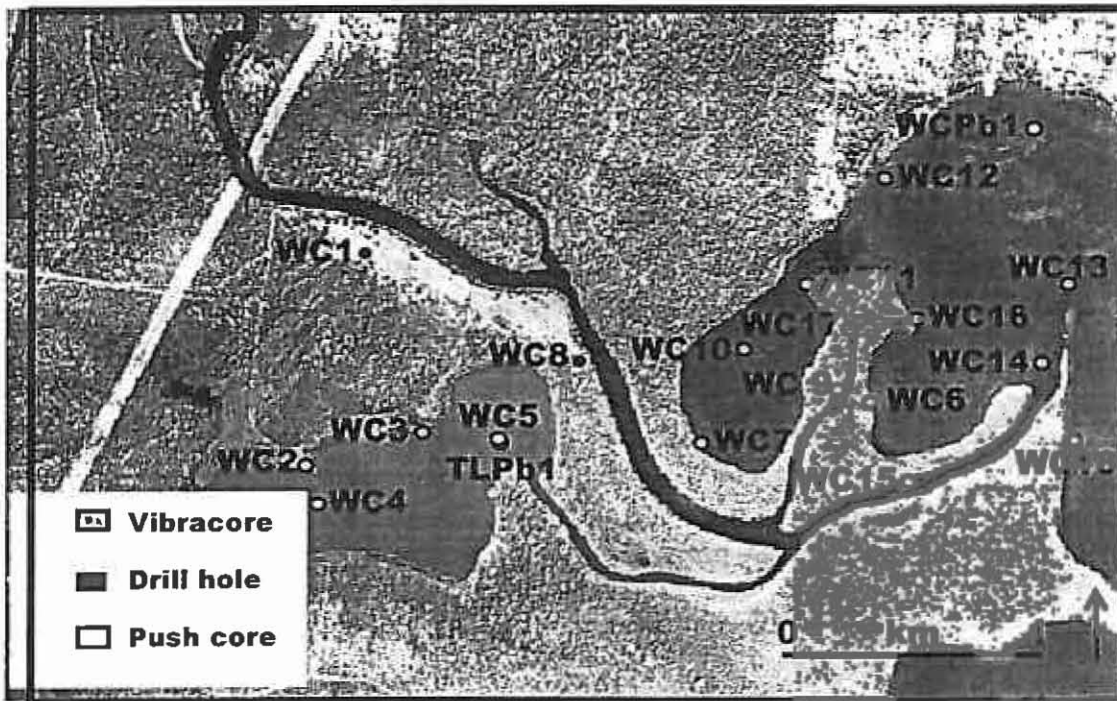


Figure 2: Location of the sixteen vibracores, two drill holes and two push cores.

### PLEISTOCENE LOW STAND DEPOSITS

During the late Pleistocene glacial period sea-level along the New South Wales coast was 110-130 m below present level (Ferland *et al.* 1995; Heap *et al.* 2004). Thus significant areas of land along Wandandian Creek were exposed resulting in the formation of highly leached and mottled sediments. These leached sediments were found at the base of vibracores WC2, 3, 12 and 13 ( Fig 2) at depths ranging from 0.6 m to 4.6 m below present mean sea-level. The lower Pleistocene sea-level facilitated the incision of waterways, such as Wandandian Creek, into earlier Pleistocene sediments and the underlying bedrock. Drill holes WC1 and WC8 suggest that the base of the Pleistocene channel had incised to depths of 10.5 m and 17.5 m, respectively, below present mean sea-level in the upper portion of the modern delta (Fig 3). This study suggests that the depth to basement of the Wandandian Creek palaeochannel is significantly deeper than the 8 m proposed by Bradshaw (1987, 1993).

Infilling the lower part of the palaeochannel is approximately 2.5 m of sub-angular very poorly sorted medium-grained sand interpreted as low-stand fluvial deposits. Overlying the fluvial sand, in WC1, is a 2 m thick palaeosol consisting of four layers with similar clay-rich lithology but differing colours. The palaeosol in this location indicates that the channel-fill sands were subaerially exposed for a lengthy period of time as Wandandian Creek moved away from this site, probably towards the northwest. In WC8 the palaeosol was not detected,

which suggests that this portion of the palaeochannel may have remained active until it was inundated by the marine transgression.

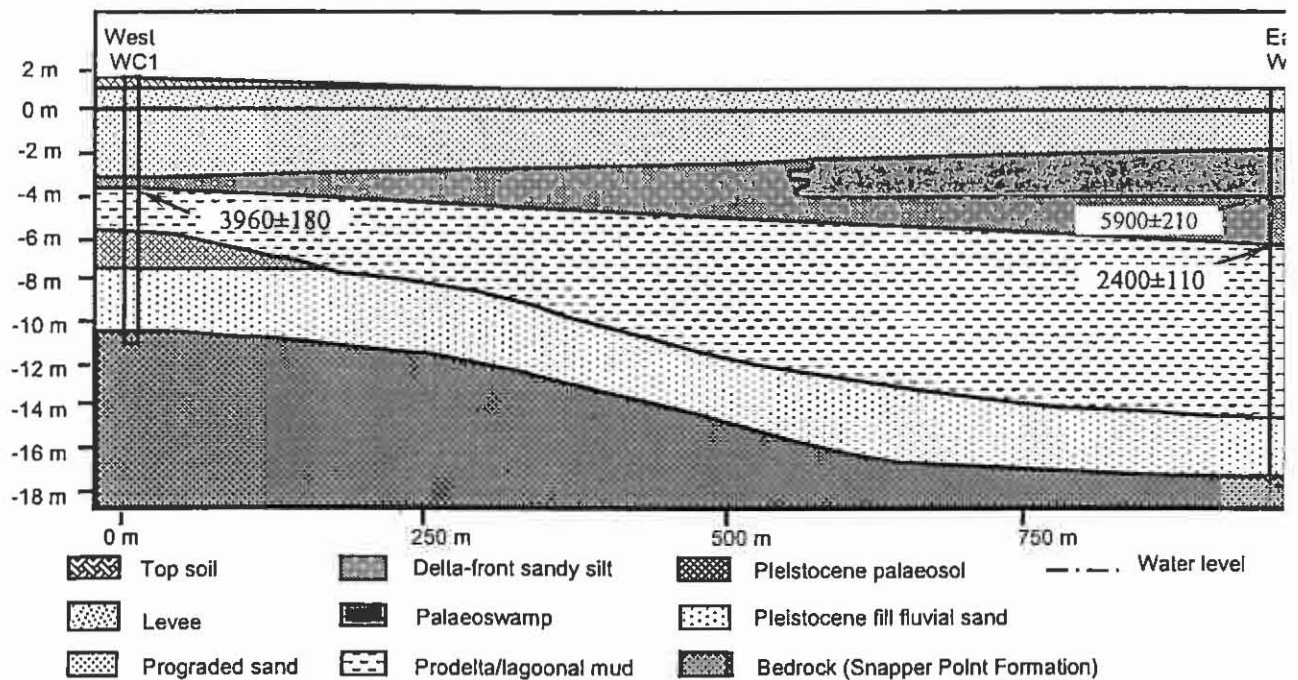


**Figure 3:** Cross-section of drill holes WC1 (NE) and WC8 (SE). The bedrock contacts were at 10.5 m and 17.15 m below mean sea-level, respectively (VE = 25).

Inherited basin morphologies significantly impact on the morphology of modern deltas (Coleman and Wright 1975; Roy *et al.* 2001). The remnant Pleistocene high detected in WC2 and WC3 (Fig 2) and the northern outcrop of Wandrawandian Siltstone limited the extent to which the delta could prograded in southerly and northerly directions, respectively. These morphological controls inevitably resulted in the formation of Tullarwalla Lagoon, a cut off sub-embayment.

### TRANSGRESSIVE DEPOSITS

The most recent post-glacial marine transgression attained present sea level around 7.7 ka and continued to rise to a maximum of +1.5 m by 7.4 ka (Sloss 2006). The increased sea-level inundated the Pleistocene land surface and resulted in deposition of an extensive transgressive sand sheet over the ancient St Georges Basin (Bradshaw 1987, 1993; Sloss 2006). However, none of the subsurface information collected in this study indicates that the transgressive sand sheet reached the westernmost portion of present day St Georges Basin. A bathometric high east of Picnic Point (Department of Land and Water Conservation 1996) limited the extent of the sand sheet and impounded western St Georges Basin. The high is tentatively thought to be the remnant of a transgressive barrier.

Impoundment of western St Georges Basin resulted in the development of a relatively calm and deep lagoonal water body that was suited to deposition, by flocculation, of muddy sediment brought down Wandandian Creek. The prodelta lagoonal mud facies is characterised by dark olive brown to black, very poorly to poorly sorted silt-sized sediment. AAR dating of a *Notospisula trigonella* ( $6380 \pm 310$  cal. yr BP) from near the base of the prodelta lagoonal

## WANDANDIAN CREEK DELTA

mud facies suggests that deposition of the silty sediment commenced prior to 6.5 ka. A date of  $3960 \pm 180$  cal. yr BP from drill hole WC1 (Fig 3), located near the contact between the prodelta lagoonal mud and delta sandy silt facies, suggests that a change in sedimentary processes occurred in the western part of the delta approximately 4 ka before present. Based on these dates, extrapolated sedimentation rates to the base of the prodelta lagoonal mud facies suggests that the Holocene high stand associated with the marine transgression ranged from approximately 7 ka to 3 ka. Young *et al.* (1993) estimated that sea-level in the vicinity of St Georges Basin during this time was approximately 1.8 m above present mean sea-level.

$^{210}\text{Pb}$  dating of push core WCPb1 indicates that subrecent prodelta sedimentation has occurred at an average rate of 0.62 mm/year. This recent sedimentation rate is similar to the prodelta sedimentation rate extrapolated for the past 1000 years at 0.51 mm/year (WC12; Fig 2). The similarity of the sedimentation rates suggests that anthropogenic impacts have had minimal affect on the sediment loads of Wandandian Creek.

### PROGRADING DELTA DEPOSITS

Progradation of the Wandandian Creek delta into the silty western part of the study area was initiated approximately 3.5 ka to 4 ka based on AAR dates of  $3960 \pm 180$  (WC1; Figs 2, 3) and  $3440 \pm 150$  (WC13; Fig 2). The dates are derived from *Notospisula trigonella* (WC1) and *Anadara trapezia* (WC13; Fig 2) located at the top of the prodelta lagoonal mud facies. It is highly probable that initial progradation of the delta would have occurred at a slower rate than at present, due to the elevated sea-level that persisted until about 3 ka (Sloss 2006). The effect of the elevated water level was to increase the accommodation space (area and depth) of St Georges Basin. However, the Late Holocene sea-level regression reduced the accommodation space, which is likely to have enabled the delta to prograde at an accelerated rate (Roy *et al.* 2001).

The initial stage of delta progradation, as observed in the Wandandian Creek delta vibracores and drill holes, is characterised by deposition of the delta sandy silt facies. This facies consists of very poorly to poorly sorted, dark olive to greyish black silt with very fine-grained sand. In the vibracores, where the nature of the contact could be determined, the delta sandy silt had a conformable contact with the prodelta lagoonal mud facies

Overlying the delta sandy silt is the prograded sand facies. The sedimentological characteristics of the prograded sand facies are more varied than the delta sandy silt facies. The basal sediments are generally very fine sand with large amounts of silt, ranging up to very coarse and relatively clean sand at the top of the facies. Distinguishing the basal sediments of the prograded facies from the delta sandy silt facies is difficult to do manually as they both appear and feel similar. However, sediment analysis using the Mastersizer clearly separates the two facies, as the basal sediments of the prograded sand facies are silty sands in contrast to the sandy silts of the delta sandy silt facies. Sedimentation rates of up to 3.12 mm/year (WC8; Figs 2, 3) were calculated for the prograded sand facies, which is considerably higher than those calculated for the prodelta lagoonal mud facies.

In several of the Wandandian Creek delta vibracores (WC6, 8, 9, 11, 16 and 17; Fig 2), an extensive, highly gaseous, organic facies was wedged between the delta sandy silt and the prograded sand facies. This facies has been interpreted to represent palaeoswamps formed in abandoned distributary channels. This facies, where intersected, generally occurs between -4 m and -1.7 m above present mean sea-level. The facies is characterised by very poorly sorted

silty sediment with minor very fine sand and clay within a porous matrix of organic material, consisting primarily of wood fragments up to 10 cm long and 5 cm in diameter. The basal portion of the facies contains significant quantities of charcoal with interspersed sandy silt lenses. Two sandy lenses are evident in the upper portion of the facies associated with the western distributary channel (WC6 and 16; Fig. 2) and are interpreted to represent flood deposits. A conventional radiocarbon ( $^{14}\text{C}$ ) date of  $910 \pm 150$  cal. yr BP indicates deposition commenced prior to 1 ka.

### **LEVEE, MOUTH BAR AND FLOODPLAIN DEPOSITS**

Overlying the prograded sand facies is a fining upward sequence of silty sand associated with the initial development of levees and floodplains. This unit developed when the gradient in the distributary channel reduced to a point where it could no longer transport the coarse sediment of the prograded sand facies resulting in overbank flooding.

Levees in the Wandandian Creek delta have accreted in some areas up to 1 m above water level. Basal sediments of the levees are relatively clean, medium-grained, buff yellow, fluvial sand. The clean fluvial sand becomes dirtier and interspersed with brownish black silty lenses which increase in frequency and thickness up profile to the extent where it is not possible to distinguish any coarse lenses. The change in sedimentary characteristics is a result of a change in the sedimentary process forming the levee from wave- and flood-washed sediment to vertically accreted mud. The muddy portions of the levees contain extensive evidence of bioturbation by plant roots and burrowing of organisms.

At the mouth of the western distributary channel, a large mouth bar has developed in response to the expansion and diffusion of the outflowing water resulting in a reduction in the channel's ability to transport sediment (Reading and Collinson 1996; Haslett 2000). Sediments deposited on the subaqueous portion of the bar are relatively clean, medium-grained, buff yellow fluvial sands.

The autocyclic process of channel avulsion, and the extension and meandering of Wandandian Creek, are the primary catalysts for the formation of the extensive subaerial floodplains in the delta. The floodplains contain several palaeochannels detected in the topographic survey of the study area. Drilling in one of these low-lying areas (WC1; Fig 2,3) intersected a 1.2 m thick fining up sequence consisting of medium- to fine-grained sand with silt overlying the prograded sand facies. The sedimentological characteristics of this fining-up sequence are similar to those of the levee and mouth bar deposits.

### **CONCLUSIONS**

The Holocene evolution of Wandandian Creek delta has been influenced by the inherited morphology of the basin, autocyclic and allocyclic processes and, to a much lesser extent, recent anthropogenic modifications. Wandandian Creek delta is a transitional delta since the bedrock and Pleistocene sediments had a significant affect on the delta's morphology. However, now that the delta has prograded into deeper water its morphology is controlled predominantly by fluvial processes and it has adopted a morphology similar to the classic birds-foot deltas as described by Bhattacharya and Walker (1992) and others.

During the late Pleistocene, lower sea-levels resulted in the development of leached and mottled sediments along the banks of the palaeo-Wandandian Creek. During this time the palaeocreek incised into earlier Pleistocene sediments and bedrock to produce a steep sided

channel with an established maximum depth of 21 m in the study area. Subsequently, rising sea-level flooded the palaeovalley. A transgressive sand sheet did not reach the study area due to a bathymetric high interpreted to represent the remains of a transgressive barrier. Instead, Holocene mud (prodelta lagoonal mud facies) directly overlies the mottled Pleistocene sediments and fluvial channel deposits; accumulation commenced at approximately 7 ka. Initial progradation of the Wandandian Creek delta into the study area commenced at 3.5 ka to 4 ka in the westernmost portion of St Georges Basin with the deposition of the delta-front sandy silt facies. This facies is then overlain by the coarsening-upward prograded sand facies followed by mouth bar and fining-up levee and floodplain deposits.

#### ACKNOWLEDGEMENTS

The fieldwork and analysis was possible due to the financial support provided by the Australian Research Council Linkage Grant (LP0347365) in conjunction with Shoalhaven Council and the School of Earth and Environmental Science University of Wollongong. The authors would like to thank Colin Murray-Wallace for allowing access to the University of Wollongong's AAR laboratory. The AMS and  $^{14}\text{C}$  dating were conducted at the University of Waikato radiocarbon dating laboratory;  $^{210}\text{Pb}$  dating was conducted at ANSTO, Lucas Heights (PGR5/02) laboratory. Seismic data was acquired with the assistance of Dave Mitchell from the University of Sydney.

#### REFERENCES

- BHATTACHARYA, J.P., AND WALKER, R.G., 1992. Deltas. In: Walker, R.G., and James, N.P. *Facies Models: Response to Sea Level Change*, p. 157-178. Geological Association of Canada, Toronto.
- BRADSHAW, B.E., 1987. *St Georges Basin – Morphology and Late Quaternary Deposits*. BSc Honours Thesis, University of Sydney.
- BRADSHAW, B.E., 1993. In: Thomas, M.C. (ed.), *Catchments and Coasts in Eastern Australia*. Department of Geography, University of Sydney, Research Monograph 5, pp. 66-71, Sydney.
- COLEMAN, J.M., AND WRIGHT, L.D., 1975. Modern river deltas: variability of processes and sand bodies. In: Broussard, M.L. (ed), *Deltas models for exploration*, p. 99-150. Huston Geological Society Davis, R.A., 1994. *The Evolving Coast*. p. 133-151. Scientific American Library, USA.
- Department of Land and Water Conservation (DLWC)., 1996. *St Georges Basin Hydrographic Survey Bathymetry*. Plan room catalogue number 10055, sheet 2. Department of Land and Water Conservation, Sydney.
- FERLAND, M.A., ROY, P.S., MURRAY-WALLACE, C.V., 1995. Glacial lowstand deposits on the outer continental shelf of southeastern Australia. *Quaternary Research*, **44**, 294-299.
- HASLETT, S.K., 2000. *Coastal systems*, p. 110-162. Routledge, London.
- HEAP, D.A., BRYCE, S., AND RYAN, D.A., 2004. Facies evolution of Holocene estuaries and deltas: A large-sample statistical study from Australia. *Sedimentary Geology*. **168**, p. 1-17.
- MURRAY-WALLACE, C.V., 1993. A review of the application of the amino acid racemisation reaction to archaeological dating. *The Artefact*. **16**, 19-26.
- READING, H.G., AND COLLINSON, J.D., 1996. Clastic coasts. In: Reading, H.G. (ed), *Sedimentary environments: processes, facies and stratigraphy*, p. 154-231.

- ROY, P.S., WILLIAMS, R.J., JONES, A.R., YASSINI, I., GIBBS, P.J., COATES, B., WEST, R.J., SCANES, P.R., HUDSON, J.P., AND NICHOL, S., 2001. Structure and function of south-east Australian estuaries. *Estuarine, Coastal and Shelf Science*, **53**, pp. 351-384.
- SLOSS, C.R., 2006. Holocene sea-level change and the aminostratigraphy of wave-dominated barrier estuaries on the southeast coast of Australia. PhD thesis, University of Wollongong, Wollongong, (unpublished).
- SLOSS, C.R., MURRAY-WALLACE, C.V., JONES, B.G., AND WALLIN, T., 2004a. Aspartic acid racemisation dating of mid-Holocene to recent estuarine sedimentation in New South Wales, Australia: a pilot study. *Marine Geology*, **212**, 45-59.
- SLOSS, C.R., JONES, B.G., AND MURRAY-WALLACE, C.V., 2004b. Aspartic acid racemisation dating of mid-Holocene to recent estuarine sedimentation in New South Wales, Australia: a pilot study. *Wetlands (Australia)*, **21**, 61-72.
- WEBB, MCKEOWN AND ASSOCIATES, 1993. *Stage 1 – Estuarine Processes St Georges Basin Management Study*. NSW Public Works and Shoalhaven City Council, Sydney.
- WEBB, MCKEOWN AND ASSOCIATES, 1996. *St Georges Basin Management Plan*. NSW Public Works and Shoalhaven City Council, Sydney.
- WEBB, MCKEOWN AND ASSOCIATES, 2001. *St Georges Basin Flood Study*. Shoalhaven City Council, Nowra.
- WINDLEY, V, 1986. *Wandrawandandian (home of lost lovers): A history of Wandandian*. Bay and Basin Printshop, Jervis Bay.
- YOUNG, R.W., BRYANT, E.A., PRICE, D.M., WIRTH, L.M., AND PEASE, M., 1993. Theoretical constraints and chronological evidence of Holocene coastal development in central and southern New South Wales, Australia. *Geomorphology*, **7**, p. 317-329.

# **MORPHOLOGICAL CHANGES, ASSESSED WITHIN A GIS FRAMEWORK, IN THE PROGRADING MACQUARIE RIVULET DELTA, NEW SOUTH WALES**

**Carl A Hopley, Brian G Jones and Marji Puotinen**

School of Earth and Environmental Sciences  
University of Wollongong  
Wollongong NSW 2522

## **ABSTRACT**

The recent morphological evolution of Macquarie Rivulet delta was assessed using historical/parish maps in conjunction with aerial photographs to map the changes within a Global Information System (GIS) framework. In the interval 1834-2002, the delta has increased in area by 14.247 ha and experienced significant morphological changes. The rates at which these morphological changes occurred fluctuated in response to land clearing and urbanisation in the catchment area and natural factors such as large rainfall events that resulted in flooding and channel avulsion.

## **INTRODUCTION**

Anthropogenic modifications to catchment areas often result in increased sediment loads and, therefore, dramatic changes in the natural rate of delta progradation. Effective mapping of these changes can greatly assist in the longer term management of the deltas. Establishing this information in the Illawarra is particularly important as development continues to encroach onto the floodplains in this area. This paper establishes the recent (1834-2002) morphological evolution of the Macquarie Rivulet delta within a GIS framework.

## **REGIONAL SETTING**

The Macquarie Rivulet delta is actively prograding into the southwestern portion of Lake Illawarra, located approximately 100 km south of Sydney (Fig. 1). Macquarie Rivulet is approximately 24 km long with a catchment area of 96.35 km<sup>2</sup> (WBM Oceanics Australia 2003), forming the largest of the five sub-catchments that drain into Lake Illawarra. Within the Macquarie Rivulet catchment area Hazelton (1993) identified six soil landscape groupings, for which the erosion potential ranges from moderate to extreme. Climate is generally warm with maximum rainfall occurring in summer to autumn (Bureau of Meteorology 2005). The proximity of the Illawarra escarpment to the delta has resulted in a well developed orographic effect in the area. Northeasterly, southwesterly and southerly winds are characteristic of the warmer months whereas in the cooler months, westerly and southwesterly winds are typical with wind velocities ranging up to 45-55 km/hr year round (WBM Oceanics Australia 2003). Between 1919 and 2003, a total of twenty-eight major or severe floods and three moderate flood events occurred in the Lake Illawarra catchment area. No other significant flood events have occurred since 2003.

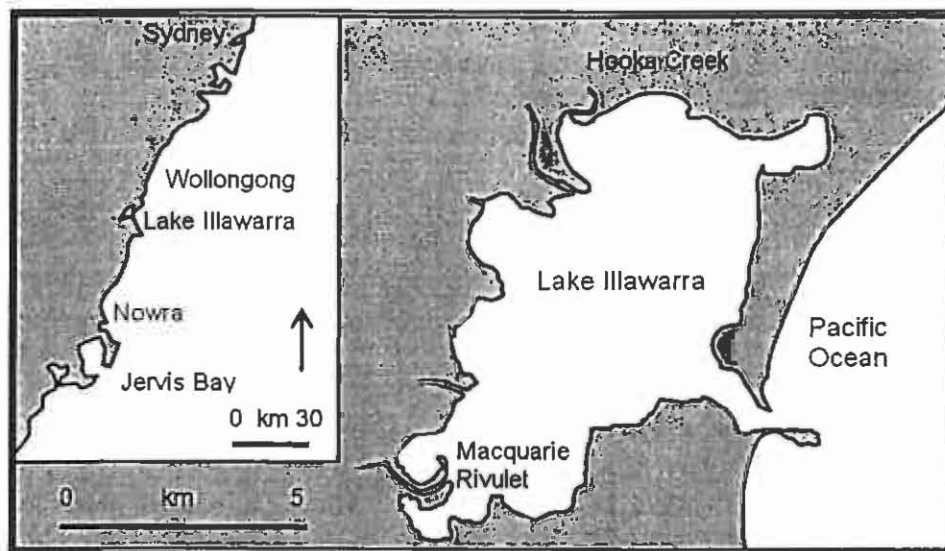


Figure 1: Location map of Lake Illawarra and the Macquarie Rivulet delta.

In the early 1800s, cedar cutters were the first known Europeans to modify the Macquarie Rivulet catchment area. Agriculture, primarily wheat, oats and potatoes, commenced in 1816 with surveying and clearing of large land grants surrounding the lakes foreshore (Lake Illawarra Authority 2005). Initially it is believed that the clearing occurred slowly due to the dense vegetation cover of the area. By the late 1800s, it was found that the area was not suitable for the growing of commercial crops and was replaced with dairy farming. Subdivision of the large land grants for residential purposes commenced in the 1920s (McDonald 1976).

#### DATA COLLECTION AND DIGITAL SCANNING

Historical/parish maps and aerial photographs were used to assess recent morphological changes on the Macquarie Rivulet delta. Each map and photograph selected for use in this study contained the entire delta within a single map/aerial photograph. Further, each map or photograph was also sufficiently detailed to facilitate the accurate delineation of the deltas boundaries (i.e., map scale of 1:25,000 or larger). The identified maps and aerial photographs were scanned at 600 dpi (following Hughes *et al.* 2006) and saved as tif files.

#### SPATIAL REFERENCING AND IMAGE PROCESSING

To accurately compare morphological changes over time in the delta, it was necessary to spatially reference the images. All images were georeferenced using ArcGIS version 9 georeferencing tools. The georeferencing process used both hard (e.g. South Coast railway line and bridge) and soft (e.g. trees and stable features of Macquarie Rivulet's channel) ground control points (GCP) as recommended by Hughes *et al.* (2006).

The selected digital images were georeferenced using 'image to image' techniques (Calzadilla *et al.* 2002). Initially, the 2002 image was georeferenced using GCPs derived from the Illawarra roads and Illawarra wetlands vector data sets (AMG 66 AGD 56 created by the School of Earth and Environmental Sciences, University of Wollongong, 1993). A polygon shapefile denoting the extent of the 2002 delta was digitised and used to georeference the 1993 image. This technique ensures that the images can be geometrically compared with accuracy. The number of GCPs used to rectify the aerial photographs and maps ranged

between 20 and 51. This variation reflects differences in the type and level of distortion present within individual images. Calculated RMS errors ranged between 5.67 and 11.19 m and were deemed acceptable as they fell within the 25 m positional accuracy standard implied by the map scale (1:25,000) of the datasets used. Second-order or quadratic transformations were used as Hughes *et al.* (2006) noted that they generally provide the best results in this type of a situation. It is important to note that it was not possible to georeference the 1834 map as it appears to be a sketch map reproduced in a report on the progress made in roads and the public works construction in NSW from the year 1827 to June 1855 (Mitchell 1856). As the map is not based on survey data, accurate GCPs could not be delineated, resulting in major root mean square (RMS) errors.

### GEOREFERENCED IMAGE PROCESSING

The georeferenced images were clipped to the extent of the study area and saved as new tif files. Onscreen digitisation within ArcGIS version 9 at a scale of no smaller than 1:2,500 was used to delineate the spatial extent of the delta. To ensure consistency between datasets, the polygon shapefile from the previous map/aerial photograph was copied, renamed and modified to reflect the morphological changes at the delta front. ArcGIS version 9 X tools were used to calculate the area of the delineated polygon shapefiles. The calculated areas enabled accurate reconstruction of the delta's growth.

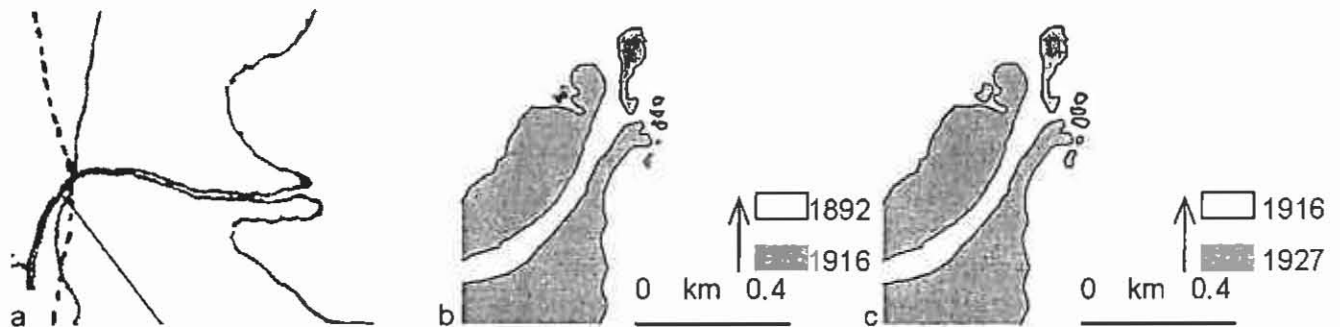


Figure 2: The extensive morphological differences in the Macquarie Rivulet delta between (a) 1834, (b) 1892-1916 and (c) 1916-1927 are illustrated. Note that the 1834 image is not georeferenced, since it appears to be a reprint of a sketch map.

Although it was not possible to georeference the 1834 map (Fig. 2), it is probable that the morphology of the delta it illustrates (Mitchell 1856) loosely reflects the morphology of the delta before extensive European modification of the catchment. This assumption is based on the fact that initial land clearing occurred relatively slowly and that it had commenced only 18 years prior to the production of the map (Lake Illawarra Authority 2005). In addition, Young's (1976) morphological interpretation of a map published in 1857 is similar to that illustrated in the 1834 map. The cusped morphology of the delta reflected in the 1834 map suggests that the dominant process acting on the delta was that of wind generated waves.

Between 1834 and 1892 it is evident that the delta changed from its east-southeast progradation direction towards the northeast (Fig. 2). This change likely represents increased influence of northeasterly winds and associated wind-wave reworking in the summer months. Furthermore, the reworking affect of the wind-waves resulted in an extensive thickening of the southern lobe of the delta. Such a significant change in the morphology of the delta is the

result of increased sediment being eroded and transported from the catchment area to the delta front. This increase in sediment was probably the result of land destabilisation due to land clearing for agricultural purposes.

In the 1892 map, several distributary channel mouth bars are evident. These formed in response to the frictional interaction between the outflowing water and the sediment interface (Suter 1994; Reading and Collinson 1996). The mouth bars resulted in the bifurcation of the Macquarie Rivulet delta, which led to the development of a morphology consistent with that of a fluvial-dominated birdsfoot delta (Coleman and Wright 1975; Bhattacharya and Walker 1992; Haslett 2000).

Minimal morphological changes were evident between 1892 and 1927 (Fig. 2). The primary changes consisted of the increases in the size of the subaerially exposed bars evident in the 1892 map and the emergence of an additional mouth bar to the south of the northeasterly-oriented channel. Between 1892 and 1927, the delta increased in area from 145.701 ha (1892) to 146.006 ha (1916) and to 146.110 ha (1927). The limited morphological changes observed are likely to reflect a lack of new survey data during this era, and may also reflect the change in focus from land clearing to pasture improvement as dairy farming replaced agriculture in the early 1900s (Young 1976; Lake Illawarra Authority 2005).

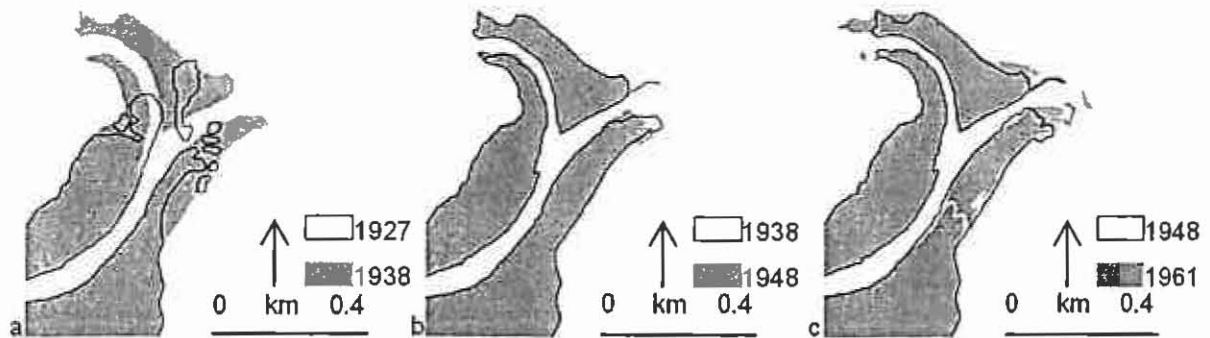


Figure 3: Morphological differences in the Macquarie Rivulet delta between (a) 1927-1938, (b) 1938-1948 and (c) 1948-1961.

Over the 11 year period between 1927 and 1938 (when the first aerial photograph became available), the area of the delta increased from 146.110 ha to 152.372 ha. In addition to the significant increase in area, the overall morphology changed dramatically (Figs 2 & 3). By 1938, the central distributary mouth bar had increased in size and had begun to hook back on itself in a northerly to northwesterly direction. The small distributary mouth bars evident in the 1927 had been reworked into the southernmost lobe of the delta. However, it is important to note the dramatic changes between 1927 and 1938 can be attributed to the fact that the digitised 1927 polygon was based on an historical map, which the authors believe is not an accurate representation of the delta, whereas the 1938 polygon is based on an aerial photograph of the delta. This highlights the need to critically review all results derived from historical maps where it is not possible to validate their accuracy.

Morphological changes are less pronounced between 1938 and 1948 (Fig. 3) than between 1927 and 1938. The main morphological change observed consists of a long thin subaerial

## MACQUARIE RIVULET DELTA

levee prograding in an easterly direction from the slightly enlarged distributary mouth bar. Continued reworking by the northeasterly wind-waves compressed the tip of the southern lobe of the delta. Young (1976) noted that between 1938 and 1948 the delta decreased in area, however, this research suggests that the delta only increased slightly in size from 152.572 ha to 152.612 ha. This discrepancy can be attributed to the improved accuracy associated with the digital mapping used in this study.

Between 1948 and 1961, the delta increased in area from 152.612 ha to 153.324 ha. Over the 11 year period, the southern lobe of the delta prograded farther into the lake and several small subaerial distributary mouth bars developed (Fig. 3). However, the morphology of the northern lobe appears to have remained relatively stable with only the tip undergoing minor reworking towards the southwest. Continued sedimentation resulted in both the northern and easternmost tips of the large distributary mouth bar prograding in westerly and northeasterly directions, respectively. The major morphological change between 1948 and 1961 was the development of a narrow crevasse splay channel, splitting the southern lobe. It is not possible to determine the actual timing of the splay development but it is likely to have occurred in response to one of the six major flood events that occurred over that time period.

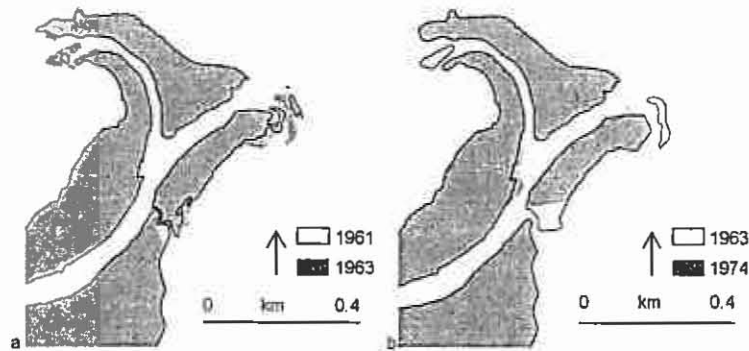


Figure 4: Morphological differences in the Macquarie Rivulet delta between (a) 1961-1963 and (b) 1963-1974.

By 1963, the small crevasse splay channel evident in the 1961 image had increased in size (Fig. 4). This increase can be attributed to erosion related to the two major flood events which occurred during this period. Sediment derived from the reworking of the splay material would have contributed to the increase in size of the northeasternmost portion of the southern lobe and the distributary mouth bar associated with the southern channel. Further, from analysis of aerial photographs of the Macquarie Rivulet catchment area from the late 1950s and 1960s, it is apparent that the urban development increased, which likely contributed to the increase size of the delta. Overall, the delta increased in size from 153.324 ha to 155.382 ha.

Between 1963 and 1974, Macquarie Rivulet delta decreased in area from 155.382 ha to 153.383 ha. This dramatic decrease in size is due to the expansion of the splay channel (Fig. 4) in response to the six major flood events that occurred over the 11 year period. The aerial photographs suggest that the expanded splay channel became the primary outlet and site of major sedimentation for Macquarie Rivulet, due to shoaling of the northern and northeastern channels. Morphological changes associated with the northern channels and the large distributary mouth bar were limited due to shoaling at the point of bifurcation. Another notable change in the delta is the absence of the large mouth bar associated with the northern

distributary channel. It is feasible that the flood events which resulted in the expansion of the splay were also responsible for the destabilization of the bar enabling it to be reworked by the northeasterly wind-waves.

Between 1974 and 1981 (Fig. 5), the delta increased in size by 2.78 ha from 153.383 ha to 156.163 ha. Continued infilling/shoaling of the northeastern and northern distributary channels blocked these two channels completely by 1981. As a consequence, the crevasse splay channel became the only active distributary channel of the delta during periods of normal flow. A further result of the shoaling was the isolation of the large distributary mouth bar and part of the southern lobe by the crevasse splay channel. Continued sedimentation resulted in the development of a large east-northeast trending distributary mouth bar in the vicinity of the splay channel. In addition to this large bar, a spit-like levee orientated in northeasterly direction extended from the most easterly point of the southern lobe. The images also illustrate that several other spit-like levees formed on the southern side of the northern lobe of the delta and were orientated in a northeast direction (Fig. 5).

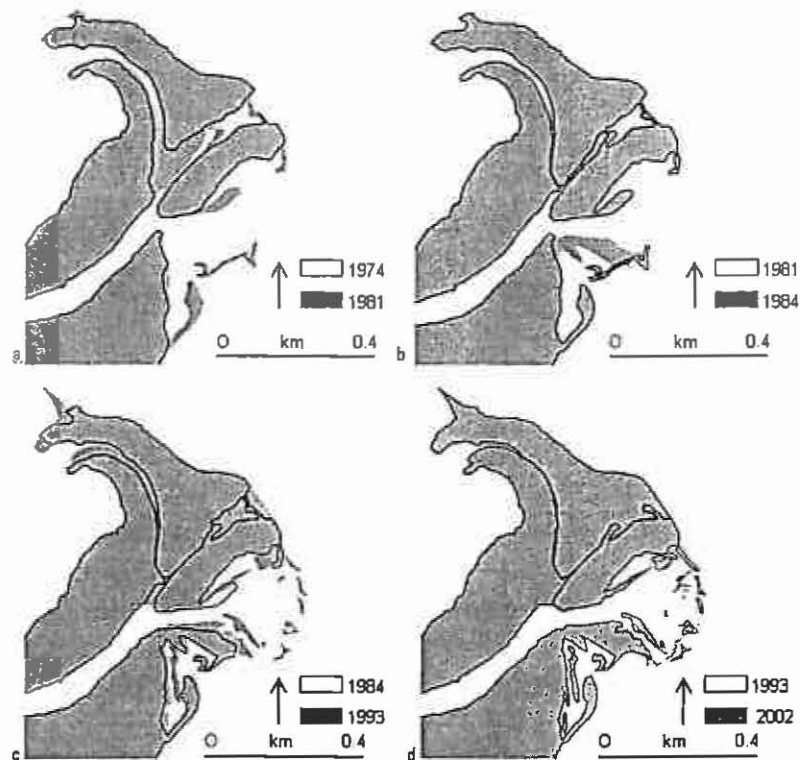


Figure 5: Morphological differences in the Macquarie Rivulet delta between (a) 1974-1981, (b) 1981-1983, (c) 1983-1993 and (d) 1993-2002.

By 1984, the area of the delta increased a further 0.982 ha to 157.125 ha. This increase can be attributed to the development of the levee extending from the northerly tip of the southern lobe. The extension of this lobe resulted in a reduction in width of the primary distributary channel and a change in orientation of its mouth towards the east. Furthermore, the prograding levee has formed a small cutoff embayment. These significant morphological changes over such a short period of time are likely to be in response to the considerable amounts of sediment introduced to the system during the large flood event that occurred in early February 1984 (Wollongong City Council 2006).

## MACQUARIE RIVULET DELTA

Between 1984-1993, morphological changes included the extension of the levee located along the southern lobe, and the development of a large elongate mouth bar roughly parallel to it (Fig. 5). Continued sedimentation within the small cutoff embayment, first observed in 1984, resulted in the formation of small subaerially exposed bars within it. Another key morphological change was the further extension of the southwestern levee on the northern lobe, which formed a small backswamp. During this period, the delta area increased from 157.125 ha to 159.812 ha. A large triangular extension off the northernmost tip of the north lobe of the delta developed due to northeasterly wind-wave reworking of sediment from the extensive delta plain and in the relatively shallow water surrounding the delta front.

From 1993 to 2002, the rate of delta growth decreased significantly, increasing in area by only 0.136 ha from 159.812 to 159.948 ha. This reduction in delta progradation was probably the result of one or more of the following factors:

- the occurrence of only one flood event;
- improvements in developmental practices which limited the amount of sediment made available to the system; and
- a possible increase in the lake level because the entrance was blocked.

The primary morphological change observed was the absence of the levee extending from the southeastern tip of the northern lobe (Fig. 5). The sediment within the levee is likely to have been reworked into the larger mouth bars and the shoreline along the northern lobe of the delta. The connection between the northern lobe and the large mouth bar was enhanced by continued shoaling of the abandoned northern distributary channel.

### CONCLUSION

An integrated approach to mapping, based on parish maps and aerial photographs within a GIS framework, can effectively assess morphological changes in deltaic environments with reasonable accuracy. This mapping approach, assuming that data of sufficient quality is available, could be applied to other deltas both in Australia and overseas. The past 168 years has seen the Macquarie Rivulet delta experience significant morphological changes. It appears that anthropogenic modifications within the catchment area have significantly affected the rate of delta progradation. For example, the rate of delta progradation generally increased during the 1970s to 1990s due to extensive development occurring in the catchment area. This study has also demonstrated the importance of natural factors, such as flooding and wind-waves, in the morphological evolution of deltas such as that of the Macquarie Rivulet.

### ACKNOWLEDGEMENTS

This research was supported by the School of Earth and Environmental Sciences at the University of Wollongong, the GeoQuEST Research Centre and an Australian Postgraduate Scholarship. John Marthick and Heidi Brown of the School of Earth and Environmental Sciences Spatial Analysis Laboratory provided valuable technical assistance.

### REFERENCES

- BHATTACHARYA, J. P., AND WALKER, R. G., 1992. Deltas. In: Walker, R. G., and James, N. P. *Facies Models: Response to Sea Level Change*, p. 157-178. Geological Association of Canada, Toronto.
- BUREAU OF METEOROLOGY, 2005. *Climate averages*. [www.bom.gov.au/climate/averages/cw-068188](http://www.bom.gov.au/climate/averages/cw-068188).

- CALZADILLA P. A., DAMEN, M. C. J., GENELETTI, D., AND HOBMA, T.W., 2002. Monitoring a recent delta formation in a tropical coastal wetland using remote sensing and GIS. Case study: Guapo River Delta, Laguna De Tacarigua, Venezuela. *Environment, Development and Sustainability*, **4**, 201-219.
- COLEMAN, J. M., AND WRIGHT, L. D., 1975. Modern river deltas: variability of processes and sand bodies. In: Broussard, M. L. (ed), *Deltas Models for Exploration*, p. 99-150. Huston Geological Society, Huston.
- HASLETT, S. K., 2000. River-dominated coastal systems. *Coastal Systems*, p. 110-162. Routledge, London.
- HAZELTON, P. A., 1993. Kiama soil landscape series, Sheet 9028. Department of Conservation and Land Management. Sydney.
- HUGHES, M. L., MCDOWELL, P. F., MARCUS, W. A., 2006. Accuracy assessment of georectified aerial photographs: implications for measuring lateral channel movement in a GIS. *Geomorphology*, **74**, 1-16.
- LAKE ILLAWARRA AUTHORITY, 2005. *History of Lake Illawarra*. [www.lia.nsw.gov.au/facts/history](http://www.lia.nsw.gov.au/facts/history).
- MCDONALD, W. G., 1976. The changing landscape of the lake. In: Turnbull, E. S., Young, R. W. (eds) *Lake Illawarra: an Environmental Assessment Project*. pp 4-9. Wollongong City Council and University of Wollongong, Wollongong.
- MITCHELL, T. L., 1856. *Report upon the progress made in roads, and in the construction of public works in NSW from the year 1827 to June 1855*. Government Printer, Sydney.
- READING, H. G., AND COLLINSON, J. D., 1996. Clastic coasts. In: Reading, H. G. (ed.), *Sedimentary Environments: Processes, Facies and Stratigraphy*, pp. 154-231. Blackwell Science, Cambridge.
- SUTER, J. R., 1994. Deltaic coasts. In: Carter, R. W. G., and Woodroffe, C. D. (eds), *Coastal Evolution: Late Quaternary Shoreline Morphodynamics*, pp. 87-120. Cambridge University Press, Cambridge.
- WBM OCEANICS AUSTRALIA, 2003. *Lake Illawarra Estuary Processes Study – Final Report*. Lake Illawarra Authority, Wollongong.
- WOLLONGONG CITY COUNCIL , 2006. website [www.wollongong.nsw.gov.au](http://www.wollongong.nsw.gov.au).
- YOUNG, R. W., 1976. Infilling of the lake. In: Turnbull, E. S., Young, R. W. (eds) *Lake Illawarra: an environmental assessment project*. p. 10-19. Wollongong City Council and University of Wollongong.

# **OH&S LEGISLATION IN THE COAL INDUSTRY – WHAT PROMPTS CHANGE?**

**Adrian Hutton**

School of Earth and Environmental Sciences  
University of Wollongong, Wollongong NSW 2522 Australia

## **ABSTRACT**

The perhaps cynical approach dictates that governments and the mines themselves react mostly to disasters or significant events, especially if these are reported to the general public. On the other hand, perhaps it is a case of “learn by mistakes” as there are loopholes and deficiencies in mine practice that only come to the fore when an unpredictable incident focuses on such loopholes or deficiencies. An examination of two major accidents, one in the Southern Coalfield, and the second in the Newcastle Coalfield of the Sydney Basin dramatically illustrate the problems posed by accidents, both to the mine operations and to the community at large. Inquiries after both accidents certainly show much was to be learned from “mistakes” and clearly show how legislators react to such well publicized disasters with amendments to mining practices and legislation especially if the inquiry that follows is unfavourable.

## **INTRODUCTION**

Safety, risk assessment and hazard mitigation have been major items on any coal mining agenda in Australia and elsewhere for the past few decades. In Australia, as elsewhere, safety in mines is covered by government legislation and in New South Wales by State government legislation. As underground mines become deeper and the risk of gas outbursts increases either due to depth or structure, research organizations have been funded for numerous projects to both gather data and to find solutions. Hanes (2004) reported that over the previous decade, the Australian Coal Association Research Program (ACARP) had funded projects for a total of \$6.5 million with increased expenditure in any year that followed a disaster. For example, in 1993, 1994 and 1995 following the South Bulli disaster in 1992 and Westcliff disaster in 1994 more than \$1.2 million, \$900,000 and \$1 million Australian dollars, respectively, were committed to research projects on outburst-related projects.

## **APPIN MINE EXPLOSION 1979**

On Tuesday, July 24, 1979, at approximately 11.00 pm, 14 coalminers were killed when a large explosion rocked Appin Colliery. Another 31 miners were underground but none suffered major injuries as most were some distance from the explosion. Ten of those killed were in the crib room which was severely damaged and the other four were in the panel where the explosion occurred. As with most mine disasters in New South Wales, a State Government inquiry, conducted by District Court Judge Goran, was held. Judge Goran was critical of Appin mine operations, and the performance of some mine employers and officers of the Department of Mines at the inquiry (Illawarra Mercury 2004).

### What Caused Ignition?

The location of the explosion (B heading inbye No 4 cut through either at the face or a point close to the face that would allow the flame to travel to the face) was relatively easy to determine. What was not straightforward was what triggered the explosion. Although the explosion “was initiated in a position from where it connected to a body of methane gas that had accumulated in B stub of K panel (Kininmonth, 1981), both the distance the flame traveled and the violence of the explosion indicated that coal dust was also a fuel.

Goran (1980) discussed three possible causes of ignition.

1. Fan Starter. Kininmonth (1981) cited observations of the fan and laboratory testing by Fisher (1979) who concluded “The fan switch was by far the most probable source of ignition that initiated the explosion of gas at Appin Colliery” although the reasons Fisher gave were a little contradictory as to whether the ignition occurred inside or outside the fan box or enclosure

2. Methanometer. The Auer methanometer normally carried by the assistant undermanager, who was killed in the explosion, was found in a damaged condition but extensive testing in inflammable gas mixtures showed it was not capable of initiating an explosion (Kininmonth, 1981).

3. Flame Safety Lamp. Two relighter type Protector Safety Lamps model GR 6S(A) were found in B heading; one along side the body of the deputy in a shuttle car at No 4 cut-through (lamp No G55) and the second attached to the body of the undermanager. Kininmonth (1981) cited investigations carried out by a Mr McKenzie-Wood in 1980 who concluded that there was no evidence that an external flammable methane atmosphere had been ignited by lamp G55, “however this lamp contained defects that would have decreased its overall efficiency and, under certain circumstances, could have ignited an external flammable methane mixture”.

Judge Goran dismissed the safety lamp as a cause of ignition with “... I cannot accept as any form of probability the proposition that the deputy’s safety lamp caused the first ignition.” Despite several counsels at the inquiry not disregarding the safety lamp and urging an open verdict (Goran, 1980). Consequently, Judge Goran concluded, “there remains only one possible culprit - the fan starter-box.” Later in the report, Judge Goran re-iterated the above conclusion when he stated, “I am left, as a result of the whole evidence, with the conviction that the explosion began by an ignition in the fan starter-box.”

In a separate inquiry, Coroner Hiatt (Hiatt 1980) found B heading stub had not been properly ventilated but he could not rule out either the safety lamp or the fan starter switch chamber as the ignition mechanism for the explosion.

Goran (1980) listed 27 recommendations or comments in his report ranging from deputies being given methanometers and magnifying glasses to examine for minute breaks in gauze, to changes in legislation. All 27 recommendations or comments were taken on board by the Minister for Mineral Resources and Development (Kininmonth 1981). Subsequently, the existing legislation under which Judge Goran was instructed to hold the inquiry was superceded by the *Coal Mines Regulation Act 1982* and the *Occupational Health and Safety Act 1983* both of which were still the legislation under which the Gretley inrush, discussed

below, was investigated. The Appin mine explosion triggered quite far-reaching ramifications.

Whether it has been the legislation or serendipity, it appears that mine safety in New South Wales has improved dramatically over the past 15 years as indicated by Department of Mineral Resources data, which show a general decline in the number of fatalities since 1990-91 and a definite decline in the number of lost time injuries per million hours worked.

#### **GRETLEY COLLIERY ACCIDENT, 1996**

About 5.30 am on 14 November, 1996, four of the eight men rostered for 50/51 panel (the other four had gone to the crib room) were operating a continuous miner when water gushed into the heading from a hole punched in the face. The continuous miner was swept 17.5 metres back down the heading where it became jammed against the ribs. The deputy, a mechanical fitter and two miners, who all had been working at the face, were swept away and drowned.

With the Gretley accident there was no dispute as to the cause of the accident. The men had been developing a roadway (C heading) in 50/51 panel with a continuous miner when they broke through the face from the working mine known as Gretley Colliery to the much older abandoned workings of the Young Wallsend Colliery. The hazard of an 'inrush' of water had turned into reality.

An inquiry chaired by Judge Staunton (Staunton 1998a) was held. From Staunton's report it is clear that no party or witness disputed that the mine plans from which the men were working led to the accident. The main dispute was which party or person should shoulder the blame for the inaccuracy of the map.

Judge Staunton made 43 recommendations following the inquiry. In the ultimate paragraph before the recommendations, Judge Staunton stated "In the view of the court the evidence disclosed a number of shortcomings in the legislation, Act and regulations, and administrative guidelines which require urgent consideration if the industry and the community is to be spared a tragedy similar to that which befell these unfortunate men on 14 November 1996." (Staunton 1998b).

The plan Gretley Colliery had been working from which had been approved by the New South Wales Department of Mineral Resources (DMR) and showed that the older colliery should have been 100 m away from the point of holing-in (Staunton 1998a). However, the inquiry on the accident concluded that at 11.00 pm in the evening when the shift started before the accident, the barrier between the two workings had only been "7 or 8 metres away". Young Wallsend Colliery workings had filled with water after having been abandoned. In addition, there was a head of water because the water surface had risen to the ground level thus increasing the water pressure.

The report lists ten contributing causes for the accident ((Staunton 1998a):

1. The DMR; it was responsible for misinterpreting a map (referred to as Sheet 1 and included in the report) of the Young Wallsend Colliery when approval to mine was sought.
2. The mine surveyor; for not researching properly the Young Wallsend Colliery before it was depicted on the Gretley mine plan.

3. A mine manager; for not recognizing and determining that the colliery had not been correctly depicted on the Gretley Colliery plan.
4. A second mine manager; who succeeded the above mine manager; and for the above reason.
5. Both mine managers; for not devising an appropriate strategy to prevent water inrush.
6. The DMR; for failing to appraise and evaluate the application to mine by the company and thus for approving a flawed system
7. A second mine surveyor; for not investigating the basis upon which the surveyor in (2) above, whom he succeeded, had depicted the Young Wallsend Colliery and had not recognized that the issue had been properly researched.
8. The second mine surveyor; for failing to properly investigate that there was an issue concerning the depiction of the Young Wallsend Colliery on the mine plan.
9. An undermanager; who failed to investigate early November reports of water in 50/51 panel made to him by two deputies
10. Two other undermanagers; who the day before the inrush failed to properly investigate issues raised by a mine deputy and failed to inform an undermanager of the contents of the report.

In addition to the causes, the report discussed 11 main issues and several subsidiary issues. The issues were raised in the hope ‘...that lessons will be learned, and similar occurrences avoided in the future.’ The issues listed by the report were:

The report devoted almost 30 pages to the issue of risk assessment and three recommendations were made concerning risk assessment. In the preface to the recommendations the report stated that “(a risk assessment) ought to have been employed by Gretley and had a risk assessment been done, ‘it probably would have exposed the inadequate research and false assumptions ...”

Of the 43 recommendations, the last six recommendations in a section of the report titled “PROSECUTION POLICY”(14% of all recommendations) clearly summarized the judge’s intent. Recommendation 38 was “That the Department (of Mineral resources) formulate a prosecution policy.” and recommendation 43, the last, was “In respect of the Newcastle Wallsend Coal Company Pty Ltd that papers be referred to the Crown Solicitor with a view to determining whether offences have been committed under sections 15 and 16 of the *Occupational Health and Safety Act 1983*.” (Staunton 1998b). Adopting a cynical approach, one could suspect that the Crown Solicitor was left in an unenviable position by Judge Staunton and he was perhaps forced to bring proceedings against persons or some entity by the judge’s recommendations.

Clearly Judge Staunton’s report on the Gretley accident had repercussion for the coal industry. In March 1999, the DMR published the first issue of the *Mine Safety News* which focused on “... the big picture - legislation, policy, and safety issues for the whole industry” (DMR 1999a) including the metaliferous industry. In the “*News*” section on the front page was the headline “CHANGES TO MINE SAFETY LEGISLATION” which announced changes to improve mine safety in the mining industry, with legislative changes reflecting new responsibilities and structures in industry (this included the metaliferous minerals industry as well as the coal industry) and the Department. In the bottom right hand corner on the front page was a graphic photograph of the notorious continuous miner in Gretley Colliery after the accident two new acts, the Mines Legislation Amendment (Mine Safety) Act, 1998 and the Mines Inspection Amendment Act, 1998 amended the Mines Inspection Act 1901,

and the Coal Mines Regulation Act, 1982. The Department acknowledged some changes followed recommendations of the Gretley Inquiry. Further on, *Mine Safety News* stated the “Gretley judicial inquiry into the deaths of four miners near Newcastle in November 1996 supported many Mine Safety Review recommendations and added further recommendations, many of which are incorporated into the new legislation.” (DMR 1999a).

The second issue (DMR 1999b) carried a flow chart of the Department’s accident response process and the headlines:

- “A NEW INVESTIGATION UNIT”
- “DRAFT OF NEW COAL REGULATIONS FOR PUBLIC REVIEW”.

The third issue (DMR 1999c) carried a message from the Minister for Mineral Resources and Fisheries (the overseeing minister for the mining industry) introducing the new regulations with:

“The new regulations put mine safety where it belongs – in the hands of the mine owners, managers, unions and workers.”

### POSTSCRIPT

Phillips (2006) wrote that in 2000 and 2005 new work safety laws were passed in New South Wales and these affected not only the mining industry but all work sites. According to Phillips in his scathing attack on the prosecutions as a result of the Gretley disaster, the “..laws are counterproductive and misconceived” and “instead of being a positive legacy to the memory of the four deceased Gretley miners, they do an injustice to their memories.” Judicial proceedings were started against some persons mentioned in Judge Staunton’s report but finality was a long way off.

In 2000 the company that owned the mine and the mine managers were prosecuted under the New South Wales OH&S laws. In 2005, almost a decade after the disaster, all were convicted. The company was fined \$1.47 million and the managers \$102,000. At the time of the disaster, the Newcastle Wallsend Coal Company Pty Ltd (Gretley mine) was owned by Oakbridge Pty Ltd, By 2005, at the time of the convictions, Xstrata had purchased Oakbridge. According to Phillips, Xstrata had inherited total responsibility for the criminal liabilities of the Newcastle Coal Company Pty Ltd, something he quite disagrees with.

Perhaps Phillips is most vehement in his questioning as to why the Department of Mineral Resources was not prosecuted despite that it had directly contributed to the disaster through its failure in relation to the maps.” No reasons were given by the then Attorney General Jeff Shaw for this.

In another vehement discussion, Phillips (2006) questions the actions of the Construction Forestry Mining and Energy Union (CFMEU), the union that had coverage of Gretley Mine. Phillips stated the CFMEU is an “OHS prosecuting authority “.. and has “the power to conduct prosecutions under the Act and to retain half of any fines imposed.” To Phillips, equally as intriguing is why the United Mining Support Services (UMSS) was not investigated since “prosecution of labour hire firms under OHS legislation is a regular occurrence around Australia.” In the Gretley case, three of the deceased miners were employed by the UMSS and the ‘employer’ has statutory total obligation for safety.” Phillips clearly sees political intrigue in the situation since the UMSS was majority-owned by the

CFMEU at the time of the disaster although since then the UMSS was sold to a Tasmanian based labour hire firm.

Since the Gretley disaster non-mining companies have been prosecuted. To Phillips (2006), the “clearest indication of the new and aggressive OHS prosecution regime is provided by the total of fines imposed”.

- In 1998-99 total NSW OHS fines for the year amounted to \$2.97 million.
- By 2003-04, the total had risen to \$13.3 million ..”.

In that period, New South Wales recorded 63% of all Australia’s OHS prosecutions, 66% of all Australia’s convictions and 64% of all Australia’s fines.

## REFERENCES

- DEPARTMENT OF MINERAL RESOURCES, 1999a. Mine Safety News, March 1999, [www.minerals.nsw.gov.au](http://www.minerals.nsw.gov.au), 8 pp.
- DEPARTMENT OF MINERAL RESOURCES, 1999b. Mine Safety News, June 1999, [www.minerals.nsw.gov.au](http://www.minerals.nsw.gov.au), 12 pp.
- DEPARTMENT OF MINERAL RESOURCES, 1999c. Mine Safety News, September-November 1999, [www.minerals.nsw.gov.au](http://www.minerals.nsw.gov.au), 12 pp.
- GORAN A.J. 1966. Accident at Bulli Colliery on 9<sup>th</sup> November, 1965. Report of Judge A.J. Goran following an Inquiry by the court of Coal Mines Regulation established under Section 33 of the Coal Mines Regulation Act, 1912, as amended. 44 pp.
- GORAN A.J. 1980. Explosion at Appin Colliery on 24<sup>th</sup> July, 1979. Report of His Honour Judge A.J. Goran Q.C. following an Inquiry by the court of Coal Mines Regulation established under Section 31 of the Coal Mines Regulation Act, 1912, as amended. 180 pp.
- HANES J., 2004. Outburst Scoping Study. Interim Report ACARP Project C10012, 170 pp.
- HARVEY C.R. 1995, The development of an outbursts data base for the Bulli coal seam; in Lama, R.D. (ed.) International Symposium-cum-Workshop on Management and Control of High Gas Emissions and Outbursts in Underground Coal Mines. 20-24 March 1995 Wollongong NSW, Australia, 405-412.
- HIATT J. 1980. Appin Inquest. Campbelltown Coroners Court, N.S.W.
- KININMONTH, R.J., 1981. Summary of Investigations into Appin Colliery explosion; in Hargraves, A.J. (ed.) Ignitions, Explosions & Fires in Coal Mines Symposium, May, 1981. The Aus.I.M.M. Illawarra Branch, Wollongong. 9-1 to 9-16.
- PHILLIPS K. 2006. The Politics of a Tragedy The Gretley Mine Disaster and the dangerous state of work safety laws in New South Wales. Institute of Public Affairs Work Reform Unit, October 2006.
- STAUNTON J.H. 1998 (a). Report of a formal investigation under section 98 of the Coal Mines Regulation Act, 1982, Volume 1, 1-342.
- STAUNTON J.H. 1998 (b). Report of a formal investigation under section 98 of the Coal Mines Regulation Act, 1982, Volume 2, 342-749.

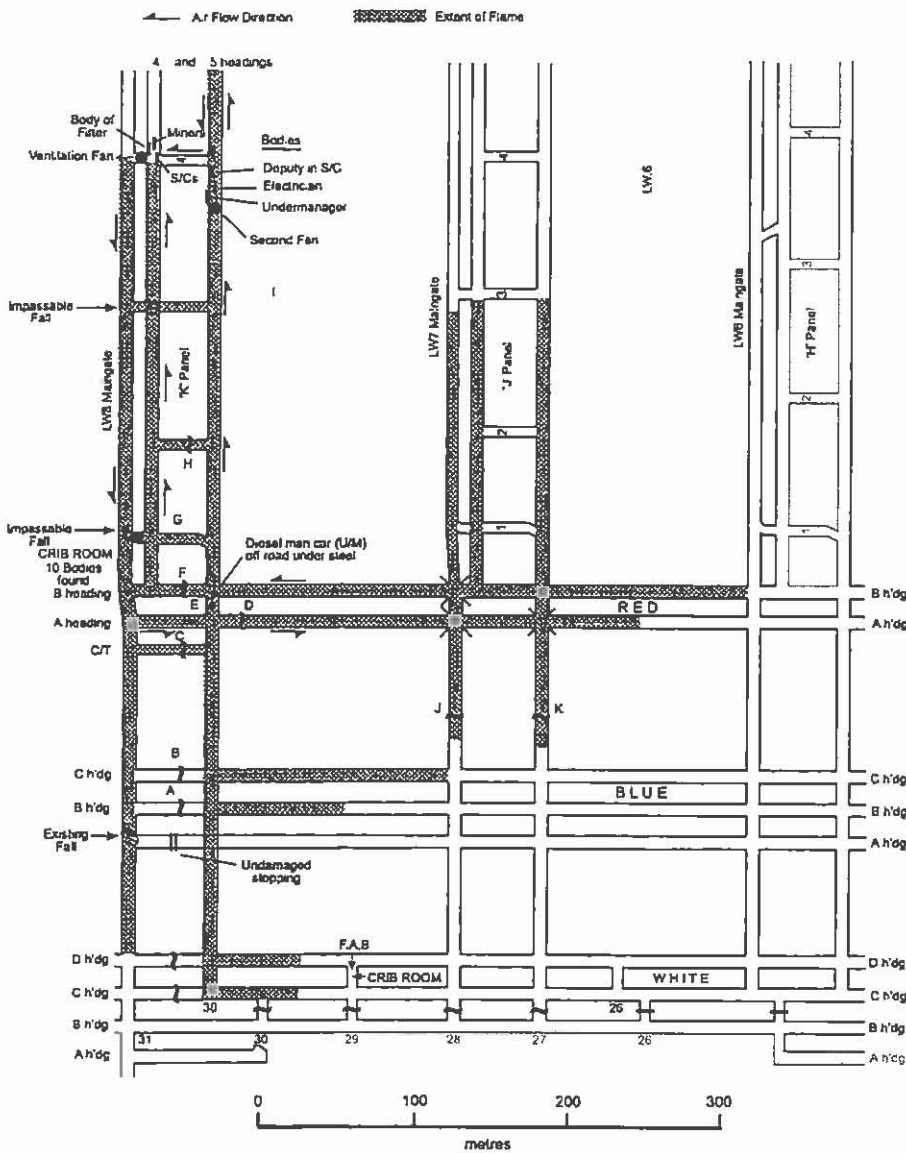


Figure 1. Plan of Appin colliery at the time of the fire in 1978. H and K panels had been developed developed and L panel was being developed at an increased rate to allow Longwall 7 to start on time. The second fan in panel B was judged to be the cause of the fire (redrawn from diagrams in Kininmonth (1981).

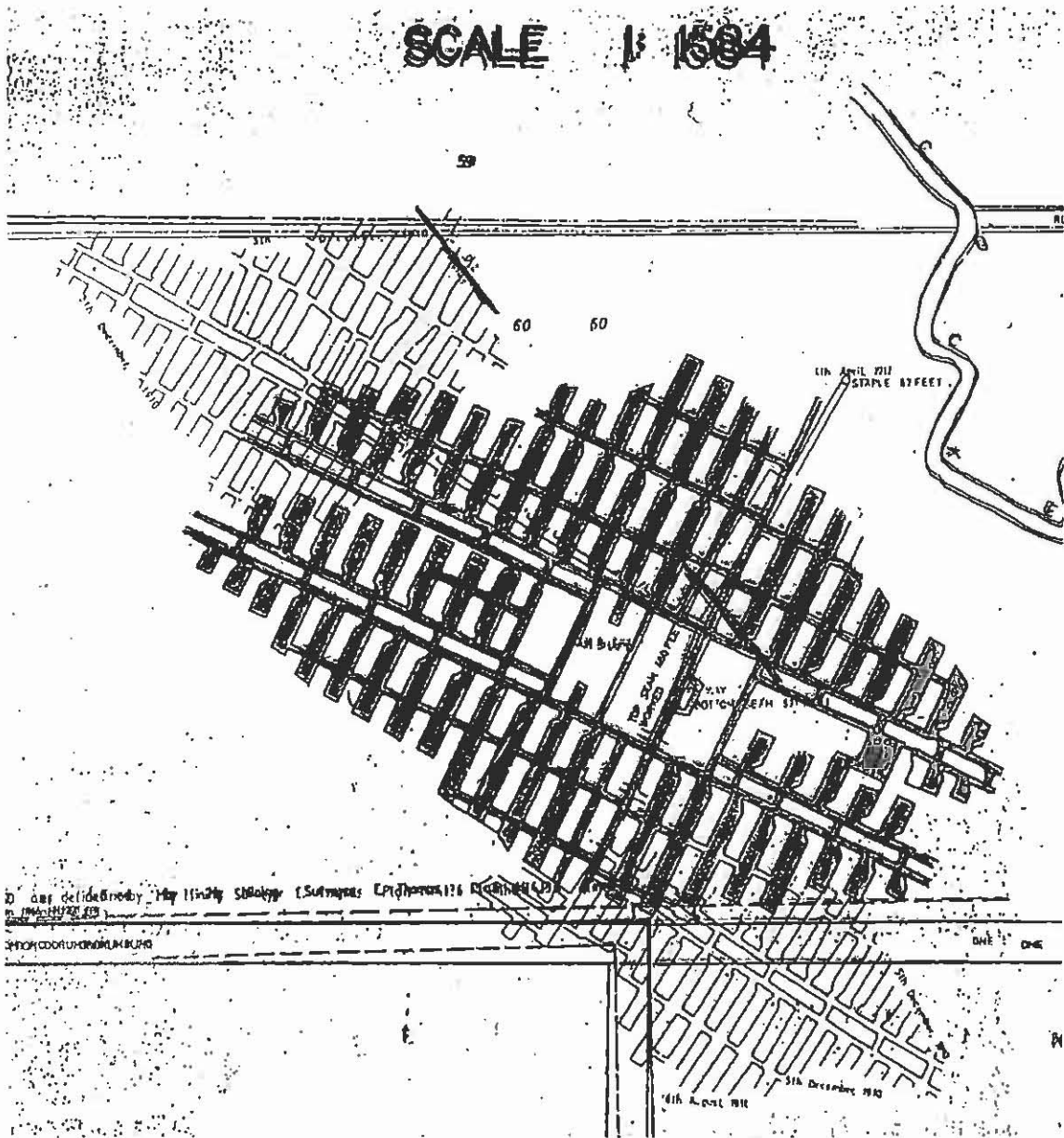


Figure 2. A composite map of the Young Wallsend mine prepared by overlaying Sheets 2 and 3 from the Gretley report by Judge Staunton. The long drives are oriented in different directions and the two plans overlap by at least 30 m in some places.

# **PETROGRAPHY OF HAWKESBURY SANDSTONE AND WATER MOVEMENT**

**Adrian Hutton, Matthew Johnson, Melissa Gentz**

School of Earth and Environmental Sciences  
University of Wollongong

## **ABSTRACT**

Hawkesbury Sandstone in the Southern Coalfield is a quartz-rich sandstone with shale layers and is discontinuous laterally as a result of bed forms produced during deposition. The matrix is mostly kaolin in the sandstone with mixed layer clays more abundant in claystone layers and lenses. During early diagenesis chert replaces some of the clay matrix. Also during diagenesis and possibly during later times, siderite and calcite were precipitated. Fluid inclusion studies indicate the quartz overgrowths, common in many samples probably formed during diagenesis as well.

Weathering of the Hawkesbury Sandstone results in solution of the clay and chert matrix and late stage precipitation of iron oxides which produce the characteristic leisegang patterns. Weathering rates increase along fractures and bedding plane surfaces and this produces increased porosity for water movement and probably contributes to cliff instability in steeply dissected terrain.

## **INTRODUCTION**

Coal mining is one of Australia's oldest major industries, second only to agriculture (Larratt and Kuru 1988), and is a major contributor to the economy of Australia at the international, national, regional and local level. Despite the significance to the economy, as concern for the environment increases the need to find a balance between mining and the environment is thought to be essential if mining is to continue in both an economically and environmentally viable manner. In 2004, the NSW Government introduced A SUBSIDENCE MANAGEMENT POLICY (SMP) to assess and reduce the impacts of longwall mining (NSW DPI 2006). Part of the Subsidence Management Policy requires that surface and groundwater management be provided for by the mining company. It is therefore important to gain an understanding of groundwater movement and characteristics to determine the effect, if any, mining has on groundwater.

Groundwater, like coal, is an important resource and its importance has increased recently due to a reduction in stored water in the Sydney Water catchment (Grey and Ross 2003) and other NSW local government areas. As surface water is depleted, alternative water sources need to be considered and groundwater is one such alternative with the result there is competition between mining companies and water providers for resources. For example, BHPBilliton Illawarra Coal has leases adjacent to the Cataract River, a source of water for the Sydney and Illawarra regions. Within a few tens of kilometres, the Hawkesbury Sandstone is now regarded as a sizable source of water for Sydney.

### **NATURE OF THE HAWKESBURY SANDSTONE**

The Hawkesbury Sandstone is not a laterally continuous unit but is composed of numerous crossbedded and planar bed sets with intermittent shale lenses that extend for more than 100 m in many cases. Conaghan and Jones (1975) and Conaghan (1980) were the first to suggest a fluvial environment in a large river such as the Brahmaputra. Jones and Rust (1983) who argued that floods of up to 15 m deposited some of the larger bed forms. All authors detailed the facies types in the Hawkesbury Sandstone and related these to flow types. Griffith (1986) proposed the Gilbert River [northern Australia] as an analogue for the Hawkesbury Sandstone precursor stream. The importance of the study by Jones and Rust (2003) is that it showed the facies types in the Hawkesbury sandstone are not laterally continuous, an important aspect when understanding water movement within the unit.

In a later study, Miall and Jones (2003) examined photomosaics of two cliff sections (one section 5.6 km long) south of Sydney. They concluded that channel elements within the Hawkesbury Sandstone were at least 2.7 km wide, and individual units 5 to 10 m high indicating that the units were deposited in water depths of up to 20 m. Significantly, the authors compared the scales of sand bodies in the Hawkesbury Sandstone with those in the Brahmaputra River and recognised 1st order to 5th order channels. The sand bodies at Kurnell Peninsula were regarded as 5th order channels 18 to 20 m thick, and sometimes with scour hollows up to 20 m deep

The degree of variability within the Hawkesbury Sandstone over a short distance, is a feature seen in the exposed cliffs of Hawkesbury Sandstone within the Illawarra region. Jones and Rust (1983) stated stacked cross bed sets represented channel fill sequences deposited by migrating straight to sinuous sand waves. Bar migration and fluvial activity was intermittent and seasonally controlled as indicated by the numerous reactivation surfaces. Bed forms were modified during the waning stages of flood events. The environment of deposition and the resulting sedimentary structures formed influence the movement of water through the Hawkesbury Sandstone and consequently the weathering of the Hawkesbury Sandstone.

### **PETROGRAPHY OF THE HAWKESBURY SANDSTONE**

Johnson (2006) described the Hawkesbury Sandstone as composed predominantly of sand-sized framework grains held together by a clay matrix. He showed that the Hawkesbury Sandstone samples were quartz-rich (range of 51.3 to 89%) (Fig. 1) which is consistent with studies undertaken by other authors where the quartz content was shown to be 51 to 72% (Franklin 2000; Freed 2005). Quartz content is not related linearly with depth. The dominant clay minerals are kaolin and illite with subordinate mixed layer clay minerals and micas. Chlorite occurs in trace amounts. Siderite, iron oxide minerals and muscovite are minor components. Clay mineral content decreases with increasing iron oxide mineral content.

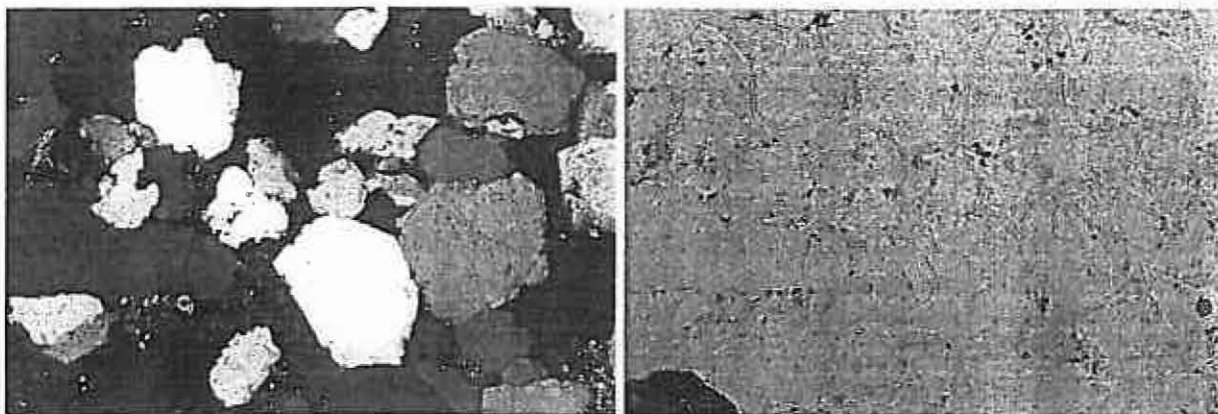


**Figure 1** Typical unweathered Hawkesbury Sandstone showing quartz framework grains with a matrix composed of kaolin and chert. Field width = 3.2 mm; RHS plane polarised light, LHS crossed polars

Gentz (2006) found quartz accounts for an average of 70.2% of the total composition of the sandstone and of the types of quartz present, fractured simple grains account for the majority of quartz grains (32.4%). The average clay mineral content of samples was 12.4% and average porosity 6.6% of sample. Siderite averaging 6.4%, muscovite 1.3% and opaque minerals 2.8% were minor constituents.

Gentz (2006) also used XRD techniques. She found an average quartz content of 78.8% in sandstone samples and 26.2% in claystone samples. Clay minerals were present within both sandstone and claystone samples and the main clay minerals identified were kaolin, illite and mixed-layer clays. Kaolin was the most common clay mineral present in sandstone and ranged from 5 to 15% in most samples. Mixed-layer clays comprised up to 14.7% of samples. Illite was present in most samples but only in small proportions with a maximum of 4.7%. The most common form of clay mineral in claystone was mixed-layer clays with other forms of clay kaolin (average 14.6%) and illite (average 7.6%) ranging from 0.3 to 23.1% and 1.9 to 15.0% respectively.

Other minerals identified using XRD analysis were siderite, muscovite, chlorite, ankerite, montmorillonite and calcite.

### **FLUID INCLUSION STUDIES**

A review of the literature shows a paucity of fluid inclusion data for studies involving quartz-rich sedimentary systems in Australia, particularly the Permo-Triassic sequence of the Sydney Basin. Data on fluid inclusions in quartz overgrowths obtained from relatively shallow samples of Hawkesbury Sandstone in three drill holes from the central-southern Sydney Basin give some insight into the temperatures and fluid parameters in quartz overgrowths. These data (Tables 2 and 3) plus information provided by McDonald and Skilbeck (1996) provide an insight into the fluids causing overgrowths in the Hawkesbury Sandstone.

**Table 1** Comparison of Mineral Contents in Sandstone versus shale (from Gentz 2006)

Mineral	Sandstone Samples		Claystone Samples	
	Average Composition (%wt)	Range (% - %)	Average Composition (%wt)	Range (% - %)
Quartz	78.8	16.9 - 95.0	26.2	2.8 - 43.9
Muscovite	1.0	0.0 - 9.1	22.8	12.3 - 31.5
Illite	1.8	0.0 - 4.7	7.6	1.9 - 15.0
Mixed-Layer Clays	1.5	0.2 - 14.7	22.6	5.5 - 40.3
Kaolin	13.4	1.7 - 72.8	14.6	0.3 - 23.1
Siderite	3.5	0.0 - 22.5	7.1	0.0 - 18.2
Chlorite*	< 0.1	0.0 - 0.9	0.4	0.0 - 1.4
Ankerite*	< 0.1	0.0 - 0.8	0.0	0.0 - 0.0
Montmorillonite*	< 0.1	0.0 - 0.1	< 0.1	0.0 - 0.2
Calcite*	< 0.1	0.0 - 0.2	< 0.1	0.0 - 0.1

**Table 2** Homogenisation temperatures for fluid inclusions in the Hawkesbury Sandstone

Drill hole	Depth	Size	Shape	Th					Tfm		
				°c					°c		
				1	2	3	4	Mean	1	2	Mean
Kurrajong Heights No 1	197.3 m	15 u	anhedral	105.1	105.6			105.4			
				90.8	92.0	94.2	92.8	92.5			
				169.0	165.9			167.5	-41.5	-41.2	-41.4
Cobbity DDH4	236 m	10 u	anhedral	104.8	104.6	106.4		105.3			
DM Liverpool DDH91	100.5 m	10 u	anhedral	98.6	98.9			98.8			

**Table 3** First-melt temperatures for fluid inclusions in the Hawkesbury Sandstone

Drill Hole	Depth	Tmi		Vapour	Remarks
		1	2		
		QC			
			Mean		
Kurrajong Heights No1	197.3 m	-2.8	-2.9	-2.9	15% Lunar shaped inclusion with gas bubble

An homogenisation temperature (Th) is that temperature where coexisting liquid and vapour phases mix to give a monophasic liquid and the temperature is taken to represent the depositional temperature of the enclosing mineral if corrections are made for the confining pressure and the salinity (measured in equivalent weight percent NaCl). The homogenisation temperatures of the fluid inclusions in the overgrowths for the three Hawkesbury Sandstone samples in this preliminary study probably indicate two temperatures of formation for the overgrowths. The lower temperatures are consistent with those obtained for fluid inclusions in the Hutton Sandstone (Queensland), which ranged from 82°C to 108 °C (Eadington *et al.* 1995), and for fluid inclusions in Narrabeen Group lithic sandstones, ranging from 62°C to 110°C and a second group ranging from 125 °C to 140.5 °C (McDonald and Skilbeck 1996). For one sample in this study, the temperature of first melting (Tfm) and the temperature of the last ice melting (Tmi) were also measured. The Tmi can be used to determine the salinity of the fluids enclosed in the fluid inclusion and represent the salinity of the fluids moving through the rock mass. Based on the data given in McDonald and Skilbeck (1996) the salinity of the fluids is approximately 5%. The one-off Th temperature of 169°C could indicate a

second higher temperature fluid invasion or a fluid inclusion formed in an earlier stage of the grain history.

## DISCUSSION

Wray (1995; 1997) attributed many of the large scale geomorphic features, such as solution basins, sandstone caves, in sandstone karst topography as a result of weathering of quartz cement and quartz framework grains in sandstone. Wray attributed etching of quartz grain surfaces, in rocks with high porosity, as a mechanism for loosening the grains and causing weathering. The studies of Johnson (2006) and Gentz (2006) showed that Wray's 'high porosity' in Hawkesbury Sandstone may be due to the solution of the clay and chert matrix. Johnson (2006) also showed that some small to microscopic scale geomorphic features formed as a result of the solution of quartz framework grains and the matrix. The pitted 'moonscape' texture on the weathered surface on some Hawkesbury Sandstone outcrop, depressions on rock surfaces covered with lichen and holes formed by root penetration are examples. In all cases, surficial quartz grains are truncated and the clay and chert matrix have been removed leaving greater porosity and basin-shaped depressions.

In her study, Gentz (2006) continued thin section studies of the Hawkesbury Sandstone and contributed additional observations. Gentz found siderite most commonly occurred within the clay matrix; as small crystals as rims on quartz grains (Fig 2) and in veins both within quartz grains and as veins through the rock samples (Fig. 3), mostly parallel or semi parallel to bedding. Siderite appears to preferentially replace clay minerals in the matrix rather than quartz framework. In the claystone, which are composed of a very high proportion of clay minerals, the preferential replacement of clay minerals results in parts of the claystone layers being almost entirely replaced by siderite. Significantly, Gentz found that in sandstone samples with thin claystone laminae/lenses, the siderite had replaced components of the claystone rather than the sandstone suggesting that the clay minerals, whether in the matrix of sandstone or as the predominant mineral in claystone layers is dissolved more readily than

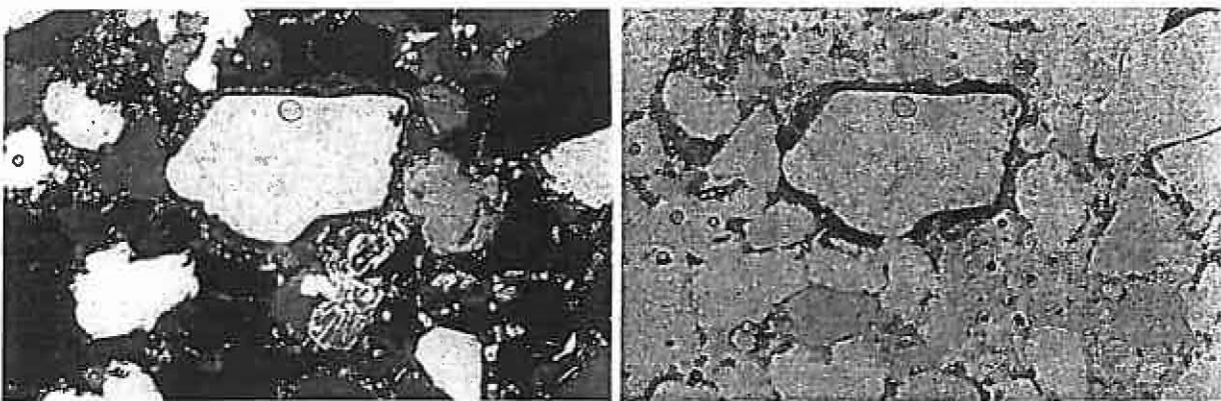


Figure 2 Siderite rim on quartz grain. Field width = 3.2 mm; RHS plane polarised light, LHS crossed polars

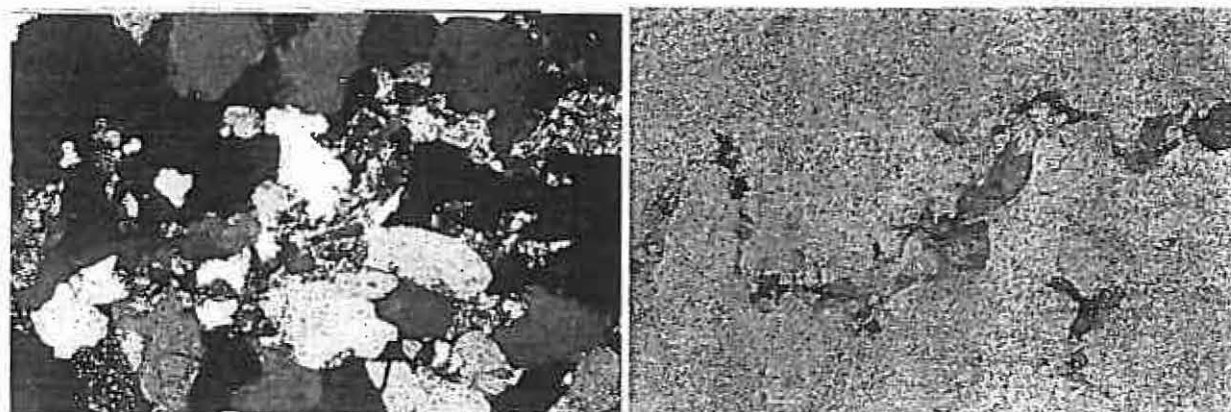


Figure 3 Siderite vein semiparallel to bedding suggesting fluid movement semiparallel to bedding. Field width = 3.2 mm; RHS plane polarised light, LHS crossed polars

quartz framework grains leading to faster weathering of finer grained beds.

### WEATHERING OF HAWKESBURY SANDSTONE

Combining the observations of Wray (1995; 1997), Gentz (2006) and Johnson (2006) the following model is proposed for the weathering of Hawkesbury Sandstone and the development of the iron stained patches and leisegang patterns in surficial Hawkesbury Sandstone:

**Stage 1** - loss of the clay matrix through solution giving fluids with increased Si ion contents

**Stage 2** - further loss of the clay matrix with precipitation of chert within the matrix; thus initially there is an increase in porosity followed by a decrease in porosity.

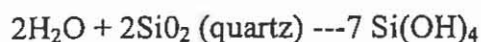
**Stage 3** - accelerated loss of the matrix with both the remaining clay minerals and the chert being dissolved, releasing more Si ions.

**Stage 4** - Precipitation of iron oxides where the rock is exposed to iron-rich fluids

**Stage 5** - Increased precipitation of iron oxide with concurrent solution of quartz framework grains, initially as small notches and surface solution followed by progressively increasing loss of the grain resulting in large embayments and alteration of the grain morphology.

The paragenesis of Hawkesbury Sandstone is complicated by the precipitation of quartz overgrowths during diagenesis and the precipitation of other secondary minerals such as siderite and calcite, during later stages of diagenesis.

Weathering agents of quartz-rich sandstones include solution, hydration and biological activity. Of these, solution appears to be the dominant process. In conditions of pH = 7 the dissolution of quartz silica can be described as follows:



### WATER MOVEMENT IN THE HAWKESBURY SANDSTONE

Published and unpublished petrographic data show that there is variability in mineralogy between different facies of the sandstone, irrespective of the facies classification used. This variability in composition is likely to be an important factor in the instability in Hawkesbury Sandstone cliffs in the Southern Coalfield. This is because the differential weathering processes may be dependent on sandstone composition.

## HAWKESBURY SANDSTONE

Thin section analysis of the Hawkesbury Sandstone provides useful data which can be used to predict the movement of water through the unit. Clay minerals are more easily weathered from the matrix allowing the development of pore space in the sandstone (Franklin 2000). Evidence in thin sections indicated that as clay minerals are removed they may be preferentially replaced by siderite which in turns reduces primary porosity. Selley (2000) found that kaolin, due to its large crystal formation, reduces porosity; illite with its fibrous crystal structure, has a greater impact on permeability due to the fact that illite crystals restrict the connectivity of pore spaces as they grow between grains.

The examination of the different facies by Johnson (2006) and the study of Griffith (1986) highlighted textural and mineralogical differences between facies in the Hawkesbury Sandstone. These differences affect the weathering of the sandstone and are important factors to consider when attempting to predict and model the likelihood of cliff instability in the Hawkesbury Sandstone.

Thin section studies clearly show that organisms such as lichens, algae and larger rooted plants accelerate the weathering of Hawkesbury Sandstone, especially on a microscale. Weathering along fractures and joints is probably accelerated thus increasing the potential for blocks to become unstable in steep-walled gorges over time because of bedding planes and tectonic joints. Block instability may be a natural process not only a mining induced process. If instability of cliff faces in gorge areas has increased as a result of mining, it would have been caused by some mechanism other than increased weathering along mining induced fractures.

It is to be expected that the most unstable cliff sections are those with sandstones that have a high porosity and loss of a majority of clay and chert matrix. These factors lead to the sandstone becoming readily friable. Facies bounded by significant bedding planes and tectonic joints would also have a high chance of becoming unstable due to the large amounts of water transported along the bedding planes causing significant solution. Rapid weathering along bedding planes allows for undercutting and results in blocks falling out of overlying strata in gorge areas. Sections of sandstone cliff with low porosity and high amounts of iron oxide filling porosity would be expected to be the most stable cliff sections.

Water movement through the Hawkesbury Sandstone is not laterally continuous over long distances Bedding plane surfaces are planes of weakness and offer porosity for water transport in the system. There are therefore several orders of water movement through the system. The 5th order bedding planes transport significant amounts of water, and therefore weather under the action of quartz solution relatively quickly. The lower order cross bed planes terminate much quicker and therefore experience much less water transport. The dominant role of bedding planes and joint systems means that horizontal water transport is more common than vertical transport in the Hawkesbury Sandstone.

### REFERENCES

- CONAGHAN P.J AND JONES J.B. 1975. The Hawkesbury Sandstone and the Brahmaputra: A depositional model for continental sheet sandstones, *Journal Geological Society of Australia*. 22, 2765-283.
- CONAGHAN P.J. 1980. The Hawkesbury Sandstone: Gross Characteristics and Depositional Environment. In: Herbert, C. and Helby, R. (eds). *A Guide to the Sydney Basin*, Geological Survey of New South Wales, Bulletin 26, Department of Mineral Resources.

- DEPARTMENT OF PRIMARY INDUSTRIES (DPI) NSW. 2006. 'Mine Subsidence', Primefact 21, <http://www.dpi.nsw.gov.au/aboutus/resources/factsheets/primefacts/?a=56763> accessed: 06/06.
- EADINGTON, P.J., HAMILTON, P.J. AND GREEN, P. 1995. Hydrocarbon fluid history in relation to diagenesis in the Hutton Sandstone, south west Queensland. Petroleum Exploration Society of Australia Conference, Adelaide, 601-618.
- FRANKLIN B.J. 2000. Sydney Dimension Sandstone: The Value of Petrography in Stone Selection and Assessing Durability. In: McNally, G.H. and Franklin, B.J. (Eds). *Sandstone City: Sydney's Dimension Stone and Other Sandstone Geomaterials*, Environmental, Engineering and Hydrogeology Group (EEHG) Geological Society of Australia, 98-117.
- FREED S.J. 2005. The Reservoir Characteristics of the Hawkesbury Sandstone in the Southern Highlands in Relation to Sydney Water Shortages, BEnvSc Honours Thesis, University of Wollongong, Wollongong.
- GENTZ M. L. 2006. A Pre-Mining Study of the Hawkesbury Sandstone and Aquifer Characteristics of Potential Longwall Mining Area, Appin Area 3. BEnvSc Honours Thesis, University of Wollongong, Wollongong.
- GREY I. AND ROSS J. 2003. Groundwater Investigation for Contingency Drought Relief in the Sydney Region, Sydney Water Corporation and Sydney Catchment Authority, Parsons Brinckerhoff.
- GRIFFITHS A. 1986. Fluvial Architecture, sedimentology, petrology and genesis of the Hawkesbury Sandstone. BSc(Hons) Thesis, University of Wollongong.
- JOHNSON M.D. 2006. Solutional Weathering of the Hawkesbury Sandstone and Cliff Instability, BEnvSc Honours Thesis, University of Wollongong, Wollongong.
- JONES B.G. AND RUST B.R. 1983. Massive Sandstone Facies in the Hawkesbury Sandstone, a Triassic Fluvial Deposit Near Sydney, Australia. *Journal of Sedimentary Petrology*, 53(4), 1249-1259.
- LARRATT H.C.O. AND KURU A. 1988. 'The Coal Industry', Back to Basics: Proceedings of a conference of the HR Nicholls Society at Newcastle (Feb19-21 1988), <http://www.hrnicholls.com.au/nicholls/nichvol4/vol49the.htm>, accessed: 06/06.
- MCDONALD S.J. AND SKILBECK C.G. 1996. Authigenic fluid inclusions in lithic sandstone: a case study from the Permo-Triassic Gunnedah Basin, New South Wales. *Australian Journal of Earth Sciences*, 43, 217-228.
- MIALL A.D. AND JONES, B.G. 2003. Fluvial Architecture of the Hawkesbury Sandstone (Triassic), Near Sydney, Australia. *Journal of Sedimentary Research*, 73(4), 531-545.
- SELLEY R.C. 2000. *Applied Sedimentology: Second Edition*, Academic Press, San Deigo.

# EFFECTS OF IGNEOUS INTRUSIONS ON COAL MEASURES OF THE SOUTH AFRICAN KAROO BASIN AND ASSOCIATED COAL SEAM GAS

Kaydy Pinetown<sup>1</sup>, Abouna Saghafi<sup>2</sup> and Phil Grobler<sup>3</sup>

<sup>1</sup> CSIRO Petroleum

PO Box 136, North Ryde, NSW, 1670, Australia

<sup>2</sup> CSIRO Energy Technology

PO Box 330, Newcastle, NSW, 2300, Australia

<sup>3</sup> Sasol Mining Ltd

Private Bag X1015, Secunda, 2302, South Africa

## ABSTRACT

Coal measures of the Highveld region of South Africa were deposited in the Karoo Basin during the Late Permian to Early Triassic. A volcanic episode that took place from the Early Jurassic until the Early Cretaceous, is of particular interest as associated intrusions are common in the coalfield and have resulted in structural complications and regional devolatilisation of the coal.

In addition to introducing structural complexities to the sedimentary succession and releasing gas into the voids, dolerite intrusions have made considerable amounts of coal reserves unsuitable for utilisation. The size of the devolatilised zone surrounding each intrusion is extremely variable ranging from <1 m to ~40 m thick, depending on intrusion size and orientation. Rocks proximal to the intrusions have commonly been contact metamorphosed such that they are brittle and porous.

Measurements of gas reservoir properties of coals in the vicinity of the intrusions indicate that localised, high gas contents are present. Measurements of porosities and methane adsorption isotherms show that gas storage capacities are increased. These increases, as well as increases in coal gas diffusivities are a result of increased pore volumes and internal surface areas due to the carbonisation. The effect of contact metamorphism is apparent in volatile matter contents which range from ~21% for distal samples to ~11% for samples adjacent to the dykes.

## INTRODUCTION

Permian coals are extensively mined in the Highveld coalfield of the Mpumalanga Province, South Africa. These coals are predominantly used for production of synthetic fuels through surface gasification and are generally classified as medium to high volatile bituminous and sub-bituminous coals. The coal seams have been intensively intruded by dolerite dykes and sills resulting in significant displacement and devolatilisation. Mining takes place at depths of ~110 m, where in situ gas contents reach up to 1.3 m<sup>3</sup>/t (Lloyd and Cook, 2004). Dangerous mining conditions are encountered around intrusion zones as the coals and other rocks surrounding the intrusions are fractured and unstable. Furthermore, these zones contain enhanced concentrations of gas, consisting predominantly of methane. This scenario is likely to give rise to outburst events and methane-dust explosions.

Anderson (1995) reported five methane outbursts at Twistdraai Mine in 1993. The outbursts were reported to be associated with dykes and sills, where pockets of gas have been encountered. Davies *et al.* (2000) also described a large methane and dust explosion from Middelbult colliery following the ignition of methane. Both these collieries are located in an area of the Highveld coalfield where numerous dolerite intrusions intersect the coal seams.

The intrusions appear to have caused entrapment of gases released from thermal metamorphism of the coals and they have also increased the friability by increasing porosity. Methane released during the dolerite intrusions was probably trapped in the coal seams and adjacent sediments, creating pockets of gas. The intrusions are likely to have increased gas storage properties as well as diffusivities such that gas release during fracturing is enhanced. The intrusions would have also reduced mechanical strengths of the coals and increased the chance of gas outbursts. Furthermore, the friability of coal in the vicinity of dykes would increase dust generation, which, combined with methane release, could lead to gas-dust explosions. Similarly, contact metamorphism of the roof rocks has led to weakness and instability, resulting in an increase in the propensity of outburst events (Anderson, 1995; Davies *et al.*, 2000).

The current study was initiated to investigate entrapment of methane in coals associated with igneous intrusions and its sudden release during mining.

#### **GEOLOGICAL SETTING AND DOLERITE INTRUSIONS IN THE HIGHVELD COALFIELD**

The Karoo Basin of South Africa contains numerous coal seams and was formed during Late Carboniferous with infilling starting during the Early Permian (see Figure 1 for location and stratigraphy). Glacial material was deposited on the undulating pre-Karoo floor, forming glacial tillite of the Dwyka Group. This marked the beginning of sedimentation of the Karoo Supergroup. The main coal seams were formed by marine transgressions during the Late Permian to Early Triassic as a result of accumulation of interbedded sandstone and siltstone cyclic units forming the Ecca Group of the succession. Coal formation was followed by deposition of the Beaufort Group, and the Molteno, Elliott and Clarens Formations. The end of formation of the Karoo Supergroup is marked by extrusive and intrusive igneous activity and represented by dolerite intrusions in the coal seams (Smith *et al.*, 1993). The most vertically extensive megasequence of the Karoo Supergroup exceeds 6 km in thickness (Catuneanu *et al.*, 1998). There are five coal seams recognised in the Highveld coalfield with the two lower seams absent towards the southern and eastern parts (Figure 2). The Number 4 Lower coal seam is the primary mined seam and is well developed throughout the Secunda area. Its average thickness varies from less than 1 m to up to 12 m (Snyman, 1998).

A volcanic episode during the Early Jurassic represents the beginning of the breakup of Gondwana (Stratten, 1986). This felsic volcanism continued until the Early Cretaceous, resulting in numerous dolerite dykes and sills intersecting the coal seams. The thickness of dolerite dykes in the region varies between ~0.1 m and ~5m, whereas the sills are up to ~40 m thick. The sizes of the devolatilised zones surrounding the intrusions are extremely variable ranging from <1 m to ~20 m thick on either side of the intrusions. The dykes do not displace the coal seams or adjacent strata and their metamorphic effect is less severe than that of the sills. Displacement caused by the sills is generally equal to the thickness of the sill. A high frequency of joints and faults occur in coal seams intersected by the dolerite sills.

## KAROO BASIN INTRUSIONS

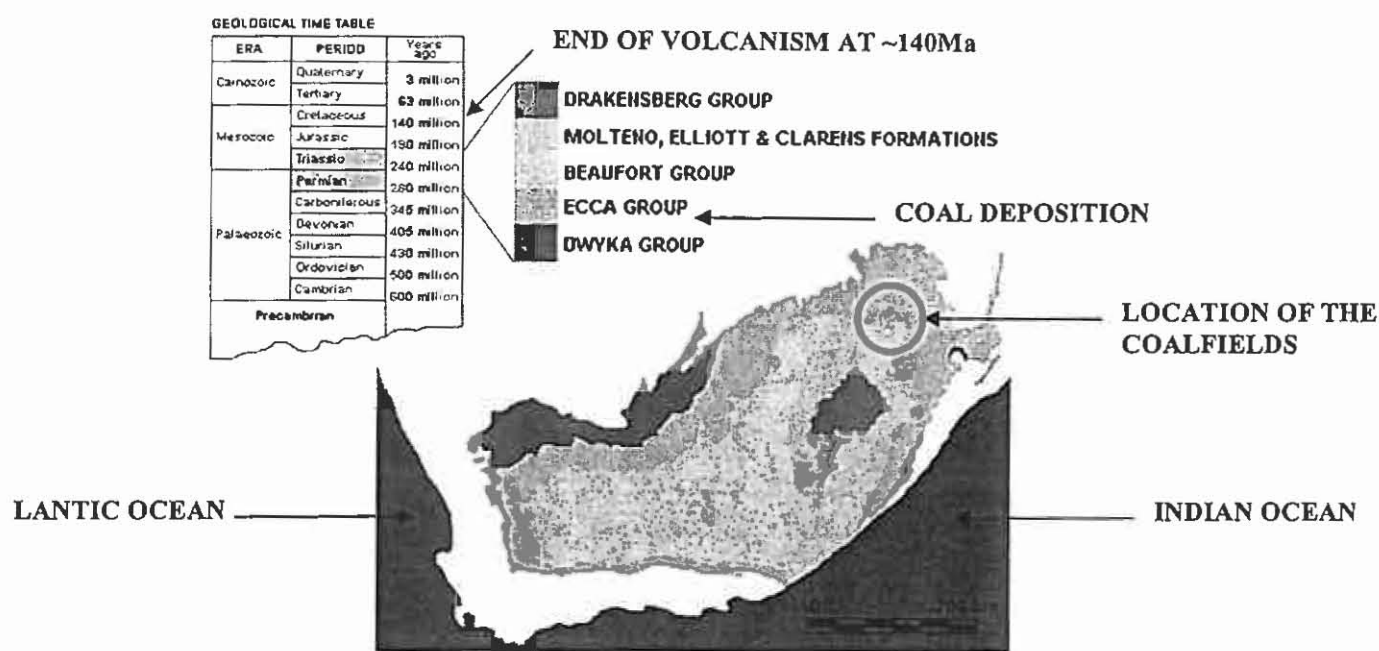


**Figure 1** Stratigraphic column showing subdivisions of the Karoo Supergroup and a map of southern South Africa showing locality of the Highveld Coalfield

The roof and floor lithologies primarily consist of sandstone and siltstone, which, in the vicinity of intrusions, have generally been contact metamorphosed and are brittle and porous. These intrusions introduced structural complications and regional devolatilisation, sterilising considerable coal reserves in terms of utilisation.

### SAMPLING AND ANALYSIS

Fourteen samples of contact metamorphosed and unaffected coals were collected from the Middelbult underground mine. At Middelbult, coal is extracted using a room and pillar mining method. The pillars are approximately 20 m x 20 m. Coal samples were obtained from the main mined seam (Number 4 Lower coal seam), including one sample of a dolerite dyke from the same locality. Samples were collected along a freshly advanced heading at various distances from a ~2.4 m wide dyke. Samples were collected ~0.5 m to ~60 m on either side of the dyke.

Visual investigation by the mine geologist and drilling information suggest that the dyke has affected and devolatilised coal up to 20 m on each side. The average coal seam thickness at the sample location is ~3.4 m and the seam is ~90 m below surface. Reservoir properties of coals, including gas adsorption isotherms, gas diffusivities, coal porosities and coal petrography were measured. For the gas adsorption isotherms a gravimetric method developed at CSIRO (Saghafi, 2003; Saghafi *et al.*, 2006a) was used whereby coal is exposed to gas pressures of up to 6 MPa at 27°C. The mass of adsorbed gas is measured against gas pressure. Crushed coal samples of ~300 g and 90 to 150 µm particle size were used for adsorption isotherm measurements.

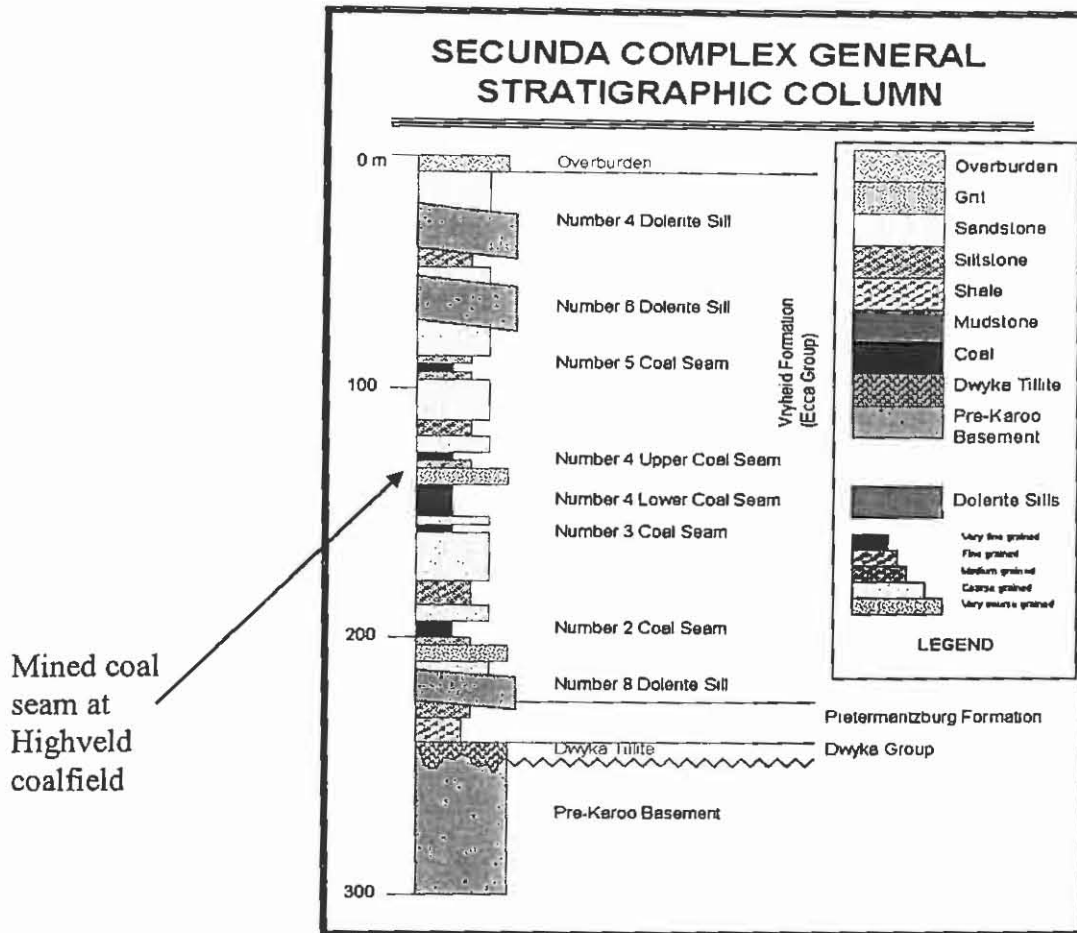


**Figure 2** Generalised stratigraphic column for the Secunda area

The diffusion coefficient of methane through solid coal was measured at the CSIRO laboratory as described in Saghafi *et al.* (2006a). Coal porosity was measured by a mercury intrusion method (Saghafi, 2003).

## RESULTS AND DISCUSSION

The samples have ash yields of 17 to 28% and moisture contents of 2 to 6%. The samples show progressive devolatilisation according to distance from the dyke (Figure 3a). The heating effect is evident in volatile matter results which range from ~21% for the more distant samples to as low as ~11% for samples adjacent to the dyke. These results differ substantially from the average volatile matter content for the area which varies between ~22% and ~26%. The volatile matter measurements are consistent with the petrographic results undertaken on six of the samples, which show increased vitrinite reflectance (VR) values for samples close to the dyke with gradual decreases away from the dyke (Figure 3b). The mean maximum vitrinite reflectance values ( $R_{v,max}$ ) for contact metamorphosed coals proximal to the dyke are ~4.0 % and for the more distant samples the values are ~0.8 %. The  $R_{v,max}$  values for unaffected coals obtained in this area is ~0.7% (Boshoff *et al.*, 1991). The VR values are in general agreement with results obtained by Stewart *et al.* (2005) for coals surrounding a 10 m thick dyke in the Springfield (No. 5) coal measures in Harrisburg, Illinois, where VR values

## KAROO BASIN INTRUSIONS

increase from 0.69%, for samples greater than one dyke thickness away, to ~5% for samples at the dyke/coal contact.

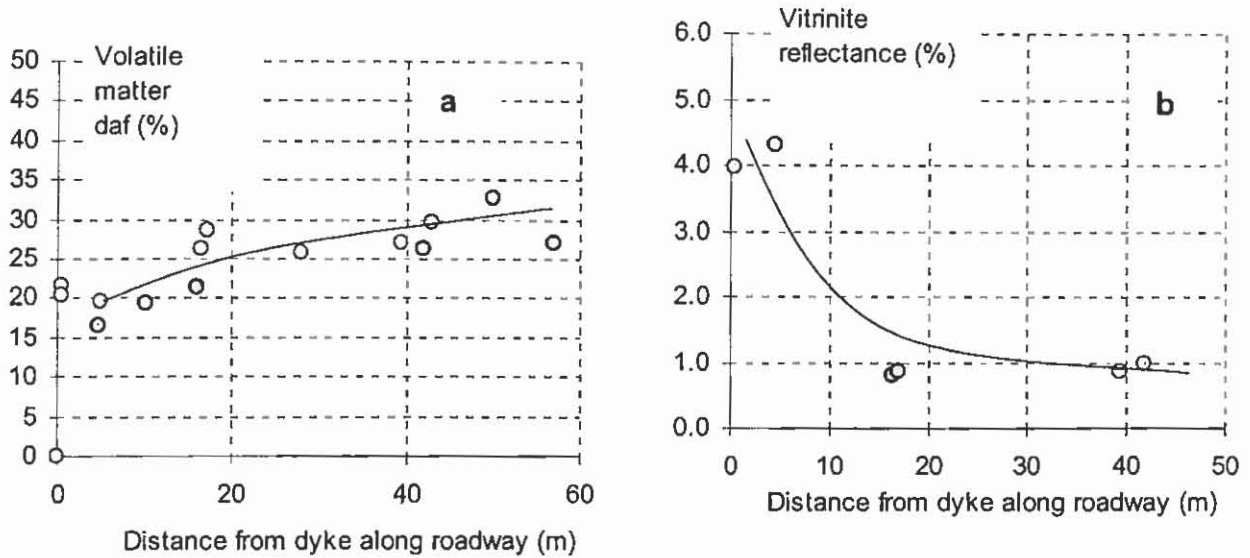


**Figure 3** Plots of coal rank parameters according to distance from dyke, showing effects of contact metamorphism on volatile matter content and VR

Gas is retained in coal by two mechanisms: free gas in macropores and adsorption on micropore surfaces (Saghafi, 1987). Measurements of porosities and methane adsorption isotherms show that gas storage capacity of the contact metamorphosed coal is increased (Figure 4a and 4b). Diffusivities are also increased for coals proximal to the intrusion (Figure 5).

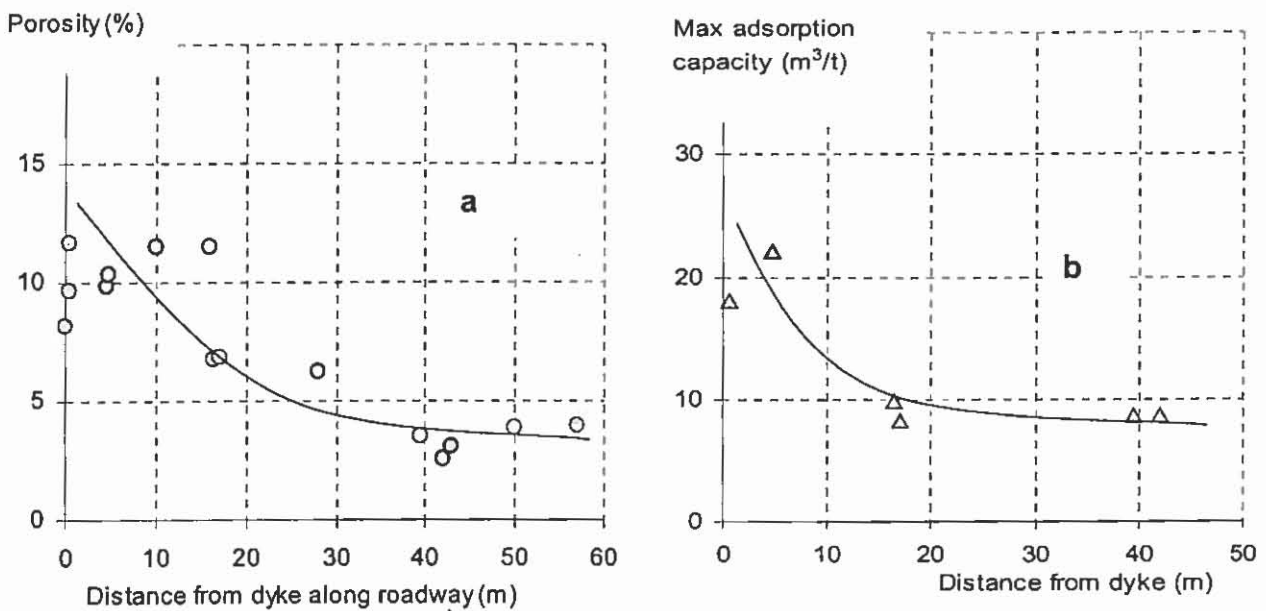


**Figure 4** Plots of gas storage parameters according to distance from dyke, showing effect of contact metamorphism on porosity and maximum methane adsorption capacity

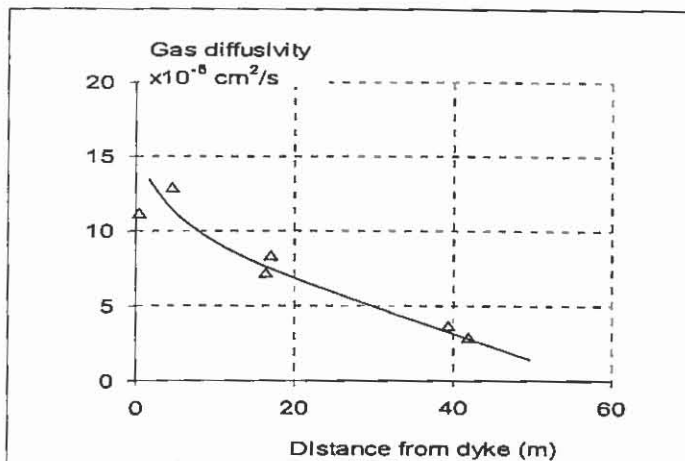


**Figure 5** Relationship between methane diffusivity and distance from dyke

The increases in storage capacity and gas diffusivity could be a result of increased in pore volumes and internal surface areas resulting from the carbonisation. The enhancement may also be due to a loss of bitumen from micro-pores during the contact metamorphism (e.g. Levine, 1992). This enhancement of methane storage capacity can partly explain the existence of high pressure gas pockets in the vicinity of dykes and the subsequent gas outbursts encountered in these areas.

The current study shows that gas released during igneous intrusion may be effectively trapped by coals because of the associated increased storage capacities and its release during mining is likely to be facilitated by increases in gas diffusivity. A recent study on CO<sub>2</sub> sequestration potential of South African coals has also shown that storage and flow properties of these coals were enhanced in proximity of igneous intrusions (Saghafi et al., 2006b). However further study on these coals and surrounding rocks are required to further elucidate factors affecting the zone of high gas contents associated with igneous intrusions.

## CONCLUSIONS

The current study assists in quantifying gas retention capacities and gas flows for coals affected by igneous intrusions to predict 'gassy' areas during mining. The results show that enhanced methane storage capacity and increased gas diffusivity of coal in the vicinity of dolerite intrusions can partly explain the occurrence of high pressure gas pockets encountered during mining through dykes in some coal mines in the Highveld region. Further studies would enable more accurate prediction of the behaviour of coal seams during mining due to gas migration and concentration, and provide better understandings of coal seam gas reservoirs.

## ACKNOWLEDGEMENTS

The authors wish to thank Douglas Roberts at CSIRO Energy Technology for the laboratory work and conducting adsorption and diffusivity tests. Our appreciation is extended to the staff and management of the Middelbult Mine and Sasol Mining for assisting with the collection of coal samples. We also thank Mr Nigel Russell and Neil Sherwood of CSIRO Petroleum for editorial comments.

## KAROO BASIN INTRUSIONS

### REFERENCES

- ANDERSON S. B. 1995. Outbursts of methane gas and associated mining problems experienced at Twistdraai Colliery. In: Lama R. ed. *Proceedings of the Int. Symposium Cum Workshop on Management & Control of High Gas Emissions & Outbursts*, pp. 423-434, Wollongong.
- BOSHOFF H. P. BERGH C. E. & KRUSZEWSKA K. J. 1991. Analyses of coal product samples of producing South African collieries. *Bulletin Division of Energy Technology, CSIR, Pretoria* **105**, 56pp.
- CATUNEANU O. HANCOX P. J. & RUBIDGE B. S. 1998. Reciprocal flexural behaviour and contrasting stratigraphies: A new basin development model for the Karoo retroarc foreland system, South Africa. *Basin Research* **10**, 417-439.
- DAVIES A.W. ISAAC A.K. & COOK P.M. 2000. Investigation of a coal-mine explosion and relevance of risk assessment. *Mining Technology: IMM Transactions section A* **109(2)**, 61-69(9).
- LEVINE J. 1992. Oversimplification can lead to faulty coalbed gas reservoir analysis. *Oil and Gas Journal* Week of November 23, 63-68.
- LLOYD P. & COOK A. 2004. Methane release from South African coal mines. *Journal of the South African Institute of Mining and Metallurgy* **105**, 483-490.
- SAGHAFI A. JEGER C. TAUZIEDE C. & WILLIAMS R. J. 1987. A new computer program for gas flow into drainage boreholes. In: *22nd International Conference of Safety in Mines Research Institutes*, pp. 147-158, Beijing.
- SAGHAFI A. 2003. Aspects of gas storage and flow properties of Australian coals. In: *The 2<sup>nd</sup> Annual Australian Coal Seam & Mine Methane Conference*, Brisbane.
- SAGHAFI A. FAIZ M. & ROBERTS D. 2006a. CO<sub>2</sub> storage and diffusivity properties of Sydney Basin coals. In Press, *the International Journal of Coal Geology*.
- SAGHAFI A. GROBLER P. PINETOWN K. & VAN HEERDEN J. 2006b. CO<sub>2</sub> storage potential of South African Coals and gas entrapment due to igneous intrusions. In: Choy C., Dai S. & Jin K. eds. *Proceedings of the 23<sup>rd</sup> Annual Meeting of the Society for Organic Petrology*, vol. 23, pp. 210-212, Beijing.
- SMITH R. M. H. ERIKSSON P. G. & BOTHA W. J. 1993. A review of the stratigraphy and sedimentary environments of the Karoo-aged basins of Southern Africa. *Journal of African Earth Sciences* **16(1/2)**, 143-169.
- SNYMAN C. P. 1998. Coal. In: Wilson M. G. C. & Anhaeusser C. R. eds. *The Mineral Resources of South Africa*, Council for Geoscience **16**, 136-205.
- STRATTEN T. 1986. Environmental and stratigraphic setting of the Karoo Basin and its mineral deposits. In: Anhaeusser C. R. & Maske S. eds. *Mineral Deposits of Southern Africa*, Geological Society of South Africa, 1863-1873.
- STEWART A. K. MASSEY M. PADGETT P. L. RIMMER S. M. & HOWER J. C. 2005. Influence of a basic intrusion on the vitrinite reflectance and chemistry of the Springfield (No. 5) coal, Harrisburg, Illinois. *International Journal of Coal Geology* **63**, 58-67.



# MULTIPLE DATA SETS USED TO EVALUATE GEOLOGY AND STRUCTURE: BOWEN AND SURAT BASINS QUEENSLAND

E. Prendergast<sup>1</sup>, B. Healy<sup>2</sup>, D. Kyan<sup>3</sup>, Z. Demidjuk<sup>2</sup>, G. McCaughan<sup>1</sup>,  
C. Woodfull<sup>1</sup> and S. Munroe<sup>2</sup>

SRK Consulting

<sup>1</sup>PO Box 2184, Greenhills NSW 2323

<sup>2</sup>Level 6, 44 Market St, Sydney NSW 2000

<sup>3</sup>Level 9, Suite 9c, 300 Adelaide Street, Brisbane QLD 4000

## ABSTRACT

A regional structural interpretation of the central Queensland Bowen, and southeastern Queensland and northern NSW Surat Basins is being used to improve the understanding between regional scale and known mine scale structures. To correlate the basement structures with the history of the basin, SRK is compiling and interrogating multiple geological and geophysical datasets to enable evaluation of basement geology, depth to basement, initiation and reactivation of structures in the Bowen and Surat Basins and surrounding areas. In order to improve the understanding of, and display, these basement features, a new 4-D regional structural/basin framework for the Bowen and Surat Basins is also being generated. This model is being constructed to provide coal exploration and mining, and oil and gas exploration, and local base and precious metals exploration with a more integrated geological framework for ongoing sub-regional to local scale geological risk based studies.

The model is being constructed from a range of available regional to lease scale geophysical and geological datasets. These datasets have been sourced from both public and company data and are being utilised together to generate a more robust structural and tectonic model than could be generated with any one single dataset.

The study area has been divided into two modules, a northern and southern module, predominantly covering the exposed Bowen Basin and Surat Basin, respectively. The study involves a number of sponsoring mining and/or exploration companies that are mainly interested in coal, coal seam methane and/or natural gas.

This paper provides some interim results from the work in progress. The results of the study are due for release to sponsors in September, 2007.

## INTRODUCTION

The Bowen Basin is located in central to southeastern Queensland and the overlying Surat Basin is in southeastern Queensland and northern NSW (Figure 1). Sedimentation in the Bowen Basin began in the Early Permian and ceased at the beginning of the Lower Jurassic. An unconformity exists between the Bowen Basin and the Surat Basin with the mid Lower Jurassic basal sediments of the Surat Basin being approximately 30 million years younger than the youngest Bowen Basin sediments. Both basins contain extensive coal measures, coal bed methane and gas and are therefore of great interest to the energy resources sector. A key focus of this study is the structural evolution and development of a regional model for these basins.

The structural evolution of the basement has an important influence on overlying sedimentary basins, including orientation of basin, depositional history of sediments, including sediment type, source rocks, palaeocurrent directions, the dominance of fluvial or marine palaeoenvironments, and concomitant and post-depositional magmatic events. Much of the tectonics/structural evolution of the basement is reflected in the structural history of the basins and early structures are commonly sites of reactivation due to new stresses resulting from reconfiguration of tectonic plates.

The basement to the Bowen and Surat Basins includes, generally from west to east, the Thompson, Lachlan and the New England Fold Belts. In places the Surat Basin sits directly on basement rocks and Bowen Basin sediments are absent. Knowledge of the types of boundaries between these fold belts, the location of sub-surface lithological boundaries and also the tectonic stresses related to ongoing plate tectonic movements is critical in the understanding of the history of the Bowen and Surat Basins. Stresses at regional scale will control small scale structures (mine site) so it is useful to be able to understand the relationship between the regional scale features and the known local structures.

### **OBJECTIVES**

The aim of the study is to provide quality geological information to resource companies interested in

- exploring for, or mining of mainly coal, coal seam methane, gas or petroleum in the Bowen or Surat Basins and
- exploring for base metals and/or gold in basement rocks such as the Drummond Basin and New England Fold Belt on the exposed margin of the basins or located under shallow <200-500m of basin and younger sediments.

The project is divided into a northern module, principally covering the Bowen Basin and a southern module that covers the southern area of the Surat Basin in Queensland and northern NSW (Figure 2). The areas were separated on the basis that many resource companies are focussed on one rather than both areas. Both modules may be obtained by clients who have interest in the two modules.

The project began by compiling and processing, where necessary, the datasets.

#### **The data sets include:**

- remotely sensed data - geophysics (magnetics, gravity, seismic, radiometrics), digital elevation and landsat/ASTER
- geological data - coal, petroleum and water drill hole records, regional geology, faults, igneous events and mapped and mine scale
- structural interpretation – based on several/all data sets.

Data has been sourced from published, open file and/or company files. The companies/government organisations currently involved in the SRK project are the Geological Survey of Queensland, BHP Coal Pty Ltd, Santos QNT Pty Ltd, Arrow Energy NL, Excel Coal Ltd, Rio Tinto Group, AMCI Australia Pty Ltd and Anglo Coal Pty Ltd.

#### **The outcomes produced will include compilations and/or interpretations of:**

- Geophysics – magnetic, gravity, seismic and radiometric data
- Basement geology – borehole data provides a view of the basement at depth, solid geology, magnetics and gravity

## GEOLOGY AND STRUCTURE BOWEN-SURAT BASINS

- Surface geology
- Structure
- Igneous
- Top of Surat Basin – Lower Cretaceous
- Base of Surat Basin – Lower Jurassic – Precipice Sandstone
- Top of Bowen Basin – top of Triassic – Moolayember Formation
- Base and/or top of several important horizons in the Surat and Bowen Basins – example Walloon Coal Measures (Surat Basin) Rangal Coal Measures (Bowen Basin)
- Depth to basement model.
- 

The GIS based product is produced in MapInfo and Arc GIS.

**Additionally the project includes and provides both a**

- Literature review and
- Time-Space Chart.

### **METHODOLOGY**

The study is divided into a compilation/processing stage and an interpretation stage.

#### **Compilation**

The compilation of datasets is integral to the study. The compilation stage is well advanced and involves obtaining datasets from company and published sources. Compilation of datasets also requires re-formatting each dataset to GIS compatible format and the same map projection. This allows all the datasets to be presented and compared with all other datasets. This is necessary for analysing and displaying datasets, for interpretations of similar datasets and comparisons to be made between different types of datasets, for example surface geology with magnetic or gravity images.

Early in the compilation stage a Time-Space Chart for the geological evolution of the basement, basins and post-basin tectonic events was produced. The chart was primarily based on published literature and now provides a preliminary guide for ongoing work. For the project area eleven tectonic events have been tentatively defined and these potentially had significant roles in producing faults and/or fault reactivation from the Early Palaeozoic to the present. Eight of these events occurred from the Early Permian. As the SRK interpretation continues the Time-Space chart will be reviewed and updated as required.

#### **Interpretation**

The interpretation stage is under way but is still in the early phases. The preliminary results include structural and basement geology interpretations. These two interpretations are based on several diverse datasets including magnetics, gravity, oil/gas/water boreholes, surface geology, seismic, published, and company mine site data and interpretations. Datasets from both NSW and QLD are being accessed.

The interpretation will:

- produce a new and unique view of the basement geology and structure
- Allocate/verify structural history

**Regional Structural Interpretation: to date**

The regional structural interpretation includes faults, folds and lineaments. Initially the interpretation is done at 1:100,000 scale. For the structural interpretation the main data sets being used are magnetics, gravity, seismic and mapped geology. Each structural feature, known and interpreted, is attributed within the GIS platform with all relevant geological information contained in the original data sets and additionally any interpretations of the datasets by the SRK team. For instance, each fault is being divided into style (for example thrust, normal, normal with strike-slip motion and so on), with geometry (dip, dip direction, orientation, displacement, sense of movement, basement/non-basement involvement) and when possible the fault is assigned an age (including age of initiation and reactivation/non-reactivation). Therefore in the GIS platform each fault has its own unique information and this is available and accessible together with the structural interpretation map on which the fault occurs.

In the final product there will be a description of each structure within the GIS platform that includes as much information as is available and/or generated from the appropriate datasets. These structural interpretations can be compared with all the appropriate datasets, for example magnetics, gravity, at any time by the client.

**Basement Geology: to date**

The preliminary basement geology interpretations for the two modules are well under way. Magnetic images are playing an important role in the interpretation of the basement geology in both modules. The sub-surface of the Southern module includes several geological domains including the Thompson Fold Belt, Lachlan Fold Belt and New England Fold Belt and the definition of their boundaries is important in establishing the structural history of the overlying basins. The northern module includes the Anakie Inlier, Drummond Basin and the northern part of the New England Fold Belt.

The gravity images are also being used to aid in establishing the sub-surface geology. The gravity interpretation includes both regional, large scale, and smaller scale structures. The interpreted large scale structures infer that there are some major continental sutures in and around the project modules.

**New view of Basement and Basins**

One of the ongoing targets of the project is to establish a 'new view' not only of the basement but of a number of marker horizons that are critical in understanding the basement of the Bowen and Surat Basins. This may lead to a re-appraisal of the resource exploration program or hydrocarbon (gas) drainage controls and/or energy related issues.

**PRELIMINARY RESULTS**

The project is in progress at the time of writing this paper so the final results are unavailable. The data sets are currently being analysed by a geological team and interpreted both separately and together to produce an integrated and iterative interpretation. This process will culminate in a structural model that incorporates the geology and structure of basement with basin and post-depositional structural and/or igneous events.

Some of the preliminary interpretations are available and include the basement geology and structural interpretations. Images of these will be displayed at the symposium along with the other data sets that will be of benefit in the final product.

## GEOLOGY AND STRUCTURE BOWEN-SURAT BASINS

### ACKNOWLEDGEMENTS

The authors would like to thank, BHP Coal Pty Ltd, Santos QNT Pty Ltd, Arrow Energy NL, Excel Coal Ltd, Rio Tinto Group, AMCI Australia Pty Ltd and Anglo Coal Pty Ltd for providing financial support and data to this project. The authors would also like to thank the Department of Natural Resources and Mines, Qld for their financial support, providing data for the project and for their ongoing interest in this project.

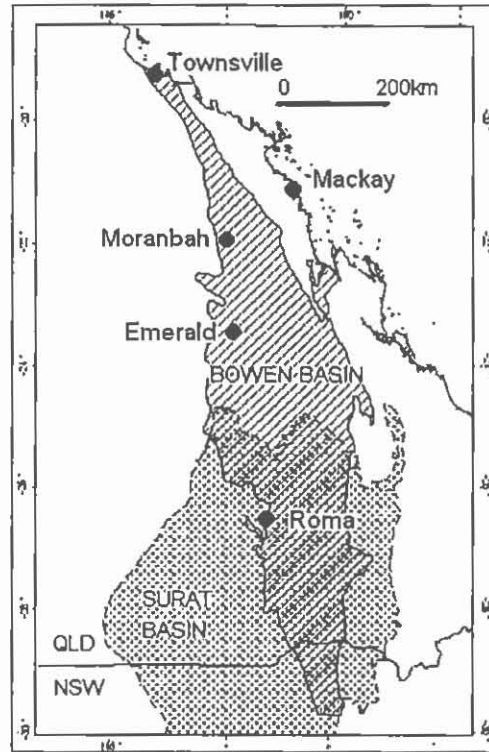


**Figure 1** Bowen and Surat Basins. Diagonal line pattern represents the Bowen Basin; shaded pattern represents the Surat Basin; Qld coastline and state border shown; Grid is GDA 94 Zone 55.

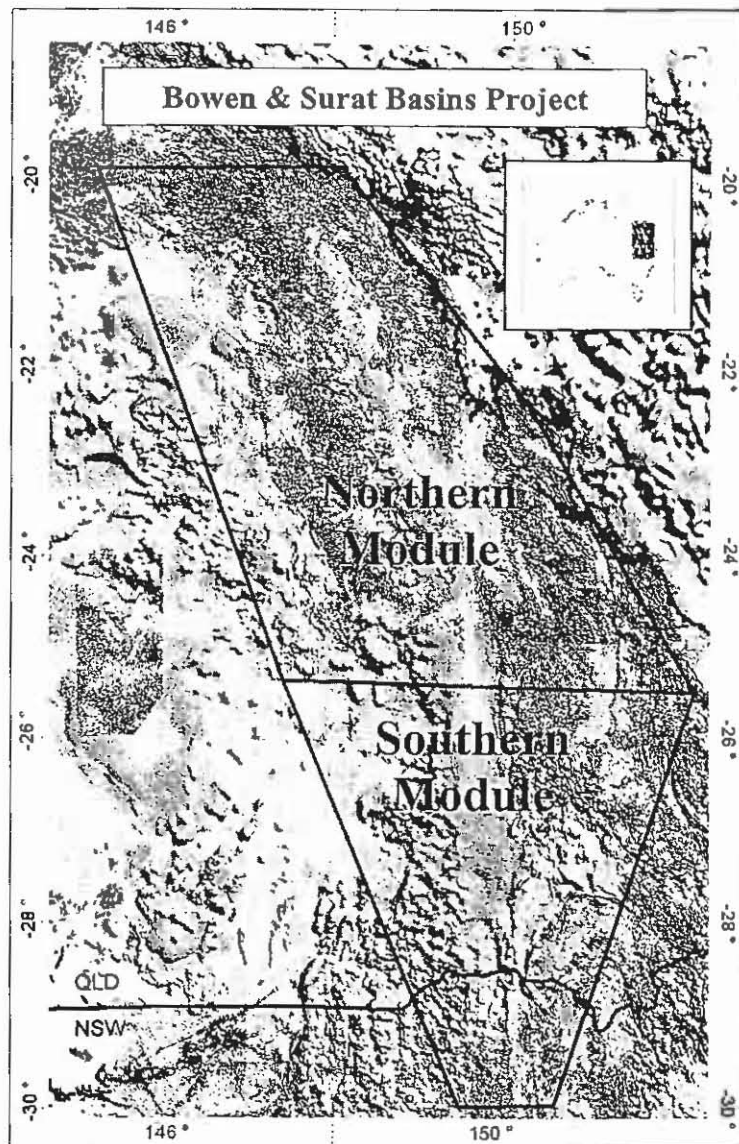


**Figure 2.** Bowen and Surat Basins Project area showing northern and southern modules with background mosaic of magnetic images. Inset shows the location of project area. Grid is GDA 94 Zone 55; coastline and state borders shown; for scale base of southern module is 110km.

# GAS RESERVOIR PROPERTIES OF SYDNEY BASIN COALS AND THEIR IMPACTS ON CO<sub>2</sub> SEQUESTRATION

Abouna Saghafi<sup>1</sup>, Mohinudeen Faiz<sup>2</sup> and Doug Roberts<sup>1</sup>

1 CSIRO Energy Technology  
P.O. Box 330, Newcastle, NSW 2300, Australia

2 CSIRO Petroleum  
P.O. Box 136, Nort Ryde, NSW 1670, Australia

## ABSTRACT

One currently investigated option for the reduction of greenhouse gases in Australia is the disposal of carbon dioxide (CO<sub>2</sub>) in coal seams. In addition to favorable geological conditions, optimal storage and flow properties of gas reservoirs are vital to the success of CO<sub>2</sub> sequestration projects. In order to study the interaction of CO<sub>2</sub> with coal seams of the Sydney Basin, forty coal samples from various Sydney Basin coalfields were measured and studied to enable the evaluation of their suitability for CO<sub>2</sub> sequestration. Coal rank for most samples studied varies from high volatile bituminous to medium volatile bituminous (R<sub>o</sub> max of 0.6 to 1.5%). The sample depths varied from less than 30 m to more than 700 m. A gravimetric method was used to measure the adsorption of gas onto coal. The Langmuir monolayer mechanism was used to represent the CO<sub>2</sub> adsorption isotherm. The Langmuir volume parameter or the theoretical maximum CO<sub>2</sub> adsorption capacity of these coals varies from about 40 m<sup>3</sup>/t to 80 m<sup>3</sup>/t (dry and ash free, daf) and the CO<sub>2</sub> storage capacity for these coals projected to in-situ seam conditions range from 5 to 50 m<sup>3</sup>/t. Different trends between gas storage and rank were observed for the southern and northern coalfields of the Sydney Basin. Based on the results, indicative assessment of the CO<sub>2</sub> sequestration potential of Sydney Basin coals can be suggested. Study of the natural occurrence of CO<sub>2</sub> in Sydney Basin coals seams showed significant under saturation relative to adsorption capacity measured in the laboratory. Further studies of the cause of the difference in gas content and measured storage capacity could lead to a more accurate estimation of the CO<sub>2</sub> sequestration potential of Sydney Basin coals.

## INTRODUCTION

Over the last five years, carbon capture and sequestration (CCS) have been increasingly considered as a means to allow Australian dependence upon coal and gas for electricity generation to continue without major, consequential increases in atmospheric carbon dioxide levels. In NSW, there is a lack of suitable geological options such as depleted oil and gas reservoirs, adjacent to the main sources of CO<sub>2</sub> emissions, to allow significant CO<sub>2</sub> storage. In the absence of these reservoirs, the extensive coal deposits present may be suitable for CO<sub>2</sub> sequestration. Many Australian coal seams contain variable methane and carbon dioxide contents. Gas composition can vary considerably across a single coal seam and in a single coal mine. At shallow depths, CO<sub>2</sub> may have a biogenic contribution, whereas at greater depths, most of the CO<sub>2</sub> is likely to be derived from igneous activity. The existence of variable volumes of CO<sub>2</sub> in Sydney Basin coals provides important information on the coal seams as natural analogues for CO<sub>2</sub> sequestration (Faiz et al, 2006a). In the present study, measurements of coal gas storage and flow properties for CO<sub>2</sub> gas in a series of Sydney Basin coals give insights on their storage potential for CO<sub>2</sub>.

### CO<sub>2</sub> STORAGE PROPERTIES FOR COAL AND INTERBEDDED ROCKS

By comparison with conventional reservoirs such as sandstone and limestone, coal differs markedly in its capacity to retain significant volumes of gas. The storage of gas in coal occurs mainly via gas adsorption onto micropore surfaces, compared to sandstone reservoirs where the gas is in a free phase and stored by compression. The adsorbed phase gas in coals adheres to the micropore surface which is very large, ranging between ~20 to 200 m<sup>2</sup>/g (Griffith and Hirst, 1944; Thomas and Damberger, 1976; Saghafi et al., 1987). The total volume of gas stored in reservoir including free and adsorbed phases per unit mass of coal or rock can be calculated from:

$$c(p,T) = f(p,T) + \frac{pM}{zRT} \frac{\epsilon}{\rho_c} \quad (1)$$

where  $c$  is the volume of gas stored per unit mass of coal which depends on temperature and pressure; the first term on the right hand side of the equation is the volume of gas adsorbed (which is almost nil for rocks) and the second term is the volume of free gas compressed in the pore system;  $p$  and  $T$  are gas pressure and temperature,  $\epsilon$  is the coal or rock porosity,  $M$  is molecular mass of gas,  $\rho_c$  is the density of the medium and  $R$  is gas constant. Both adsorbed and free phase volumes are expressed at atmospheric pressure and at standard temperature.

For comparison of CO<sub>2</sub> storage capacities of sandstone and coal reservoirs, the volumes required to store a tonne of CO<sub>2</sub> in an Australian coal and sandstone is shown in Figure 1. Significantly less coal is required to store a tonne of CO<sub>2</sub> compared to storage in sandstone reservoirs. For example, at a depth of 400 m, less than 8 m<sup>3</sup> of coal is required to store one tonne of CO<sub>2</sub>, while about 90 m<sup>3</sup> sandstone with a porosity of 15% is required to store the same mass of CO<sub>2</sub>. Coal in this example has a porosity of 5%.

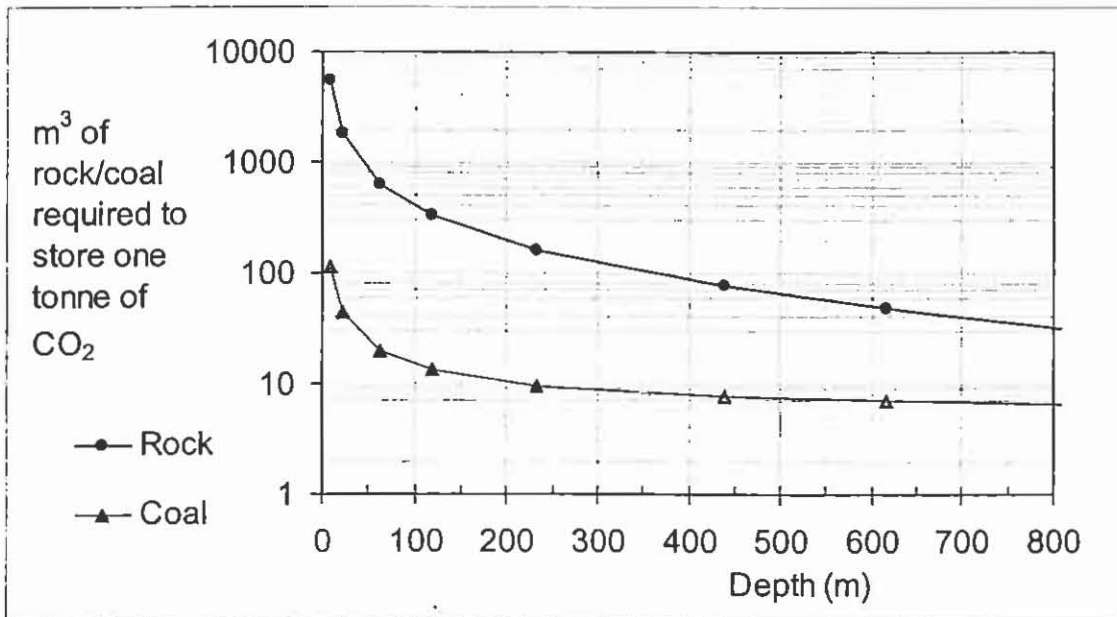


Figure 1. CO<sub>2</sub> storage in sandstone and coal: storage capacity ratio

**COAL SAMPLES AND MEASUREMENT METHODOLOGY**

Forty coal samples from 17 coal seams in Sydney basin were measured. The sample locations span across Southern, Newcastle and Hunter coalfields. Samples were obtained from coal face in mines and from drill holes from <30 m to >700 m. The volatile matter content of these samples varies from 13.5 to 42.6% (daf; Figure 2), ash content from 3.3 to 57% and moisture from 0.4 to 7.9%. Three contact metamorphosed coals with volatile matter contents of <20% were also measured. The maximum mean vitrinite reflectance ( $R_o$  max) for measured coals varies from 0.66 to 1.50% and for contact metamorphosed coals up to 11.2%.

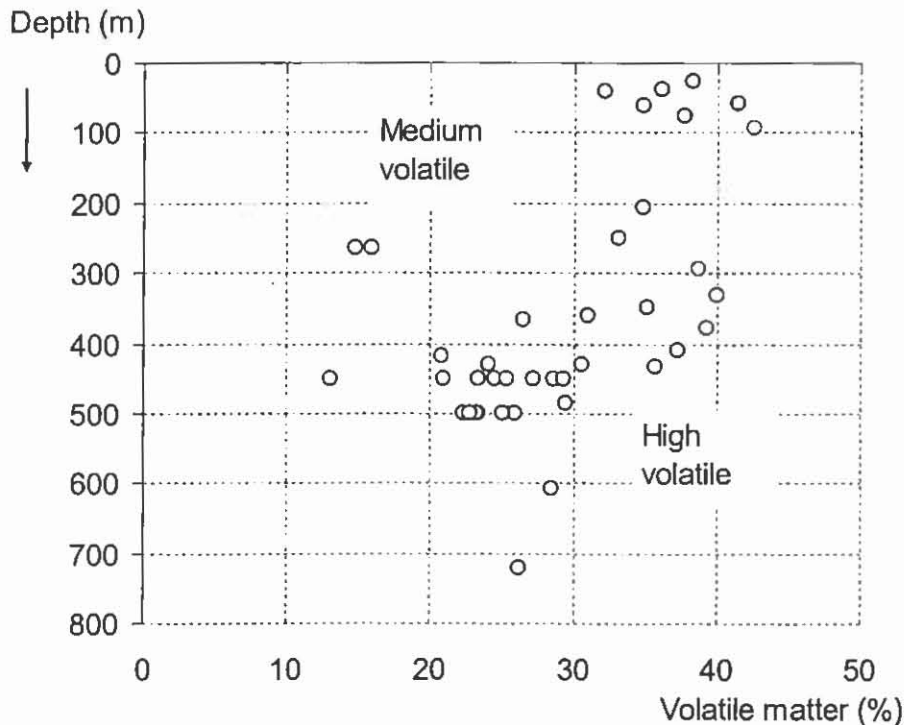


Figure 2. Distribution of coal samples measured in this study

**Measurement methodology**

A gravimetric method was used to measure the adsorption isotherms of these coals. Gas pressures of up to 6 MPa were used to determine the adsorption isotherms at 27°C using ~300 g of crushed coal per sample. The crushed coal used in the measurement of adsorption consists of particle sizes of 90 to 150 μm. The adsorption isotherm equipment and methodology used in this study is described in previous papers (Saghafi, 2003; Saghafi et al. 2006a). Coal petrology, ash, moisture and volatile matter contents were measured according to standard methods.

**Isotherm model**

Most coal adsorption isotherms observed to date can be classified as Type I isotherm. Gregg and Sing (1982) give a detailed description of various isotherm types and their interpretation. The Langmuir model (1918) can be obtained by interpreting the Type I using the kinetic theory of gases. This model assumes that a monolayer adsorption occurs at the coal and gas interface. The model also assumes:

- the energy of adsorption is constant over all adsorption sites,
- the adsorbate molecules are held at localized and definite sites and each site can accommodate only one adsorbate molecule, and
- there is no interaction between neighboring adsorbate molecule.

Assuming a dynamic equilibrium between the adsorption and desorption rate the Langmuir equation is described as:

$$c = \frac{V_L p}{p + P_L} \quad (2)$$

where  $p$  is pore pressure and  $V_L$  and  $P_L$  are the Langmuir volume and pressure parameters.  $V_L$  represents the maximum capacity of coal to store gas and  $P_L$  is the pressure at which half of the storage capacity of coal is reached.

### RESULTS OF ADSORPTION PROPERTIES OF COALS

The distribution of the adsorption capacity for Sydney Basin coals used in this study is shown in Figure 3 (coal as received). The measured adsorption isotherms show that these coals can adsorb 30 to 78 m<sup>3</sup>/t ( $V_L$  parameter for coal as received; Figure 3) of CO<sub>2</sub> gas. Moisture and ash corrected (daf) adsorption capacity for most of these coals range from 60 to 80 m<sup>3</sup>/t.

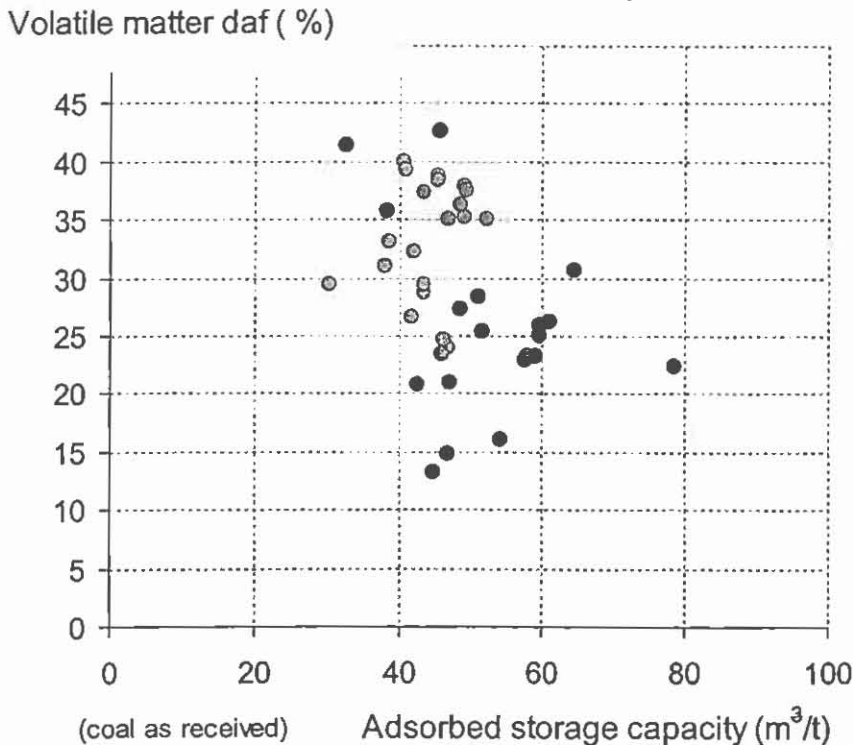


Figure 3. CO<sub>2</sub> adsorption capacity of Sydney Basin coals

#### CO<sub>2</sub> adsorption and coal rank

Coal petrology was examined for more than half of the coal samples. As shown in Figure 4, the higher rank coals of southern coalfield and lower rank coals of the northern Sydney Basin show separate groupings according to adsorption capacities. The CO<sub>2</sub> adsorption capacity of coals from each of these regions (represented by the Langmuir volume parameter  $V_L$ ) show broad increases with vitrinite reflectance.

## SYDNEY BASIN COALS AND CO<sub>2</sub> SEQUESTRATION

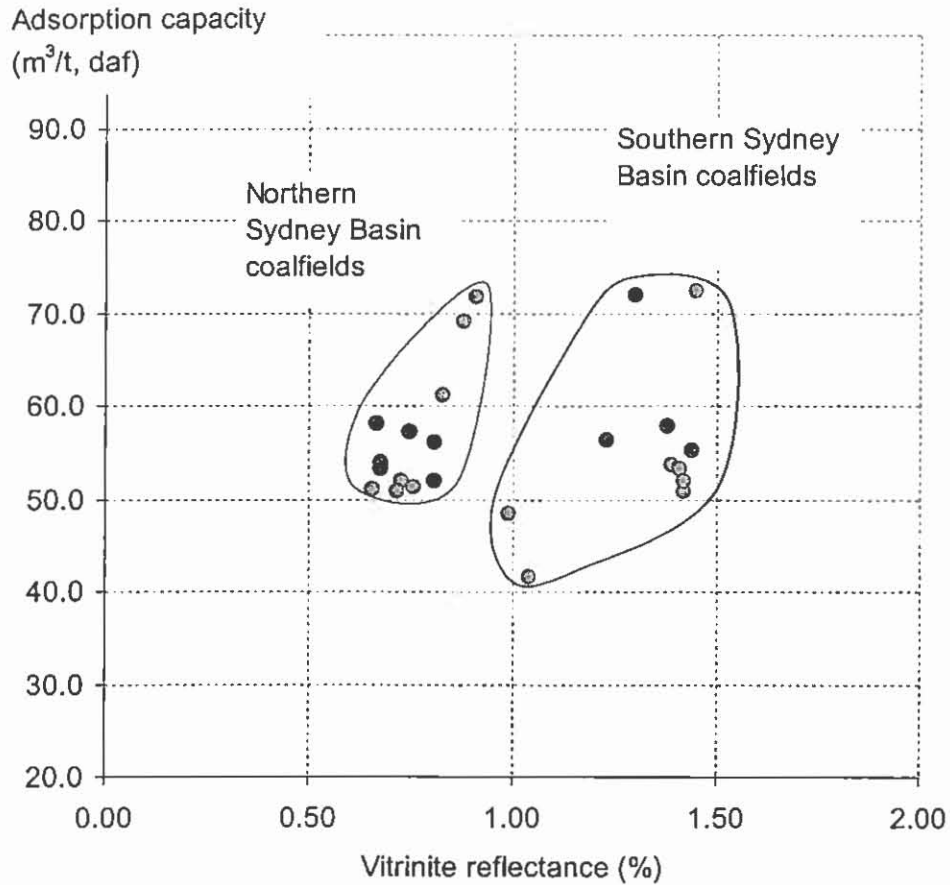


Figure 4. Adsorption of CO<sub>2</sub> as a function of coal rank for Sydney Basin coals

### CO<sub>2</sub> STORAGE POTENTIAL AND IMPLICATION FOR SEQUESTRATION IN COAL SEAMS

Based on the results of adsorption measurements of coals from the Sydney Basin, a model describing the storage capacity for Sydney Basin coals can be formulated. In this study, a model and preliminary estimations of the storage capacities was produced according to coal seam depths and measured isotherm data assuming that the hydrostatic pressure equals the gas pressure at a given depth. In Figure 5, the results of estimation of CO<sub>2</sub> storage capacity with depth based on the assumptions described above are shown. The analysis of data shows that the storage capacity in the adsorbed phase on coal can be expressed in terms of depth by a power function:

$$c = C_0 \left( \frac{h}{H_0} \right)^\alpha \quad (3)$$

where  $c$  is the adsorption capacity of coal at depth  $h$  and  $C_0$  and  $H_0$  are the reference depth and its corresponding storage value. The values for parameters in equation 3 for the Sydney Basin coals are:

$C_0 = 30.1 \text{ m}^3/\text{t}$ ,  $H_0 = 400 \text{ m}$  and  $\alpha = 0.63$ .

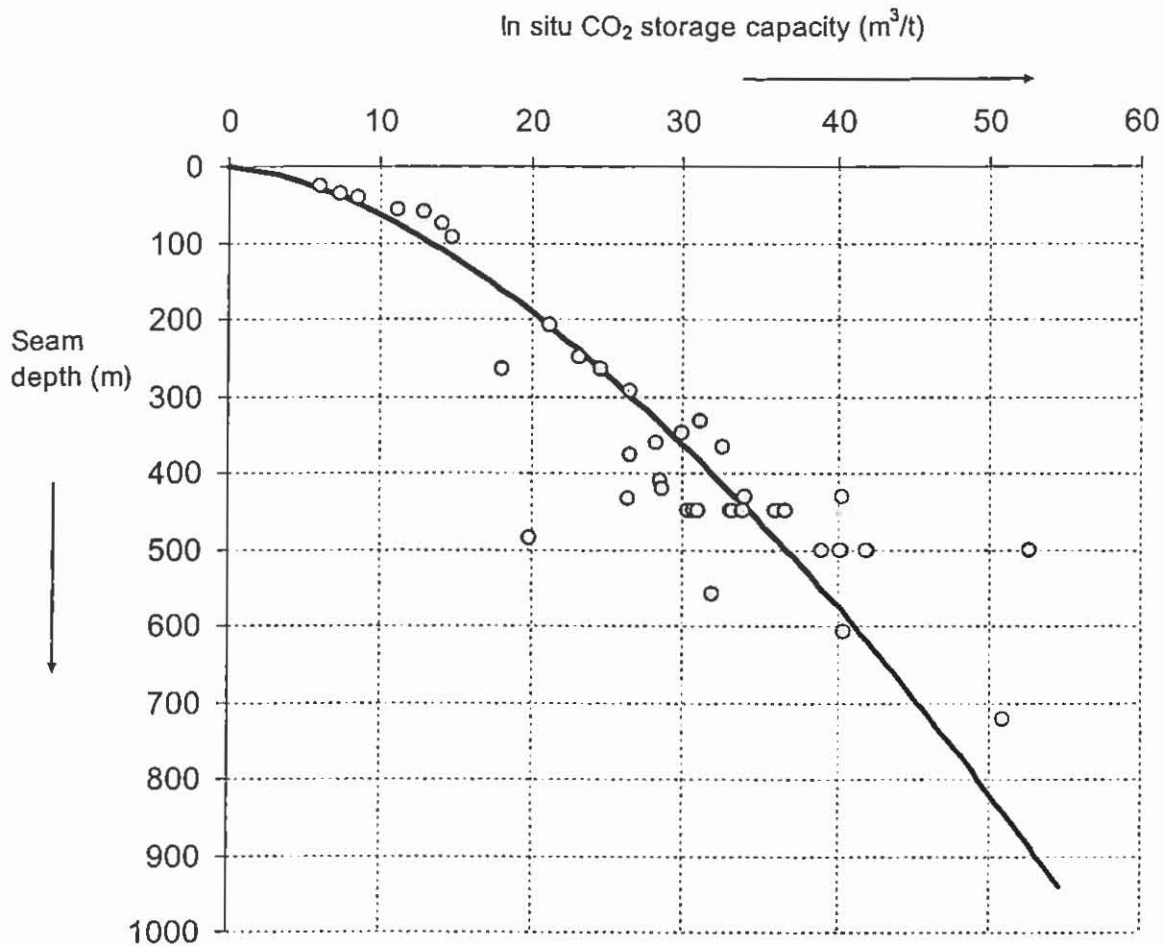


Figure 5. Estimated in situ CO<sub>2</sub> storage capacity as a function of depth for Sydney Basin coals (modified from Saghafi et al., 2006a)

## DISCUSSION

Sydney Basin coals contain large amounts of CO<sub>2</sub> and in some instances the gas in the coals consists of almost pure CO<sub>2</sub>. This natural occurrence of CO<sub>2</sub> in large quantities provides an important opportunity to study the in-situ behavior of CO<sub>2</sub> in geological systems and its interactions with coal. For instance, it is observed that coals in the Sydney Basin are under saturated in their CO<sub>2</sub> content compared to their laboratory saturated values (Faiz et al., 2006b). Though this phenomenon also occurs for CH<sub>4</sub>, the level of under saturation is generally much smaller for methane. Measurements of CO<sub>2</sub> and CH<sub>4</sub> storage capacities of Sydney Basin coals (Saghafi et al., 2006b) show that up to twice as much CO<sub>2</sub> can be stored relative to CH<sub>4</sub>. Measurements of the gas contents of these coals, however, show that CH<sub>4</sub> and CO<sub>2</sub> have similar upper storage limits and the seams are largely under-saturated with respect to predicted CO<sub>2</sub> contents on the basis of adsorption isotherms that were measured in the laboratory (Figure 6). The reasons for this under-saturation are currently being assessed. Studies on the effects of mixed gases on the storage capacity of a Bowen Basin coal showed that considerably less CO<sub>2</sub> may be stored if small amounts of methane are present (Saghafi et al., 2006b). This may have implications for CO<sub>2</sub> storage in coal seams which generally contain other adsorbed gases (Faiz et al., 2006b). The observations indicate that under optimal conditions, only half or less of the laboratory measured capacity may be reached. Additional laboratory evaluations of CO<sub>2</sub> interactions with coal, coupled with observations of naturally

occurring CO<sub>2</sub> in coal seams should allow a more accurate quantification of the potential for CO<sub>2</sub> storage in deep coal seams.

Saturated CO<sub>2</sub> content

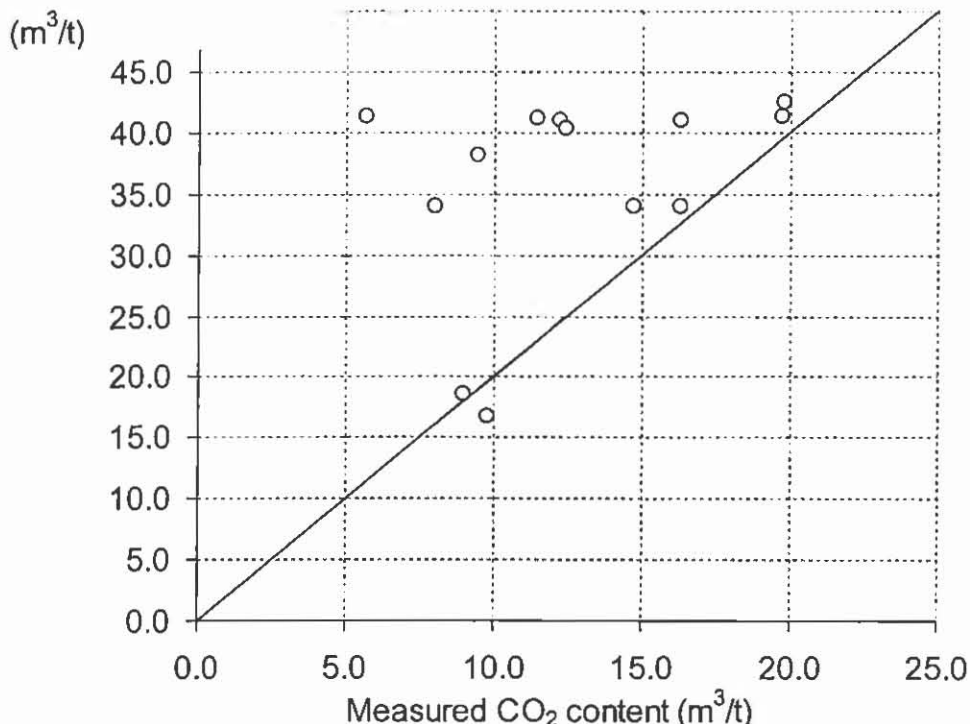


Figure 6. Measured CO<sub>2</sub> contents compared with estimated saturation levels based on measured isotherms, for hydrostatic pressures, with a suite of southern Sydney Basin coals (after Saghafi et al., 2006b).

#### ACKNOWLEDGEMENTS

The authors wish to thank CSIRO Energy Transformed Flagship for funding part of this research. We acknowledge the valuable assistance from coal companies operating in Sydney Basin for providing coal samples used in this study. We extend our thanks to Dr Graeme Batley and Dr Greg Duffy from CSIRO Energy Technology for their valuable editorial comments.

#### REFERENCES

- FAIZ M.M., BARCLAY, S.A., SHERWOOD, N., STALKER L., SAGHAFI A., WHITFORD., D.J., 2006a. Natural accumulation of CO<sub>2</sub> in coals from the Southern Sydney Basin: implications for geosequestration. *Journal of the Australian Petroleum Production and Exploration Association* 46, 455-474.
- FAIZ, M., SAGHAFI, A., BARCLAY, S.A., STALKER, L., SHERWOOD, N. AND WHITFORD, D.J. 2006b. Distribution of Juvenile CO<sub>2</sub> in the Sydney Basin, Australia: A Natural Analogue for CO<sub>2</sub> Storage in Bituminous Coals. *Eighth International Conference on Greenhouse Gas Control Technologies (GHGT-8)*, Trondheim, Norway.
- GREGG, S. J. AND SING, K. S. W., 1982. *Adsorption, Surface Area and Porosity*, New York, Academic Press.
- GRIFFITH, M. AND HIRST, W., 1944. *Proceedings of a conference on the ultra fine structure of coals and coke*. The British Coal Utilisation Research Association, London, p. 80.
- LANGMUIR, I. 1918. *Journal of American Chemical Society*, 40, 1361.

- SAGHAFI A, JEGER C, TAUZIEDE C, WILLIAMS R J, 1987. A new computer program for gas flow into drainage boreholes. In: 22nd International Conference of Safety in Mines Research Institutes, Beijing, China, 147-158.
- SAGHAFI, A., 2003. Aspects of gas storage and flow properties of Australian coals. In: The 2<sup>nd</sup> Annual Australian Coal Seam & Mine Methane Conference, 19-20 February 2003, Brisbane, Australia.
- SAGHAFI, A., FAIZ, M. AND ROBERTS, D. 2006a. CO<sub>2</sub> storage and diffusivity properties of Sydney Basin coals. In Press, the International Journal of Coal Geology.
- SAGHAFI, A., FAIZ, M., ROBERTS, D. AND SHERWOOD, N. 2006b. CO<sub>2</sub> storage potential and enhanced coal seam methane recovery with respect to mixed gas conditions for eastern Australian coals. In: Proceedings of the 23<sup>rd</sup> Annual meeting of the Society for organic Petrology (TSOP), Beijing China, September 15-22, Volume 23, pp. 207-209.
- THOMAS, J., JR. AND DAMBERGER, H. H., 1976. Internal surface area, moisture content and porosity in Illinois coal: variation with coal rank. Illinois State Geological Survey Circ. 493, 38 pp.

## FLY ASH – WASTE OR RESOURCE?

Colin R. Ward<sup>1,2</sup>, David French<sup>2</sup>, Craig Heidrich<sup>3</sup> and Harry Bowman<sup>4</sup>

<sup>1</sup>School of Biological, Earth and Environmental Sciences  
UNSW, Sydney 2052

<sup>2</sup>CSIRO Division of Energy Technology  
PMB 7, Menai 2234

<sup>3</sup>Ash Development Association of Australia  
PO Box 1194, Wollongong 2500

<sup>4</sup>Consultant Geologist, 16 Viburnum Rd, Loftus 2232

### ABSTRACT

Although traditionally regarded as an industrial waste, the solid products of coal combustion in pulverised fuel power stations, fly ash and bottom ash, are increasingly being recognised as a useful mineral resource, with applications and potential applications that include the cement and concrete industries, stabilisation of engineered soils for construction purposes, production of synthetic aggregates and zeolites, and improvement of soils for agriculture and horticulture. The material also has potential for use in different ways as backfill in mining operations, providing benefits to the mine through rehabilitation, subsidence control and other mechanisms, and to the community by reducing the area of land otherwise required for ash disposal associated with power production. The mineralogical, geotechnical and geochemical characteristics of individual ashes may vary, depending on the coal feedstock and combustion conditions. The mobility of particular elements may also vary, depending in part of the environmental conditions into which the ash is placed. Site-specific studies of the chemical interactions between ash, rock and water may be significant in establishing the environmental risks, if any, associated with mine-site ash use. The regulatory framework within which ash might be used for mine backfill also needs to be taken into account.

### INTRODUCTION

When coal is burnt in a pulverised fuel (pf) furnace for electric power production, two types of solid residue or ash are produced. The fine particles, which remain in suspension with the combustion gases and are recovered by fabric filters or electrostatic precipitators, form material with mainly silt-sized particles known as fly ash. This fraction typically represents up to 90% of the total solid materials, collectively referred to as coal combustion products (CCPs), that are produced from modern pf combustion systems. The coarser fraction is mainly represented by sand- or gravel-size aggregates that have fallen to the bottom of the combustion chamber to form material known as furnace ash or bottom ash.

### NATURE OF FLY ASH

The fly ashes produced in Australian power stations are light to mid grey or grey-brown in colour, with irregular to spherical particles ranging from  $<1 \mu\text{m}$  to  $>200 \mu\text{m}$  in size. A bimodal size distribution is typically present, with one peak 10-20  $\mu\text{m}$  and the other 35-80  $\mu\text{m}$ . The particles are generally spherical in shape (Fig. 1), and range from vesicular materials made up mainly of aluminosilicate glass to crystalline aggregates (ferrospheres) consisting mainly of iron oxide or spinel minerals. Other components include essentially

unaltered quartz and other mineral grains, unburnt carbon particles of different types derived from incompletely combusted coal, and thin-walled, hollow silicate spheres called cenospheres, that float when the ash is placed in water. The cenospheres are often harvested separately from ash ponds, and used to produce a range of high-value industrial products.

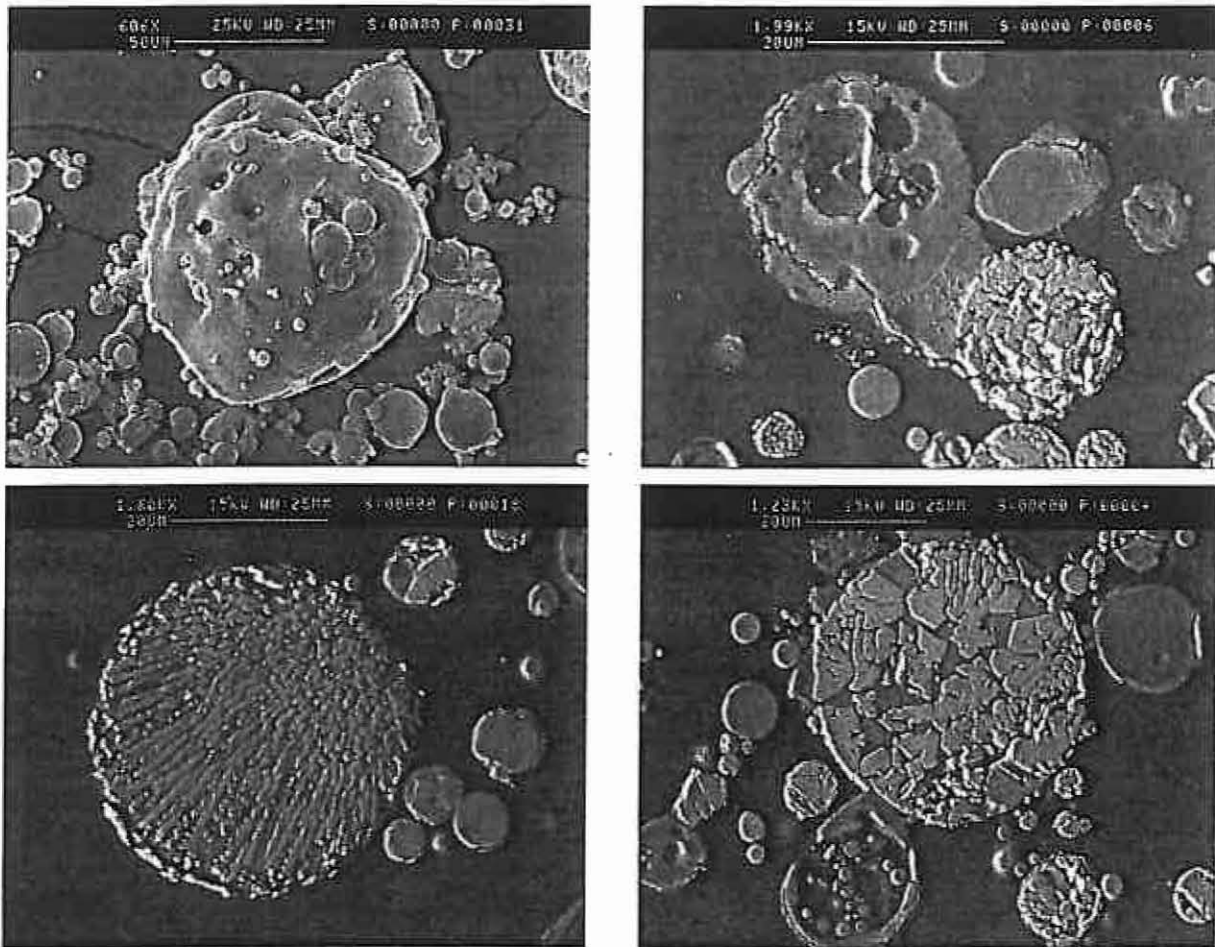


**Figure 1** Scanning electron microscope images of a range of fly ash particles.

The chemical composition of typical fly ashes from New South Wales and Queensland power stations is summarised in Table 1. Most of the material is categorised as Class F under the ASTM system (ASTM 1999), with 80-85%  $\text{SiO}_2$  and  $\text{Al}_2\text{O}_3$  and <10%  $\text{CaO}$ . The other principal group under this system, class C, has a higher  $\text{CaO}$  content, and is most commonly derived from combustion of lignites and other low-rank coals.

The mineralogy of fly ash, including the proportion of amorphous or non-crystalline glassy material, can be evaluated using modern X-ray diffraction techniques (Ward & French 2006). The main crystalline components are quartz, mullite and magnetite (Table 2), with cristobalite also occurring in ashes from plants with higher combustion temperatures. Most of the material, however, is made up of crystallographically amorphous aluminosilicate glass. The abundance of the different minerals, and also the inferred composition of the glassy phase, can be related to the mineral matter in the original feed coal. Gypsum, calcite and a number of calcium aluminate minerals may also be present in some cases, especially in the ashes from calcium-rich, lower-rank coal seams.

FLY ASH – WASTE OR RESOURCE?

Table 1 Chemical composition of selected NSW and Queensland fly ashes.

Station No.	New South Wales						Queensland			
	1	2	3	12	13	4	5	6	7	14
SiO <sub>2</sub>	65.9	65.78	61.5	67.0	57.5	50.83	53.23	74.66	62.9	44.5
Al <sub>2</sub> O <sub>3</sub>	27.6	26.93	22.4	24.8	28.2	31.73	25.89	22.90	29.3	30.7
Fe <sub>2</sub> O <sub>3</sub>	1.1	1.64	7.6	3.1	5.6	12.30	9.74	0.45	1.8	14.4
CaO	0.4	0.35	3.3	1.0	3.8	1.40	4.36	0.07	1.3	4.2
BaO	0.0	0.0	0.1	0.0	0.1	0.03	0.23	0.02	0.1	0.1
MgO	0.3	0.30	1.1	0.6	1.2	1.02	1.17	0.13	1.1	1.6
Na <sub>2</sub> O	0.2	0.41	0.9	0.6	0.2	0.15	0.35	0.07	0.8	0.4
K <sub>2</sub> O	2.9	3.0	1.9	1.6	1.1	0.28	1.40	0.20	0.5	0.9
TiO <sub>2</sub>	1.3	1.15	0.9	1.0	1.6	1.95	1.24	1.40	1.8	1.9
P <sub>2</sub> O <sub>5</sub>	0.2	0.11	0.2	0.2	0.5	0.05	1.81	0.06	0.1	1.0
SO <sub>3</sub>	0.1	0.30	0.1	0.1	0.2	nd	0.41	0.03	0.2	0.3
<b>Total</b>	<b>100.0</b>	<b>100.0</b>	<b>100.0</b>	<b>100.0</b>	<b>100.0</b>	<b>100.0</b>	<b>100.0</b>	<b>100.0</b>	<b>100.0</b>	<b>100.0</b>

A range of trace elements is also present in Australian fly ashes, although the concentrations are generally low compared, for example, to European or Chinese materials (Moreno *et al.* 2005; Liu *et al.* 2004). Some of the more significant elements from the environmental viewpoint appear to occur as coatings on the surfaces of the ash particles, formed by condensation or adsorption of volatile elements with cooling of the combustion stream (Kutschko and Kim, 2006). The potential mobility of these elements in water under different environmental conditions may be significant in the management of ash emplacements, and relevant research for Australian ashes is discussed more fully by Jankowski *et al.* (2006).

Table 2 Mineralogy of New South Wales and Queensland fly ashes.

Station Number	New South Wales				Queensland			
	1	2	3	12	13	5	7	14
Quartz	4.9	11.2	9.7	5.2	5.3	7.2	10.0	2.3
Mullite	8.5	16.0	10.2	8.9	18.5	7.2	21.3	8.9
Cristobalite			0.1	0.1				
Magnetite		0.2	0.7		0.3	1.1		1.9
Other spinel		0.2					0.5	
Maghemite	0.1		0.8	0.4	1.1	1.0	0.4	1.3
Hematite	0.0	0.4	0.4			0.7	0.0	0.5
Calcite						0.3		
Glass	86.4	72.0	78.1	85.4	74.8	82.2	68.2	85.0

Australian fly ash typically has geotechnical characteristics similar to those of medium to dense sand, but a compacted density of only ~60% that of dense sand. It therefore represents material with a high strength and relatively a low bulk density, the combination of which enhances its applicability for backfilling retaining walls or for use in construction embankments on soft soil materials. Other mechanical properties relevant to such applications include:

- high internal angle of friction;
- low compressibility;
- ease of compaction; and
- low settlement when used as a fill material.

Australian ashes are generally pozzolanic (i.e. when added to water and calcium hydroxide it forms compounds with cementitious properties), and can be used in conjunction with other cementitious materials (e.g. Portland and slag cements) to enhance the characteristics and performance of concrete. Use of ash in this way, in preference to extraction of other raw materials, has additional benefits in reducing Australia's nett greenhouse gas emissions (Heidrich *et al.* 2005).

### **BENEFICIAL USE OF FLY ASH**

Approximately 13 million tonnes of fly ash and other CCP's are currently produced in Australia and New Zealand each year. Around 6.1 Mt or 47% are used to provide a range of value-added products or for some other beneficial purpose, generating annual revenues of more than \$100 million. A total of 1.46 Mt (11%) of ash are used in high-value applications such as cement or concrete manufacture, resulting in an annual reduction of more than 1.1 Mt of CO<sub>2</sub> equivalent greenhouse gas emissions through savings in the requirement for clinker manufacture. Other activities involving beneficial use of ash, such as mine-site remediation and haul road construction, consume ~4.1 Mt (32%), typically generating only cost recovery. The surplus (6.9 Mt) is mainly placed into storage ponds or dry emplacements near the power station awaiting future opportunities for economic use.

In the USA 57.1 Mt of fly ash and 15.4 Mt of bottom ash, together with boiler slag and flue gas desulphurisation (FGD) residues, were produced in 2000 from combustion of ~1 billion tonnes of coal (Kalyoncu 2001). Over 18 Mt of this fly ash (31.9%) was used, mainly in cement and concrete, structural fills, waste stabilization, road base/sub-base, and mining applications. The member countries of the European Coal Combustion Products Association (ECOBA) generated 37 Mt of fly ash in the same year, and profitably used >18 Mt (48% usage rate). Raw material shortages and favourable state regulations account for this higher use rate. The main usage was in concrete (37%), followed by Portland cement manufacture (31%) and road construction (21%). An additional 15.43 Mt of fly ash and 2.05 Mt of bottom ash were used in landfill applications.

A number of barriers exist in Australia that inhibit wider use of fly ash for beneficial purposes. Regardless of any recycling or use of the material, coal ash is still considered in the regulatory environment to be an industrial waste, and as such is subject to greater controls than equivalent virgin (e.g. directly mined) materials. This has the effect of making virgin materials more attractive than recycled materials, even though the recycled materials (ash) may be equally if not more suitable for the purpose in question.

As an example, during early 2005 a large development project close to a fly ash source site required ~500,000 tonnes of engineering fill. The design engineers agreed that fly ash met the physical and chemical properties of the project. Nevertheless, additional testing at considerable additional cost was required by the local regulator, above and beyond the requirements for virgin materials. The additional test requirements were met, after which the regulator deemed that "land fill levies" were payable if the prescribed waste material was used, as the project required >20,000 tonnes of such material. The resulting levy made use of the ash commercially unviable, resulting in the use of traditional quarried and virgin excavated natural materials for the project.

### **Cement and Concrete Products**

A significant part of the fly ash sold from Australian power stations is used in pre-mixed concrete, either as a cement replacement or as a fine aggregate supplement. A key factor is the calcium content of the ash, which significantly affects its pozzolanic nature. Another is the unburnt carbon content, too much of which may impact adversely on the concrete properties.

Australian Standards for pre-mixed concrete allow up to 40% of the portland cement to be replaced by fly ash (Heeley & Shirtley 2001). The ash may be incorporated either by mixing it with other ingredients at the concrete batching plant or by use of blended cements in the concrete mix. The cost of Portland cement in NSW is >\$100 per tonne, and hence incorporation of fly ash can provide significant savings to the concrete industry. The savings are, however, offset by the transport distance required to transfer the fly ash from the power stations to the major Sydney and Newcastle concrete markets.

### **Soil Stabilisation, Engineered Fills and Road Bases**

Fly ash may be added to otherwise well-sorted (poorly graded) sandy soils to fill the void spaces, increasing the overall density and aiding in compaction. In some cases the self-cementing properties of the ash may help to bind the soil together. Such stabilisation will help the soil to support roads (road base), bridges, buildings and other man made structures, and maintain the soil's stability for the lifetime of the structure. The fly ash and soil may be compacted into layers (structured fills), or a mixture of fly ash, soil, water and Portland cement may be placed like a liquid (flowable fills) to solidify as a low-strength but effective engineered fill material.

### **Agricultural Materials**

Due to the dominance of silt sized particles and the porous nature of the components, addition of fly ash may help to increase the water-holding capacity and modify the permeability of otherwise unfavourable soils, and hence increase the level of water infiltration and retention and decrease the rate of water loss in agricultural and horticultural applications. Addition of ash to sandy soils, for example, can reduce episodes of moisture deficit, and also aid the retention of nutrients such as nitrate, ammonium and phosphorus in the rooting zone, leading to increases in plant yield and a range of associated economic and environmental benefits. Ash may also be used to increase the porosity and permeability of clay-rich soils, lowering bulk density, providing better water infiltration and increasing the aeration level (Yunusa *et al.* 2006).

Addition of ash may change the soil pH, and also provide chemical nutrients otherwise lacking in the soil, making up for deficiencies that might arise due to prolonged weathering or extended cropping. Some elements, however, such as B, Mo, Se, while beneficial if not essential at certain concentrations, may become toxic at higher concentration levels, and the mobility of these components under soil conditions may need to be taken into account.

### **Ash in Mine Backfill**

Coal ash and other combustion products may be used as backfill in open-cut or underground coal mines for a number of beneficial purposes. These include:

- void infilling, spoil pile re-contouring or highwall reclamation;
- grouting or infilling to control subsidence, ground movement or water flow;
- amelioration of unfavourable water quality (e.g. acid pH) associated with mining;

- provision of construction materials for mine access and haulage roads;
- stabilisation of exposed rock, tailings or soil to prevent wind or water erosion;
- control of contaminant migration, underground fires or spontaneous combustion; and
- improvement of natural or artificial soils in mine-site rehabilitation programs.

The main beneficial use of ash for mine backfill, especially in overseas countries, has traditionally been derived from the interaction of alkaline ash with mine solids, mine waters or in mining voids to ameliorate acid mine drainage (AMD) conditions. However, ash is also routinely emplaced in open-cut mines as part of void infill programs in the western USA, without necessarily an AMD involvement, and this may provide a better parallel for similar use in Australian conditions. In underground mines ash-based backfill may be used for ground support and subsidence control, an area in which the critical factors are flowability, density, porosity, abrasiveness, strength and pozzolanic properties. Australian examples of the use of power station ash in this way include Olympic Dam and Mt Isa. Fly ash has also been used for the control of mine fires, as a contaminant barrier to reduce the escape of waterborne contaminants from potentially toxic mine products such as preparation tailings, and as an additive to enhance the fertility of mine soils in reclamation programs.

#### **Aggregates and Geopolymers**

Coarse (gravel-size) and fine (sand-size) aggregates for concrete and other applications can be produced from fly ash by partially or completely melting the ash, typically with the aid of a flux to lower the melting temperature, and either forming the melt into appropriately-sized particles or crushing it on cooling. Alternatively, aggregates can be produced by binding ash particles together into larger masses with a cementing agent.

Another approach is to transform the ash into geopolymers, which are artificial rock-like silicate materials produced by synthetic reactions between the ash and other agents at temperatures below 100°C (Swanepoel & Strydom 2002). Geopolymerisation involves the dissolution of Al and Si from the surfaces of waste materials as well as the surface hydration of undissolved waste particles, followed by the polymerisation of active surface groups and soluble species to form a gel and subsequently a hardened geopolymer structure.

#### **Zeolite Production**

A range of zeolite minerals may be produced by reacting SiO<sub>2</sub>, Al<sub>2</sub>O<sub>3</sub> and cations under hydrothermal conditions (pH 10-14, >100°C), and the abundant aluminosilicate glass component in fly ash provides a potential raw material for zeolite synthesis (Querol *et al.* 2002; Elliot 2005). Zeolites are used as controlled-release fertilisers, soil conditioners and ion exchange media, and also as detergent builders, pesticide carriers, and animal dietary supplements. Although natural zeolites are also available, synthetic zeolites, including materials made from fly ash, may be tailored more specifically to meet particular market requirements.

#### **REGULATORY ISSUES IN MINE BACKFILL APPLICATIONS**

The emplacement of fly ash or bottom ash from a power station into either an operating or a closed coal mine in New South Wales would need approval under part 3A of the Environmental Planning and Assessment Act before it could routinely be undertaken. The consent authority for such approval would be the Minister for Planning, who would act on the recommendation of the Department of Planning. Other affected agencies, such as the Department of Primary Industries, would also be consulted, and a planning focus meeting

## FLY ASH – WASTE OR RESOURCE?

would be needed. If ash emplacement were to become a normal part of the operations, the Department of Primary Industries would have a regulatory role in its capacity of controlling mine-site rehabilitation.

Emplacement of fly ash into the final void of a closed coal mine would, however, probably not require a part 3A approval as it would not be a major development. The approval would be under part 4 of the Environment and Planning Act with the consent authority being the local Council.

Gaining approval to emplace fly ash into an existing mine would need the technical information required for any EIS. This would include:

- the chemistry of the material;
- likely contamination from the ash and how it would be contained;
- dust suppression, noise, truck movements etc;
- impact on ground water;
- impact on the community.

Emplacement of fly ash into an operating or worked-out mine, rather than establishing a separate ash emplacement area in otherwise undisturbed or productive terrain, does have environmental advantages. For this reason ash emplacement proposals meeting the requirements would probably be supported by the approving authority. Given that all mines in New South Wales will need to have a part 3A approval in the near future, there is currently a unique opportunity to incorporate approval for ash emplacement into mining operations.

The separate ownership of coal mines and power stations in NSW and Queensland requires co-operation between the two for disposal of fly ash as part of mine rehabilitation. Because ash emplacement adds environmental risk to the mine's operation, mining companies would also require some benefit to their operations. Such benefits might include payment for accepting the ash, a condition for coal purchase by the generator, or operational benefits such as truck back-loading. The best chance for co-disposal is where the power station and the mine are commonly owned, and where the responsible authorities strongly encourage co-disposal, and where technical studies show that the ash is neutral if not beneficial in its environmental impact.

### CONCLUSIONS

Despite being regarded as an industrial waste and therefore a potential source of environmental problems, the ash produced from coal-fired power stations represents a useful source of raw material for a range of industrial products. In addition to the new ash produced each year, the ash already emplaced in ponds and other disposal sites represents a shallow-lying mineral deposit that is more readily accessible than many equivalent geological materials, and should thus be factored into mineral resource evaluations.

Emplacement of ash into mine excavations, either during mine operation or as part of final void rehabilitation, provides advantages to the community in minimising the area set aside for waste disposal, and is therefore worthy of closer investigation. Geological studies associated with such proposals should include hydrogeochemical evaluations of the ash-rock-water system, as well as a range of geotechnical and other assessments. Overseas experience in more challenging environments has shown few negative impacts, and in many cases significant benefits, from the use of ash in mine backfilling operations.

**ACKNOWLEDGEMENTS**

The authors wish to acknowledge financial support provided by the Co-operative Research Centre for Coal in Sustainable Development, which is funded in part by the Cooperative Research Centres Program of the Commonwealth Government of Australia.

**REFERENCES**

- ASTM. 1999. Standard specification for coal fly ash and raw or calcined natural pozzolan for use as a mineral admixture in concrete. *ASTM C618-99*, Philadelphia, PA, USA, 4pp.
- ELLIOT, A. D. & ZHANG, D. K. 2005. Controlled release zeolite fertilizers: a value-added product produced from fly ash. *Proceedings of World of Coal Ash Symposium*, Lexington, Kentucky, USA, 32 pp. (CD publication).
- HEELEY, P., & SHIRTLEY, R. 2001. The Eraring ash utilisation success story. *Proceedings of 20th Pittsburgh International Coal Conference*, Newcastle, Australia, 11 pp. (CD publication).
- HEIDRICH, C., HINCZAK, I. & RYAN, B. 2005. Case study: CCPs' potential to lower greenhouse gas emissions for Australia. *Proceedings of World of Coal Ash Symposium*, Lexington, Kentucky, USA, 20 pp. (CD publication).
- JANKOWSKI, J., WARD, C. R., FRENCH, D. & GROVES, S. 2006. Mobility of trace elements from selected Australian fly ashes and its potential impact on aquatic ecosystems. *Fuel* **85**, 243-256.
- KALYONCU, R. S. 2001. Coal combustion products – production and uses. *Proceedings of 18th Pittsburgh International Coal Conference*, Newcastle, Australia, 16 pp. (CD Publication).
- KUTSCHKO, B. & KIM, A. G. 2006. Fly ash characterization by SEM–EDS. *Fuel* **85**, 2537–2544.
- LIU, G., ZHANG, H., GAO, L., ZHENG, L. & PENG, Z. 2004. Petrological and mineralogical characterizations and chemical composition of coal ashes from power plants in Yanzhou mining district, China. *Fuel Processing Technology* **85**, 1635-1646.
- MORENO, N., QUEROL, X., ANDRES, J. M., STANTON, K., TOWLER, M., NUGTEREN, H., JANSSEN-JURKOVICOVA, M. & JONES, R. 2005. Physico-chemical characteristics of European pulverized coal combustion fly ashes. *Fuel* **84**, 1351-1363.
- QUEROL, X., MORENO, N., UMANA, J. C., ALASTUEY, A. HERNANDEZ, E., LOPEZ-SOLER, A. & PLANA, F. 2002. Synthesis of zeolites from coal fly ash: an overview. *International Journal of Coal Geology* **50**, 413– 423.
- SWANEPOEL, G. C. & STRYDOM, C. A. 2002. Utilisation of fly ash in a geopolymeric material. *Applied Geochemistry* **17**, 1143–1148
- WARD, C. R. & FRENCH, D. 2006. Determination of glass content and estimation of glass composition in fly ash using quantitative X-ray diffractometry. *Fuel* **85**, 2268–2277.
- YUNUSA, I. A. M., EAMUS, D. DESILVA, D. L., MURRAY, B. R., BURCHETT, M. D., SKILBECK, C. G. & HEIDRICH, C. 2006. Fly-ash: An exploitable resource for management of Australian agricultural soils. *Fuel* **85**, 2337–2344.

# RANK AND MACERAL CHEMISTRY OF THE GRETA COAL MEASURES IN THE SYDNEY AND CRANKY CORNER BASINS

Colin R. Ward, Zhongsheng Li and Lila W. Gurba\*

School of Biological, Earth and Environmental Sciences  
University of New South Wales, Sydney 2052

\*Present Address: CRC for Coal in Sustainable Development  
PO Box 883, Kenmore, Qld

## ABSTRACT

Analysis of maceral chemistry using electron microprobe techniques shows that the seams of the Greta Coal Measures on the Lochinvar Anticline and in the Cranky Corner Basin are significantly higher in rank than is indicated by their mean maximum vitrinite reflectance values. The vitrinite in the Greta Coal Measures on the Muswellbrook Anticline has ~78% C and a reflectance ( $R_{v_{max}}$ ) of ~0.7%, following a relationship consistent with that shown by most other coals in the Sydney-Bowen Basin. The vitrinite in the coals of the Cranky Corner Basin has much lower reflectance values ( $R_{v_{max}} = 0.4-0.5\%$ ), but a similar C content to the Muswellbrook Anticline material. Despite the large difference in reflectance the C contents of the vitrinite macerals indicate a similar rank level for the Greta coals on both sides of the Hunter Thrust structure.

Compared to the Muswellbrook Anticline material, the vitrinite macerals in the Greta seam of the Cessnock area have similar to slightly lower reflectance values ( $R_{v_{max}} = 0.6-0.7\%$ ). These decrease still further near the top of the seam profile, due to overlying marine influence. The vitrinite in the Greta seam, however, has higher C content (83%) than that of the Muswellbrook or Cranky Corner Basin coals, suggesting a significantly higher rank level. Vitrinite C contents are also constant throughout the seam profile, despite the upwardly decreasing reflectance. Although the coals in both the Cessnock and Cranky Corner areas have anomalously low reflectance due to marine influence, the magnitude of the anomaly is significantly greater than the relatively small deviation indicated by the reflectance profile within the Greta seam. Elemental analysis of the macerals, using electron microprobe techniques, therefore appears to provide a better indicator of rank for such coals than the vitrinite reflectance values.

The vitrinite macerals in the coals with the more extreme anomalies in reflectance (i.e. those with more strongly suppressed reflectance values) also have high proportions of organic S. The additional organic S apparently occurs in place of O in the maceral structure. The high-S vitrinite with anomalously low reflectance also contains significant proportions of Al and Ca, incorporated into the organic material. Similar proportions of Ca, Al and other elements occur in the organic matter of many lower-rank coals, but these elements are typically lost from the coals as the rank increases. The coals of the Greta Coal Measures with high organic S and strong marine influence therefore have many of the properties of lower-rank coals (low vitrinite reflectance, high proportion of inherent inorganic elements), despite being metamorphosed to a higher rank level.

## INTRODUCTION

Rank (degree of metamorphism), type (nature of original organic components) and grade (freedom from mineral and inorganic matter) are the three independent variables that control coal properties. They are, however, in themselves concepts, and different individual properties of the coal are used as indicators of the fundamental parameters. Properties used as rank indicators include the C or H content, volatile matter and specific energy of the whole coal, expressed to an appropriate basis (*e.g.* dry, ash-free). However, because the different organic constituents (macerals) in the coal each have different characteristics, these properties are also influenced by coal type. The optical reflectance of the vitrinite, and in Australian Standards the telocollinite, is therefore widely used to provide a rank indicator that is essentially independent of the mixture of macerals (coal type) or mineral matter present.

With the development of special techniques for measurement of light elements (C, O, N), electron microprobe analysis, widely used to study other geological materials, has also been used in recent studies to evaluate the chemical constitution of individual coal macerals (*e.g.* Bustin *et al.* 1993, 1996; Ward & Gurba 1998, 1999, Gurba & Ward 2000; Mastalerz & Gurba 2002). These studies have shown, *inter alia*, that the vitrinite macerals have lower proportions of C, organic S and N, and higher proportions of O, than the inertinite macerals in the same coal samples. The technique was used by Ward *et al.* (2005) to identify the progressive changes in elemental composition with rank for the individual macerals in a series of Bowen Basin coals, covering a range from sub-bituminous to semi-anthracite materials.

## CHARACTERISTICS OF THE GRETA COAL MEASURES

The Early Permian Greta Coal Measures are exposed on the Lochinvar and Muswellbrook Anticlines in the northern Sydney Basin, and also in the Cranky Corner Basin a short distance to the north. The unit is underlain and overlain by marine strata (Dalwood and Maitland Groups respectively), and many of the coals have unusually high S contents due to this marine influence. The upper part of the Greta seam in the Lochinvar Anticline area typically has visible pyrite, and also a higher S content (both pyritic and organic) than the lower 2-3 m section. The Tangorin seam in the Cranky Corner Basin has up to 6% total S, much of which occurs in organic form.

The marine origin of the overlying strata has also resulted in anomalously low (suppressed) vitrinite reflectance in the seams of the Greta Coal Measures. Diessel (1992) and Diessel and Gammidge (1998) indicate that the mean random reflectance of telocollinite in the Greta seam decreases from 0.6-0.7% at the base to around 0.5% at the top as a result of marine transgression. Diessel and Gammidge (2003) also indicate that the mean random vitrinite (telocollinite) reflectance decreases from ~0.77% at the base of the Greta Coal Measures in the Cranky Corner Basin to 0.42% just above the Stanhope seam, due in large part to marine influence on the original coal formation.

The purpose of the present study was to investigate more fully the nature of the coals in the Greta Coal Measures, focusing on the relation between maceral chemistry and vitrinite reflectance in coals showing the effects of marine influence. Another objective was to investigate the partitioning of organic sulphur among the individual macerals within the high-sulphur coals of the sequence, especially those in the Cranky Corner Basin, due to the significance of organic S in coal marketing and utilisation.

### SAMPLES AND ANALYTICAL METHODS

A series of coal samples from Southland Colliery, 10 km west of Cessnock, was provided to represent the upper, middle and lower sections of the Greta seam. Total S in the coal (daf basis) increases from ~1% in the lower part of the section to a little over 4% in the upper part, due to increases in both pyritic and (whole-coal) organic S content. A second series of samples was provided from the Tangorin seam and the underlying Stanhope seam near Great Greta Colliery in the Cranky Corner Basin. The Stanhope and Tangorin seams both have relatively high total S (6.0-7.5%). Most of the S in the Stanhope seam appears to be pyritic in nature, but most of the sulphur in the Tangorin seam is organic, and pyritic S makes up only 1% (air-dried) of the section studied. A ply sample from the Puxtrees seam at Drayton Colliery, on the Muswellbrook Anticline, was also used as part of the test program.

Individual points on the different macerals in carbon-coated polished sections of each coal were analysed using a Cameca SX-50 electron microprobe, using conditions and calibration standards as described by Ward *et al.* (2005). The percentages of C, O, N, S, Si, Al, Ca and Fe were measured for each point, with a note on the type of maceral represented in each case. Points that apparently included mineral contaminants (*e.g.* points with high Si or points with particularly high percentages of both Fe and S) were excluded from consideration; so, too, were points that included some of the mounting epoxy resin, indicated by unusual O and high N contents. Average compositions of the individual macerals in each sample are summarised in Table 1. Other polished sections of the coals were subjected to conventional petrographic studies using optical microscopy, including measurement of the mean maximum vitrinite (telocollinite) reflectance. Further details of the study and a more comprehensive discussion of the results are provided by Ward *et al.* (in press).

### VITRINITE CHEMISTRY, REFLECTANCE AND RANK

Figure 1 shows the relation between the C content of the telocollinite in the coals studied, as measured by microprobe analysis, and the mean maximum telocollinite reflectance for the same samples, in comparison to similar data for a number of other Australian coals based on previous studies (*e.g.* Ward *et al.* 2005). The relationship between vitrinite composition and vitrinite reflectance for the Puxtrees seam on the Muswellbrook Anticline is consistent with that of other Sydney-Bowen Basin coals, and thus the vitrinite reflectance appears to provide a reasonable basis for rank evaluation. The vitrinites in the seams of the Cranky Corner Basin, however, have similar carbon contents, suggesting a similar rank level to the Puxtrees material (*i.e.* equivalent to ~0.7%  $R_{v_{max}}$ ), but have much lower vitrinite reflectance values. If used as a rank indicator, the vitrinite reflectance would therefore significantly underestimate the thermal history of the Crank Corner Basin seams.

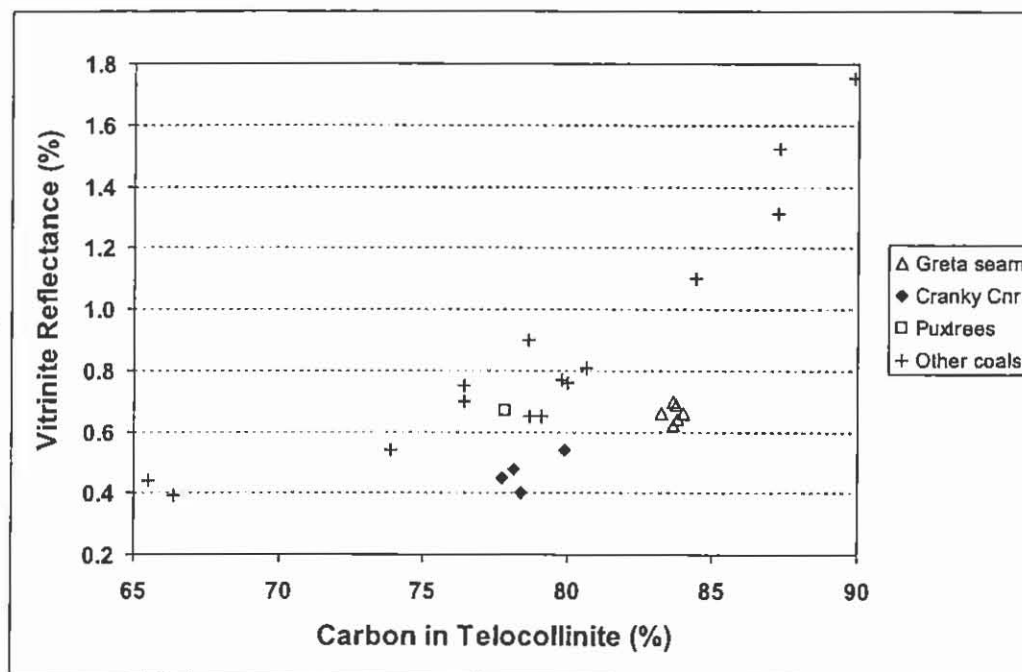
The vitrinite macerals in the Greta seam samples from Southland Colliery all have similar C contents, despite the upward decrease in reflectance within the seam section. The vitrinite carbon content for these coals is higher than for the Puxtrees or Cranky Corner materials (Fig. 1), indicating a higher rank for the Greta Coal Measures on at least this part of the Lochinvar Anticline than on the Muswellbrook Anticline or in the Cranky Corner Basin. The vitrinite reflectance values, even in the lower part of the seam, thus also provide an under-estimate of the actual thermal maturity level.

Table 1 Elemental composition of macerals in coal samples (after Ward *et al.* in press)

	Rv <sub>max</sub>	Maceral	No	C%	O%	N%	S%	Al%	Si%	Ca%	Fe%
Greta seam	0.62%	TC	24	83.66	8.35	1.82	2.44	0.20	0.04	0.12	0.04
Southland Colliery		DSC	13	83.60	8.46	1.86	2.56	0.20	0.06	0.17	0.01
Top section		SP	3	89.49	4.77	1.30	2.03	0.07	0.08	0.04	0.04
2.2 m		SF	9	86.74	6.66	1.80	1.16	0.14	0.03	0.13	0.04
		FUS	15	90.21	4.01	1.40	0.74	0.04	0.02	0.19	0.04
		IND	3	92.95	2.58	0.92	0.50	0.03	0.09	0.19	0.09
Greta seam	0.69%	TC	18	83.25	8.91	1.97	1.39	0.14	0.03	0.06	0.02
Southland Colliery		DSC	16	83.75	8.56	1.99	1.40	0.16	0.03	0.05	0.03
Middle section		SP	3	89.03	4.88	1.42	1.12	0.02	0.01	0.01	0.04
1.0 m		SF	19	86.68	6.81	1.37	0.86	0.01	0.02	0.10	0.03
		FUS	18	90.65	4.10	0.94	0.49	0.02	0.04	0.09	0.04
		IND	4	93.49	2.65	0.33	0.42	0.00	0.01	0.19	0.06
Greta seam	0.70%	TC	17	83.64	8.59	1.71	1.08	0.14	0.03	0.05	0.03
Southland Colliery		DSC	10	83.33	8.84	1.95	1.09	0.18	0.08	0.18	0.04
Bottom section		CUT	3	88.58	5.48	0.84	0.77	0.06	0.04	0.05	0.00
2.0 m		SF	6	84.87	8.20	1.08	0.86	0.01	0.02	0.09	0.00
		FUS	18	90.78	4.24	0.95	0.51	0.08	0.12	0.13	0.04
		IND	4	93.86	2.31	0.75	0.35	0.03	0.02	0.05	0.06
Tangorin seam	0.40%	TC	15	78.37	10.87	1.62	6.23	0.28	0.04	1.05	0.01
Cranky Cnr Basin		DSC	6	78.91	10.06	0.96	6.15	0.33	0.15	1.08	0.05
Ply 1		SF	9	84.41	7.07	1.31	2.97	0.09	0.10	0.93	0.01
		FUS	9	90.82	4.01	0.70	1.66	0.07	0.03	0.21	0.02
		IND	2	93.38	2.62	0.23	1.33	0.01	0.02	0.22	0.00
Tangorin seam	0.48%	TC	17	78.12	10.77	1.33	6.46	0.49	0.08	0.66	0.01
Cranky Cnr Basin		DSC	3	84.56	7.69	1.30	4.00	0.15	0.12	0.21	0.00
Ply 4		SP	6	84.06	6.34	0.62	6.77	0.15	0.11	0.31	0.02
		SF	11	85.43	7.36	0.96	2.75	0.03	0.03	0.29	0.03
		FUS	8	89.71	4.91	0.54	2.00	0.01	0.02	0.19	0.02
		IND	2	91.59	3.61	0.54	1.65	0.00	0.02	0.13	0.06
Tangorin seam	0.45%	TC	17	77.73	11.04	1.04	5.59	0.29	0.06	0.83	0.04
Cranky Cnr Basin		DSC	5	78.34	11.09	1.16	5.21	0.31	0.06	0.74	0.00
Composite		SF	15	87.41	5.90	1.27	1.59	0.02	0.06	0.18	0.02
		FUS	4	89.93	3.06	0.83	2.08	0.18	0.05	0.31	0.00
Stanhope seam	0.54%	TC	11	79.90	10.32	1.48	2.93	0.29	0.07	0.57	0.02
Cranky Cnr Basin		DSC	8	79.56	10.21	1.65	3.25	0.28	0.06	0.67	0.04
Ply 2		SF	6	84.95	7.47	1.07	1.28	0.02	0.04	0.30	0.03
		FUS	4	87.45	6.00	0.82	0.95	0.01	0.08	0.26	0.00
		IND	4	91.71	3.25	0.51	0.98	0.01	0.01	0.22	0.04
Puxtrees seam	0.67%	TC	8	77.85	15.65	2.06	0.76	0.04	0.05	0.01	0.03
Ply 1		DSC	11	79.32	14.36	1.76	0.75	0.05	0.06	0.01	0.02
Drayton Colliery		SP+DSC	6	81.51	13.56	1.57	1.00	0.07	0.08	0.01	0.01
		SP	5	86.19	8.34	1.10	0.56	0.02	0.09	0.02	0.03
		CUT	4	88.57	6.18	0.68	0.38	0.01	0.01	0.01	0.05
		SF	9	81.35	12.89	1.36	0.26	0.04	0.05	0.03	0.06
		FUS	7	86.62	7.73	0.77	0.28	0.02	0.01	0.14	0.02
		IND	4	89.91	4.61	1.03	0.27	0.01	0.01	0.10	0.00

TC = telocollinite; DSC = desmocollinite; SP = sprorinite; CUT = cutinite; SF = semifusinite; FUS = fusinite; IND = inertodetrinite

The lateral variation in vitrinite C content across the three areas (Fig. 2) is consistent with higher rank and deeper burial of the Greta Coal Measures on the southern end of the Lochinvar Anticline, away from the Hunter Thrust and towards the structural axis of the basin. Uplift on the anticline has subsequently brought the higher-rank Greta seam coals closer to the present-day ground surface. The seams on the Muswellbrook Anticline and in the Cranky Corner Basin apparently have a similar rank levels and burial histories, despite the contrasts in their vitrinite reflectance and tectonic setting.



**Figure 1.** Relation between mean maximum vitrinite (telocollinite) reflectance and C content of telocollinite for samples studied, in comparison to similar data from other Australian coal seams (Ward *et al.* in press).

### ORGANIC SULPHUR AND OTHER ELEMENTS

The coals in the study with anomalously low vitrinite reflectance also tend to have relatively high total S and organic S contents, with organic S being especially abundant in the vitrinite components. Figure 3 further suggests that the vitrinites in the coals from the Cranky Corner Basin, which have particularly high organic S contents, also have anomalously low proportions of O in relation to their C contents. The magnitude of the anomaly is close to the additional percentage of organic S in the vitrinites of these coals, which suggests that the additional S has replaced O in the molecular structure of the macerals concerned.

Electron microprobe analysis also shows that the vitrinites with high levels of organic S have significant percentages of Al and Ca within the organic structure. Such organically-associated inorganic elements are common in lower-rank coals (Miller & Given 1986; Ward 1992), but in other coals are typically lost at higher rank levels (Ward *et al.* 2005). The coals containing these elements, the Cranky Corner and upper Greta seam samples, therefore have elemental compositions (especially vitrinite carbon contents) consistent with a high-volatile bituminous rank, but the vitrinite reflectance and organically-associated inorganic elements of lower rank materials.

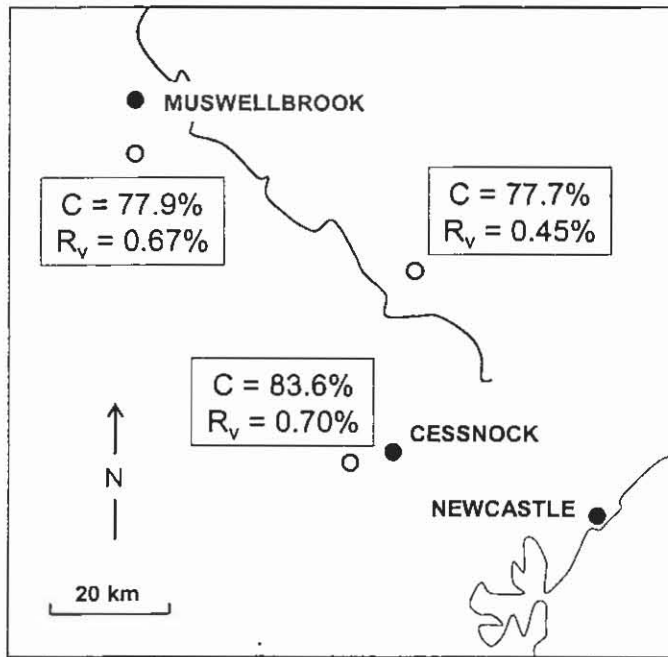


**Figure 2.** Lateral variation in vitrinite carbon content and vitrinite (telocollinite) reflectance in seams of the Greta Coal Measures (after Ward *et al.* in press).

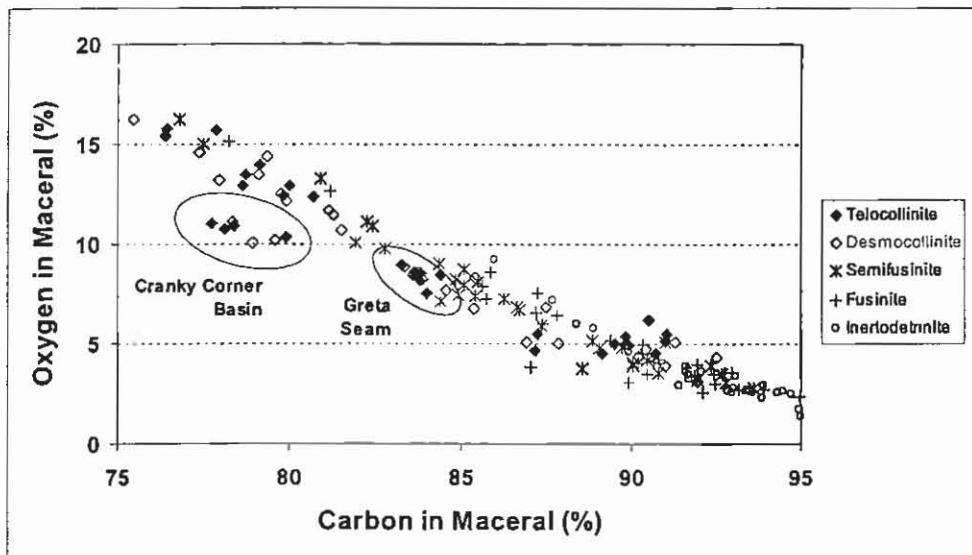


**Figure 3.** C-O plot for macerals in Greta Coal Measures and other Australian coal samples (Ward *et al.*, in press). Note the low O content of the high-S vitrinites in the Cranky Corner Basin coals, relative to other vitrinites with equivalent C contents.

Plotting the proportions of Al and Ca in the vitrinite macerals against the organic S content of the vitrinites in the same coal samples (Fig. 4) suggests that the proportions of these elements in the vitrinite both tend to increase with increasing organic S content. The total proportion of the two elements (i.e. Al + Ca), moreover, shows an essentially linear increase with the vitrinite's organic sulphur content. The slope of the regression line (0.21) further suggests that the Ca and Al consistently make up a combined total representing ~20% of the organic S in the vitrinite components.

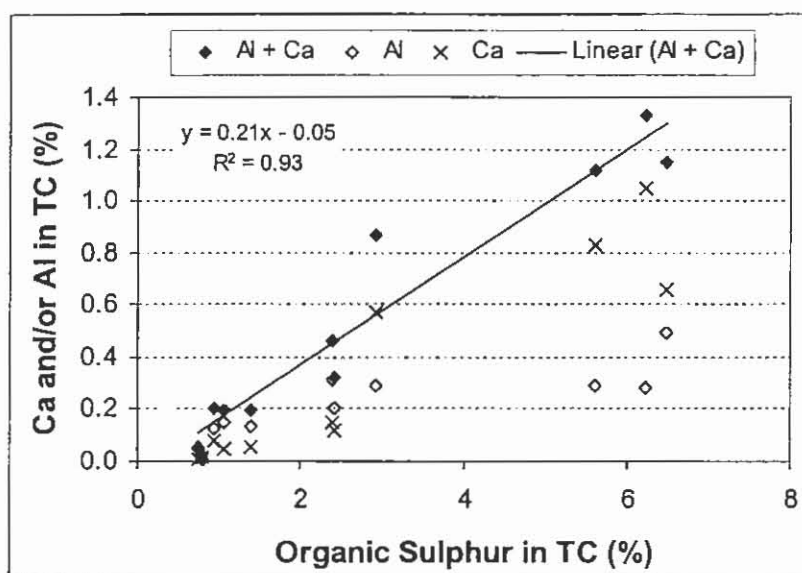


**Figure 4.** Abundance of Al, Ca and total Al + Ca in telocollinite in relation to (organic) S content of telocollinite for all samples from the Greta Coal Measures (Ward *et al.* in press). Linear regression correlation line and equation for Al + Ca against sulphur in telocollinite is also shown.

Inorganic elements occurring in the chemical structure of coal macerals may be expected to react in a different way to the same elements occurring in the coal in mineral form (e.g. Ca as carbonates or Al in clay minerals). The significant abundance of such elements in the macerals of some (but not all) parts of the Greta Coal Measures therefore needs to be taken into account in assessing the behaviour of the coal in different market applications, including the possibility of slagging associated with conventional (pulverised fuel) combustion and future development of processes based on gasification systems.

#### ACKNOWLEDGEMENTS

Financial support for the study was provided under the Large Grants Scheme of the Australian Research Council. Thanks are expressed to Rad Flossman for polished section preparation, Maria Mastalerz for provision of the carbon standard used in the microprobe study, and Barry Searle for assistance with the electron microprobe analyses. Thanks are also expressed to the relevant mining and exploration companies, and to Guy Palese, Ron Slocombe, Luc Daigle and Anton Crouch, for provision of the coal samples. Thanks also to the referees for their constructive comments.

#### REFERENCES

- BUSTIN, R. M., MASTALERZ, M. & WILKS, K. R. 1993. Direct determination of carbon, oxygen and nitrogen content in coal using the electron microprobe. *Fuel* **72**, 181-185.
- BUSTIN, R. M., MASTALERZ, M. & RAUDSEPP, M. 1996. Electron-probe microanalysis of light elements in coal and other kerogen. *International Journal of Coal Geology* **32**, 5-30.
- DIESSEL, C. F. K., 1992. *Coal-Bearing Depositional Systems*. Springer Verlag, Berlin, 721 pp.
- DIESSEL, C. F. K. & GAMMIDGE, L. 1998. Isometamorphic variations in the reflectance and fluorescence of vitrinite – a key to depositional environment. *International Journal of Coal Geology* **36**, 167-222.
- DIESSEL, C. F. K. & GAMMIDGE, L. C. 2003. Downhole vitrinite reflectance in DM Tangorin DDH 1. In: Facer, R. A. & Foster, C. B. eds. *Geology of the Cranky Corner Basin*, New

- South Wales Department of Mineral Resources, Coal and Petroleum Bulletin 4, 107-114.
- GURBA, L. W. & WARD, C. R. 2000. Elemental composition of coal macerals in relation to vitrinite reflectance, Gunnedah Basin, Australia, as determined by electron microprobe analysis. *International Journal of Coal Geology* 44, 127-147.
- MASTALERZ, M. & GURBA, L. W. 2001. Determination of nitrogen in coal macerals using electron microprobe technique – experimental procedure. *International Journal of Coal Geology* 47, 23-30
- MILLER, R.N. & GIVEN, P. H. 1986. The association of major, minor and trace inorganic elements with lignites: I – Experimental approach and study of a North Dakota lignite. *Geochimica et Cosmochimica Acta* 50, 2033-2043.
- WARD, C. R. 1992. Mineral matter in Triassic and Tertiary low-rank coals from South Australia. *International Journal of Coal Geology* 20, 185-208.
- WARD, C. R. & GURBA, L. W. 1998. Occurrence and distribution of organic sulphur in macerals of Australian coals using electron microprobe techniques. *Organic Geochemistry* 28, 635-647.
- WARD, C. R. & GURBA, L. W. 1999. Chemical composition of macerals in bituminous coals of the Gunnedah Basin, Australia, using electron microprobe techniques. *International Journal of Coal Geology* 39, 279-300.
- WARD, C. R., LI, Z. S. & GURBA, L. W. 2005. Variations in coal maceral chemistry with rank advance in the German Creek and Moranbah Coal Measures of the Bowen Basin, Australia, using electron microprobe techniques. *International Journal of Coal Geology* 63, 117-129.
- WARD, C. R., LI, Z. S. & GURBA, L. W., in press. Variations in elemental composition of macerals with vitrinite reflectance and organic sulphur in the Greta Coal Measures, New South Wales, Australia, *International Journal of Coal Geology*.

# IDENTIFICATION OF THE PERMIAN-TRIASSIC BOUNDARY IN THE SOUTHERN SYDNEY BASIN

Megan L. Williams, Paul F. Carr and Brian G. Jones

School of Earth and Environmental Sciences  
University of Wollongong, Wollongong, NSW, 2522

## ABSTRACT

The identification of the Permian-Triassic (P-Tr) boundary in eastern Australia is based primarily on palynological and plant fossil evidence with limited  $\delta^{13}\text{C}_{\text{org}}$  data from the northern part of the Sydney Basin. This boundary in the Sydney Basin has been placed at the top of the last Permian coal measures. Here we report preliminary  $\delta^{13}\text{C}_{\text{org}}$ , total organic carbon (TOC), and major and trace element data for a continuous non-marine P-Tr section from the southern Sydney Basin. The boundary is identified by a negative shift in  $\delta^{13}\text{C}_{\text{org}}$  of  $\sim 3.8\%$  occurring  $\sim 1$  m above the Bulli Coal. Lack of correlation between  $\delta^{13}\text{C}_{\text{org}}$  and TOC indicates that the isotopic signature has not been affected by contamination or diagenetic processes. Positive excursions in Ni, Cr and Co concentrations are coincident with the negative  $\delta^{13}\text{C}_{\text{org}}$  shift, and are most likely a reflection of oxygen availability and changing mineral proportions.

## INTRODUCTION

The negative shift in  $\delta^{13}\text{C}$  of carbonates ( $\delta^{13}\text{C}_{\text{carb}}$ ), particularly in marine sections, is widely accepted as a marker for the P-Tr boundary and in many cases this occurs in conjunction with the first appearance of the Triassic index fossil conodont *Hindeodus parvus* (Yin *et al.* 2001). A negative shift in  $\delta^{13}\text{C}$  of organic matter ( $\delta^{13}\text{C}_{\text{org}}$ ) is recognised in both marine and non-marine sections – in the case of marine sections this shift is coincident with that seen in carbonates (Morante *et al.* 1994; Wang *et al.* 1994; de Wit *et al.* 2002; Sakar *et al.* 2003; Peng *et al.* 2005). The magnitude of these  $\delta^{13}\text{C}$  shifts ranges from 2‰ to 10‰. Identification of the boundary in non-marine sections is hampered by a lack of appropriate index fossils, and this also makes correlation between marine and non-marine sections difficult (Foster *et al.* 1998). The negative shift in  $\delta^{13}\text{C}_{\text{org}}$ , however, together with fossil and palynological evidence for some more widespread species and the global cessation of coal formation have been used to identify the P-Tr boundary in a number of non-marine sections (Morante *et al.* 1994; Retallack 1995; Morante 1996; de Wit *et al.* 2002; Sakar *et al.* 2003).

The Sydney Basin contains thick, continuous non-marine sections spanning the P-Tr boundary. The most recent studies have shown that the P-Tr boundary occurs at the top of the last Permian coals, coincident with a change in lithology to siliciclastic strata, the last known occurrence of *Glossopteris* flora, and near the base of the *Protohaploxylinus microcorpus* palynozone (Retallack 1995, 1999; Morante 1996). As part of a larger study encompassing several Australian basins, Morante (1996) examined a core from the northern part of the Sydney Basin and found a negative  $\delta^{13}\text{C}_{\text{org}}$  shift of 4‰  $\sim 20$  m above the last Permian coal,

whereas in a section from the Bowen Basin the negative shift was 6‰ ~1m above the last Permian Coal. In both cases the negative shifts are coincident with palynological and plant fossil markers. Here we examine a section from the southern Sydney Basin in an attempt to gather further isotopic and geochemical evidence for the position of the P-Tr boundary.

### SAMPLING & ANALYSES

Samples were taken every 20-30 cm from a drill core (Douglas DDH15) supplied by BHP Billiton. The core had been recently drilled and stored under cover, ensuring the material had not been subjected to weathering. Logging was carried out by personnel from Strata Control Technology Pty Ltd, and thus the positions of the samples relative to the Bulli Coal are accurately known. The samples were split with one fraction crushed to a fine powder in a tungsten-carbide mill and another in a chrome-steel mill.

XRD analyses were performed at the University of Wollongong using a Philips 1150 PW Bragg-Brentano diffractometer with Cu K $\alpha$  radiation and a graphite monochromator. The TRACES software package was used for phase identification, and quantitative results were obtained using SIROQUANT quantitative analysis software.

Major and trace element concentrations were determined by XRF by Bruce Chappell at Macquarie University. Analyses for the rare earth element (REE), platinum group elements (PGE), Au and Re were performed by Activation Laboratories Ltd, Canada, using a combination of INAA and ICP-MS.

$\delta^{13}\text{C}_{\text{org}}$  and total organic carbon (TOC) analyses were performed at ANSTO on a Eurovector Euro EA 3000 and GV Instruments MicroMass IsoPrime mass spectrometer. Samples were treated with dilute HCl, rinsed with high purity water, and dried prior to measurement. Results are reported relative to the V-PDB standard ( $\delta^{13}\text{C}_{\text{org}}$ ) and in % (TOC).

### RESULTS

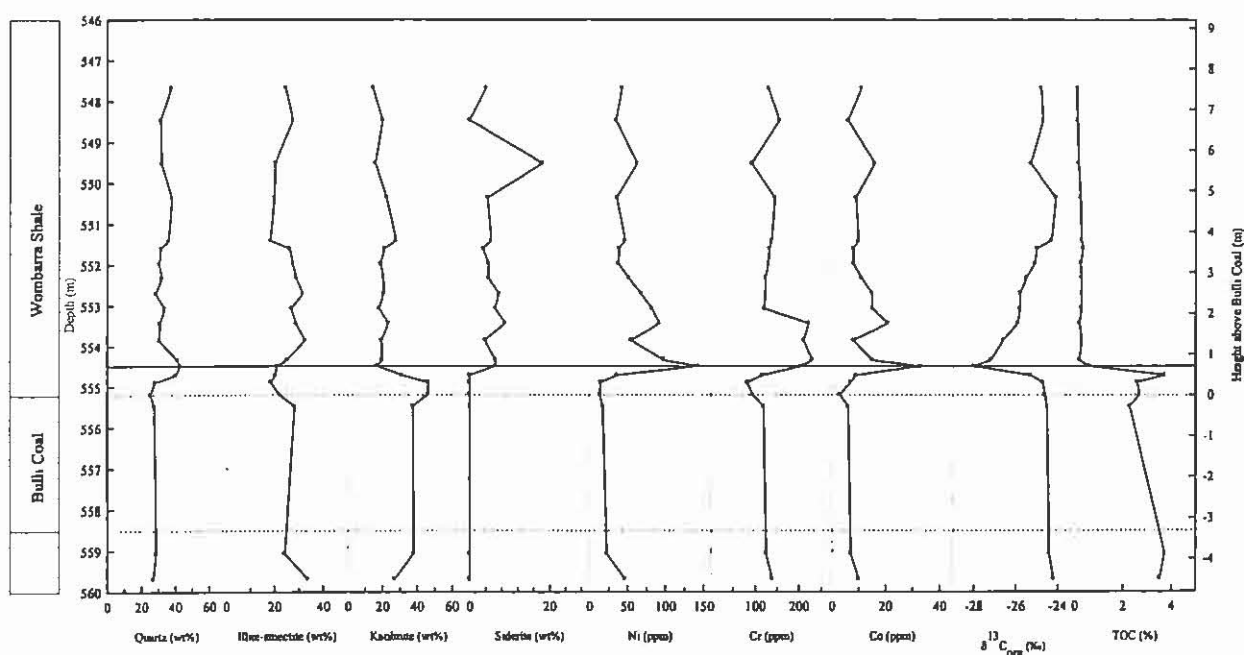
The material sampled from ~1.5 m below to ~9 m above the Bulli Coal is a fine- to very fine-grained shale that varies from massive to very finely laminated. Laminations are parallel to subparallel. The contact with the underlying coal is gradational. The colour varies from very dark grey/black adjacent to the Bulli Coal, becoming slightly paler upwards. Plant fragments occur throughout but have their highest density near the Bulli Coal.

Figure 1 shows variations in selected mineralogical and geochemical data with height above the top of the Bulli Coal. The  $\delta^{13}\text{C}_{\text{org}}$  data show a clear negative shift of 3.8‰ at 0.8 m and a gradual recovery by 4 m. The TOC data show a spike followed by a shift to lower values at 0.8 m with values subsequently remaining consistently low. No statistically significant correlation exists between TOC and  $\delta^{13}\text{C}_{\text{org}}$  (Fig. 2).

The mineralogy is dominated by quartz and clays with muscovite and minor siderite. Quartz, siderite, and (to a lesser extent) muscovite and illite-smectite all show increases in abundance at ~0.8 m, whereas kaolinite decreases. The major element distributions are linked to the changes in mineralogy. Increases in SiO<sub>2</sub>, Fe<sub>2</sub>O<sub>3</sub>, MnO and MgO at 0.8 m reflect the quartz and siderite contents, and the decrease in Al<sub>2</sub>O<sub>3</sub> is related to the kaolinite decrease. The slight increase in K<sub>2</sub>O at 0.8 m is most likely linked to slight increases in muscovite and illite-smectite.

## P-TR BOUNDARY IDENTIFICATION

Notable in the trace element results are the increases in Ni, Cr and Co at 0.8 m. Th/U ratios reflect the prevailing redox conditions with high values indicating more oxic conditions (Jones & Manning 1994; Dypvik & Harris 2001; Dypvik *et al.* 2006). Here they show some variability with lower values occurring at 0.8 m, coincident with the increases in Ni, Cr and Co. Zr/Rb ratios are low (<3) and show little variation, an indication of shales with near-constant grain size. Where slight variations occur they correlate with SiO<sub>2</sub> fluctuations, reflecting periods of relative increases and decreases in slightly coarser grained material (Dypvik & Harris 2001). (Zr+Rb)/Sr ratios are relatively constant between 2 and 4, indicating the clastic to carbonate balance is reasonably steady with relatively low carbonate input (Dypvik & Harris 2001). This is consistent with the XRD results for carbonate content.



**Figure 1.** Selected mineralogical and geochemical data, including carbon isotope results. The solid line running across all plots delineates the position of the P-Tr boundary based on the  $\delta^{13}\text{C}_{\text{org}}$  results and is ~0.8 m above the Bulli Coal.

REE patterns normalised to the NASC standard (Fig. 3) do not show much deviation from standard shale with the exception of those samples from very close to the coal. The only Eu anomaly is a negative anomaly for the sample at -4.49 m. Measurements of contents of PGE, Au and Re for the samples from 0.31 m to 1.76 m were all below the detection limits with the exception of the sample at 1.76 m which contains 15.3 ppb Au.

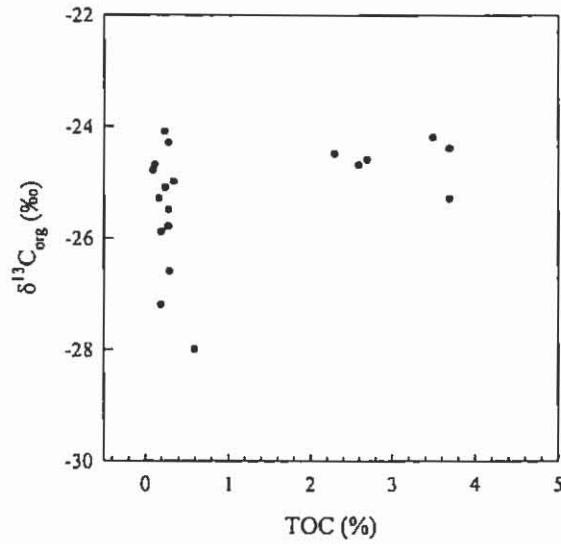


**Figure 2.** Plot of  $\delta^{13}C_{org}$  vs TOC for samples spanning the P-Tr boundary in the southern Sydney Basin. Those with higher TOC are closest to the Bulli Coal.

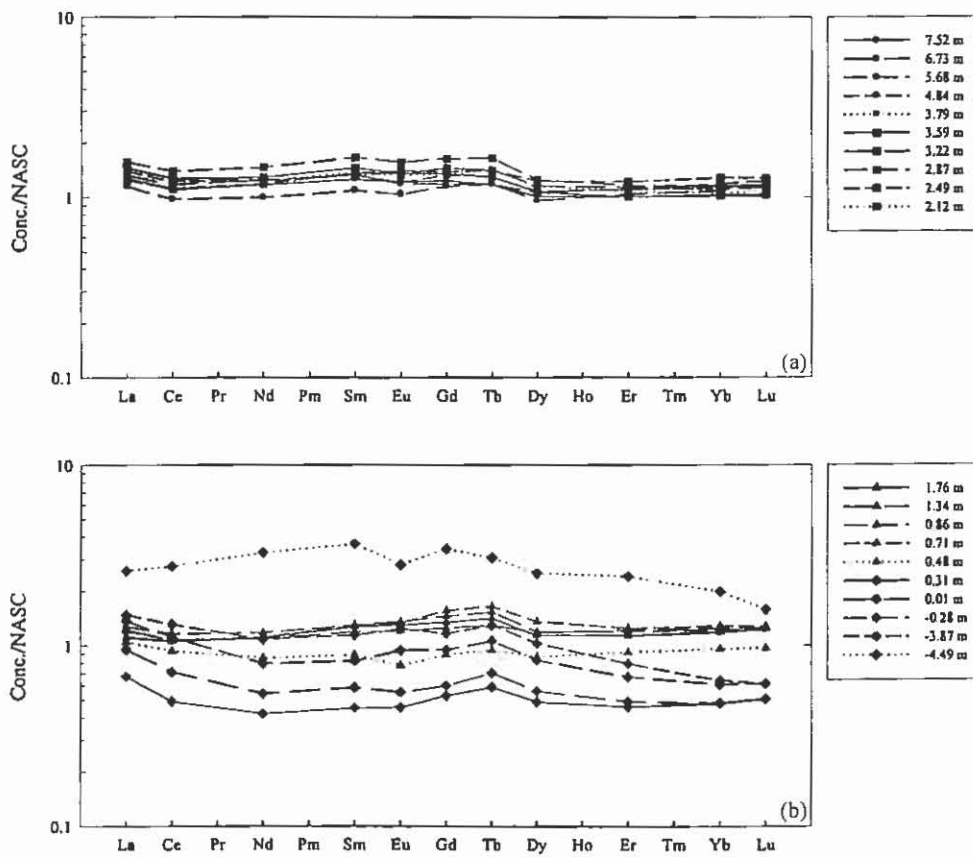


**Figure 3.** REE patterns for samples from the southern Sydney Basin normalised to NASC.

## DISCUSSION

Macropetrographic and micropetrographic data indicate that sedimentation across the P-Tr boundary was continuous; evidence of palaeosol development is absent. The laminations, organic matter content, bulk mineralogy, and trace element ratios all indicate a predominantly low energy fluvial, lacustrine or lagoonal environment subject to minor fluctuations in energy and oxygen levels. This is consistent with the findings of Dehghani (1994) for the lower fine-grained unit of the Wombarra depositional system.

The magnitude of the negative  $\delta^{13}\text{C}_{\text{org}}$  shift is similar to that found in numerous, worldwide, marine and non-marine P-Tr sections (e.g. Holser *et al.* 1989; Morante *et al.* 1994; Wang *et al.* 1994; Morante 1996; Krull & Retallack 2000; de Wit *et al.* 2002; Peng *et al.* 2005). The stratigraphic position of the shift (~1 m above the last Permian coal) also coincides with that found in the northern Sydney Basin (Morante 1996) and Antarctica (Krull & Retallack 2000). The lack of correlation between  $\delta^{13}\text{C}_{\text{org}}$  and TOC signifies that the isotope measurements have not been affected by contamination or thermally driven loss of hydrocarbons during diagenesis (Krull & Retallack 2000; Sandler *et al.* 2006). We thus conclude that our evidence shows the position of the P-Tr boundary in the southern Sydney Basin to be ~1 m above the top of the last Permian coal.

Coincident with the negative shift in  $\delta^{13}\text{C}_{\text{org}}$  are enrichments in Ni, Cr and Co. These, together with low Th/U ratios, could be explained by changes in carbonate content, TOC, clay content, oxygen levels or a meteorite impact (Jones & Manning 1994; Ellwood *et al.* 2003; Muñoz-Espadas *et al.* 2003; Abanda & Hannigan 2006; Dypvik *et al.* 2006). The trace element ratios V/Cr and Ni/Co are often used to identify the relevant enrichment process with oxidising conditions being characterised by V/Cr <2 and Ni/Co <5 (Jones & Manning 1994). The samples from the southern Sydney Basin have V/Cr values of 0.5-1.5 suggesting more oxic conditions. The Ni/Co values are  $\leq 5$  up to 0.8 m above the coal seam after which they jump to ~7 before falling back to ~5. These values indicate that oxygen levels fluctuated, becoming more dysoxic at the P-Tr boundary. A recent study by Abanda and Hannigan (2006) has shown that the different mineral fractions in shales show different enrichment patterns of trace elements due to diagenesis, with the carbonate fraction enriched in Co and the organic fraction enriched in Cr and Ni. The results presented here are whole rock measurements which negate distinction between contributions from the carbonate and organic fractions. The relative amounts of illite-smectite and kaolinite are variable and may also be significant in affecting the trace element enrichment patterns. Thus the changes in Ni, Cr and Co are most likely a reflection of oxygen levels during deposition coupled with some influence from changing mineral proportions.

Meteorite impact can also result in the kinds of changes in geochemical and isotopic behaviour observed in the southern Sydney Basin section. For an impact to be considered as a feasible explanation, however, further support from evidence such as shocked quartz, microspherules and PGE anomalies (especially Ir) is typically required. The available data do not show detectable levels of PGEs. A study of a continental section in India reported a positive Eu anomaly which was considered to be a sign of a meteorite impact (Sakar *et al.* 2003). No such anomaly was recognised in the current study.

## CONCLUSIONS

The P-Tr boundary in the southern Sydney Basin appears to occur ~1 m above the Bulli Coal in the basal shales of the Narrabeen Group and is defined by a negative shift in  $\delta^{13}\text{C}_{\text{org}}$  of

3.8‰. This is consistent with evidence from the northern Sydney Basin and other sections worldwide.

Major and trace element data, including the REE, indicate a mainly low energy fluvial, lacustrine or lagoonal depositional environment with continuous sedimentation and no paleosol development. No conclusive evidence for a meteorite impact at the P-Tr boundary has been identified. Further investigations of additional physical and geochemical data are being pursued to clarify the cause of the extinction event.

## REFERENCES

- ABANDA, P. A. & HANNIGAN, R. E. 2006. Effect of diagenesis on trace element partitioning in shales. *Chemical Geology* **230**, 42-59.
- DEGHANI, M. H. 1994. *Sedimentology, Genetic Stratigraphy and Depositional Environment of the Permo-Triassic Succession in the Southern Sydney Basin, Australia*. PhD thesis, University of Wollongong, Wollongong (unpubl.).
- DE WIT, M. J., GHOSH, J. G., DE VILLIERS, S., RAKOTOSOLOFO, N., ALEXANDER, J., TRIPATHI, A. & LOOY, C. 2002. Multiple organic carbon isotope reversals across the Permo-Triassic boundary of terrestrial Gondwana sequences: clues to extinction patterns and delayed ecosystem recovery. *Journal of Geology* **110**, 227-240.
- DYPVIK, H. & HARRIS, N. B. 2001. Geochemical facies analysis of fine-grained siliciclastics using Th/U, Zr/Rb and (Zr+Rb)/Sr ratios. *Chemical Geology* **181**, 131-146.
- DYPVIK, H., SMELROR, M., SANDBAKKEN, P. T., SALVIGSEN, O. & KALLESON, E. 2006. Traces of the marine Mjølner impact event. *Palaeogeography, Palaeoclimatology, Palaeoecology* **241**, 621-636.
- ELLWOOD, B. B., BENOIST, S. L., EL HASSANI, A., WHEELER, C. & CRICK, R. E. 2003. Impact ejecta layer from the Mid-Devonian: Possible connection to global mass extinctions. *Science* **300**, 1734-1737.
- FOSTER, C. B., LOGAN, G. A. & SUMMONS, R. E. (1998) The Permian-Triassic boundary in Australia: where is it and how is it expressed? *Proceedings of the Royal Society of Victoria* **110**, 247-266.
- HOLSER, W. T., SCHÖNLAUB, H.-P., ATTREP, M., BOECKELMANN, K., KLEIN, P., MAGARITZ, M., ORTH, C. J., FENNINGER, A., JENNY, C., KRÁLIK, M., MAURITSCH, H., PAK, E., SCHRAMM, J.-M., STATTEGGER, K. & SCHMÖLLER, R. 1989. A unique geochemical record at the Permian/Triassic boundary. *Nature* **337**, 39-44.
- JONES, B. & MANNING, D. A. C. 1994. Comparison of geochemical indices used for the interpretation of palaeoredox conditions in ancient mudstones. *Chemical Geology* **111**, 111-129.
- KRULL, E. S. & RETALLACK, G. J. 2000.  $\delta^{13}\text{C}$  depth profiles from paleosols across the Permian-Triassic boundary: Evidence for methane release. *Geological Society of America Bulletin* **112**, 1459-1472.
- MORANTE, R. 1996. Permian and Early Triassic isotopic records of carbon and strontium in Australia and a scenario of events about the Permian-Triassic Boundary. *Historical Biology* **11**, 289-310.
- MORANTE, R., VEEVERS, J. J., ANDREW, A.S. & HAMILTON, P.J. 1994. Determination of the Permian-Triassic boundary in Australia from carbon isotope stratigraphy. *Australian Petroleum Exploration Association Journal* **34**, 330-336.
- MUÑOZ-ESPADAS, M.-J., MARTÍNEZ-FRÍAS, J. & LUNAR, R. 2003. Main geochemical signatures related to meteoritic impacts in terrestrial rocks: A review. In: Koeberl C. & Martínez-Ruiz F.C. eds. *Impact Markers in the Stratigraphic Record*, pp. 65-90.

## P-TR BOUNDARY IDENTIFICATION

Germany: Springer-Verlag]

- PENG, Y., ZHANG, S., YU, T., YANG, F., GAO, Y. & SHI, G. R. 2005. High-resolution terrestrial Permian-Triassic eventostratigraphic boundary in western Guizhou and eastern Yunnan, southwestern China. *Palaeogeography, Palaeoclimatology, Palaeoecology* **215**, 285-295.
- RETALLACK, G. J. 1995. Permian-Triassic life crisis on land. *Science* **267**, 77-80.
- RETALLACK, G. J. 1999. Postapocalyptic greenhouse paleoclimate revealed by earliest Triassic paleosols in the Sydney Basin, Australia. *Geological Society of America Bulletin* **111**, 52-70.
- SAKAR, A., YOSHIOKA, H., EBIHARA, M. & NARAOKA, H. 2003. Geochemical and organic carbon isotope studies across the continental Permo-Triassic boundary of Raniganj Basin, eastern India. *Palaeogeography, Palaeoclimatology, Palaeoecology* **191**, 1-14.
- SANDLER, A., ESHET, Y. & SCHILMAN, B. 2006. Evidence for a fungal event, methane-hydrate release and soil erosion at the Permian-Triassic boundary in southern Israel. *Palaeogeography, Palaeoclimatology, Palaeoecology* **242**, 68-89.
- WANG, K., GELDSETZER, H. H. & KROUSE, H. R. 1994. Permian-Triassic extinction: Organic  $\delta^{13}\text{C}$  evidence from British Columbia, Canada. *Geology* **22**, 580-584.
- YIN, H., ZHENG, K., TONG, J., YANG, Z. & WU, S. 2001. The global stratotype section and point (GSSP) of the Permian-Triassic Boundary. *Episodes* **24**, 102-114.



# ORGANIC GEOCHEMICAL CHARACTERISTICS OF LATE PERMIAN COALS FROM THE SOUTHERN SYDNEY BASIN, AUSTRALIA

Manzur Ahmed<sup>1</sup>, Herbert Volk<sup>1</sup>, Simon C. George<sup>2</sup> and Mohinudeen Faiz<sup>1</sup>

<sup>1</sup>CSIRO Petroleum  
PO Box 136, North Ryde, NSW 1670, Australia

<sup>2</sup>Australian Centre for Astrobiology  
Macquarie University, Sydney, NSW 2109, Australia

## ABSTRACT

This paper presents results of organic geochemical analyses of solvent extracts of four Late Permian coals and shaly coals from the Appin, Tahmoor and Metropolitan mines in the southern Sydney Basin, Australia. The aliphatic hydrocarbon fractions of these samples are characterised by the presence of high relative abundances of pristane, C<sub>19</sub> tricyclic terpane, C<sub>20</sub> tricyclic terpane, C<sub>24</sub> tetracyclic terpane, C<sub>29</sub> steranes and diasteranes, and the absence of C<sub>30</sub> steranes and extended tricyclic terpanes. This is consistent with peat deposition in a relatively oxic depositional environment under non-marine conditions. The coals are geochemically similar, and consistent with their Permian age contain coniferous organic matter with no input from flowering plants and no significant contribution from Araucariaceae conifers. However, the Metropolitan coal exhibits some biomarker characteristics usually found in organic matter associated with carbonates. This is very likely due to the adsorption of some allochthonous hydrocarbons produced in the interbedded calcareous rocks. The molecular maturities of the Sydney Basin coals as assessed by a variety of aliphatic and aromatic hydrocarbon biomarkers are similar to their measured vitrinite reflectance (1.0 to 1.4 %). This indicates that most of the hydrocarbons extracted from these samples are indigenous to the host Late Permian coals, or in the case of the Metropolitan coal are partly derived from intercalated shales of similar maturity. High organic matter extractabilities (>6,000 ppm), hydrogen contents of 4.9 to 5.4%, liptinite contents up to 2.5% and the peak to late oil window thermal maturities suggest that these high volatile to medium volatile bituminous coals may have generated significant and possibly commercial amounts of petroleum.

## INTRODUCTION

Unambiguous evidence of petroleum expulsion from coal is limited, and only a few commercial oil discoveries can be confidently correlated to coals (Wilkins and George 2002). Southeast Asia, Australia and New Zealand are the main regions with significant coal-sourced oil provinces (e.g. MacGregor 1994). The source sequences for these oils are generally Tertiary (e.g. Indonesian Basins: Matchette-Downes *et al.* 1994; Thompson *et al.* 1994; Taranaki Basin: e.g. Killops *et al.* 1994) or Jurassic/Cretaceous (e.g. Gippsland Basin, Australia: Powell and Boreham 1994) in age, with the Permian coals of the Cooper Basin, Australia (e.g. Powell and Boreham 1994; Curry *et al.* 1994) being notable exceptions. Based on pyrolysis studies Boreham *et al.* (1999) suggested that the Permian coals in the Bowen and Surat basins also have oil potential.

The presence of an active petroleum system in the Sydney Basin is strongly suggested by the occurrence of numerous gas and oil shows in both petroleum and coal exploration wells (Herbert 1984; Stewart and Alder 1995; Alder *et al.* 1998). Nevertheless, there have been no discoveries of economic or sub-economic petroleum accumulations in this coal-rich basin.

In this study, four Late Permian coals/shaly coals from the Appin, Tahmoor and Metropolitan Mines of the southern Sydney Basin have been studied using organic geochemistry and organic petrology so as to assess their thermal maturities and source rock potential for generating liquid hydrocarbons.

**SAMPLES**

The four samples were obtained from in-seam gas drainage boreholes in the Appin, Tahmoor and Metropolitan underground coal mines (Figure 1). Petrological and elemental composition of these medium to high volatile bituminous coals/shaly coals are summarised in Table 1. Present-day coal ranks were attained in the early Cretaceous during maximum burial associated with high heat flow during rifting along the eastern coast of Australia (Dumitru *et al.* 1991).

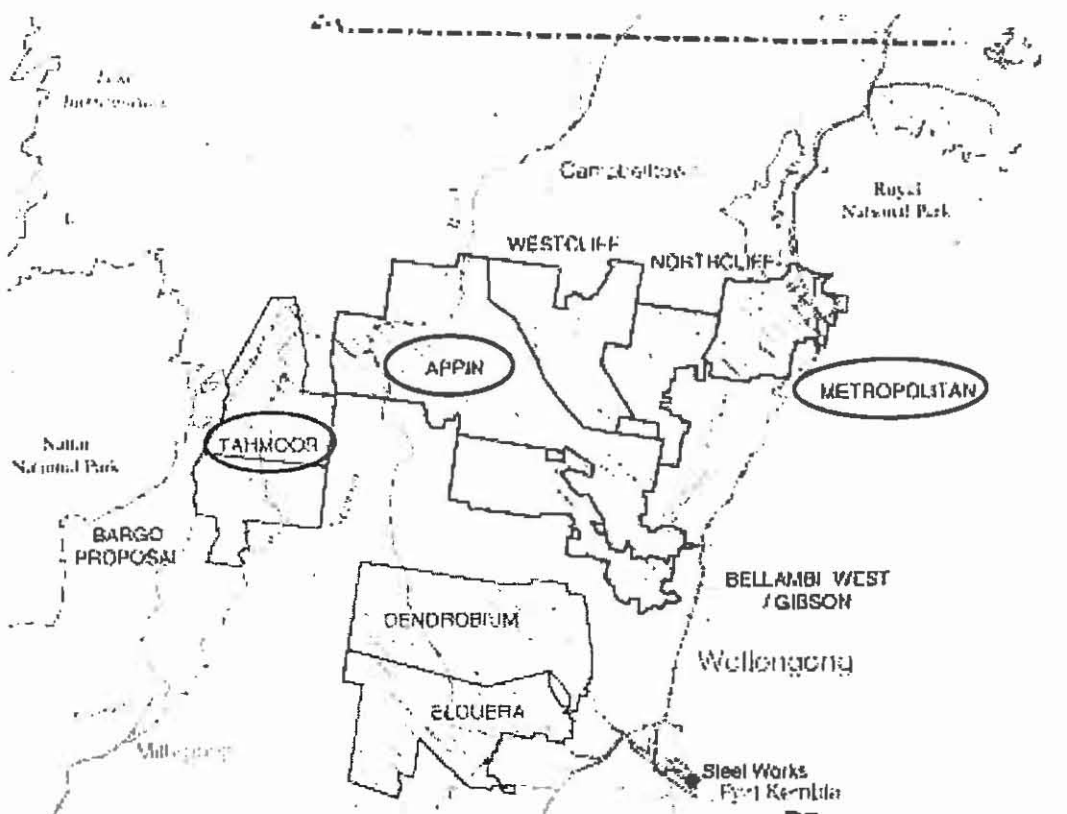


Figure 1 Coal mine lease boundaries in the Southern Sydney Basin (after Moffit 2000).

## GEOCHEMISTRY OF SYDNEY BASIN COALS

**Table 1** Petrological and elemental composition of the southern Sydney Basin coals/shaly coals.

Coals/Shaly Coals	Depth (m)	VR%	Extractability (ppm of coal)	Petrological Composition (volume %)				Elemental Composition (weight%, dry ash free)				
				Vitrinite	Inertinite	Liptinite	Minerals	% C	H	N	S	O
Appin GAP 1130	485	1.3	6000	30	13	<0.1	57	71	5.4	1.7	0.6	21
Tahmoor GB01	434	1.0	11000	80	15	2.5	2.3	88	5.4	2.0	0.5	4.3
Tahmoor GWS05	434	1.0	9000	45	49	1.3	5.0	90	4.9	1.8	0.4	3.5
Metropolitan	430	1.4	10000	66	28	<0.1	6.0	90	4.9	1.7	0.4	3.2

VR = Vitrinite Reflectance, C = Carbon, H = Hydrogen, N = Nitrogen, S = Sulphur, O = Oxygen

### METHODS

Vitrinite reflectance, maceral composition and elemental composition of the coals were determined following standard procedures (Standards Association of Australia 1997, 1998, 2000a, 2000b). The coals were crushed into a fine powder, solvent extracted and the extractable organic matter (EOM) was fractionated into asphaltene, aliphatic hydrocarbons, aromatic hydrocarbons and polar compounds using the procedures described in Stalker et al. (2001). The aliphatic and aromatic hydrocarbon fractions were analysed by gas chromatography (GC) and GC-mass spectrometry for detailed molecular compositions (Stalker et al. 2001).

### RESULTS AND DISCUSSION

#### Characteristics of organic matter

Most coals are formed under non-marine conditions (Tissot and Welte 1984). Likewise, the four Permian coals/shaly coals of the southern Sydney Basin exhibit the following organic geochemical characteristics which are consistent with their formation under relatively oxic, non-marine conditions containing predominantly land-derived higher plant organic matter:

- ◆ Significantly higher abundances of pristane compared to phytane,
- ◆ High abundances of the C<sub>19</sub> and C<sub>20</sub> tricyclic terpanes and C<sub>24</sub> tetracyclic terpane relative to other tricyclic terpanes,
- ◆ Predominance of C<sub>29</sub> steranes and diasteranes over C<sub>27</sub> steranes and diasteranes, and
- ◆ Absence or low abundances of C<sub>30</sub> steranes and extended tricyclic terpanes.

Despite the overall similarity of these organic geochemical characteristics, the coals/shaly coals show some subtle and distinctive variations in their molecular compositions. This is demonstrated in the spider diagram (Figure 2) of eighteen source-related molecular geochemical parameters.

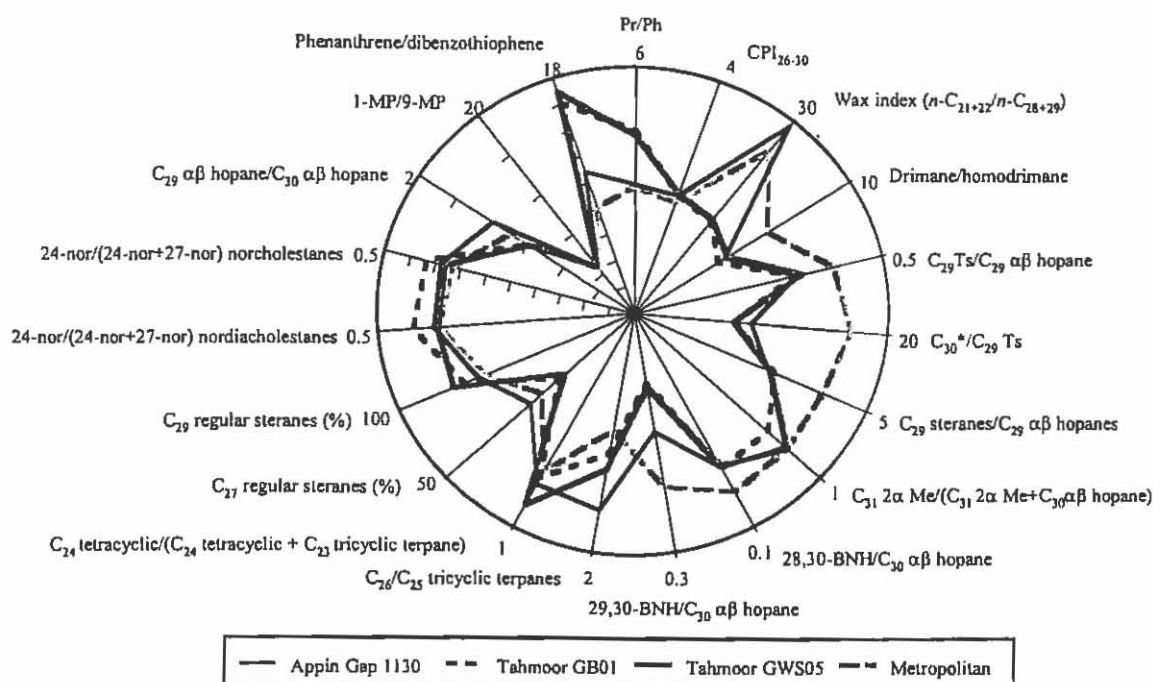


**Figure 2** Spider diagram illustrating the source differences and similarities for the coal samples (Pr = Pristane, Ph = Phytane, CPI = Carbon Preference Index).

For example, Appin Gap, Tahmoor GB01 and Tahmoor GWS05 coals are dominated by  $C_{30}$   $\alpha\beta$  hopane and contain moderate abundances of rearranged hopanes, whereas the Metropolitan coal contains very high abundances of rearranged hopanes. Interestingly, higher abundances of  $C_{29}$   $\alpha\beta$  hopane (30-norhopane), slightly higher abundances of 29,30-BNH and significant amounts of  $C_{30}$  30-norhopanes and 2 $\alpha$ -methylhopanes for the Metropolitan coal may indicate the adsorption of calcareous-sourced hydrocarbons produced in the interbedded calcareous shales or siltstones. However, relatively higher thermal maturity of this sample (Figure 4) may be, partly, responsible for the enhanced abundances of these compounds.

Oleanane, the biomarker for angiosperm flowering plants that evolved during the cretaceous (Moldowan *et al.* 1994), is absent in all the coals. This is consistent with the low content of 1,2,7- and 1,2,5-trimethylnaphthalenes (Figure 3) suggesting that these coals do not contain any contribution from angiosperm-derived terrestrial organic matter. Relatively low abundances of aromatic land plant markers, 1-methylphenanthrene, 1,7-dimethylphenanthrene and retene (Figure 3), are consistent with insignificant input of *Araucariacean* higher plants, conifer trees that became particularly abundant in the Jurassic (Alexander *et al.*, 1988). Therefore the aromatic land plant markers are also consistent with the Permian age of the coals and the Gondwana plant communities which were present in Australia at the time.

## GEOCHEMISTRY OF SYDNEY BASIN COALS

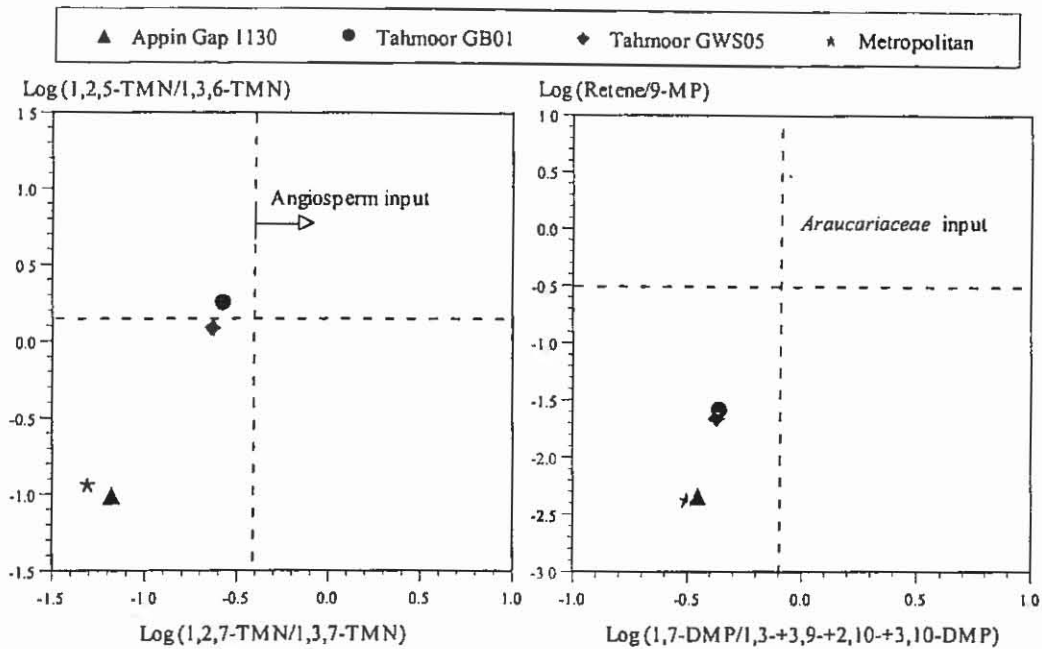


**Figure 3** Cross plots of aromatic land plant markers showing the absence of angiosperm and *Araucariaceae* plant inputs in the coal/shaly coal samples

### Thermal Maturity

Molecular parameters derived from the aliphatic hydrocarbon distributions in the southern Sydney Basin coals show some differences in their thermal maturities (Figure 4). The CPI<sub>26-30</sub> values (~1) of the Appin, Tahmoor GB01,

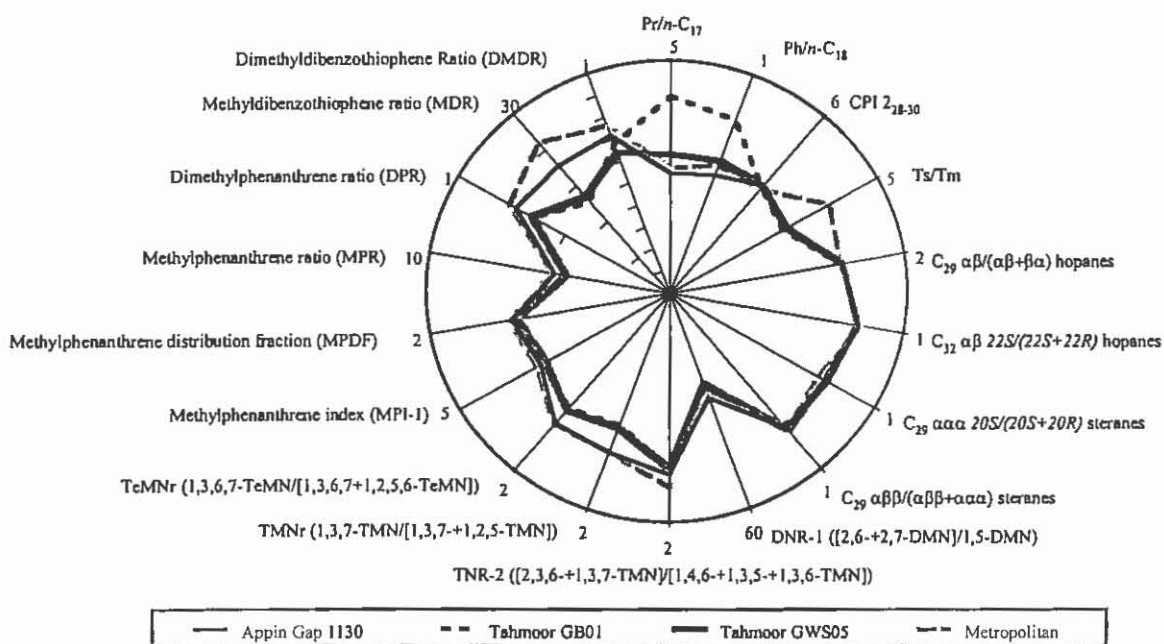


**Figure 4** Spider diagram illustrating the maturity differences and similarities for the coal samples. The plot is configured in a way that more mature samples plot more towards the outside of the diagram (DMN= Dimethylnaphthalene, TMN = Trimethylnaphthalene, TeMN = Tetramethylnaphthalene).

Tahmoor GWS05 and Metropolitan coals are indicative of a maturity in the peak to late stage of the oil generation window. This is consistent with low abundances of thermally unstable moretanes ( $\beta\alpha$  hopanes) and Tm. The configurational isomeric ratios of  $\alpha\beta$  and  $\beta\alpha$  hopanes, 22*S* and 22*R* hopanes,  $\beta\alpha$  20*S* and 20*R* diasteranes,  $\alpha\alpha\alpha$  20*S* and 20*R* steranes and  $\alpha\beta\beta$  and  $\alpha\alpha\alpha$  steranes have all reached their equilibrium values, consistent with oil window or greater thermal maturities. The majority of the aromatic hydrocarbon parameters derived from alkylnaphthalenes and alkylphenanthrenes indicate maturities of ca. 0.9 to 1.2% vitrinite reflectance equivalent (VRE), and consistent with vitrinite reflectance measurements; the Metropolitan sample is the most mature coal based on these parameters.

Therefore, it is apparent that the thermal maturities of the Sydney Basin coals estimated from the molecular distribution of various biomarkers and aromatic hydrocarbons are either close to or slightly lower than their measured vitrinite reflectance values (VR = 1.0 to 1.4%). This lack of maturity imbalance between the molecular maturities and vitrinite reflectance indicates that most of the hydrocarbons extracted from these samples are indigenous to the host Late Permian coals.

### Hydrocarbon Generation Potential

High extractabilities of organic matter (>6,000 ppm of rock, Table 1), hydrogen contents of 4.9 to 5.4 % and liptinite contents of up to 2.5 % (Table 1) indicate that the Permian coals in the southern Sydney Basin may have some potential for generating liquid hydrocarbons. Furthermore, both the molecular and measured vitrinite reflectance values demonstrate that these coals have thermal maturities within or beyond the oil generation window. Therefore the Late Permian coals of the southern Sydney Basin may have generated significant and possibly commercial amounts of petroleum hydrocarbons. What is still unclear is whether oil has been expelled in large-enough volumes to produce commercial deposits.

### CONCLUSIONS

- ◆ Like most coals the southern Sydney Basin coals were formed in a relatively oxic depositional environment under non-marine conditions.
- ◆ The coals contain coniferous organic matter with no input from angiosperm flowering plants that evolved during the Upper Cretaceous.
- ◆ The coals do not have any significant contribution from *Araucariaceae*, conifer trees that became particularly abundant in the Jurassic.
- ◆ The aromatic land plant markers are consistent with the Permian age of the coals and the Gondwana plant communities which were present in Australia at the time.
- ◆ The calcareous signatures of the Metropolitan coal may be due to the adsorption of traces of allochthonous petroleum produced in the interbedded calcareous shales or siltstones.
- ◆ The Late Permian Sydney Basin coals have experienced molecular maturities in the peak to late stage of the oil generation window.
- ◆ The lack of imbalance between the molecular and measured maturities confirms that most of the hydrocarbon extracts are indigenous and were sourced from the host Late Permian coals.
- ◆ Thermally mature Late Permian coals of the southern Sydney Basin may have generated significant and possibly commercial amounts of petroleum.

## ACKNOWLEDGEMENTS

We thank Centennial Coal Company Ltd, Excel Coal Pty Ltd and BHP Billiton Pty Ltd for providing us samples and permission to publish this work. Thanks are also due to Robinson Quezada for analytical supports.

## REFERENCES

- ALDER J. D., HAWLEY S., MAUNG T., SCOTT J., SHAW R. D., SINELIKOV A. & KOUZMINA G. 1998. Prospectivity of the offshore Sydney Basin: A new perspective. *APPEA Journal* **38**(1), 68-92.
- ALEXANDER R., LARCHER A. V., KAGI R. I. & PRICE P. L. 1988. The use of plant derived biomarkers for correlation of oils with source rocks in the Cooper/Eromonga Basin System, Australia. *APEA Journal* **28**(1), 310-324.
- BOREHAM C. J., HORSFIELD B. & SCHENK H. J. 1999. Predicting the quantities of oil and gas generated from Australian Permian coals, Bowen Basin using pyrolytic methods. *Marine and Petroleum Geology* **16**, 165-188.
- CURRY D. J., EMMETT J. K. & HUNT J. W. 1994. Geochemistry of aliphatic-rich coals in the Cooper Basin, Australia, and Taranaki Basin, New Zealand: implications for the occurrence of potentially oil-generative coals. In: Scott, A.C. and Fleet, A.J. (Eds.). *Coal and coal bearing strata as oil-prone source rocks?* The Geological Society, London, pp. 149-182.
- DUMITRU T. A., HILL K. C., COYLE D. A., DUDDY I. R., FOSTER D. A., GLEADOW A. J.W., GREEN P.F., KOHN B.P., LASLETT G.M. & O'SULLIVAN A. J. 1996. Fission track thermochronology: application to continental rifting of south-eastern Australia. *Australian Petroleum Exploration Association, Journal*, **31**(1), 131-142.
- KILLOPS S. D., WOOLHOUSE A. D., WESTON R. J. & COOK R. A. 1994. A geochemical appraisal of oil generation in the Taranaki Basin, New Zealand. *The American Association of Petroleum Geologists Bulletin* **78**, 1560-1585.
- HERBERT C. 1984. Oil in the Sydney Basin. Methane Drainage Pty Ltd. NSW *Department of Mineral Resources Report PGR 1984/02*.
- MATCHETTE-DOWENS C. J., FALICK A. E., KARMAJAYA A. E. & ROWLAND S. A. 1994. A maturity and palaeoenvironmental assessment of condensates and oils from the North Sumatra Basin, Indonesia. In: Scott A. C. and Fleet A. J. (Eds.) *Coal and coal bearing strata as oil-prone source rocks?* The Geological Society, London, pp. 139-148.
- MACGREGOR D. S. 1994. Coal bearing strata – a global overview. In: Scott A. C. and Fleet A. J. (Eds.) *Coal and coal bearing strata as oil-prone source rocks?* The Geological Society, London, pp. 107-118.
- MOFFIT R. S. (2000). A compilation of the geology of the Southern Coalfield. *Geological Survey of NSW Report No. GS1998/277*. Department of Mineral Resources.
- MOLDOWAN J. M., DAHL J., HUIZINGA, B. J., FAGO F. J., HICKEY L. J., PEAKMAN T. M. & TAYLOR D. W. (1994) The molecular fossil record of oleanane and its relation to angiosperms. *Science*, **265**, 768-771.
- POWELL T. G. & BOREHAM C. J. 1994. Terrestrially sourced oils: where do they exist and what are our limits of knowledge? In: Scott A. C. and Fleet A. J. (Eds.) *Coal and coal bearing strata as oil-prone source rocks?* The Geological Society, London, pp. 11-30.
- RADKE M. & WELTE D. H. 1983. The methylphenanthrene index (MPI): a maturity parameter based on aromatic hydrocarbons. In: M. Bjorøy *et al.* eds. *Advances in Organic Geochemistry*, pp. 504-512. John Wiley, Chichester.

- RADKE M., RULLKÖTTER J. & VRIEND S. P. 1994. Distribution of naphthalenes in crude oils from the Java Sea: source and maturation effects. *Geochimica et Cosmochimica Acta* 58, 3675-3689.
- STALKER, L., AHMED, M., VOLK, H. & GEORGE S. C. 2001. Best practise document: organic geochemical methods at CSIRO Petroleum. *Australian Petroleum Cooperative Research Centre*, Unrestricted Report No. 01-001.
- STANDARDS ASSOCIATION OF AUSTRALIA 1997. Australian standards AS1038.6.1: Higher rank coal and coke - ultimate analysis. Standards Association of Australia, Sydney.
- STANDARDS ASSOCIATION OF AUSTRALIA 1998. Australian Standards AS2856.2: coal maceral analyses. Standards association of Australia, Sydney.
- STANDARDS ASSOCIATION OF AUSTRALIA 2000a. Australian Standards AS1038.3: Proximate analysis of higher rank coal. Standards Association of Australia, Sydney.
- STANDARDS ASSOCIATION OF AUSTRALIA 2000b. Australian standards AS2456.3: Microscopical determination of the reflectance of coal macerals. Standards Association of Australia, Sydney.
- THOMPSON S., COOPER B.S. & BARNARD P.C. 1994. Some examples and possible explanations for oil generation from coals and coaly sequences. *In*: Eds. Scott A. C. & Fleet A. J. *Coal and coal bearing strata as oil-prone source rocks?* The Geological Society, London, pp. 119-138.
- STEWART R. & ALDER D. (Eds.) 1995. *New South Wales Petroleum Potential*, New South Wales Department of Mineral Resources, Sydney, 188 pp.
- TISSOT B. P. & WELTE D. H. 1984. *Petroleum Formation and Occurrence*. Second Edition. Springer-Verlag, Berlin.
- WILKINS R. W. . & GEORGE S. C. 2002. Coal as a source rock for oil: A review. *International Journal of Coal Geology* 50, 317-361.

# THE USE OF ACOUSTIC SCANNER RESULTS FOR MINE DESIGN

K E Bartlett<sup>1</sup> and J L Edwards<sup>2</sup>

<sup>1</sup>Consultant Geologist, MINARCO

<sup>2</sup>Consultant Geologist, Collective Experience

## ABSTRACT

High resolution acoustic scanning technology has emerged in recent years as a powerful wireline tool for identifying the occurrence and orientation of structures and borehole breakout – the latter being a strong indicator of horizontal stress directions.

As is often the case with such technology it is one thing to generate a data set that describes the attributes of the various features apparent in a log, and another to be able to analyse those data in such a way that their individual and collective impact on mine planning issues can be readily assessed.

This paper describes a process for the interactive manipulation and visualisation of joint and breakout data to enable them to be effectively included in the mine design process.

## INTRODUCTION

This review details the development of the joint and breakout database, from acoustic scanner results, as part of the broader geotechnical assessment undertaken for the Wyong Project. The main aim in developing the database was twofold:

- to assist in assessing the impact of jointing on face stability
- to assist in assessing the impact of horizontal stress on longwall gateroad stability

## AVAILABLE DATA

Of the 159 holes relevant to the Primary Target Area, 53 were logged with an acoustic scanner – 48 of these holes were logged by Groundsearch Australia, and 5 were logged by Reeves Wireline. Two of the Groundsearch logs yielded corrupted data, whilst no joint data was available from the Reeves logs. The joint database was therefore compiled from a total of 46 holes and the breakout database included 51 holes.

## DATABASE

### Joints database

The focus of the joints database was to assess the potential impact of jointing on longwall face stability and caving characteristics of the longwall goaf.

Initially, the joint data for each hole were incorporated into a data set where they could be displayed to show their attributes, depth and stratigraphic relationship (see Table 1). The

magenta line indicates the seam horizon; the yellow line represents the top of the Munmorah Conglomerate and the red dotted line indicates the depth to which the hole was logged.

The data were then incorporated into the database format where they were characterised by type, rotated to true north, related to a specific stratigraphic unit, and assigned a height above seam. The database was designed to enable various subsets to be sorted and filtered for the purposes of comparison.

B800W350

FRACTURE NUMBER	DIP (DEG)	AZIMUTH (DEG)	TO ( M)	FROM ( M)	CATEGORY	
1	79	336	149.74	150.26	Possible joint	168
26	44	306	180.08	180.18	Joint - open	138
78	44	67	243.96	244.05	Possible joint	79
96	63	312	265.25	265.44	Joint - open	144
124	52	214	335.17	335.29	Possible joint	46
126	79	198	351.85	352.32	Joint - open	30
139	74	38	356.12	356.45	Joint - closed	50
142	79	7	356.51	356.99	Joint - closed	19
146	85	19	356.78	357.80	Joint - open	31
159	76	39	368.27	368.63	Joint - open	51
168	55	295	369.29	369.42	Joint - closed	127

MUN		WGN		Logged depth	
0	191.9	0	351.975	0	374.06
180	191.9	180	351.975	180	374.06

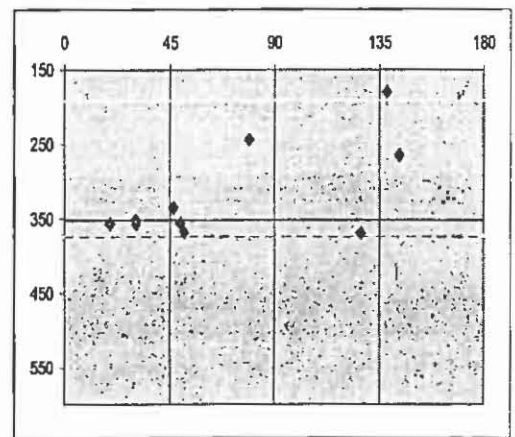


Table 1 – B800W350 joints in initial format

**Breakout database**

The focus of the breakout database was to assess the potential impact of the maximum horizontal stress direction on longwall gateroad stability, both during development and on retreat .

Initially, the breakout data for each hole were incorporated into a data set where they could be displayed to show their attributes, depth and stratigraphic relationship (see Table2). The magenta line indicates the seam horizon; the yellow line represents the top of the Munmorah Conglomerate, the brown line represents the top of the Dooralong Shale and the red dotted line indicates the depth to which the hole was logged.

The data were then incorporated into the database format where they were rotated to true north, related to a specific stratigraphic unit, and assigned a height above seam. This database was also designed to enable various subsets to be sorted and filtered for the purposes of comparison.

## ACOUSTIC SCANNER RESULTS FOR MINE DESIGN

B800W350					MUN	WGN	Logged depth		DOOR			
TOP (M)	BASE (M)	BREAKOUT AZIMUTH (DEG)	SIGMA 1 AZIMUTH (DEG)	SIGMA 1 TRUE (DEG)	0 180	191.9 191.9	0 180	351.975 351.975	0 180	374.06 374.06	0 180	318.3 318.3
203.94	204.06	300	210	42								
205.90	206.02	300	210	42								
207.20	207.63	300	210	42								
228.31	228.44	290	200	32								
235.86	236.84	300	210	42								
239.92	240.55	310	220	52								
240.66	240.72	320	230	62								
244.41	245.44	300	210	42								
245.67	246.25	295	205	37								
246.42	246.48	305	215	47								
246.85	247.78	300	210	42								
264.76	265.33	315	225	57								
269.50	269.83	270	180	12								
271.22	271.4	335	245	77								
290.01	290.82	305	215	47								
291.14	291.44	300	210	42								
300.03	300.61	295	205	37								
301.83	302.34	300	210	42								
302.73	302.92	295	205	37								
303.10	304.51	295	205	37								
318.71	318.95	290	200	32								
362.20	362.29	330	240	72								
366.26	366.55	340	250	82								
367.32	367.75	335	245	77								

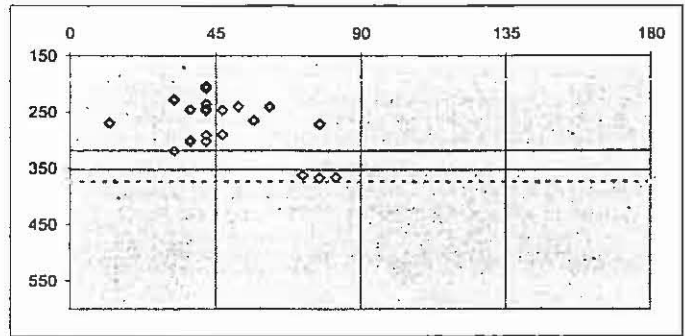


**Table 2 – B800W350 breakout in initial format**

### RESULTS

#### Joints

The final analysis of the joint data was based around a number of basic assumptions:

- sub-vertical joints will have greater impact than low angle joints
- near-seam joints will impact on face stability
- rock mass joints will impact on caving
- 'open' joints will have greater impact than 'closed' joints

Consequently, the main emphasis was placed on high angle joints in the stratigraphic units below the Tuggerah Formation. A plot of all of the joints contained in the database is shown in Figure 1.

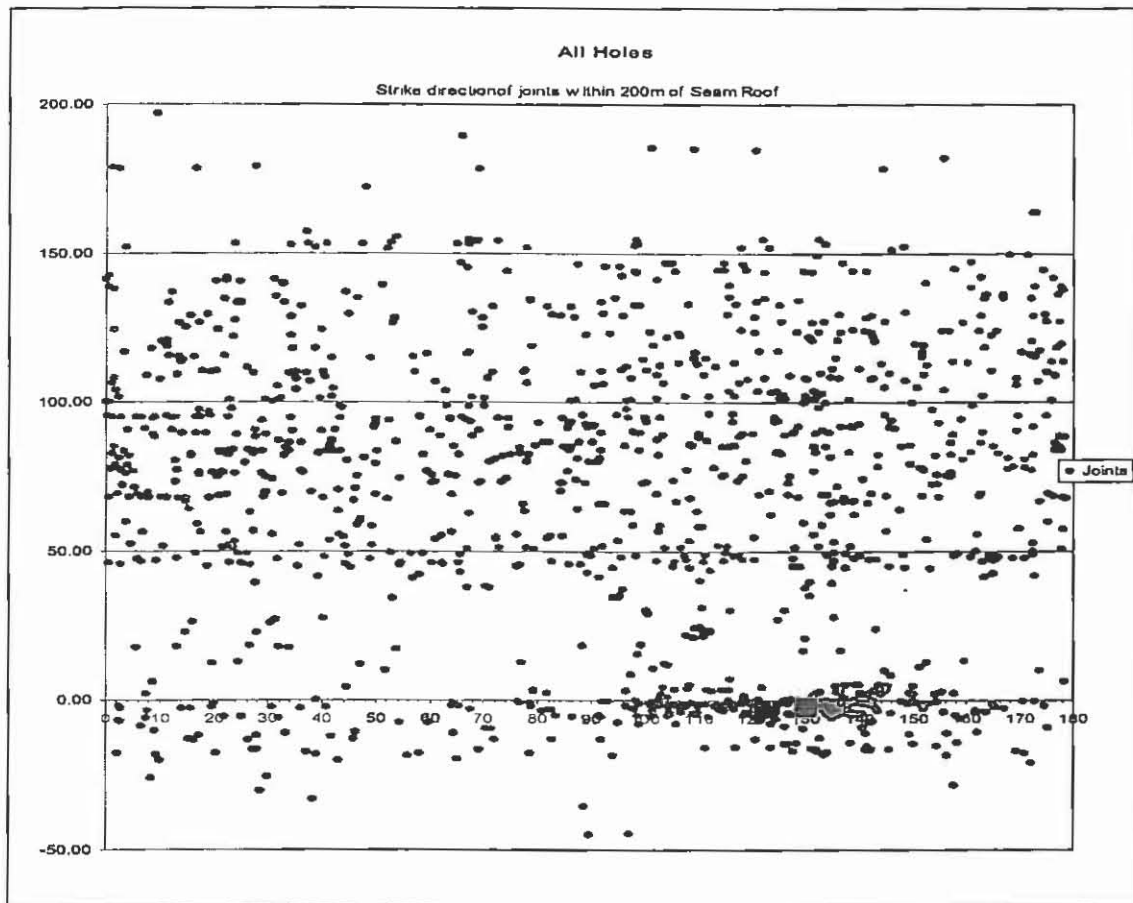


**Figure 1 – Joint occurrences up to 200m above seam roof**

Figure 1 exhibits three key features:

- the cluster of near seam joints occurring in the range of  $100^{\circ}$  to  $145^{\circ}$
- the relatively few joints in the Dooralong Shale i.e. the interval of approx. 40m above the seam
- the random orientation of joints in the Munmorah Conglomerate

To investigate the joint distributions further, the Primary Target Area was divided into four logical sub-areas, namely the NE, SE, NW and SW areas - each of which corresponded to a discrete area of the proposed mine plan. Of these four areas, only the NE and SE area have been assessed at this stage, due largely to the distribution of available data and the current planning requirements. Particular emphasis has been placed on the NE area, as it is the area of more immediate concern in terms of the finalisation of the mine layout.

Interactive graphics have been employed to enable a rapid, visual analysis of the distribution and orientation of various combinations of joint type on an area-by-area basis, as shown in Figure 2 and 3.

# ACOUSTIC SCANNER RESULTS FOR MINE DESIGN

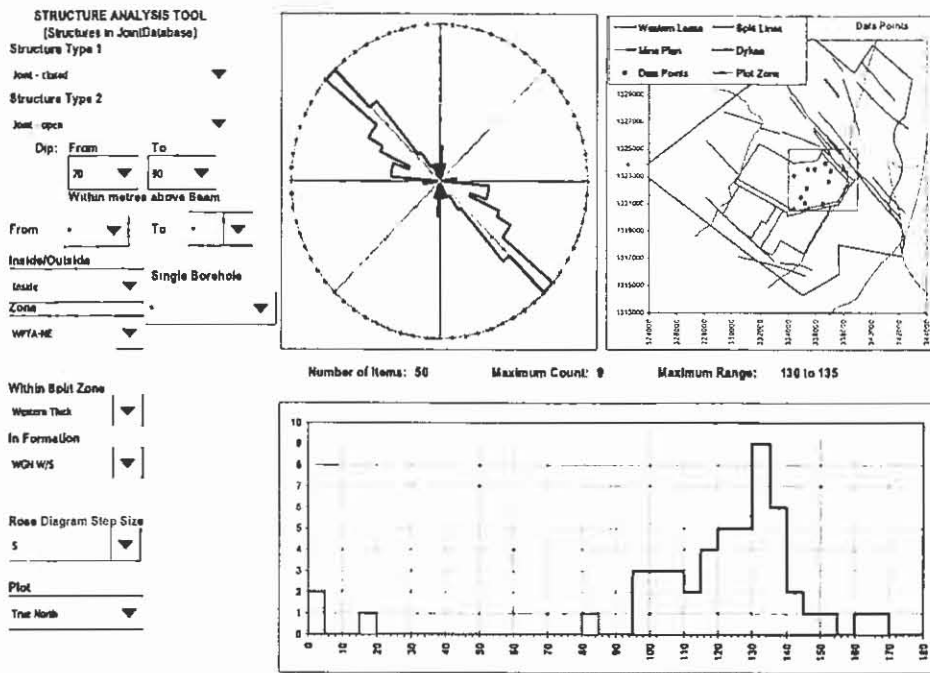


Figure 2: NE Area - Open and closed joints within working section, with >70° dip

Table 3: Joint Orientations in the NE Area

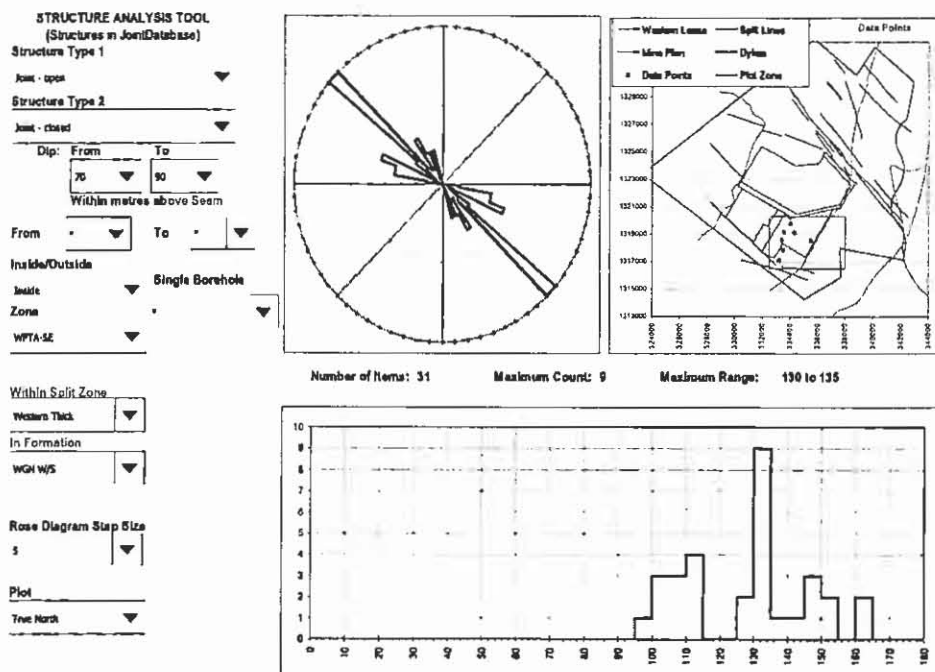


Figure 3: SE Area - Open and closed joints within working section, with >70° dip

These sheets enable joints of various types within each area to be plotted for a variety of depth intervals or stratigraphic horizons to produce a rose diagram and histogram of orientations. In

the NE Area, a total of 50 high-angle joints exist within the WGN working section with a summary of their orientations shown in Table 3.

Joint Type	Number	Orientation (True)
Open	21	115-135°
Closed	29	120-140°

In the SE Area, a total of 31 high-angle joints exist within the WGN working section with a summary of their orientations shown in Table 4.

Joint Type	Number	Orientation (True)
Open	10	100-135°
Closed	21	110-155°

**Table 4: Joint Orientations in the SE Area**

It can be seen that not only are there fewer joints in the SE Area compared to the NE Area, they are also slightly more scattered in their orientation.

#### **Breakout**

The final analysis of the breakout data was based around two basic assumptions:

- breakout associated with jointing may be erroneous
- near-seam breakout will be most significant to roadway behaviour

Consequently, any breakout that occurred within 0.5m of a recorded joint was excluded from the database, and particular emphasis was placed on analysing breakout within 50m of the seam. A plot of all unjointed Sigma H orientations contained in the database is shown in Figure 4.

The key features exhibited in this figure are:

- relatively fewer occurrences in the Dooralong Shale
- the cluster of orientations between 20° and 50°

# ACOUSTIC SCANNER RESULTS FOR MINE DESIGN

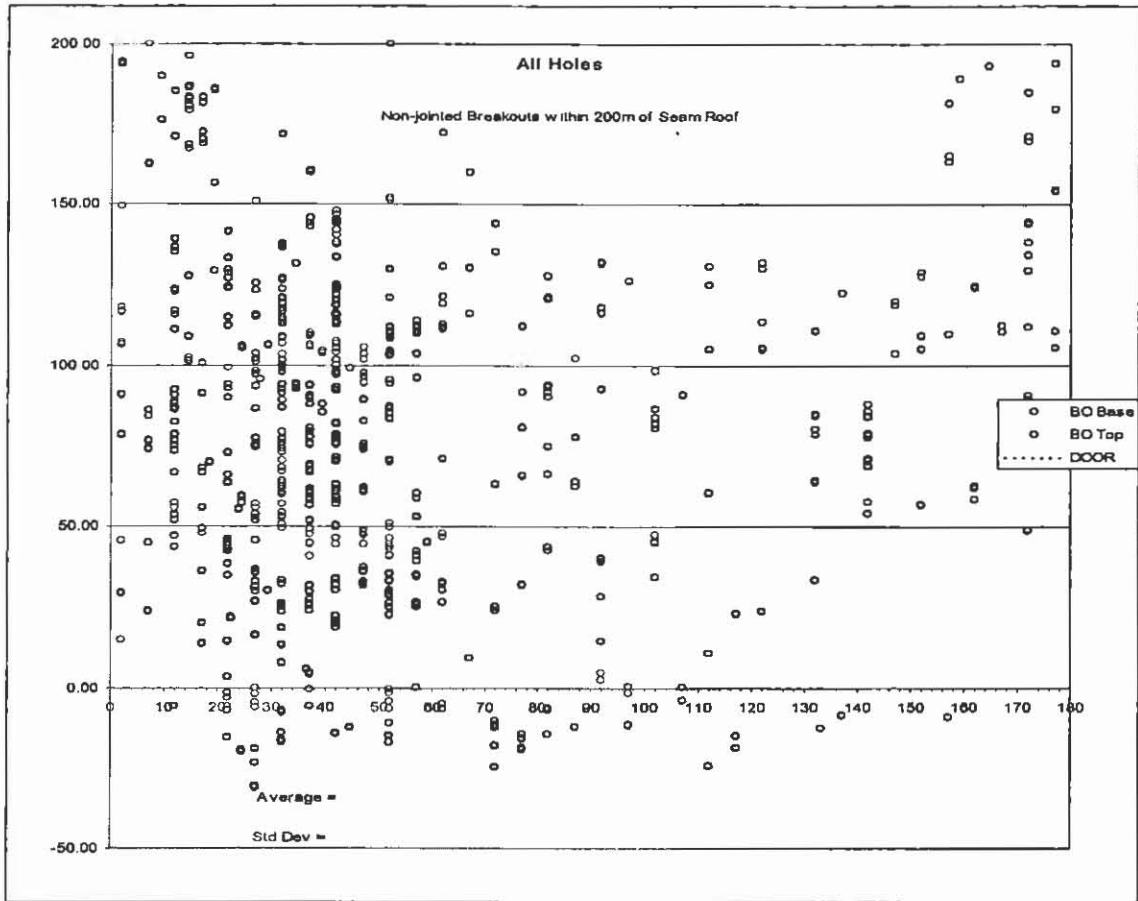


Figure 4: Unjointed Sigma H occurrences within 200m of seam roof

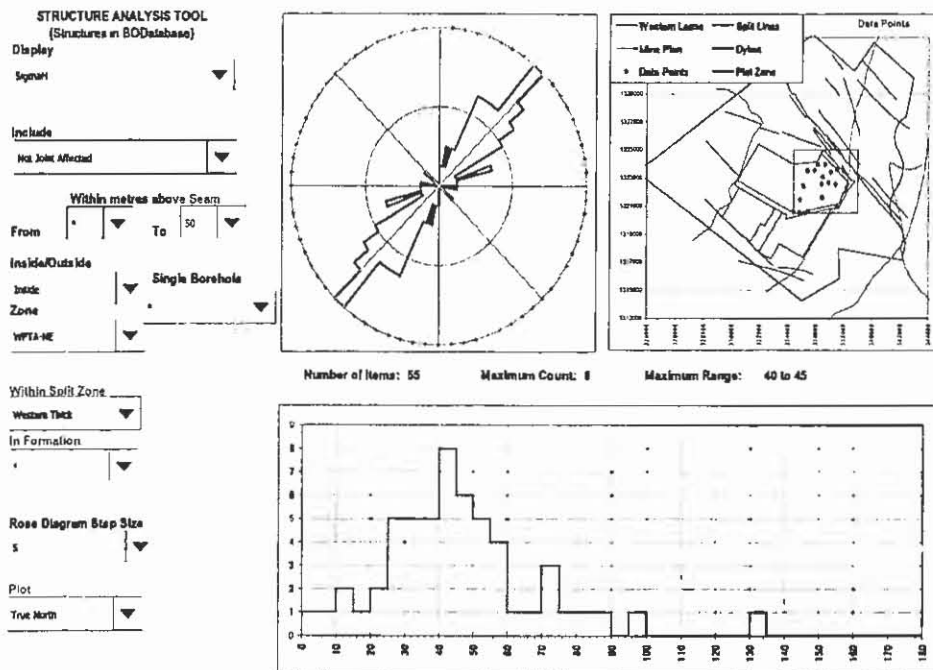
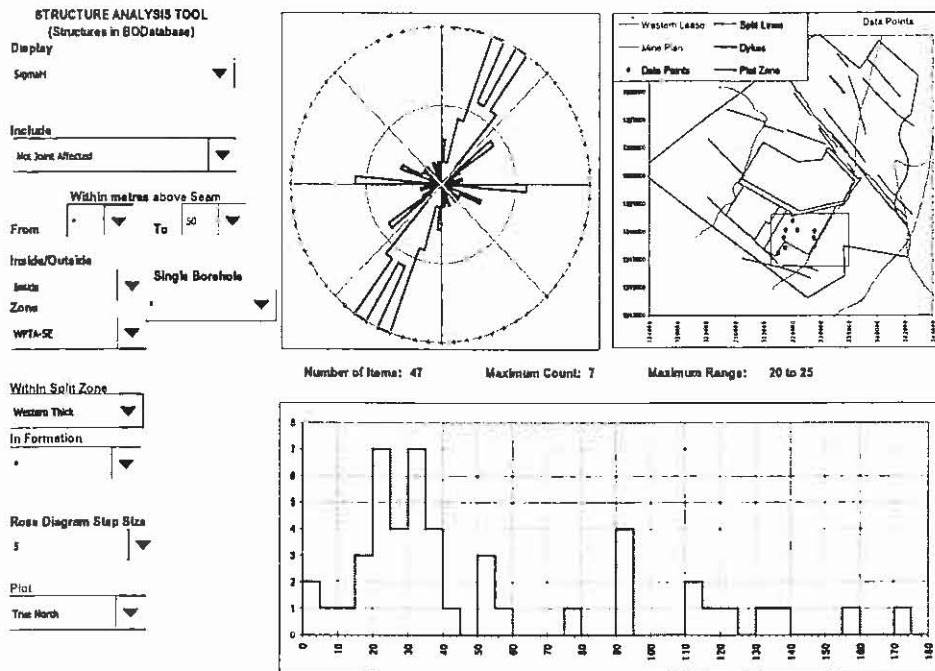


Figure 5: NE Area – Maximum horizontal stress direction within 50m of seam

Figure 5 indicates that in the NE Area, the maximum horizontal stress direction is predominantly within the range of 25° to 60°.



**Figure 6: SE Area – Maximum horizontal stress direction within 50m of seam**

As in the case of the joint analysis, there are less occurrences of breakout in the SE Area than in the NE Area. Figure 6 also indicates that the stress orientations SE Area are not only more scattered but also show a significant element of E-W compression.

Further analysis resolved this anomaly by identifying that virtually all of the E-W stress indicators were associated with the three holes located adjacent to the Central Channel. This led to the subdivision of the SE Area into the ESE Area and WSE Area, as shown in Figures 7 and 8. These Figures suggest that the stress orientations in the WSE Area are essentially consistent with those on the NE Area (in the range 15° to 55°) whilst those in the ESE Area are dominantly E-W (90° to 110°).

# ACOUSTIC SCANNER RESULTS FOR MINE DESIGN

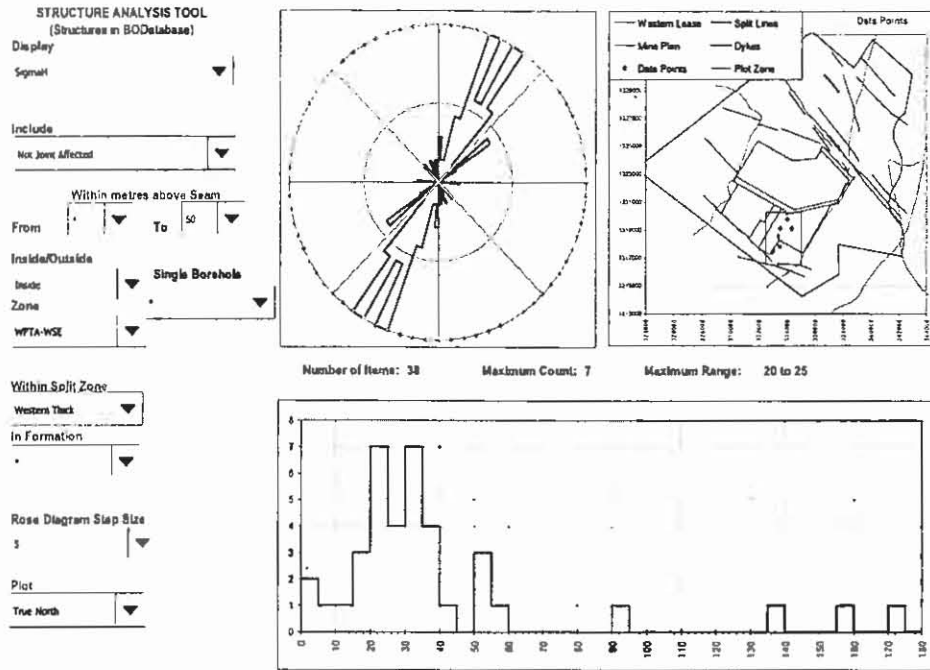


Figure 7: WSE Area – Maximum horizontal stress direction within 50m of seam

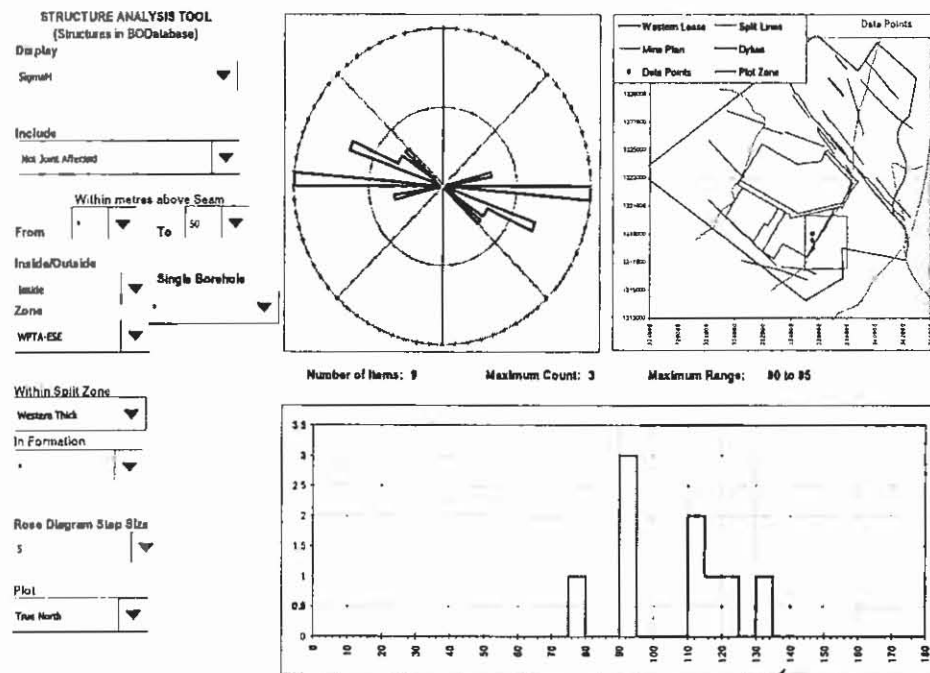


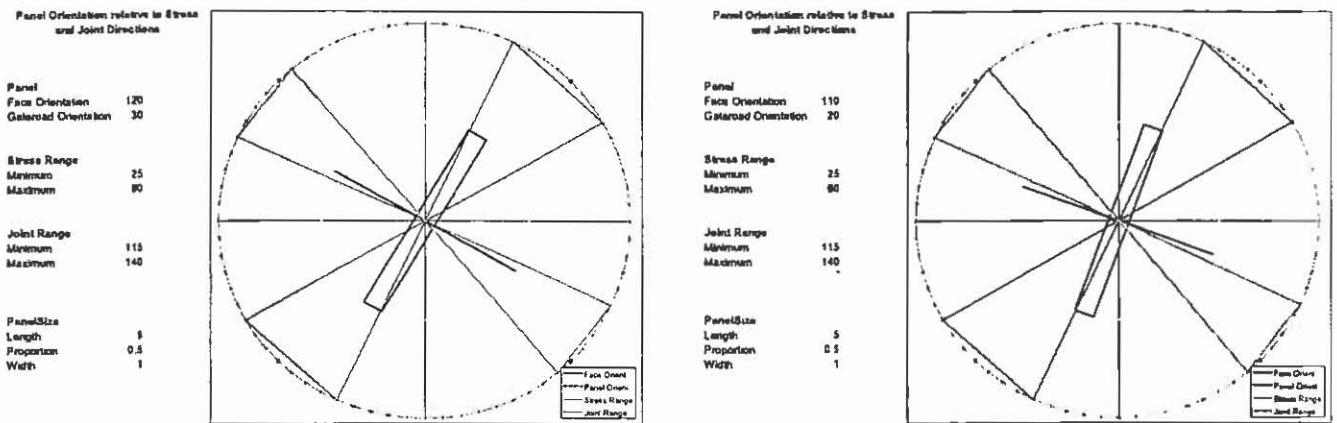
Figure 8: ESE Area – Maximum horizontal stress direction within 50m of seam

The lack of E-W stress associated with the flank of the Central Channel in the NE Area suggests that the anomaly is associated with the Vales Point seam split line which runs in an E-W direction across the lower third of the SE Area.

**CONCLUSIONS**

The joint analysis clearly indicated that joints are much more consistent in the near-seam environment than in the overlying rock mass. This implies that jointing will have a much more predictable influence on face stability than on caving characteristics.

The current longwall gate road direction will see the face oriented at 120°, which falls within the range of both the open and closed joints in the NE Area (Figure 9). To minimise the risk of persistent spalling on the longwall face, it would be ideal to rotate the face anti-clockwise 20° to 30° into a more E-W orientation. Face conditions in the SE Area would also benefit



from a similar rotation.

**Figure 9: NE Area - Current and Alternative face orientations of 120° and 110°**

The breakout analysis indicated that the maximum horizontal stress in the NE Area is operating predominantly within a range of 25° to 60° with an average of approximately 40°. This becomes a limiting factor to the amount that the longwall face can be rotated to minimise the affect of jointing. Figure 9 shows the general range of joint and stress orientation with respect to the current face direction of 120° and a possible revised layout of 110°.

**ACKNOWLEDGEMENTS**

The authors wish to thank Kores Australia Pty Ltd, the managers of the Wallarah 2 Coal Project, for their kind permission to publish and present this paper.

**REFERENCES**

MACGREGOR S. 2002, Acoustic Scanner Analysis of Borehole Breakout to Define the Stress Field Across Mine Sites in the Sydney and Bowen Basins, Proceedings of 21<sup>st</sup> International Conference on Ground Control in Mining, Morgantown, WV, USA.  
 MACGREGOR S. 2003, Definition of Stress Regimes at Borehole, Mine and Regional Scale in the Sydney Basin Through Breakout Analysis, Proceedings of 36<sup>th</sup> Sydney Basin Symposium, Wollongong, Australia, pp. 223-232.

# RIP: THE WOLLOMBI COAL MEASURES

Michael Creech

Excel Coal Limited  
Level 9, 1 York St, Sydney, NSW, 2000, Australia

## INTRODUCTION

Exploration of the upper seams of the Wollombi Coal Measures in the late 1990's at both Broke and, more recently, at Ridglands by the DPI (Brunton & Moore 2004), and at Anvil Hill by Powercoal highlighted several issues that rendered the use of Wollombi Coal Measure nomenclature problematic and requiring considerable modification. Among these issues was the miscorrelation of seams in the nominated Type Bore for the Wollombi Coal Measures first identified by Stevenson (1997). These miscorrelations included the Greig's Ck seam, which unfortunately was the only seam that had precedence prior to the ratification of the Wollombi Coal Measures (Standing Committee on Coalfield Geology of NSW 1975). The miscorrelation of this seam and the adjacent tuff also rendered the nomenclature of the target seams being explored by the DPI and Powercoal unusable.

The Wollombi Coal Measures of the Hunter Valley Coalfield and the Newcastle Coal Measures of the Newcastle Coalfield have long been recognized as equivalent (David 1907; Booker 1954; Britten 1972 & 1975), however detailed correlations have only recently been proposed (Stevenson 1997 & 1999; Beckett et al.; 1999 Creech 2000; Weatherall 1999; Kramer 1999; Kramer et al. 2001).

In order to address these issues the Coalfield Geology Council of NSW established the Wollombi Coal Measures Working Party in August 2000. Using geophysical logs and detailed descriptions of drill core the Working Party identified excellent correlations of both major tuffs and seams of the Newcastle Coal Measures across the Hunter Valley. Seam profiles that incorporated numerous tonsteins provided further evidence to support the notion that both the Wollombi and Newcastle Coal Measures were not merely equivalent but were identical.

Since Newcastle Coal Measure nomenclature was better understood, more practical in its application (preference in correlating tuffs rather than clastic units) and had historical precedence, replacement of the Wollombi Coal Measures with Newcastle Coal Measure nomenclature was proposed by the Working Party in November 2004.

At the November meeting of the Coalfield Geology Council the following resolutions were subsequently ratified:

- That the entire Wollombi Coal Measure nomenclature be replaced with Newcastle Coal Measure nomenclature in the northern Sydney Basin.

- That Amoco Wybong DDH1 be adopted as the “Reference Bore” for the Newcastle Coal Measures in the Hunter Valley. This bore has been photographed, geophysically logged and all seams remain intact with the core currently available for inspection at Londonderry.
- That the base of the Newcastle Coal Measures in the Hunter Valley be raised to the top of the Watts Sandstone so as to conform to the same nomenclature in the Newcastle Coalfield. (The Watts Sandstone is therefore retained in Hunter Valley nomenclature and is recognised as the equivalent of the Waratah Sandstone in the Newcastle Coalfield.)
- That the Singleton Supergroup in the Hunter Valley now consists of the Newcastle Coal Measures, the Watts Sandstone and the Wittingham Coal Measures.

This stratigraphic review can be downloaded from DIGS (GS Report No.2004/415), along with the supporting data and background information. May the Wollombi Coal Measures rest in peace (Table 1.1).

#### **THE NEWCASTLE COAL MEASURES IN THE HUNTER VALLEY**

Correlations using Newcastle Coal Measure nomenclature are primarily based upon the identification of major tuffs as stratigraphic markers. This contrasted with the emphasis that was placed on seams and the intervening clastic units in the nomenclature of the Wollombi Coal Measures. The identification of regionally significant tuffaceous units is however strengthened if a coal bearing sequence is recognised immediately above or below the unit (such as the Great Northern seam above, or the Fassifern seam below the Awaba Tuff). If a correlatable tuff lies within clastic strata then its identification can only be by reference to its position between coal bearing strata some distance above and below (i.e. it is in about the right location). In these instances the correlation is less certain.

A table of suggested correlations for all bores studied by the Working Party was prepared to assist future workers in using Newcastle Coal Measure nomenclature in the Hunter Valley. Due to the sparse spacing of relevant bores it is anticipated that such correlations will be subject to review in the future.

The Newcastle Coal Measures in the Hunter Valley are more uniform in thickness than their Newcastle Coalfield equivalents. Commensurate with this more uniform development there is a lack of conglomeratic strata that is such a predominant feature of the Newcastle Coal Measures. In this regard the Hunter Valley equivalents are more akin to the southern Newcastle Coalfield where conglomerates are less dominant and the lower seams in the Lambton Formation are poorly developed. Similarly the upper seams of the Newcastle Coal Measures are the most widespread and best developed.

By considering the similarities between the two stratum (including the size, direction and migration of palaeochannels) regional exploration strategies can be undertaken. In addition this review promotes a more regional perspective to understanding peat formation in the Sydney Basin.

## VOLCANISM

The five fold increase in the known extent of the various seams and tuffs of the Newcastle Coal Measures (Figure 1) suggests a re-evaluation of the scale and potential source(s) of volcanism may be warranted. Studies after the Mt St Helens eruption of May 1980 (Francis 1985) suggested that ash falls compact 2:1 within 2 months of deposition, a process that involves the reduction of pore spaces and expulsion of water. Subsequent compaction during diagenesis and further burial, has been estimated to be an additional 2:1 (Bohor & Triplehorn 1981). Therefore assuming a mapped extent of 160km by 50km, an average thickness of 5cm (0.00005 km) and a total compaction ratio of 4:1, it can be estimated that the average tonstein records an original ash discharge of at least 1.6 cubic kilometres. Similarly at an average preserved thickness of 3 metres, the interseam tuffs of the Newcastle Coal Measures may have originally represented an ash deposit well in excess of the 100 cubic kilometres.

These ash volumes however may represent a considerable underestimate of the volume of the original ash discharge. Firstly we do not have preserved the ash that would have been deposited on the flanks of the source volcano. In ultraplanean events this ash may comprise a volume equal to the more distal ash deposits (Francis 1985). We also do not appear to be able to identify the potential limits of the original ash deposit from the current data. With reference to the extents of similar ash deposits identified in Europe it would seem likely that the preserved deposits are only a portion of the original potential ash deposit and that they may very well have covered the entire Sydney Basin. This proposition may be supported by the recently proposed correlation of the Awaba, Warners Bay and Nobbys Tuffs in the southern Sydney Basin Basin (Hill 1994; Hill et al. 1994; Grevenitz et al. 2003; Carr et al. 2003).

These volumes suggest that the source eruptions were of the scale of at least a "cataclysmic" ultraplanean (VEI 5+) for the tonsteins and may have been as large as a "colossal" ultraplanean event (VEI 7) for the thicker tuffs. As a comparison, the Mt St Helens eruption of 1980 had a VEI of 5 and an ash volume of more than 1 cubic kilometre, whereas Krakatau (1883) had a VEI of 6 with ten times the amount of ash deposited (Volcanoes of the World (VOW) website 2004). The Taupo eruption of 180AD is a 6+ eruption and the study area fits easily within the lateral extents of the resultant Taupo ignimbrite.

Assuming a time period of approximately 2 to 6 million years for the deposition of the Newcastle Coal Measures (estimated using data published by Gulson et al. 1990; Theveniaut et al. 1994; Brakel & Totterdell 1988; Roberts et al. 1994), the six major tuffs of the Newcastle Coal Measures represent one large and/or close eruption episode every 330,000 to one million years. There are of the order of 165 tonsteins in the Newcastle Coal Measures suggesting a frequency of one smaller and/or more distant eruption every 10,000 - 35,000 years. This frequency should however be regarded as a minimum as not all the ash falls have been preserved and of those preserved, some units may also represent multiple events.

The volcanic frequency represented by intraseam tonsteins may be more accurately assessed by considering the number of tonsteins preserved in a single thick coal seam such as the Fassifern seam. Although preserving only a small time frame compared to the entire extent of the Newcastle Coal Measures, it has the benefit of providing a continuous record with a series of individual tonsteins that can be correlated across the study area. Assuming a 10:1 compaction ratio for coal (Ryer & Langer 1980) and to 2mm/yr peat growth for the

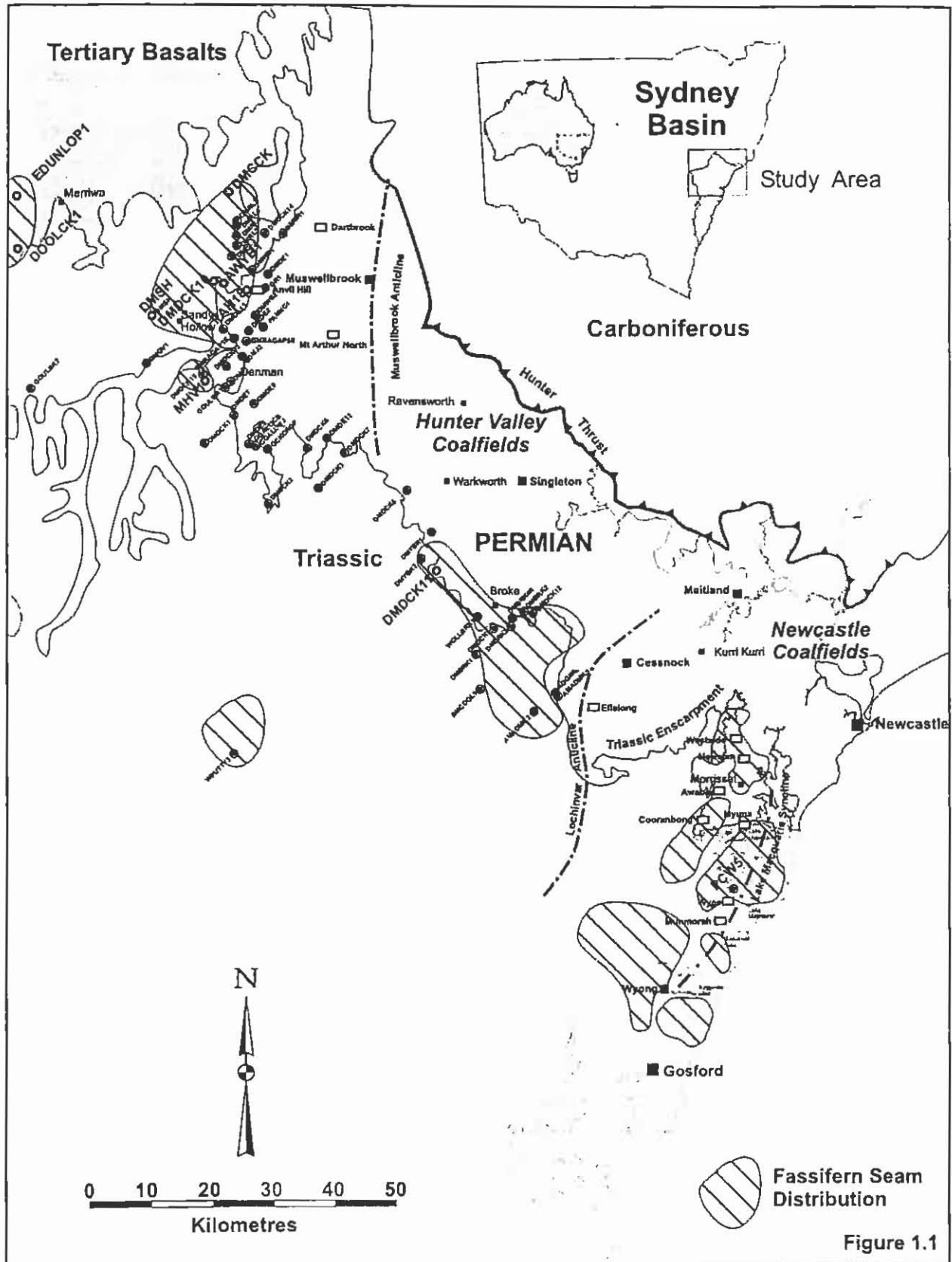


Figure 1 Distribution of the Fassifern seam, northern Sydney Basin.

Newcastle Coal Measures (Diessel 1992), it is estimated that 1 metre of coal accumulated every 5 to 10,000 years. The inclusion of 15 correlatable tonsteins in the 6 to 7 metre thick Fassifern seam therefore represents an average ash fall frequency of one event every 2,000 to 5,000 years.

Consistent with their chemistry (Diessel 1985, Kramer 1999), this range of eruption frequencies compares satisfactorily with more recent plinian-style volcanism associated with destructive plate margins. For instance over the last 200,000 years tonsteins preserved in deep sea cores of the Mediterranean preserve an eruptions of similar scale once every 10,000 years (Keller et al., 1978; McCoy 1981). Tephra deposits near Mayor Island, New Zealand, preserve an eruption frequency of one every 4000 years (Wilson et al., 1995).

Records from around the world suggest that there have also been 46 eruptions of VEI 6 or greater recorded over the last 12,000 years (VOW 2004), and only 4 eruptions of 6+ VEI. By grouping all 5+ eruptions to their relevant volcanic districts around the globe, the average frequency of eruptions of this size from each source area over the last 12,000 years, is one every 4000 years. This compares with the estimate herein of one every 2 to 5,000 years calculated from the distribution of tonsteins in the Fassifern seam profile. Almost all eruptions of this intensity have occurred at destructive plate margins.

There is some chemical evidence in tonsteins and evidence of thinning in tuffs across the study area to suggest that the source volcano(s) may be located to the east of the study area. It is proposed that the volcanic source may be associated with the destructive Panthalassan plate margin that was active in the Late Permian and located 1000 kilometres to the east of the study area (Veevers et al., 1994 and 2000). The volcanoes themselves may have been located further west but potentially 100-500km east of the study area.

#### **SEAM PROGRADATION OR AGGRADATION**

The correlation of seam profiles of the Newcastle Coal Measures across the northern Sydney Basin contradicts the notion that the precursor peat formed from behind a shoreline that retreated to the south (Warbrooke 1981; Herbert et al., 1976; Herbert 1980a). Although the long axis of the correlations is perpendicular to this direction, the width of these correlations exceeds 50km. In this distance the tonsteins would be expected to show some evidence of transgressing the seam profile, such as merging below the floor of the seam and/or significant changes in the character of individual coal plies (Fig 1.2). Indeed it is proposed that if the seams formed from progradation rather than vertical aggradation then the detail of the correlations found could not be preserved, and the recommendations regarding replacement of the Wollombi Coal Measures could not be supported.

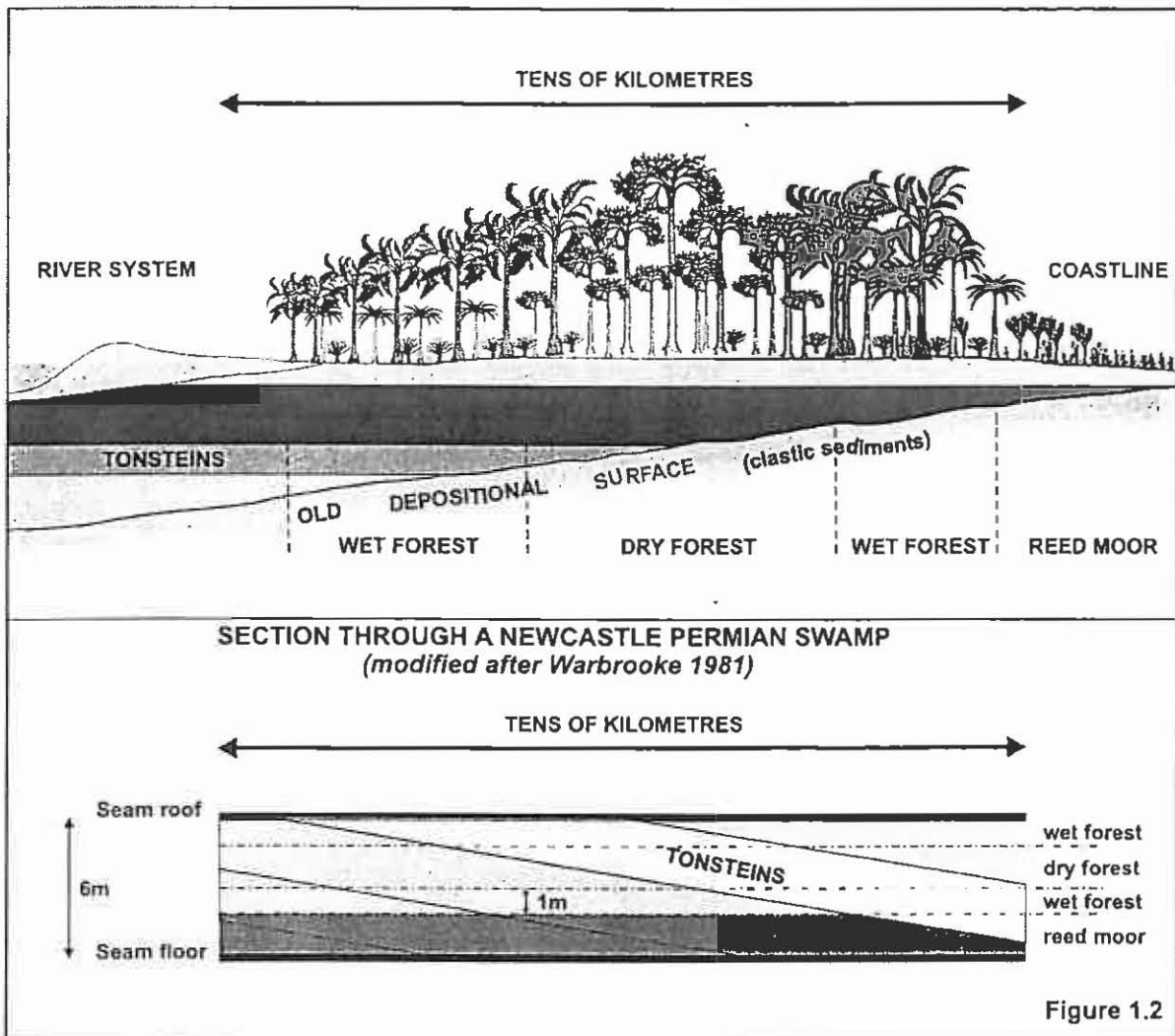


Figure 2 Section through a Newcastle Permian Swamp.

### DETRITALS MAY NOT ALWAYS INDICATE FLUVIAL DISPERSAL

The extended correlation of seams of the Newcastle Coal Measures has enabled detailed ply correlations to be made across the northern Sydney Basin. The uniform distribution of detrital components such as ash, inertodetrinite, sporinite, liptinite and fusinite suggests that not only is their dispersal mechanism uniform but that both the supply of and preservation of these various components is relatively constant. That the extent of the correlated seams now extends a considerable distance either side of the Lochinvar Anticline suggests that multiple fluvial systems would have influenced the northern Sydney Basin. It could be argued that flooding occurred simultaneously across the entire area however it is difficult to envisage how fluvial distribution could supply equivalent proportions of various plant material.

The potential for dispersal by wind may offer a more likely scenario. There is no reason to discount the possible introduction of dust (as well as volcanic ash) from adjacent environments as well as fine plant remains, leaves and cuticles as well as fine charcoal. The suggestion that detrital components may be predominantly dispersed in the air suggests a cautionary note regarding the assumed link between high proportions of detrital material and flooding of the peat.

WOLLOMBI COAL MEASURES

TABLE 1 Proposed stratigraphy of the northern Sydney Basin

<b>NARRABEEN GROUP</b>				
<b>NEWCASTLE</b>	Moon Beach	Island	Vales Point seam	
			Wallarah seam	
	Formation		Great Northern seam	
	Awaba Tuff			
	Boolaroo	Formation	Fassifern seam	
			Upper Pilot seam	
			Mt Hutton tuff	
			Lower. Pilot seam	
	Hartley Hill seam			
	Warners Bay Tuff			
	Adamstown	Formation	Australasian seam	
			Stockrington tuff	
			Montrose seam	
			Wave Hill seam	
			Edgeworth tuff	
			Fern Valley seam	
Victoria Tunnel seam				
Nobbys Tuff				
Lambton	Formation	Nobbys seam		
		Dudley seam		
		Yard seam		
		Borehole seam		
Watts Sandstone		Waratah Sandstone		
<b>WITTINGHAM</b> <b>COAL MEASURES</b>	Denman Formation	<b>TOMAGO</b> <b>COAL</b> <b>MEASURES</b>	Dempsey Formation	

REFERENCES

- BECKETT J., CREECH M., STEVENSON D., MOLONEY J., PRATT W., WILES L. & TADROS V. 1999. *One Basin – One Stratigraphy. Newcastle to Narrabri Core Display*. 33<sup>rd</sup> Newcastle Symposium on Advances in the Study of the Sydney Basin, July 30, Newcastle Univ. NSW.
- BOHOR B. F. & TRIPLEHORN D. M. 1981. Volcanic Origin of the Flint Clay Parting in the Hazard N. 4 (Fire Clay) Coal Bed of the Breathitt Formation in Eastern Kentucky. *In: Coal and coal-bearing rocks of Eastern Kentucky*. Geological Society of America Annual Coal Division Field Trip Guidebook, Kentucky Geological Survey, pp. 49-54.

- BOOKER F. W. 1954. *Coal at Martindale Creek, near Denman*. Report of the Department of Mines, to the Parliament of NSW for 1950, p.71.
- BRUNTON J. & MOORE A. 2004. *The Ridgeland Core Drilling Programmes 2001 and 2003, Hunter Coalfield NSW*. NSW Department of Mineral Resources Report GS2004/123 (unpublished).
- CARR P., FANNING M., JONES B. & HUTTON A. 2003. *Geochronology of Coal Measures in the Sydney Basin from U-Pb SHRIMP Dating of Airfall Tuffs*. Proceedings of the 35<sup>th</sup> Sydney Basin Symposium on "The Advances in the Study of the Sydney Basin" Sept. 29-30, 2003, Wollongong University, pp. 303-305.
- CREECH M. K. 2000. *The Wollombi Coal Measures – Refugees from Newcastle*. 34<sup>th</sup> Newcastle Symposium on Advances in the Study of the Sydney Basin, 15<sup>th</sup> AGC Convention, Univ. Tech. Sydney, July 2000.
- DAVID T. W. E. 1907. *The Geology of the Hunter River Coal Measures*. Geological Survey of NSW Memoir (Geology) 4, 372pp.
- DIESSEL C.F.K. 1985. *Tuffs and Tonsteins in the Newcastle Coal Measures of NSW Australia*. Comptes Rendus Dixieme Congress Int. de Stratigraphie et de Geologie du Carboneferre. Madrid 12-17 Sept 1983, Vol 4, pp. 197-210.
- DIESSEL C.F.K. 1992. *Coal Bearing Depositional Systems*. Springer Verlag Berlin, 721pp.
- FRANCIS E.H. 1985. *Recent Ash Fall: A Guide to Tonstein Distribution*. Proceedings of the 10<sup>th</sup> Int. Congress on Carboniferous Stratigraphy and Geology, (Dixieme Congress Int. de Stratigraphie et de Geologie du Carboneferre.) Madrid 12-17 Sept 1983, Vol 4, pp.189-195.
- GREVENITZ P., CARR P.F. & HUTTON A.C. 2003. *Geochemical Correlation of Late Permian Airfall Tuffs in Coal Measures, Sydney Basin, Australia*. Proceedings of the 35<sup>th</sup> Sydney Basin Symposium on "The Advances in the Study of the Sydney Basin" Sept. 29-30, 2003, Wollongong University, pp 25-32.
- HILL M.B.L. 1994. *Sydney Basin Coal Seam Correlations*. Minfo Magazine 45, 48-50. NSW Departement of Mineral Resources.
- HILL M.B.L., ARMSTRONG M., COZENS S. & BYRNES J. 1994. *Tracing the Bulli & Balgownie Seams across the Sydney Basin*. Proceedings of the 28<sup>th</sup> Sydney Basin Symposium on "The Advances in the Study of the Sydney Basin" April 15-17, Newcastle University, pp. 142-150.
- HERBERT C. 1980a. Depositional Development of the Sydney Basin. In Herbert C. & Helby R. eds. "A Guide to the Sydney Basin" NSW Geological Survey Bulletin 26, 11-52.
- HERBERT C., LANGFORD-SMITH T. & BRANAGAN D. eds 1976. *An Outline of the Geology and Geomorphology of the Sydney Basin*. 25<sup>th</sup> Int. Geological Congress, Sydney, University of Sydney, Science Press.
- KELLER J., RYAN W.B.F., NINKOVITCH D., ALTHERR R. 1978. *Explosive Volcanic Activity in the Mediterranean over the past 200,000 years as Recorded in Deep Sea Sediments*. Geological Society of America Bulletin 89, 591-604.
- KRAMER W. 1999. *Stratigraphic Correlation of the Tuffs in the Newcastle Coal Measures*. Honours Thesis, University of Newcastle (unpublished).
- KRAMER W., WEATHERALL G. & OFFLER R. 2001. *Origin and Correlation of Tuffs in the Permian Newcastle and Wollombi Coal Measures, NSW, Australia, using Chemical Fingerprinting*. International Journal of Coal Geology 47 115-135.
- MCCOY F.W. 1981. Areal Distribution, Redosition and Mixing of Tephra within Deep Sea Sediments of the Eastern Mediterranean Sea. In McCoy F.W. & Sparks R.S.J. eds. *Tephra Studies*, Reidel Co., pp. 245-254.

- NEWCASTLE COALFIELD SUBCOMMITTEE – Standing Committee on Coalfield Geology. 1995. *Proposed Revision of the Stratigraphy of the Newcastle Coal Measures – ratified in June 1992*) Geological Survey of NSW Report GS1995/256.
- RYER T.A. AND LANGER A.W. 1980. *Thickness Change Involved in the Peat- to-Coal Transformation for a Bituminous Coal of Cretaceous Age in Central Utah*. *Journal of Sedimentary Petrology* **50**, 987-992.
- STANDING COMMITTEE ON COALFIELD GEOLOGY OF NSW. 1975. *Stratigraphy of the Singleton Supergroup – ratified 1971*. Records of the Geological Survey of NSW, Vol. 16, Part 1 3/3/75.
- STEVENSON D. 1997. *Broke Drilling Program August 1996 – February 1997*. Notes to accompany Core Display at Wyee Bay Core Shed, 8/5/97.
- STEVENSON D. 1999. *The Wollombi Coal Measures*. 33<sup>rd</sup> Newcastle Symposium – Advances in the Study of the Sydney Basin, July 30 – Aug 1, Newcastle University.
- VEEVERS J.J., CONAGHAN P.J., & POWELL C. MCA. 1994. Eastern Australia. In Veevers J.J. and Powell C. McA. Eds. *Permian-Triassic Pangean Basins and Foldbelts along the Panthalassan Margin of Gondwanaland*, pp. 12-171. Geological Society of America Memoir **184**.
- VEEVERS J.J., MORGAN P., O'REILLY S.Y., WALTER M.R., & SCHEIBNER E. 2000. In: Veevers J.J. (ed), *Billion year Earth History of Australia and Neighbours in Gondwanaland*. GEMOC Press Sydney, 388pp.
- VOLCANOES OF THE WORLD. 2004. [www.volcano.si.edu/world](http://www.volcano.si.edu/world) [Accessed 17/03/04].
- WARBROOKE P.R. 1981. *Depositional Environments of the Upper Tomago and Lower Newcastle Coal Measures, NSW*. PhD Thesis, University of Newcastle, NSW (unpublished).
- WEATHERALL G. D. 1999. *Stratigraphic Correlation of the Tuffs of the Wollombi Coal Measures using Geochemical Fingerprinting*. BSc Honours Thesis, University of Newcastle.
- WILSON C.J.N, HOUGHTON B.F., PILLANS B.J. & WEAVER S.D. 1995. *Taupo Volcanic Zone Calc-alkaline tephra on the peralkaline Mayor Island volcano, New Zealand: Identification and uses as Marker Horizons*. *Journal of Volcanology and Geothermal Research* **69**, 303-311.



# PRIMARY FABRIC AND FRACTURE DISTRIBUTION WITHIN THE CORDEAUX CRINANITE INTRUSIVE

Luc Daigle

Senior Engineering Geologist  
Strata Control Technology Pty. Ltd.  
P.O. Box 824, Wollongong N.S.W. 2520

## ABSTRACT

Recent diamond drill hole coring by BHP Billiton Illawarra Coal was used to characterise the distribution of fracturing within the Cordeaux Crinanite intrusive body. Geological data obtained from boreholes Dendrobium DDH 36, 37, 51, 52 and 53 provided sufficient information to determine the pattern and history of fracture emplacement within the intrusive body.

Geological logging of the cored holes was complimented by acoustic scanner log analysis of each hole, Petrological and geochemical analysis of samples from Dendrobium DDH 36 and Dendrobium DDH 37, and field inspection of outcrop exposures.

The Cordeaux Crinanite is an intrusive sill complex consisting primarily thick olivine rich dolerite (Crinanite) sills and thinner olivine cumulate (Picritic) sills. Outcrop exposures of the complex are present along parts of Cordeaux Reservoir and forms the bedrock to the Upper Cordeaux Number 1 Dam and Upper Cordeaux Number 2 Dam and much of their catchments.

The intrusive body is roughly circular in shape and has a domed top and largely planar base which however does locally exhibit a bowl shaped base. The intrusive is commonly referred to as a sill but is demonstrated by drilling to gradually cross cut stratigraphy, the base ranges from approximately the Balgownie Seam to above the Bulli Seam into the Coalcliff, the roof may extend up to the Stanwell Park Claystone.

The shape of the body may be best defined as a laccolith due to the doming, circular geometry and roughly concordant stratigraphic position, the height to width ratio is more characteristic of a laccolith than a sill. The localised bowl shaped section of the base may form part of the feeder dyke system for the complex. Several probable associated feeder dykes have been intersected beneath the crinanite complex in underground workings, these may coalesce to form the basal neck of the complex. The main body of the complex exceeds 100m in thickness, near the margins thickness rapidly decreases and terminates in thin sills which pinch out, the maximum width of the body approaches 3 kilometres.

Layering within the body can be defined by lithologic change and contact chill margins, these form the primary fabric of the complex. Four distinct intrusive phases (units) were identified in the boreholes examined; their emplacement from top to bottom is as follows:

1. Coarse grained crinanite (approximately 50m thick).
2. Medium to coarse grained crinanite (approximately 12m - 25m thick).
3. Picrite (approximately 4m thick)
4. Picritic Crinanite (approximately <1m – 2m thick)

The order of intrusive emplacement was determined from chilled margin relationships and minor cross cutting relationships.

Outcrop exposures of the complex only consist of the coarse grained crinanite which forms the upper stratigraphy of the intrusive (units 1 and 2). The crinanite exposures are characterised by a thin weathering profile of bright red-orange soil (<1 to 3m thick) and the base of the soil weathering in boreholes is typically at 3m to 7m. Thin zones of oxidation continue along some joint planes and fault planes to 35m depth. The crinanite is highly resistant to weathering, mineral filled joints tend to weather out at surface and a thin rind of oxidation forms on outcrops in areas of deep weathering. Geomechanical testing completed shows the intrusive rocks have a typical UCS of >300MPa, as weathering is shallow the high strength rock extends to surface exposures. The topography over the exposed crinanite may largely reflect the original intrusive roof geometry due to its high strength and resistance to weathering relative to the surrounding sediments.

Fracturing in the crinanite complex is characteristic of thin bodied intrusives. Two distinct primary fracture sets are discernible; an early-formed set of columnar joints followed by late-formed cooling joint sets and hydrothermal mineralisation (Analcime-calcite-zeolite) which fills all the early-formed fractures. Secondary fracture sets created by post emplacement tectonics are present and are represented by regional faulting and jointing, these are not filled with hydrothermal mineral. A final late-formed fracture set present is an exfoliation joint set, this is present in most outcrops and is typical of intrusive rocks of uniform character. These fractures are sub-parallel to the surface topography and are formed as a result of de-burial de-stressing of the igneous body. These form thin sheet like layers near the surface and quickly diminish in frequency with depth. They cross cut the primary fractures and contain no mineralisation. The cored boreholes show exfoliation joints become rare below 15m depth.

### **CORE LOGGING**

Five fully cored holes intersecting the Cordeaux Crinanite were logged and photographed to capture the fracture characteristics and internal stratigraphy of the intrusive body.

### **Field Inspection Of Outcrop Exposures**

Outcrop exposures of the Cordeaux Crinanite is mainly limited to the drainage system, subcrop was present at drill sites Dendrobium DDH 36, in the paddock adjacent Dendrobium DDH 37, in the paddock and sump of Dendrobium DDH 51 and in the drainage adjacent to Dendrobium DDH 53.

Recognisable columnar jointing is present on surface at Dendrobium DDH 51 as large (>50cm diameter) polygonal blocks in the weathered soil profile. In the drainage adjacent to Dendrobium DDH 53 a nearly continuous outcrop is present from the Upper Cordeaux No. 2 Dam wall downstream for nearly 500m. In this section the columnar joints are observed to decrease in diameter as the Crinanite margin is approached. Variation in columnar joint dimensions are influenced by the latent heat within the body and rate of cooling, cooling is more rapid near the margins and produces small diameter columns while greater thickness of

intrusive results in slower cooling and the formation of large diameter columns. At Dendrobium DDH 36 columnar jointing is not readily recognised in the surface exposures.

Low angle, surface parallel exfoliation joints are present on most outcrop exposures (Photographs 1 and 2). These are seen to cross cut primary fabric and early and late formed joint sets including the columnar joint sets.

### Petrographic Analysis Of Core

Nine samples of core were submitted for petrological, mineralogical and chemical analysis, five are from Dendrobium DDH 36 and four from Dendrobium DDH 37. These are reported by Barron (2005). The Cordeaux Crinanite is described as an olivine dolerite with alkaline affinity cut by veins of analcime (+/- calcite +/- zeolite). An intrusive sill is found intruding the Tongarra Seam in Dendrobium DDH 37, two samples of this rock contain significant K-feldspar and is of syenitic affinity. Secondary minerals (analcime +/- calcite +/- zeolite) found in veins within the crinanite are located on the majority of fractures, particularly the moderate to high angle defect planes. This mineralisation represents a hydrothermal event during the cooling stages of the intrusive body. Shrinkage fractures emplaced as a result of cooling provided pathways for fluid circulation and mineral deposition.

Geochemical and trace element analysis of both intrusive types (Figure 1) demonstrate probable fractionation of a single primary parent magma was the source of these rocks.

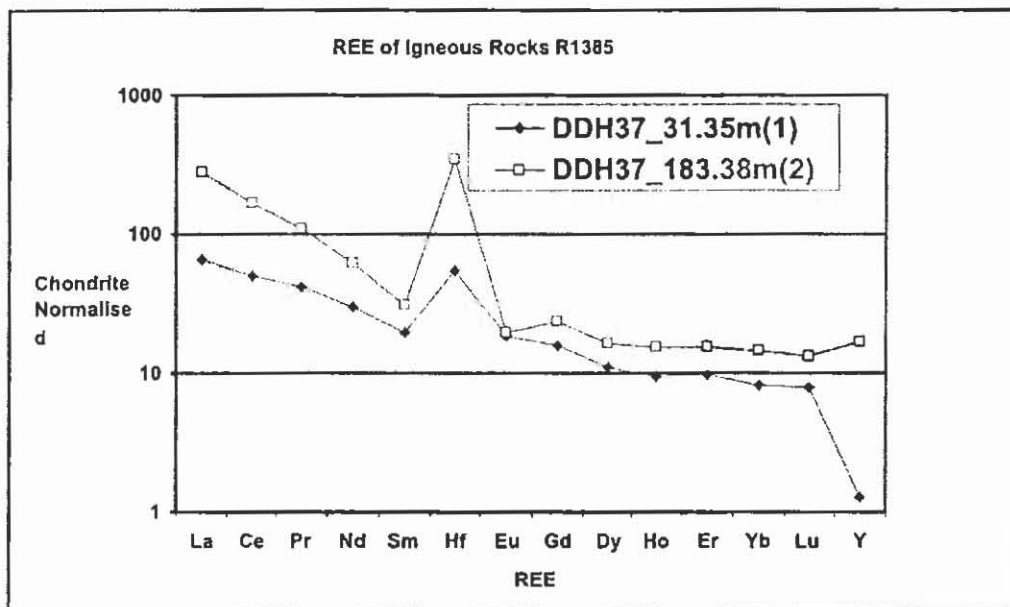


Figure 1 Rare earth and trace element analysis indicates both intrusives are sourced from a single parent melt (from Barron 2005 (Report No. 3/04/1385)).

### Analysis of Core

Acoustic scanner images from Dendrobium DDH 36, 51, 52 and 53 data were used by SCT Operations to identify 447 defect orientations (dip and dip-direction) within the Cordeaux Crinanite.

Frequency distribution of the defects (Figure 2) is plotted and indicates distinct populations are present.

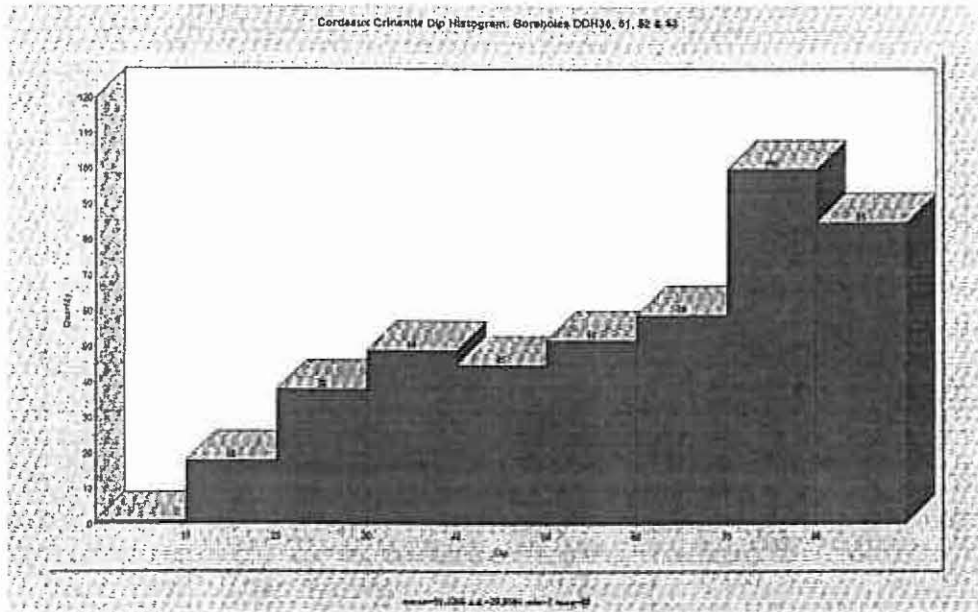


Figure 2 Dip histogram of fractures within the clinanite.

Three distinct groupings of data are apparent in the histogram:

- a) A small group (19) of very low angle dipping defects less than  $20^{\circ}$ .
- b) A large group (241) of moderate angle dipping defect planes between  $20^{\circ}$  and  $70^{\circ}$ .
- c) A large group (185) of high angle dipping defect planes between  $70^{\circ}$  and  $90^{\circ}$ .

Plotting of the defect poles as a scatter plot in an equal angle stereo net then contouring of the poles permits viewing and selection of the dominant trends within the large data set (Figures 3). This methodology provides geostatistical determination of significant groupings within the data set.

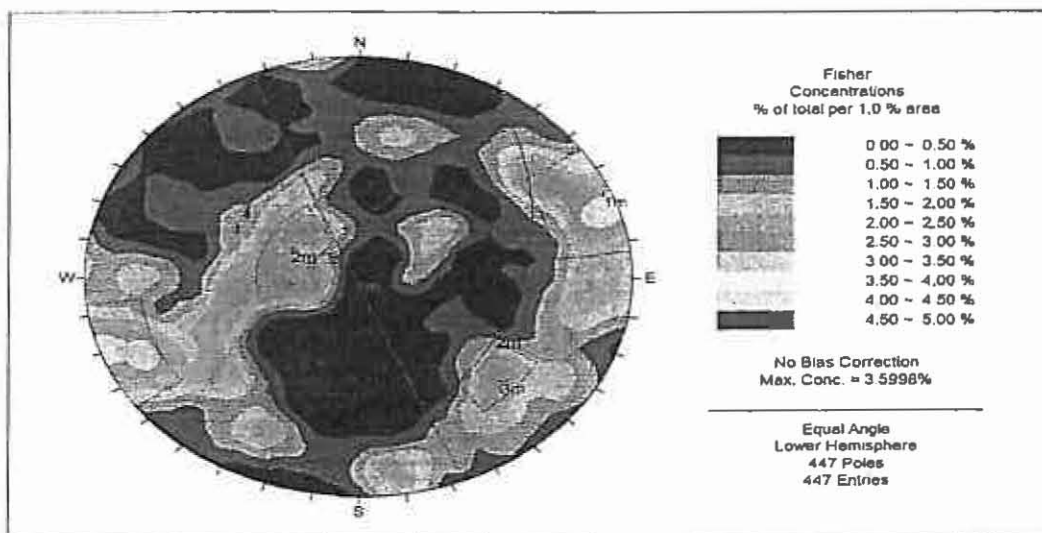


Figure 3 Contour plot of defect holes.

Three dominant trends were identified within the data set.

- 1) The first set was a sub-vertical fracture set striking  $337^{\circ}$
- 2) The second set were relatively moderate dip ( $30^{\circ}$ ) striking  $027^{\circ}$
- 3) The third major set was also moderate dip ( $70^{\circ}$ ) and striking  $227^{\circ}$

Additional sets are likely present, but are dominated by the three identified trends.

Further refinement of the data requires greater understanding of the formation of these defect planes and their emplacement history. The fracture analysis reviews models of fracture formation and application to the observed Cordeaux Crinanite.

### FRACTURE ANALYSIS

Fracturing systems within various igneous bodies are well documented and encountered fractures can readily be interpreted. Defect planes within an intrusive can be divided into an emplacement history based on their cross cutting relationship, orientation, morphology, and mineralisation. The typical division of defects in an intrusive is as follows:

- a) **Primary Fabric:** internal flow structures, crystal alignment, lithological variation, emplacement fractures and faulting. Often identified by chill margins and shape contacts.
- b) **Cooling Fractures:** fracture sets which developed as the intrusive cools and shrinks, these include columnar joints in a thin bodied intrusive. Cooling fractures can form as early and late stage events.
- c) **Secondary Fractures:** these form after the emplacement and cooling of the intrusive, they are typically related to regional tectonics and can usually be identified by their lack of hydrothermal mineralisation and cross cutting relationship with the early formed defects. Additional defects may develop due to de-burial and de-stressing of the rock mass, surface exposures of igneous rocks are commonly affected by exfoliation joints which disperse quickly with increased depth.

Exposures of the Cordeaux Crinanite readily display the typical defect sets expected within igneous rocks. The following describes the defect planes identified.

#### Determination of Primary Fabric

Primary fabric is not readily observed in outcrop, however, in core the Crinanite is readily divided into a complex of several sub-horizontal sill like bodies of varying thickness. These are defined by changes in lithology and by the nature of their contacts, drill core intersection of the Cordeaux Crinanite in closely spaced holes (Dendrobium DDH 36, 37, 51, 52, and 53) has resulted in the identification of the following stratigraphy in order of emplacement and position from top to bottom of the intrusive complex:

- |        |                                    |
|--------|------------------------------------|
| Unit 1 | Medium to Coarse Grained Crinanite |
| Unit 2 | Fine to Medium Grained Crinanite   |
| Unit 3 | Picrite                            |
| Unit 4 | Picritic Crinanite                 |

These individual units are separated by variation in composition, grain size and chill margins which assist in determining emplacement history. Figure 1 shows idealised geology between holes Dendrobium DDH 36 and Dendrobium DDH 37, additional holes northeast of this position confirm the limited extent of the Cordeaux Crinanite. Figure 2 depicts the observed stratigraphy within the Cordeaux Crinanite between holes Dendrobium DDH 36, Dendrobium DDH 51, Dendrobium DDH 52 and Dendrobium DDH 53.

The contact between Unit 1 and 2 is a thin chill margin which is indistinct in some holes but is also supported by changing grain size over the contact zone. The emplacement of these two units is likely not separated by much time as petrographic studies indicate that there is little change in the initial magma. Compositional similarity and minor chill margin development supports rapid intrusion of individual units. Unit 2 has a gradual fining in grain size towards the base over a 5 to 6 metre interval which forms its base and is a thick chill margin representing gradual cooling over a greater length of time. Sub-vertical joints at the base of Unit 2 are truncated by the underlying Unit 3.

Unit 3 is a coarse grain picrite (olivine cumulate) its upper and lower contacts are sharp with distinct thin chill margins indicating it intruded the sill complex after substantial chilling of the overlying units. Thin dykes of the picrite intrude the overlying units, supporting the emplacement sequence determined.

Unit 4 is a mixture of coarse grained picrite and crinanite, this thin sill forms the base of the sill complex and varies from distinct chilled top and bottom contacts to completely chilled where it is thin. In hole Dendrobium DDH 51 the units lower contact has mixed with the underlying sedimentary rocks and has the appearance of a pepperite. Pepperites normally form where magmatic rocks contact wet unconsolidated sediments. If this is a true pepperite, the timing of emplacement of the Cordeaux Crinanite may be very early and predate complete lithification of the sediments, more likely is a softening of the enclosing sediments has occurred during the process of emplacement.

#### **Early Formed Cooling Fracture Sets**

Columnar jointing is prevalent throughout the body and represents initial early cooling of the intrusive when magma has begun to congeal and final crystallisation occurs. Polygonal fracture patterns are identifiable at most outcrop localities, distribution of the columns by size is discernible with smaller columns dominating towards the complex margins and larger columns prevailing towards the centre of the complex (Photograph 1).

Size distribution of the columns reflects the thermal dynamics of the body with the margins cooling and crystallising more quickly than the thick central part which cooled slowly and developed much larger diameter columns. Columns formed roughly perpendicular to the contact margins and may plunge back towards the magma source direction as demonstrated by Waters (1960), this is apparent in outcrop near the Cordeaux Manor. Growth striations are discernible on some columns and represent progressive crack propagation during cooling, these can give an appearance of sub-horizontal layering within individual columns.

The intrusive complex is similar in character to a composite basalt flow, classic subdivision of column architecture into an upper colonnade, entablature and lower colonnade may be possible. The upper colonnade here is represented by the smaller columns (.25m to .5m diameter) on the complex margins and possibly extends as a thin skin over the entire complex, the entablature is represented by the much larger diameter columns (>.5m diameter) and more

## CORDEAUX CRINANITE

massive central core of the complex. The lower colonnade although not exposed in outcrop may be represented by the jointing developed in the basal picrite sills and chill margins of the complex. Figure 4 illustrates the conceptual model of columnar architecture.

### DISTRIBUTION OF COLUMNAR JOINTS

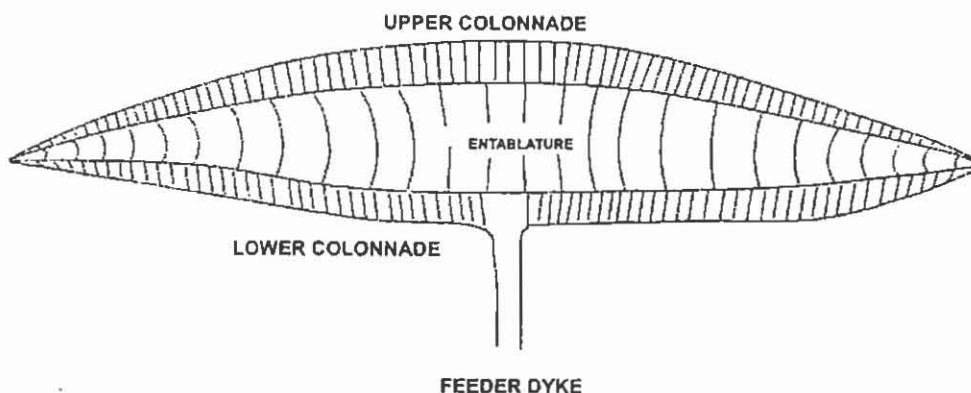
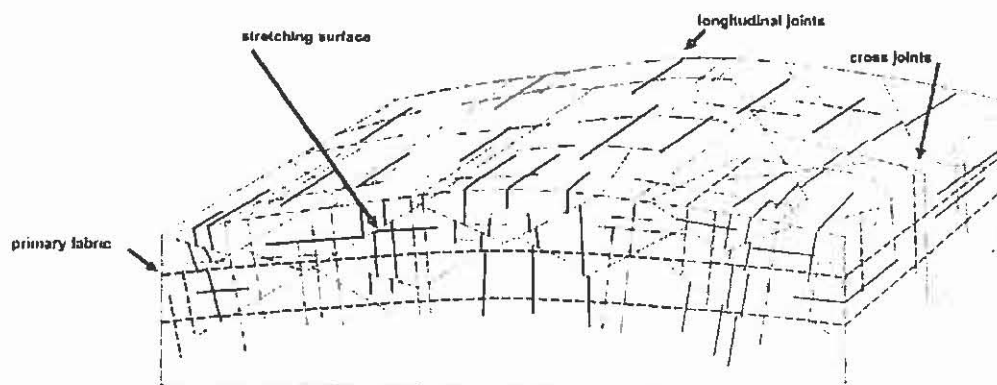


Figure 4 Columnar jointing conceptual model of columnar architecture.

Nearly all early formed fractures are filled by a later hydrothermal mineralizing event. Even on the tight columnar joints a thin film of analcime +/- calcite +/- zeolite is present.

### LATE FORMED COOLING FRACTURE SETS

Progressive cooling and resultant shrinking of the Cordeaux Crinanite has resulted in the formation of additional fracturing. These fractures propagate throughout the entire body and their orientation is influenced by the geometry of the sill complex. Cloos (1922), described the idealised pattern of defects that may develop within an igneous body (Figure 5), these ranged from low-moderate dip conjugate sets through to high angle fractures perpendicular to the cooling surface and running longitudinal to the body. These fractures are most commonly filled with hydrothermal minerals (analcime +/- calcite +/- zeolite) deposited as latent heat from the body inducing hydrothermal circulation systems. These fractures cross cut the primary fabrics (sill contacts) and early formed cooling joints (columnar set).



Idealised fracture distribution in an igneous body as described by Cloos (1922)

**Late stage Fracturing:**

Related to the thermal dynamics of the intrusion, Hans Cloos (1922) recognised the following fundamental types of primary fracturing: cross fracturing, longitudinal fractures, stretching fractures, marginal fissures, and marginal thrusts.

Figure 5 Igneous body conceptual model of late stage cooling fractures.

Numerous fractures observed in the core and in outcrop are readily identifiable as late cooling fractures. These are particularly notable in outcrop exposures where the cross cutting nature can be seen more clearly.

### Regional Tectonic Fracturing

Regional tectonic deformations are well documented in the area, faulting and jointing are the best examples. Within the Cordeaux Crinanite, these defect planes should be present. However, they were not readily determined in the core or in outcrop. These late features are post igneous emplacement and also post date the hydrothermal event associated with the cooling of the sill complex. Thus regional tectonic fabrics should be notable by the absence of hydrothermal mineralisation. Preservation of the mineral fill in fractures within surface exposures is poor within the weathering horizons, some of the mineral (calcite) is readily susceptible to leaching, however, sufficient residue is present to determine if the fracture was mineralised. Detailed surface mapping and extrapolation of known structures from surface and underground mapping may better delineate the presence of these features.

### De-burial Stress Relief Fracturing

Exfoliation jointing is a common feature of outcropping igneous bodies. De-burial due to surface weathering and erosion unload the rock and stress relief manifests as surface parallel joints which form thin layered sheets. These fractures rapidly decrease in frequency with depth, in the cored holes they occur to approximately 15m depth. Price and Cosgrove (1990) provide a good description of exfoliation fracturing. The extent of these joints is limited by the degree of surface erosion (depth of overburden) and topography. Exfoliation joints are observed to cross cut primary and early formed fabrics such as columnar joints and mineral filled fractures. This relationship is demonstrated in Photographs 1 and 2.

## SUMMARY AND CONCLUSIONS

Petrologic examination of the Cordeaux Crinanite has identified the rock mass is composed mainly of olivine dolerite and olivine cumulate. These rocks can be classified in different igneous nomenclature systems of which crinanite can be used for olivine dolerite and picrite for olivine cumulate. These rocks were emplaced as thick to thin intrusive sills forming a stack complex of multiple sills.

The geometry of the intrusive complex suggests it is approximately concordant to slightly discordant within the coal measures. The intrusive is circular in its footprint and its roof is broadly domed and quickly slopes at the margins to thin sills. The base is roughly planar, a broad neck zone of source dykes may form a bulged protrusion of the base, this feature is not yet fully delineated. Based on the overall geometry observed the complex is best referred to as a loccolith, a concordant intrusive with a planar sole and the magma has domed the overlying rocks (Davis, 1984).

Fracturing of the intrusive complex is strongly influenced by the shape and dimensions of the body, the relative sill like layering and moderate thickness of the body has permitted the development of columnar jointing to form as an early cooling feature of the complex. Continued cooling has produced late stage cooling fractures characteristic of most intrusive bodies and associated development of hydrothermal circulation with vein mineralisation. Progressive deformation of the complex post emplacement by regional tectonics, has produced fault and joint sets which cross cut the emplacement fabrics, but are less conspicuous. A final set of fractures formed as erosion exposed the complex and de-stressed the rock resulting in exfoliation joints forming sheet like bodies near outcrop surfaces.

Compilation of the core log data and review of outcrop exposures combined with petrologic relationships permitted the identification of five fracture types within the Cordeaux Crinanite and their emplacement history, these are listed in their order of formation and summarised in Table 1.

Frequency distribution of the fracture sets is variable throughout the intrusive complex and has highly variable orientation. An analysis of all 447 oriented defects in core indicates three distinct groups high angle ( $70^{\circ}$  to  $90^{\circ}$ ), moderate angle ( $20^{\circ}$  to  $70^{\circ}$ ), and lastly a number of fractures are low angle  $<20^{\circ}$ . This analysis resulted in an asymmetrical frequency distribution of fractures, however, if structure defects are modelled as depth related intervals the plot will be bimodal near the surface and quickly progress to a more asymmetrical plot at depth, this is due to greater frequency of the near surface exfoliation defect planes. Figure 6 illustrates the expected fracture distribution within the Cordeaux Crinanite.

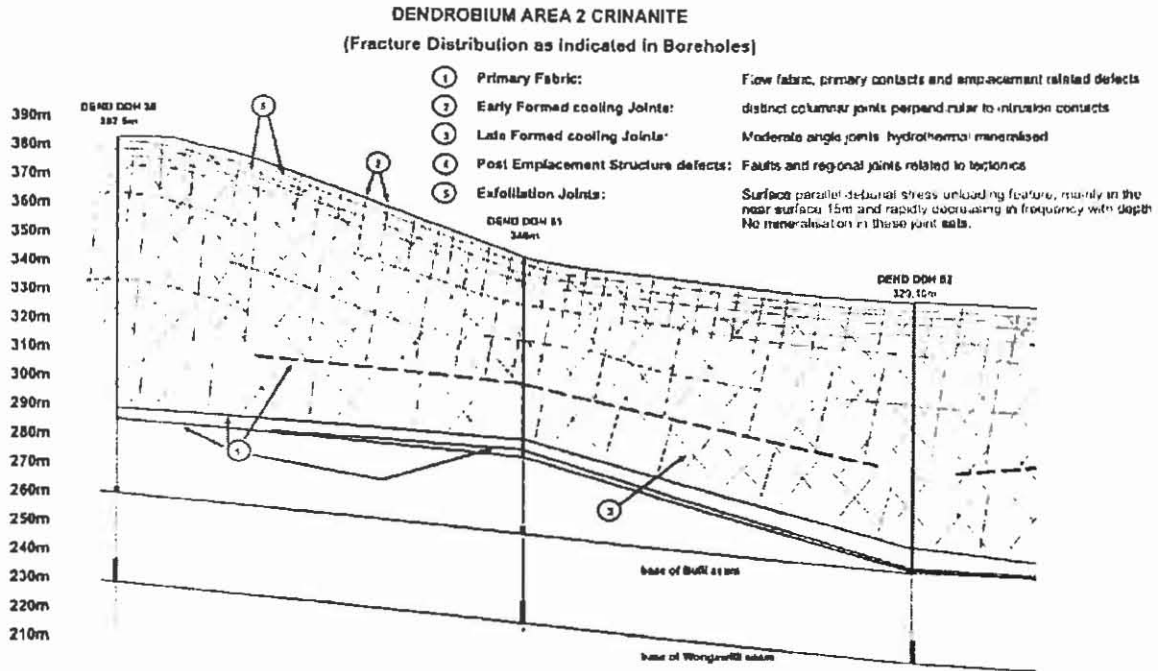


Figure 8 Fracture distribution within the Cordeaux Crinanite.

Table 1: Fracture Types and Emplacement History within the Cordeaux Crinanite

<b>Primary Fracturing</b>	
<b>1.</b>	<b>Emplacement Foliation</b> Fracturing and foliation related to emplacement of the intrusive body. These may include joints and faults formed which affect the enclosing stratigraphy inflated by the displacing intrusive. Individual sill boundaries defined by chill margins, changed grain size and lithology.
<b>2.</b>	<b>Early Cooling (Columnar Jointing)</b> Begin to form as the melts congeals and cools, size distribution and orientation affected by proximity to intrusive body margins and geometry.
<b>3.</b>	<b>Late Cooling Fracturing</b> Influence of regional stresses, intrusive body geometry and thermal dynamics result in fracturing characterised by thin dykes and veining. Major fracture sets include cross fracturing, longitudinal fractures, stretching fractures, marginal fissures and marginal thrusts.
<b>Secondary Fracturing</b>	
<b>4.</b>	<b>Regional Stresses (Tectonic)</b> Regional jointing and faulting related to post emplacement tectonics.
<b>5.</b>	<b>De-burial Stress Relief (Exfoliation)</b> Surface parallel fracturing related to de-burial, cross cuts primary fracture sets and forms thin sheets. These fractures are restricted to near surface of the outcrop and decrease rapidly in frequency with depth.

## CORDEAUX CRINANITE

### REFERENCES

- CLOOS, H., 1922, Über Ausbau und Anwendung der granittektonischen Methode: Preussischen Geologischen Landesanstalt, v. 89, p. 1-18.
- DAVIS, G.H., 1984, Structural Geology of Rocks and Regions, p 215-216.
- PRICE, N.J., AND COSGROVE, J.W., 1990, Analysis of geological structures, Cambridge University Press.
- WATERS, A.C., 1960, Determining direction of flow in basalts: American Journal of Science, v. 258a, p. 350-366.

### CORDEAUX CRINANITE Outcrop Exposures Along Cordeaux No 2 Dam Spillway



**Photograph 1.** Dipping columnar joints are present on the margin of the crinanite complex along Cordeaux No 2 Dam Spillway. Columns in this area are approximately 25cm to 35cm in diameter, these are intersected by various later formed fracture sets. Particularly, a complex of low angle, surface parallel fractures are prominent. Some of these fractures which intersect the columns are exfoliation joints sub-parallel to the weathering surface. Some of these planes intersect and form ramping and stepped outcrop exposures.



**Photograph 2.** Variable planes of the exfoliation joints cross cutting continuous columns.

# GEOLOGY OF THE WILLOW TREE-ARDGLEN AREA, NEW SOUTH WALES: A REAPPRAISAL

M.W. DAWSON<sup>1,2</sup>

<sup>1</sup>Department of Earth Sciences  
University of New England, NSW 2350.

<sup>2</sup>Whitehaven Coal Mining  
Boggabri Road, Gunnedah, NSW 2380.

## ABSTRACT

The Willow Tree-Ardglen area marks the boundary between the structural Gunnedah and Werrie Basins in northern New South Wales. This area encompasses complex structural relationships between Cainozoic Volcanics, Surat Basin, Werrie Basin, Gunnedah Basin and Tamworth Belt. Detailed outcrop mapping has been undertaken to resolve basin boundary relationships.

Sedimentologically, the Permian sequence in the Willow Tree area has similar characteristics to that of the Hunter Coalfield. The ~300 metre thick coal-bearing Greta Coal Measures (Skeletal Formation, Oaklyn Siltstone, Key Band Conglomerate and Rowan Formation) interval is overlain by the ~500 metre thick marine Maitland Group (Branxton Formation and Mulbring Formation) interval which is in turn overlain by an unknown thickness of coal-bearing Singleton Supergroup (Vane Subgroup) interval.

New structural interpretation shows that the Mooki Thrust is low-angle and cut by later upright faults that are concealed by coluvium and alluvium. A vertical to subvertical coal seam in the Permian Vane Subgroup is unconformably overlain by shallow (<15°) southwest dipping Early Triassic Digby Formation at the Willow Tree tip. This unconformity constrains the development of the Mooki Thrust to the latest Permian. Neotectonics in the area is manifest as vertical faulting of Palaeogene basalts against Carboniferous Volcanics.

## INTRODUCTION

Willow Tree is located approximately 300 km north of Sydney, New South Wales (Figure 1). The area hosts a complex interaction between the New England Orogen, Werrie Basin, Gunnedah Basin, Surat Basin and Cainozoic volcanics. No detailed geological studies have been undertaken in the Willow Tree to Ardglen area since that of Hanlon (1948). Therefore, a revision of stratigraphic terminology is needed to keep in line with the recent advances in the study of the Sydney and Gunnedah Basins. The geology in the Willow Tree area is investigated as part of a project to form a regional sequence stratigraphic interpretation of the Greta Coal Measures in the Werrie Basin.

## REGIONAL SETTING AND PREVIOUS WORK

The Werrie Basin is a structural basin containing Permian sedimentary and volcanic rocks that unconformably overlies Middle Cambrian (Cawood 1980) to earliest Permian (Roberts et al 2006) basement of the Tamworth Belt, Southern New England Orogen (Gilligan and Brownlow 1988). Briefly, the Werrie Basin consists of the basal terrestrial Temi Formation

that comprises up to ~220 m of mudstones, sandstones, pebble conglomerates and minor felsic to intermediate volcanics and coal (Roberts *et al.* 2006; Hanlon 1948). Overlying the Temi Formation are a series mafic to intermediate volcanics and associated intrusives (Werrie Basalt and Warrigundi Igneous Complex) up to 2 km thick that were deposited in both marine and terrestrial regimes (Carey 1935; Hanlon 1948). The Werrie Basalt is unconformably overlain by late Early Permian coal-bearing sequence of the Willow Tree Formation (Oversby 1971; Pratt 1996) (herein renamed the Greta Coal Measures – Willow Tree area).

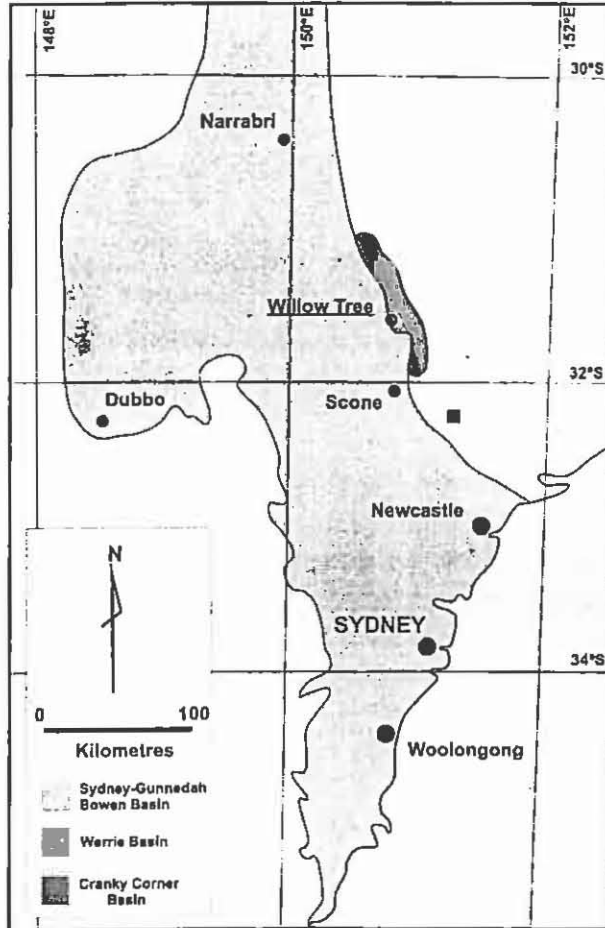


**Figure 1** The location of Willow Tree, New South Wales.

Conformably overlying the Willow Tree Formation is the early Late Permian marine conglomerates and sandstones of the Borambil Creek Formation (herein renamed the Maitland Group, Branxton Formation – Willow Tree area). This unit consists of basal, poorly-sorted conglomerates and diamictites with sandy and fossiliferous horizons (Hanlon 1948). The youngest unit in the Werrie Basin is the Late Permian Toll Bar Formation (herein renamed the Maitland Group, Mulbring Siltstone (lower) and Singleton Supergroup (upper) – Willow Tree area). This unit is both terrestrial and marine contains sandstone, siltstone, mudstone and coal with localised pods of limestone (Hanlon 1948).

## METHODS

Fieldwork entailed detailed creek traverses of the Permian and Triassic sedimentary rocks in the areas to the west and southwest of Willow Tree. No coal exploration drilling has been undertaken in the Willow Tree area. All coordinates discussed in this paper are in Geodetic Datum of Australia 1994, Map Grid Australia Zone 56.

## LITHOLOGY

The Permian formations in the Willow Tree area occur on the western edge of the structural Werrie Basin. Due to the lithological similarities between the Permian at Willow Tree, to those in the Hunter Valley to the south, a new stratigraphy is to include nomenclature from the Hunter Coalfield (Beckett 1988). Table 1 shows a revised stratigraphy of the Willow Tree area. Figure 2 is a map of the area to the northwest of Willow Tree.

At the Willow Tree to Ardglan area, the Werrie Basalt is approximately 500 metres thick and outcrops poorly. Lithologies comprise altered basalt, and basaltic volcanoclastics, with minor ignimbrites, spherulitic ashflow tuffs and polymictic conglomerates. Plagioclase laths altered to carbonate and clays are a distinguishing feature within the mafic phases of the Werrie Basalt at Willow Tree. In a railway cutting next to the New England Highway at Ardglan (GR 290100 6487900), vertically dipping basaltic flows of the Werrie Basalt are unconformably

## WILLOW TREE-ARDGLEN AREA

overlain by subhorizontal Cainozoic basalts of the Liverpool Range Volcanics. A deep weathering surface on the Werrie Basalt is also present at this contact, indicating early Cainozoic weathering episode.

The Greta Coal Measures is 300 metres thick and outcrops in two areas in the Willow Tree-Ardglen district. The first area occurs as a semicontinuous, four kilometre long line of outcrop, immediately to the west of Borambil Creek at Willow Tree. The second area occurs one kilometre to the west of Kankool as a 500 metre long, northwest striking, vertically dipping outcrop.

**Table 1** Revised Permian to Cainozoic stratigraphy in the Willow Tree area.

QUATERNARY	ALLUVIUM AND COLLUVIUM		
PALAEOGENE	LIVERPOOL RANGE VOLCANICS		
TRIASSIC	NAPPERBY FORMATION		
	DIGBY FORMATION		
PERMIAN	SINGLETON SUPERGROUP	WITTINGHAM COAL MEASURES	VANE SUBGROUP
	MAITLAND GROUP	MULBRING SILTSTONE	
		BRANXTON FORMATION	
	GRETA COAL MEASURES	ROWAN FORMATION	
		KEY BAND CONGLOMERATE	
		OAKLYN SILTSTONE	
	DALWOOD GROUP	SKELETAR FORMATION	
		WERRIE BASALT	

A five metre wide outcrop of the Skeletar Formation was observed in a gully to the north of 'Oaklyn' immediately to the west of an outcrop of weathered Werrie Basalt. The Skeletar Formation comprises almost wholly of kaolinitic peletoidal claystone with angular to subrounded claystone clasts up to 6 mm (Figure 3). Conformably overlying the Skeletar Formation is 150 metres of massive friable siltstone herein named the Oaklyn Siltstone. A type section is proposed in the erosion gully 800 metres to the north northwest of 'Oaklyn' homestead. An unnamed coal seam within the Oaklyn Siltstone occurs on the edge of Borambil Creek on 'Oaklyn'. The seam is split and occurs as a 60 cm upper and a 30 cm lower coal ply separated by 30 cm of siltstone. Siderite replaced to iron oxides is quite common throughout the section. Minor laminated, fine grained lithic sandstone occurs sporadically throughout the type section.

The Key Band Conglomerate (after Hanlon's 1948 'Key Band of Conglomerate') is the most easily identifiable unit within the Greta Coal Measures and is up to 30 metres thick. Lithologies are typified by poorly-sorted, well-rounded, lithic cobble conglomerates. Outcrop of the Key Band Conglomerate is manifest as a prominent ridge of conglomerate and can be followed for up to three kilometres on the western side of Borambil Creek. The Key Band Conglomerate is usually split into two conglomeratic sections each 10 metres thick, separated by approximately 10 metres of coarse lithic sandstone. Overlying the Key Band Conglomerate are upward fining cycles of pebble conglomerate, lithic, sandstone, siltstone and coal of the Rowan Formation. The clasts within the Rowan Formation are dominated by red jasper, and green chert typical of the Greta Coal Measures in the Musswellbrook Anticline (Beckett 1988; Boyd and Leckie 2000), and the Cranky Corner Basin (Stevenson 2003).

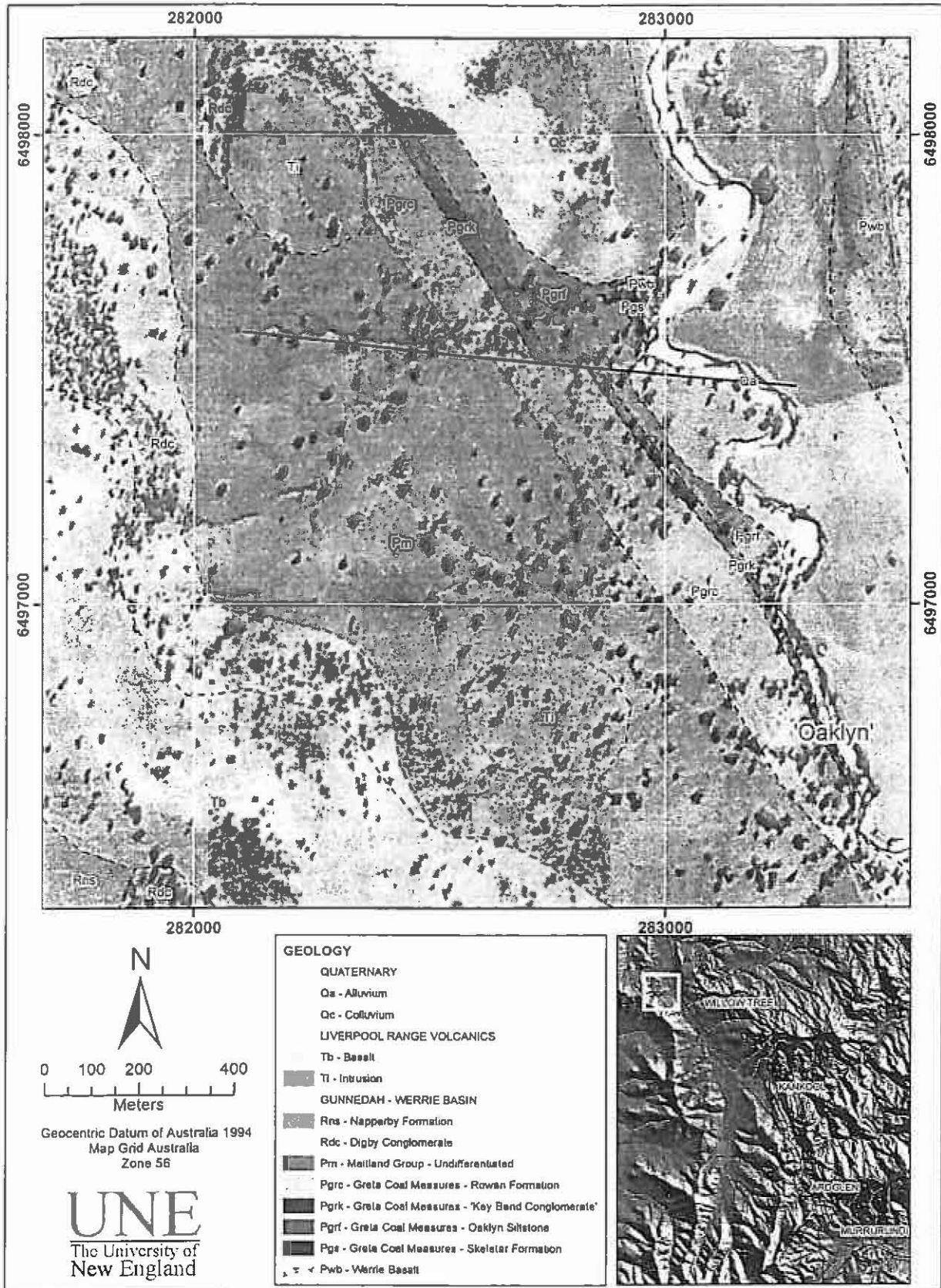
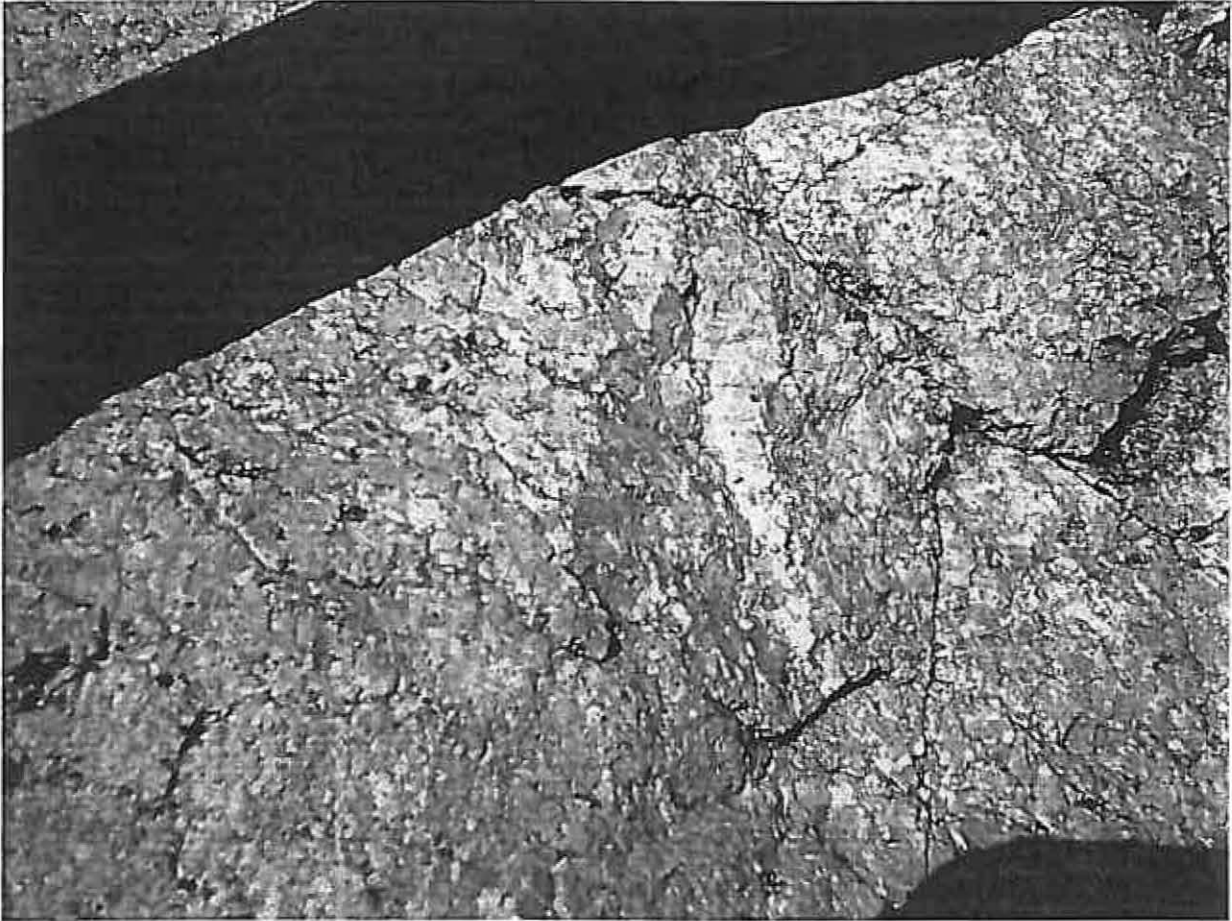


Figure 2 Geology of the area to the northwest of Willow Tree.



**Figure 3** A slightly weathered peletoidal claystone (Skeletal Formation) cropping in an erosion gully on 'Oaklyn' property (GR 282940 6497670).

A poorly cropping, 500 metre thick Maitland Group (Branxton Formation and Mulbring Siltstone) overlies the Greta Coal Measures at Willow Tree. The Branxton Formation comprises poorly sorted, lithic, pebble conglomerate with minor sandstone and siltstone. The Mulbring Siltstone comprises a monotonous series of grey siltstone. A thin, laterally extensive limestone (marl) horizon exists within the upper part of the Mulbring Siltstone to the west of Willow Tree.

Hanlon (1948) noticed weathered carbonaceous sedimentary rocks on the western side of 'Oaklyn' and attributed these to the Late Permian coal measures. The recent uncovering of the Singleton Supergroup in the floor of the local council gravel quarry to the west of Willow Tree has provided more lithological data on these coal measures. The Singleton Supergroup rocks in the Willow Tree area comprise pebble conglomerate, lithic sandstone, siltstone, tuff and coal.

Rocky outcrops of subhorizontal to shallowly dipping cobble conglomerates typify the Digby Formation in the Willow Tree area. Clast compositions of conglomerates are used for the distinction between the Digby Formation and the Greta Coal Measures in the field. The Digby Formation can be identified due to the presence of black chert, an increase in the abundance of jasper and an absence of green chert.

## STRUCTURE

The Mooki Thrust from this study is inferred to exist to the west of Toll Bar Ridge, and to be low angle similar to the Hunter Thrust (Beckett 1988) and that intersected to the north on the AGSO Seismic Section (Korsch 1999). A large scale hanging wall anticline to the east of the Mooki Thrust has been mapped by previous authors (Hanlon 1949; Roberts *et al.* 2006), the hinge of which plunges slightly to the south southeast and can be observed along the New England Highway 2 kilometres to the north of Willow Tree (GR 284500 6498100). On the west limb of this anticline, the Permian strata dip quite steeply (70 to 90 degrees).

A 90 degree angular unconformity exists between the Early Triassic Digby Formation and the Late Permian Vane Subgroup at the Willow Tree tip. This constrains the timing of deformation for the Late Permian Hunter Orogeny which must predate the deposition of the Digby Formation and post date the deposition of the lower Singleton Supergroup.

At the northern entrance to the railway tunnel at Ardglen (GR 291140 6486130), a vertically dipping fault line (Murrurundi Thrust) is exposed striking 100 degrees (Dawson *et al.* 2003). This fault is interpreted to be oblique slip and juxtaposes the Carboniferous Currabubula Formation against the Cainozoic Liverpool Range Volcanics. The oblique slip fault comprises approximately 200 metres of dip slip component and up to 3 kilometres of sinistral strike slip movement. This estimate is based on the amount of displacement of the Permian and Cainozoic Volcanics to the north and south of the Murrurundi Fault. Investigations of the 1997 Liverpool Plains airborne geophysical survey shows the magnetic lineament expressions of the Murrurundi Thrust which stretches for over 100 kilometres from east of Murrurundi through to Tambar Springs.

A fault previously interpreted as the Mooki Thrust (Offenberg 1971, Gilligan and Brownlow 1987) is inferred to exist beneath Borambil Creek. Evidence for this fault is manifest as changes in the heights for the base of Cainozoic Liverpool Range Volcanics either side of the creek. Moreover, the volcanics on the eastern side are more than 100 metres higher than those on the western side of Borambil Creek.

## COAL GEOLOGY

There are a number of occurrences of coal in the Willow Tree area. For example:

- A thin coal seam outcrops on the banks of Borambil Creek on 'Oaklyn' property (GR 282970 6497570).
- An eight metre thick coal seam has been unearthed at the base of a local council road base quarry, adjacent to the Willow Tree tip (Figure 4).
- A three metre thick coal seam with low ash contents (Raggatt 1939) was excavated during the sinking of a well near the Willow Tree School.

No coal exploration drilling has occurred in the Willow Tree area, therefore a resource estimate is difficult to ascertain. Pratt (1996) identified a resource of 3.5 million tonnes along the eight kilometres of subcrop for the Greta Coal Measures in the Willow Tree area. This estimate is based on a coal thickness of 3 metres, to a depth of 100 metres. Due to the similarities in lithologies of the Greta Coal Measures and Singleton Supergroup at Willow Tree to those in the Werris Creek and Blandford areas, coal thickness can also be assumed to be similar. Therefore, a cumulative thickness of coal in the order of 30 metres within two coal

measures (Greta Coal Measures and Singleton Supergroup) is expected. Factors limiting the size of the economic extraction of coal in the Willow Tree area include: The extreme dips of the coal; Cainozoic igneous intrusions; a significant portion of the coal measures subcrop beneath Borambil Creek.



**Figure 4** A vertically dipping, eight metre thick (wide) coal seam in the local council quarry next to the Willow Tree Tip (GR 283300 6494760). Note: subhorizontal Digby Formation in the quarry walls.

### ACKNOWLEDGEMENTS

Thanks to the landowners in the Willow Tree area for providing access for mapping.

### REFERENCES

- BECKETT J. 1988. The Hunter Coalfield. Notes to accompany the 1:100 000 Geological Map, *Geological Survey of New South Wales, Report GS1988/51*.
- BOYD R. & LECKIE D. 2000. The Greta Coal Measures in the Muswellbrook Anticline area, New South Wales. *Australian Journal of Earth Sciences* 47, 259-279.
- CAREY S.W.1934. The Geological Structure of the Werrie Basin. *Journal and proceedings of the Linnean Society of New South Wales* 59, 351-374.
- CAREY S.W.1935. Note on the Permian Sequence in the Werrie Basin. *Journal and proceedings of the Linnean Society of New South Wales* 60, 447-456.

- CAWOOD P.A. 1980. Geological development of the New England Fold Belt in the Woolomin-Nemingha and Wisemans Arm regions. The evolution of a Palaeozoic fore-arc terrain. PhD thesis, University of Sydney.
- DAWSON M.W., VICKERY N.M., BARNES R.G., TADROS V.N. & WILES L.A. 2004. Nandewar geology – integration and upgrade, Nandewar Western Regional Assessment. Resource and Conservation Assessment Council. 169pp.
- GILLIGAN L.B. & BROWNLOW J.W. eds 1987. *Tamworth-Hastings 1:250 000 metallogenic map. Sheets SH 56-13, SH 56-14 (plus parts of SI 56-1 and SI 56-2). Mineral deposit data sheets and metallogenic study.* Geological Survey of New South Wales, 438 pp.
- HANLON F.N. 1948. Geology of the north-western coalfield. Part II. Geology of the Willow Tree—Temi district. *Royal Society of New South Wales, Journal and Proceedings* **81**, 291-297.
- LOUGHNAN F.C. 1975. Correlatives of the Greta Coal Measures in the Hunter Valley and Gunnedah Basin, New South Wales., *Geological Society of Australia. Journal*, **22(2)**, 243-253.
- OFFENBERG A.C. 1971. *Tamworth 1:250,000 Geological Sheet SH 56-13*, Geological Survey of New South Wales, Sydney.
- PRATT W. 1996. Coal resources of the Werrie Basin NSW. Department of Mineral Resources, **GS1996/528**, pp19.
- PRATT W. 1998. Gunnedah Coalfield (South) Regional Geology 1:100 000 - First edition, Geological Survey of New South Wales, Map.
- RAGGATT H.G. 1939. Coal Discovery at Willow Tree. *Department of Mines New South Wales, Annual report*. 107-108.
- ROBERTS J., OFFLER R. & FANNING M. 2006. Carboniferous to Lower Permian stratigraphy of the southern Tamworth Belt, southern New England Orogen, Australia: boundary sequences of the Werrie and Rouchel blocks. *Australian Journal of Earth Sciences* **53(2)**, 249-284.
- STEVENSON D.K. 2003. Stratigraphy, lithology and depositional setting of the Cranky Corner Basin. pp. 15-50 *In: Facer R.A. & Foster C.B. eds. Geology of the Cranky Corner Basin. New South Wales Department of Mineral Resources, Coal and Petroleum Bulletin* **4**, iv + 252.

# EXPLORATION OF COAL DEPOSITS

J Edwards<sup>1</sup>, K Bartlett<sup>2</sup>, P Hatherly<sup>3</sup> and J Lea<sup>4</sup>

<sup>1</sup> Consultant Geologist, Collective Experience

<sup>2</sup> Project Geologist, BHP Billiton

<sup>3</sup> Prof. Geophysics, University Of Sydney

<sup>4</sup> Managing Director, Groundsearch Australia Pty Ltd

## INTRODUCTION

Coal exploration has traditionally involved the acquisition of data to enable a resource to be quantified and qualified to the extent that its economic potential can be determined. This process commonly relied on:

- drilling to determine the depth and thickness of coal seams, broad characterisation of the overburden and interburden, and provide cores for coal quality analyses.
- basic wireline logging to crosscheck the depth and thickness of coal seams and provide some indication of rock mass strength.
- basic surface geophysics and remote sensing to identify major geological structures.

In recent years, the adoption of the JORC Code as a basis for the reporting of resources and reserves has placed a greater emphasis on the need for detailed, reproducible data sets that not only satisfy the traditional requirements of mine planners, but also satisfy the governance requirements of corporate and financial institutions. Similarly, the development of sophisticated numerical modelling techniques for use in both open-cut and underground mine design, has seen a greater demand for precise geotechnical data, in-situ stress characterisation and hydrological information as routine input to the design process.

These requirements, coupled with the prevailing trend toward high capital, relatively inflexible mining techniques less tolerant of geological surprises, and the need for consideration of environmental issues such as groundwater impacts and surface subsidence, requires modern exploration programs to be more multifaceted, and designed to commence capturing data relevant to 'downstream issues' during even the initial phases of exploration planning.

### Objective

The ultimate objective of any exploration program is to strategically and cost-effectively provide the data required to design and/or maintain an economic mining operation. This guideline serves to list and summarise key techniques, and indicate how and when they may be applied during the various phases of coal exploration, to coincide with the assessment and approval stages of a project, so as to provide the essential inputs in a timely manner for the purposes of detailed resource assessment as well as mine related planning.

Resource definition and the likely conversion to reserves can be categorised into several stages and processes. The broad relationship between the project, reporting and approval stages is outlined in Figure 1. In summary, the company process for resource definition and

reserve utilisation (shown in red in Figure 1) must be compatible with the industry-accepted process (shown in orange in Figure 1), to allow compliance with the political process (shown in green in Figure 1). Whilst it is acknowledged that some of these elements do not perfectly align, they offer a reasonable indication of the level of exploration data that should be available at each stage of the project.

### Scope

This guideline considers coal exploration activities relevant to:

- green fields exploration - aimed at defining a virgin resource for the purpose of developing a new mine.
- brown fields exploration - aimed at revising the definition of an existing resource for the purpose of re-developing an existing mine.
- operational exploration - aimed at providing data for geological risk definition and the detailed design of an existing operation.
- underground and open-cut projects.

Whilst the guideline is not intended to be exhaustive, it does attempt to identify the majority of the exploration techniques that are commonly available, as well as some of the issues that may be considered in their implementation. Similarly, the techniques have only been briefly described since detailed descriptions are readily available in the literature.

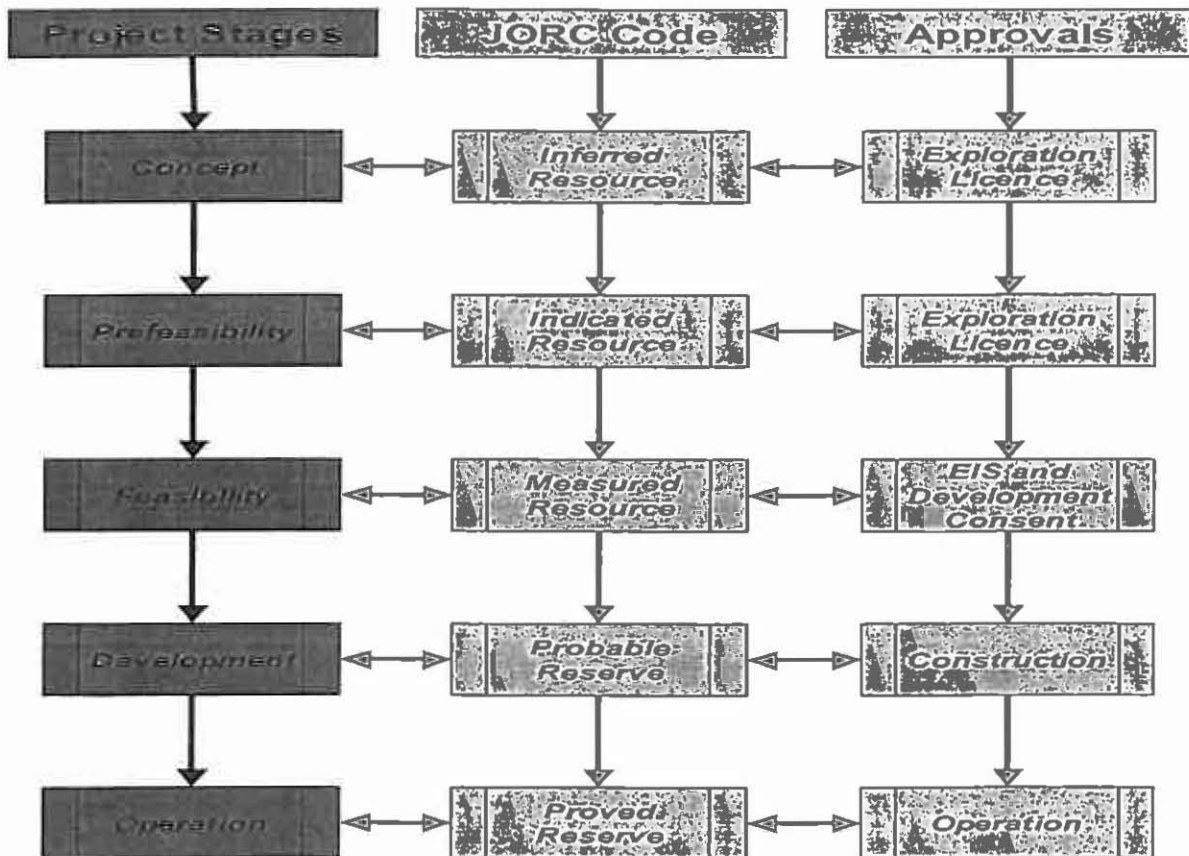


Figure 1. The broad relationship between the stages of exploration, the categories of the JORC Code and the stages of the approval process

### PLANNING

The overall strategy in exploration should begin with identifying a broad understanding of the deposit and then progressively developing a more detailed understanding of the issues that are considered pivotal to its exploitation. It should not simply focus on developing a traditional geological model, as it is also the mechanism by which all of the input data necessary to provide a sound engineering basis for sophisticated mine design techniques are acquired.

The planning phase therefore commences with a synthesis of all available pre-existing data and some conceptual understanding of the project goal. From this it is possible to identify the data that are required to achieve that goal and the techniques that should be employed. Key considerations at this stage of the program should include the:

- suite of data that will ultimately be required from geological, environmental and engineering perspectives
- data acquisition techniques that will best provide those data
- the staged approach by which the data will be acquired .
- database management of inter-related data sets
- modelling techniques that are likely to be employed
- development of baseline data sets for environmental modelling
- community liaison and involvement

Forward thinking at this stage of the program may well avoid considerable expense and hardship further into the project should systems prove to be inadequate or it is identified that an issue has been overlooked or underestimated.

### TECHNIQUES

The choice of exploration techniques to be included in a program will depend largely on the stage of the project. Whilst not all of these techniques will necessarily be deemed relevant to a particular project, those that are must be incorporated into the program at the appropriate stage so as to enable their results to impact on the planning of the subsequent exploration stage.

The techniques outlined below may arguably have relevance across virtually all stages of a project, however an attempt is made here to identify the key stages at which selected techniques may best contribute. Clearly the intention should be to increase the resolution of the data provided by a particular technique as it is applied to each subsequent stage of the project.

Figure 2 serves to indicate at which stages of the project the various techniques should be considered to provide a minimum and meaningful level of coverage.

Techniques	JORC Code	Inferred Resource	Indicated Resource	Measured Resource/ Reserve	Probable Reserve	Proved Reserve
	Approvals	Exploration Licences	Exploration Licences	EIS and Development Consent	Construction	Operation
	<b>Research</b> Literature Searches Maps, Air Photos & Satellite Imagery Geographical Information Systems Field Mapping <b>Geophysics</b> <b>Airborne</b> Magnetometer Radiometric Gravity <b>Surfaces</b> Magnetometer Seismic Reflection Seismic Refraction Micro-seismics Resistivity Gravity RIM Ground probing radar Tomography <b>Borehole</b> Natural gamma Density Sonic Resistivity Neutron Caliper Dip meter/breakout Deviation Acoustic scanner Magnetometer Induction <b>Drilling</b> Site procedures Non-core Slim Core Logging/Photography Coal quality Groundwater Gas Stress Large diameter Size distributions Detailed washability Specialty Surface to in-seam Longhole Rotary Downhole motor (DHM) <b>Community Liaison</b>					

Figure 2 Key techniques and the stages at which they should be incorporated into the exploration program

**Research**

Adequate research will not only provide a compilation of the available pre-existing data, but should also seek to provide a basic framework on which to build and develop future models.

Literature Searches – This is the fundamental starting point from which any exploration program should be developed, and should include:

- database searches
- company records
- departmental reports
- mine record tracings
- open file reports
- conference papers

## EXPLORATION OF COAL DEPOSITS

- journal articles
- university theses
- water bore reports

Whilst only some of these may be available for a particular area they will generally serve as sound background for ongoing activities provided they are reliable and applicable.

**Maps, Air Photos & Satellite Imagery** – These provide a fundamental basis for planning exploration activities. Not only do they provide information regarding access and terrain, detailed air photo and satellite imagery interpretation often identify structural features and trends that may offer significant bearing on the initial exploration strategy. Air photo interpretation, for example, is quick and cheap and its value as an exploration tool is often under-rated. The cyclical nature of satellite imagery and the use of multispectral analysis make it particularly useful for identifying changes in the distribution of Recent sediments and drainage patterns as well as for infrastructure planning.

**Geographical Information Systems (GIS)** – These types of data sets have emerged as being particularly useful as a basis for:

- Topographical modelling of pre and post mining surfaces
- Landownership databases
- Infrastructure planning
- Providing a record of the location of exploration activities
- Preparation of approvals

**Field Mapping** – In conjunction with air photo interpretation, field mapping remains a cheap and valuable basis for initial exploration planning which is often overlooked for the sake of more highly technical methods. The surface expression of geological features and the availability of even limited dip and strike data will significantly enhance any structural interpretation as well as potentially enhance the strategic use of any proposed remote sensing techniques.

### **Geophysics**

By comparison to drilling, geophysical techniques are relatively non-invasive though they tend to be qualitative rather than truly quantitative. The various methods by which they remotely sense properties of the rock mass enable them to identify geological structures and features, which are difficult and expensive to define by drilling. They provide supplementary interpretations that often assist in determining the drilling strategy. Early use of airborne techniques, followed by surface surveys, invariably provides information on intruded and structured zones within an area thereby enabling the drilling program to be modified to define these zones and focus on areas of greater economic potential.

**Airborne** - Airborne geophysical techniques involve the use of low flying fixed wing aircraft or helicopters to measure a variety of geophysical parameters to identify broad scale features for more detailed, ground-based definition. Surveys are recorded in a grid of closely spaced profile lines with occasional tie lines to link these data strings together. Flying heights and line spacings need to be selected according to the survey objectives and logistical considerations. Processed results are usually presented in an image form that allows analysis using image processing and visualisation software. The evolution of highly accurate satellite

location technology in recent years has added a new dimension to the usefulness of airborne data.

- **Magnetometer** - In coal mining applications, aeromagnetic surveys are used to detect the presence of magnetic bodies in the near surface such as igneous intrusions and surface flows; however, the determination of the exact location of intrusives at depth, and their vertical extent, is non-unique.
- **Radiometric** - Radiometric surveys are frequently flown in conjunction with airborne magnetic surveys and record the presence of gamma radiation from radioactive isotopes from potassium, uranium and thorium. The radioactivity at the immediate ground surface has the main influence on these surveys so their use is mainly directed towards mapping different soil types and identifying transported soils from those due to in-situ weathering. The procedure is also very useful for lithological interpretation in areas of outcrop.
- **Gravity** - Precision airborne gravity surveying is a development used in minerals exploration where concentrations of dense economic minerals cause local fluctuations in the earth's gravity field.

**Surface** - Surface geophysical techniques are usually quite detailed and focused on defining a feature that has been indicated by a broader scale technique. Surveys are usually undertaken along profile lines or within a grid, with measurements taken with hand held instruments or suitably equipped all-terrain vehicles.

- **Magnetometer** - Magnetometer surveys across the ground surface allow detailed mapping of the earth's magnetic field. These surveys are useful for detecting igneous dykes and sills providing they have a sufficient magnetic signature. Felsic mineralogy, weathering and alteration may significantly reduce any expected magnetic effect, whilst the extrapolation of surface anomalies to infer dyke properties at depth is still non-unique.
- **Seismic Reflection** - Seismic surveys rely on the refraction and reflection of seismic waves within the earth. Waves can be introduced using explosive charges, falling weights, earth tampers (mini-sosie) or truck mounted vibrating plates (vibrois). The waves are detected using arrays of geophones arranged on either a profile line (2D seismic surveying) or in a grid (3D seismic surveying). In reflection seismic surveying, waves are reflected off subsurface interfaces when there is change in the acoustic impedance (product of seismic velocity and density) between layers. Multiple shots are required to develop a map of the subsurface. Generally these data require intensive computer processing before they can be interpreted, preferably using interactive computer methods. Coal seams are very good reflectors of seismic energy and seismic reflection surveys have an important role in determining coal seam structure. Seismic reflection surveying works best when the depths of interest are greater than about 50 m, and problems may exist in multi-seam environments or when basalts are present on the surface in multiple flows. In both cases, the wave propagation patterns become more difficult to analyse.
- **Seismic Refraction** - Seismic refraction surveys allow the mapping of near surface layers within the weathering profile. Results provide depths to layers, and velocities, which can be related to rock strength. The method requires that the seismic velocities of the layers increase with depth.
- **Micro-seismics** - Micro-seismic monitoring uses the same geophone sensors as other seismic methods but the sources of the seismic energy are the emissions of seismic energy associated with the fracturing of rock caused by stress induced rock failure,

particularly in caving situations. This method mainly finds its use in monitoring mining operations when it is necessary to understand the ground response and predict roof falls, however it can also assist in predicting outburst zones. The locations of microseismic events are determined using standard seismological methods. Failure mechanisms may also be determined by this technique.

- ***Inseam Seismic***- These surveys exploit the wave guiding of seismic energy that occurs on account of the low seismic velocities in coal compared to the surrounding roof and floor strata. Waves are partially trapped in the coal seam and travel within it some hundreds of metres. Reflection will occur when faults, dykes and other discontinuities cut the coal seam. Surveys can be undertaken from underground workings or between boreholes where sources and geophones are placed within boreholes. To ensure that reflection signals return to the geophones, the reflecting targets need to be oriented sub parallel to the line of the geophone array.
- ***Resistivity*** - There is a wide range of geophysical techniques designed to map the variations in the resistivity (inverse of conductivity) within the earth. These techniques are mainly used for mineral exploration where metallic minerals are typically highly conductive in comparison to the host rocks. In coal mining, cindered coal in the vicinity of igneous intrusions may be a conductive target. The resistivity of coal is also typically greater than the host rocks allowing coal seams to be mapped at varying resolutions. Old workings (dry and flooded) in the near surface may also be detected using these methods. Signal is introduced into the ground either in the form of an electric current, or through the generation of an electromagnetic field within a wire loop laid out on the ground surface or around an aircraft (airborne em). Detection is based on measuring the potential difference between electrodes or by the strength of induced fields in suitable electric or magnetic field sensors.
- ***Gravity*** - In a coal-mining context, gravity surveys conducted from the ground surface can be used to map deep bedrock channels and detect old workings when they are within a few tens of metres of the surface. Gravity surveying is relatively slow and all stations need to be accurately located. For the detection of old workings, very accurate measurements and careful reduction is required. Such surveys are normally referred to as microgravity surveys.
- ***RIM (Radio Imaging Method)*** is an electromagnetic counterpart to in-seam seismic surveying. Just as coal seams act as seismic waveguides, they also allow the wave guiding of electromagnetic waves because of their typically elevated resistivities. Electromagnetic waves, typically in the range 20 – 200 KHz range are introduced into the coal seam and detected using magnetic field antennas. Abnormal losses in the electromagnetic energy can be interpreted in terms of likely disruptions to the waveguide – faults, dykes and sills, washouts, changes in fluid saturation etc. Surveys can be undertaken between boreholes and between underground headings.
- ***Ground probing radar*** is an electromagnetic equivalent to seismic reflection surveying. Electromagnetic waves at frequencies over 50 MHz are launched into the ground and reflect off boundaries where there are contrasts in electrical properties. Penetration is generally only a few metres in conductive weathered layers, but by using borehole antennas located below the weathering, ranges of a few tens of metres can be achieved. Applications include the location of old workings and abandoned (metal cased) bores
- ***Tomography*** – This technique allows the mapping of geological features between boreholes or underground workings in a similar way to medical imaging. Multiple source and receiver positions are needed. Tomography can involve seismic waves,

electromagnetic waves (RIM) and direct electrical currents. Ambiguity and artefacts are unfortunate features of geological tomography because surveys are usually conducted with sources and receivers to just two sides of the region of interest. Features parallel to those sides may not be mapped; other features will be mapped with distorted edges.

**Borehole** – Borehole, downhole, or wireline geophysics offers a suite of tools that are run within a completed borehole. When used in conjunction with each other, or calibrated with laboratory results such as rock strength or ash, these techniques are crucial in characterising coal seams, aquifers, and the overall rockmass itself, thereby adding significantly to the program's geological, geotechnical and environmental databases.

- **Natural gamma** - This technique detects naturally occurring gamma rays from K, U & Th to identify rock type boundaries. It is a good coal/sand/shale/clay delineator and hence a very useful correlation tool. The data can be acquired through rods and casing in problem holes and the tool requires no radioactive source.
- **Density** - The in situ apparent bulk densities are calculated from backscattered gamma radiation emitted from a source attached to the tool. The tools are generally calibrated to give data in g/cc units and provide an accurate delineation of rock type boundaries. Data can be used also in conjunction with sonic properties to enable rock strengths to be calculated. However, the method requires a radioactive source and is affected by variations in borehole diameter (washouts).
- **Sonic** - This method uses variations in formation sonic travel times that are then translated into sonic velocities of the wall rock materials. Some tools produce full waveform data and are particularly useful for indicting relative rock strengths, cement bond logs, porosity and fractured zones. The tool requires water in the borehole and is affected washouts.
- **Resistivity** - This method measures the electrical resistance of wall rock materials and it is the inverse of conductivity. It can be used to identify weathered coal, hydrocarbon zones and conductive compounds. It requires water in the borehole and is affected by salinity and washouts.
- **Neutron** - This method bombards wall rock nuclei with neutrons from a source on the tool that then emit various amounts of measurable energy. It is particularly useful in hydrocarbon detection and porosity determinations even through steel casing. It requires a radioactive source and can be affected by PVC casing.
- **Caliper** – This tool uses a single mechanical arm to provide a profile of the borehole wall. It is usually incorporated with a density tool and is crucial for identifying washout zones in the hole, which may otherwise be misinterpreted as lithological changes.
- **Dip meter/breakout** - The tool uses mechanical arms (usually 4 act as XY calipers) to measure the micro resistivity of wall rocks. It is used to calculate the dip angle and dip direction of features such as bedding and possibly borehole breakout. The method requires water in the borehole and relatively good wall conditions.
- **Deviation** – this tool provides information regarding the direction and distance that the hole has deviated from the vertical.
- **Acoustic scanner** - The tool measures the variations in sonic transit times and amplitudes to produce on-screen images of planar features such as bedding, jointing and borehole breakout. The wall rock images are used with software to interpret dip and dip directions of planar features, whilst breakout provides a valuable indicator of in-situ stress direction. Stress magnitude may be estimated from the degree of failure

## EXPLORATION OF COAL DEPOSITS

of units of known strength. The tool requires water in the borehole and relatively good wall conditions.

- **Magnetometer** - The tool measures variations in the bulk magnetic susceptibility of wall rocks. It indicates the occurrence of magnetic material such as some igneous intrusions, siderite and magnetite. The tool is affected by steel casing.
- **Induction** - The tool measures the rock conductivity in boreholes and wells within a zone of 25 to 125 cm from the borehole, but can be compensated for borehole fluid, PVC casing, or grouting materials. The tool can also be used in air filled holes to measure the conductivity response. Resistivity can generally be calculated as the inverse of conductivity. The tool is severely affected by steel rods and casing.

### Drilling

Drilling is by far the most expensive, labour intensive and time consuming component of any exploration program. Consequently it is crucial that a preliminary geological interpretation of the deposit, based on research and geophysical data, is generated prior to finalising drill hole locations. This will serve to identify potential anomalies, low to zero potential areas and prime target areas where detailed exploration can be focused.

The minimum requirements for reporting under the JORC Code are outlined in the Australian Guidelines for Estimating and Reporting of Inventory Coal, Coal Resources and Coal Reserves. Whilst that guideline deals with the spatial distribution of drill holes this section considers the practical aspects of the drilling program itself.

**Initial considerations** - At the outset of the program consideration should be given to:

- **Staged Exploration** - Initial drilling on a broad spacing followed by infill drilling enables the geological interpretation to be progressively refined. The choice of fully and/or partially cored and/or non-cored holes can also be incorporated into the staging strategy to achieve the most cost effective result. The initial stage should utilise fully cored holes to accurately characterise the geological and geotechnical attributes of the rock sequence by establishing a correlation between physical samples and borehole geophysics. These relationships can then be used to enable the progressive reduction of the amount of coring in later stages of the program.
- **Pattern and Spacing** - Accepted practice is usually an orthogonal grid. Different spacings are required for the various stages of resource definition, both underground and open cut, as outlined in the Guideline referred to above.
- **Borehole Naming Conventions** - Historically, boreholes have often been named sequentially. With the increasing dependence on computer-based interpretation, there is a greater tendency toward the use of a grid-based nomenclature.
- **Seam/Ply Naming Conventions** - The use of a flexible system to allow additions/alterations to correlatable units at a later stage is strongly recommended to cater for modifications that may emerge as the program progresses.

**Site procedures** - In this day and age it is crucial that the complete range of Health, Safety, Environmental and Community (HSEC) issues be addressed when planning any exploration activity. A number of these requirements are specifically included in the Exploration Licence conditions. Key issues which may require the development and implementation of detailed site procedures include:

- **Access agreements** - The use of a standard access agreement such as the "Rural Land Access Agreement for Mineral Exploration" developed by NSW Minerals Council in conjunction with the NSW Farmers Association is strongly recommended. Such

agreements include details of compensation that will be paid for various exploration activities that may be undertaken.

- **Site management plans** – The plans should address the following issues:
  - Leasehold and land access conditions
  - Special requirements from landholders
  - Hours of operation
  - Livestock control measures
  - Environmental considerations which should also be extended to neighbouring properties
  - Containment/control measures for environmental mishaps
  - Containment/control measures comply with government regulations
  - Noise control including equipment soundproofing
  - Dust control from vehicle movements and RC/PCD drilling
  - Wet weather access
  - Waste disposal
  - Water – use of onsite water or water trucks
  - Photography before, during, after and six months after leaving site
  - OH&S issues - contractors comply with regulations, safety fencing, sanitation requirements, supply of material safety data sheets and preparation of safe operating procedures.
  - Rehabilitation of both the drill site and access tracks
  - Borehole sealing and grouting

**Non-core drilling** - This is the quickest and cheapest form of drilling, using either air or water circulation in conjunction with hammer, blade or roller bits. This technique is normally applied to:

- **“Wildcat”** exploration to simply determine the presence of coal in an area.
- **Pre-collaring** – This can be undertaken through non-coal bearing sequences to reduce costs during later stages of the exploration program. These sections of a partially cored hole should also be geophysically logged for comparison to neighbouring fully cored holes.
- **LOX line** – to identify the limit of oxidation/sub-crop in open cut deposits.
- **In-fill and hazard detection drilling** – where geophysically logged, non-cored holes are drilled within an area of cored holes to confirm seam continuity or to locate faults or intrusions.

**Core drilling** - The accepted standard in coal exploration to provide intact physical samples of both coal and non-coal sequences, for geological, geotechnical and analytical purposes is HQ (or Slimline). There is an increasing recognition for process-orientated information, which is best achieved from large diameter core samples.

- **Slimline (HQ or similar)** – The following data sets can be generated from a HQ drilling program:
  - Lithological data - A strict logging standard needs to be adhered to to ensure repeatability of standard descriptors and rock types from different loggers. Particular attention needs to be paid to an efficient and safe core storage and handling facility.
  - Core Photography –This allows information from different holes to be compared quickly and requires standardised camera settings and position.

## EXPLORATION OF COAL DEPOSITS

- Geotechnical data – This can be derived from direct observations, laboratory testing and wireline logs. It should include fracture logging, RQD, physical specimen testing (ISRM Standard – Uniaxial, Triaxial, Shear)
- Coal quality - The range of analyses to be performed should be determined in line with the expected coal type (thermal or metallurgical). Whilst some should be undertaken on a ply-by-ply basis, some cost savings can be achieved by restricting others to composite samples. Slimline testing should also include basic washability analyses, though this should be supplemented by large diameter core testing.
- Groundwater – This should be undertaken to characterise the hydrological regime of the deposit. Results from the following techniques can be used to calibrate wireline log interpretations:
  - core testing to determine strata porosity and permeability
  - Packer testing for downhole/in situ porosity and permeability determinations
  - Piezometer monitoring for water quality and standing water levels
  - Pump testing for determination of water flow characteristics.
- Gas – Desorption testing of coal seams and other strategic units provides essential data regarding gas types and quantities for mine ventilation design.
- Stress – Detailed quantification of the in situ stress field is an important input for effective mine design. This has traditionally been determined through the use of hydrofracturing, however the cost of such determination generally restricted its use to one or two site tests per project. The routine use of downhole acoustic scanners run in conjunction with the standard suite of geophysical tools, however, provides an extensive coverage of stress determinations, both vertically and horizontally throughout the deposit. Overcoring techniques may also be employed to measure stress magnitude and direction.
- **Large diameter** – Potential working sections can be determined from the results of slim core analyses. However, to enable truly representative size distributions and washability analyses to be undertaken for detailed wash plant design, larger diameter cores are required. Ideally these should be 200mm, though in the case of deep deposits, closely spaced 100mm cores may suffice provided a representative size distribution is assured.
- **Downhole Water Jet drilling** – This technique has been applied satisfactorily to generate bulk samples from drill holes though great caution and control is required to ensure that the sample is representative of the desired seam section. In open cut projects, a trial box cut is the best means of obtaining a representative bulk sample.

**Specialty Drilling** - A variety of specialised drilling techniques have been developed to address particular mining related issues and are mainly used for the identification of mining hazards:

- **Surface to in-seam** – This usually takes the form of medium radius drilling (MRD) and is primarily used for gas drainage
- **Longhole** - This is an underground technique used for gas drainage and/or hazard identification.
- **Rotary drilling** is limited to relatively short holes due to poor directional control
- **Downhole motor (DHM) drilling** has the capability of drilling in excess of 1 km and offers much better directional and survey control.

**DATABASE MANAGEMENT**

It is essential that every piece of data that is collected is incorporated into a database, and standardised formats should be determined for the supply of data from external sources. Databases (Figure 3) need to have the facility to export selected data in standard formats, eg comma separated data, to enable the data to be transferred to other packages for modelling and statistical analysis.

Techniques	Databases							
	GIS	Geological	Geotechnical	Quality	Gas	Groundwater	Environment	Community
<b>Research</b>								
Literature Searches	■	■	■	■	■	■	■	■
Maps, Air Photos & Satellite Imagery	■	■	■	■	■	■	■	■
Geographical Information Systems	■	■	■	■	■	■	■	■
Field Mapping	■	■	■	■	■	■	■	■
<b>Geophysics</b>								
<b>Airborne</b>								
Magnetometer	■	■	■	■	■	■	■	■
Radiometric	■	■	■	■	■	■	■	■
Gravity	■	■	■	■	■	■	■	■
<b>Surface</b>								
Magnetometer	■	■	■	■	■	■	■	■
Seismic Reflection	■	■	■	■	■	■	■	■
Seismic Refraction	■	■	■	■	■	■	■	■
Micro-seismics	■	■	■	■	■	■	■	■
Resistivity	■	■	■	■	■	■	■	■
Gravity	■	■	■	■	■	■	■	■
RIM	■	■	■	■	■	■	■	■
Ground probing radar	■	■	■	■	■	■	■	■
Tomography	■	■	■	■	■	■	■	■
<b>Borehole</b>								
Natural gamma	■	■	■	■	■	■	■	■
Density	■	■	■	■	■	■	■	■
Sonic	■	■	■	■	■	■	■	■
Resistivity	■	■	■	■	■	■	■	■
Neutron	■	■	■	■	■	■	■	■
Caliper	■	■	■	■	■	■	■	■
Dip meter/breakout	■	■	■	■	■	■	■	■
Deviation	■	■	■	■	■	■	■	■
Acoustic scanner	■	■	■	■	■	■	■	■
Magnetometer	■	■	■	■	■	■	■	■
Induction	■	■	■	■	■	■	■	■
<b>Drilling</b>								
<b>Site procedures</b>								
Non-core	■	■	■	■	■	■	■	■
Slam Core	■	■	■	■	■	■	■	■
<b>Logging/Photography</b>								
Coal quality	■	■	■	■	■	■	■	■
Groundwater	■	■	■	■	■	■	■	■
Gas	■	■	■	■	■	■	■	■
Stress	■	■	■	■	■	■	■	■
<b>Large diameter (200mm)</b>								
Size distributions	■	■	■	■	■	■	■	■
Detailed washability	■	■	■	■	■	■	■	■
<b>Specialty</b>								
Surface to in-seam	■	■	■	■	■	■	■	■
Longhole	■	■	■	■	■	■	■	■
Rotary	■	■	■	■	■	■	■	■
Downhole motor (DHM)	■	■	■	■	■	■	■	■
<b>Community Liaison</b>								

**Figure 3.** Key databases and the techniques that support them

Collected data should be gathered, validated and input once only. That is to say, if the data are to be used in multiple applications it should be transferred electronically between packages using standardised, documented procedures. This will overcome the risk of transcription errors and the potential for inconsistencies between datasets.

Where possible individual master databases should be developed for each data type. Databases can then be integrated by use of project standard reference fields and nomenclature, eg bore names, survey grids, height datum, seam names. This will facilitate the seamless integration of lithological, geotechnical, geophysical and coal quality databases for the purposes of modelling and mine design.

This process should also be applied to the collation and use of geographical and environmental data for ultimate use in the preparation of an EIS.

### MODELLING

The traditional concept of a model for a deposit was a series of plans, sections, tables and supporting documentation that could be presented in hard copy. Today a model begins with the development of a strategy/philosophy to combine numerous sets of data from a myriad of sources and disciplines. These include borehole data, geophysical data, geotechnical data, design data, environmental data and financial data. It should be stressed that none of these parameters can be effectively modelled in isolation. While some of these data sets will be site specific some may be generic, such as equipment production rates and cost estimates. The model then becomes the instrument by which these data sets are integrated and interrogated to produce a range of outcomes for various mining options.

**Geological** - The geological model is a series of files containing three-dimensional data of numerous parameters relating to the stratigraphy, structure and quality of the deposit. The modelling software is able to graphically display and interrogate this information to produce traditional plans, sections and resource estimates. It can also generate derived information to be passed to other software and specialists for further assessment.

The complex and sophisticated modelling tools that are available today require an ordered geographic distribution of adequate, valid data. The processes used to model a deposit need to be applied by an experienced user who has detailed knowledge of the capability and limitations of the package, guided by the geologist who has the detailed knowledge of the deposit in question. Modelling packages generally contain a variety of facilities, which can be used to help control the geological model so that it most accurately reflects the known geological characteristics of the deposit. The final modelling process may eventually combine a number of steps.

As new models are generated an extensive validation process should be invoked. Contour plans of as many and as varied parameters and intervals as possible should be generated and inspected (on screen may be sufficient without producing hard copy) to ensure that unrealistic "bull's eyes" have not been introduced by dramatic trends in data. Some of these anomalies may need to be controlled by extent lines that are manually input by the geologist with the best knowledge of the deposit. Anomalies may also reflect miscorrelations, which need to be corrected in the raw data, whilst real anomalies should become the targets for follow-up exploration. New models should not be released for use by other disciplines until they have been thoroughly checked and signed off. Access controls to the data and authorisation to edit/modify geological models needs to be carefully controlled and documented in line with the appointment of a designated Competent Person for reporting purposes (see JORC Code). This is the fundamental basis of the repeatability that is required to satisfy the requirements of the JORC Code.

**Geophysical** - Throughout the course of an exploration program, a number of different geophysical techniques are likely to be used. Normal practice would be to incorporate and reprocess any pre-existing data with newly acquired results to produce the best possible interpretation by taking advantage of the most current processing techniques. It is the final interpretations of this modelling that should then be incorporated into the geological model.

**Geotechnical** - Rock property data generated from laboratory testing of core is point data. The statistical linkage of these data to various wireline data sets enables 'continuous data' to be interpreted throughout the entire rock mass. This is particularly useful for incorporation

into numerical modelling techniques that are commonly available for various aspects of mine design, such as subsidence predictions, stability analyses and support or slope designs.

**Environmental** - Environmental models provide a strategic assessment of the planning and environmental issues associated with the project. They should build on historical data and baseline studies to address statutory requirements and provide preliminary environmental assessment of impacts and environmental management. In the case of hydrological assessments, wireline logs, core test results and piezometric data are incorporated into the modelling process.

**Process and Design** - Very sophisticated tools exist for this stage of planning and that sophistication should be considered during the entire program to ensure that the appropriate level of data is being generated to meet their requirements. Typical models that are readily available include:

- Numerical modelling for roadway and layout design, subsidence prediction and slope stability
- Coal handling and transport simulations
- Coal preparation plant design

**Financial** - Once a conceptual mine plan and production schedule have been produced, detailed financial modelling should be undertaken to identify and analyse the various capital options. Confidence in the financial model will progressively increase in line with the precision of the resource definition, particularly as it moves from a resource to a reserve with the advent of a mine plan.

## COMMUNITY

The local community is now recognised as an important participant of any project. Many Exploration Licences include in their conditions the requirement to establish a Community Liaison Committee very early in the life of the project. It should be remembered that the reputation generated during initial exploration has the potential to taint, either favourably or unfavourably, the project for the rest of its duration. Open and honest communication and consultation is essential. No issue can be seen as unimportant and should be addressed immediately.

A contact database should be established at the outset of the program to record names, addresses, points of concern (positive and negative), and follow-up actions. This will prove extremely valuable during the life of the project and an essential piece of information at any public enquiry to demonstrate how the project involves the local community in the evaluation process.

## GENERAL COMMENTS

Exploration is no longer the simple acquisition of geological data. It is an integrated process by which the input to all of the elements of a project are gathered and analysed. By adopting some simple philosophies and considerations at the outset it is often possible to improve efficiency and avoid false economics. These may include:

- Remain focused on the objective: to provide sufficient data, of an appropriate quality at the appropriate time
- Aim to mitigate the risk of surprises and adverse performance of the business

## EXPLORATION OF COAL DEPOSITS

- Maximise the data from each hole to avoid the need for additional drilling at later stages
- Minimise the number of contractors and build good working relationships
- Select contractors on capability and performance rather than price
- Treat contractors and other project participants professionally
- Data are not necessarily absolute and are likely to require reassessment and reinterpretation at various stages during the project.
- Ensure that all data and reports are properly archived. Digital data in particular should be backed up onto current computer media as technology changes.
- A mine may be in operation for many years so the relevance of data collected now may not become obvious until some time into the future as mine geology takes over from exploration geology.

### ACKNOWLEDGEMENTS

The authors, acting as a committee of the Coalfield Geology Council of NSW, originally prepared this article to assist the AusIMM in their latest revision of Monograph 12. The authors wish to thank the Coalfield Geology Council of NSW for their collective contribution to this article, and their kind permission for it to be presented at this symposium.



# VARIABILITY IN COAL SEAM GAS CONTENTS THAT IMPACTS ON FUGITIVE GAS EMISSIONS ESTIMATIONS FOR AUSTRALIAN BLACK COALS

Joan Esterle<sup>1</sup> Ray Williams<sup>2</sup> Renate Sliwa<sup>1</sup> Meredith Malone<sup>2</sup>

<sup>1</sup> CSIRO Exploration and Mining  
<sup>2</sup> GeoGAS Pty Ltd

## ABSTRACT

This study was prompted by a need to understand the factors influencing estimates of fugitive greenhouse gas emissions generated from black coal as a by-product during the mining process. Although they comprise some 3% of Australia's net greenhouse gas emissions, they will be increasingly significant with the increase in coal production. Fugitive gas emissions from coal mining and handling are generally estimated by the amount of gas released per tonne of coal mined and handled, less any abatement through gas capture and utilisation. Ideally, each mine monitors, measures and reports their annual emissions that are then tallied at a coalfield, state or basin scale. Where country or basin specific emissions factors are known, this factor can be applied, else a global average is used as a default.

Although gas emissions behaviour is due to an interplay of factors, virgin coal seam gas content is used as a proxy to demonstrate the inherent variability that will impact upon default estimations of fugitive greenhouse gas emissions from black coals. A database of some 2000 boreholes with confidential measurements of gas reservoir parameters of various seams from mines across the Hunter Valley and Central Bowen Basin coalfield were compiled and analysed. These coalfields were chosen as they are known to be different in coal rank, grade and gas reservoir behaviour.

Previous studies demonstrate that gas sorption capacity follows measurable coal properties such as rank and type for differing pressures and temperatures. Actual gas contents do not always match theoretical capacity and all reservoir properties, in particular gas content, vary greatly at the mine scale. This *in situ* variability at the mine scale, coupled with varying approaches to mine gas management makes it almost impossible to develop emissions factors for coalfield or basin scales with a reasonable level of certainty, much more be extrapolated to state and country scales.

As has been suggested by various guidelines for the estimation of fugitive greenhouse gas emissions, the most reliable estimations are made at the mine scale from measurement and monitoring. Mine scale estimations can be improved by taking a domain approach, where depth and pressure relationships are relatively stable and within which the variability of reservoir parameters is reduced to some degree.

## INTRODUCTION

This study was prompted by a need to understand the factors influencing estimates of fugitive gas emissions<sup>1</sup> generated from black coal as a by-product of the mining process. Fugitive emissions from fossil fuels were reported to represent 5.5% of Australia's net greenhouse gas emissions, of which the mining and handling of black coal accounted for 58% (National Greenhouse Gas Inventory NGGI 2002; Australian Greenhouse Office AGO 2005). Guidelines for fugitive emissions estimations from coal mining and handling can be found in the document "Australian Methodology for the Estimation of Greenhouse Gas Emissions and Sinks 2003", published by the Australian Greenhouse Office, Department of the Environment and Heritage<sup>2</sup>.

Fugitive gas emissions from coal mining and handling are generally estimated by the amount of gas released per tonne of coal mined and handled, less any abatement through gas capture and utilisation.

$$\begin{aligned} \text{Total Emissions} = & \text{Emissions from Underground Mines} \\ & + \text{Emissions from Surface Mines} \\ & + \text{Post-Mining Emissions} \\ & - \text{Emissions Avoided Due to Gas Recovery}^3 \end{aligned}$$

Ideally, each mine monitors, measures and reports their annual emissions which are then tallied at a coalfield, state or basin scale (termed the Tier 3 approach). For underground mines, gas emissions can be measured from ventilation and degasification systems. Where mine-specific emissions data aren't available, emissions are estimated based on *in situ* gas contents or a generalised class of gassiness. For surface or open cut mines and post-mining activities, the methodology for estimating gas emissions consists of multiplying coal production by basin-specific emissions factors. Where country or basin specific emissions factors are known, the approach is termed Tier 2. Many of these methods were derived by a series of studies conducted in different countries in the early 1990's (IPCC 1997; for Australia Williams *et al.* 1993). Where they are unknown, a global averaging or Tier 1 method can be used with default emissions factors proposed by the IPCC based on these different studies (Irving *et al.* 2004). In summary, the Tier approach is as follows:

Tier 1	Global averaging
Tier 2	Basin or country-scale estimate
Tier 3	Coalfield, basin, state from mine scale

The range of emissions factors derived for different countries is discussed in Saghafi *et al.* (2005) and in the Guidelines for National Greenhouse Gas Inventories (IPCC 2004). These factors will vary as more data become available, so it is best to use the most recent of reports

---

<sup>1</sup> Fugitive coal seam gas, commonly methane, which is liberated from geological 'enclosure' as a function of mining activity, is seen to be a fugitive greenhouse emission, if not captured and combusted in the form of waste coal mine gas ([http://www.greenhousegas.nsw.gov.au/acp/generation\\_faqs.asp#coal](http://www.greenhousegas.nsw.gov.au/acp/generation_faqs.asp#coal)).

<sup>2</sup> The Australian document and updated workbooks can be downloaded from <http://www.greenhouse.gov.au/inventory>; guidelines can also be obtained from the Intergovernmental Panel on Climate Change *Guidelines for National Greenhouse Gas Inventories* are at <http://www.ipcc-nggip.iges.or.jp>.

<sup>3</sup> A review of mine methane mitigation and utilisation strategies can be found in Shi *et al.* 2005.

## VARIABILITY IN COAL SEAM GAS

and visit the website for updates (AGO 2005)<sup>4</sup>. For Australia, Tier 2 emissions factors do not differ between Queensland and New South Wales for gassy underground mines, but do for open cut black coal mining (Table 1; AGO 2005).

**Table 1** Tier 2/3 fugitive emission factors for the production of raw coal as carbon dioxide, methane and carbon dioxide equivalence (source NGGI 2005 cited in AGO 2005)

	CO <sub>2</sub>	CH <sub>4</sub>	CO <sub>2</sub> -e
COAL	m <sup>3</sup> /t raw coal	m <sup>3</sup> /t raw coal	m <sup>3</sup> /t raw coal
Gassy underground mines NSW	NA	25.43	534.06
Gassy underground mines QLD	NA	25.76	540.86
Less gassy underground mines	NA	0.80	16.70
Open cut mines NSW	NA	3.21	67.24
Open cut mines Queensland	NA	1.20	25.27
Open cut mines Tasmania	NA	1.00	20.98

The main sources of uncertainty in the Tier 1 and 2 estimates, and projections from them, include the level of coal production and, more so, the emissions intensity of that production (AGO 2003). For underground coal mines there is sufficient data from exploration drilling to examine this variability and model potential emissions factors as a function of the mining process. Models can be validated by auditing gas emissions during pre-mining drainage programs and in the ventilation streams during mining. For open cut mines gas contents are rarely measured as gas contents are commonly too low for safety concerns at these shallow depths. However, due to the need to quantify greenhouse gas emissions and the significant number of open cut coal mines in Australia, work is underway to develop more direct Tier 3 methods of measuring and monitoring gas emissions from open cut mines (Saghafi *et al.* 2003; 2005).

Levels of production from coal mines with high intrinsic emission intensities have a dominating effect on the total level of fugitive emissions; the higher the total demand for coal production from emissions intensive mines the higher will be the emissions without abatement strategies. What is not well documented is the variability in the emission intensity of different coals and the underlying factors that control it. The objective of this study was to examine the variability of *in situ* or virgin coal seam reservoir properties in Australian black coal that may impact upon future emissions intensity calculations in the absence of mine-site specific reporting. Only the gas content and permeability data are presented here.

### DATA AND METHODS

The approach of this study was to determine relationships between *in situ* coal seam reservoir properties (gas content, composition, and sorption capacity and, where available, permeability, coal seam character and geological parameters) for Australian coals through compiling and analysing available company data in different geological/gas domains in Queensland and New South Wales. The two chosen coalfields were the Central Bowen Basin

<sup>4</sup> <http://www.greenhouse.gov.au/workbook/pubs/workbook-2005.pdf>

and Hunter Valley, as these two fields have known differences in coal seam rank and gas reservoir behaviour, and contain abundant gas measurement data from coal exploration drilling data (Williams *et al.* 2002; Esterle *et al.* 2002). Coals in the Hunter Valley are commonly high volatile bituminous A<sup>5</sup> in rank whereas those in the Central Bowen Basin range from high to low volatile bituminous<sup>6</sup>.

Gas content data for different seams were available for some 1300 boreholes across sixteen mines and deposits in the Central Bowen Basin, and for some 1000 boreholes across six mines in the Hunter Valley drilled over the past 5 to 10 years. All gas contents are reported in cubic metres per ton (m<sup>3</sup>/t) and normalised to 15% ash at 20°C and 101.3 kPaa (Qm15), unless otherwise stated.

## RESULTS AND DISCUSSION

Figure 1 shows the variability in coal seam gas content as a function of depth for samples available to this study. For a coal of given rank, gas content commonly increases with depth of cover but variability can be very high at the scale of a basin, a mine site or even a single borehole. Gas content should increase with depth because the gas adsorption capacity of a given rank of coal will increase with increasing pore pressure (assuming that temperature variation is minor). In early fugitive gas emission studies in the United States, it was hoped that variation in rank between basins could be used as a guideline for estimating gas contents (Masemore *et al.* 1996). Given the difference in coal rank ranges between the Hunter Valley and the Central Bowen Basin samples, one would expect better discrimination between the two basins, but the scatter is too great.

Although volumes of gas, in particular CH<sub>4</sub> and CO<sub>2</sub>, are produced during coalification, only a fraction is retained in the coal. Gas retention in the coal is dependent upon a complex interplay of factors (Levine 1993) controlling the gas holding capacity of the coal, its permeability, the sealing nature of the overlying rocks, and the pressure of the rocks and fluids in the overburden. Areas or domains where gas content appears to be “abnormally” low or high for a given depth are indicative of geological (and hydrological) irregularities at some point in the geological history of that seam (Scott 2002). For example, the extremely low gas contents (<2%) across depths down to 500 m in the Hunter Valley data (Figure 1) reflect the gas loss across all seams approaching the Mt Arthur monocline (from Williams in Esterle *et al.* 2006).

---

<sup>5</sup> random vitrinite reflectance R<sub>vo</sub> ~ 0.75%; volatile matter, dry ash free basis V<sub>mdaf</sub> ~ 39%

<sup>6</sup> R<sub>vo</sub>=1.9%, V<sub>mdaf</sub>=14% random vitrinite reflectance R<sub>vo</sub> ~ 0.9% to 1.92%; volatile matter, dry ash free basis V<sub>mdaf</sub> ~ 31 to 14%

## VARIABILITY IN COAL SEAM GAS

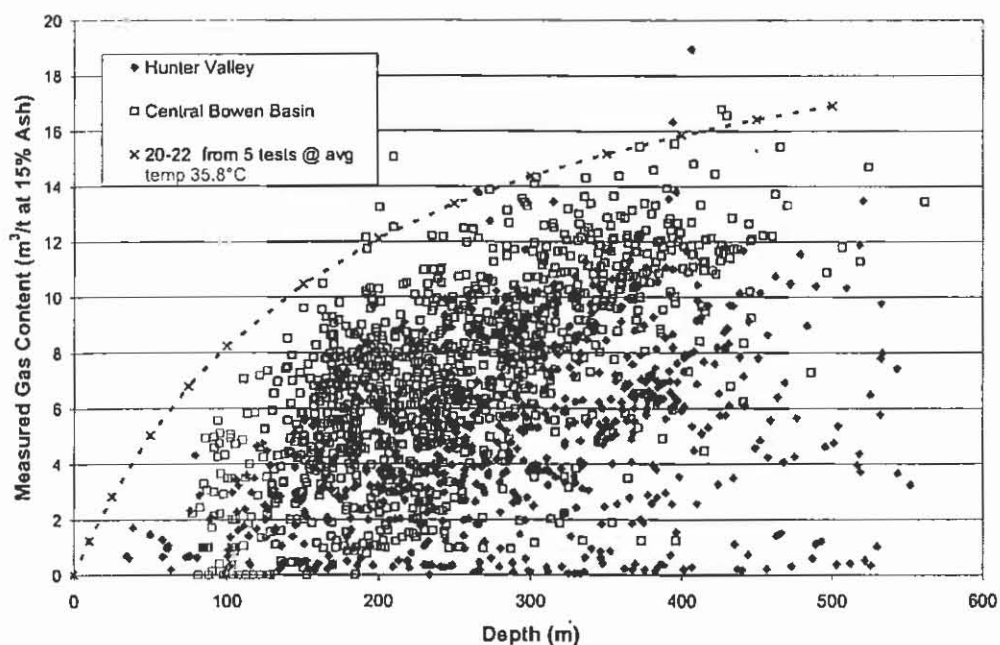


**Figure 1** Variation of coal seam gas content against depth for Bowen Basin and Hunter Valley sample sets, overlain by a methane gas isotherm at the boundary of medium and low volatile rank coal (volatile matter =20- 22% dry ash free)

The change in gas content with depth or cover can be used to identify domains in which the gas gradient is relatively uniform (**Figure 2**). In such domains, the gas content is normally predictable to within  $\pm 0.7 \text{ m}^3/\text{t}$ , according to depth and ash yield, and it is mappable as defined areas on a plan (Williams and Yurakov 2003). Domain boundaries can be related to geological features, usually faults or changes in the geometry and character of the seam (Esterle *et al.* 2000). The gas domain approach was examined as a method for improving the allocation of gas emission intensity for a given basin or area.

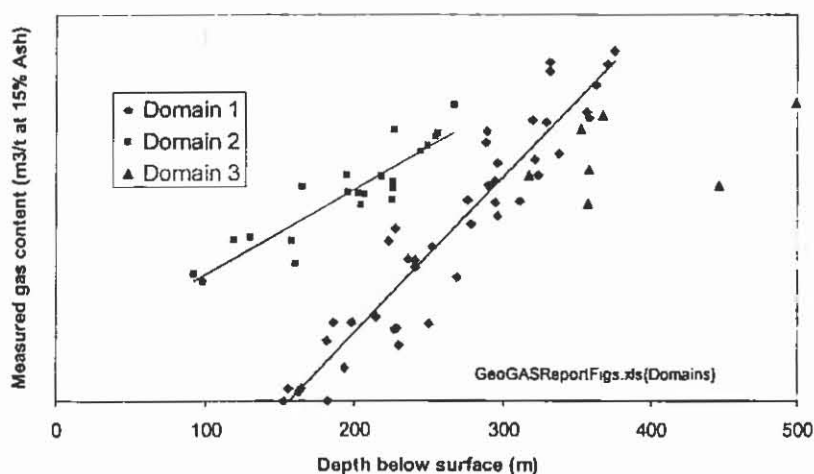


**Figure 2** Example of Gas Content Depth Gradients Grouped As Domains

The Bowen Basin and Hunter Valley coals exhibit a wide range of gas contents as indicated by the depth/gas content gradient trend lines from gas domains across the different minesites (**Figure 3**). In the Bowen Basin, some relatively high gas contents occur at shallow depths

(e.g. 6-8 m<sup>3</sup>/t at 100 m depth). In other cases, depths of up to 190 m need to be reached before there is any measurable gas content in the coal. The single trend line of reducing gas content with depth is supported by extensive data, and occurs over a wide area in the Bowen Basin. This aberrant loss of saturation with depth occurs in an area of complex coal seam splitting and subsequent faulting.

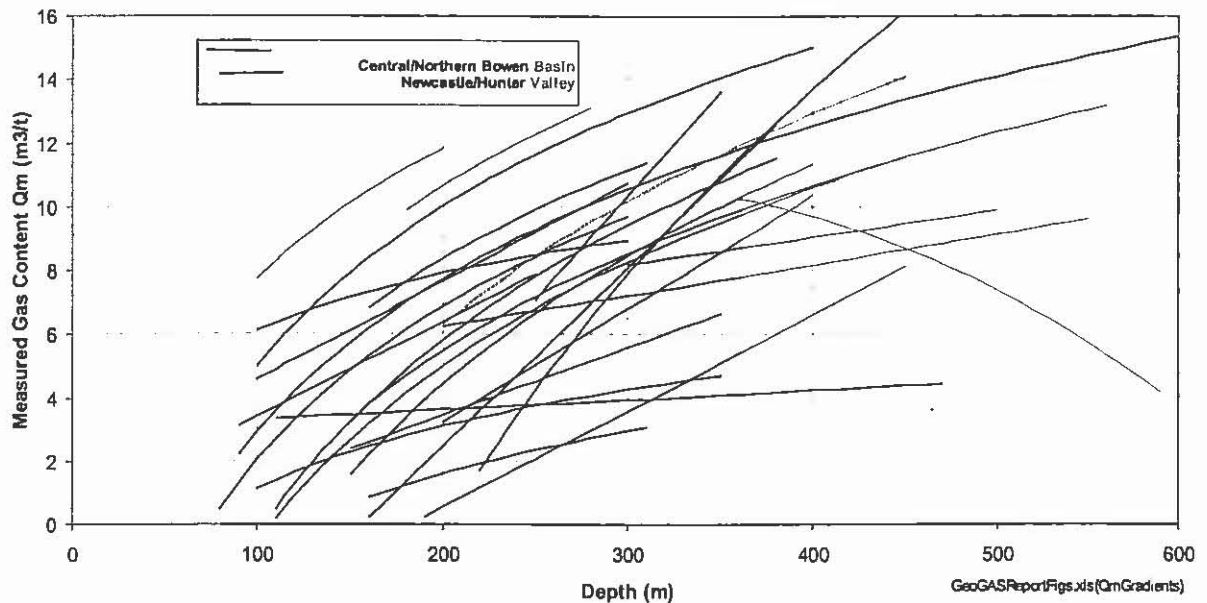


**Figure 3** Gas Content Gradients from Gas Domains in Coals from Hunter Valley and Bowen Basin

Gas content data for both basins are sparse at the shallow depth range of 0-120 m, which would represent the limit of open cut mining with current practice, but can be extrapolated to vary from <1 to 8 m<sup>3</sup>/t (Figure 3). This variability demonstrates the difficulty in applying an average factor at a coalfield or basin scale. Gas content increases in the deeper ranges but at different rates in each of the mines, which is also reflected in the gas gradient plots. Variability in the 220-281 m depth range, where sample numbers are generally good for each mine, is also high ranging from <2 to 11 m<sup>3</sup>/t for the Bowen Basin mines and 3 to 9 m<sup>3</sup>/t for the Hunter Valley mines. Considering the tight rank range for the Hunter Valley coals, R<sub>vo</sub> ~ 0.78-0.8%, versus those in the Bowen coal samples, R<sub>vo</sub> ~ 0.9 to 1.92%, the range in gas contents is quite wide.

Gas content gradients are highly variable between mine sites for both basins, ranging from 0.5 m<sup>3</sup>/t to 4.7 m<sup>3</sup>/t per 100 m depth of cover. The number of mine sites in the Hunter Valley data set are too few to derive a frequency distribution, but the spread of gradients is narrower and with lower values than the Bowen Basin data set. Again, standard deviations are high, making it difficult to state differences between the mines.

Gas content gradients were averaged for the different coal-bearing stratigraphic units in the two basins (Figure 4). Younger coals don't necessarily mean shallower coals in this analysis, as each unit traverses the depth range of shallow to deep. Variability in gradients between units is greater in the lower rank Hunter Valley coals, but on average, lower than the higher rank Bowen coals. The Fort Cooper Coal Measure has a surprisingly high gas gradient, but

the sample is small (only 3). Coal in these measures is not currently mined due to its quality, but it is exposed in some open pits.

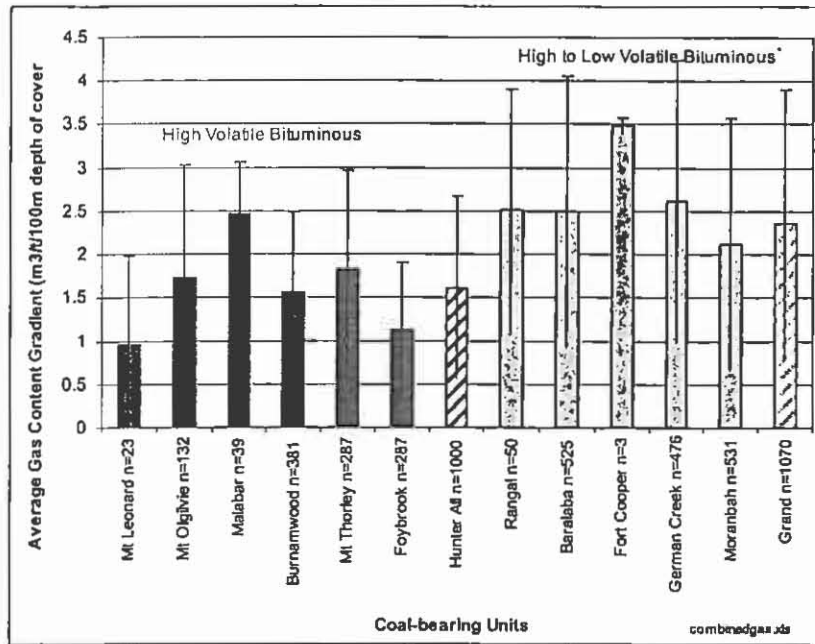


Figure 4 Average gas content gradients for coal-bearing stratigraphic units in the Hunter Valley (red) and Bowen Basin (blue). Units are ordered older to the right. Error bars show standard deviations.

Data were not available to examine the detailed relationship between gas content gradients and coal rank and type for all samples from each of the basins. Therefore samples were assigned an average rank (by vitrinite reflectance) to investigate relationships (Figure 5). Again, the variability in gas content gradients for the Hunter Valley samples is high, given the narrow range in rank. The Bowen Basin samples show more of an increase in gradient with increasing rank. Enough samples with maceral composition data were available in the medium volatile coals from the Bowen Basin to suggest that gradients may also increase with increasing vitrinite content, albeit with high standard deviations (Figure 6).

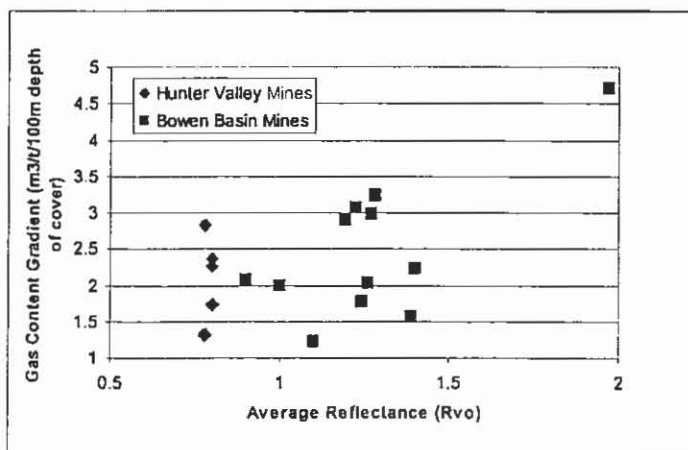
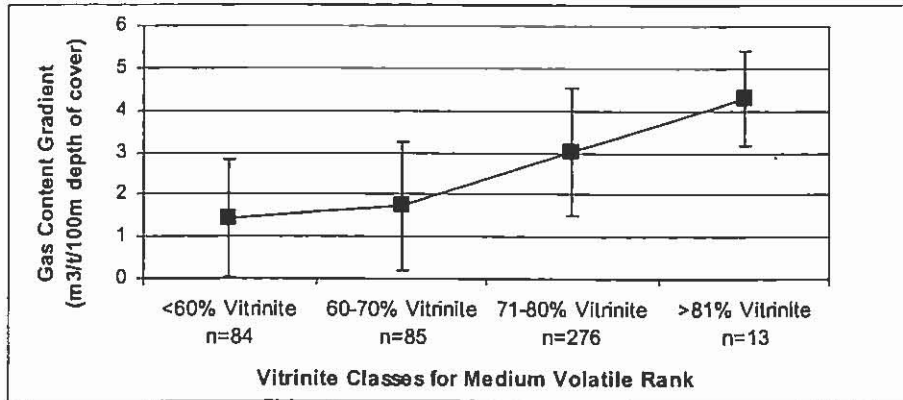
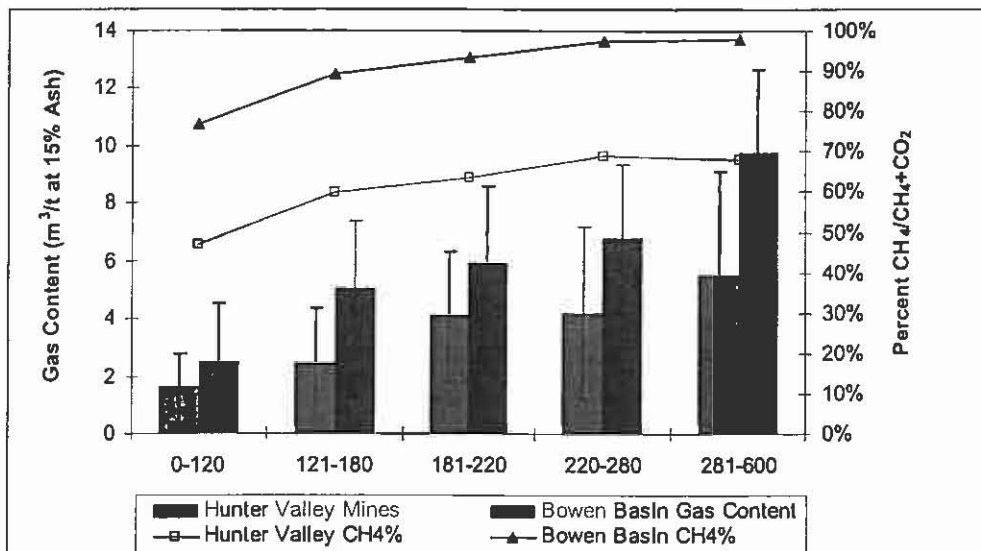


Figure 5 Gas content gradient for coals of varying ranks



**Figure 6** Gas content gradient for coals of varying vitrinite contents for Bowen Basin data set, medium volatile bituminous rank.

Data can be summarised for Bowen Basin and Hunter Valley mine sites using a depth range approach (**Figure 7**) and some gross generalisations made. In the shallow depth range 0-120 m the average gas contents are low and standard deviation too high to discriminate between the areas with any certainty. Again, this reduces the reliability of a Tier 2 and Tier 1 approach to estimating emissions intensity, even using the domain approach. At greater depths the average gas contents are higher in the Bowen Basin, and this probably reflects the increased rank (gas sorption capacity) plus higher gas saturation.



**Figure 7** Gas content and composition averages for depth ranges in the Bowen Basin and Hunter Valley mines. Standard deviations overlain on gas contents.

The domain approach may be a better method for deriving Tier 2 estimations of emissions as it takes into account the strong, albeit variable, depth control on gas contents.

### CONCLUSIONS

Based on the data analysed in this study, the gas content variability is so high that existing emission factors are unreliable even at a regional level and should not be used as estimates from individual mines. As has been suggested by various guidelines for the estimation of fugitive greenhouse gas emissions, the most reliable estimations are made at the mine scale

from measurement and monitoring. Mine scale estimations can be improved by taking a domain approach, where depth and pressure relationships are relatively stable and within which the variability of reservoir parameters is reduced to some degree. However, even this approach will not allow a blanket emissions factor to be derived.

Methods should be developed to allow individual mines to estimate their emissions, which would need to allow for the following factors - local variation in gas content, rates of release of gas during and post mining, and gas retained in coal as it leaves the mine lease (and projects such as this are being conducted). Although it was outside the scope of this study, the next logical step is to conduct a series of Tier 3 mine scale studies and then compare them to estimations made by applying Tier 2 formulae and/or to develop of calibrated emission models that take account of both the varying reservoir properties and the mining process.

### ACKNOWLEDGEMENTS

The authors are indebted to the coal companies in the Hunter Valley and Bowen Basin that made confidential and sensitive data available to this project. They also thank ACARP and its monitors for their financial support and patience through this project.

### REFERENCES

- AUSTRALIAN GREENHOUSE GAS OFFICE. 2003. National Greenhouse Gas Inventory 2003. Available on the internet at <http://www.greenhouse.gov.au/inventory/2003/index.html>.
- AUSTRALIAN GREENHOUSE OFFICE. 2003 Australian Methodology for the Estimation of Greenhouse Gas Emissions and Sinks 2003. available on the internet at <http://www.greenhouse.gov.au/inventory/methodology/fugitive.html>.
- AUSTRALIAN GREENHOUSE OFFICE.2005. AGO Factors and Methods Workbook December 2005. Available on the internet at <http://www.greenhouse.gov.au/workbook/pubs/workbook-2005.pdf>.
- CROSDALE P.J., BEAMISH B.B. & VALIX M. 1998, Coalbed methane sorption related to coal composition, in R.M. Flores, ed., Coalbed methane: from coal-mine outbursts to a gas resource. *International Journal of Coal Geology* **35**, 147-158.
- ESTERLE J.S., SLIWA R., LE BLANC SMITH G., YAGO J., WILLIAMS R., LI S. & DIMITRAKOPOULOS R., 2002. Bowen Basin Supermodel 2000. Final Report for ACARP Project C9021. 180pp. + posters and CD.
- ESTERLE J.S., WILLIAMS R.J., SLIWA R. & MALONE M. 2006. Variability in Gas Reservoir Parameters that Impact on Emissions Estimations for Australian Black Coals. Final Report for ACARP Project C13071. 36pp.
- FAIZ M.M. & HUTTON A.C., 1997. Coal seam gas in the southern Sydney Basin, New South Wales. *APEA Journal* **37**, 415-428.
- IRVING W.N. & TAILAKOV O. 2004 (draft). Expert Group Meeting on Good Practice in Inventory Preparation- Energy:CH<sub>4</sub> Emissions Coal Mining and Handling (draft). IPCC/OECD/IEA Programme on National Greenhouse Gas Inventories.
- IPCC 1997. Revised 1996 IPCC Guidelines for National Greenhouse Gas Inventories, Reference Manual (Vol 3), Intergovernmental Panel on Climate Change. Available on the internet at <http://www.ipcc-nggip.iges.or.jp/public/gl/invs1.htm>.
- LAXMINARAYANA C. & CROSDALE P.J. 1999. Role of coal type and rank on methane sorption characteristics of Bowen basin, Australia coals. *International Journal of Coal Geology* **40**, 309-325.

- LEVINE J.R. 1993. Coalification: the evolution of coal as source rock and reservoir rock for oil and gas. *In: Law B.E & Rice D.D. eds. Hydrocarbons from coal: AAPG Studies in Geology* 38, pp. 39-77.
- MASEMORE S., PICCOT S., RINGLER E. & DIAMOND W.P. 1996. Evaluation and analysis of gas content and coal properties of major coal bearing regions of the United States. US Environmental Protection Agency Report EPA-600/R-96-065. Available on the internet at <http://www.p2pays.org/ref/07/06340.pdf>.
- SAGHAFI A., DAY S.J., FRY R., QUINTANAR A., ROBERTS D., WILLIAMS D.J. & CARRAS J.N. 2005. Development of an improved methodology for estimation of fugitive seam gas emissions from open cut mining. Final Report for ACARP Project C12072.
- SAGHAFI A., SAY S.J., WILLIAMS D.W. & CARRAS J.N. 2003. Towards the development of an improved methodology for estimating fugitive seam gas emissions from open cut coal mining. Final Report for ACARP Project C9063.
- SCOTT A.R., 2002. Hydrogeologic factors affecting gas content distribution in coal beds. *International Journal of Coal Geology* 50, 363– 387.
- SHI S., BEATH A., GUO H. & MALLETT C. 2005. An assessment of mine methane mitigation and utilisation technologies. *Progress in Energy and Combustion Science* 31 (2), 123-170.
- WILLIAMS D.J., SAGHAFI A., LANGE A.L. & DRUMMOND M. 1993. Methane emissions from open-cut mines and post-mining emissions from underground coal. Report to the Department of Environment, Sport and Territories, CSIRO Investigation Report CET/IR 173.
- WILLIAMS R.J., CASEY D.A. & YURAKOV E. 2000. Gas reservoir properties for mine gas emission assessment. *In: Beeston J.W. (ed.) Bowen Basin Symposium 2000-the New Millennium-Geology*. Geological Society of Australia Inc., Coal Geology Group and the Bowen Basin Geologists Group, Rockhampton, October 2000, 325-334.
- WILLIAMS R.J. & YURAKOV 2003. Improved Application of Gas Reservoir Parameters. Final Report for ACARP Project C10008.

# THE PORT BOTANY HAWKESBURY SANDSTONE LPG CAVERN: AN OVERVIEW OF CAVERN DESIGN, OPERATION AND MONITORING

Wendy McLean and Andrea Averkiou

Hydrogeology Unit, Parsons Brinckerhoff, Ernst & Young Centre  
Level 27, 680 George St, Sydney, NSW 2000

## ABSTRACT

Globally, unlined rock caverns have been successfully used to store liquefied petroleum gas (LPG) underground. Elgas Limited owns and operates Australia's first and only unlined LPG cavern storage facility located at Port Botany, Sydney. Excavation of the unlined cavern within the Hawkesbury Sandstone commenced in 1996, and the cavern was commissioned in 2000. This facility allows Elgas to store 65,000 tonnes of propane LPG 130 metres underground in four unlined, parallel galleries, securing the supply of LPG for Australia's eastern states.

The gas storage design relies on the water pressure in the surrounding saturated rock mass being greater than the pressure inside the cavern. This pressure is caused by the temperature and volume of the LPG. As a result of this difference in pressure, LPG will not flow from the cavern or escape into the surrounding saturated rock. Instead, there will be a small but steady migration of water from the surrounding rock into the cavern, which is subsequently removed by pumping. Approximately 100 tonnes of water per day is pumped from the cavern.

As there is no possibility of access to the caverns after commissioning, continuous and regular groundwater monitoring data are used to analyse whether the gas containment condition is satisfied or not. Water levels are monitored daily in a number of monitoring piezometers and groundwater chemistry is analysed every three months. Water levels are monitored to ensure the hydraulic margin (safety margin) around the cavern is maintained. Groundwater and process water samples are analysed for a range of analytes, in particular dissolved gases to ensure migration of gas from the cavern is not occurring. Over the last three years, a piezometer replacement program has been implemented, with the construction of eight new vertical monitoring piezometers to depths of 163 metres. The piezometer replacement program, hydraulic testing and ongoing water level and water quality monitoring have provided valuable insights into the aquifer properties of the Hawkesbury Sandstone, as well as providing the necessary data for analysis to ensure hydraulic containment of the LPG cavern.

## INTRODUCTION

In countries lacking natural geological conditions for gas storage, the use of caverns excavated in hard rock for the storage of natural gas is becoming more popular (Kim *et al.* 2000; Ko *et al.* 2002; Lee *et al.* 2002; Lindholm 1989; Linag & Lindblom 1994; Nielson & Olsen 1989; Tek 1989). In Sweden, in particular, unlined underground storages for fuel are very common (Larsson *et al.* 1977).

The principal of LPG storage in unlined rock caverns is based on the constraining effect of groundwater in rock fractures surrounding the cavern. The pressure of LPG in the cavern must be less than the actual groundwater pressure surrounding the cavern to prevent outward migration of gas from the cavern. One way to maintain groundwater pressure is to install a water curtain above the cavern periphery.

The Elgas underground LPG storage cavern at Port Botany, Sydney, operates using this principle of hydraulic containment. The cavern is the first unlined gas storage facility in Australia, and commenced operations in 2000. Hydraulic containment is maintained by controlling the hydraulic head of the water curtain situated 14.5 metres above the cavern. The water curtain is composed of tunnels for water distribution and an array of drilled holes tapped into the tunnel which inject water into the cavern through the rock system.

Groundwater pressure and flow around the cavern is influenced by natural factors such as the distribution of faults and joints, topographical features (recharge and discharge zones), artificial factors such as water curtains, and seasonally variable factors such as rainfall and fluctuating cavern gas pressures. It is necessary to monitor the effects of these natural and artificial factors on the hydraulic head and hydraulic containment of the gas.

Since caverns cannot be accessed once commissioned, it is necessary to monitor groundwater levels and groundwater chemistry to ensure hydraulic containment is maintained. This paper outlines the installation of the piezometer monitoring network undertaken at the Sydney underground LPG cavern, details of the regular groundwater monitoring program and presents findings from the testing and monitoring program on the aquifer properties and hydrogeochemistry of the Hawkesbury Sandstone.

### **GEOLOGICAL SETTING**

The local geology comprises unconsolidated sand deposits (Botany Sands) which overlie Hawkesbury Sandstone. At this location, dredged sand from Botany Bay has been used to reclaim the Port Botany site. The unconsolidated sand is up to 40 metres thick across the Elgas site, and comprises dredged fill to around 14 metres depth, with a variable thickness of Botany Sands (9 metres to 30 metres thick). The base of the unconsolidated sand sequence is at around minus 17 metres Australian Height Datum (mAHD) on the southern boundary of the site, and around minus 40 mAHD on the northern site boundary. The cavern site has a ground elevation of approximately 5 mAHD.

The Hawkesbury Sandstone is Mid-Triassic in age. It is flat-lying, extends 20,000 square kilometres in area, and can be up to 250 metres thick. The sandstone is a hard and durable rock composed of very fine to coarse quartz sand grains (although mostly medium grained) cemented with silica, clay and iron oxides or carbonates to form massive sandstone (Conaghan 1980; Herbert 1983; Pells 1985). Occasional shale bands occur within the sandstone, and at the cavern site there is a continuous shale layer around 10 metres in thickness, occurring approximately between minus 90 and minus 100 mAHD. This band appears to be present beneath most of the site, but is thin or absent on the eastern side of the cavern.

**HYDROGEOLOGICAL SETTING**

Conceptually, there are three aquifer systems at the Sydney LPG Cavern: the unconfined aquifer in the dredged sand/Botany Sands unit, and the underlying upper and lower Hawkesbury Sandstone aquifers.

The shallow aquifer system within the fill and sand material is dominated by saline water. The water table is only a few metres below ground level and there is a strong tidal influence. The main recharge of the shallow sand aquifer is from precipitation (and irrigation), with the groundwater flowing in a south-westerly direction, leading to discharge into Botany Bay.

In the Port Botany area, the Hawkesbury Sandstone is interpreted to behave as a leaky confined aquifer, comprising two main aquifer units separated by a thin shale band. Parsons Brinckerhoff (2003) interpreted the Hawkesbury Sandstone as a layered aquifer system, with groundwater occurring in discrete horizons that occasionally have vertical hydraulic connection. Groundwater movement is interpreted to be variable, with both primary granular flow and secondary flow along fractures.

The current Hawkesbury Sandstone water levels range from around 0 to -5 mAHD (upper sandstone) and from about -12 to -38 mAHD (lower sandstone) (Figure 1). The main influence on water levels and pressure heads is tidal movements for the shallow sandstone aquifer, and cavern pressure for the deep sandstone aquifer.

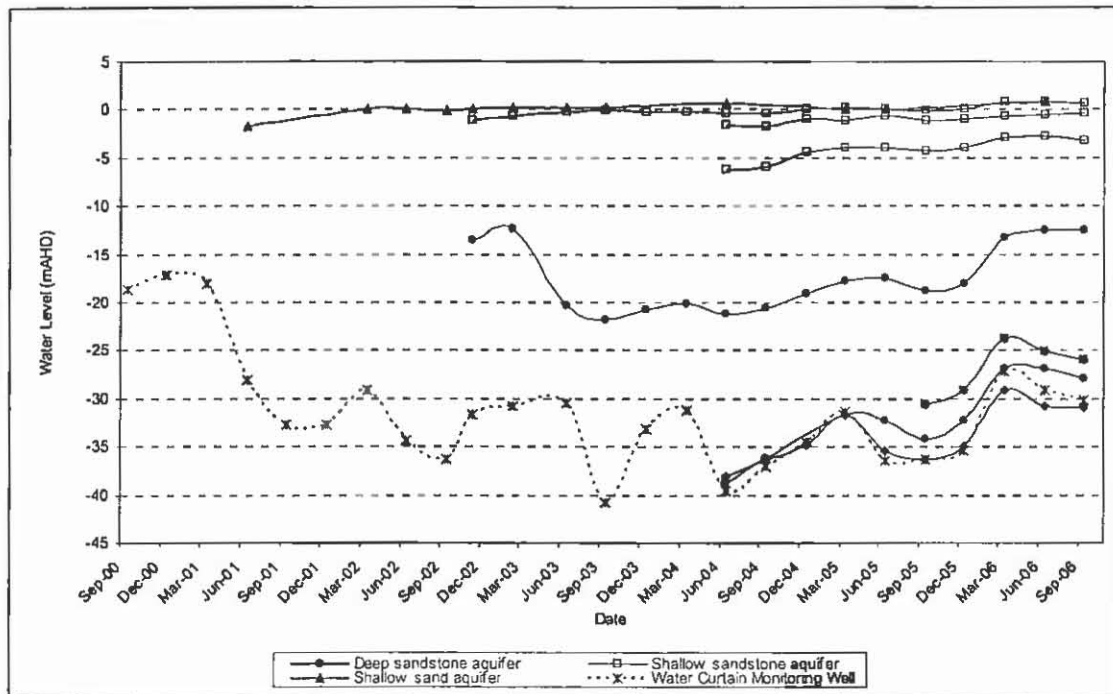


**Figure 1** Groundwater hydrographs from a number of monitoring piezometers at the cavern site.

From pre-construction water quality data, the Hawkesbury Sandstone aquifers contain low salinity water with low nutrient concentrations. The water is often acidic (with a pH range from 3.5 to 5.5), however at this site, pHs of between pH 7 and pH 9 were noted after construction of the piezometers (however near neutral pHs have been observed in other

Hawkesbury Sandstone bores in the Sydney Basin). The Hawkesbury Sandstone aquifers often contain elevated iron levels but low heavy metal concentrations. Low major ion concentrations (sodium chloride dominant) also occur within the Hawkesbury Sandstone aquifers (McKibbin and Smith, 2000).

Naturally, the recharge of the sandstone aquifers is from the eastern exposed sandstone along the coastline, with water discharging to Botany Bay through the Botany Sands. Both flow velocities and aquifer permeabilities are generally low, with hydraulic conductivities in the sandstone on-site of  $4.5 \times 10^{-4}$  to  $7.7 \times 10^{-2}$  m/day, and off-site of  $8.5 \times 10^{-2}$  to  $1.9 \times 10^{-1}$  m/day (PB, 2004). The flow direction is expected to be predominantly from the north-east to the south-west. Locally, the LPG Cavern has influenced these natural velocities and flow directions.

### ELGAS LPG CAVERN

The Elgas LPG cavern was excavated with a top elevation of -124 m AHD, so that the pressure of the surrounding groundwater will remain in excess of the gas pressure in the cavern, thus ensuring the containment of the LPG. The cavern volume is obtained by four parallel, unlined galleries, which are 14 metres wide, 11 metres high and about 230 metres in length. They are interconnected at the upper and lower level by smaller connection galleries (5.5 metres by 5.5 metres) so as to allow the interconnection of the vapour and liquid phase of the LPG (Geostock, 2000).

A 'water curtain' was constructed 14.5 metres above the top of the storage galleries to maintain saturation of the rock and to ensure permanent groundwater flow towards the storage, thus helping to retain the LPG within the caverns. The water curtain is made up of small tunnels and boreholes drilled into the surrounding rock. Town water is injected into the water curtain via a pipe in the Access Shaft. A cross-section of the cavern is shown in Figure 2.

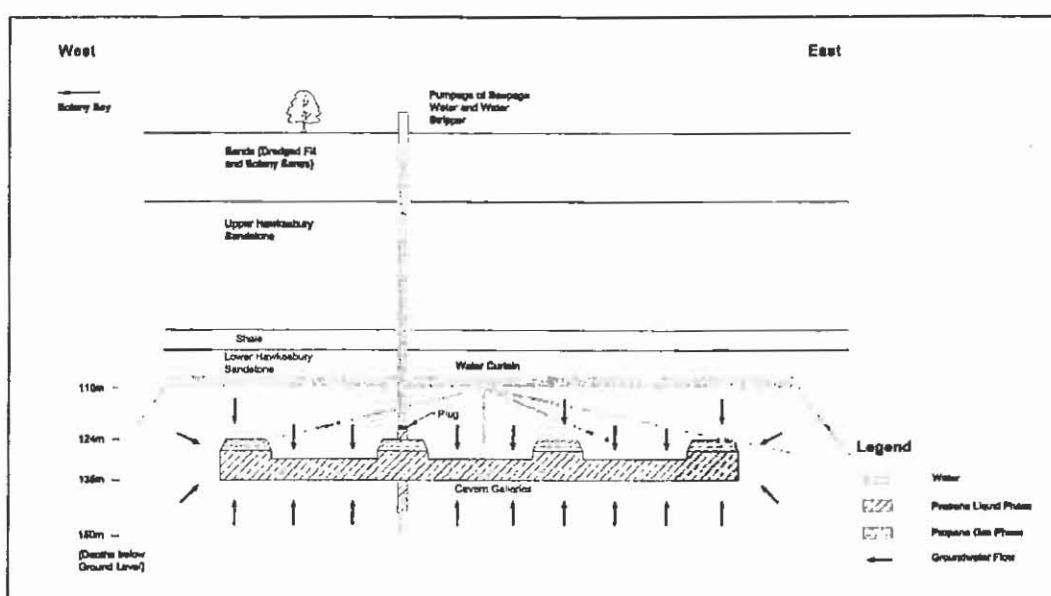


Figure 2: Cross-section of Elgas LPG cavern.

LPG is discharged from LPG ships at  $-42^{\circ}\text{C}$ . In order to prevent shattering of the sandstone around the cavern, the discharged LPG is heated to approximately  $7^{\circ}\text{C}$  prior to entering the

underground cavern. The stored LPG eventually reaches a temperature of 15°C. Once the LPG is loaded for distribution, a dryer removes any moisture.

Groundwater seepage into the cavern is directed to a 38 cubic metre sump located at a depth of 150 metres below ground level, and pumped to surface by pumps under level control. LPG in the seepage water is removed by a flash drum and water stripper once pumped to surface.

So as to assure the adequate functioning of the underground storage, the cavern requires frequent monitoring. The levels of seepage water and LPG liquid product, together with temperature and pressure within the cavern, are continuously monitored.

### **CAVERN MONITORING PROGRAM – WATER QUALITY AND WATER LEVELS**

Since commissioning of the cavern, there has been no possibility of access to the cavern, so continuous and regular groundwater monitoring data are used to analyse whether the gas containment condition is satisfied or not. Groundwater samples have been collected from a network of on-site and off-site piezometers, and process water samples have been taken from cavern operation and access shafts and the water treatment unit (water stripper) on a quarterly basis. Water quality of the water curtain is monitored by taking samples from a monitoring piezometer which penetrates the water curtain. Water levels are collected from piezometers on a daily to weekly basis. The monitoring network comprises four deep sandstone piezometers, four shallow sandstone piezometers, a shallow sand piezometer, the water curtain monitoring well, access and operation shafts and cavern seepage water from the water treatment plant (water stripper).

Originally the monitoring network comprised piezometers that were converted from geotechnical boreholes and were sampled using bailers. Due to the non-standard PVC size, pumps could not be used and the water could not be purged. There was also concern regarding the integrity of these piezometers. These piezometers were replaced in stages from 2002 to 2006 with standard vertical piezometers. Depths of piezometers penetrating the upper sandstone aquifer range between 55 and 86 metres, and between 127 and 164 metres in the deep sandstone aquifer.

Low flow dedicated MicroPurge pumps are used to sample the on-site piezometers in the sandstone. The pumps were installed at the depths of the screened sections, which corresponds to the main water-bearing zones in each aquifer. The flow rate of the MicroPurge pumps is set at a rate below the recharge capacity of the formation, thus only water from the aquifer is pumped. A portable submersible pump (Grundfos MP1) is used to purge and sample off-site monitoring piezometers.

A large analytical suite is analysed on a quarterly basis to monitor whether the gas containment condition is maintained, to monitor any potential groundwater contamination from surrounding industries, and water quality impacts due to cavern operation. The analytical suite includes: field parameters (including electrical conductivity (EC), redox potential (Eh), temperature and pH), major ions, metals, nutrients, hydrocarbon gases, BTEX compounds, total petroleum hydrocarbons and polyaromatic hydrocarbons.

To assure gas containment by the water curtain system, the water curtain drilled holes and surface of the cavern must be prevented from microbial clogging. The rupture of a cavern system by microbial clogging was reported in the caverns storing crude oil (Barbo and

Danielson 1980). Potential microbial clogging is monitored by laboratory analysis of bacteria (nitrate reducing, sulphate and sulphite reducing and iron depositing *Gallionella spp.* and *Sphaerotilus spp.*).

### HYDROGEOCHEMICAL PROPERTIES

Long term groundwater monitoring has provided valuable information on the hydrogeochemistry of the Hawkesbury Sandstone aquifers and also the Botany Sands aquifer in the Port Botany region. The chemistry of groundwater in the study area are presented in Table 1 and in the Piper diagram in Figure 3, which is a plot of the relative concentration (%meq/l) of the major cations and anions. Distinct geochemical differences occur in groundwater from the three aquifers.

**Table 1** Chemical compositions of groundwaters and seepage waters in the study area (June 2006 results).

Aquifer Type Sample Location	Lower Sandstone			Upper Sandstone			Sand	Seepage Water
	RepBHB2(L) Sep-06	RepBHG(L) Sep-06	RepMP3(L) Sep-06	RepBHB2(U) Sep-06	RepBHG(U) Sep-06	RepMP3(U) Sep-06	SP5 Jun-06	WS(inlet) Sep-06
pH	8.03	7.95	7.46	6.09	5.74	6.4	6.86	6.8
Redox Potential (mV)	-119	-147	-112	-76	-47	-86	-67	37
Temperature (°C)	19.2	19.8	20.8	18.6	20.7	23.8	18.4	19.9
EC (µS/cm)	1,604	1,166	3,415	13,680	15,060	27,260	51,090	5,233
Na (mg/L)	325	254	340	1,381	1,788	3,870	12,000	818
K (mg/L)	6	5	8	47	46	122	468	24
Mg (mg/L)	10	3	9	411	381	491	1,380	76
Ca (mg/L)	20	6	25	595	672	1,160	505	146
Cl (mg/L)	322	185	363	4,640	5,620	9,970	20,000	1,680
SO <sub>4</sub> (mg/L)	<1	1	2	68	114	560	2,320	90
Alkalinity as CaCO <sub>3</sub> (mg/L)	388	362	353	6	2	16	660	78
SiO <sub>2</sub> (mg/L)	9.1	10.2	8.8	12	10.4	9.6	4.45	5.5
Fe <sup>2+</sup> (mg/L)	0.08	<0.05	2.92	51.5	86	173	4.4	18.9
Mn (mg/L)	0.006	0.013	0.047	0.943	1.41	2.21	0.103	0.507

Groundwater from both the Botany Sands aquifer and the upper Hawkesbury Sandstone aquifer are both dominated by Na and Cl, however the sand aquifer is substantially more saline and has an EC approaching that of seawater. The upper Hawkesbury Sandstone groundwater has a naturally high salinity due to the mixing with groundwater from the overlying sand aquifer, and its proximity to Botany Bay. The EC of groundwater from the upper sandstone aquifer ranges from approximately 12,000 to 30,000 µS/cm. The pH conditions in this aquifer are acidic to neutral (pH 5 to 7) and redox conditions are typically reducing. Groundwater from the Hawkesbury Sandstone typically has elevated concentrations of iron and manganese (McKibbin and Smith 2000) and groundwater from the upper aquifer at the Elgas cavern site have dissolved iron concentrations up to 630 mg/L and manganese concentrations up to 8.25 mg/L. Sources of iron include siderite (iron carbonate, FeCO<sub>3</sub>) and iron oxyhydroxides and oxides.

Groundwater from the lower Hawkesbury Sandstone aquifer in the vicinity of the cavern site is typically Na-HCO<sub>3</sub>-Cl as shown on the Piper diagram in Figure 3. It has a lower salinity than the upper sandstone aquifer (EC approximately 1,000 to 3,500 µS/cm), has a higher pH (pH 7.5 to 12.5), and more reducing conditions (Eh -150 to -300 mV). Dissolved iron and manganese concentrations are lower than in the upper sandstone aquifer, with iron and manganese concentrations ranging from detection limit to 0.5 mg/L and detection limit to 0.15 mg/L, respectively. Methane is naturally present in deep sandstone piezometers and is believed to be due to methane generated in the underlying coal seams. Methane is detected at

concentrations up to 13,800  $\mu\text{g/L}$ . No other dissolved hydrocarbon gases (butane, ethane, ethene, propane or propene) have been detected in groundwater, indicating gas containment has been maintained.

The chemical composition of seepage water pumped out of the cavern represents a composite of fresh water injected into the water curtain and groundwater from the Hawkesbury Sandstone aquifers. Salinity of cavern seepage water varies with the volume of water pumped into the water curtain, and is currently 5,233  $\mu\text{S/cm}$ . The pH of seepage water is circumneutral, and redox conditions typically oxidising. Seepage water is dominated by sodium and chloride.

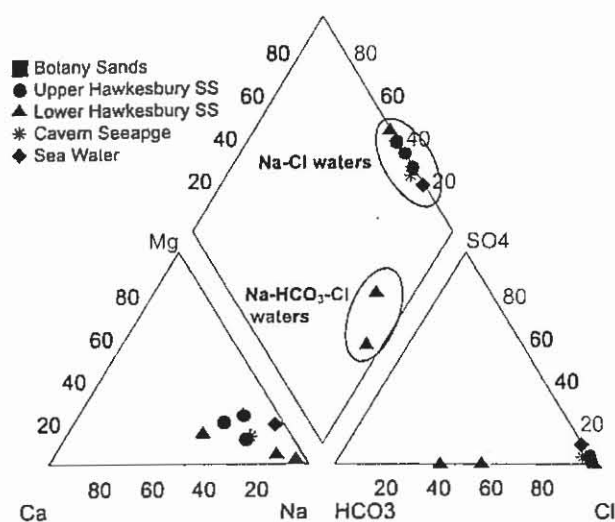


Figure 3 Piper diagram showing chemical composition of cavern seepage and groundwater.

## CONCLUSIONS

The Sydney underground LPG storage cavern is Australia's first unlined storage cavern. The cavern is excavated 130 metres underground in the Hawkesbury Sandstone and up to 65,000 tonnes of LPG can be stored in the four unlined, parallel galleries. The gas storage design relies on the principle of water pressure in the surrounding saturated rock mass being greater than the pressure of the stored gas inside the cavern. Regular monitoring of water quality and water levels are undertaken from a piezometer monitoring network to ensure gas containment is maintained. Data obtained from the piezometer replacement program undertaken from 2002 to 2006 and long term monitoring data has provided valuable information on the aquifer properties and hydrogeochemistry of the Hawkesbury Sandstone and Botany Sands aquifer, as well as providing the necessary data for analysis to ensure the hydraulic containment of the LPG cavern.

## ACKNOWLEDGEMENTS

The authors wish to thank Aldo Costabile (Cavern Terminal Manager, Elgas Ltd) and Elgas Ltd for permission to publish the data and for technical review of this paper.

## REFERENCES

- BARBO T. F. & DANIELSEN S. W. 1980. Bacterial impairment of water curtain between oil storage caverns in rock. In: Bergman, M. (ed.) *Subsurface space: environmental protection, low cost storage energy savings*. Pergamon Press, Oxford, 245-250.

- CONAGHAN, P.J. 1980. The Hawkesbury sandstone: Gross Characteristics and Depositional Environment. In: Herbert, C., and Helby., R. (Eds) *A Guide to the Sydney Basin*. Geological Survey of New South Wales, Bulletin 26, Department of Mineral Resources.
- GEOSTOCK 2000. *Elgas LPG Cavern – Hydrogeological Management Plan for Operation*.
- HERBERT C. 1983 (Ed). *Geology of the Sydney 1:100,000 Sheet 9130*, NSW Department of Mineral Resources.
- KIM T., LEE K-K., CHANG H. W. & KO K. S. 2000. Groundwater flow system inferred from hydraulic stresses and heads at an underground LPG storage cavern site. *Journal of Hydrology* 236 165-184.
- KO K-S., CHANG H, KIM T., & LEE, K-K. 2002. Factors affecting the underground system around an underground LPG storage cavern. *Quarterly Journal of Engineering Geology and Hydrogeology* 35 279-290.
- LARSON I., FLEXER A., AND ROSEN B. 1977. Effects on ground water caused by excavation of rock store caverns. *Engineering Geology* 11 279-294.
- LEE J., KIM R-H. & CHANG H-W. 2002. Interaction between groundwater quality and hydraulic head in an area around an underground LPG storage cavern, Korea. *Environmental Geology* 43 901-912.
- LIANG J. & LINDBLUM U. 1994. Analyses of gas storage capacity in unlined rock. *Rock Mechanics and Rock Engineering* 27(3) 115-134.
- LINDBLUM U. 1989. The performance of water curtains surrounding rock caverns used for gas storage. *International Journal of Rock Mechanics and Mining Sciences and Geomechanics Abstracts* 26(1) 85-97.
- MCKIBBIN D. & SMITH P.C. 2000. *Sandstone Hydrogeology of the Sydney Region*. In: McNally G.H & Franklin B.J. (Eds.) *Sandstone City – Sydney's Dimension Stone and other Sandstone Geomaterials*. Proceedings of a symposium held on 7th July 2000, during the 15th Australia Geological Convention at the University of technology Sydney.
- NIELSEN B. & OLSEN J. 1989. *Storage of gases in rock caverns*. A.A. Balkema, Rotterdam.
- PARSONS BRINCKERHOFF AUSTRALIA 2003. *Groundwater investigation for contingency relief in the Sydney Region. Results of desktop study December 2003*. Report 2114271A PR\_2984 RevE, dated December 2003.
- PARSONS BRINCKERHOFF AUSTRALIA 2004. *Water Quality Monitoring Program Annual Report July 2003 to July 2004, Sydney LPG Cavern*. 2116471A PR\_9344, dated September 2004.
- PELLS P.J.N 1985. Engineering Properties of the Hawkesbury Sandstone. In: Pells P.J.N (Ed.) *Engineering Geology of the Sydney Region*. Published on behalf of the Australian Geomechanics Society.
- TEK M. R. 1989. *Underground storage of natural gas*. NATO ASI Series. Kluwer Academic Publishers, Dordrecht.

# EXPLORATORY BLEND OPTIMISATION MODELLING

**Chris McMahon**

Principal Consultant, McMahon Coal Quality Resources  
12 Chiswick Place Forest Lake, Queensland, 4078

## **ABSTRACT**

Optimisation of the mining and delivery process at various production stages can result in significant physical and financial gains for the mining company using such technology. For set constraints an optimised solution can be found that will increase revenue, save physical resources, increase staff time and reduce frustration.

This paper describes two optimisation examples that utilised the SOLVER<sup>™</sup> routine from Microsoft Excel's spreadsheet program. The Microsoft Excel SOLVER<sup>™</sup> tool finds an optimum solution to a mathematical problem based on known constraints. It can maximise, minimise or use optimal resources to achieve a predefined target. The developed software also had associated software infrastructure as designed by the author to make the process user friendly.

An additional benefit of optimisation is that the process assists in the identification of tonnage and quality bottlenecks, shortfalls in supply and critical processes.

The optimisation examples given are for two projects: 1) the first representing a very long term (one year to twenty year) period; and 2) the second a very short term (intra-day) period.

Optimisation can be applied practically over any time frame in a myriad of situations including but not limited to the applications of blending in mine planning and production and stockpile modelling, as are displayed herein. Any situation which has variables with limits that need to be imposed and a maximum, minimum or exact outcome can have optimisation applied.

## **INTRODUCTION**

Many areas of coal mining from exploration to coal export have subjective logistical decisions made on processing. Through optimisation, significant performance enhancements and resulting revenue savings can be made when applied to a multi-variant process.

Optimisation processes applied to reality often fail from over planning and lack of flexibility. That is, trying to control too many variables in a process, in too constrained a manner, resulting in models that are unsustainable in the real world. MCQR has applied optimisation in the real world utilising key variables and practical constraints that can be used repeatedly and effectively. The methodology has been applied over very short term (intra-day) periods up to very long term (multiple years) periods.

The goal of optimising a mining process can be maximisation or minimisation to a certain value or the achievement of the best allocation of resources within specified limits to meet a specific target value. This paper gives actual optimisation processes performed by McMahon Coal Quality Resources and the resulting efficiency increases and revenue savings.

## **METHOD**

The basic process of optimisation requires defining the goal to be achieved (the optimisation outcome), defining the process variables that affect the goal and defining the limits of those variables to perform the optimisation. The information is then compiled, fitted to software and the optimisations produced.

Mine site tonnage and quality inventory and predictions were obtained from the sites themselves with McMahon Coal Quality Resources (MCQR) managing the projects.

The Microsoft Excel Solver tool utilised in these simulations uses the Generalized Reduced Gradient (GRG2) nonlinear optimization code developed by Leon Lasdon, University of Texas at Austin, and Allan Waren, Cleveland State University.

Linear and integer problems use the simplex method with bounds on the variables, and the branch-and-bound method, implemented by John Watson and Dan Fylstra, Frontline Systems, Inc.

## **OPTIMISATION PROJECT 1 - TWENTY YEAR MINE PLAN OPTIMISATION**

### **Process**

#### Overview

The spreadsheet input and outputs are summarised in the Figure 1.

## OPTIMISATION MODELLING

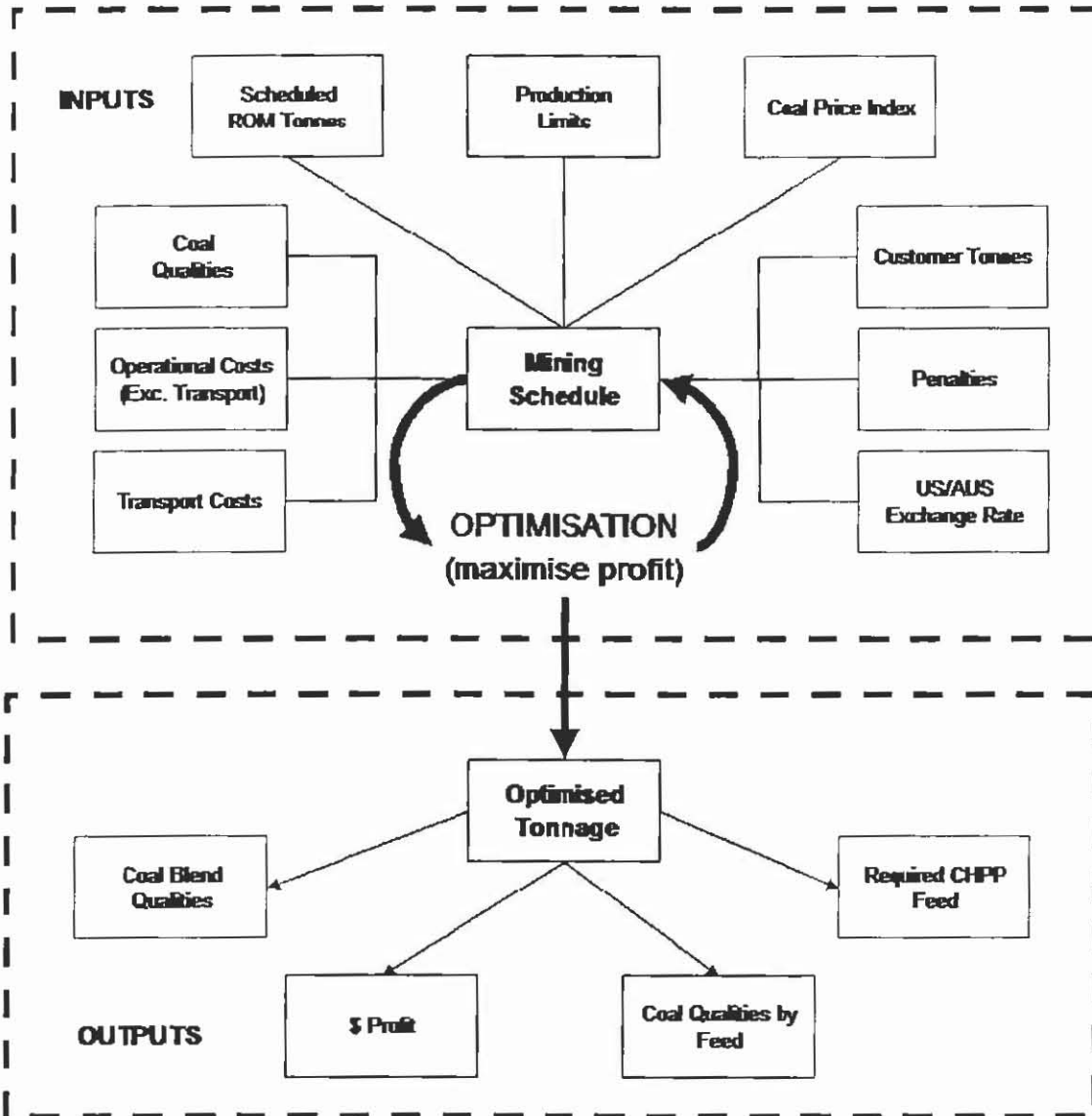


Figure 1 Inputs and Outputs for Optimisation Model.

### Spreadsheet Setup

The premise of the inputs as displayed above is to maximise dollar return by adjusting mine production from the “Base” Mining Schedule using limits for tonnage and quality. Feed back from outputs (iterations) eventually produces an “Optimised Tonnage” feed that satisfies the limits set and maximises profit.

MCQR performed the spreadsheet setup for the schedule so the solver routine could extract the relevant information.

### Options Used

Tonnage limits for different areas, mining costs, customer tonnage requirements, prices and penalties and coal quality information (with limits if required though none were set for this set of results) all on a tonnage weighted basis were evaluated.

Allocation for coal purchases was also produced in the model.

Penalty adjustments were included in the calculations so within tolerance quality decreases are compensated for to obtain the best financial return.

#### Further Options Available

Further options that were available but not utilised in the initial optimisation runs were as follows:

The criteria of the ROM coal mining having to be greater than or equal to the customer sales was disabled.

The coal quality information rejection criteria (quality for a particular parameter having to be made in order for the optimisation to proceed) was disabled.

Optimisation for the best markets to chase based on pit to port flow through costs (mining costs versus cost of sale) were not evaluated.

#### **Solver Routine**

The optimisation process is summarised in the following flow diagram (Figure 2).

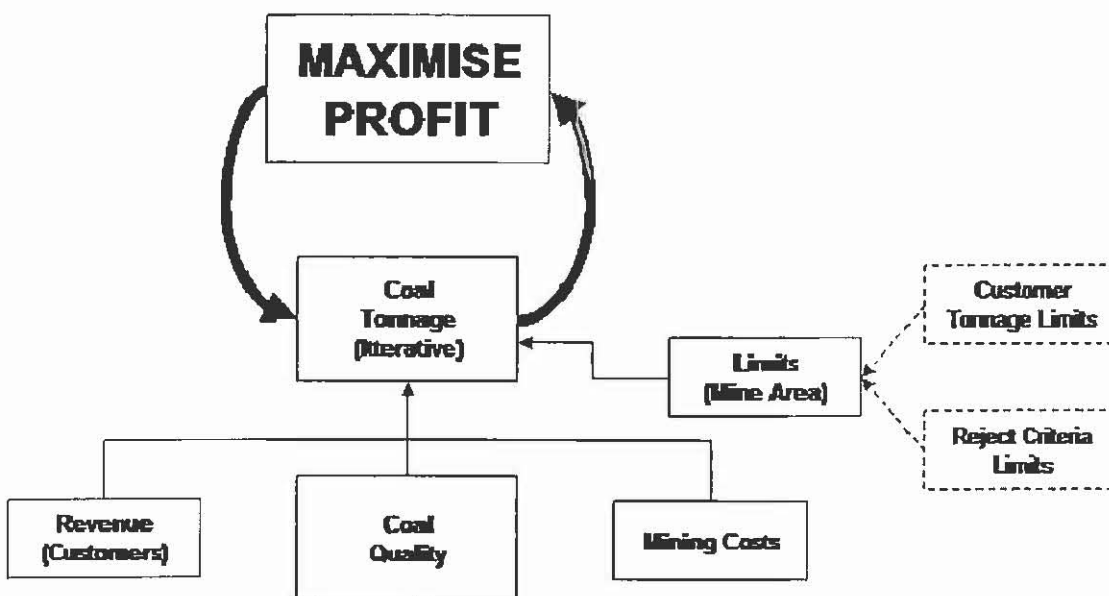


Figure 2 Optimisation Process.

To Maximise Profit, the solver routine examined the Revenue (from Customers), Coal Quality, Mining Costs and Limits (CHP Feed limitations only in this iteration) for the Coal (ROM) Tonnages. The starting Coal Tonnages were changed in an iterative fashion until successive iterations showed no significant increase in overall profit (profit maximised). A brief description of each data input/calculation tab is given following.

#### **Data Input & Calculations**

##### Revenue

The Customers contract information determined overall revenue. All the coal mines customers were listed individually on a yearly basis with inputs made for their respective price per product tonne of coal (US\$) and volume (tonnage) with calculations for penalties for

coal quality where applicable. The input prices were corrected for penalties based on the yearly average quality (Figure 3).

The corrected prices were linked to the tonnage change cells of the solver routine in the same tab to produce a yearly tonnage weighted average dollar result. The prices were finally converted to Australian dollars (allocation for different exchange rates on a per year basis was made with a default conversion rate).

Customer	Average Price (US\$)	Sales Tonnage K	Penalties (per tonne of product coal, US\$)					Sum of Penalties	Average Penalty Adjusted Price (US\$)	Average Penalty Adjusted Price (AUS\$)	
			TM% (ar)	Ash% (ad)	Sulphur (%)	Phos% (ad)	CSN				
A	\$72.10	482	\$0.80	\$0.00	\$0.00			\$0.80	\$71.30	\$95.07	
B	\$74.90	40	\$0.83	\$0.00	\$0.00			\$0.83	\$74.07	\$98.76	
C	\$74.00	60	\$0.82	\$0.00	\$0.00			\$0.82	\$73.18	\$97.57	
D	\$71.50	1,558	\$0.79	\$0.00	\$0.05			\$0.84	\$70.66	\$94.21	
E	\$72.70	274	\$0.80	\$0.00	\$0.00			\$0.80	\$71.90	\$95.86	
F	\$74.00	150	\$0.08	\$0.00	\$0.00			\$0.08	\$73.92	\$98.56	
G	\$71.30	195	\$2.21	\$0.00	\$0.00		\$0.46	\$2.67	\$68.63	\$91.50	
H	\$71.90	1,195	\$0.80	\$0.00	\$0.00			\$0.80	\$71.10	\$94.81	
I	\$73.90	607	\$0.82	\$0.00	\$0.00			\$0.82	\$73.08	\$97.44	
J	\$72.90	116	\$0.81	\$0.00	\$0.00			\$0.81	\$72.09	\$96.12	
K	\$74.50	212	\$0.08	\$0.14	\$0.00			\$0.22	\$74.28	\$99.04	
L	\$72.30	151	\$0.80	\$0.00	\$0.00		\$2.18	\$1.50	\$70.80	\$94.40	
M	\$72.20	200	\$0.09	\$0.00	\$0.00	\$0.00		\$0.09	\$72.11	\$96.14	
N	\$72.70	100	\$0.80	\$0.00	\$0.00			\$0.80	\$71.90	\$95.86	
SUM		5,340	US\$ to AUS\$=							AVG	\$95.31

Figure 3 Customer Information Page of Optimisation Model.

Mining Costs

The Mining Costs determined overall mining (and rehabilitation) costs per ROM tonne (calculated yields being used to give product tonnes). Costs for each mine area were input (AUS\$ / tonne) and rose by a “CPI” (coal price index) every subsequent year (each year has its own CPI input variable, though a default was used). Coal handling plant capacity was also input in this section (though no restrictions on coal handling plant feed or other logistics were made).

Coal Quality

Inputs for yield and quality were made on a yearly basis for the tonnage variables.

Coal Tonnage

The inputs for tonnage by area were made on a yearly basis for the tonnage variables.

Limits

Upper and lower bounds were placed at the user's discretion to limit the maximum and minimum amount of material (tonnage) that can be retrieved from a mining area. The solver routine works within these limits to obtain the best financial return and outputs the optimised tonnages. In the tested model only six mine areas had limits applied, the other areas having fixed tonnages.

Customer Tonnage Limits

The Customer Tonnage Limits were not enabled in the initially processed simulations. Upper and lower bounds can be placed at the user's discretion to limit the maximum and minimum amount of product that can be sent to a particular customer. Coupled with the mine area optimisation, the solver routine would work within these limits to not only give the most profitable mining scenarios but to identify the most profitable combination of mining scenarios and customer supply and/or most profitable markets.

### Reject Criteria Limits

The Reject Criteria Limits were not enabled in the processed simulations. Maximum and minimum rejection criteria limits can be set for quality.

### **Outcomes**

The following outcomes were achieved from the twenty year mine optimisation.

The model results showed that the optimised solution took more of some coal allocations, and less of others to give a maximum dollar per tonne return based on the information and constraints it was given.

An additional profit of AUS\$54M over the twenty year period was produced using the results of the first pass optimisation. That is, a 0.47c / product tonne improvement was made which equated to an on average AUS\$2.6 million per annum profit.

The wash plant capacity was found to be far less than the coal planned to be mined. Consequently a coal handling plant upgrade was scheduled to accommodate this and the full set of tonnages for the set of simulations was able to be run.

A shortfall in coal for predicted market demand was also noted and alternative strategies developed for such.

Several other strategies emerged from issues flagged by the optimisation including options for selective marketing, additional coal supplies to fill gaps (blending options) and increased production in some areas and decrease in others (cost benefit).

## **OPTIMISATION PROJECT 2 – INTRA-DAY STOCKPILE OPTIMISATION**

### **Project Rationale**

At the Jellinbah mine in Central Queensland, various seams and areas within the mine yield different quality products. At the time of the development of the optimisation tool described in this paper, Jellinbah was a raw coal mine using selective mining and stockpile blending to achieve product specification.

Some twenty odd different quality product stockpiles existed at any one time and the on-site coal quality engineer (being Chris McMahon of MCQR at the time) had to at least once a day decide the blend to meet the following criteria:

- to meet product specification in ash and sulphur,
- minimise use of good quality coal,
- maximise use of poorer quality stockpiles,
- ensure the depletion of stockpiles periodically to allow for new coal and
- provide a simple ratio from several stockpiles for blending using the front end loaders.

Thus the need for a tool to simplify and optimise products in a practical manner was devised by MCQR while on site. The following describes the operation of the tool developed for such.

**Control Interface**

Figure 4 depicts the control interface developed in Excel for loading relevant data and running the optimisation tool.

<p><b>1. Set product constraints</b></p> <table border="1"> <tr> <th colspan="5">SET / OPTIMISE PRIMARILY ON ASH</th> </tr> <tr> <th>Tonnage</th> <th colspan="2">Ash</th> <th colspan="2">Sulphur</th> </tr> <tr> <td>SET</td> <td>MIN</td> <td>MAX</td> <td>MIN</td> <td>MAX</td> </tr> <tr> <td>16,000</td> <td>9.8</td> <td></td> <td>0.68</td> <td>0.70</td> </tr> </table> <table border="1"> <tr> <th colspan="5">SET / OPTIMISE PRIMARILY ON SULPHUR</th> </tr> <tr> <th>Tonnage</th> <th colspan="2">Sulphur</th> <th colspan="2">Ash</th> </tr> <tr> <td>SET</td> <td>MIN</td> <td>MAX</td> <td>MIN</td> <td>MAX</td> </tr> <tr> <td>6,500</td> <td>0.45</td> <td></td> <td>12.0</td> <td>15.0</td> </tr> </table>						SET / OPTIMISE PRIMARILY ON ASH					Tonnage	Ash		Sulphur		SET	MIN	MAX	MIN	MAX	16,000	9.8		0.68	0.70	SET / OPTIMISE PRIMARILY ON SULPHUR					Tonnage	Sulphur		Ash		SET	MIN	MAX	MIN	MAX	6,500	0.45		12.0	15.0	<p><b>3. Add/remove samples and change tonnages as required on "SOLVER"</b> <b>GO TO SOLVER</b></p>	
SET / OPTIMISE PRIMARILY ON ASH																																															
Tonnage	Ash		Sulphur																																												
SET	MIN	MAX	MIN	MAX																																											
16,000	9.8		0.68	0.70																																											
SET / OPTIMISE PRIMARILY ON SULPHUR																																															
Tonnage	Sulphur		Ash																																												
SET	MIN	MAX	MIN	MAX																																											
6,500	0.45		12.0	15.0																																											
<p><b>4. Optimise for constraints chosen</b></p> <p><b>OPTIMISE PRIMARY ASH</b></p> <p><b>OPTIMISE PRIMARY SULPHUR</b></p> <p><b>OPTIMISE &amp; MINIMISE USE OF A STOCKPILE</b></p> <p><b>OPTIMISE &amp; MAXIMISE USE OF A STOCKPILE</b></p>																																															
<p><b>MINIMISE MAX (OR OTHER) STOCKPILE</b></p> <table border="1"> <tr> <th>Tonnage</th> <th colspan="2">Ash</th> <th colspan="2">Sulphur</th> <th rowspan="2">Stockpile to MINIMISE</th> </tr> <tr> <td>SET</td> <td>MIN</td> <td>MAX</td> <td>MIN</td> <td>MAX</td> </tr> <tr> <td>16,000</td> <td>9.8</td> <td>10.00</td> <td>0.68</td> <td>0.70</td> <td>C07</td> </tr> </table> <p>Correct stockpile code?&gt; C07</p>					Tonnage	Ash		Sulphur		Stockpile to MINIMISE	SET	MIN	MAX	MIN	MAX	16,000	9.8	10.00	0.68	0.70	C07	<p><b>5. Refine optimisation by adding/removing/changing samples as appropriate</b></p>																									
Tonnage	Ash		Sulphur		Stockpile to MINIMISE																																										
SET	MIN	MAX	MIN	MAX																																											
16,000	9.8	10.00	0.68	0.70	C07																																										
<p><b>MAXIMISE STOCKPILE</b></p> <table border="1"> <tr> <th>Tonnage</th> <th colspan="2">Ash</th> <th colspan="2">Sulphur</th> <th rowspan="2">Stockpile to MAXIMISE</th> </tr> <tr> <td>SET</td> <td>MIN</td> <td>MAX</td> <td>MIN</td> <td>MAX</td> </tr> <tr> <td>17,000</td> <td>9.2</td> <td>9.40</td> <td>0.66</td> <td>0.80</td> <td>C12</td> </tr> </table> <p>Correct stockpile code?&gt; C12</p>					Tonnage	Ash		Sulphur		Stockpile to MAXIMISE	SET	MIN	MAX	MIN	MAX	17,000	9.2	9.40	0.66	0.80	C12																										
Tonnage	Ash		Sulphur		Stockpile to MAXIMISE																																										
SET	MIN	MAX	MIN	MAX																																											
17,000	9.2	9.40	0.66	0.80	C12																																										
<p><b>2. Import Required Data</b></p> <p><b>CRUSHED STOCKPILES</b></p> <p><b>CENTRAL ROM PILES</b></p> <p><b>4 WEEK COAL PLAN (THIS WEEK'S ONLY + PLAINS ROM)</b></p>																																															

**Figure 4** Control Interface for Data Loading and Optimisation.

The process involved firstly setting the type of optimisation. This was done by setting the necessary product constraints for either ash or sulphur or minimising or maximising the use of a particular stockpile.

Next the most up-to-date information for optimisation was found. This was done by macros developed to find and/or access certain programs that would then have the data imported into the optimisation program. Three such programs existed:

- The “Crushed Coal Stockpiles” program which was the program used to manage the product stockpiles on a daily basis.
- The “Central ROM Piles” which was a record of the run of mine (ROM) stockpiles.
- The “4 Week Coal Plan” which was the coal predicted to come out of the various mining pits in the next four weeks.

“Solver” Control Sheet

Next specific criteria for the optimisation were accessed in the SOLVER sheet. This is given following.

SOURCE DATA	BLEND OPTIMISATION Jellinbah Resources										BLEND	Original VALUES - Central & Plains					SAMPLE INPUT
	CENTRAL & PLAINS											Central & Plains					
	SP#	Date	PL	TS	ASH	TS	CSW	SE d/d	TS	ASH		TS	CSW	SE d/d			
CENTRAL Stockpiles (per Stockpiles. xls)	C01	01-May-00	PL#00	0.0	20.3	1.02	0.9	7.74	0	21.2	1.04	0.9	7.742	C01			
	C02	28-May-00	Romp 1 ROM	0	21.3	0.93	0.6	8.37	0	21.7	0.93	0.6	8.375	C02			
	C03	07-Jun-00	Romp 2 ROM	0	14.0	1.54	1.2	7.87	0	14.15	1.54	1.2	7.87	C03			
	C04	30-May-00	R2M	0	14.8	1.50	1.9	8.87	0	14.55	1.50	1.9	8.850	C04			
	C05	08-May-00	R2M Bench 2	0	15.1	1.42	1.1	8.85	0	15.7	1.42	1.1	8.850	C05			
	C06	28-May-00	R2M	0	15.5	1.38	2.0	8.85	0	15.30	1.38	2.0	8.850	C06			
	C07	28-Jun-00	R2M 1/2 Bench 1	4.350	7.9	0.52	2.1	8.850	26%	4.350	7.9	0.52	2.1	8.850	C07		
	C08	28-Jun-00	R2M 2 Bench 2	5.316	18.9	0.75	1.8	8.550	31%	14.179	10.9	0.75	1.8	8.550	C08		
	C09	00-Jan-00	0	0	0.00	0.0	0	0	0	0	0.00	0.0	0	C09			
	C10	18-Jun-00	R2M 1/2 Bench 1	0	0	0.00	0.0	0	0	0	0.00	0.0	0	C10			
	C11	04-Jun-00	R2M 1/2	0	16.3	0.64	0.5	8.55	0	16.55	0.64	0.5	8.550	C11			
	C12	00-Jan-00	0	0	0.00	0.0	0	0	0	0	0.00	0.0	0	C12			
	C13	22-Jun-00	Min 7 Bench 1 & 2	0	0	0.00	0.0	0	0	0	0.00	0.0	0	C13			
	C14	02-Apr-00	R2M 2 Bench 2	0	13.3	2.25	2.7	8.55	0	23.400	15.3	2.25	2.7	8.528	C14		
	C15	00-Jan-00	0	0	0.00	0.0	0	0	0	0	0.00	0.0	0	C15			
	C16	23-May-00	R2M 1/2 Bench 1	7.25	11.9	1.55	2.3	8.55	4%	6.548	11.9	1.55	2.3	8.550	C16		
	C17	25-Jun-00	R2M 2 Bench 2	1.181	11.3	0.96	1.1	8.550	7%	11.258	11.3	0.96	1.1	8.550	C17		
	C18	22-May-00	R2M 1/2 Bench 1	7.17	11.9	1.57	2.0	8.550	4%	6.144	11.9	1.57	2.0	8.550	C18		
	C19	00-Jan-00	0	0	0.00	0.0	0	0	0	0	0.00	0.0	0	C19			
	C20	00-Jan-00	0	0	0.00	0.0	0	0	0	0	0.00	0.0	0	C20			
	C21	17-Apr-00	R2M 2 Bench 2	0	14.1	1.80	3.2	8.550	0	10.596	14.1	1.80	3.2	8.550	C21		
	C22	28-Jun-00	R2M 1/2 Bench 1	0	15.5	1.41	1.1	8.550	0	3.831	15.5	1.41	1.1	8.550	C22		
	C23	28-Jun-00	R2M 1/2 Bench 2	0	15.8	1.45	1.1	8.550	0	7.518	15.2	1.45	1.1	8.550	C23		
	C24	00-Jan-00	0	0	0.00	0.0	0	0	0	0	0.00	0.0	0	C24			
	C25	00-Jan-00	0	0	0.00	0.0	0	0	0	0	0.00	0.0	0	C25			
	C26	00-Jan-00	0	0	0.00	0.0	0	0	0	0	0.00	0.0	0	C26			
	C27	00-Jan-00	0	0	0.00	0.0	0	0	0	0	0.00	0.0	0	C27			
	C28	00-Jan-00	0	0	0.00	0.0	0	0	0	0	0.00	0.0	0	C28			
	C29	00-Jan-00	0	0	0.00	0.0	0	0	0	0	0.00	0.0	0	C29			
	C30	00-Jan-00	0	0	0.00	0.0	0	0	0	0	0.00	0.0	0	C30			
	C31	00-Jan-00	0	0	0.00	0.0	0	0	0	0	0.00	0.0	0	C31			
	C32	00-Jan-00	0	0	0.00	0.0	0	0	0	0	0.00	0.0	0	C32			
	C33	00-Jan-00	0	0	0.00	0.0	0	0	0	0	0.00	0.0	0	C33			
	C34	00-Jan-00	0	0	0.00	0.0	0	0	0	0	0.00	0.0	0	C34			
	C35	00-Jan-00	0	0	0.00	0.0	0	0	0	0	0.00	0.0	0	C35			
C36	00-Jan-00	0	0	0.00	0.0	0	0	0	0	0.00	0.0	0	C36				
C37	00-Jan-00	0	0	0.00	0.0	0	0	0	0	0.00	0.0	0	C37				
C38	00-Jan-00	0	0	0.00	0.0	0	0	0	0	0.00	0.0	0	C38				
C39	00-Jan-00	0	0	0.00	0.0	0	0	0	0	0.00	0.0	0	C39				
C40	00-Jan-00	0	0	0.00	0.0	0	0	0	0	0.00	0.0	0	C40				
C41	00-Jan-00	0	0	0.00	0.0	0	0	0	0	0.00	0.0	0	C41				
C42	00-Jan-00	0	0	0.00	0.0	0	0	0	0	0.00	0.0	0	C42				
C43	00-Jan-00	0	0	0.00	0.0	0	0	0	0	0.00	0.0	0	C43				
C44	00-Jan-00	0	0	0.00	0.0	0	0	0	0	0.00	0.0	0	C44				
C45	00-Jan-00	0	0	0.00	0.0	0	0	0	0	0.00	0.0	0	C45				
C46	00-Jan-00	0	0	0.00	0.0	0	0	0	0	0.00	0.0	0	C46				
C47	00-Jan-00	0	0	0.00	0.0	0	0	0	0	0.00	0.0	0	C47				
C48	00-Jan-00	0	0	0.00	0.0	0	0	0	0	0.00	0.0	0	C48				
C49	00-Jan-00	0	0	0.00	0.0	0	0	0	0	0.00	0.0	0	C49				
C50	00-Jan-00	0	0	0.00	0.0	0	0	0	0	0.00	0.0	0	C50				
C51	00-Jan-00	0	0	0.00	0.0	0	0	0	0	0.00	0.0	0	C51				
C52	00-Jan-00	0	0	0.00	0.0	0	0	0	0	0.00	0.0	0	C52				
C53	00-Jan-00	0	0	0.00	0.0	0	0	0	0	0.00	0.0	0	C53				
C54	00-Jan-00	0	0	0.00	0.0	0	0	0	0	0.00	0.0	0	C54				
C55	00-Jan-00	0	0	0.00	0.0	0	0	0	0	0.00	0.0	0	C55				
C56	00-Jan-00	0	0	0.00	0.0	0	0	0	0	0.00	0.0	0	C56				
C57	00-Jan-00	0	0	0.00	0.0	0	0	0	0	0.00	0.0	0	C57				
C58	00-Jan-00	0	0	0.00	0.0	0	0	0	0	0.00	0.0	0	C58				
C59	00-Jan-00	0	0	0.00	0.0	0	0	0	0	0.00	0.0	0	C59				
C60	00-Jan-00	0	0	0.00	0.0	0	0	0	0	0.00	0.0	0	C60				
C61	00-Jan-00	0	0	0.00	0.0	0	0	0	0	0.00	0.0	0	C61				
C62	00-Jan-00	0	0	0.00	0.0	0	0	0	0	0.00	0.0	0	C62				
C63	00-Jan-00	0	0	0.00	0.0	0	0	0	0	0.00	0.0	0	C63				
C64	00-Jan-00	0	0	0.00	0.0	0	0	0	0	0.00	0.0	0	C64				
C65	00-Jan-00	0	0	0.00	0.0	0	0	0	0	0.00	0.0	0	C65				
C66	00-Jan-00	0	0	0.00	0.0	0	0	0	0	0.00	0.0	0	C66				
C67	00-Jan-00	0	0	0.00	0.0	0	0	0	0	0.00	0.0	0	C67				
C68	00-Jan-00	0	0	0.00	0.0	0	0	0	0	0.00	0.0	0	C68				
C69	00-Jan-00	0	0	0.00	0.0	0	0	0	0	0.00	0.0	0	C69				
C70	00-Jan-00	0	0	0.00	0.0	0	0	0	0	0.00	0.0	0	C70				
C71	00-Jan-00	0	0	0.00	0.0	0	0	0	0	0.00	0.0	0	C71				
C72	00-Jan-00	0	0	0.00	0.0	0	0	0	0	0.00	0.0	0	C72				
C73	00-Jan-00	0	0	0.00	0.0	0	0	0	0	0.00	0.0	0	C73				
C74	00-Jan-00	0	0	0.00	0.0	0	0	0	0	0.00	0.0	0	C74				
C75	00-Jan-00	0	0	0.00	0.0	0	0	0	0	0.00	0.0	0	C75				
C76	00-Jan-00	0	0	0.00	0.0	0	0	0	0	0.00	0.0	0	C76				
C77	00-Jan-00	0	0	0.00	0.0	0	0	0	0	0.00	0.0	0	C77				
C78	00-Jan-00	0	0	0.00	0.0	0	0	0	0	0.00	0.0	0	C78				
C79	00-Jan-00	0	0	0.00	0.0	0	0	0	0	0.00	0.0	0	C79				
C80	00-Jan-00	0	0	0.00	0.0	0	0	0	0	0.00	0.0	0	C80				
C81	00-Jan-00	0	0	0.00	0.0	0	0	0	0	0.00	0.0	0	C81				
C82	00-Jan-00	0	0	0.00	0.0	0	0	0	0	0.00	0.0	0	C82				
C83	00-Jan-00	0	0	0.00	0.0	0	0	0	0	0.00	0.0	0	C83				
C84	00-Jan-00	0	0	0.00	0.0	0	0	0	0	0.00	0.0	0	C84				
C85	00-Jan-00	0	0	0.00	0.0	0	0	0	0	0.00	0.0	0	C85				
C86	00-Jan-00	0	0	0.00	0.0	0	0	0	0	0.00	0.0	0	C86				
C87	00-Jan-00	0	0	0.00	0.0	0	0	0	0	0.00	0.0	0	C87				
C88	00-Jan-00	0	0	0.00	0.0	0	0	0	0	0.00	0.0	0	C88				
C89	00-Jan-00	0	0	0.00	0.0	0	0	0	0	0.00	0.0	0	C89				
C90	00-Jan-00	0	0	0.00	0.0	0	0	0	0	0.00	0.0	0	C90				
C91	00-Jan-00	0	0	0.00	0.0	0	0	0	0	0.00	0.0	0	C91				
C92	00-Jan-00	0	0	0.00	0.0	0	0	0	0	0.00	0.0	0	C92				
C93	00-Jan-00	0	0	0.00	0.0	0	0	0	0	0.00	0.0	0	C93				
C94	00-Jan-00	0	0	0.00	0.0	0	0	0	0	0.00	0.0	0	C94				
C95	00-Jan-00	0	0														

## OPTIMISATION MODELLING

The above sheets (which formed one continuous sheet in the program; Figures 5 & 6) showed the data imported from the previous load for the crushed coal stockpiles, ROM coal and 4 week projections.

These were given to supply the operator with the option of using upcoming coal extractions or ROM stockpile reserves that still require crushing to be utilised. This program was used on a daily basis but had the option to be run on any time frame.

The operator could opt to use certain stockpiles or not by pushing one of the buttons under the "SAMPLE IN/OUT" column (stockpiles not being used having the cell being highlighted in blue). Pushing the button a second time would restore the current value to the sheet.

The optimisation routine used these as starting values. The stockpile limits and options set in the previous sheet were then used to find the best solution for blending.

When this sheet was complete, the operator returned to the Interface Control page and selected the appropriate optimisation. Optimisations available were as follows.

- to optimise to meet a specification in ash,
- to optimise to meet a specification in sulphur,
- optimise to minimise use of a certain (good quality) stockpile,
- optimise to maximise use of a certain (poor quality) stockpile.

### **Optimisation Report**

Once the optimisation was selected, a blend optimisation report was produced as follows (Figures 7 & 8).

BLEND OPTIMISATION REPORT												
Jellinbah Resources												
CENTRAL & PLAINS												
INPUT COM TYPE NAME: SSB (Product 2) to the Slot												
SAP#	Date	PK	Splice & Results	Stockpile & Not Used	USED Tonnes	LEFT Tonnes	Ash	TS	CSW	SE dal	BWdX	Approx No of Trucks / Loads
C01	04-May-00	R12S06				3.532	20.3	1.04	0.9	7.742		
C02	26-May-01	Ramp 9 RDM				1.317	21.7	0.93	0.6	8.376		
C03	07-Jun-01	R8N10 Beh 2				18.315	14.0	1.54	1.2	7.877		
C04	20-May-01	R09 N10				14.758	14.8	1.58	1.9	8.550		
C05	04-May-01	R1004 Bench 2				3.887	15.1	1.42	1.4	8.550		
C06	31-May-01	R08 N10				9.300	15.6	1.68	2.0	8.550		
C07	28-Jun-01	R12 S09 Beh 1			4.390	0	7.9	0.52	2.4	8.550	26%	29
C08	26-Jun-01	R8N10 Bench 2			5.316	8.863	10.9	0.75	1.8	8.550	21%	35
C09						0						
C10	28-Jun-01	R12 S09 Beh 1		X		4.825	8.1	0.52	2.2	8.550		
C11	04-Jun-01	R1 S08 L				2.955	16.3	0.84	0.5	8.550		
C12						0						
C13	22-Jun-01	Max 7 Bench 2 & 3		X		6.316	7.8	0.36	4.0	8.550		
C14	02-Apr-01	R12S08 Bench 2				23.400	13.2	2.28	2.7	8.528		
C15						0						
C16	23-May-01	R1004 Beh 2			725	6.933	11.9	1.58	2.3	8.550	4%	5
C17	26-Jun-01	R8N10 Bench 2			1.181	10.287	11.3	0.99	1.1	8.550	7%	5
C18	22-May-01	R1004 Beh 2			747	5.396	11.9	1.57	2.0	8.550	4%	5
C19	16-Jun-01	MAX 7 Ltr 2		X		2.352	6.2	0.36	3.7	8.550		
C20	10-Dec-00	R9S09 Beh 1				10.555	14.1	1.60	3.2	8.550		
C21	17-May-01	R1004 Beh 2 less part				3.831	15.6	1.41	1.4	8.550		
C22	20-Jun-01	R8N10 Pts Lwr Bench 2				7.548	13.8	1.49	1.1	8.550		
C23	03-Jun-01	R12 S08				850	12.6	1.95	0.5	8.550		
C24						0						
ST6						0						
ST52						0						
STM						0						
STM2						0						
STM	28-Jun-01	R12 S09 Beh 1		X		190	8.1	0.52	2.2	8.550		
STM2						0						
						0						
Max 07				X		3.500	6.6	0.37				
R12S08						0						
R1004						0						
R6N12				X		17.000	9.7	0.66				
Max 08				X		3.500	6.6	0.37				
R15N06						0						
R8N10 Beh 2				X		12.000	11.2	0.92				
R8N10 Beh 3				X		36.000	11.0	1.00				

Figure 7 Report Sheet 1 of 2.

## OPTIMISATION MODELLING

BLEND OPTIMISATION REPORT												
Jellinbah Resources												
CENTRAL & PLAINS												
INPUT COAL TYPE HERE: SSB (Product 2) to the Slot												
S/Pile	Date	PK	Spillou s Results	Stockpile s Not Used	USED Tonnes	LEFT Tonnes	AsH	YS	CSW	SE dal	BlendX	Approx No of Trucks / Loads
Top of Ramp 1	07-Jun-01	Max Stup8		X		3 000	9.5	0.35				
Top of Ramp 1	pre 18/05/01	Ramp 1		X		1 000	15.0	0.56				
Top of Ramp 6	pre 18/05/01	Ramp 6		X		3 000	20.0	0.84				
Top ROM / ROM 1		RO8N10 Bch 2				0	14.0	1.60				
ROM 2	04-Apr-01					0						
ROM 3	08-Jun-01	RO8 N10 Bch 2		X		4 134	15.0	1.25				
ROM 4						0						
ROM 5						0						
ROM 6						0						
ROM 7						0						
ROM 8		Dirty Coal		X		6 000	15.0	0.80				
ROM 9	01-Jun-99	Really Dirty Coal		X		66 500	23.0	1.00				
P01	26-Jun-01	Px 1 Block 1 Lit 7 & 8			2 287	863	8.9	0.52	1.0	8 550	13%	15
P02	29-Jun-01	Px 1 Block 1 Lit 7 & 8			2 254	146	8.8	0.46	1.0	8 550	14%	16
P03						0						
P04						0						
P05						0						
P06						0						
P07						0						
P08						0						
P09						0						
P10						0						
P11						0						
P12						0						
P13						0						
P14						0						
P15						0						
P16						0						
P17						0						
P18						0						
P19						0						
P20	25-May-01	Clean up "FOR S/Pile Base"		X		1 151	15.6	0.02		7 325		
P21						0						
P22						0						
Good ROM INVENTORY						0						
Int ROM INVENTORY				X		41 770	9.4	0.44				
Bad ROM INVENTORY				X		6 569	15.0	0.50				
<b>TOTAL</b>		<b>Central + Plains</b>				<b>17,000</b>	<b>10</b>	<b>9.7</b>	<b>0.71</b>		<b>100%</b>	<b>113</b>

Figure 8 Report Sheet 2 of 2.

The above sheets (which again formed one continuous sheet in the program) gave the following outputs.

- percentage break up and number of trucks / loads to be used for each stockpile.
- the quality associated with each stockpile,
- an overall quality.

### Intra-Day Stockpile Modelling Outcomes

Testing this program made stockpile strategies simpler and more efficient.

Several trials indicated that using the program produced a blend that minimised the use of the mostly valuable high quality blend component by 10 to 20% over conventional user methods. That is, 10 to 20% less high quality coal was used.

This had a complimentary effect of utilising an equivalent amount less of the poorer quality coals. This in turn greatly aided in producing more space for stockpiling and faster turn over of old stockpiles.



# GREATER SYDNEY REGION AUDIT AND GAPS ANALYSIS

David J Och

Geological Survey of New South Wales,  
Department of Primary Industries

## ABSTRACT

The Geological Survey of New South Wales (GSNSW), has commenced an audit and gaps analysis of geoscience data for the Greater Sydney Region (GSR). This task was initiated following concerns expressed by the New South Wales Committee for the Coordination Government Geological Program regarding the potential loss of important geoscientific data and the need for a new generation of geological maps for the region.

The audit and gaps analysis report will be used to inform a future program of geological mapping and resources assessment. Data will ultimately be compiled into a comprehensive 3D data set for application in land use, infrastructure and resource planning embracing Australia's largest population centre.

## CURRENT MAP SERIES

The Greater Sydney Region geological map series comprises:

- Five published 1:250,000 geological maps covering Singleton, Newcastle, Sydney, Wollongong and Ulladulla (Table 1; Figure 1). All these maps date back to 1966; with exception of the Ulladulla metallogenic map. Explanatory notes only exist for Sydney and Newcastle.
- Seven published 1:100,000 geological maps (Table 1; Figure 2) covering the populated coastal zone of Gosford – Sydney – Penrith – Wollongong and to the north Bulahdelah – Dungog – Camberwell, exist out of the possible 23 1:100,000 geological sheets for the Greater Sydney Region. Although all these maps are greater than 20 years old, many are widely used by government agencies, councils and geoconsultancies, to name a few. Some unpublished 1:100,000 maps (Newcastle, Cessnock and Port Stephens) also exist. Separate explanatory notes exist for Sydney, Wollongong – Port Hacking, and the Penrith sheets with a combined explanatory notes volume for the other three maps to the north.
- A limited number of 1:50,000 geological maps (Table 1; Figure 3) were published in the early 1970's, (Coricudgy, Glen Alice, Glen Davis, Katoomba, Kiama, Mellong, Olinda, Robertson, Windsor, and Wollongong), as a result of the Central Coast construction material studies. Other maps (Avon, Burragorang, Jamison, Jervis Bay – Currarong, Mittagong – Bullio, Moss Vale – Wingello, Nowra – Toolijooa and Yerranderie) also exist in unpublished form. Only explanatory notes exist for

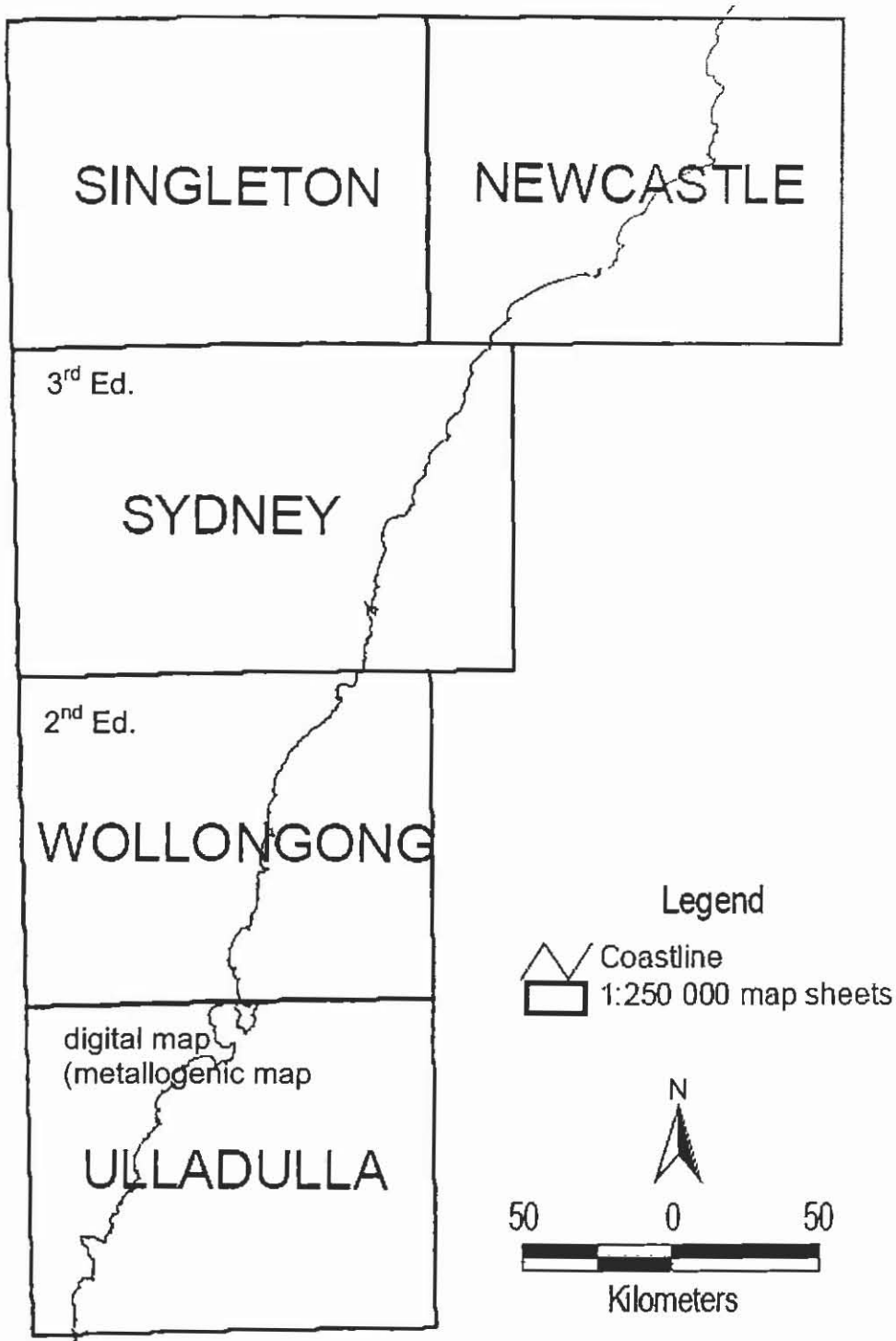


Figure 1. Coverage of published 1:250,000 geological map series for the Greater Sydney Region

GREATER SYDNEY REGION AUDIT

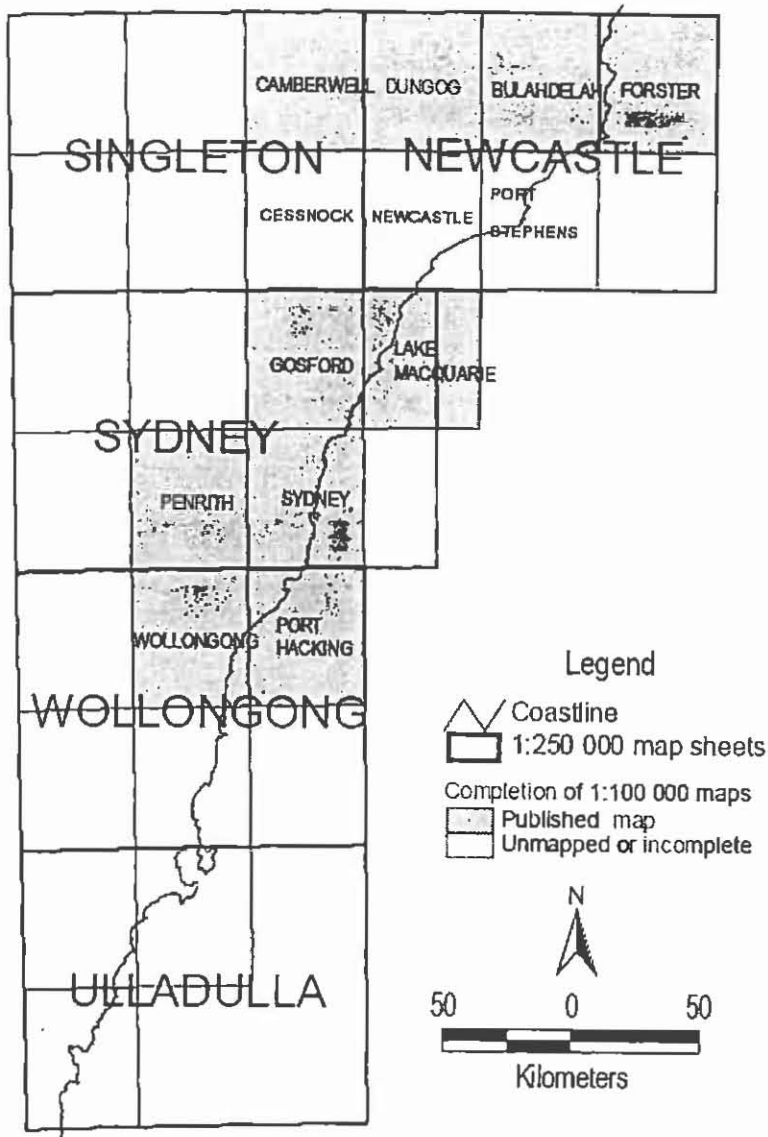


Figure 2. Extent of published 1:100,000 geological map sheet series for the Greater Sydney Region.

**GEOLOGICAL MAPS  
1:50 000**

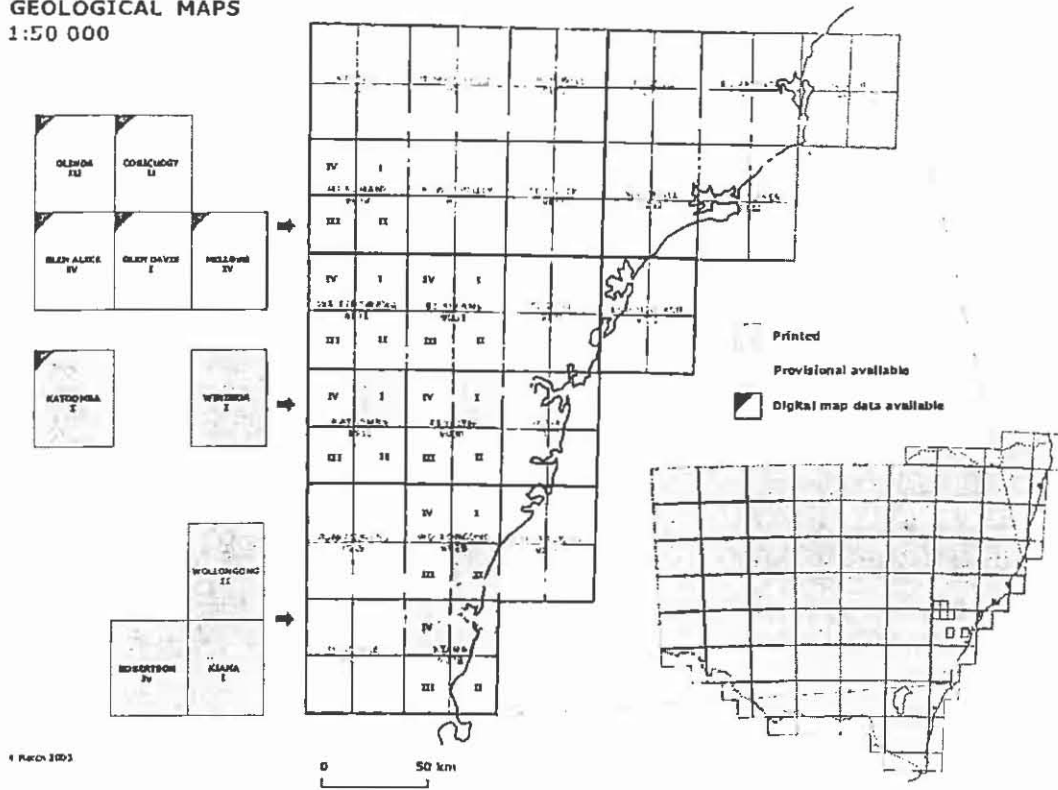


Figure 3. Extent of published 1:50,000 geological map sheets for the Greater Sydney Region.

**GEOLOGICAL MAPS  
1:25 000**

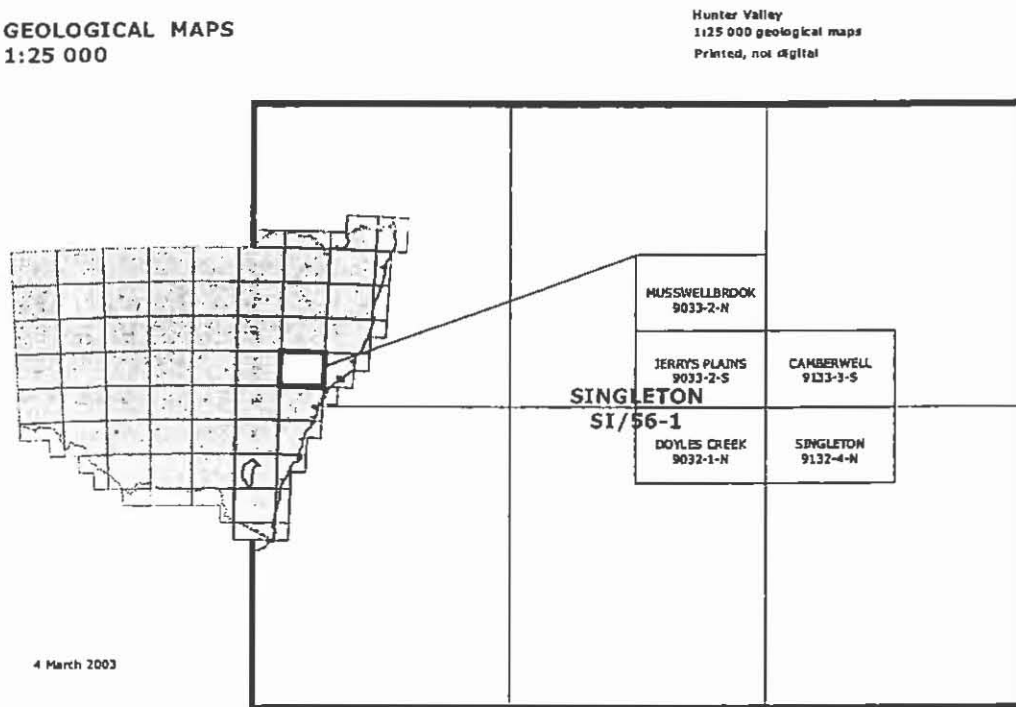


Figure 4. Extent of published 1:25,000 geological map sheets for the Greater Sydney Region.

## GREATER SYDNEY REGION AUDIT

A comprehensive literature study is now underway for the region with results being compiled into a citation manager called Endnote. This software has the ability to store multiple data on any publication. It allows and PDF's of publications or their URL's where they can be obtained from, to be linked. Images such as maps can be stored on file for easy access. Also, most publication (conference proceedings, journals, books etc.) entered into this software have had their abstracts or summaries scanned as text. All data entered is associated with a map sheet number and keywords. This and the GSNSW's DIGS database allows for easy retrieval of data relevant to an individual map sheet, geological feature or location (Figure 5, 6, and 7). These data will also be compiled into ArcGIS to provide a spatial relationship of all these data collected e.g. publications, theses (Figure 8(a)), geochemistry, geophysics (Figure 8(b)), maps, cross sections and bore logs. Once these data are all compiled a gaps analysis will be undertaken and used to inform the selection of areas of future work.

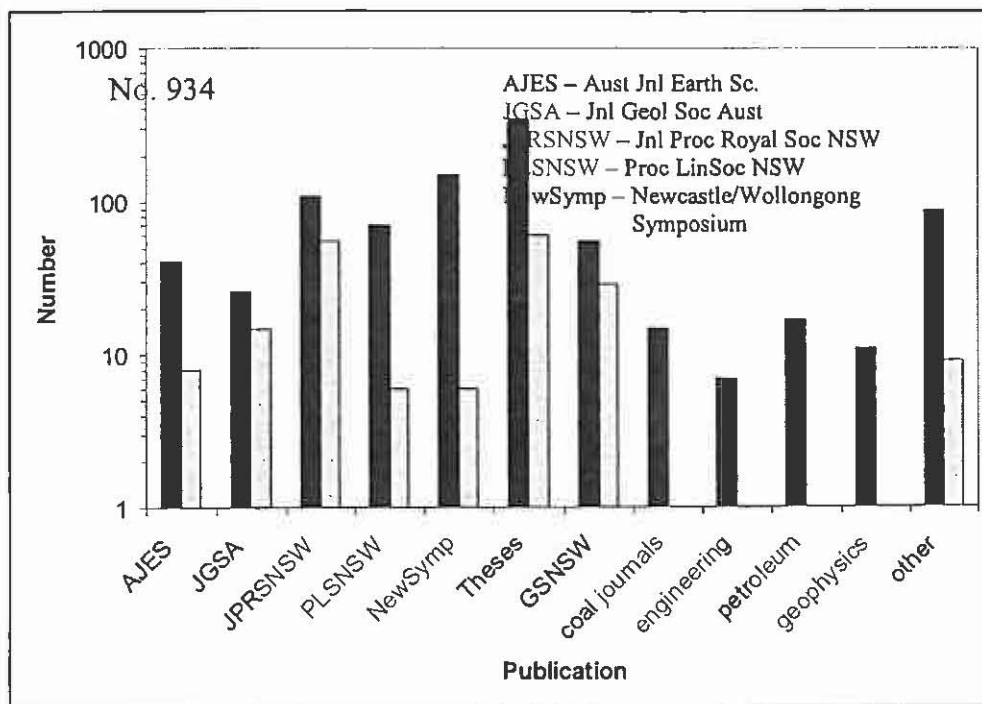


Figure 5. Histogram plotting the number of sourced published journals and theses (maps) for the Greater Sydney Region. Black – publications; grey – maps.

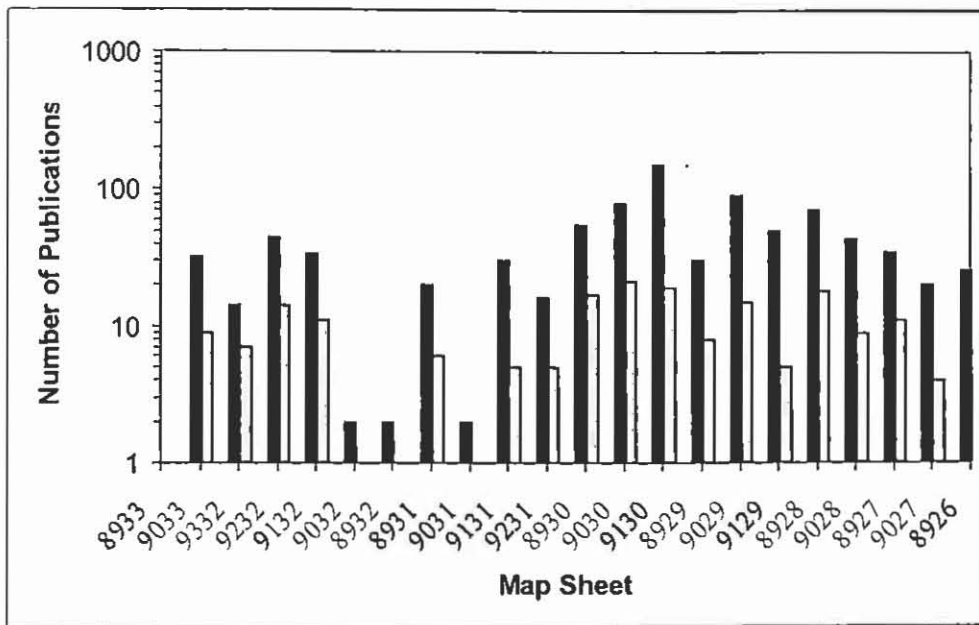


Figure 6. Histogram plotting sourced non GSNSW Publications against Greater Sydney Region 1:100,000 geological map sheets. Black – publications; grey – maps.

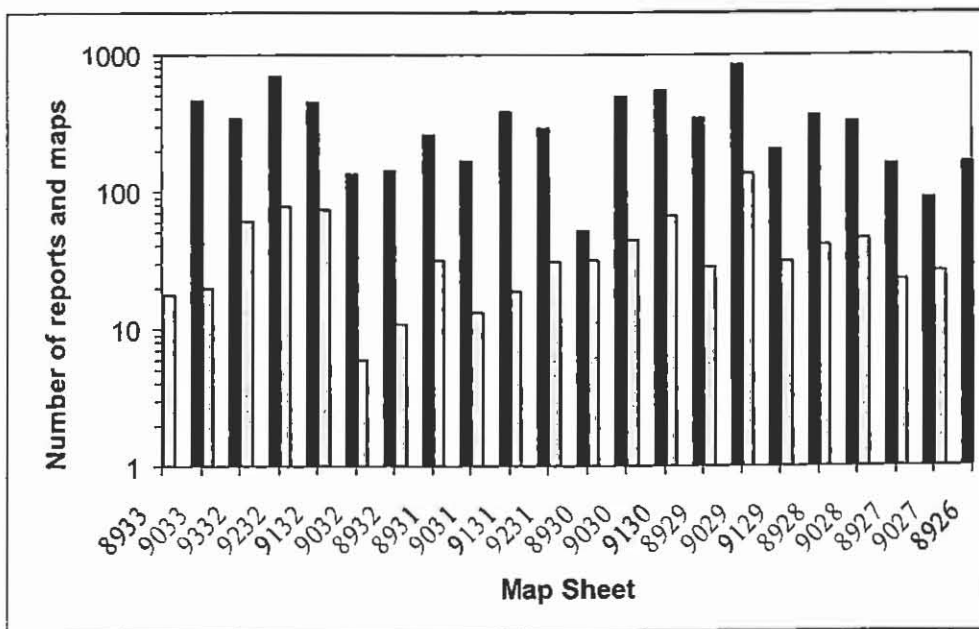


Figure 7. Histogram plotting sourced GSNSW reports and maps (DIGS) against Greater Sydney Region 1:100,000 geological map sheets. Black – reports; grey – maps.

## GREATER SYDNEY REGION AUDIT

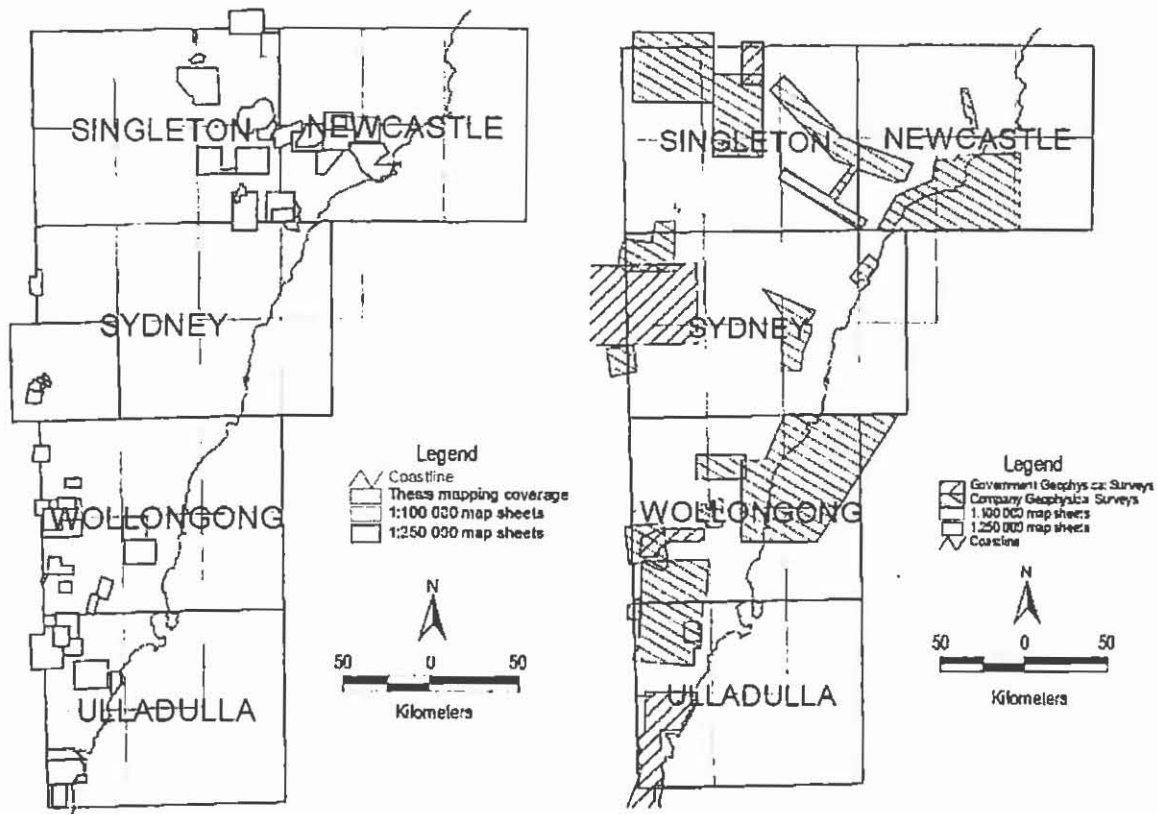


Figure 8. ArcGIS compilation of (a) theses and (b) geophysical data (after MacRae (2003)).

### WHERE TO FROM HERE?

The audit and gaps analysis report for the Greater Sydney Region is due for completion in March 2008. Once completed, the report will be circulated to a range of government agencies and councils etc for information and comment. It is hoped the report will provide the basis for a well informed plan to upgrade the geoscientific data for the Greater Sydney Region.

### THE POTENTIALS FOR SUCH A MAPPING PROGRAMME

This process of information assessment and collation will be the first step in a project to provide a world class geoscience information framework to advise the future growth of this world class city.

### ACKNOWLEDGEMENTS

Published with permission of the Deputy Director-General, NSW Department of Primary Industries – Mineral Resources.

### REFERENCE:

MACRAE, G. P. 2003. *Brief review of requirements for remapping of Greater Sydney Region 1:250 000 Standard Geological Maps*. Department of Mineral Resources Sydney, pp. 1-16.



# FACTORS AFFECTING WATER QUALITY IN THE WINGECARRIBEE SHIRE COUNCIL LOCAL GOVERNMENT AREA.

M. O'Donnell<sup>1</sup>, G. O'Brien<sup>2</sup>, A. Hutton<sup>1</sup>

<sup>1</sup>School of Earth and Environmental Sciences, University of Wollongong,  
NSW 2522

<sup>2</sup>Department of Chemistry, University of Wollongong,  
NSW 2522

## ABSTRACT

Wingecarribee Local Government Area (LGA) comprises approximately 2700 km<sup>2</sup> of chiefly agricultural and undeveloped land with scattered towns and villages. The Wingecarribee LGA includes the headwaters of several regionally significant rivers and some of Sydney's water catchment. Good water quality is therefore important for the local and wider community, as well as for ecological health.

The University of Wollongong staff and students undertook a water quality monitoring program on behalf of Wingecarribee Shire Council between May 2002 and July 2004. A large range of chemical, physical and biological parameters was measured. Dissolved oxygen, turbidity, pH, ORP, temperature, nutrients, conductivity and faecal coliforms were collected for the entire, 26 approximately monthly sampling trips. Chlorophyll a, pheophyton, alkalinity and blue-green algae were determined over a shorter period. Sediment samples were collected and analysed for the determination of pesticides and metal contamination.

The sampling period included the particularly hot and dry summer of 2002/2003 and a return to less extreme conditions after March 2003. A comparison of water quality results from these different climatic regimes facilitates the discussion of the possible environmental impact to stream water quality, of continued drying and warming, as is predicted by some models (Whetton et al. 2005) for S.E.Australia.

## INTRODUCTION AND BACKGROUND

Wingecarribee LGA (Fig 1) is located 110 to 200 km southwest of Sydney, at approximate latitude 34°30'S and longitude 150°30'E. The majority of the LGA is above 630 m in elevation and is therefore often referred to as the Southern Highlands.

Waterways include the Nepean, Wollondilly, Wingecarribee, Shoalhaven and Paddy's Rivers. Several of these rivers have cut deep gorges. Almost all the flow of these rivers is impounded in water storage reservoirs for use in Sydney and the region, with some released for environmental flows. Wingecarribee and Fitroy Falls Reservoirs are within the LGA and local rivers are used currently to transfer significant amounts of water northwards. Such water transfers can impact stream biota.

The local climate is generally cooler than the neighbouring coastal areas due to elevation and distance from the moderating effect of the sea. Rainfall is highest in the east, with an average

of 1600 mm per annum, due to orographic effects, but decreases to 850 mm per year in the west. Precipitation is generally evenly spread throughout the year.

The surface geology of the region is dominated by the Wianamatta Shale, Tertiary volcanics and the Hawkesbury Sandstone. The type and utility of the soil developed is strongly related to these parent materials with the shale and volcanic rocks producing sought after agricultural soils. Water quality is also strongly effected by geology, soil type and land use. Water quality is lower on the shale and volcanic derived soils in agricultural and urban areas and higher on the undeveloped sandstone country. The underlying Triassic and Permian sedimentary rocks are exposed in the deep gorges and at the margins of the LGA.

Land use includes urban (4.2% of the LGA), agriculture, grazing and cropping (43.7% combined) state forest, water catchment and national parks (52.1% combined). There is limited manufacturing.



Figure 1. Wingecarribee Shire LGA showing sites discussed in this paper.

#### PARAMETERS MEASURED AND QUALITY CONTROL

Physicochemical water quality parameters, including, temperature, pH, dissolved oxygen (% and mg/L), oxidation-reduction potential (ORP), turbidity and conductivity/salinity were determined on either a YeoCal 711 or a YSI 6820 multi-probe. Logbooks were kept on daily calibrations and checks, with standard solutions. In all cases, samples and data were collected either by, or under the direct supervision of, a trained and experienced employee the university.

Samples for nutrients and metals were field filtered and kept on ice, then immediately frozen on return to the laboratory. Separate samples for total metals and nutrients were treated in the same way.

## WINGECARRIBEE WATER QUALITY

Alkalinity samples were field filtered into a gas tight glass tube with no headspace, kept cool and analysed as soon as possible. Chlorophyll samples were wrapped in aluminium foil, kept on ice and filtered immediately on return to the laboratory. The glass fibre filter was then frozen for later analysis. Faecal coliform samples were collected with due regard for contamination, using gloves and avoiding contact with the lip of the sterilised jar. Samples were kept cool with an air gap in the jar. Analysis was conducted within 24 hours.

All external analyses, such as for nutrients and faecal coliforms, were performed by NATA accredited laboratories. Quality control samples were routinely included in all sample despatches and included certified standards, internal standards, replicates, blanks and inter-laboratory comparisons. Data quality objectives were exceeded on all occasions.

### RESULTS AND DISCUSSION

The state of a water body can be measured and described using a range of physical, chemical and biological properties. As our understanding increases these parameters can be used to explain the processes operating in such a body. As the balance of our interest moves from science to management, water quality indicators can be used to evaluate the quality of the water body against guidelines such as those of the Australian and New Zealand Environment and Conservation Council (ANZECC 2000). Obtaining values outside of these guidelines does not necessarily infer poor water quality, but may only indicate the need for further investigations. If further investigations are mandated, guideline values become trigger values, facilitating efficient management of the environment. Local guideline values should be developed reflecting local geology, environments and climate, rather than relying on default values (ANZECC & ARMCANZ 2000).

No individual measured parameter can characterize the quality of a water body and the selection of parameters is dependant on the water body's values or uses. Thus the design of water quality sampling programs is dependent on a range of factors including the ecological values and human uses of the water body, cost, and the utility, relevance and scientific credibility of parameters.

The comparison of different water quality studies is hampered by differing sample design, as well as data quality and availability. The complexity of this task is increased by the lack of appropriate statistical tools for data that varies in sample size and other attributes. Many studies restrict analysis to a comparison of means, ranges and other simple statistical tools. This is the approach adopted here, with the inclusion of medians for non-normally distributed and log transformed data such as faecal coliforms and pH.

Wingecarribee Shire Council Integrated Water Quality Study data is compared with two other studies: Wollongong Wide Water Quality Study (WWWQS) (conducted by the University of Wollongong in collaboration Wollongong City Council and Sydney Water) and data from a Shellharbour City Council River Study. Comparison has been facilitated by similar sampling methodology, parameters, equipment and training. Limitations include differences in duration, frequency and timing.

### Parameters and Indicators

#### pH

The ANZECC (2000) guidelines recommend generally neutral pH values (between 6.5 and 7.5) for upland rivers. Divergences from these values can influence the solubility and/or

Table 1. Comparison of Council Water Quality Monitoring Projects

Indicator	Wollongong*1			Wingecaribee*2			Shellharbour*3		
	33 sites			15 sites			2 sites		
	Mean or median ^	Range	n	Mean or median ^	Range	n	Mean or median ^	Range	n
<i>Physical</i>									
Conductivity uS/cm	552	21-2941	723	231	36-750	195	195	65-464	55
Turbidity ntu	38	0.1-600	419	20	0-491	195	8	0-187	58
Temperature °C	17	9.3-34	741	15.4	6.6-31.6	195	16.6	8.8-26.6	63
<i>Microbiological</i>									
Faecal Coliforms cfu/100ml	350^	0-140,000	733	90^	0-36000	207	62^	0-650	53
<i>Chemical</i>									
pH	7.82^	3.33-9.16	671	7.11^	5.95-9.41	195	7.19^	6.01-8.71	59
ORP mv	289	-65-524	358	332	16.7-570	195			
<i>Dissolved</i>									
Oxygen %	76	94-212	314	76	10.4-169	195	99	36-163	59
Dissolved Oxygen mg/L	8	0.82-18	739	7.7	0.9-13.5	195	9.7	3-17.7	59
Total Phosphorous mg/L	0.08	0.004-2.4	303	0.1	0.1-19.94	211	0.048	0-0.44	69
Total Nitrogen mg/L	0.56	0-5.05	261	2.29	0.16-27	211	0.45	0-1.28	69
TKN mg/L	0.37	0-2.75	302	1.2	0-22.4	211			
Ammonia mg/L	0.03	0-1.94	719	0.45	0-16.58	204			
Nitrate mg/L	0.18	0-3.6	544	1.06	0-13.11	210			

\*1 Wollongong Wide Water Quality Study 2000-2003, \*2 Wingecaribee Integrated Water Quality Study 2002-2004 (this paper), \*3 Shellharbour River Study 1999-2003

toxicity of many compounds. The pH of the streams in the WSC area is generally neutral and is closer to pH of 7 than other areas listed in Table 1. In general lower pH was accompanied by lower alkalinity values and this was found to occur mostly at sites dominated by Hawkesbury sandstone.

The Nepean River at the Tourist Rd (Fig 2) has low levels of dissolved salts such as carbonate that can buffer pH, due to the sandstone derived soils. The correlation between the dissolved salts and pH reflects this. Increasing atmospheric carbon dioxide will lower stream pH and increase weathering of parent material, releasing more dissolved salts.

## WINGECARRIBEE WATER QUALITY

### Conductivity

In freshwater, the concentration of dissolved salts (usually ionic species, such as, chloride, carbonate, bicarbonate, sulphate, sodium, calcium, magnesium and potassium) is usually determined indirectly as electrical conductivity (referred to hereafter as conductivity). Salts, while essential to life, can have a detrimental effect at high concentrations. Excessive salt reduces agricultural productivity and can destroy infrastructure such as roads and buildings

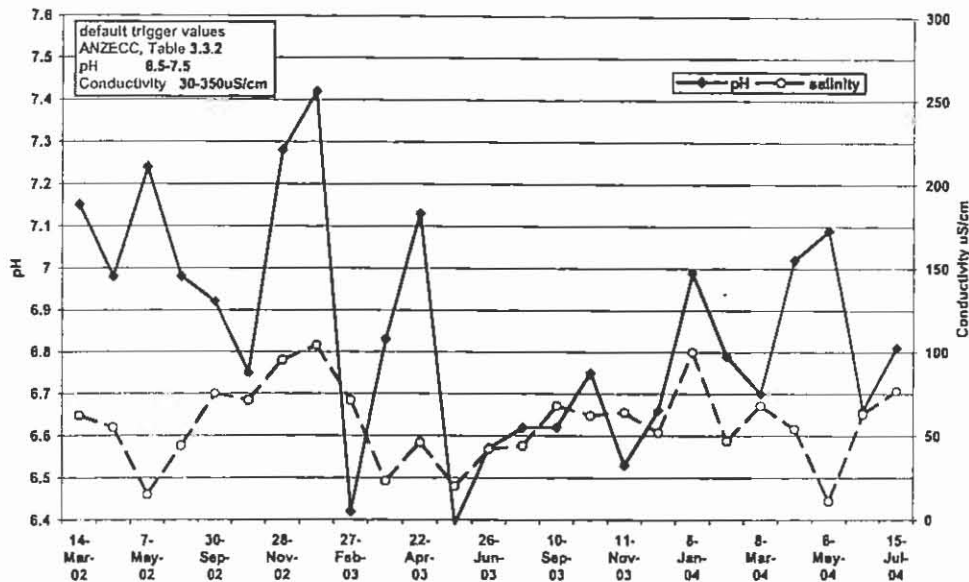


Figure 2. pH and Conductivity values, Nepean River at Tourist Rd.

through efflorescence, the process whereby the growth of salt crystals destroys the fabric of masonry and other materials (NSW EPA, 2000).

ANZECC (2000) guidelines provide a large range for conductivity values in lowland rivers (33-350  $\mu\text{S/cm}$ ) reflecting the natural variability of this parameter. In this study the lowest values in the region occur on the Hawkesbury Sandstone and the highest on the Wianamatta Shale. The sources for the high conductivity include connate salt within the Wianamatta Shales of marine origin, atmospheric deposition and storage of marine salt over long periods of time and dissolution of minerals within the volcanic rocks. The sewage treatment plants also release elevated salt. Salinisation is predicted to become a significant problem in the region if current land practices continue.

### Temperature

Temperature values followed the expected seasonal patterns with small additional variations linked to the degree of shading at any particular site. In this study free flowing streams are all generally within a few degrees of each other on any sampling occasion. The 2003/2004 summer maximum stream temperatures are typically 18-21 $^{\circ}\text{C}$  similar to the average maximum temperature of 18.9 $^{\circ}\text{C}$  (State of the Environment, 2003). Similarly winter minimum values, 7-8 $^{\circ}\text{C}$  reflect ambient conditions.

The summer 2002/2003 reached 32  $^{\circ}\text{C}$  during sampling in January at Nepean River. Increased temperature has the following effects on the ecological functioning of streams:

- Lowers the saturated concentration of oxygen,
- Increases metabolic functioning of plants, possibly increasing oxygen production,
- Increases metabolic functioning of cold blooded animals and bacteria, increasing oxygen demand,
- Increases the rate of bacterial decay releasing organic bound nutrients,
- Increases the likelihood that these factors will combine to produce algal blooms and collapses.

Many of these processes are observed in the data collected over the summer of 2002/2003, such as:

- Elevated oxygen due to eutrophic conditions, Nepean River at Tourist Rd. (Fig 3)
- Anoxia at Lake Alexandra. (Fig 4)
- Elevated ammonia at Lake Alexandra.

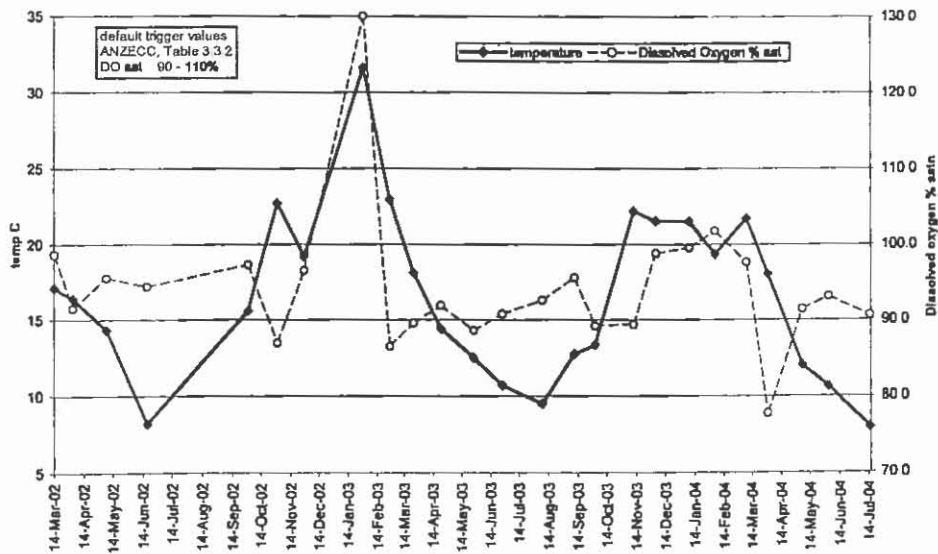


Figure 3. Temperature and Dissolved Oxygen: Nepean River at Tourist Rd.

## WINGECARRIBEE WATER QUALITY

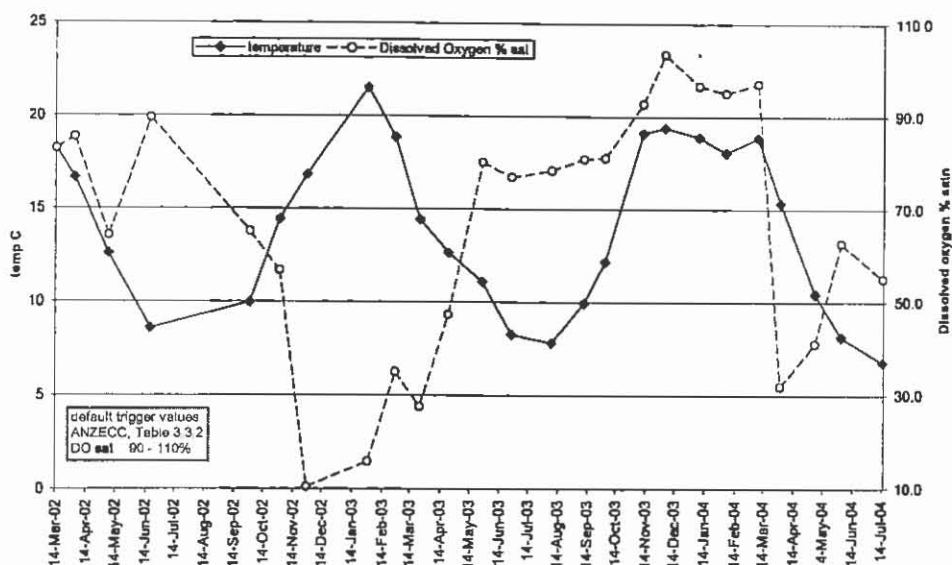


Figure 4. Temperature and Dissolved Oxygen values, Paddy's River at Quarry Rd.

### Dissolved Oxygen (DO)

Adequate oxygen is essential to almost all aquatic ecosystems. Low dissolved oxygen is the cause of many fish kills, and can result from decomposition of organic material, stagnation or elevated temperatures. In a stable aquatic ecosystem, the two central chemical reactions of life: respiration and photosynthesis, deplete and replenish oxygen in a diurnal cycle that keeps the average DO concentrations relatively close to saturation. The ANZECC (2000) guidelines suggest DO saturation concentrations be in the range 90-110% saturation.

The low dissolved oxygen often found during drought can also magnify ecosystem stress from sources such as salinity, temperature and high turbidity.

The use of dissolved oxygen, as a water quality indicator is problematic, as it varies considerably in space and time, particularly diurnally. Systematic studies, can be skewed significantly by the time of day sampling occurs if regular. The aggregate data can, however, serve as a useful tool in assessing water quality in a given system if this limitation is accepted.

### Turbidity

Turbidity has been measured in these studies using turbidity probes with readings in nephelometric turbidity units (NTU). Turbidity is used as an economic and credible replacement for the measurement of total suspended solids (TSS). Suspended particulate matter, particularly clay, reduces water quality directly by limiting light penetration and also indirectly, because once deposited, the solids can provide an important source of phosphorus enhancing biological activity. Soil and bank erosion have been identified as the major degrading process in Australian rivers (Olley 1995).

Turbidity correlates with level of development in the catchments and particularly to impervious surfaces. The median value for this study, 20 ntu is large and reflects the need to increase riparian vegetation, limit cattle access to streams and reduce impervious areas.

### Faecal Coliforms

Traditionally the microbiological suitability of water for drinking, recreation and stock watering has been determined by the presence of faecal coliform bacteria. Faecal coliforms are found in the gut of warm-blooded animals, their faeces and in material contaminated with these faeces. These bacteria are not pathogenic, but indicate the level of risk associated with contact or ingestion. This tool was developed to determine the likelihood of human faecal contamination to drinking water due to the threat of the bacteria *Vibrio cholerae*, *Campylobacter*, *Salmonella*, *Shigella* and others. These bacteria do not persist in water storages, are filtered out and are killed by chlorination. However, *Cryptosporidium* and *Giardia* are not hindered by storage, filtration and chlorination. Moreover, they are present in local cattle. Elevated faecal coliform levels, during dry weather, in grazing country indicates that cattle have direct access to streams. During wet weather spores are washed through the soil and into rivers and dams. Heavy rain after a drought is particularly effective at delivering spores to the waterways.

The ANZECC (2000) guidelines for recreational waters vary based on the level of contact with water. Primary contact (eg swimming) and secondary contact (eg. boating) are 150 and 1000 colony forming units per 100 mL (cfu/100 mL), respectively. Stock drinking water guidelines are lower at 100 cfu/100 mL.

Concentrations of faecal coliform bacteria in WSC streams are high (Figs 5 and 6). Faecal coliform concentrations in most streams respond dramatically to rain events. Increases of several orders of magnitude, or more, are normal after heavy rain. Wet weather sources are probably animal faeces and sewage. Dry weather sources are probably direct faecal contamination of the water by unfenced stock (Nepean River at Tourist Rd.) and ducks (Lake Alexandra), or cracked or corroded sewage mains.

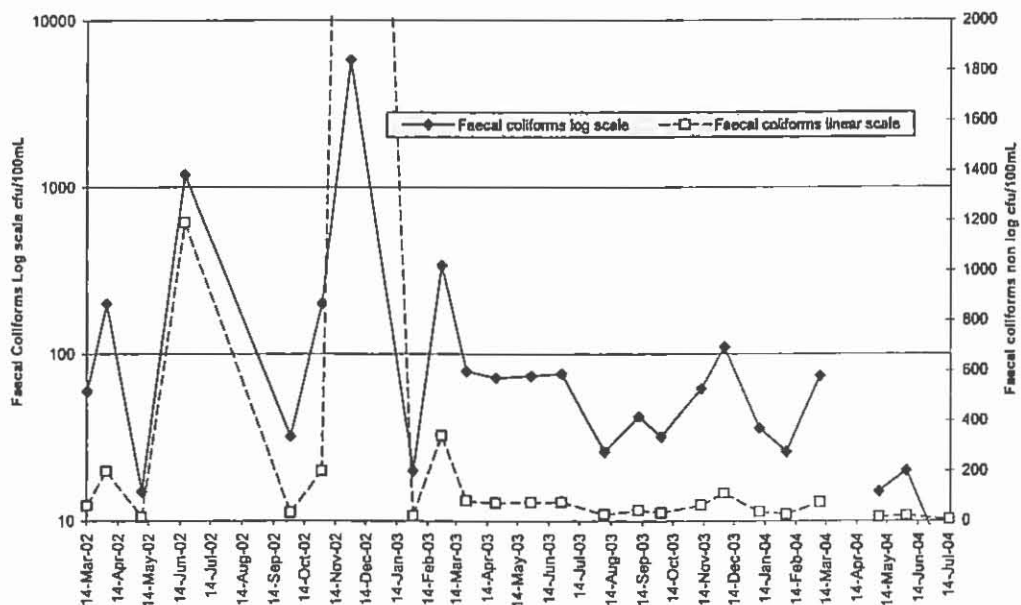


Figure 5. Faecal Coliform values, Nepean River at Tourist Rd.

## WINGECARRIBEE WATER QUALITY

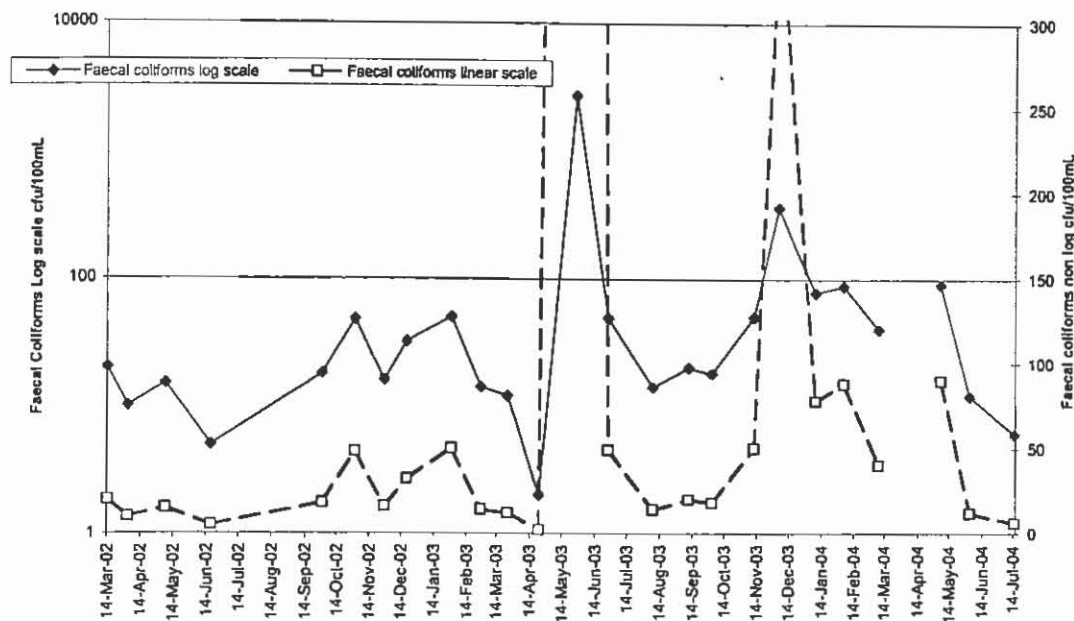


Figure 6. Faecal Coliform values, Wingecarribee River at Bongbong

### Nutrients

Nutrients in aquatic systems include those chemical species that are required by plants for growth and survival, and include various chemical forms of nitrogen (N), phosphorus (P), potassium, iron and silicon. Interest is usually focussed on those nutrients that, when in limited supply, limit the growth of plants and algae. This is usually P and N, but their relative importance changes with the environment being studied.

In a water quality program, the choice of parameters to study is dependent on the aims of the study. In the case of nutrients, with a range of chemical forms, the choice is primarily between dissolved and total nutrients. Phosphorus is usually measured as total P and dissolved P (variously called reactive phosphorus or ortho-phosphate or dissolved inorganic P - DIP). Total phosphorus may include dissolved, sediment bound and organic forms, with the dissolved phosphorus usually being the minor component. Thus, increases in sediment load or algal biomass will influence total phosphorus measurements in ways that are difficult to interpret. Total phosphorus (and total nitrogen) measurements, however, facilitate the calculation of nutrient budgets that assist management responses. Dissolved P and weakly bound P are readily utilized by algae and higher plants and are therefore important parameters to measure in process studies. Nitrogen species include ammonium, nitrite and nitrate (all dissolved) and an organic form (Kjeldahl nitrogen, TKN). The concentration of dissolved reactive phosphorus (DRP) frequently correlates strongly with algal growth, with elevated levels often leading to algal blooms. The DRP to DIN ratio is also an indicator of the risk of blue-green algal blooms, particularly if it is high. This is due to these algae not being limited by access to DIN as they can convert atmospheric nitrogen to organic nitrogen.

In Figures 7 to 9 DRP correlates to TKN, which reflects the algal biomass. DRP is in most instances elevated before the bloom. Nitrate has an inverse relationship with TKN and is elevated after the blooms crash probably as a result of biomass mineralisation.

ANZECC (2000) guidelines for upland rivers, for total P and DIP are 0.02 and 0.015 mg/L respectively. The mean value for total P routinely exceeded these guidelines in many locations. The likely sources of phosphorus include eroded soil, stream banks and fertilizer applications.

Unlike phosphorus, nitrogen and its chemical forms are not always conserved within an aquatic system. Blue-green algae and bacteria can fix nitrogen. Nitrogen can also be lost from the system as nitrogen gas in reducing conditions, and through denitrification in the sediments and at the sediment-water interface. Sources of nitrogen include fertilizer applications, sewage overflows and leakage, naturally fixed nitrogen and dissolved oxides of nitrogen from internal combustion engines and lightning. The contribution from motor vehicles, particularly nitrogen dioxide from Sydney, makes it difficult to determine the background for nitrogen species in water, locally.

### Chlorophyll *a*

Chlorophyll *a* and total P correlate strongly at Nepean River (Fig 10). Both correlate with algal biomass which is the parameter of direct interest. All three parameters vary in the degree of difficulty of measurement and utility. DRP is probably the most predictive. The direct measurement of chlorophyll *a* by fluorometer offers advantages in terms of speed, ease and the ability to do a large number of samples.

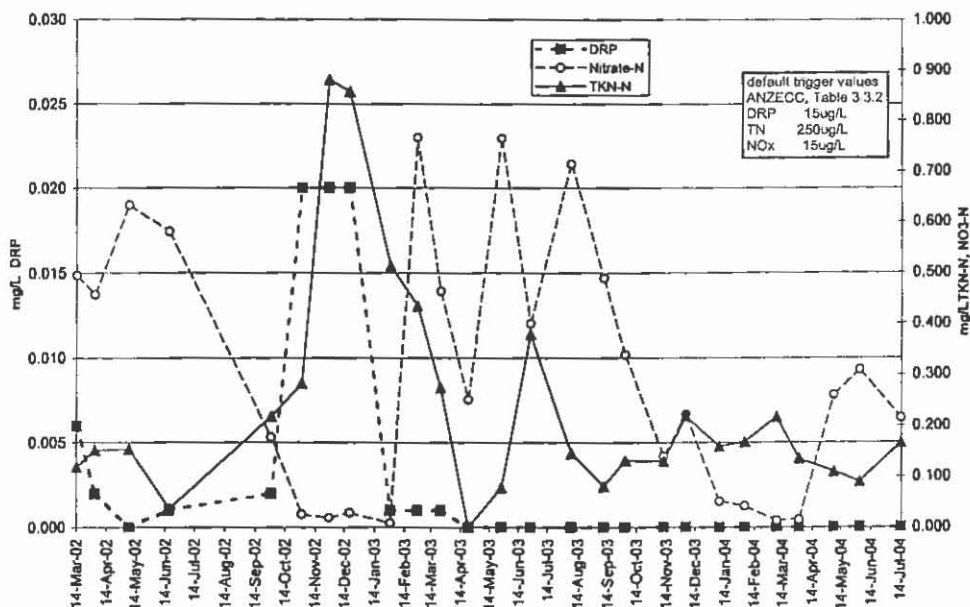


Figure 7. Nutrient values, Nepean River at Tourist Rd.

# WINGECARRIBEE WATER QUALITY

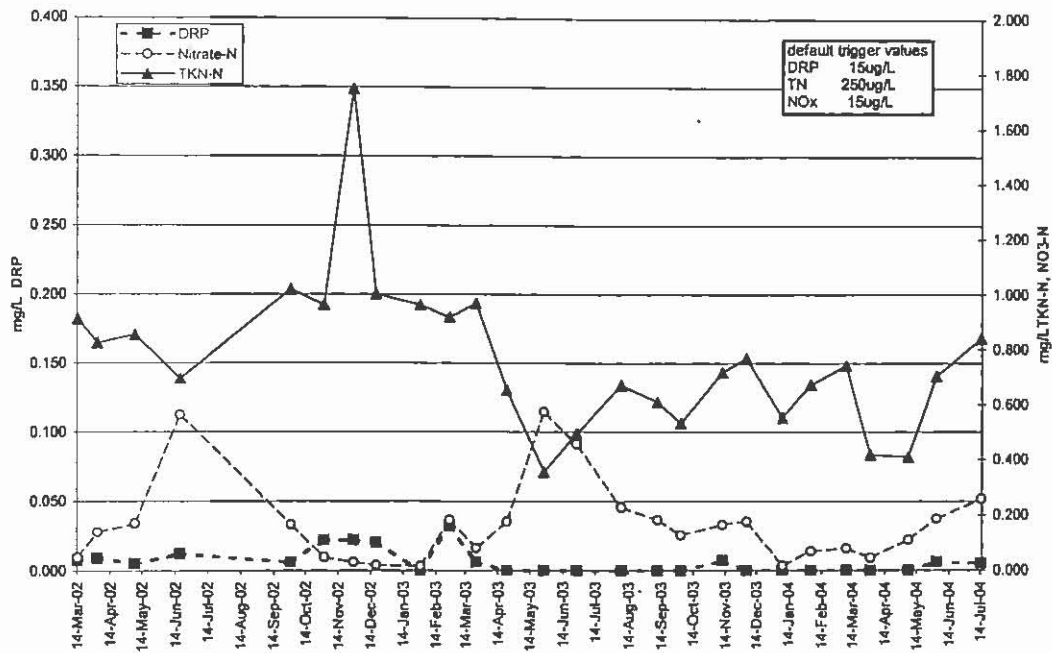


Figure 8. Nutrient values, Paddy's River at Quarry Rd.

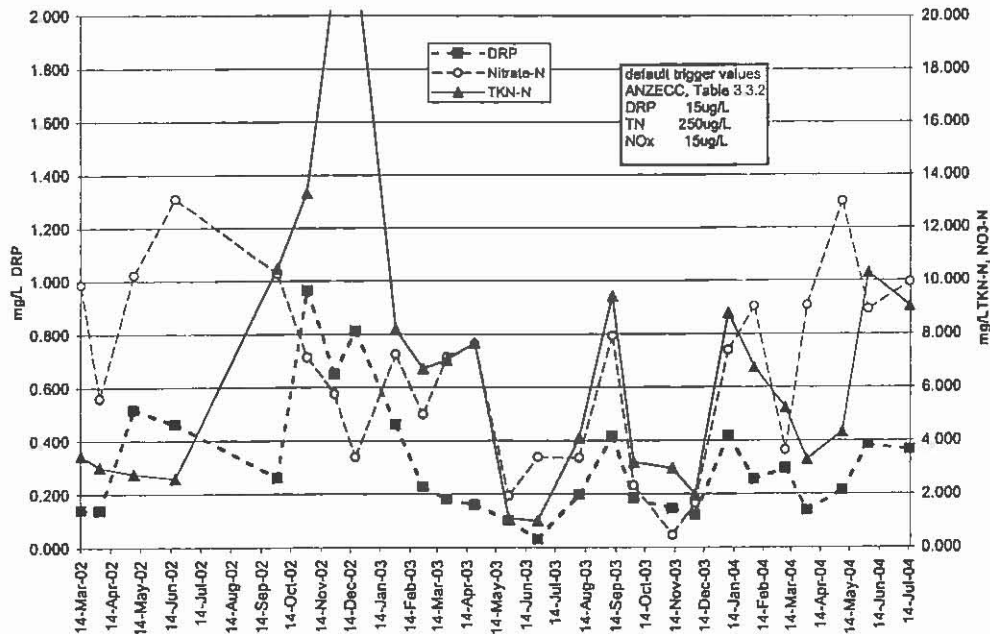


Figure 9. Nutrient values, Mittagong Cr at Burradoo.

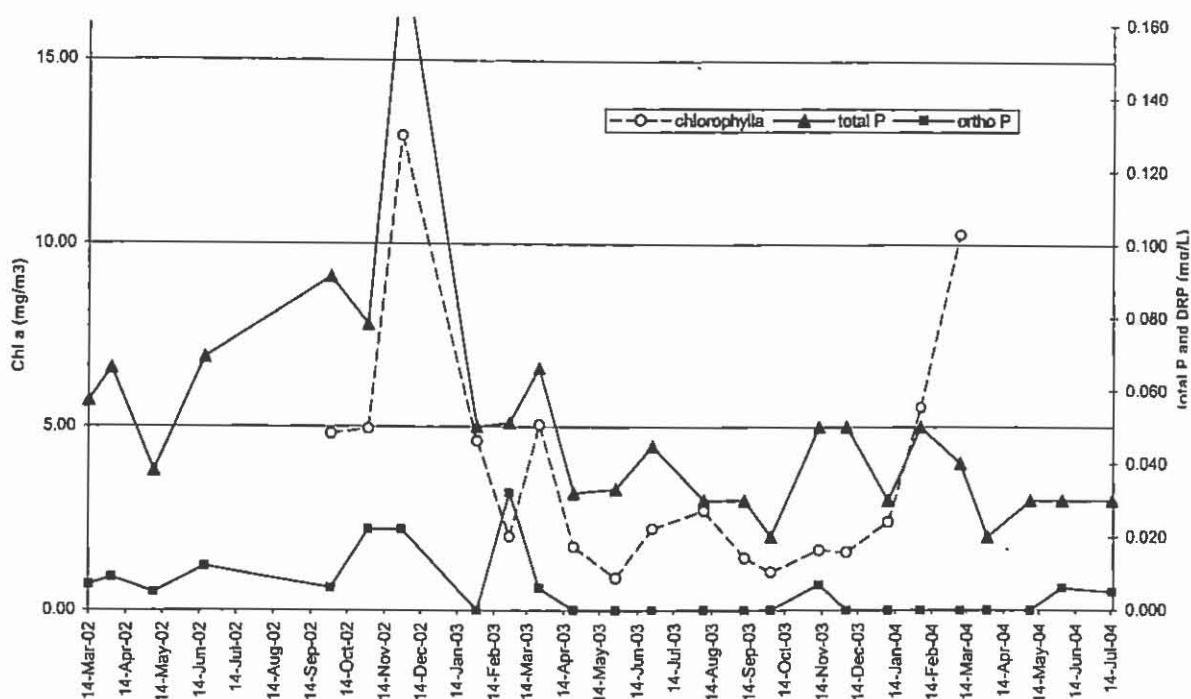


Figure 10. Nutrients and chlorophyll a values, Nepean River at Tourist Rd.

## CONCLUSIONS

The naturally rich agricultural soils of the Wingecarribbee LGA, prolonged application of super-phosphate after the Second World War and extensive soil and subsoil erosion has left this region with a legacy of potentially eutrophic streams and rivers. Lower flows, stagnation and increasing temperatures will facilitate the development of algal blooms and anoxic conditions degrading ecosystem health, lowering amenity and the suitability of water for human consumption.

Salinisation is an environmental issue of national significance and is present in Wingecarribbee LGA. The effects of salinisation are predicted to increase.

The presence of cattle within the Sydney water catchment area is problematic given the known occurrence of *Cryptosporidium* and *Giardia*. Reducing cattle access to streams will reduce this health threat.

## REFERENCES

- ANZECC & ARMCANZ (1996) *National Water Quality Management Strategy: Draft Rural Land Uses and Water Quality*. Australia and New Zealand Environment and Conservation Council & Agriculture and Resource Management Council of Australia and New Zealand, Canberra.
- ANZECC/ANZECC & ARMCANZ (2000) *Australian Guidelines for Water Quality Monitoring and Reporting – Summary*. National Water Management Strategy, Paper No. 7a, Australia and New Zealand Environment and Conservation Council & Agriculture and Resource Management Council of Australia and New Zealand, Canberra.

## WINGECARRIBEE WATER QUALITY

- AMERICAN WATER WORKS ASSOCIATION, AMERICAN PUBLIC HEALTH ASSOCIATION & WATER ENVIRONMENT FEDERATION (1999) *Standard Methods for the Examination of Water and Wastewater. Twentieth Edition*. American Water Works Association, American Public Health Association & Water Environment Federation, America.
- Olley, J. 1995, *Sources of Suspended Sediment and Phosphorus in the Murrumbidgee River*, Consultancy Report No. 95-32, CSIRO Division of Water Resources, Canberra
- SHELLHARBOUR CITY COUNCIL (1999-2003) Shellharbour River Study, Shellharbour City Council. (Unpublished Data)
- WOLLONGONG CITY COUNCIL (2003). Surface Water Quality Monitoring Data, Wollongong City Council, Wollongong, NSW. (Unpublished Data)
- WHETTON, P.H. et al (2005) *Australian Climate Change Projections. For Impact Assessment and Policy Application : A Review*. CSIRO Marine and Atmospheric Research. Canberra.
- STATE OF THE ENVIRONMENT REPORT 2002-2003 (2004) Wingecarribee Shire Council



# APPLICATIONS OF SEISMIC REFLECTION IN THE COAL ENVIRONMENT

Troy Peters and Natasha Hendrick

Velseis Pty Ltd  
PO Box 118, Sumner Park, Qld 4074

## ABSTRACT

Seismic reflection has grown to become a valuable geophysical tool for the accurate and cost-effective imaging of coal seams, and is now of significant importance to the economics and safety of coal mining in Australia. This paper provides an essential, up-to-date overview of the advantages and potential pitfalls of using the seismic method in the coal environment based on the experiences of a number of Australian coal mines. The major advantage of using seismic data is its ability to produce a more continuous image of a target coal seam than can be achieved via borehole drilling. Seismic-derived elevation surfaces, and information about faults and other stratigraphic anomalies located via seismic imaging, can be used by mines to target borehole drilling for fault evaluation and grout pattern design, and help predict changing roof, floor and seam conditions. Recent developments in advanced 3D seismic interpretation and converted-wave seismology focus on detecting more subtle stratigraphic features, locating gas, and mapping lithology away from borehole locations. However, the accuracy to which the seismic method can recover structural and stratigraphic information is controlled by the inherent limitations in the technology and the geological environment in which the seismic survey is conducted. Vertical and lateral resolution limits of a seismic dataset restrict the size of a feature that can be imaged using seismic data, and the ability to resolve closely spaced structures. Unfavourable near-surface geology (e.g. thick Tertiary sediments or basalts) will have a negative impact on seismic image quality and reduce the ability of the seismic data to resolve faults and other stratigraphic anomalies. Seismic reconciliation is a calibration process that enables a mine to gain a greater understanding of the uncertainties of the seismic method in characterising faults and stratigraphic anomalies in their particular environment. A proactive approach to using and assessing seismic data throughout the mine planning and development process will maximise the benefits of a seismic survey to a coal mine.

## INTRODUCTION

Seismic reflection data have been acquired for coal mining operations in Australian coal basins for over 30 years. Originally used solely as a resource exploration tool, the seismic method now routinely contributes to coal-mine design and development. In the decades since seismic reflection data were first acquired for coal applications, there have been remarkable developments in the acquisition, processing and interpretation of seismic data. Today significant amounts of high-resolution information extracted from seismic datasets contribute to reducing mine downtime and increasing the safety of mine operations. This paper provides a concise summary of the fundamental concepts of seismic reflection, details the type of information that can now be extracted from seismic data and discusses the effective use of

## SEISMIC REFLECTION IN THE COAL ENVIRONMENT

all of them believed to be in the Bowen Basin, Queensland. No 3D-3C seismic reflection surveys have been undertaken for coal exploration.

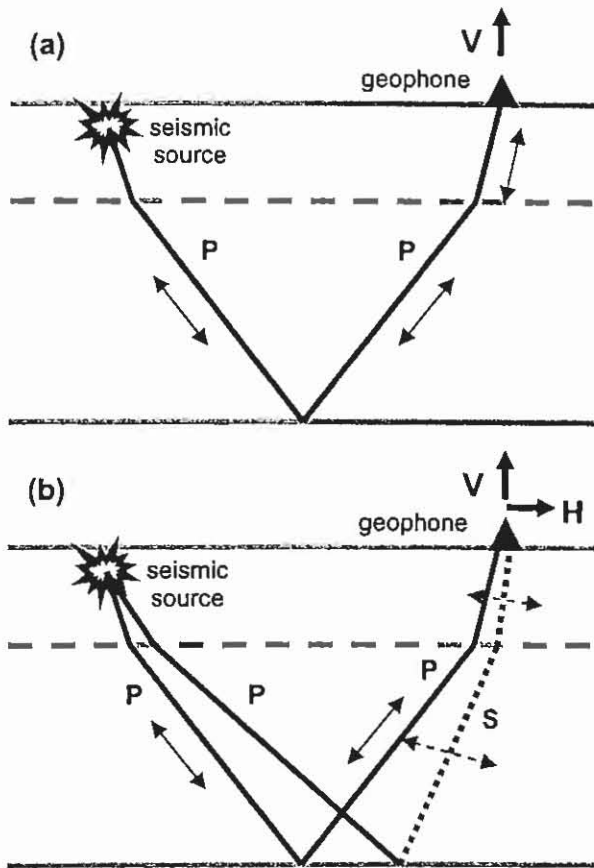


**Figure 1** (a) Conventional seismic reflection assumes that only P waves arrive at the surface. Since the particle motion of an upward travelling P wave is largely vertical (indicated by the solid arrows), a vertically-oriented geophone is used for acquisition. (b) Multi-component seismic recording recognises that both P and mode-converted PS waves will arrive at the surface. The particle motion of an upward travelling S wave is largely horizontal (indicated by the dashed arrows). Thus both the vertical (V) and horizontal (H) components of ground motion must be recorded to take advantage of both wave types.

### SEISMIC INTERPRETATION

A 2D seismic image or 3D seismic volume is a graphical representation of the geological boundaries in the survey area as a function of two-way reflection time. In simple terms, seismic interpretation is the process of tracking significant geological boundaries (e.g. target coal seams) in the seismic data and producing two-way time (TWT) horizons or surfaces. Whereas the interpretation of 2D seismic data is confined to a single vertical plane, the spatial redundancy of 3D data provides the user with high-density maps of the coal seam topology. In both instances, the major advantage of seismic exploration is the ability to produce a more continuous image of the target coal seam than can be achieved via borehole drilling.

#### Depth Surfaces

Provided sufficient geological control exists (e.g. borehole data), a reliable time-to-depth conversion can be performed on the interpreted seismic TWT horizons to yield coal-seam elevation surfaces. These surfaces can give a more accurate indication of relative changes in coal-seam elevation that can be extracted from widely-spaced borehole data. Conventional P-

seismic data in the coal environment – knowledge that all mine staff using seismic data should have. Traditionally, application of the seismic method in the coal environment has involved delineating structures that have the potential to impact on mining operations. More recently, seismic depth conversion has gained popularity as a tool for deriving detailed coal elevation surfaces, and efforts are being directed towards extracting stratigraphic information from seismic data. This paper also highlights new converted-wave coal-seismic applications, such as imaging very shallow coal seams, detecting zones of fracturing via shear-wave splitting analysis, and mapping lithology away from boreholes using integrated P/PS interpretation.

### FUNDAMENTAL CONCEPTS OF SEISMIC REFLECTION

In brief, seismic reflection involves imaging the sub-surface using artificially-generated sound waves. Typically, small dynamite explosions or vibratory sources (e.g. mini-SOSIE or Vibroseis) are used to generate seismic waves at or near the surface. Receiving devices (geophones) are placed on the surface to detect the seismic energy that originates from the seismic source, travels down into the earth and gets partially reflected back to the surface at each geological boundary. 2D seismic exploration involves acquiring seismic data along a single line of receivers. The resultant 2D seismic image can be used to detect features in the subsurface along the particular survey line. 3D seismic exploration involves using a grid of surface receivers to detect the reflected seismic energy generated by each seismic source. 3D seismic data yield a much more extensive and higher-resolution image of the subsurface than 2D seismic data. This makes 3D seismic more attractive in terms of being able to contribute significantly to the structural and stratigraphic understanding of a mine area.

Conventional coal-seismic acquisition assumes that typical coal-seismic sources will result in only compressional (P) waves arriving at the surface. P waves are longitudinal sound waves that have particle motion in the direction of travel. Hence reflected P-wave energy travelling upwards from a geological boundary will have particle motion with a strong vertical component at the surface receiver (Figure 1a). Conventional 2D and 3D seismic acquisition records only the vertical component of seismic energy arriving back at the receivers. This type of seismic recording can also be referred to as single-component (1C) recording, and is by far the most common method of seismic exploration used in the coal environment (e.g. there have been approximately fifty conventional 3D seismic surveys acquired in the Bowen and Sydney Basins since 1997).

In reality, both reflected P and shear (S) waves typically arrive at the surface during a seismic survey. S waves are transverse sound waves that have particle motion perpendicular to the direction of travel. Since coal-seismic sources dominantly produce P-wave energy, most of the S energy arriving at the surface is in fact mode-converted PS energy. That is, energy from a wave that travels down to a geological boundary as a P wave, gets partially converted to S energy at the boundary, and then travels back to the surface as an S wave. Any PS-wave energy arriving at the surface will have a strong horizontal component of particle motion (Figure 1b). Multi-component seismic recording measures both the vertical and horizontal components of ground motion to enable exploitation of both the P and PS energy arriving at the surface. Note that, multi-component recording may also be referred to as three-component (3C) recording since the vertical and two orthogonal horizontal components (inline and crossline components) of ground motion are generally recorded. To date, less than ten 2D-3C seismic reflection surveys have been conducted for coal exploration in Australia –

wave coal-seismic data can typically map coal seams from depths of approximately 50 m, down to depths of approximately 800 m. Due to differences in the way P and S waves propagate in the subsurface (e.g. Hendrick 2004), PS seismic data can image much shallower coal seams. Our experience indicates that PS data can map coal seams as shallow as 25 m (Figure 2), making multi-component seismic data particularly useful for opencut coal exploration.

Seismic-derived elevation surfaces can be integrated with borehole information about the mine and used to assist with grout pattern design, flight plan design for longwall cutting profiles, and guiding in-seam drilling for the purpose of gas drainage.

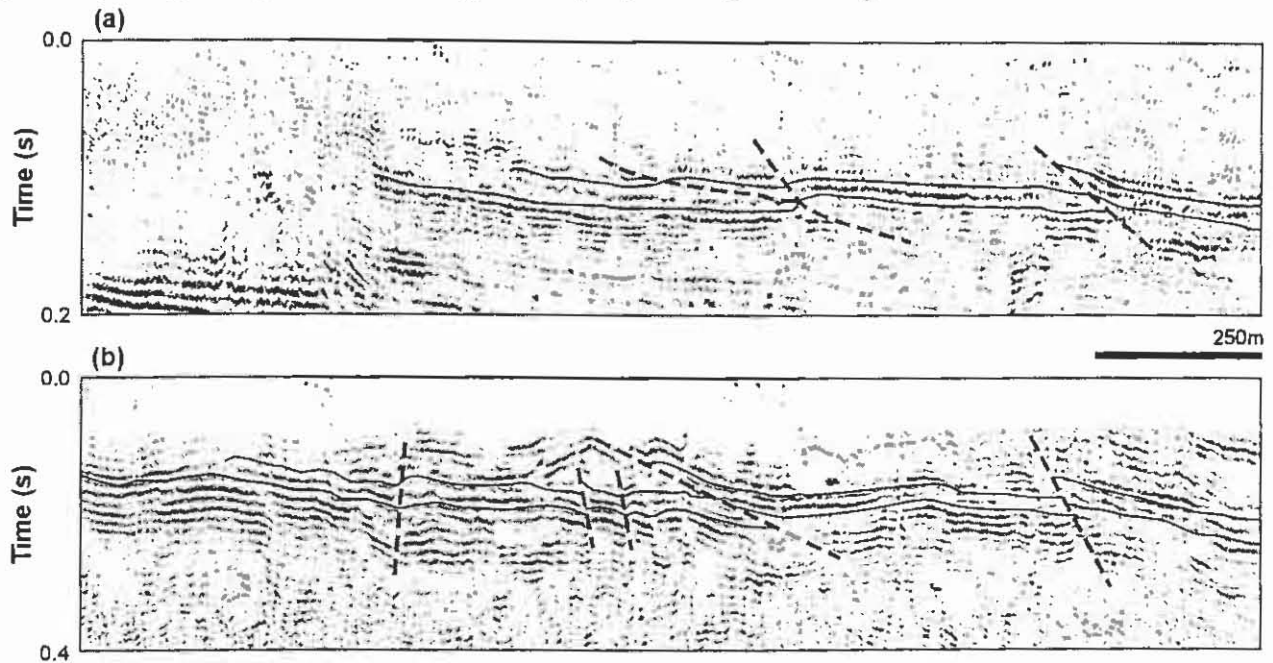


**Figure 2** (a) Conventional P-wave image and (b) PS image from a 2D multi-component seismic survey in the Bowen Basin, Queensland. The target coal seams are indicated by the solid lines. Interpreted faults are approximately marked by the dashed lines. For this trial, the PS section is able to image the shallow coal seams to depths of approximately 25 – 30 m (left-hand edge of image).

### Structural Information

Typically, accurate delineation of structure is the primary objective of a seismic reflection survey. Seismic TWT horizons, together with the seismic data, can be used to derive a number of seismic attribute maps (e.g. TWT gradient, seismic amplitude, instantaneous frequency, semblance) that can be used to highlight structural features that may impact on mining operations (Figure 3). Seismic data provide a dense sampling of the subsurface and so can detect a greater number of structures than borehole drilling. Estimates of fault throw, fault width and the location of a structure can be computed from the seismic data. Our experience indicates that faults as small as 2-3 m can often be detected using 3D seismic data. Velseis has recently undertaken research (Hendrick 2006) to utilise the phenomenon of shear-wave splitting (SWS), as a method of detecting fracturing or faulting at a smaller scale than that obtained from conventional P-wave seismic. Shear wave splitting is the process whereby S waves split into two approximately orthogonally-polarised shear waves with different velocities in fractured media. The potential of SWS to contribute useful information about minor, localised faulting is still being evaluated.

## SEISMIC REFLECTION IN THE COAL ENVIRONMENT

Once mine staff have gained a better understanding of local structure from a seismic survey, drilling programs can be targeted for fault evaluation and grout pattern design. If necessary, mine plans can be designed or amended to avoid significant structures. In this way, fault information derived from seismic data can help reduce longwall downtime and increase the safety of mine operations.

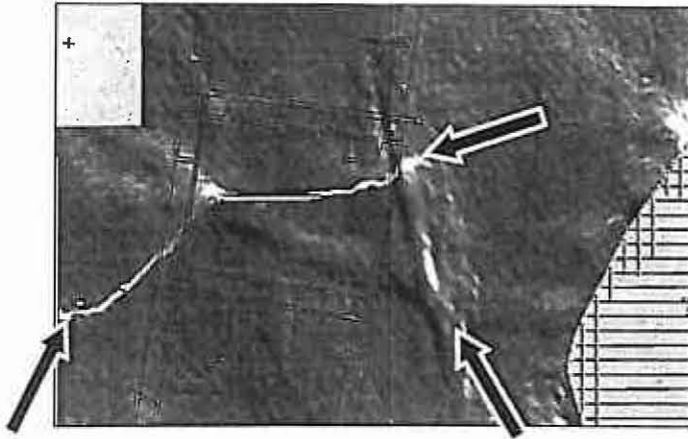


**Figure 3** Map view of the semblance attribute derived from a 3D seismic volume acquired in the Bowen Basin, Queensland. Rapid changes in the seismic attribute map (highlighted by the arrows) delineate structures cutting the proposed mining panel.

### Stratigraphic Information

Recently there has been an increasing desire to obtain more than just structural information from seismic data. Careful examination of seismic waveform variations, and anomalous features in seismic attribute maps, can contribute to the stratigraphic interpretation of a seismic dataset. Often reconciliation drilling is required to gain an understanding of what a seismic anomaly represents in real physical terms. Nevertheless, highlighting such features can contribute to the greater geological understanding of the mine area. Our experiences indicate that seam splitting and igneous intrusions (sills) are two of the most prevalent stratigraphic anomalies detected via conventional 3D seismic interpretation (often detected in the instantaneous frequency attribute map). There are a number of more complex seismic interpretation procedures being developed and tested that involve full seismic waveform analysis, geological inversion or integrated P and PS interpretation. Such tools attempt to provide additional information on rock type and pore fluids, for example. A recent ACARP research project completed by Velseis (Hendrick 2006) presents the first attempts to map lithology away from borehole locations using integrated P/PS seismic interpretation. The interpretation results from many of these more advanced seismic tools are still being evaluated in the context of remote imaging in the coal environment.

Stratigraphic anomalies and lineaments derived from seismic data can be used by mines to design targeted drilling programs to help optimise mine plans, avoid intruded coal, prepare for weak roof/floor conditions or accommodate changes in seam thickness during mining.

### EFFECTIVE USE OF YOUR SEISMIC DATA

In order to maximise the advantage of conducting a seismic survey, it is imperative to have an understanding of both the inherent limitations of the seismic method, and the impact the local geological environment can have on the seismic data. Armed with this knowledge, and the resources to actively integrate seismic data into mine planning and development, any potential pitfalls associated with using seismic can be minimised, resulting in considerable technical and cost benefits to the mine.

### Understanding Seismic Resolution

The ability of a seismic dataset to image a geological feature is largely a function of the frequency content of the seismic data – with higher frequency content leading to greater resolution. The frequency content of a seismic dataset is controlled by the seismic source type (with a dynamite source resulting in a higher-resolution seismic dataset than a mini-SOSIE source), the receiving device and the near-surface and subsurface geological conditions.

The vertical resolution of a seismic dataset is often indicated by two measures – the ‘detectable limit’, which is defined as the minimum layer thickness required to produce an observable seismic reflection (Sheriff 1991), and the ‘resolvable limit’, which is defined as the minimum separation of two discrete seismic reflectors at which one can determine there is more than one interface present (Sheriff 1991). Good quality 3D coal-seismic datasets will have a ‘detectable limit’ of the order of 1-2 m and a ‘resolvable limit’ between 2.5-5 m. This implies that the seismic volume won’t be able to detect structures with displacements less than approximately 1-2 m, and seam splits and/or faults are unlikely to be properly imaged in the seismic volume until the interburden and/or displacement becomes greater than approximately 2.5 m. Obviously, these resolution limits become larger in the presence of noise. The dangers in not understanding the vertical resolution limits of your seismic dataset are assuming that your seismic data will detect all geological features that could impact mine operations and placing too much significance on the computed physical dimension of seismic anomalies with very small displacements.

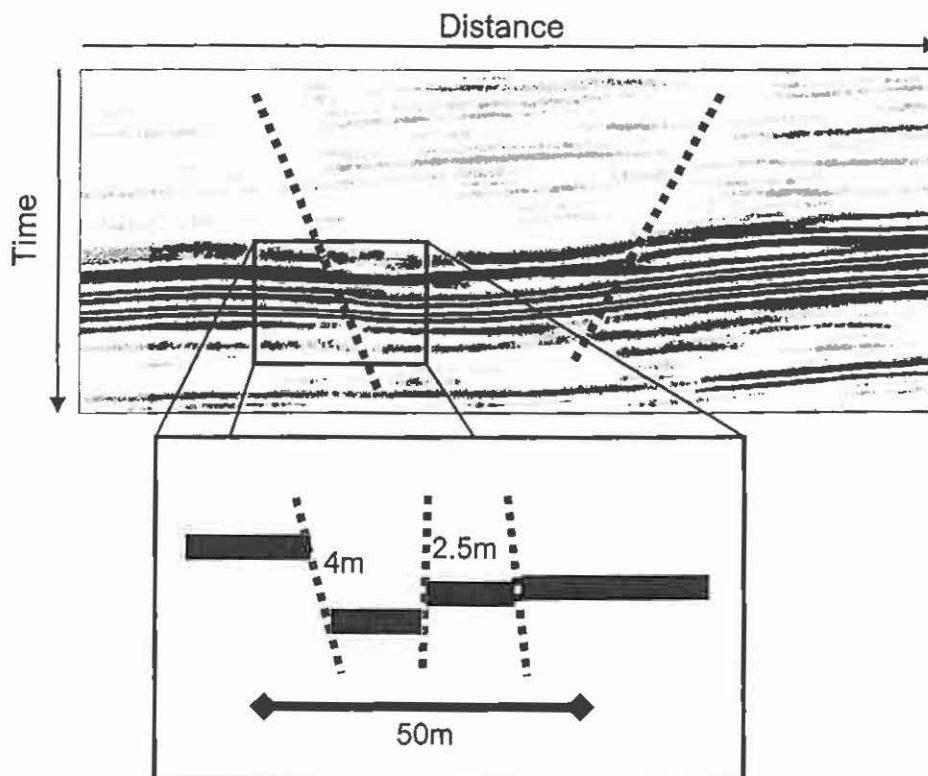


**Figure 4** Interpretation of these seismic data acquired in the Bowen Basin, Queensland indicates there are two faults present. Subsequent mapping during underground mining reveals that the left-hand seismic structure is in fact three closely-spaced faults. The lateral resolution limits of the seismic data prevent the three faults from being imaged clearly.

The lateral resolution limit of a seismic dataset is generally indicated by the 'Fresnel zone' – the zone over which any two or more reflecting points are considered indistinguishable from the Earth's surface (Sheriff, 1991). In practical terms, this means a disruption in a target coal seam can influence the recorded seismic reflection event across a broad area. The implication of this for imaging structures with seismic data is two-fold – first, we can expect errors of up to  $\pm 15$  m in the interpreted locations of geological features and structures. The potential pitfall in this instance is to not accommodate this magnitude of error in seismic fault locations when including seismic data on mine maps or determining detailed cutting profiles. Secondly, seismic data will generally not be able to detect multiple faults that occur within close proximity (e.g. within a zone of 40-50 m). Rather, the seismic image will likely show a single, broad displacement with a throw equivalent to the net throw of the fault zone (Figure 4). Mine staff must avoid the trap of always interpreting a single line on a seismic fault map as a single structure. Referencing fault widths supplied by the interpreter will help highlight locations where multiple faults may exist.

### **The Influence of Coal-Mine Geology**

As noted above, coal-mine geology can have a negative impact on the frequency content of a seismic dataset. Unconsolidated, thick surface layers will cause significant attenuation of high-frequency seismic energy, which in turn reduces the resolution of the seismic dataset (Peters and Hearn 2001). In addition, near-surface geology can affect the ability of energy from the seismic source to penetrate downwards to the target coal seam/s. For example, thick near-surface basalts and other high-velocity layers will result in a very poor signal-to-noise ratio in the resultant seismic image (Figure 5). In these situations, the above-defined resolution limits become less relevant, and the ability of seismic data to detect faults and other geological features can be dramatically reduced. Obviously, if near-surface geology is understood prior to a seismic survey being undertaken, steps can be taken to minimise any negative effect (e.g. the seismic source may be able to be positioned below thick Tertiary or interbedded basalt layers). Nevertheless, care must be taken to avoid the assumption that all faults and stratigraphic anomalies on a seismic interpretation map are equally reliable. Referencing fault confidence levels supplied by the seismic interpreter will indicate the significance that should be given to a fault interpretation. Mines should also be careful about assuming no structures exist when a seismic dataset does not detect any structures, particularly through areas flagged as poor-quality data areas by the seismic interpreter.

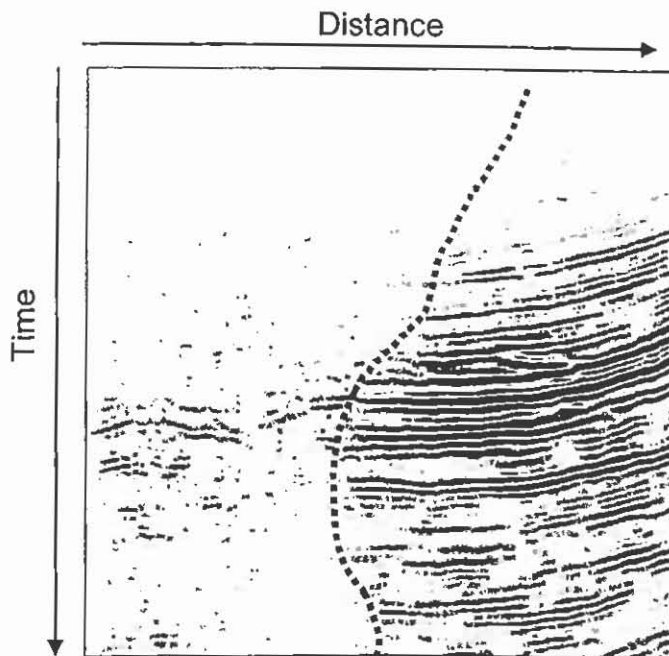


**Figure 5** Clearly the seismic data on the left-hand side of this image suffers from a poorer signal-to-noise ratio than the data on the right-hand side. The seismic data on the left have been acquired beneath a thick, near-surface basalt layer. The high-velocity layer attenuates the seismic energy as it propagates down to the target coal layers, and again on its return to the seismic receivers. Seismic structures and other anomalies are more difficult to detect in the data on the left.

Perhaps surprisingly, the stratigraphy of the coal seams can also influence a seismic dataset. For a single-seam environment, the depth of the coal seam will only marginally alter the seismic response (with deeper reflection events suffering only a minor reduction in high-frequency energy compared to shallow reflection events). However, in a multi-seam environment, it becomes progressively more difficult to extract a clean, high-resolution image of coal seams at depth. Seismic energy will suffer severe transmission loss as it passes through multiple coal seams in a geological sequence. Thus, seismic reflection events for deeper seams in a multi-seam environment can be affected by a poor signal-to-noise ratio. This can lead to false structures in the data or the potential for real structures to be inaccurately imaged. Mine staff must have a good understanding of their local geology to assess the relative robustness of any seismic interpretation results and take this, as well as observations from the seismic interpreter and lessons learnt from the seismic reconciliation process, into consideration when utilising their seismic data.

### Time-to-Depth Conversion

Initially, all seismic interpretation is conducted with reference to two-way reflection time. However, in order to integrate seismic information into mine-planning packages, often seismic surfaces, and sometimes the seismic trace volume itself, are converted to depth. Time-to-depth conversion relies on borehole information to compute conversion velocities (since the depth of a geological boundary at a certain point is equal to the average seismic velocity multiplied by half the TWT of the interpreted horizon at that point). Away from borehole locations, the conversion velocities are extrapolated via sophisticated gridding algorithms. Nevertheless, these velocities are not necessarily accurate away from the borehole locations and the seismic depth horizons should not be assumed to be absolutely correct. Our experience is that while absolute seismic-derived depths can be erroneous away from boreholes, the *relative* changes in coal seam elevation are quite reliable.

### Integrating Seismic Data into the Mining Process

The interpretation of a coal-seismic dataset results in a significant quantity of additional information that needs to be incorporated into traditional mine-planning packages. Such information will include, but not be limited to, coal-seam elevations (ASCII format), fault

## SEISMIC REFLECTION IN THE COAL ENVIRONMENT

characterisation files (DXF format) and interpreted seismic images (TIFF images). Effective integration of seismic data into the mine planning and development process not only requires that these data be included in maps and software used daily at the mine site, but also requires that mine staff gain an understanding of the uncertainties inherent in their local seismic data.

The process of gaining a better understanding of the uncertainties of the seismic method in characterising faults and stratigraphic anomalies in a particular environment is commonly referred to as seismic reconciliation. Reconciliation involves comparing seismic interpretation results with hard geological data available from either validation drilling or underground mine mapping. Mines that most effectively integrate seismic into their mine planning and development are those who are proactive about reconciliation (Peters 2005). Clearly, seismic data cannot be considered in isolation from all other geological and geophysical information available at a mine site – the more information that is fed into the seismic interpretation process, the better the outcomes. The reconciliation process enables mine staff and the seismic interpreter to develop realistic expectations about what seismic data can deliver to a particular mine. This process of reconciliation should continue throughout the working life of a mine.

### CONCLUSIONS

Seismic reflection data can produce a more continuous image of a target coal seam than can be achieved via borehole drilling. Seismic-derived elevation surfaces, and locations of faults and other stratigraphic anomalies can be used by mines to target drilling programs, assist with grout pattern design, guide inseam drilling for gas drainage, contribute to flight plan design for longwall cutting profiles, and help mines prepare for changing roof, floor or seam conditions. Recent developments in advanced 3D seismic interpretation techniques and converted-wave seismology are tackling the more difficult problems of detecting fracturing, zones of gas, and seam intrusions, and mapping coal quality and lithology away from borehole locations. To optimise technical and cost benefits to the mine, staff using seismic data must understand the inherent limitations of the seismic method. Care must be taken to not assume that seismic data will detect all geological features that can impact mine operations. When faults are closely spaced, or seismic data suffer from significant noise contamination or frequency attenuation, structures and other geological features can be missed by the seismic data. An active seismic reconciliation program will enable mine staff to develop a greater understanding of the uncertainties of the seismic method in characterising faults and stratigraphic anomalies in their particular environment. In this way, mine staff can develop realistic expectations about what seismic data can deliver to their mine.

### ACKNOWLEDGEMENTS

The authors would like to thank all those coal-mine staff who have supported and facilitated the use of seismic reflection for improving their mine planning and development process. Velseis' converted-wave seismic research has been supported with funds from ACARP (Projects C10020 and C13029).

### REFERENCES

- HENDRICK N. 2006. Integrated P-Wave / PS-Wave Seismic Imaging for Improved Geological Characterisation of Coal Environments: ACARP Project C13029.
- HENDRICK N. 2004. Shallow, high-resolution converted-wave seismology for coal exploration: AIG Bulletin 41, 85-91.

- PETERS T., 2005. The successful integration of 3D seismic into the mining process: Practical examples from Bowen Basin underground coal mines, pp. 165-169.
- PETERS T. & HEARN S. 2001. The influence of coal-mine geology on seismic data quality in the Bowen Basin: 15<sup>th</sup> ASEG Geophysical Conference and Exhibition, Expanded Abstracts, CD-ROM.
- SHERIFF R.E. 1991. Encyclopedic Dictionary of Exploration Geophysics: SEG, Tulsa, Oklahoma.

# ORGANIC PETROLOGY – STATE OF THE ART (AN OVERVIEW)

Walter Pickel

Coal & Organic Petrology Services P/L  
23/80 Box Road, Taren Point, NSW 2229

## ABSTRACT

This presentation will outline some of the recent developments in Organic and Coal Petrology with regard to technical developments, results in recent research and modifications in International Standards. The possible outcome of these changes will be discussed. The focus is on the microscopical determination of the coal parameters rank, type and grade and on maturity/kerogen type determination of dispersed organic matter in sedimentary rocks. Variations and differences in methods will be presented and compared.

The new ISO Standard 11760 (2005) has provided a comprehensive frame to classify coals by rank, type and grade and overcome the problems with various different standards/classification systems. The standard also coincides with the new maceral definitions as issued by the ICCP. The International Standards dealing with the petrographic analysis of coal (ISO7404) is recently being revised extending the scope of the Standard from bituminous coals and anthracite to coals of all rank.

New developments in microscope design will especially change the way vitrinite reflectance analysis is performed. The lack of precise and robust rotating stages in new microscopes has already put the determination of maximum vitrinite reflectance analysis under question for the future. The replacement of photomultipliers by grey level determination on video screens will further push the switch to random vitrinite reflectance analysis. Automated reflectance analysis systems also exclusively can be used to determine random reflectance and their fast advance especially in routine quality analysis is very probable.

The especially Australian (and American) preference of maximum vitrinite reflectance analysis is however not really at risk, as results from both analyses on crushed samples can be easily re-calculated (Figure 1) for the rank of most commercial coals.

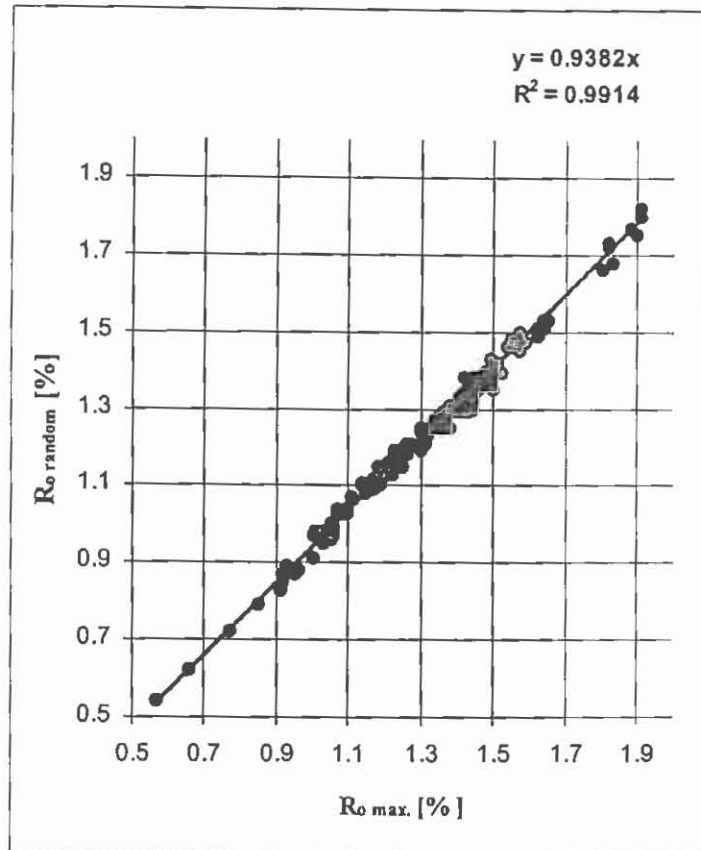


**Figure 1** Relation between  $R_{\max}$  and  $R_r$  with results from Australian coals.

Automated systems, which are capable of more sophisticated analyses like grain size and grain shape related characterization of coals are worked on intensively since years. They are not yet commercial for standard analyses. But they certainly present one promising – and exciting - way for the future.

The accreditation of organic petrologists is other significant improvement, which in combination with more accurate new definitions of the microscopic coal components, is of great benefit to allow comparison of results from different analysts/laboratories. A single coal analysis accreditation has been successfully offered since 2000 by the ICCP with more than 80 analysts accredited by now. This year two additional accreditation programs, for coal blends and dispersed organic matter analysis have been added to the scheme.

# ENHANCED GEOLOGICAL MODELLING THROUGH ADVANCES IN LOGGING AND INTERPRETATION OF INSEAM BOREHOLES

Scott Thomson<sup>1</sup>, Scott Adam<sup>2</sup>, Peter Hatherly<sup>3</sup>

<sup>1</sup> CRC Mining; Principal, CoalBed Concepts

<sup>2</sup> Senior Mechanical Engineer, CRC Mining

<sup>3</sup> CRC Mining; Professor of Geophysics, University of Sydney

## ABSTRACT

The Australian coal industry drills many kilometers of inseam boreholes every year, largely for degasification purposes. The geological data that may be obtained from the geophysical logging of these inseam boreholes is largely overlooked. This paper presents a case for detailed logging of inseam boreholes and highlights the value of the integration of this data into the geological modelling process. Work is currently underway to develop tailored geophysical logging instrumentation to suit Australian Medium Radius Surface to Inseam and underground inseam boreholes.

## INTRODUCTION

To date the assessment of a prospective underground coal mining lease has been predicated on traditional forms of exploration, involving vertical boreholes, physical sampling and regional structural determinations largely based on interpretation from geophysical methods such as seismic and magnetics. Although this methodology has been generally adequate in defining the resource, geological surprises in underground longwall mining still do occur, often with costly outcomes.

The recent development of Medium Radius Drilling (MRD) primarily for gas extraction purposes has provided a hitherto unforeseen opportunity for gaining valuable geological data from the plane of the coal seam itself, rather than relying on surface based geophysical methods or interpolation between vertical boreholes. This outcome is fortuitous, as with rare exceptions, MRD boreholes are designed with one specific purpose in mind – to provide a means of degasifying the coal seam so that mining can proceed unhindered. Exploration benefits are considered purely secondary.

Many mining operations are committing to the 'up front' expense of the MRD approach as a long term solution to coal seam degasification requirements. The commitment requires near term capital, and relies upon lead time and management advantages over the more conventional 'just in time' underground degasification drilling. The method has been particularly supported in Queensland where relatively open surface access and generally favourable coal seam permeability and gas content conditions suit the application of MRD.

The key to successful geological interpretation from inseam boreholes is geophysical logging of the borehole. Currently no equipment has been specifically designed for the current application. However, geophysical logging of vertical boreholes is commonplace and Measure While Drilling (MWD) and Logging While Drilling (LWD) has been a standard part

of oilfield exploration for many years. The challenge is to transfer the techniques and equipment from oilfield experience to the specific requirements of horizontal in-seam boreholes in coal seams, at a reasonable cost, and to ensure that the data provided can be usefully and conveniently adopted for coal mine exploration.

Recent work in this field (see ACARP Projects C12024 and C14034) has clearly established the benefits of using in-seam logging to assist geological interpretation from in-seam boreholes. The field work associated with these projects has also established that the available logging tools are not suitable for deployment in Australian in-seam logging configurations. The tools that have provided the best results to date are the Deutsche Montan Technologie (DMT) shuttles (from Germany), which are designed to be run in HQ or NQ cored boreholes. In-seam logging tools incorporating the best features of the DMT shuttles need to be tailored to suit the application in Australia.

## INSEAM DRILLING PRACTICE

### Underground Drilling

In-seam directional drilling, given current equipment configurations, is possible to distances of about 1600 m. In reality, boreholes greater than 1000 m in length are rare in Australian (and international) coalfield drilling. In the majority of degasification drilling boreholes are drilled to a maximum of 500 m, and 300-350 m is most usual. Exploration boreholes are only in rare cases planned to drill 1000 m+, and due to geological factors, rig performance limitations, and time constraints they do not always achieve their designated target.

An NQ or CHD (or similar) rod string is usual in underground in-seam drilling, and an electronic survey tool and downhole motor (Figure 1). Electronic survey tools have effectively replaced the use of single shot cameras due to the speed at which survey information can be processed and acted upon by the drill operator. Electronic survey tools are an integral component in the process of steering the drill. The increased reliability of the survey result has generally assisted the geological interpretation process.

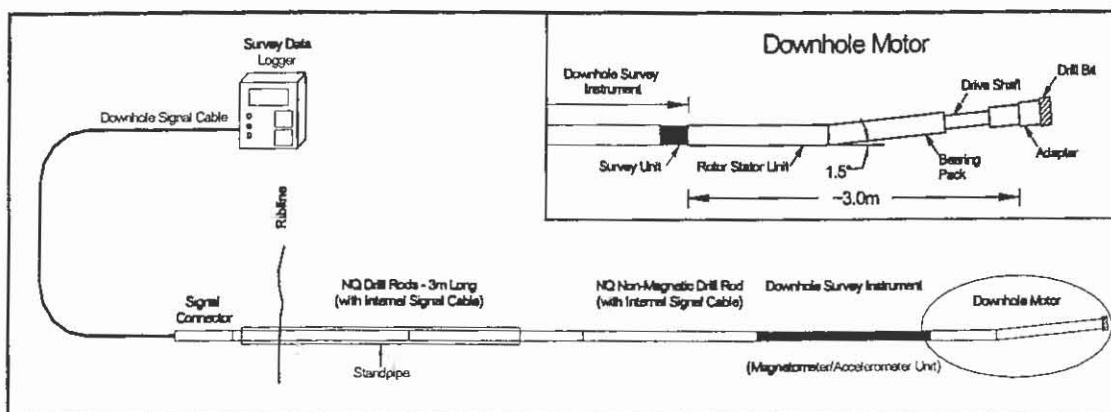


**Figure 1** Schematic representation of standard practice underground directional drilling downhole equipment

The equipment limits the distance the hole can be drilled. The thrust / pull back capacity of the rig may be important but the major limiting factor is the frictional forces acting on the drill rod string with depth. The act of directional drilling involves the use of a downhole motor with a bent sub. The continual process of correcting the path of the borehole by

## ENHANCED GEOLOGICAL MODELLING

modification of the orientation of the bend angle results in a borehole path that is tortuous. The stiff NQ rod string fights a constant battle with the borehole walls and ultimately the frictional forces negate the ability of the drill machine to push the rods further. Soft or fractured ground may further limit the depth capacity of the directional-drilling project. Borehole collapse is a frequent cause of abandonment of a drilling exercise. The reasons for borehole failure in in-seam drilling are developed more fully in Thomson and MacDonald, 2003.

With directional drilling there is no core, and cuttings from the borehole are not normally collected. The only formal record of the borehole is contained in the data from the electronic survey instrument and the written records of the driller (Figure 2). This is the essence of the problem as these records are extremely subjective.

The driller records changes in drill machine performance and 'feel' as the string advances. This is recorded by the driller on hand written log sheets. According to the skills of the operator, the notes can be quite detailed or basic in the extreme. The driller is well aware of

SURVEY									
DEPTH	DIRECT	DP	ORIENT	DTRACK	COMMENTS	LR	VD	FLOW	DRET RIG DAY
33	125.7	-2.6	15	31.5	Branch 27m 1p 3cm	2.4	1.3	150	500 2000
39	126.2	-2.9	6	32.4	COAL	2.7	1.6	0	
45	125.2	-1.9	33.9	43.2	COAL	2.1	1.9	"	
51	122.5	-0.9	311	49.0	COAL	2.1	2.0	"	
57	121.4	-0.6	322	54.8	COAL	1.5	2.3	"	
63	120.4	-0.2	343	60.5	COAL	1.6	2.4	"	
69	118.4	-1.3	262	66.3	COAL	1.7	2.3	"	
75	117.2	-1.6	324	71.9	COAL	2.0	2.4	"	
81	116.6	-0.9	0	77.5	COAL	2.1	2.5	"	
87	114.6	-0.9	2.9	83.1	COAL	2.5	2.6	"	
93	113.5	-0.6	321	87.6	COAL	2.4	2.8	"	
99	113.0	1.2	69	94.6	COAL	2.3	2.9	"	
105	112.2	1.3	287	99.6	COAL	3.3	2.9	"	
111	110.0	1.5	282	104.6	COAL / BAVIS' HAND	3.5	2.7	"	
					AT 111m about 300mm long LAST 3m			180	700 2200
117	106.4	1.2	313	110.2	COAL / LAST 2m HARD	3.7	2.1	180	500 2000
					Grey Strk	4.6	1.9	170	700 2200
123	105.5	2.3	344	115.2	STRAK / Grey Strk	4.6	1.9	180	600 2700
129	105.2	3.3	324	120.4	STRAK / COAL LAST 2m	4.2	1.8	180	600 2700
135	104.6	4.1	326	125.3	COAL	4.7	1.7	180	500 2000
141	103.7	5.5	326	130.5	COAL / HARDER BAVIS' HAND Grey Strk	5.0	0.7	180	500 2100
147	102.4	7.0	349	135.4	COAL / BLACK RTN	5.0	0.0	180	500 2000
153	101.6	9.4	353	140.3	COAL	5.2	0.3	180	"
159	101.4	10.5	15	145.0	COAL / STRAK LAST 3m. Mudstone	6.0	1.8	180	500 2000

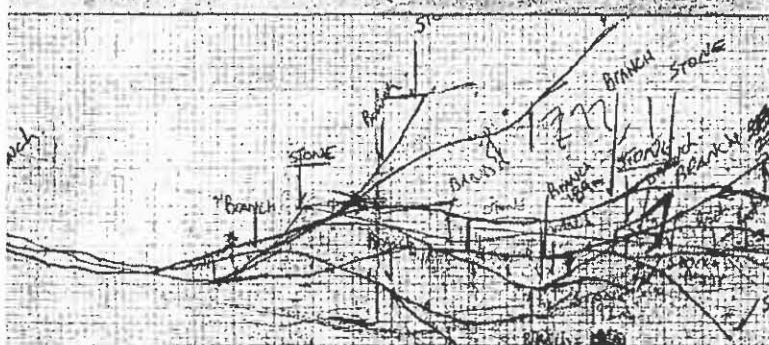


Figure 2 Typical underground in-seam driller's log; note driller's comments, the main clue to geological variability down hole.

hardness variation and also the colour change of the drilling fluid exiting the borehole. Thus, in most cases geological interpretation is carried out post-drilling - from viewing the drill logs - and using intuition to resolve the true meaning of "hard", "soft", "sticky", "grey" etc.

Using in-seam boreholes for exploration purposes alone is limited by the cost of the drilling exercise, the risk of losing tools down hole, and the quality of the data gathered during drilling. The last factor is the main reason for the lack of success in exploration drilling from in-seam, and this is why data from in-seam drilling is rarely used for geological modelling purposes. Geophysical logging of in-seam boreholes directly addresses this issue.

### Medium Radius Surface to Inseam Drilling (SIS)

This discussion deals only with surface to seam drilling of the Medium Radius Drilling (MRD) variety (Figure 3). MRD is a loose term but relates to a radius of curvature which can be drilled with standard drill pipe and standard rigs. This generally equates to a bend radius in the range 200 – 400 m (or 3° - 7° per 30 m). The application of MRD Surface to Inseam Drilling (SIS) has flourished in Australian coal mining over the past 3-5 years, primarily as a means of degasifying coal seams well in advance of mine workings, and as an alternative to inseam underground drilling. The relative cost benefits of this approach remains open to debate, and depends upon a number of geological factors, drilling performance factors, lead time issues, and economic decisions regarding the time value of money.

The application of MRD SIS has also been embraced in many Coal Seam Methane (CSM) fields. Here, directional drilling offers an alternative to more conventional extraction technologies such as Vertical Boreholes (fractured, cavity completed or under-reamed) and emerging technologies such as Tight Radius Drilling (TRD). For a summation of the pros and cons of the various drilling techniques for CSM applications refer to Thomson *et al.* 2003.

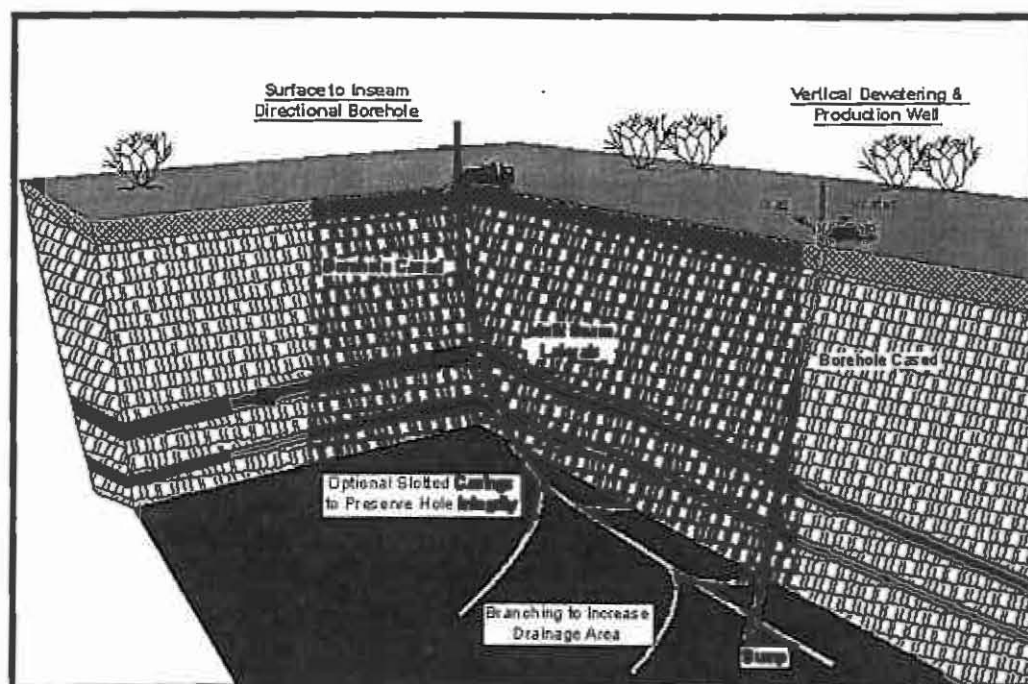


Figure 3 Schematic MRD configuration for gas extraction (from Thomson *et al.* 2003).

In SIS projects, cost has traditionally been controlled by utilising small mobile multipurpose rigs, which are standard mining industry equipment. In addition, as the sweet spot for MRD resides shallower than 500 m depth (see Thomson & MacDonald, 2002) MRD requirements suit the use of top drive rigs with lightweight drill pipe. The relatively “cheap” drill equipment and the fact that MRD SIS holes do not require stimulation suggests tailoring the methodology to shallower high permeability zones may prove successful, and this premise has been borne out by recent experience.

Another recent development has been the use of civil engineering Horizontal Directional Drilling (HDD) rigs to extend the reach of the SIS process. This variety of SIS utilises 60 t push / pull rigs to drill boreholes in excess of 2000 m inseam.

The key advantage of MRD as an extraction method is that the path of the drill hole opens up a large drainage area, impossible to replicate even with the largest hydraulic fracture from a vertical well. Boreholes with an in-seam section from 1000 – 2000 m are now commonplace and a large area of the resource can be drained from a single horizontal hole.

In coal mining applications of SIS the long in-seam section of the borehole is usually orientated parallel to mine gate roads, and down the axis of the proposed longwall panels. The location of these boreholes provides a great opportunity to gather geological data from the plane of the seam, in the area of most interest to the mine, and geophysical logging of these boreholes can provide detailed information impossible to replicate through surface based geophysical methodologies.

Gathering geological data from SIS boreholes – which have been drilled primarily for degasification purposes – is currently carried out crudely, relying on real time gamma data (at best) used for steering purposes and survey records. Whilst interpretation on this basis is better than nothing, the confidence in the outcomes of this process will be significantly enhanced using geophysical logging technologies.

The challenge remains to develop logging technology that can be easily adapted to SIS drilling systems, and the range of drill pipes in common use in Australia. In addition, the system should ideally also be suitable for deployment in underground in-seam boreholes.

### **EXPERIENCE OF LOGGING IN-SEAM BOREHOLES**

A number of field trials have been conducted over the past 2-3 years from a highwall at the German Creek mine in Central Queensland. The German Creek site was selected because (apart from being suitable in terms of access and availability) the research program could be used to explore a proposed underground mining area, an extension of Central Colliery. The site was expected to traverse a number of igneous intrusions and could therefore potentially provide valuable mine planning data. Two long in-seam horizontal boreholes were completed and logged in separate work phases (see ACARP Projects C12024 and C14034). The relative location of the two boreholes is presented in Figure 4.

A range of geophysical techniques were demonstrated at the German Creek site but the most useful proved to be the Directional Gamma System (DGS) and the Coal Combi Sonde (CCS) developed by Deutsche Montan Technologie (DMT) of Germany. These systems were designed for application in NQ and HQ cored boreholes in the Germany underground coal industry and had to be modified for use with Australia in-seam equipment at German Creek, and later for SIS field work completed in the Illawarra region of NSW. The most useful sondes were:

- Directional Gamma: Invaluable for determining position of the borehole path relative to the roof and floor, and the trend of the borehole through horizontal geological layers.
- Gamma-Gamma (or Density): Reinforces the directional gamma data by clearly identifying the difference between dense non-coal material and coal, but most importantly is the means to distinguish hard, crystalline igneous material from normal sedimentary lithologies.

- Acoustic calliper: Helps by establishing borehole diameter variation and ensuring correct interpretation of the gamma and density results, also assists by identifying zones of hole 'blow out' which may be related to geological structure.

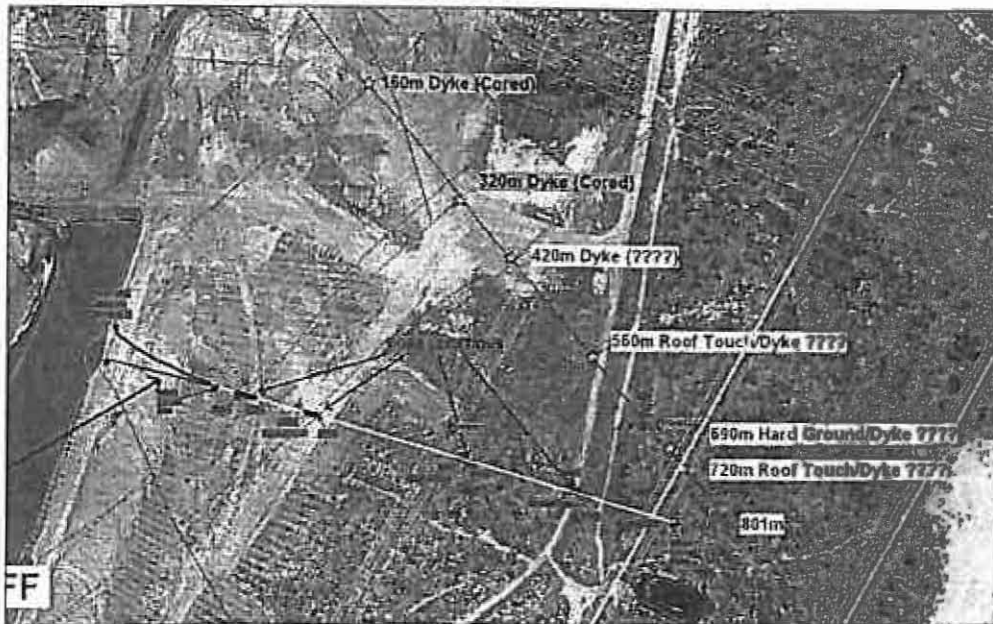


**Figure 4** Location of two in-seam boreholes used to evaluate geophysical logging technologies at German Creek. The most northern hole (blue) was drilled to the SE through a number of projected dykes (red). The second borehole (yellow) was drilled ESE.

The directional gamma results from the first survey at German Creek provide the best introduction to the value of the natural gamma results. Results for the first 260 m of borehole are shown in Figure 5. Also shown are the natural gamma results from the Surtech survey tool and an estimate of the position of the hole from mid-seam inferred from the Surtech data.

The natural gamma responses are in keeping with the results usually obtained in vertical exploration holes. In most circumstances, natural gamma data (recorded as either counts per second) or converted to a calibrated measure of API, become elevated in roof and floor rocks when compared with the coal. Figure 6 shows an example of a typical gamma ray log recorded from a vertical borehole at German Creek in the German Creek seam<sup>1</sup>. Key points to note is the gamma difference between coal and non-coal, and the presence of a mid seam band approximately 1m from the base of the seam – this also shows up clearly in the logging of the horizontal borehole.

When the borehole touches the floor between 50 and 90 m, there is a significant increase in the natural gamma radiation from the sensor directed to the floor but not to the same extent in the sensor directed upwards. Similarly, between 112-146 m where the hole touches the roof, there is a preferential increase in the radiation from the sensor directed upwards compared to the sensor directed down, except between 134-138 m where it appears that the hole has gone into the roof and the up and down sensors are reporting similar levels of radiation.

<sup>1</sup> Natural gamma radiation does not occur at a constant rate. As a result, natural gamma logs typically have a noisy appearance. The results become smoother if larger detecting crystals and longer measurement periods (slower logging rates) are used.

## ENHANCED GEOLOGICAL MODELLING

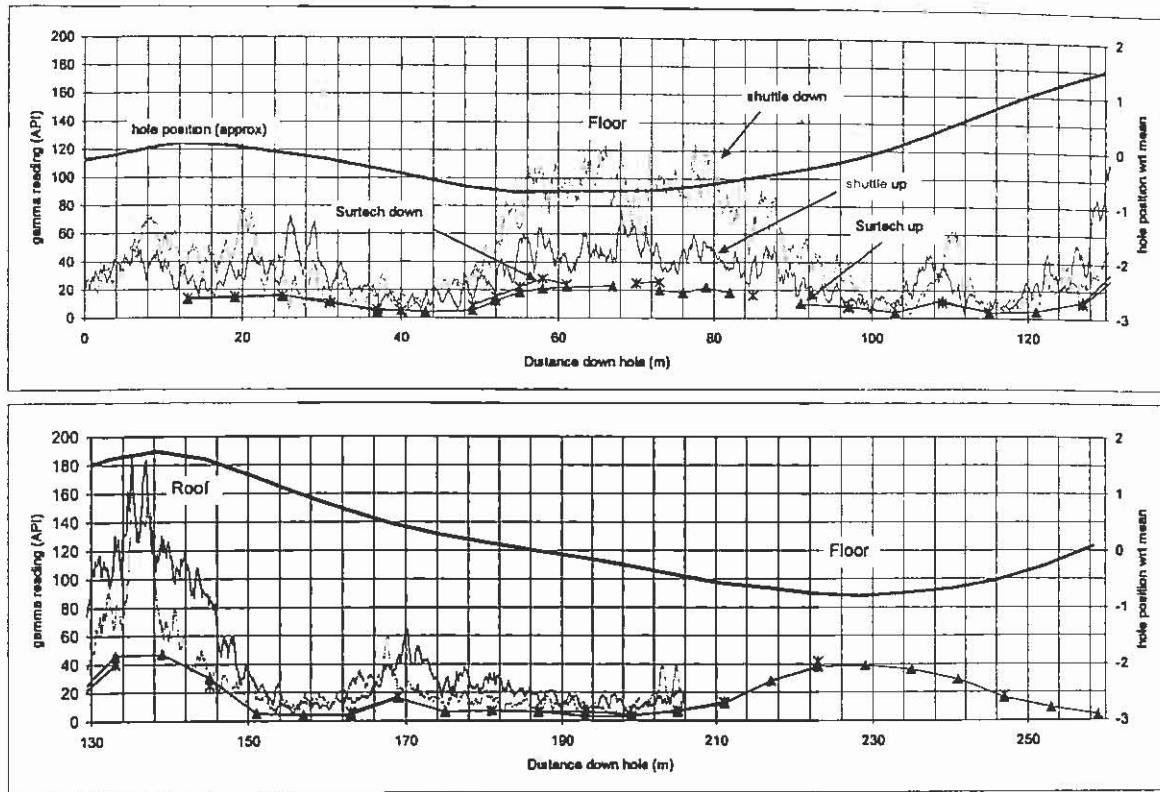


**Figure 5** Directional gamma results for the DMT directional gamma shuttle and Surtech tools for the first survey. The black line indicates the approximate position of the hole as inferred by the Surtech survey tool.

Note also the responses at 108-112 m and 166-174 m where it is inferred that the hole passes through a mid-seam ash band. At 108-112 m, the hole is trending upwards and the ash band is detected first by the detector directed upwards. The converse applies when the hole trends down through the ash band at 166-174 m. On the basis of these observations, it also appears that the hole has been collared in the vicinity of the ash band and remains at this relative position though to about 30 m.

A similar interpretation is possible from the Surtech natural gamma readings but the data are incomplete and the intensity of the signal is much reduced. The differences between the 'up' and 'down' readings are also correspondingly reduced. The factors that are affecting this log are the 6 m sampling interval (ie at rod changes), the size of the gamma ray detection crystal, and the time over which readings were taken and the shielding effect of the drill rods.

The density data for the first section of the hole is shown in Figure 7. These data have been converted from the measured gamma ray counts to approximate density using the formula:

$$\text{Density} = -\ln(\text{counts}) + 7.3$$

This is an empirical formula chosen because it placed the coal density at approximately 1.5 g/cc and the roof density at 135 m (where the hole is inferred to have passed into the roof) at slightly more than 2.5 g/cc.

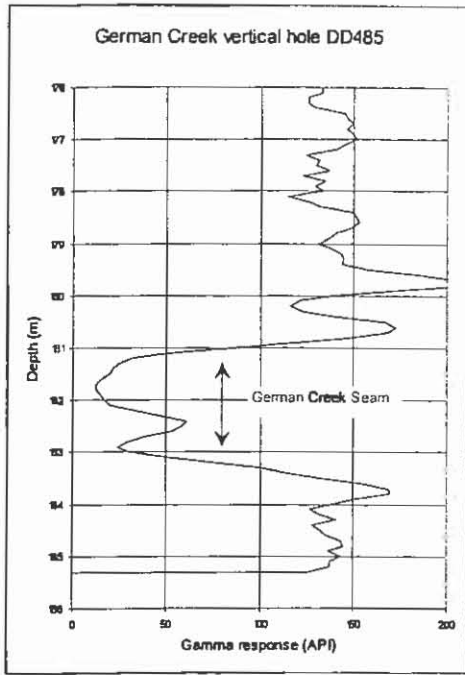


Figure 6 Typical gamma ray log from a vertical exploration hole at German Creek.

The density data in Figure 7 are consistent with the interpretation derived from the natural gamma data. When the hole is in the vicinity of the floor (50-90 m), the density lies between the coal and roof values. It is also slightly elevated in the vicinity of the ash bands in the first 30 m and at 107 m.

At the ash band at 165 m, a dyke was also intersected. The density at this point is much higher and has a value of about 3.1 g/cc – a value typical of a volcanic rock. This single point establishes the true value of the density reading, it unequivocally denotes the presence of igneous rock in a sedimentary coal environment, one of the main hazards to longwall coal extraction.

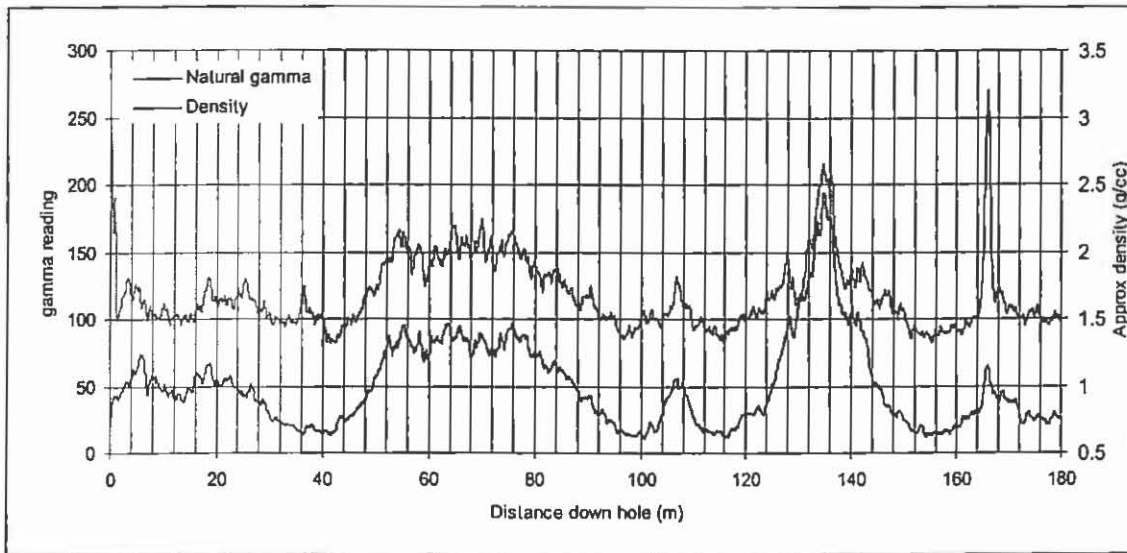


Figure 7 Density data from the Coal-Combi Shuttle for the first 180 m of the borehole with natural gamma data for reference.

### INTEGRATION WITH THE MINE PLANNING PROCESS

Currently, there is limited use of MRD borehole information for interpretation of geological structure, and probably even less use of underground drilling data. Reasons given for failure to include data from in-seam boreholes essentially revolve around a lack of confidence in the quality of data received. As a result, geological models use vertical borehole data almost exclusively to develop a grid surface that reflects seam characteristics. Vertical borehole spacing is usually on a grid with 500 m+ spacing. MRD borehole information – provided the data can be interpreted with confidence – offers the opportunity to input seam control points

at an almost infinitely detailed level along a linear section that corresponds with the path of the borehole. This could be similarly achieved in underground in-seam drilling provided logging and survey data was available for review.

An example is presented in Figure 9. This example uses real data from an Australian longwall operation. Here, the model generated from the vertical borehole data (green line) underestimates the severity of the dip change at 680 m and an upthrow fault at around 1560 m. Seam profile interpretation here is based on physical roof intersections (of which there are many). No horizontal in-seam logging data was available for this interpretation. The seam profile has been crudely generated, and even at this level shows areas of improvement on the original geological model. If this borehole had been logged the level of certainty would be much higher.

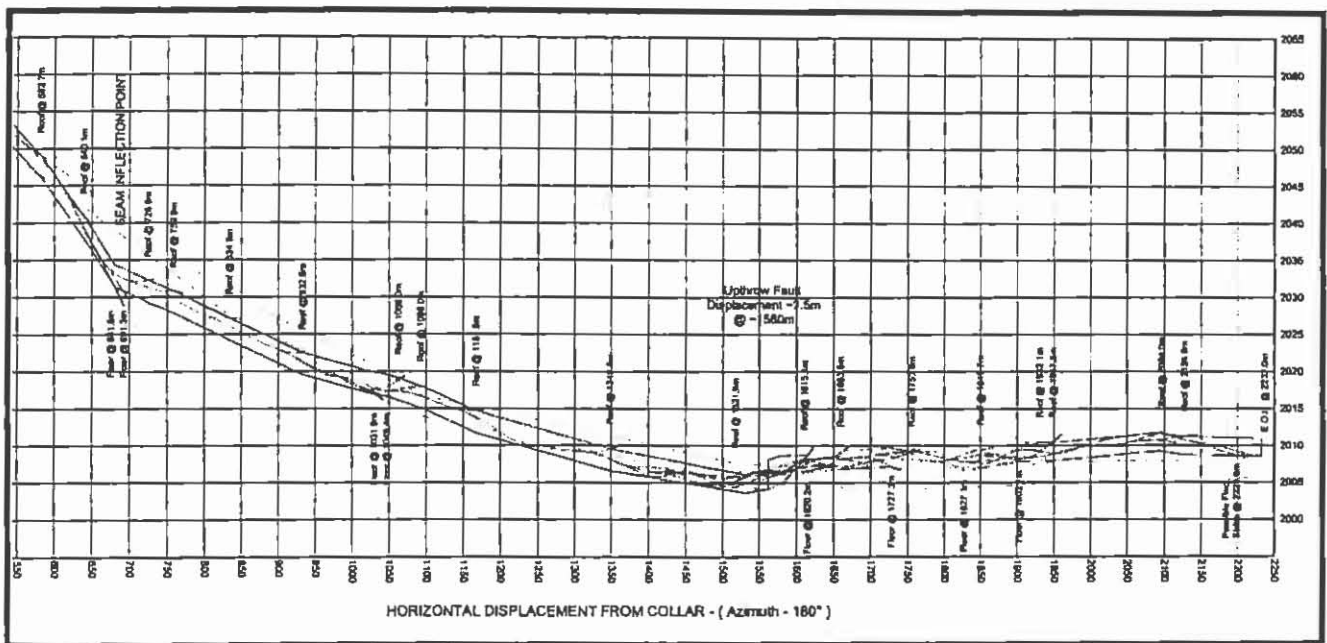


**Figure 9** A sectional view through a MRD SIS borehole showing the change to the geological model wrought by the interpretation of the in-seam borehole. The original model contours are in green.

In plan view (Figure 10), arbitrary seam control points along the path of the same borehole (established at 100 m centres) results in a re-contoured surface that more clearly reflects geological reality than the model that relied on vertical boreholes alone. The SIS data reveals faulting previously undetected, and provides a much clearer picture of seam morphology.

**CONCEPTS FOR DEVELOPMENT**

**What tools are important?**

For successful in-seam logging interpretation it has been established that the use of directional gamma, density and acoustic calliper are important. This combination satisfies most practical requirements of in-seam logging from horizontal boreholes. It establishes with a high level of confidence the position of the borehole path within the seam, the presence or absence of hard igneous intrusions, and provides the necessary tools to evaluate displacement structures. In short, this suite of tools is enough to elevate in-seam drilling geological interpretation from the

current status of rudimentary to non-existent, through to a high confidence interpretation that can be used to validate and improve the geological model.

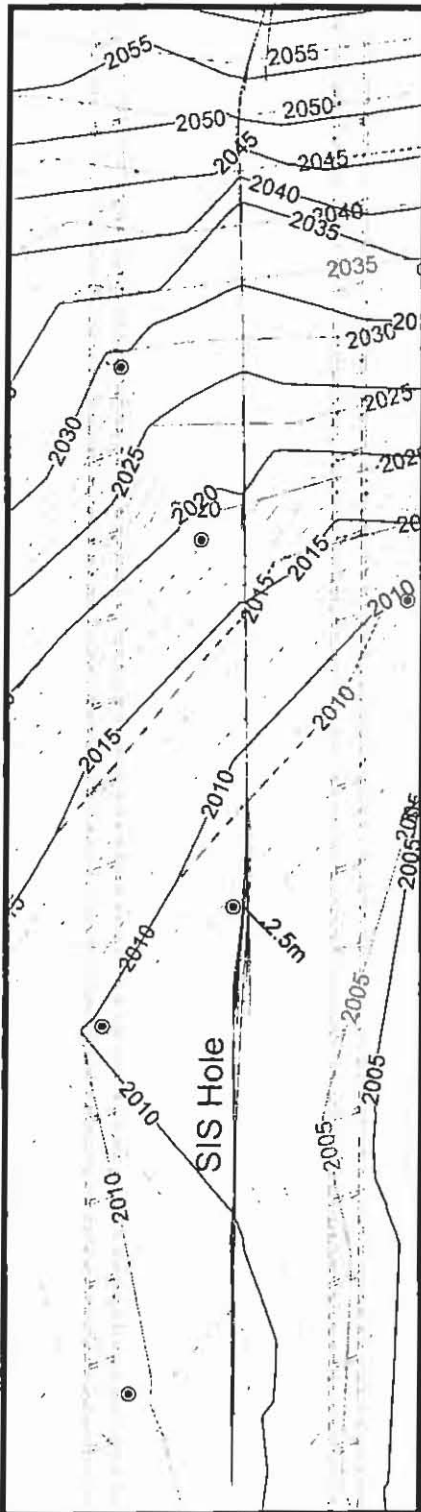


**Figure 10** Geological contours of top of seam showing variance between 500 m centres (brown) and with addition of SIS data (cyan).

However, these tools do not currently exist in a combined tool. The DMT systems have been designed specifically for the requirements of German coal mining, and are not suited to the Australian range of applications. The key components are also split, the directional gamma residing in the DGS and the density sonde within the CCS. In addition, recent work by CRC Mining in developing rig performance monitoring systems such as the Pressure Logger (a device that measures real time annular pressure down hole) and Torque Thrust Sensor (an objective means of evaluating rig performance parameters) should possibly be included in a specifically designed logging system for Australian MRD SIS and underground coal applications.

The precise configuration of the ideal logging tool needs to incorporate a flexibility of design that addresses both the deployment issues of MRD and underground in-seam drilling. It needs to incorporate (at a minimum) directional gamma, density and calliper capability, and ideally, also be linked to developments in rig performance systems such as the Torque/Thrust Sensor and Pressure Logger.

#### **Deployment issues**

Despite the technical success of the field programs utilising the DMT shuttles, it must be stressed that in each case, specific and unique modifications needed to be made to enable the work to proceed. The DMT shuttles are designed to be deployed by pumping down the inside of drill rods, however no MRD SIS rigs in Australia currently run large enough drill rods to accommodate the geophysical shuttles.

In addition, the CCS is designed to be used with HQ rods and the DGS with NQ, neither of which are suitable for use in MRD applications. NQ is relatively common underground but underground in-seam rods incorporate a MECCA connection (a hard wired rod that occupies a position within the inner wall of the rods). With the MECCA connection pump down logging is impossible.

A further unique feature of the CCS is the deployment of an acoustic calliper which protrudes from the front of the core barrel in normal HQ applications. In order to achieve this in the field work a dedicated run with an open (core barrel) ended rod was required. This enabled the shuttle to protrude during logging. The running of a dedicated rod string introduced unnecessary risk to the process and proved to be extremely time consuming (and expensive)

In short, the DMT shuttles provided valuable data but were clearly not designed for easy application in in-seam directionally drilled boreholes of the type common in Australia. A logging tool that addressed this ease of deployment issue is required. Other issues that also influenced this decision included the size of the DMT shuttles (large modules with some now out-of-date electronics), limited battery life for pump down and retraction from long MRD SIS boreholes, mechanical engineering problems associated with the deployment of a radioactive source in a non-vertical borehole, and the non-IS (intrinsically safe) nature of the CCS probe.

### **Concepts for an improved logging system**

The key ingredients for an improved logging system for Australian in-seam drilling purposes include:

- Compatibility with all popular drill pipes (therefore must be capable of being run in drill rods of 'N' size at a minimum).
- Must be designed IS in order to be used in underground boreholes.
- Must incorporate directional gamma, density and acoustic calliper sondes (at a minimum).
- Ideally should be linked to drill performance sensors such as Torque / Thrust and the Pressure Logger.
- Must be easily deployed in order to minimise rig down time during data acquisition.

As a consequence of these deliberations, the CRC Mining has lodged a patent application for a logging tool that satisfies these requirements, and incorporates some unique features that specifically address the requirements of logging in a horizontal borehole predominantly drilled in coal (Figure 10).

### **CONCLUSIONS**

The changing nature of in-seam drilling practice in Australian coal mining applications has provided an improved opportunity to gather geophysical logging data from long in-seam boreholes. Field work has established the particular value of directional gamma, density, and calliper data for the evaluation of geology from horizontal in-seam boreholes. This information can be used to significantly improve the quality of the geological model for prospective longwall operations.

Work is underway to develop a logging tool suitable for application in Australian in-seam boreholes.

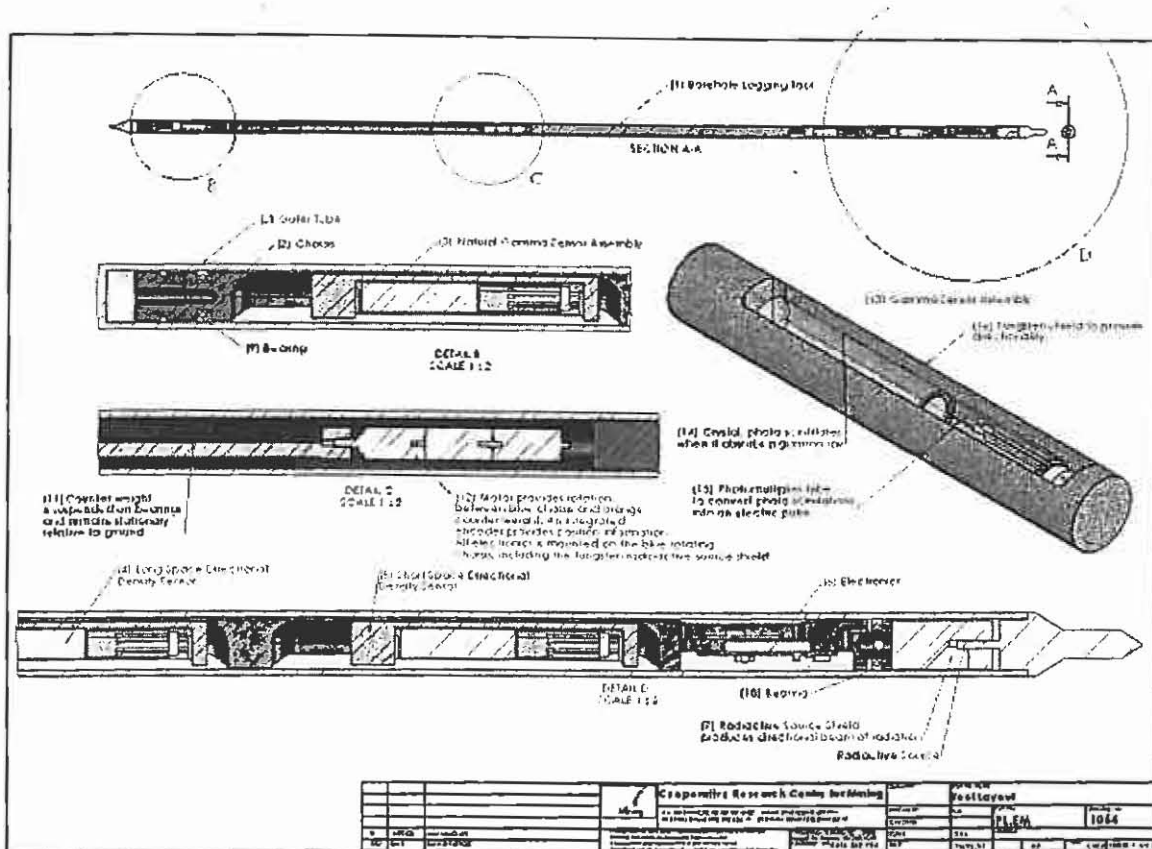


Figure 10 Patented design for a geophysical logging tool that will be suitable for deployment in all current Australian in-seam drilling applications.

**ACKNOWLEDGEMENTS**

This work has been supported by the Australian coal industry through ACARP Projects C1204 and C14034. Anglo Coal and BHPB Illawarra have assisted with site preparation and partly funded the field work. The contribution of DMT of Germany to the research program is gratefully acknowledged.

**REFERENCES**

AUSTRALIAN DRILLING INDUSTRY TRAINING COMMITTEE LTD. 1997, *Drilling: the Manual of Methods, Applications, and Management*, Lewis Publishers, CRC Press LLC.

BPB COAL INTERPRETATION MANUAL. 1981. BPB Instruments Limited, Loughborough, UK.

HATHERLY P., DIXON R., TCHEN T., JECNY Z., CERAVOLO C., MURRAY W., POLLOCK J.T.A. & WILLIAMS C.J. 1996. *Sensing and logging for in-seam boreholes*. Final report, ACARP project C4037.

GRAY I., CLEMENCE P., PARADISE G., CHARLTON S., DIXON R. & HATHERLY P. 2002. *The development of geosteering sensors for in-seam drilling* Final Report ACARP, Projects C5029, C7023, C10007.

RIDER M. 1996. *The Geological Interpretation of Well Logs*, Whittles Publishing, Caithness, UK.

THOMSON S. 1999. *In-seam exploration drilling: mine planning applications*, Bowen Basin Geological Symposium, submitted paper.

## ENHANCED GEOLOGICAL MODELLING

- THOMSON S. & ADAM S. 2006. *Intelligent Drilling Systems*, Final report, ACARP project C14034 (in press).
- THOMSON S., ADAM, S. & HATHERLY P. 2005. *Comparative Study of In-Seam Surveying Technology (Coal Interface Detection Project)*, Final report, ACARP project C12024.
- THOMSON S. & MACDONALD D. 2002. *The Application of Medium Radius Drilling for Coal Bed Methane Extraction*, 1<sup>st</sup> Australian Coal Seam and Mine Methane Conference, 25-26 June 2002.
- THOMSON S. & MACDONALD D. 2003. *A Question of Balance - dispelling the myth of 'boggy ground' and other spurious claims in coal seam drilling*, 35<sup>th</sup> Sydney Basin Symposium, 29-30 Sep 2003, University of Wollongong.
- THOMSON, S. & MACDONALD D. 2004. *Extended Surface to Seam Drilling; Design and Control*, 2<sup>nd</sup> Coal Seam Methane and Mine Methane Summit, 18-19 March 2004.
- THOMSON, S., LUKAS A. & MACDONALD D. 2003. *Maximising Coal Seam Methane Extraction through Advanced Drilling Technologies*, 2<sup>nd</sup> Australian Coal Seam and Mine Methane Conference, 19-20 February 2003.



## List of Authors

<b>Author</b>	<b>Page</b>
Adam, S.	279
Ahmed, M.	149
Armstrong, M.	59
Averkiou, A.	223
Bartlett, K.	157, 197
Beamish, B.	1
Bowman, H.	125
Clarkson, F.	1
Carr, P.	9, 141
Coxhead, C.	37
Creech, M.	167
Daigle, L.	177
David, K.	15
Davis, B.	27
Dawson, M.	37, 189
Demidjuk, Z.,	111
Edwards, J.	157, 197
Esterle, J.	27, 213
Faiz, M.	117, 149
Fergusson, C.	45
French, D.	125
Gentz, M.	95
George, S.	149
Griffin, J.	51
Grobler, P.	103
Gurba, L.	133
Hatherly, P.	59, 197, 279
Healy, B.,	111
Heidrich, C.	125
Hendrick, N.	267
Hopley, C.	71, 79
Hutton, A.	51, 87, 97, 253
Jones, B.	9, 71, 79, 95, 141
Johnson, M.	95
Keilar, D.	27
Kyan, D.,	111
Lea, J.	197
Li, Z.	133
Malone, M.	213
McCaughan, G.,	111
McLean, W.	223

**List of Authors (cont.)**

McMahon, C.	231
McMinn, A.	37
Munroe, S.	111
O'Brien, G.	253
Och, D.	243
O'Donnell, M.	253
Peters, T.	267
Pickel, W.	277
Pinetown, K.	103
Prendergast, E.	111
Puotinen, M.	79
Roberts, D.	117
Saghafi, A.	105, 117
Selleck, B.	9
Sliwa, R.	213
Thomson, S.	59, 2793
Volk, H.	149
Ward, C.	125, 133
Williams, M.	141
Williams, R.	213
Woodfull, C.	111